Emergency Medicine International

Application of Image Processing Technology in Emergency Medicine

Lead Guest Editor: Hang Chen
Guest Editors: Zhendong Mu, Yi Liang, and Naeem Akhtar Qaisrani

Application of Image Processing Technology in Emergency Medicine

Emergency Medicine International

Application of Image Processing Technology in Emergency Medicine

Lead Guest Editor: Hang Chen
Guest Editors: Zhendong Mu, Yi Liang, and Naeem Akhtar Qaisrani

Contents

Retracted: Establishment of a Finite Element Model of Normal Nasal Bone and Analysis of Its Biomechanical Characteristics
Emergency Medicine International
Retraction (1 page), Article ID 9814568, Volume 2023 (2023)

Retracted: Key Technology of the Medical Image Wise Mining Method Based on the Meanshift Algorithm
Emergency Medicine International
Retraction (1 page), Article ID 9809046, Volume 2023 (2023)

Retracted: Risk Factors of Catheter-Related Infection in Unplanned Extubation of Totally Implantable Venous-Accessportsin Tumor Patients
Emergency Medicine International
Retraction (1 page), Article ID 9805374, Volume 2023 (2023)

Retracted: Related Factor Analysis and Nursing Strategies of Diarrhea in Critically Ill Patients with Enteral Nutrition
Emergency Medicine International
Retraction (1 page), Article ID 9803698, Volume 2023 (2023)

Retracted: A Multimodel Fusion Method for Cardiovascular Disease Detection Using ECG
Emergency Medicine International
Retraction (1 page), Article ID 9803581, Volume 2023 (2023)

Retracted: Diagnostic Predictive Value of Tryptase, Serum Amyloid A and Lipoprotein-Associated Phospholipase A2 Biomarker Groups for Large Atherosclerotic Cerebral Infarction
Emergency Medicine International
Retraction (1 page), Article ID 9798523, Volume 2023 (2023)

Retracted: Application Value of Management Model Based on "Zero Tolerance" Concept in Pressure Ulcer Management
Emergency Medicine International
Retraction (1 page), Article ID 9786387, Volume 2023 (2023)

Retracted: An Auxiliary Scoring Model for Patients with Acute Pulmonary Embolism Complicated with Atrial Fibrillation Was Established Based on Random Forests
Emergency Medicine International
Retraction (1 page), Article ID 9784847, Volume 2023 (2023)

Retracted: Application of Melatonin with N-Acetylcysteine Exceeds Traditional Treatment for Acetaminophen-Induced Hepatotoxicity
Emergency Medicine International
Retraction (1 page), Article ID 9783815, Volume 2023 (2023)

Contents

Retracted: The Influence of Sports Dance on the Physical and Mental Development of Contemporary College Students Based on Health Detection
Emergency Medicine International
Retraction (1 page), Article ID 9803639, Volume 2023 (2023)

Retracted: Application of Low-Intensity Laser in the Treatment of Skeletal Muscle Injury in Runners
Emergency Medicine International
Retraction (1 page), Article ID 9801869, Volume 2023 (2023)

Retracted: Analysis of the Effect of Quality Nursing on Recovery after Thoracic Surgery
Emergency Medicine International
Retraction (1 page), Article ID 9794070, Volume 2023 (2023)

Retracted: Effects of Amiodarone and Esmolol for Heart Rate and Cardiovascular Changes
Emergency Medicine International
Retraction (1 page), Article ID 9789785, Volume 2023 (2023)

Retracted: Application of Computer-Based Simulation Teaching Combined with PBL in Colorectal Tumor Hemorrhage
Emergency Medicine International
Retraction (1 page), Article ID 9763530, Volume 2023 (2023)

Retracted: 3D Automatic Segmentation of Brain Tumor Based on Deep Neural Network and Multimodal MRI Images
Emergency Medicine International
Retraction (1 page), Article ID 9754041, Volume 2023 (2023)

Retracted: Font Design in Visual Communication Design of Genetic Algorithm
Emergency Medicine International
Retraction (1 page), Article ID 9896378, Volume 2023 (2023)

Retracted: A Study on the Relationship between Sense of Disease Uncertainty and Family Strength and Mental Resilience in Guardians of Children with Inflammatory Bowel Disease
Emergency Medicine International
Retraction (1 page), Article ID 9879027, Volume 2023 (2023)

Retracted: Association of β2-Agonist Receptor Gene Polymorphisms with Acute Exacerbations of COPD: A Prospective Observational Study
Emergency Medicine International
Retraction (1 page), Article ID 9874658, Volume 2023 (2023)

Retracted: Influence of Aerobic Exercise Load Intensity on Children's Mental Health
Emergency Medicine International
Retraction (1 page), Article ID 9869764, Volume 2023 (2023)

Contents

[Retracted] Effect of Zhuyun I Recipe Capsule Enema on the Immune Microenvironment of the Endometrium during Implantation Window in Rats
Hang Zhou, Pei Guo, Pengfei Zeng, Zhixing Yin, Li Yan, Jinzhu Huang, Yi Wang, Juan Li, Wanting Xia, Yang Wang, Chang Liu, and Qian Zeng
Research Article (11 pages), Article ID 4746121, Volume 2022 (2022)

[Retracted] Systematic Review and Meta-Analysis of the Evaluation of the Efficacy of Manipulation and Cervical Traction in the Treatment of Radical Cervical Spondylosis
Jianquan Chen, Rongbin Chen, Yong Li, Maoshui Chen, Zhouming Lv, Haobin Zeng, and Qiang Lian
Research Article (10 pages), Article ID 3837995, Volume 2022 (2022)

[Retracted] Diagnostic Predictive Value of Tryptase, Serum Amyloid A and Lipoprotein-Associated Phospholipase A2 Biomarker Groups for Large Atherosclerotic Cerebral Infarction
Wenhui Jia, Xia Li, Fang Lei, Fengyun Hu, Fenglian Li, Xueying Zhang, Siyu Liu, Feifei Huang, and Changxin Li
Research Article (7 pages), Article ID 5784909, Volume 2022 (2022)

[Retracted] A Meta-Analysis of How Nonalcoholic Fatty Liver Disease Affect Antiviral Treatment of Patients with e Antigen-Positive Chronic Hepatitis B
Yandong Chen, Qiang Liu, Jing Han, Siyu Gao, Qian Xiao, Xiaoli Huang, Lu Lu, and xiaolin Zhou
Research Article (7 pages), Article ID 4774195, Volume 2022 (2022)

[Retracted] Clinical Evaluation of Unilateral Vertebroplasty for OVCF
Xiaoming Wen, Yan Zhang, Wei Jiang, Wenbo An, Binggang Zhang, and Jianjun Liu
Research Article (6 pages), Article ID 2037185, Volume 2022 (2022)

[Retracted] Efficacy and Safety of Glycosides of Tripterygium wilfordii Combined with Renin-Angiotensin System in the Treatment of IgA Nephropathy: A Systematic Review and Meta-Analysis
Ming Chen, Peiqing Zhang, Lianhua Li, Zhuo Yu, Na Liu, and Lifan Wang
Research Article (12 pages), Article ID 5314105, Volume 2022 (2022)

[Retracted] Effect of Risk-Focused Diversified Safety Management Mode in Patients with Major Artery Stent Implantation
Yan Shao, Cai-Juan Wu, Youjun Mao, Dong-Mei Li, Yun-Zhou Wang, and Kang Zhu
Research Article (9 pages), Article ID 1284254, Volume 2022 (2022)

[Retracted] Clinical Efficacy and Safety Analysis of Levofloxacin for the Prevention of Infection after Traumatic Osteoarthrosis and Internal Fixation: Systematic Review and Meta-Analysis
Weiliang Wang, ChuanQi Zou, and Jie Zhang
Research Article (9 pages), Article ID 8788365, Volume 2022 (2022)

[Retracted] Risk Factors of Catheter-Related Infection in Unplanned Extubation of Totally Implantable Venous-Accessportsin Tumor Patients
Min Xu, Lie Deng, Yanyi Zhu, Yuanfang Li, Fan Wang, Hui Li, and Ying Zhou
Research Article (7 pages), Article ID 4235316, Volume 2022 (2022)

Contents

Contents

Hindawi
Emergency Medicine International
Volume 2023, Article ID 9813103, 1 page
https://doi.org/10.1155/2023/9813103

Retraction

Retracted: An Image Fusion Algorithm Based on Improved RGF and Visual Saliency Map

Emergency Medicine International

Received 19 December 2023; Accepted 19 December 2023; Published 20 December 2023

This article has been retracted by Hindawi following an investigation undertaken by the publisher [1]. This investigation has uncovered evidence of one or more of the following indicators of systematic manipulation of the publication process:

(1) Discrepancies in scope

(2) Discrepancies in the description of the research reported

(3) Discrepancies between the availability of data and the research described

(4) Inappropriate citations

(5) Incoherent, meaningless and/or irrelevant content included in the article

(6) Manipulated or compromised peer review

The presence of these indicators undermines our confidence in the integrity of the article's content and we cannot, therefore, vouch for its reliability. Please note that this notice is intended solely to alert readers that the content of this article is unreliable. We have not investigated whether authors were aware of or involved in the systematic manipulation of the publication process.

Wiley and Hindawi regrets that the usual quality checks did not identify these issues before publication and have since put additional measures in place to safeguard research integrity.

We wish to credit our own Research Integrity and Research Publishing teams and anonymous and named external researchers and research integrity experts for contributing to this investigation.

The corresponding author, as the representative of all authors, has been given the opportunity to register their agreement or disagreement to this retraction. We have kept a record of any response received.

References

[1] Y. Li, H. Yang, and Y. Gao, "An Image Fusion Algorithm Based on Improved RGF and Visual Saliency Map," *Emergency Medicine International*, vol. 2022, Article ID 1693531, 10 pages, 2022.

Hindawi
Emergency Medicine International
Volume 2023, Article ID 9754073, 1 page
https://doi.org/10.1155/2023/9754073

Retraction

Retracted: Study on the Changes of Liver and Kidney Function-Related Indicators and Clinical Significance in Patients with OSAHS

Emergency Medicine International

Received 19 December 2023; Accepted 19 December 2023; Published 20 December 2023

This article has been retracted by Hindawi following an investigation undertaken by the publisher [1]. This investigation has uncovered evidence of one or more of the following indicators of systematic manipulation of the publication process:

(1) Discrepancies in scope
(2) Discrepancies in the description of the research reported
(3) Discrepancies between the availability of data and the research described
(4) Inappropriate citations
(5) Incoherent, meaningless and/or irrelevant content included in the article
(6) Manipulated or compromised peer review

The presence of these indicators undermines our confidence in the integrity of the article's content and we cannot, therefore, vouch for its reliability. Please note that this notice is intended solely to alert readers that the content of this article is unreliable. We have not investigated whether authors were aware of or involved in the systematic manipulation of the publication process.

In addition, our investigation has also shown that one or more of the following human-subject reporting requirements has not been met in this article: ethical approval by an Institutional Review Board (IRB) committee or equivalent, patient/participant consent to participate, and/or agreement to publish patient/participant details (where relevant).

Wiley and Hindawi regrets that the usual quality checks did not identify these issues before publication and have since put additional measures in place to safeguard research integrity.

We wish to credit our own Research Integrity and Research Publishing teams and anonymous and named external researchers and research integrity experts for contributing to this investigation.

The corresponding author, as the representative of all authors, has been given the opportunity to register their agreement or disagreement to this retraction. We have kept a record of any response received.

References

[1] R. Liu and X. Kong, "Study on the Changes of Liver and Kidney Function-Related Indicators and Clinical Significance in Patients with OSAHS," *Emergency Medicine International*, vol. 2022, Article ID 9536617, 7 pages, 2022.

Hindawi
Emergency Medicine International
Volume 2023, Article ID 9870169, 1 page
https://doi.org/10.1155/2023/9870169

Retraction

Retracted: Analysis of the Effectiveness of Transradial Access Puncture in the Application of Complications and Comfort after Cerebral Angiography

Emergency Medicine International

Received 28 November 2023; Accepted 28 November 2023; Published 29 November 2023

This article has been retracted by Hindawi, as publisher, following an investigation undertaken by the publisher [1]. This investigation has uncovered evidence of systematic manipulation of the publication and peer-review process. We cannot, therefore, vouch for the reliability or integrity of this article.

Please note that this notice is intended solely to alert readers that the peer-review process of this article has been compromised.

Wiley and Hindawi regret that the usual quality checks did not identify these issues before publication and have since put additional measures in place to safeguard research integrity.

We wish to credit our Research Integrity and Research Publishing teams and anonymous and named external researchers and research integrity experts for contributing to this investigation.

The corresponding author, as the representative of all authors, has been given the opportunity to register their agreement or disagreement to this retraction. We have kept a record of any response received.

References

[1] H. Wan, L. Gao, and D. Huang, "Analysis of the Effectiveness of Transradial Access Puncture in the Application of Complications and Comfort after Cerebral Angiography," *Emergency Medicine International*, vol. 2022, Article ID 3457034, 6 pages, 2022.

Hindawi
Emergency Medicine International
Volume 2023, Article ID 9864247, 1 page
https://doi.org/10.1155/2023/9864247

Retraction

Retracted: Clinical Efficacy and Safety Analysis of Levofloxacin for the Prevention of Infection after Traumatic Osteoarthrosis and Internal Fixation: Systematic Review and Meta-Analysis

Emergency Medicine International

Received 28 November 2023; Accepted 28 November 2023; Published 29 November 2023

This article has been retracted by Hindawi, as publisher, following an investigation undertaken by the publisher [1]. This investigation has uncovered evidence of systematic manipulation of the publication and peer-review process. We cannot, therefore, vouch for the reliability or integrity of this article.

Please note that this notice is intended solely to alert readers that the peer-review process of this article has been compromised.

Wiley and Hindawi regret that the usual quality checks did not identify these issues before publication and have since put additional measures in place to safeguard research integrity.

We wish to credit our Research Integrity and Research Publishing teams and anonymous and named external researchers and research integrity experts for contributing to this investigation.

The corresponding author, as the representative of all authors, has been given the opportunity to register their agreement or disagreement to this retraction. We have kept a record of any response received.

References

[1] W. Wang, C. Zou, and J. Zhang, "Clinical Efficacy and Safety Analysis of Levofloxacin for the Prevention of Infection after Traumatic Osteoarthrosis and Internal Fixation: Systematic Review and Meta-Analysis," *Emergency Medicine International*, vol. 2022, Article ID 8788365, 9 pages, 2022.

Hindawi
Emergency Medicine International
Volume 2023, Article ID 9863185, 1 page
https://doi.org/10.1155/2023/9863185

Retraction

Retracted: The Impact of 3S2E Nursing Management on the Psychological Status of Respiratory Function and Quality of Life of Patients with Severe Pneumonia in the ICU

Emergency Medicine International

Received 28 November 2023; Accepted 28 November 2023; Published 29 November 2023

This article has been retracted by Hindawi, as publisher, following an investigation undertaken by the publisher [1]. This investigation has uncovered evidence of systematic manipulation of the publication and peer-review process. We cannot, therefore, vouch for the reliability or integrity of this article.

Please note that this notice is intended solely to alert readers that the peer-review process of this article has been compromised.

Wiley and Hindawi regret that the usual quality checks did not identify these issues before publicationand have since put additional measures in place to safeguard research integrity.

We wish to credit our Research Integrity and Research Publishing teams and anonymous and named external researchers and research integrity experts for contributing to this investigation.

The corresponding author, as the representative of all authors, has been given the opportunity to register their agreement or disagreement to this retraction. We have kept a record of any response received.

References

[1] Y. Xu, X. Li, Q. Yang, and X. Ma, "The Impact of 3S2E Nursing Management on the Psychological Status of Respiratory Function and Quality of Life of Patients with Severe Pneumonia in the ICU," *Emergency Medicine International*, vol. 2022, Article ID 4949498, 5 pages, 2022.

Hindawi
Emergency Medicine International
Volume 2023, Article ID 9840632, 1 page
https://doi.org/10.1155/2023/9840632

Retraction

Retracted: Meta-Analysis of Predictive Role of Early Neurological Deterioration after Intravenous Thrombolysis

Emergency Medicine International

Received 28 November 2023; Accepted 28 November 2023; Published 29 November 2023

This article has been retracted by Hindawi, as publisher, following an investigation undertaken by the publisher [1]. This investigation has uncovered evidence of systematic manipulation of the publication and peer-review process. We cannot, therefore, vouch for the reliability or integrity of this article.

Please note that this notice is intended solely to alert readers that the peer-review process of this article has been compromised.

Wiley and Hindawi regret that the usual quality checks did not identify these issues before publication and have since put additional measures in place to safeguard research integrity.

We wish to credit our Research Integrity and Research Publishing teams and anonymous and named external researchers and research integrity experts for contributing to this investigation.

The corresponding author, as the representative of all authors, has been given the opportunity to register their agreement or disagreement to this retraction. We have kept a record of any response received.

References

[1] H. Jiang, J. Zuo, D. Wang, Y. Huang, C. Gao, and Y. Wan, "Meta-Analysis of Predictive Role of Early Neurological Deterioration after Intravenous Thrombolysis," *Emergency Medicine International*, vol. 2022, Article ID 2894426, 11 pages, 2022.

Hindawi
Emergency Medicine International
Volume 2023, Article ID 9840485, 1 page
https://doi.org/10.1155/2023/9840485

Retraction

Retracted: *C*-Reactive Protein, Procalcitonin, and a Novel Pathogenesis and Therapeutic Target of Thrombocytopenia in Sepsis

Emergency Medicine International

Received 28 November 2023; Accepted 28 November 2023; Published 29 November 2023

This article has been retracted by Hindawi, as publisher, following an investigation undertaken by the publisher [1]. This investigation has uncovered evidence of systematic manipulation of the publication and peer-review process. We cannot, therefore, vouch for the reliability or integrity of this article.

Please note that this notice is intended solely to alert readers that the peer-review process of this article has been compromised.

Wiley and Hindawi regret that the usual quality checks did not identify these issues before publication and have since put additional measures in place to safeguard research integrity.

We wish to credit our Research Integrity and Research Publishing teams and anonymous and named external researchers and research integrity experts for contributing to this investigation.

The corresponding author, as the representative of all authors, has been given the opportunity to register their agreement or disagreement to this retraction. We have kept a record of any response received.

References

[1] J. Li, L. Hu, and L. Li, "*C*-Reactive Protein, Procalcitonin, and a Novel Pathogenesis and Therapeutic Target of Thrombocytopenia in Sepsis," *Emergency Medicine International*, vol. 2022, Article ID 2498435, 9 pages, 2022.

Hindawi
Emergency Medicine International
Volume 2023, Article ID 9831045, 1 page
https://doi.org/10.1155/2023/9831045

Retraction

Retracted: Nursing of Vulvar Cancer Radical Operation Combined with Laparoscopic Inguinal Lymph Node Dissection

Emergency Medicine International

Received 28 November 2023; Accepted 28 November 2023; Published 29 November 2023

This article has been retracted by Hindawi, as publisher, following an investigation undertaken by the publisher [1]. This investigation has uncovered evidence of systematic manipulation of the publication and peer-review process. We cannot, therefore, vouch for the reliability or integrity of this article.

Please note that this notice is intended solely to alert readers that the peer-review process of this article has been compromised.

Wiley and Hindawi regret that the usual quality checks did not identify these issues before publication and have since put additional measures in place to safeguard research integrity.

We wish to credit our Research Integrity and Research Publishing teams and anonymous and named external researchers and research integrity experts for contributing to this investigation.

The corresponding author, as the representative of all authors, has been given the opportunity to register their agreement or disagreement to this retraction. We have kept a record of any response received.

References

[1] S. Huang and F. Qiu, "Nursing of Vulvar Cancer Radical Operation Combined with Laparoscopic Inguinal Lymph Node Dissection," *Emergency Medicine International*, vol. 2022, Article ID 8091114, 6 pages, 2022.

Hindawi
Emergency Medicine International
Volume 2023, Article ID 9826874, 1 page
https://doi.org/10.1155/2023/9826874

Retraction

Retracted: Total Thoracoscopic versus Robotic Surgery for Repair of Atrial Septum Defect: A Propensity Matching Score Analysis

Emergency Medicine International

Received 28 November 2023; Accepted 28 November 2023; Published 29 November 2023

This article has been retracted by Hindawi, as publisher, following an investigation undertaken by the publisher [1]. This investigation has uncovered evidence of systematic manipulation of the publication and peer-review process. We cannot, therefore, vouch for the reliability or integrity of this article.

Please note that this notice is intended solely to alert readers that the peer-review process of this article has been compromised.

Wiley and Hindawi regret that the usual quality checks did not identify these issues before publication and have since put additional measures in place to safeguard research integrity.

We wish to credit our Research Integrity and Research Publishing teams and anonymous and named external researchers and research integrity experts for contributing to this investigation.

The corresponding author, as the representative of all authors, has been given the opportunity to register their agreement or disagreement to this retraction. We have kept a record of any response received.

References

[1] Y. Liu, Z. Liu, X. Li et al., "Total Thoracoscopic versus Robotic Surgery for Repair of Atrial Septum Defect: A Propensity Matching Score Analysis," *Emergency Medicine International*, vol. 2022, Article ID 5371493, 6 pages, 2022.

Hindawi
Emergency Medicine International
Volume 2023, Article ID 9820756, 1 page
https://doi.org/10.1155/2023/9820756

Retraction

Retracted: Clinical Features and Surgical Strategies of Distal Radius Posttraumatic Deformity

Emergency Medicine International

Received 28 November 2023; Accepted 28 November 2023; Published 29 November 2023

This article has been retracted by Hindawi, as publisher, following an investigation undertaken by the publisher [1]. This investigation has uncovered evidence of systematic manipulation of the publication and peer-review process. We cannot, therefore, vouch for the reliability or integrity of this article.

Please note that this notice is intended solely to alert readers that the peer-review process of this article has been compromised.

Wiley and Hindawi regret that the usual quality checks did not identify these issues before publication and have since put additional measures in place to safeguard research integrity.

We wish to credit our Research Integrity and Research Publishing teams and anonymous and named external researchers and research integrity experts for contributing to this investigation.

The corresponding author, as the representative of all authors, has been given the opportunity to register their agreement or disagreement to this retraction. We have kept a record of any response received.

References

[1] N. Zhang and J. Fang, "Clinical Features and Surgical Strategies of Distal Radius Posttraumatic Deformity," *Emergency Medicine International*, vol. 2022, Article ID 5268822, 7 pages, 2022.

Hindawi
Emergency Medicine International
Volume 2023, Article ID 9814568, 1 page
https://doi.org/10.1155/2023/9814568

Retraction

Retracted: Establishment of a Finite Element Model of Normal Nasal Bone and Analysis of Its Biomechanical Characteristics

Emergency Medicine International

Received 28 November 2023; Accepted 28 November 2023; Published 29 November 2023

This article has been retracted by Hindawi, as publisher, following an investigation undertaken by the publisher [1]. This investigation has uncovered evidence of systematic manipulation of the publication and peer-review process. We cannot, therefore, vouch for the reliability or integrity of this article.

Please note that this notice is intended solely to alert readers that the peer-review process of this article has been compromised.

Wiley and Hindawi regret that the usual quality checks did not identify these issues before publication and have since put additional measures in place to safeguard research integrity.

We wish to credit our Research Integrity and Research Publishing teams and anonymous and named external researchers and research integrity experts for contributing to this investigation.

The corresponding author, as the representative of all authors, has been given the opportunity to register their agreement or disagreement to this retraction. We have kept a record of any response received.

References

[1] L. Zhang, X. Wang, Y. Sun, S. Wang, F. Zhang, and Z. Zhang, "Establishment of a Finite Element Model of Normal Nasal Bone and Analysis of Its Biomechanical Characteristics," *Emergency Medicine International*, vol. 2023, Article ID 3783051, 8 pages, 2023.

Hindawi
Emergency Medicine International
Volume 2023, Article ID 9809046, 1 page
https://doi.org/10.1155/2023/9809046

Retraction

Retracted: Key Technology of the Medical Image Wise Mining Method Based on the Meanshift Algorithm

Emergency Medicine International

Received 28 November 2023; Accepted 28 November 2023; Published 29 November 2023

This article has been retracted by Hindawi, as publisher, following an investigation undertaken by the publisher [1]. This investigation has uncovered evidence of systematic manipulation of the publication and peer-review process. We cannot, therefore, vouch for the reliability or integrity of this article.

Please note that this notice is intended solely to alert readers that the peer-review process of this article has been compromised.

Wiley and Hindawi regret that the usual quality checks did not identify these issues before publication and have since put additional measures in place to safeguard research integrity.

We wish to credit our Research Integrity and Research Publishing teams and anonymous and named external researchers and research integrity experts for contributing to this investigation.

The corresponding author, as the representative of all authors, has been given the opportunity to register their agreement or disagreement to this retraction. We have kept a record of any response received.

References

[1] J. Cui, Y. Wang, and K. Wang, "Key Technology of the Medical Image Wise Mining Method Based on the Meanshift Algorithm," *Emergency Medicine International*, vol. 2022, Article ID 6711043, 8 pages, 2022.

Hindawi
Emergency Medicine International
Volume 2023, Article ID 9805374, 1 page
https://doi.org/10.1155/2023/9805374

Retraction

Retracted: Risk Factors of Catheter-Related Infection in Unplanned Extubation of Totally Implantable Venous-Accessportsin Tumor Patients

Emergency Medicine International

Received 28 November 2023; Accepted 28 November 2023; Published 29 November 2023

This article has been retracted by Hindawi, as publisher, following an investigation undertaken by the publisher [1]. This investigation has uncovered evidence of systematic manipulation of the publication and peer-review process. We cannot, therefore, vouch for the reliability or integrity of this article.

Please note that this notice is intended solely to alert readers that the peer-review process of this article has been compromised.

Wiley and Hindawi regret that the usual quality checks did not identify these issues before publication and have since put additional measures in place to safeguard research integrity.

We wish to credit our Research Integrity and Research Publishing teams and anonymous and named external researchers and research integrity experts for contributing to this investigation.

The corresponding author, as the representative of all authors, has been given the opportunity to register their agreement or disagreement to this retraction. We have kept a record of any response received.

References

[1] M. Xu, L. Deng, Y. Zhu et al., "Risk Factors of Catheter-Related Infection in Unplanned Extubation of Totally Implantable Venous-Accessportsin Tumor Patients," *Emergency Medicine International*, vol. 2022, Article ID 4235316, 7 pages, 2022.

Hindawi
Emergency Medicine International
Volume 2023, Article ID 9803698, 1 page
https://doi.org/10.1155/2023/9803698

Retraction

Retracted: Related Factor Analysis and Nursing Strategies of Diarrhea in Critically Ill Patients with Enteral Nutrition

Emergency Medicine International

Received 28 November 2023; Accepted 28 November 2023; Published 29 November 2023

This article has been retracted by Hindawi, as publisher, following an investigation undertaken by the publisher [1]. This investigation has uncovered evidence of systematic manipulation of the publication and peer-review process. We cannot, therefore, vouch for the reliability or integrity of this article.

Please note that this notice is intended solely to alert readers that the peer-review process of this article has been compromised.

Wiley and Hindawi regret that the usual quality checks did not identify these issues before publication and have since put additional measures in place to safeguard research integrity.

We wish to credit our Research Integrity and Research Publishing teams and anonymous and named external researchers and research integrity experts for contributing to this investigation.

The corresponding author, as the representative of all authors, has been given the opportunity to register their agreement or disagreement to this retraction. We have kept a record of any response received.

References

[1] D. Liu, Q. Liu, and X. Wen, "Related Factor Analysis and Nursing Strategies of Diarrhea in Critically Ill Patients with Enteral Nutrition," *Emergency Medicine International*, vol. 2022, Article ID 8423048, 8 pages, 2022.

Hindawi
Emergency Medicine International
Volume 2023, Article ID 9803581, 1 page
https://doi.org/10.1155/2023/9803581

Retraction

Retracted: A Multimodel Fusion Method for Cardiovascular Disease Detection Using ECG

Emergency Medicine International

Received 28 November 2023; Accepted 28 November 2023; Published 29 November 2023

This article has been retracted by Hindawi, as publisher, following an investigation undertaken by the publisher [1]. This investigation has uncovered evidence of systematic manipulation of the publication and peer-review process. We cannot, therefore, vouch for the reliability or integrity of this article.

Please note that this notice is intended solely to alert readers that the peer-review process of this article has been compromised.

Wiley and Hindawi regret that the usual quality checks did not identify these issues before publication and have since put additional measures in place to safeguard research integrity.

We wish to credit our Research Integrity and Research Publishing teams and anonymous and named external researchers and research integrity experts for contributing to this investigation.

The corresponding author, as the representative of all authors, has been given the opportunity to register their agreement or disagreement to this retraction. We have kept a record of any response received.

References

[1] G. Song, J. Zhang, D. Mao, G. Chen, and C. Pang, "A Multimodel Fusion Method for Cardiovascular Disease Detection Using ECG," *Emergency Medicine International*, vol. 2022, Article ID 3561147, 10 pages, 2022.

Hindawi
Emergency Medicine International
Volume 2023, Article ID 9798523, 1 page
https://doi.org/10.1155/2023/9798523

Retraction

Retracted: Diagnostic Predictive Value of Tryptase, Serum Amyloid A and Lipoprotein-Associated Phospholipase A2 Biomarker Groups for Large Atherosclerotic Cerebral Infarction

Emergency Medicine International

Received 28 November 2023; Accepted 28 November 2023; Published 29 November 2023

This article has been retracted by Hindawi, as publisher, following an investigation undertaken by the publisher [1]. This investigation has uncovered evidence of systematic manipulation of the publication and peer-review process. We cannot, therefore, vouch for the reliability or integrity of this article.

Please note that this notice is intended solely to alert readers that the peer-review process of this article has been compromised.

Wiley and Hindawi regret that the usual quality checks did not identify these issues before publication and have since put additional measures in place to safeguard research integrity.

We wish to credit our Research Integrity and Research Publishing teams and anonymous and named external researchers and research integrity experts for contributing to this investigation.

The corresponding author, as the representative of all authors, has been given the opportunity to register their agreement or disagreement to this retraction. We have kept a record of any response received.

References

[1] W. Jia, X. Li, F. Lei et al., "Diagnostic Predictive Value of Tryptase, Serum Amyloid A and Lipoprotein-Associated Phospholipase A2 Biomarker Groups for Large Atherosclerotic Cerebral Infarction," *Emergency Medicine International*, vol. 2022, Article ID 5784909, 7 pages, 2022.

Hindawi
Emergency Medicine International
Volume 2023, Article ID 9786387, 1 page
https://doi.org/10.1155/2023/9786387

Retraction

Retracted: Application Value of Management Model Based on "Zero Tolerance" Concept in Pressure Ulcer Management

Emergency Medicine International

Received 28 November 2023; Accepted 28 November 2023; Published 29 November 2023

This article has been retracted by Hindawi, as publisher, following an investigation undertaken by the publisher [1]. This investigation has uncovered evidence of systematic manipulation of the publication and peer-review process. We cannot, therefore, vouch for the reliability or integrity of this article.

Please note that this notice is intended solely to alert readers that the peer-review process of this article has been compromised.

Wiley and Hindawi regret that the usual quality checks did not identify these issues before publication and have since put additional measures in place to safeguard research integrity.

We wish to credit our Research Integrity and Research Publishing teams and anonymous and named external researchers and research integrity experts for contributing to this investigation.

The corresponding author, as the representative of all authors, has been given the opportunity to register their agreement or disagreement to this retraction. We have kept a record of any response received.

References

[1] Y. Liu, C. Zhou, N. Li, and X. Gong, "Application Value of Management Model Based on "Zero Tolerance" Concept in Pressure Ulcer Management," *Emergency Medicine International*, vol. 2022, Article ID 6792584, 6 pages, 2022.

Hindawi
Emergency Medicine International
Volume 2023, Article ID 9784847, 1 page
https://doi.org/10.1155/2023/9784847

Retraction

Retracted: An Auxiliary Scoring Model for Patients with Acute Pulmonary Embolism Complicated with Atrial Fibrillation Was Established Based on Random Forests

Emergency Medicine International

Received 28 November 2023; Accepted 28 November 2023; Published 29 November 2023

This article has been retracted by Hindawi, as publisher, following an investigation undertaken by the publisher [1]. This investigation has uncovered evidence of systematic manipulation of the publication and peer-review process. We cannot, therefore, vouch for the reliability or integrity of this article.

Please note that this notice is intended solely to alert readers that the peer-review process of this article has been compromised.

Wiley and Hindawi regret that the usual quality checks did not identify these issues before publication and have since put additional measures in place to safeguard research integrity.

We wish to credit our Research Integrity and Research Publishing teams and anonymous and named external researchers and research integrity experts for contributing to this investigation.

The corresponding author, as the representative of all authors, has been given the opportunity to register their agreement or disagreement to this retraction. We have kept a record of any response received.

References

[1] C. Zhang, Q. Guan, J. Qin, D. Huang, and J. Wu, "An Auxiliary Scoring Model for Patients with Acute Pulmonary Embolism Complicated with Atrial Fibrillation Was Established Based on Random Forests," *Emergency Medicine International*, vol. 2022, Article ID 2596839, 8 pages, 2022.

Hindawi
Emergency Medicine International
Volume 2023, Article ID 9783815, 1 page
https://doi.org/10.1155/2023/9783815

Retraction

Retracted: Application of Melatonin with N-Acetylcysteine Exceeds Traditional Treatment for Acetaminophen-Induced Hepatotoxicity

Emergency Medicine International

Received 28 November 2023; Accepted 28 November 2023; Published 29 November 2023

This article has been retracted by Hindawi, as publisher, following an investigation undertaken by the publisher [1]. This investigation has uncovered evidence of systematic manipulation of the publication and peer-review process. We cannot, therefore, vouch for the reliability or integrity of this article.

Please note that this notice is intended solely to alert readers that the peer-review process of this article has been compromised.

Wiley and Hindawi regret that the usual quality checks did not identify these issues before publication and have since put additional measures in place to safeguard research integrity.

We wish to credit our Research Integrity and Research Publishing teams and anonymous and named external researchers and research integrity experts for contributing to this investigation.

The corresponding author, as the representative of all authors, has been given the opportunity to register their agreement or disagreement to this retraction. We have kept a record of any response received.

References

[1] M. Chen, J. Ke, S. Ma, H. Chai, L. Zhang, and L. Zhang, "Application of Melatonin with N-Acetylcysteine Exceeds Traditional Treatment for Acetaminophen-Induced Hepatotoxicity," *Emergency Medicine International*, vol. 2022, Article ID 2791743, 8 pages, 2022.

Hindawi
Emergency Medicine International
Volume 2023, Article ID 9783534, 1 page
https://doi.org/10.1155/2023/9783534

Retraction

Retracted: Clinical Observation of Computer Vision Technology Combined with Music Therapy in the Treatment of Alzheimer's Disease

Emergency Medicine International

Received 28 November 2023; Accepted 28 November 2023; Published 29 November 2023

This article has been retracted by Hindawi, as publisher, following an investigation undertaken by the publisher [1]. This investigation has uncovered evidence of systematic manipulation of the publication and peer-review process. We cannot, therefore, vouch for the reliability or integrity of this article.

Please note that this notice is intended solely to alert readers that the peer-review process of this article has been compromised.

Wiley and Hindawi regret that the usual quality checks did not identify these issues before publication and have since put additional measures in place to safeguard research integrity.

We wish to credit our Research Integrity and Research Publishing teams and anonymous and named external researchers and research integrity experts for contributing to this investigation.

The corresponding author, as the representative of all authors, has been given the opportunity to register their agreement or disagreement to this retraction. We have kept a record of any response received.

References

[1] A. Zhang, Y. Yang, and M. Xu, "Clinical Observation of Computer Vision Technology Combined with Music Therapy in the Treatment of Alzheimer's Disease," *Emergency Medicine International*, vol. 2022, Article ID 2567340, 12 pages, 2022.

Hindawi
Emergency Medicine International
Volume 2023, Article ID 9780649, 1 page
https://doi.org/10.1155/2023/9780649

Retraction

Retracted: Effect of Risk-Focused Diversified Safety Management Mode in Patients with Major Artery Stent Implantation

Emergency Medicine International

Received 28 November 2023; Accepted 28 November 2023; Published 29 November 2023

This article has been retracted by Hindawi, as publisher, following an investigation undertaken by the publisher [1]. This investigation has uncovered evidence of systematic manipulation of the publication and peer-review process. We cannot, therefore, vouch for the reliability or integrity of this article.

Please note that this notice is intended solely to alert readers that the peer-review process of this article has been compromised.

Wiley and Hindawi regret that the usual quality checks did not identify these issues before publication and have since put additional measures in place to safeguard research integrity.

We wish to credit our Research Integrity and Research Publishing teams and anonymous and named external researchers and research integrity experts for contributing to this investigation.

The corresponding author, as the representative of all authors, has been given the opportunity to register their agreement or disagreement to this retraction. We have kept a record of any response received.

References

[1] Y. Shao, C. Wu, Y. Mao, D. Li, Y. Wang, and K. Zhu, "Effect of Risk-Focused Diversified Safety Management Mode in Patients with Major Artery Stent Implantation," *Emergency Medicine International*, vol. 2022, Article ID 1284254, 9 pages, 2022.

Hindawi
Emergency Medicine International
Volume 2023, Article ID 9845275, 1 page
https://doi.org/10.1155/2023/9845275

Retraction

Retracted: Electron Microscope Observation of Acupuncture and Nerve Repair in the Treatment of Peripheral Facial Paralysis

Emergency Medicine International

Received 8 August 2023; Accepted 8 August 2023; Published 9 August 2023

This article has been retracted by Hindawi following an investigation undertaken by the publisher [1]. This investigation has uncovered evidence of one or more of the following indicators of systematic manipulation of the publication process:

(1) Discrepancies in scope
(2) Discrepancies in the description of the research reported
(3) Discrepancies between the availability of data and the research described
(4) Inappropriate citations
(5) Incoherent, meaningless and/or irrelevant content included in the article
(6) Peer-review manipulation

The presence of these indicators undermines our confidence in the integrity of the article's content and we cannot, therefore, vouch for its reliability. Please note that this notice is intended solely to alert readers that the content of this article is unreliable. We have not investigated whether authors were aware of or involved in the systematic manipulation of the publication process.

In addition, our investigation has also shown that one or more of the following human-subject reporting requirements has not been met in this article: ethical approval by an Institutional Review Board (IRB) committee or equivalent, patient/participant consent to participate, and/or agreement to publish patient/participant details (where relevant).

Wiley and Hindawi regrets that the usual quality checks did not identify these issues before publication and have since put additional measures in place to safeguard research integrity.

We wish to credit our own Research Integrity and Research Publishing teams and anonymous and named external researchers and research integrity experts for contributing to this investigation.

The corresponding author, as the representative of all authors, has been given the opportunity to register their agreement or disagreement to this retraction. We have kept a record of any response received.

References

[1] Z. Shan, "Electron Microscope Observation of Acupuncture and Nerve Repair in the Treatment of Peripheral Facial Paralysis," *Emergency Medicine International*, vol. 2022, Article ID 5432223, 10 pages, 2022.

Hindawi
Emergency Medicine International
Volume 2023, Article ID 9843571, 1 page
https://doi.org/10.1155/2023/9843571

Retraction

Retracted: Clinical Treatment and Nursing Intervention Study of Clipping Treatment of Cerebral Aneurysm under the Health Model of Data Analysis

Emergency Medicine International

Received 8 August 2023; Accepted 8 August 2023; Published 9 August 2023

This article has been retracted by Hindawi following an investigation undertaken by the publisher [1]. This investigation has uncovered evidence of one or more of the following indicators of systematic manipulation of the publication process:

(1) Discrepancies in scope
(2) Discrepancies in the description of the research reported
(3) Discrepancies between the availability of data and the research described
(4) Inappropriate citations
(5) Incoherent, meaningless and/or irrelevant content included in the article
(6) Peer-review manipulation

The presence of these indicators undermines our confidence in the integrity of the article's content and we cannot, therefore, vouch for its reliability. Please note that this notice is intended solely to alert readers that the content of this article is unreliable. We have not investigated whether authors were aware of or involved in the systematic manipulation of the publication process.

In addition, our investigation has also shown that one or more of the following human-subject reporting requirements has not been met in this article: ethical approval by an Institutional Review Board (IRB) committee or equivalent, patient/participant consent to participate, and/or agreement to publish patient/participant details (where relevant).

Wiley and Hindawi regrets that the usual quality checks did not identify these issues before publication and have since put additional measures in place to safeguard research integrity.

We wish to credit our own Research Integrity and Research Publishing teams and anonymous and named external researchers and research integrity experts for contributing to this investigation.

The corresponding author, as the representative of all authors, has been given the opportunity to register their agreement or disagreement to this retraction. We have kept a record of any response received.

References

[1] Y. Huang and L. Huang, "Clinical Treatment and Nursing Intervention Study of Clipping Treatment of Cerebral Aneurysm under the Health Model of Data Analysis," *Emergency Medicine International*, vol. 2022, Article ID 8178963, 12 pages, 2022.

Hindawi
Emergency Medicine International
Volume 2023, Article ID 9836710, 1 page
https://doi.org/10.1155/2023/9836710

Retraction

Retracted: Clinical Evaluation of Unilateral Vertebroplasty for OVCF

Emergency Medicine International

Received 8 August 2023; Accepted 8 August 2023; Published 9 August 2023

This article has been retracted by Hindawi following an investigation undertaken by the publisher [1]. This investigation has uncovered evidence of one or more of the following indicators of systematic manipulation of the publication process:

(1) Discrepancies in scope
(2) Discrepancies in the description of the research reported
(3) Discrepancies between the availability of data and the research described
(4) Inappropriate citations
(5) Incoherent, meaningless and/or irrelevant content included in the article
(6) Peer-review manipulation

The presence of these indicators undermines our confidence in the integrity of the article's content and we cannot, therefore, vouch for its reliability. Please note that this notice is intended solely to alert readers that the content of this article is unreliable. We have not investigated whether authors were aware of or involved in the systematic manipulation of the publication process.

In addition, our investigation has also shown that one or more of the following human-subject reporting requirements has not been met in this article: ethical approval by an Institutional Review Board (IRB) committee or equivalent, patient/participant consent to participate, and/or agreement to publish patient/participant details (where relevant).

Wiley and Hindawi regrets that the usual quality checks did not identify these issues before publication and have since put additional measures in place to safeguard research integrity.

We wish to credit our own Research Integrity and Research Publishing teams and anonymous and named external researchers and research integrity experts for contributing to this investigation.

The corresponding author, as the representative of all authors, has been given the opportunity to register their agreement or disagreement to this retraction. We have kept a record of any response received.

References

[1] X. Wen, Y. Zhang, W. Jiang, W. An, B. Zhang, and J. Liu, "Clinical Evaluation of Unilateral Vertebroplasty for OVCF," *Emergency Medicine International*, vol. 2022, Article ID 2037185, 6 pages, 2022.

Hindawi
Emergency Medicine International
Volume 2023, Article ID 9835949, 1 page
https://doi.org/10.1155/2023/9835949

Retraction

Retracted: Systematic Review and Meta-Analysis of the Evaluation of the Efficacy of Manipulation and Cervical Traction in the Treatment of Radical Cervical Spondylosis

Emergency Medicine International

Received 8 August 2023; Accepted 8 August 2023; Published 9 August 2023

This article has been retracted by Hindawi following an investigation undertaken by the publisher [1]. This investigation has uncovered evidence of one or more of the following indicators of systematic manipulation of the publication process:

(1) Discrepancies in scope
(2) Discrepancies in the description of the research reported
(3) Discrepancies between the availability of data and the research described
(4) Inappropriate citations
(5) Incoherent, meaningless and/or irrelevant content included in the article
(6) Peer-review manipulation

The presence of these indicators undermines our confidence in the integrity of the article's content and we cannot, therefore, vouch for its reliability. Please note that this notice is intended solely to alert readers that the content of this article is unreliable. We have not investigated whether authors were aware of or involved in the systematic manipulation of the publication process.

Wiley and Hindawi regrets that the usual quality checks did not identify these issues before publication and have since put additional measures in place to safeguard research integrity.

We wish to credit our own Research Integrity and Research Publishing teams and anonymous and named external researchers and research integrity experts for contributing to this investigation.

The corresponding author, as the representative of all authors, has been given the opportunity to register their agreement or disagreement to this retraction. We have kept a record of any response received.

References

[1] J. Chen, R. Chen, Y. Li et al., "Systematic Review and Meta-Analysis of the Evaluation of the Efficacy of Manipulation and Cervical Traction in the Treatment of Radical Cervical Spondylosis," *Emergency Medicine International*, vol. 2022, Article ID 3837995, 10 pages, 2022.

Hindawi
Emergency Medicine International
Volume 2023, Article ID 9823909, 1 page
https://doi.org/10.1155/2023/9823909

Retraction

Retracted: Application of Image Processing Technology in Aerobics Injury Diagnosis

Emergency Medicine International

Received 8 August 2023; Accepted 8 August 2023; Published 9 August 2023

This article has been retracted by Hindawi following an investigation undertaken by the publisher [1]. This investigation has uncovered evidence of one or more of the following indicators of systematic manipulation of the publication process:

(1) Discrepancies in scope
(2) Discrepancies in the description of the research reported
(3) Discrepancies between the availability of data and the research described
(4) Inappropriate citations
(5) Incoherent, meaningless and/or irrelevant content included in the article
(6) Peer-review manipulation

The presence of these indicators undermines our confidence in the integrity of the article's content and we cannot, therefore, vouch for its reliability. Please note that this notice is intended solely to alert readers that the content of this article is unreliable. We have not investigated whether authors were aware of or involved in the systematic manipulation of the publication process.

In addition, our investigation has also shown that one or more of the following human-subject reporting requirements has not been met in this article: ethical approval by an Institutional Review Board (IRB) committee or equivalent, patient/participant consent to participate, and/or agreement to publish patient/participant details (where relevant).

Wiley and Hindawi regrets that the usual quality checks did not identify these issues before publication and have since put additional measures in place to safeguard research integrity.

We wish to credit our own Research Integrity and Research Publishing teams and anonymous and named external researchers and research integrity experts for contributing to this investigation.

The corresponding author, as the representative of all authors, has been given the opportunity to register their agreement or disagreement to this retraction. We have kept a record of any response received.

References

[1] D. Zhang and Y. Tian, "Application of Image Processing Technology in Aerobics Injury Diagnosis," *Emergency Medicine International*, vol. 2022, Article ID 2553048, 13 pages, 2022.

Hindawi
Emergency Medicine International
Volume 2023, Article ID 9821382, 1 page
https://doi.org/10.1155/2023/9821382

Retraction

Retracted: Effect of Bodybuilding and Fitness Exercise on Physical Fitness Based on Deep Learning

Emergency Medicine International

Received 8 August 2023; Accepted 8 August 2023; Published 9 August 2023

This article has been retracted by Hindawi following an investigation undertaken by the publisher [1]. This investigation has uncovered evidence of one or more of the following indicators of systematic manipulation of the publication process:

(1) Discrepancies in scope
(2) Discrepancies in the description of the research reported
(3) Discrepancies between the availability of data and the research described
(4) Inappropriate citations
(5) Incoherent, meaningless and/or irrelevant content included in the article
(6) Peer-review manipulation

The presence of these indicators undermines our confidence in the integrity of the article's content and we cannot, therefore, vouch for its reliability. Please note that this notice is intended solely to alert readers that the content of this article is unreliable. We have not investigated whether authors were aware of or involved in the systematic manipulation of the publication process.

In addition, our investigation has also shown that one or more of the following human-subject reporting requirements has not been met in this article: ethical approval by an Institutional Review Board (IRB) committee or equivalent, patient/participant consent to participate, and/or agreement to publish patient/participant details (where relevant).

Wiley and Hindawi regrets that the usual quality checks did not identify these issues before publication and have since put additional measures in place to safeguard research integrity.

We wish to credit our own Research Integrity and Research Publishing teams and anonymous and named external researchers and research integrity experts for contributing to this investigation.

The corresponding author, as the representative of all authors, has been given the opportunity to register their agreement or disagreement to this retraction. We have kept a record of any response received.

References

[1] M. Sun and L. Wang, "Effect of Bodybuilding and Fitness Exercise on Physical Fitness Based on Deep Learning," *Emergency Medicine International*, vol. 2022, Article ID 3891109, 2 pages, 2022.

Hindawi
Emergency Medicine International
Volume 2023, Article ID 9816329, 1 page
https://doi.org/10.1155/2023/9816329

Retraction

Retracted: Effect of Zhuyun I Recipe Capsule Enema on the Immune Microenvironment of the Endometrium during Implantation Window in Rats

Emergency Medicine International

Received 8 August 2023; Accepted 8 August 2023; Published 9 August 2023

This article has been retracted by Hindawi following an investigation undertaken by the publisher [1]. This investigation has uncovered evidence of one or more of the following indicators of systematic manipulation of the publication process:

(1) Discrepancies in scope
(2) Discrepancies in the description of the research reported
(3) Discrepancies between the availability of data and the research described
(4) Inappropriate citations
(5) Incoherent, meaningless and/or irrelevant content included in the article
(6) Peer-review manipulation

The presence of these indicators undermines our confidence in the integrity of the article's content and we cannot, therefore, vouch for its reliability. Please note that this notice is intended solely to alert readers that the content of this article is unreliable. We have not investigated whether authors were aware of or involved in the systematic manipulation of the publication process.

Wiley and Hindawi regrets that the usual quality checks did not identify these issues before publication and have since put additional measures in place to safeguard research integrity.

We wish to credit our own Research Integrity and Research Publishing teams and anonymous and named external researchers and research integrity experts for contributing to this investigation.

The corresponding author, as the representative of all authors, has been given the opportunity to register their agreement or disagreement to this retraction. We have kept a record of any response received.

References

[1] H. Zhou, P. Guo, P. Zeng et al., "Effect of Zhuyun I Recipe Capsule Enema on the Immune Microenvironment of the Endometrium during Implantation Window in Rats," *Emergency Medicine International*, vol. 2022, Article ID 4746121, 11 pages, 2022.

Hindawi
Emergency Medicine International
Volume 2023, Article ID 9814961, 1 page
https://doi.org/10.1155/2023/9814961

Retraction

Retracted: Efficacy and Safety of Glycosides of Tripterygium wilfordii Combined with Renin-Angiotensin System in the Treatment of IgA Nephropathy: A Systematic Review and Meta-Analysis

Emergency Medicine International

Received 8 August 2023; Accepted 8 August 2023; Published 9 August 2023

This article has been retracted by Hindawi following an investigation undertaken by the publisher [1]. This investigation has uncovered evidence of one or more of the following indicators of systematic manipulation of the publication process:

(1) Discrepancies in scope
(2) Discrepancies in the description of the research reported
(3) Discrepancies between the availability of data and the research described
(4) Inappropriate citations
(5) Incoherent, meaningless and/or irrelevant content included in the article
(6) Peer-review manipulation

The presence of these indicators undermines our confidence in the integrity of the article's content and we cannot, therefore, vouch for its reliability. Please note that this notice is intended solely to alert readers that the content of this article is unreliable. We have not investigated whether authors were aware of or involved in the systematic manipulation of the publication process.

Wiley and Hindawi regrets that the usual quality checks did not identify these issues before publication and have since put additional measures in place to safeguard research integrity.

We wish to credit our own Research Integrity and Research Publishing teams and anonymous and named external researchers and research integrity experts for contributing to this investigation.

The corresponding author, as the representative of all authors, has been given the opportunity to register their agreement or disagreement to this retraction. We have kept a record of any response received.

References

[1] M. Chen, P. Zhang, L. Li, Z. Yu, N. Liu, and L. Wang, "Efficacy and Safety of Glycosides of Tripterygium wilfordii Combined with Renin-Angiotensin System in the Treatment of IgA Nephropathy: A Systematic Review and Meta-Analysis," *Emergency Medicine International*, vol. 2022, Article ID 5314105, 12 pages, 2022.

Hindawi
Emergency Medicine International
Volume 2023, Article ID 9803639, 1 page
https://doi.org/10.1155/2023/9803639

Retraction

Retracted: The Influence of Sports Dance on the Physical and Mental Development of Contemporary College Students Based on Health Detection

Emergency Medicine International

Received 8 August 2023; Accepted 8 August 2023; Published 9 August 2023

This article has been retracted by Hindawi following an investigation undertaken by the publisher [1]. This investigation has uncovered evidence of one or more of the following indicators of systematic manipulation of the publication process:

(1) Discrepancies in scope
(2) Discrepancies in the description of the research reported
(3) Discrepancies between the availability of data and the research described
(4) Inappropriate citations
(5) Incoherent, meaningless and/or irrelevant content included in the article
(6) Peer-review manipulation

The presence of these indicators undermines our confidence in the integrity of the article's content and we cannot, therefore, vouch for its reliability. Please note that this notice is intended solely to alert readers that the content of this article is unreliable. We have not investigated whether authors were aware of or involved in the systematic manipulation of the publication process.

In addition, our investigation has also shown that one or more of the following human-subject reporting requirements has not been met in this article: ethical approval by an Institutional Review Board (IRB) committee or equivalent, patient/participant consent to participate, and/or agreement to publish patient/participant details (where relevant).

Wiley and Hindawi regrets that the usual quality checks did not identify these issues before publication and have since put additional measures in place to safeguard research integrity.

We wish to credit our own Research Integrity and Research Publishing teams and anonymous and named external researchers and research integrity experts for contributing to this investigation.

The corresponding author, as the representative of all authors, has been given the opportunity to register their agreement or disagreement to this retraction. We have kept a record of any response received.

References

[1] H. Huang, "The Influence of Sports Dance on the Physical and Mental Development of Contemporary College Students Based on Health Detection," *Emergency Medicine International*, vol. 2022, Article ID 3715150, 11 pages, 2022.

Hindawi
Emergency Medicine International
Volume 2023, Article ID 9801869, 1 page
https://doi.org/10.1155/2023/9801869

Retraction

Retracted: Application of Low-Intensity Laser in the Treatment of Skeletal Muscle Injury in Runners

Emergency Medicine International

Received 8 August 2023; Accepted 8 August 2023; Published 9 August 2023

This article has been retracted by Hindawi following an investigation undertaken by the publisher [1]. This investigation has uncovered evidence of one or more of the following indicators of systematic manipulation of the publication process:

(1) Discrepancies in scope
(2) Discrepancies in the description of the research reported
(3) Discrepancies between the availability of data and the research described
(4) Inappropriate citations
(5) Incoherent, meaningless and/or irrelevant content included in the article
(6) Peer-review manipulation

The presence of these indicators undermines our confidence in the integrity of the article's content and we cannot, therefore, vouch for its reliability. Please note that this notice is intended solely to alert readers that the content of this article is unreliable. We have not investigated whether authors were aware of or involved in the systematic manipulation of the publication process.

Wiley and Hindawi regrets that the usual quality checks did not identify these issues before publication and have since put additional measures in place to safeguard research integrity.

We wish to credit our own Research Integrity and Research Publishing teams and anonymous and named external researchers and research integrity experts for contributing to this investigation.

The corresponding author, as the representative of all authors, has been given the opportunity to register their agreement or disagreement to this retraction. We have kept a record of any response received.

References

[1] Y. Chen and Q. Li, "Application of Low-Intensity Laser in the Treatment of Skeletal Muscle Injury in Runners," *Emergency Medicine International*, vol. 2022, Article ID 1211602, 9 pages, 2022.

Hindawi
Emergency Medicine International
Volume 2023, Article ID 9794070, 1 page
https://doi.org/10.1155/2023/9794070

Retraction

Retracted: Analysis of the Effect of Quality Nursing on Recovery after Thoracic Surgery

Emergency Medicine International

Received 8 August 2023; Accepted 8 August 2023; Published 9 August 2023

This article has been retracted by Hindawi following an investigation undertaken by the publisher [1]. This investigation has uncovered evidence of one or more of the following indicators of systematic manipulation of the publication process:

(1) Discrepancies in scope
(2) Discrepancies in the description of the research reported
(3) Discrepancies between the availability of data and the research described
(4) Inappropriate citations
(5) Incoherent, meaningless and/or irrelevant content included in the article
(6) Peer-review manipulation

The presence of these indicators undermines our confidence in the integrity of the article's content and we cannot, therefore, vouch for its reliability. Please note that this notice is intended solely to alert readers that the content of this article is unreliable. We have not investigated whether authors were aware of or involved in the systematic manipulation of the publication process.

In addition, our investigation has also shown that one or more of the following human-subject reporting requirements has not been met in this article: ethical approval by an Institutional Review Board (IRB) committee or equivalent, patient/participant consent to participate, and/or agreement to publish patient/participant details (where relevant).

Wiley and Hindawi regrets that the usual quality checks did not identify these issues before publication and have since put additional measures in place to safeguard research integrity.

We wish to credit our own Research Integrity and Research Publishing teams and anonymous and named external researchers and research integrity experts for contributing to this investigation.

The corresponding author, as the representative of all authors, has been given the opportunity to register their agreement or disagreement to this retraction. We have kept a record of any response received.

References

[1] Y. Zhou and M. Xu, "Analysis of the Effect of Quality Nursing on Recovery after Thoracic Surgery," *Emergency Medicine International*, vol. 2022, Article ID 6204832, 10 pages, 2022.

Hindawi
Emergency Medicine International
Volume 2023, Article ID 9789785, 1 page
https://doi.org/10.1155/2023/9789785

Retraction

Retracted: Effects of Amiodarone and Esmolol for Heart Rate and Cardiovascular Changes

Emergency Medicine International

Received 8 August 2023; Accepted 8 August 2023; Published 9 August 2023

This article has been retracted by Hindawi following an investigation undertaken by the publisher [1]. This investigation has uncovered evidence of one or more of the following indicators of systematic manipulation of the publication process:

(1) Discrepancies in scope
(2) Discrepancies in the description of the research reported
(3) Discrepancies between the availability of data and the research described
(4) Inappropriate citations
(5) Incoherent, meaningless and/or irrelevant content included in the article
(6) Peer-review manipulation

The presence of these indicators undermines our confidence in the integrity of the article's content and we cannot, therefore, vouch for its reliability. Please note that this notice is intended solely to alert readers that the content of this article is unreliable. We have not investigated whether authors were aware of or involved in the systematic manipulation of the publication process.

In addition, our investigation has also shown that one or more of the following human-subject reporting requirements has not been met in this article: ethical approval by an Institutional Review Board (IRB) committee or equivalent, patient/participant consent to participate, and/or agreement to publish patient/participant details (where relevant).

Wiley and Hindawi regrets that the usual quality checks did not identify these issues before publication and have since put additional measures in place to safeguard research integrity.

We wish to credit our own Research Integrity and Research Publishing teams and anonymous and named external researchers and research integrity experts for contributing to this investigation.

The corresponding author, as the representative of all authors, has been given the opportunity to register their agreement or disagreement to this retraction. We have kept a record of any response received.

References

[1] H. Wang, F. Lei, L. Bai, and A. Zhang, "Effects of Amiodarone and Esmolol for Heart Rate and Cardiovascular Changes," *Emergency Medicine International*, vol. 2022, Article ID 9197369, 7 pages, 2022.

Hindawi
Emergency Medicine International
Volume 2023, Article ID 9763530, 1 page
https://doi.org/10.1155/2023/9763530

Retraction

Retracted: Application of Computer-Based Simulation Teaching Combined with PBL in Colorectal Tumor Hemorrhage

Emergency Medicine International

Received 8 August 2023; Accepted 8 August 2023; Published 9 August 2023

This article has been retracted by Hindawi following an investigation undertaken by the publisher [1]. This investigation has uncovered evidence of one or more of the following indicators of systematic manipulation of the publication process:

(1) Discrepancies in scope
(2) Discrepancies in the description of the research reported
(3) Discrepancies between the availability of data and the research described
(4) Inappropriate citations
(5) Incoherent, meaningless and/or irrelevant content included in the article
(6) Peer-review manipulation

The presence of these indicators undermines our confidence in the integrity of the article's content and we cannot, therefore, vouch for its reliability. Please note that this notice is intended solely to alert readers that the content of this article is unreliable. We have not investigated whether authors were aware of or involved in the systematic manipulation of the publication process.

Wiley and Hindawi regrets that the usual quality checks did not identify these issues before publication and have since put additional measures in place to safeguard research integrity.

We wish to credit our own Research Integrity and Research Publishing teams and anonymous and named external researchers and research integrity experts for contributing to this investigation.

The corresponding author, as the representative of all authors, has been given the opportunity to register their agreement or disagreement to this retraction. We have kept a record of any response received.

References

[1] Y. Zhang, J. Hu, L. Li, and Y. Zhao, "Application of Computer-Based Simulation Teaching Combined with PBL in Colorectal Tumor Hemorrhage," *Emergency Medicine International*, vol. 2022, Article ID 1251388, 10 pages, 2022.

Hindawi
Emergency Medicine International
Volume 2023, Article ID 9754041, 1 page
https://doi.org/10.1155/2023/9754041

Retraction

Retracted: 3D Automatic Segmentation of Brain Tumor Based on Deep Neural Network and Multimodal MRI Images

Emergency Medicine International

Received 8 August 2023; Accepted 8 August 2023; Published 9 August 2023

This article has been retracted by Hindawi following an investigation undertaken by the publisher [1]. This investigation has uncovered evidence of one or more of the following indicators of systematic manipulation of the publication process:

(1) Discrepancies in scope
(2) Discrepancies in the description of the research reported
(3) Discrepancies between the availability of data and the research described
(4) Inappropriate citations
(5) Incoherent, meaningless and/or irrelevant content included in the article
(6) Peer-review manipulation

The presence of these indicators undermines our confidence in the integrity of the article's content and we cannot, therefore, vouch for its reliability. Please note that this notice is intended solely to alert readers that the content of this article is unreliable. We have not investigated whether authors were aware of or involved in the systematic manipulation of the publication process.

In addition, our investigation has also shown that one or more of the following human-subject reporting requirements has not been met in this article: ethical approval by an Institutional Review Board (IRB) committee or equivalent, patient/participant consent to participate, and/or agreement to publish patient/participant details (where relevant).

Wiley and Hindawi regrets that the usual quality checks did not identify these issues before publication and have since put additional measures in place to safeguard research integrity.

We wish to credit our own Research Integrity and Research Publishing teams and anonymous and named external researchers and research integrity experts for contributing to this investigation.

The corresponding author, as the representative of all authors, has been given the opportunity to register their agreement or disagreement to this retraction. We have kept a record of any response received.

References

[1] Z. Qian, L. Xie, and Y. Xu, "3D Automatic Segmentation of Brain Tumor Based on Deep Neural Network and Multimodal MRI Images," *Emergency Medicine International*, vol. 2022, Article ID 5356069, 9 pages, 2022.

Hindawi
Emergency Medicine International
Volume 2023, Article ID 9896378, 1 page
https://doi.org/10.1155/2023/9896378

Retraction

Retracted: Font Design in Visual Communication Design of Genetic Algorithm

Emergency Medicine International

Received 8 August 2023; Accepted 8 August 2023; Published 9 August 2023

This article has been retracted by Hindawi following an investigation undertaken by the publisher [1]. This investigation has uncovered evidence of one or more of the following indicators of systematic manipulation of the publication process:

(1) Discrepancies in scope
(2) Discrepancies in the description of the research reported
(3) Discrepancies between the availability of data and the research described
(4) Inappropriate citations
(5) Incoherent, meaningless and/or irrelevant content included in the article
(6) Peer-review manipulation

The presence of these indicators undermines our confidence in the integrity of the article's content and we cannot, therefore, vouch for its reliability. Please note that this notice is intended solely to alert readers that the content of this article is unreliable. We have not investigated whether authors were aware of or involved in the systematic manipulation of the publication process.

Wiley and Hindawi regrets that the usual quality checks did not identify these issues before publication and have since put additional measures in place to safeguard research integrity.

We wish to credit our own Research Integrity and Research Publishing teams and anonymous and named external researchers and research integrity experts for contributing to this investigation.

The corresponding author, as the representative of all authors, has been given the opportunity to register their agreement or disagreement to this retraction. We have kept a record of any response received.

References

[1] Y. Wang and W. Chung, "Font Design in Visual Communication Design of Genetic Algorithm," *Emergency Medicine International*, vol. 2022, Article ID 6897115, 10 pages, 2022.

Hindawi
Emergency Medicine International
Volume 2023, Article ID 9879027, 1 page
https://doi.org/10.1155/2023/9879027

Retraction

Retracted: A Study on the Relationship between Sense of Disease Uncertainty and Family Strength and Mental Resilience in Guardians of Children with Inflammatory Bowel Disease

Emergency Medicine International

Received 8 August 2023; Accepted 8 August 2023; Published 9 August 2023

This article has been retracted by Hindawi following an investigation undertaken by the publisher [1]. This investigation has uncovered evidence of one or more of the following indicators of systematic manipulation of the publication process:

(1) Discrepancies in scope

(2) Discrepancies in the description of the research reported

(3) Discrepancies between the availability of data and the research described

(4) Inappropriate citations

(5) Incoherent, meaningless and/or irrelevant content included in the article

(6) Peer-review manipulation

The presence of these indicators undermines our confidence in the integrity of the article's content and we cannot, therefore, vouch for its reliability. Please note that this notice is intended solely to alert readers that the content of this article is unreliable. We have not investigated whether authors were aware of or involved in the systematic manipulation of the publication process.

Wiley and Hindawi regrets that the usual quality checks did not identify these issues before publication and have since put additional measures in place to safeguard research integrity.

We wish to credit our own Research Integrity and Research Publishing teams and anonymous and named external researchers and research integrity experts for contributing to this investigation.

The corresponding author, as the representative of all authors, has been given the opportunity to register their agreement or disagreement to this retraction. We have kept a record of any response received.

References

[1] J. Yan and L. Luo, "A Study on the Relationship between Sense of Disease Uncertainty and Family Strength and Mental Resilience in Guardians of Children with Inflammatory Bowel Disease," *Emergency Medicine International*, vol. 2022, Article ID 4797281, 6 pages, 2022.

Hindawi
Emergency Medicine International
Volume 2023, Article ID 9874658, 1 page
https://doi.org/10.1155/2023/9874658

Retraction

Retracted: Association of β2-Agonist Receptor Gene Polymorphisms with Acute Exacerbations of COPD: A Prospective Observational Study

Emergency Medicine International

Received 8 August 2023; Accepted 8 August 2023; Published 9 August 2023

This article has been retracted by Hindawi following an investigation undertaken by the publisher [1]. This investigation has uncovered evidence of one or more of the following indicators of systematic manipulation of the publication process:

(1) Discrepancies in scope
(2) Discrepancies in the description of the research reported
(3) Discrepancies between the availability of data and the research described
(4) Inappropriate citations
(5) Incoherent, meaningless and/or irrelevant content included in the article
(6) Peer-review manipulation

The presence of these indicators undermines our confidence in the integrity of the article's content and we cannot, therefore, vouch for its reliability. Please note that this notice is intended solely to alert readers that the content of this article is unreliable. We have not investigated whether authors were aware of or involved in the systematic manipulation of the publication process.

Wiley and Hindawi regrets that the usual quality checks did not identify these issues before publication and have since put additional measures in place to safeguard research integrity.

We wish to credit our own Research Integrity and Research Publishing teams and anonymous and named external researchers and research integrity experts for contributing to this investigation.

The corresponding author, as the representative of all authors, has been given the opportunity to register their agreement or disagreement to this retraction. We have kept a record of any response received.

References

[1] F. Lu, N. Xu, and J. Zheng, "Association of β2-Agonist Receptor Gene Polymorphisms with Acute Exacerbations of COPD: A Prospective Observational Study," *Emergency Medicine International*, vol. 2022, Article ID 2711489, 5 pages, 2022.

Hindawi
Emergency Medicine International
Volume 2023, Article ID 9869764, 1 page
https://doi.org/10.1155/2023/9869764

Retraction

Retracted: Influence of Aerobic Exercise Load Intensity on Children's Mental Health

Emergency Medicine International

Received 8 August 2023; Accepted 8 August 2023; Published 9 August 2023

This article has been retracted by Hindawi following an investigation undertaken by the publisher [1]. This investigation has uncovered evidence of one or more of the following indicators of systematic manipulation of the publication process:

(1) Discrepancies in scope
(2) Discrepancies in the description of the research reported
(3) Discrepancies between the availability of data and the research described
(4) Inappropriate citations
(5) Incoherent, meaningless and/or irrelevant content included in the article
(6) Peer-review manipulation

The presence of these indicators undermines our confidence in the integrity of the article's content and we cannot, therefore, vouch for its reliability. Please note that this notice is intended solely to alert readers that the content of this article is unreliable. We have not investigated whether authors were aware of or involved in the systematic manipulation of the publication process.

Wiley and Hindawi regrets that the usual quality checks did not identify these issues before publication and have since put additional measures in place to safeguard research integrity.

We wish to credit our own Research Integrity and Research Publishing teams and anonymous and named external researchers and research integrity experts for contributing to this investigation.

The corresponding author, as the representative of all authors, has been given the opportunity to register their agreement or disagreement to this retraction. We have kept a record of any response received.

References

[1] S. Zhao, "Influence of Aerobic Exercise Load Intensity on Children's Mental Health," *Emergency Medicine International*, vol. 2022, Article ID 7827980, 11 pages, 2022.

Hindawi
Emergency Medicine International
Volume 2023, Article ID 9862919, 1 page
https://doi.org/10.1155/2023/9862919

Retraction

Retracted: The Effect of Comprehensive Rehabilitation Nursing on the Rehabilitation of Sports-Induced Ankle Joint Injuries

Emergency Medicine International

Received 8 August 2023; Accepted 8 August 2023; Published 9 August 2023

This article has been retracted by Hindawi following an investigation undertaken by the publisher [1]. This investigation has uncovered evidence of one or more of the following indicators of systematic manipulation of the publication process:

(1) Discrepancies in scope
(2) Discrepancies in the description of the research reported
(3) Discrepancies between the availability of data and the research described
(4) Inappropriate citations
(5) Incoherent, meaningless and/or irrelevant content included in the article
(6) Peer-review manipulation

The presence of these indicators undermines our confidence in the integrity of the article's content and we cannot, therefore, vouch for its reliability. Please note that this notice is intended solely to alert readers that the content of this article is unreliable. We have not investigated whether authors were aware of or involved in the systematic manipulation of the publication process.

Wiley and Hindawi regrets that the usual quality checks did not identify these issues before publication and have since put additional measures in place to safeguard research integrity.

We wish to credit our own Research Integrity and Research Publishing teams and anonymous and named external researchers and research integrity experts for contributing to this investigation.

The corresponding author, as the representative of all authors, has been given the opportunity to register their agreement or disagreement to this retraction. We have kept a record of any response received.

References

[1] Y. Qiao, B. Zhang, and L. Zhang, "The Effect of Comprehensive Rehabilitation Nursing on the Rehabilitation of Sports-Induced Ankle Joint Injuries," *Emergency Medicine International*, vol. 2022, Article ID 4004965, 12 pages, 2022.

Hindawi
Emergency Medicine International
Volume 2023, Article ID 9849537, 1 page
https://doi.org/10.1155/2023/9849537

Retraction

Retracted: A Meta-Analysis of How Nonalcoholic Fatty Liver Disease Affect Antiviral Treatment of Patients with e Antigen-Positive Chronic Hepatitis B

Emergency Medicine International

Received 8 August 2023; Accepted 8 August 2023; Published 9 August 2023

This article has been retracted by Hindawi following an investigation undertaken by the publisher [1]. This investigation has uncovered evidence of one or more of the following indicators of systematic manipulation of the publication process:

(1) Discrepancies in scope
(2) Discrepancies in the description of the research reported
(3) Discrepancies between the availability of data and the research described
(4) Inappropriate citations
(5) Incoherent, meaningless and/or irrelevant content included in the article
(6) Peer-review manipulation

The presence of these indicators undermines our confidence in the integrity of the article's content and we cannot, therefore, vouch for its reliability. Please note that this notice is intended solely to alert readers that the content of this article is unreliable. We have not investigated whether authors were aware of or involved in the systematic manipulation of the publication process.

Wiley and Hindawi regrets that the usual quality checks did not identify these issues before publication and have since put additional measures in place to safeguard research integrity.

We wish to credit our own Research Integrity and Research Publishing teams and anonymous and named external researchers and research integrity experts for contributing to this investigation.

The corresponding author, as the representative of all authors, has been given the opportunity to register their agreement or disagreement to this retraction. We have kept a record of any response received.

References

[1] Y. Chen, Q. Liu, J. Han et al., "A Meta-Analysis of How Nonalcoholic Fatty Liver Disease Affect Antiviral Treatment of Patients with e Antigen-Positive Chronic Hepatitis B," *Emergency Medicine International*, vol. 2022, Article ID 4774195, 7 pages, 2022.

Hindawi
Emergency Medicine International
Volume 2023, Article ID 9847534, 1 page
https://doi.org/10.1155/2023/9847534

Retraction

Retracted: Study on the Influencing Factors of Osteoarthritis in Southern China

Emergency Medicine International

Received 8 August 2023; Accepted 8 August 2023; Published 9 August 2023

This article has been retracted by Hindawi following an investigation undertaken by the publisher [1]. This investigation has uncovered evidence of one or more of the following indicators of systematic manipulation of the publication process:

(1) Discrepancies in scope
(2) Discrepancies in the description of the research reported
(3) Discrepancies between the availability of data and the research described
(4) Inappropriate citations
(5) Incoherent, meaningless and/or irrelevant content included in the article
(6) Peer-review manipulation

The presence of these indicators undermines our confidence in the integrity of the article's content and we cannot, therefore, vouch for its reliability. Please note that this notice is intended solely to alert readers that the content of this article is unreliable. We have not investigated whether authors were aware of or involved in the systematic manipulation of the publication process.

Wiley and Hindawi regrets that the usual quality checks did not identify these issues before publication and have since put additional measures in place to safeguard research integrity.

We wish to credit our own Research Integrity and Research Publishing teams and anonymous and named external researchers and research integrity experts for contributing to this investigation.

The corresponding author, as the representative of all authors, has been given the opportunity to register their agreement or disagreement to this retraction. We have kept a record of any response received.

References

[1] D. Lu, X. Ding, and W. Lu, "Study on the Influencing Factors of Osteoarthritis in Southern China," *Emergency Medicine International*, vol. 2022, Article ID 2482728, 6 pages, 2022.

Hindawi
Emergency Medicine International
Volume 2023, Article ID 9814568, 1 page
https://doi.org/10.1155/2023/9814568

Retraction

Retracted: Establishment of a Finite Element Model of Normal Nasal Bone and Analysis of Its Biomechanical Characteristics

Emergency Medicine International

Received 28 November 2023; Accepted 28 November 2023; Published 29 November 2023

This article has been retracted by Hindawi, as publisher, following an investigation undertaken by the publisher [1]. This investigation has uncovered evidence of systematic manipulation of the publication and peer-review process. We cannot, therefore, vouch for the reliability or integrity of this article.

Please note that this notice is intended solely to alert readers that the peer-review process of this article has been compromised.

Wiley and Hindawi regret that the usual quality checks did not identify these issues before publication and have since put additional measures in place to safeguard research integrity.

We wish to credit our Research Integrity and Research Publishing teams and anonymous and named external researchers and research integrity experts for contributing to this investigation.

The corresponding author, as the representative of all authors, has been given the opportunity to register their agreement or disagreement to this retraction. We have kept a record of any response received.

References

[1] L. Zhang, X. Wang, Y. Sun, S. Wang, F. Zhang, and Z. Zhang, "Establishment of a Finite Element Model of Normal Nasal Bone and Analysis of Its Biomechanical Characteristics," *Emergency Medicine International*, vol. 2023, Article ID 3783051, 8 pages, 2023.

Hindawi
Emergency Medicine International
Volume 2023, Article ID 3783051, 8 pages
https://doi.org/10.1155/2023/3783051

Research Article

Establishment of a Finite Element Model of Normal Nasal Bone and Analysis of Its Biomechanical Characteristics

Liuqing Zhang,[1] XinYue Wang,[2] Yiyuan Sun,[3] Shuqin Wang,[4] FuLong Zhang,[5] and Zhen Zhang [6]

[1]*Department of Otolaryngology Head and Neck Surgery, The First Affiliated Hospital of Bengbu Medical College, Bengbu, Anhui 233000, China*
[2]*Department of Ophthalmology, The First Affiliated Hospital of Anhui Medical University, Hefei, Anhui 230022, China*
[3]*Department of Otolaryngology Head and Neck Surgery, ShangHai Nineth Hospital, School of Medicine, Shanghai Jiaotong University, Shanghai 200001, China*
[4]*Department of Imaging, The First Affiliated Hospital of Bengbu Medical College, Bengbu, Anhui 233000, China*
[5]*Department of Emergency Surgery, The First Affiliated Hospital of Bengbu Medical College, Bengbu, Anhui 233000, China*
[6]*Department of Pediatric, The First Affiliated Hospital of Bengbu Medical College, Bengbu, Anhui 233000, China*

Correspondence should be addressed to Zhen Zhang; 15040140207@xs.hnit.edu.cn

Received 17 August 2022; Revised 7 September 2022; Accepted 14 September 2022; Published 31 March 2023

Academic Editor: Hang Chen

Nasal bone is a long, paired series of small bones, which is narrow at the top and broad at the bottom, that forms the base of the nasal dorsum. Together with the nasal part of the frontal bone, the frontal process of the maxilla and the middle plate of the ethmoid bone constitute the bone scaffold of the external nose. In this paper, the DICOM image data file was imported into the Mimics software for 3D reconstruction. At the same time, the Geomagic software was used for relevant image processing, and the finite element software ANSYS was used to establish a finite element model to analyze the stress characteristics of the naso-maxillary complex. *Results.* The maximum principal stress and maximum strain force at the lower segment of nasal bone and the junction of nasal bone and maxilla were relatively large. When the same external force acts on the lower segment of the nasal bone and the angle is 0° (sagittal force), the maximum principal stress and maximum strain force are the smallest. When the angle continues to increase, the maximum principal stress and maximum strain force continue to increase.

1. Introduction

Nasal bone is one of the important components of maxillofacial bone cartilage scaffold. Because it independently protrudes in the center of maxillofacial region and its structure is relatively thin, it is particularly prone to fracture under the action of external force [1]. Its biomechanical mechanism is very important for understanding its biological characteristics, which is also the basis for solving related clinical problems. Normal nasal bones are divided into left and right parts, which are roughly rectangular in shape [2]. The left and right parts cannot be completely symmetrical, and the connection between them is also very close. When an external force acts on the nasal bone, it is easy to cause nasal deformity, thus affecting the appearance of the maxillofacial region, and in serious cases, it will lead to nasal ventilation disorders. Accurate and rapid establishment of a three-dimensional finite element model of nasal bone is helpful to understand its biomechanical properties and analyze its stress mechanism [3]. In recent years, the finite element method has been widely used in the related research of human limbs, spine, or various soft tissues, while the establishment of the finite element model of nasal bone and the biomechanical research are few [4]. The correlation analysis of the biomechanical characteristics of nasal bone provides a basis for the clinical diagnosis and treatment of nasal bone fracture and also lays a foundation for the related biomechanical research of otolaryngology and craniomaxillofacial surgery.

This study also has certain limitations. First of all, the number of materials collected is limited. The materials of this study are from hospitalized patients in our hospital. The selection of materials is relatively random, and there is no large-scale research, which has certain limitations. Second, the results of finite element analysis of nasal bone depend on the quality of modeling to a certain extent [5, 6]. Due to the influence of soft tissue, muscle, ligament, and other structures around the nasal bone, there is certain subjectivity in a series of processes such as image segmentation and image processing in the research process. In addition, some steps can be simplified in the modeling process, which may also lead to the model established in the research not being completely consistent with the real tissue structure characteristics. The biomechanical environment that completely simulates the nasomaxillary complex cannot be achieved at present. Finally, at present, most bone modeling still endows materials with a single modulus [7], but there is no unified evaluation standard in finite element modeling, material properties, and algorithms. The same is true in this study. The finite element model calculated through experiments is different from the substantive structural stress situation [8]. Some scholars calculate the elastic modulus of different materials based on different gray values of different bones. However, the relevant empirical formulas need to be further amended and improved.

2. Data and Methods

2.1. Modeling Data Collection. 100 normal adult nasal bone imaging data were randomly collected. The patient had no history of maxillofacial trauma and surgery, and no history of related maxillofacial diseases.

2.2. Equipment Selection and CT Scanning Three-Dimensional Reconstruction. 64 slice spiral CT was used to scan the nasal bones of healthy adults, and the CT plain scan image data of patients were obtained [9]. The scanning range is from the frontal bone to the bottom of the nose and from both sides to the lateral margin of the bilateral maxilla. The scanning layer thickness is 0.625 mm. First, the extracted imaging data are saved in DICOM (digital imaging and communications in medicine) format [10, 11]. The collected nasal bone imaging data were reconstructed by using the medical 3D reconstruction software mimics (material's interactive medical image control system) 20.0, and the appropriate gray threshold was set to segment the obtained image, establish the normal nasal bone and surrounding bone imaging model, and temporarily output it as a STL format file.

2.3. Postprocessing. Because the obtained STL format file is relatively rough, it is imported into Geomatic studio (American Geomatic company) for smooth noise reduction and surface processing. After relevant details are repaired, a smooth surface model is constructed. After the surface model is converted into a solid model, the file is saved in IGES format (as shown in Figure 1).

2.4. Establishment of Mesh Solid Model of Nasomaxillary Complex. The postprocessing three-dimensional model of nasomaxillary complex is imported into the finite element analysis software ANSYS workbench'19.0 (analysis system) [12], the boundary and contour lines of the three-dimensional solid model are established, and the tiny points, lines, and surfaces that have or may have an impact on the modeling are manually processed, and the model is divided into regular modules. When delimiting, the element size is set to 1 mm, 2 mm, and 3 mm, respectively. After repeated calibration, it is found that the 1 mm grid is the most suitable for this study. After division, the divided volume mesh is synthesized. After manual calibration, the mesh model of the nasomaxillary complex with 162086 units and 202528 nodes is finally generated (as shown in Figure 1).

2.5. Setting of Boundary Constraints and Stress Analysis. We treat the nasomaxillary complex as a whole, remove the constraints of surrounding soft tissue, muscles, ligaments, and other structures on the nasomaxillary complex, and fix the upper end of the nasal bone and the lateral edge of the double maxilla, and the lower end is the free edge. The nasal bone is divided into upper, middle, and lower parts (Figure 2). The upper end is the part above the level of the anterior inner segment of the frontomaxillary suture, the middle part is the narrowest part, and the lower part is from the lower segment of the medial edge of the nasal bone to the outer edge of the nasal bone. Figure 3 shows the distribution of the maximum principal stress and strain force generated by the 100 N vertical external force at the junction of the upper, middle, and lower segments of the nasal bone and the lateral nasal bone and maxilla. It is necessary to further select the lower segment of the nasal bone to simulate the stress and strain distribution of the nasal bone under the action of 100 N external force environment at different angles of 0°, 30°, 45°, 60°, 75°, and 90° (0° parallel to the sagittal plane), as shown in Figure 4. In this study, the author refers to relevant studies to define relevant parameters and selects the elastic modulus of 137000 MPa and Poisson's ratio of 0.326.

3. Results

In this study, the structure of nasomaxillary complex can be vividly reproduced by modeling. After simulating the vertical stress of 100 N at the junction of the upper, middle, and lower segments of the nasal bone and the lateral nasal bone and maxilla, the results show that (as shown in Table 1) the maximum principal stress at the upper and middle segments of the nasal bone is relatively less than that at the junction of the lower segment of the nasal bone and the lateral nasal bone and maxilla, and the strain force at the upper and middle segments of the nasal bone is relatively less than that at the junction of the lower segment of the nasal bone and the lateral nasal bone and maxilla. When different angular forces are applied to the lower segment of the nasal bone (the magnitude of the force is equal to 100 N), when the angle is 0°, that is, when the direction of the force is parallel to the sagittal plane, the maximum principal stress and maximum

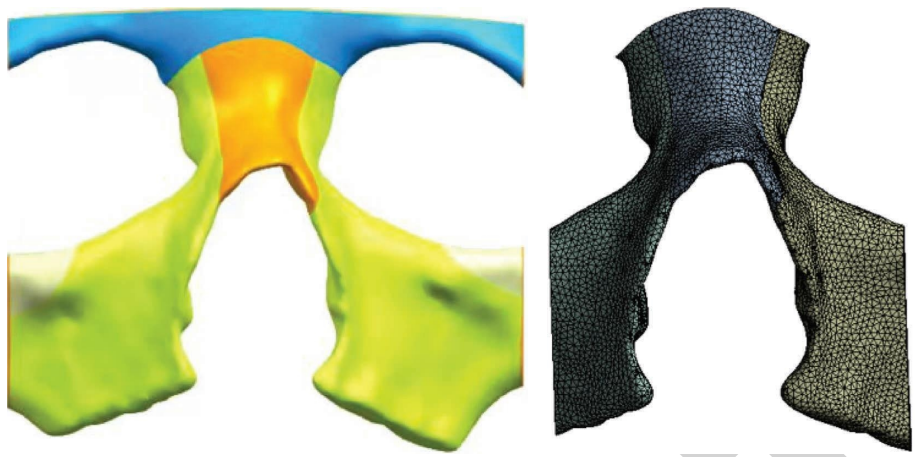

Figure 1: Nasomaxillary complex model and mesh model.

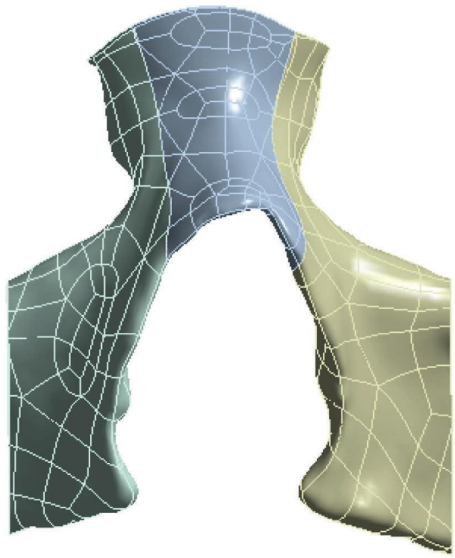

Figure 2: Positioning of the upper, middle, and lower segments of nasal bone and the junction of nose and maxilla.

strain force are the smallest, and when the angle is 90°, that is, when the force is perpendicular to the sagittal plane, the maximum principal stress and maximum strain force are the smallest. During this period, the angle is that with the continuous increase of the angle, the maximum principal stress and the maximum strain force are also increasing (as shown in Table 2).

4. Discussion

With the continuous development of biomechanics, the finite element method is gradually applied to various fields, and bone stress analysis is one of the main application fields of FEM [13, 14]. In this study, the results of FEM analysis can not only explain the biomechanical mechanism of nasomaxillary complex injury [15] but also provide some theoretical guidance for nasomaxillary complex injury in future clinical diagnosis and treatment. In this study, the stress of nasal trauma was simulated and analyzed by the finite element method [16]. Combined with the research results in Figure 3 and Table 1, it can be found that under the same external force conditions, the maximum principal stress of the upper middle segment of nasal bone is relatively less than that of the lower segment of nasal bone and the junction of lateral nasal bone and maxilla, and the strain force of the upper middle segment of nasal bone is relatively less than that of the lower segment of nasal bone and the junction of lateral nasal bone and maxilla [17]. Considering that the lower segment of the nasal bone protrudes in the center of the maxillofacial region, the structure is relatively thin, so it is relatively prone to fracture under the action of external force [18, 19]. In addition, the junction of nasal bone and maxilla, that is, the nasomaxillary suture, is the bone junction, which runs through the whole length of the lateral edge of nasal bone and the medial edge of maxilla. The bone in the suture junction area is relatively weak, and it is also prone to fracture or separation under the action of external force, and the maxillary sinus cavity of adults will become more protrusive after maturity [20]. Therefore, the maximum stress, that is, the maximum strain force, measured at the lower segment of the nasal bone; that is, the side in this study is relatively large.

Combined with the research results in Figure 4 and Table 2, it can be found that under the same external force, the maximum principal stress and maximum strain force gradually increase with the increasing angle of the lower nasal bone. Considering that when the angle is 0°, that is, when an external force is applied in the sagittal direction, the vertical external force acts directly on the nose, and the force direction is parallel to the nasal septum. As an external nasal support, the nasal septum has a certain supporting effect, and the space of the upper and lower diameters of the nasal septum suddenly decreases under the action of the external force, and the nasal septum can resolve the impact of some external forces in a deflected way to a certain extent. When the angle increases continuously, according to the principle of force decomposition, the lateral force of the external nasal bracket increases continuously. When the direction is perpendicular to the nasal bone bracket, that is, the angle is 90°, the

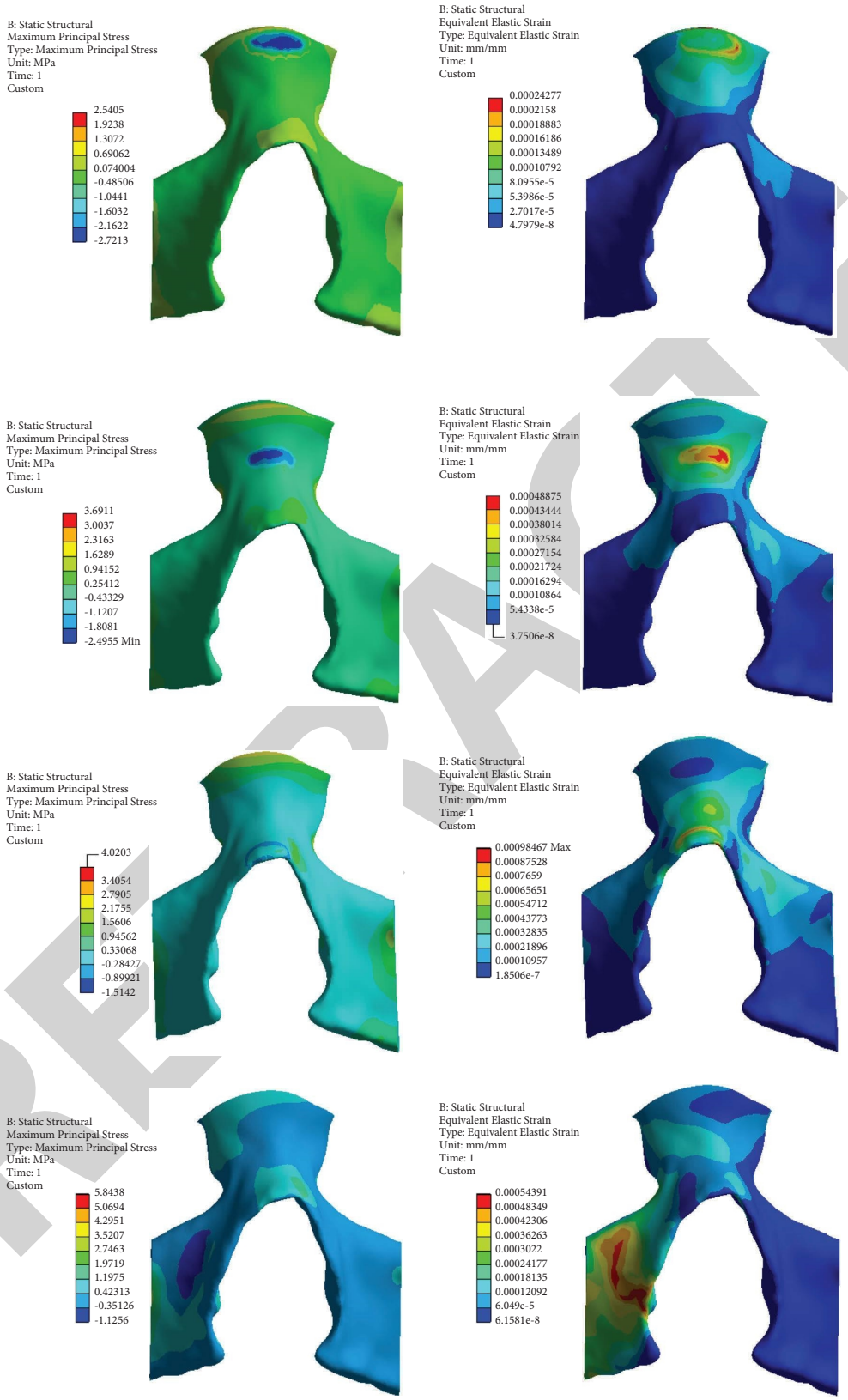

Figure 3: Stress and strain distributions of the upper, middle, and lower nasal bone and nasomaxillary junction under 100 N vertical external force.

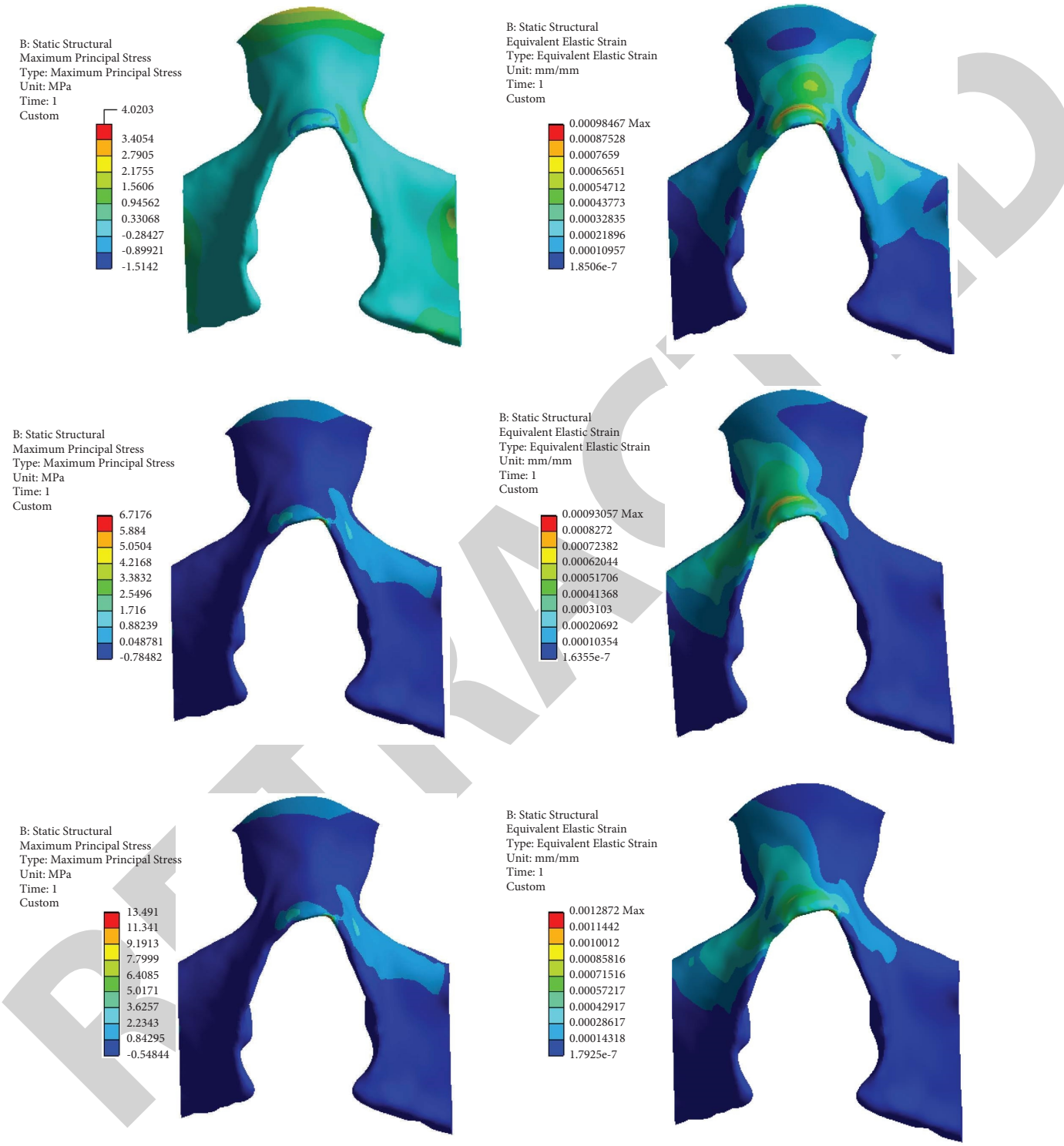

(a)

Figure 4: Continued.

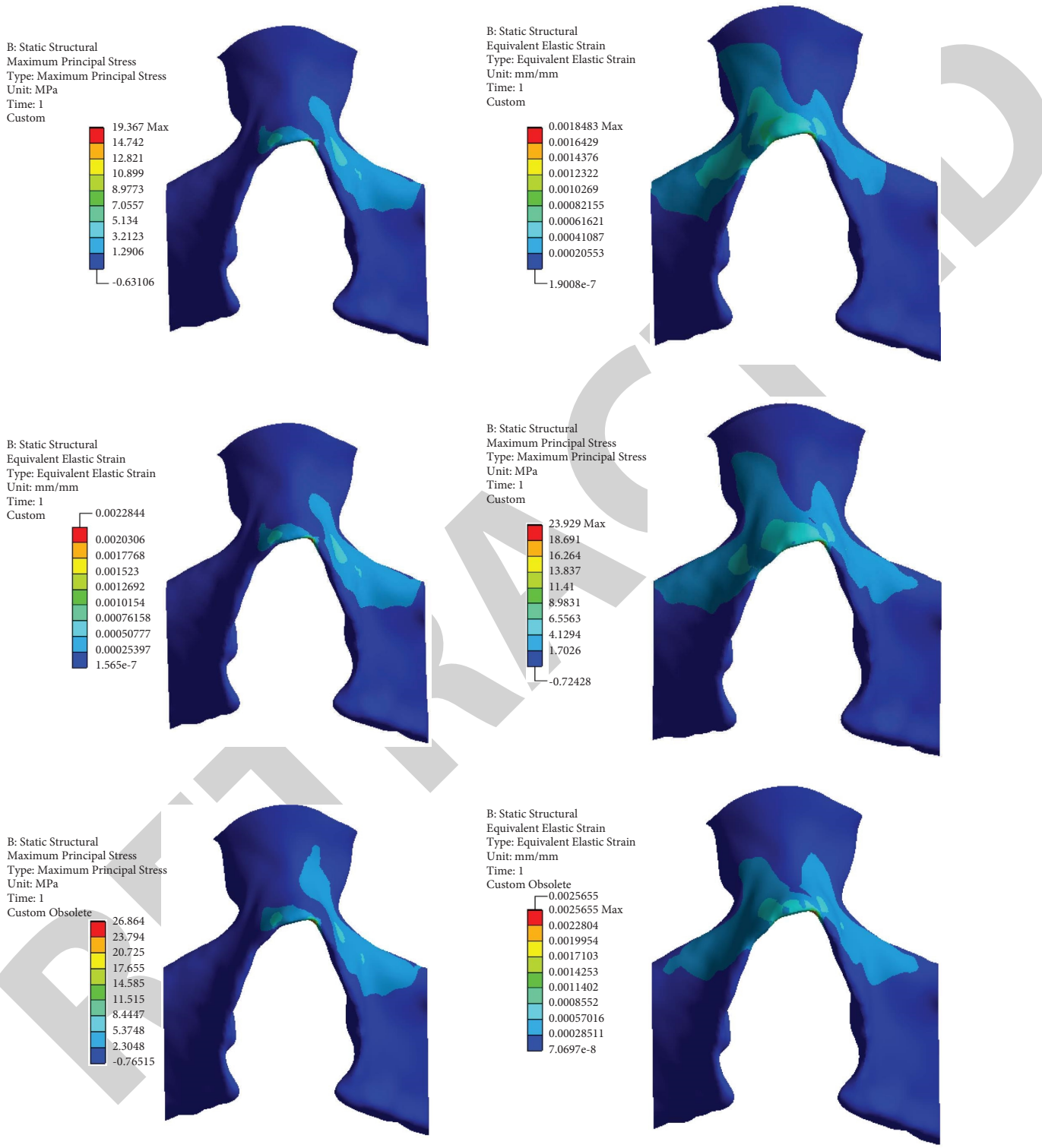

(b)

Figure 4: Distribution of stress and strain at the lower end of nasal bone at different angles.

lateral force is the largest, and the squeeze nasal bone shifts sideways, and the supporting structure of the external nasal skeleton is more likely to be damaged. At this time, the maximum principal stress of the external nose, that is, the maximum strain force, is the largest; that is, it is more prone to fracture.

Table 1: Stress and strain distributions of nasal bone and its surrounding parts.

	Maximum principal stress (PA)	Maximum strain force (mm/mm)
Upper segment	2.54	0.000243
Middle part	3.69	0.000489
Lower segment	4.02	0.000985
Flank	5.84	0.000544

Table 2: Stress and strain distributions of nasal bone at different angles.

	Maximum principal stress (PA)	Maximum strain force (mm/mm)
0°	4.02	0.000085
30°	6.71	0.000931
45°	13.49	0.001287
60°	19.37	0.001848
75°	23.93	0.002284
90°	26.86	0.002566

5. Conclusion

The stress of nasal bone under the same external force at different action points and angles is studied by finite element analysis, and the combination of three-dimensional reconstruction and finite element analysis provides a certain theoretical basis for the study of the stress mechanism of nasal maxillary complex and also provides a basis for the clinical diagnosis and treatment of nasal trauma, nasal bone, and surrounding structural fractures.

Data Availability

The data used to support the findings of this study are included in the article.

Conflicts of Interest

The authors declare that they have no conflicts of interest.

Acknowledgments

The authors would like to show sincere thanks to those technicians who have contributed to this research.

References

[1] L. Zhang, Y. sun, P. Wang, R. Shi, and D. Chen, "Epidemiological analysis of 2881 patients with nasal bone fracture," *Journal of Clinical Otorhinolaryngology Head and neck surgery*, vol. 34, no. 3, pp. 239–243, 2020.

[2] B. Zhang, M. Cai, F. Ruan, and Z. Chen, "Study on the effects of orthodontics on anterior tooth displacement in patientsy," *Evidence-Based Complementary and Alternative Medicine*, vol. 2022, Article ID 6544895, 5 pages, 2022.

[3] X. Xie, X. Pan, W. Zhang, and J. An, "A context hierarchical integrated network for medical image segmentation," *Computers and Electrical Engineering*, vol. 101, Article ID 108029, 2022.

[4] M. Daas, G. Dubois, A. S. Bonnet, P. Lipinski, and C. Rignon-Bret, "A complete finite element model of a mandibular implant-retained overdenture with two implants:Comparison between rigid and resilient attachment configurations," *Medical Engineering and Physics*, vol. 30, no. 2, pp. 218–225, 2008.

[5] B. Miles, A. J. Ruys, E. Kolos et al., "Subject specific finite element modeling of periprosthetic femoral fracture using element deactivation to simulate bone failure," *Medical Engineering and Physics*, vol. 37, no. 6, pp. 567–573, 2015.

[6] X. Chen, C. A. Myers, C. W. Clary et al., "Simplified mechanical tests can simulate physiological mechanics of a fixation construct for periprosthetic femoral fractures," *Journal of Biomechanical Engineering*, vol. 144, no. 3, Article ID 031003, 2022.

[7] X. Xie, X. Pan, F. Shao, W. Zhang, and J. An, "Mci-net: multiscale context integrated network for liver ct image segmentation," *Computers and Electrical Engineering*, vol. 101, Article ID 108085, 2022.

[8] H. Yu, M. Jeon, Y. Kim, and Y. Choi, "Epidemiology of violence in pediatric and adolescent nasal fracture compared with adult nasal fracture: an 8-year study," *Archives of Craniofacial Surgery*, vol. 20, no. 4, pp. 228–232, 2019.

[9] X. Xie, W. Zhang, H. Wang et al., "Dynamic adaptive residual network for liver CT image segmentation," *Computers and Electrical Engineering*, vol. 91, Article ID 107024, 2021.

[10] K. S. Kim, H. G. Lee, J. H. Shin, J. H. Hwang, and S. Y. Lee, "Trend analysis of nasal bone fracture," *Archives of Craniofacial Surgery*, vol. 19, no. 4, pp. 270–274, 2018.

[11] H.-H. Zhou, D. Ongodia, Q. Liu, R. T. Yang, and Z. B. Li, "Incidence and pattern of maxillofacial fractures in children and adolescents: a 10 years retrospective cohort study," *International Journal of Pediatric Otorhinolaryngology*, vol. 77, no. 4, pp. 494–498, 2013.

[12] O. Tepper and J. Schreiber, "Invited discussion on: the anatomical study of the nasal septal cartilage with its clinical implications," *Aesthetic Plastic Surgery*, vol. 45, no. 04, pp. 1712-1713, 2021.

[13] M. S. Hur, H. S. Won, D. S. Kwak, I. H. Chung, and I. B. Kim, "Morphological patterns and variations of the nasal septum components and their clinical implications," *Journal of Craniofacial Surgery*, vol. 27, no. 8, pp. 2164–2167, 2016.

[14] M. Xu, L. Deng, Y. Zhu et al., "Risk factors of catheter-related infection in unplanned extubation of totally implantable venous-accessportsin tumor patients," *Emergency Medicine International*, vol. 2022, Article ID 4235316, 7 pages, 2022.

[15] J. Zhao, Y. H. Zhou, Y. Q. Zhao et al., "Oral cavity-derived stem cells and preclinical models of jaw-bone defects for bone tissue engineering," *Stem Cell Research & Therapy*, vol. 14, no. 1, pp. 1–20, 2023.

[16] S. R. Lauesan, J. Daugaard-Jensen, E. F. Lauridsan, and I. Kjær, "Localised scleroderma en coup de sabre affecting the skin, dentition and bone tissue within craniofacial neural crest fields, Clinical and radiographic study of six patients," *European Archives of Paediatric Dentistry*, vol. 20, pp. 339–350, 2019.

[17] Y. Liang, C. Jiang, L. Wu, W. Wang, Y. Liu, and X. Jian, "Application of combined osteotomy and reconstruction prebent plate position (CORPPP) technology to assist in the precise reconstruction of segmental mandibular defects(-CORPPP) technology to assist in the precise reconstruction of segmental mandibular defects," *Journal of Oral and Maxillofacial Surgery*, vol. 75, no. 9, pp. 2026.e1–2026.e10, 2017.

Hindawi
Emergency Medicine International
Volume 2023, Article ID 9879027, 1 page
https://doi.org/10.1155/2023/9879027

Retraction

Retracted: A Study on the Relationship between Sense of Disease Uncertainty and Family Strength and Mental Resilience in Guardians of Children with Inflammatory Bowel Disease

Emergency Medicine International

Received 8 August 2023; Accepted 8 August 2023; Published 9 August 2023

This article has been retracted by Hindawi following an investigation undertaken by the publisher [1]. This investigation has uncovered evidence of one or more of the following indicators of systematic manipulation of the publication process:

(1) Discrepancies in scope

(2) Discrepancies in the description of the research reported

(3) Discrepancies between the availability of data and the research described

(4) Inappropriate citations

(5) Incoherent, meaningless and/or irrelevant content included in the article

(6) Peer-review manipulation

The presence of these indicators undermines our confidence in the integrity of the article's content and we cannot, therefore, vouch for its reliability. Please note that this notice is intended solely to alert readers that the content of this article is unreliable. We have not investigated whether authors were aware of or involved in the systematic manipulation of the publication process.

Wiley and Hindawi regrets that the usual quality checks did not identify these issues before publication and have since put additional measures in place to safeguard research integrity.

We wish to credit our own Research Integrity and Research Publishing teams and anonymous and named external researchers and research integrity experts for contributing to this investigation.

The corresponding author, as the representative of all authors, has been given the opportunity to register their agreement or disagreement to this retraction. We have kept a record of any response received.

References

[1] J. Yan and L. Luo, "A Study on the Relationship between Sense of Disease Uncertainty and Family Strength and Mental Resilience in Guardians of Children with Inflammatory Bowel Disease," *Emergency Medicine International*, vol. 2022, Article ID 4797281, 6 pages, 2022.

Hindawi
Emergency Medicine International
Volume 2022, Article ID 4797281, 6 pages
https://doi.org/10.1155/2022/4797281

Research Article

A Study on the Relationship between Sense of Disease Uncertainty and Family Strength and Mental Resilience in Guardians of Children with Inflammatory Bowel Disease

Jun Yan[1] **and Lin Luo**[2]

[1]*Wuhan Children's Hospital (Wuhan Maternal and Child Healthcare Hospital), Tongji Medical College, Huazhong University of Science&Technology, Wuhan 430014, China*
[2]*ICU, Fifth Hospital in Wuhan, Wuhan 430050, China*

Correspondence should be addressed to Lin Luo; luolin19710721@126.com

Received 22 August 2022; Revised 23 September 2022; Accepted 29 September 2022; Published 12 October 2022

Academic Editor: Hang Chen

Background. Inflammatory bowel disease is difficult to cure, which seriously affects the physical and mental health of children and brings negative psychological stress to guardians. Uncertainty in illness of guardians reduces the ability of care and is not conducive to the treatment and recovery of children. Therefore, it is of great significance to explore the related factors of uncertainty in illness. *Objective*. The aim of this study is to explore the relationship between sense of disease uncertainty and family strength and mental resilience in guardians of children with inflammatory bowel disease (IBD). *Method*. A total of 146 guardians of 88 children with inflammatory bowel disease were investigated. The guardians' sense of disease uncertainty, family strength, and mental resilience were evaluated by Mishel uncertainty in illness scale-family member (MUIS-FM), family hardiness index (FHI), and Connor–Davidson resilience sca1e (CD-RISC), respectively. Spearman correlation was used for analyzing the correlation between the guardian's sense of disease uncertainty and family resilience. *Results*. The guardian's MUIS-FM score from lowest to highest was complexity, unpredictability, lack of information, and uncertainty. The average scores of FHI and CD-RISC were lower than the average score of CD-RISC of the general community in China 65.4 ($t = -4.36$, $P < 0.05$). The score of MUIS-FM was significantly correlated with the scores of FHI and CD-RISC ($P < 0.05$). Multiple linear regression analysis showed that the challenge score in the FHI scale and the fortitude score and the strength score in the CD-RISC scale were the main influencing factors of guardians' sense of disease uncertainty in children with IBD ($P < 0.05$). *Conclusion*. The guardians of children with IBD had a more serious sense of disease uncertainty, which was related to family strength and mental resilience.

1. Introduction

Inflammatory bowel disease (IBD) is a type of chronic nonspecific inflammation of the intestine with unknown etiology [1, 2]. It mainly includes Crohn's disease (CD) and ulcerative colitis (UC), which is often manifested as abdominal pain, diarrhea, bloody stools, weight loss, and so on. The disease is difficult to cure and has repeated attacks, with potential cancer risk. In recent years, the incidence of IBD among children has been increasing. IBD seriously affects growth, development, physiological function, and mental healthof children [3, 4]. Moreover, it is also a heavy negative stress event and psychological impact on the guardians, which leads to a series of psychological problems of the guardians, which has attracted more and more social attention [5, 6]. The psychological problems of guardians are often related to the family members' low understanding and awareness of the specific condition, treatment process, and prognosis of IBD. Uncertainty in illness refers to the lack of ability to determine disease information, including the etiology, pathogenesis, treatment plan, nursing measures, and prognosis of the disease, which is one of the main factors causing psychological pressure on patients or guardians and may lead to the weakening of guardians' ability to seek

disease information. It is easy to cause a large number of adverse psychological states and extreme behaviors if guardians are prevented from playing their normal caregiving functions [7]. The uncertainty of the disease will adversely affect the normal living status and quality of life of the guardian, thus damaging the mental health of the guardian and is not conducive to the treatment and rehabilitation of the children [8]. Therefore, it is of great clinical significance to pay attention to the sense of disease uncertainty of guardians of children with IBD. Current studies on family members' sense of disease uncertainty mainly focused on comprehensive clinical specialties such as internal medicine, surgery, and oncology [9], while there were few reports on guardians of IBD children. This study mainly studied the correlation between the guardian's sense of disease uncertainty and family strength and mental resilience in children with IBD. The report was as follows.

2. Materials and Methods

2.1. General Data. A total of 146 guardians of 88 children with inflammatory bowel disease were investigated. This study was approved by the Wuhan Children's Hospital (Wuhan Maternal and Child Healthcare Hospital) Ethics Committee. Children inclusion criteria were (1) the children were diagnosed as IBD according to the expert consensus on diagnosis and treatment of IBD in children in 2019 [10]; (2) 1–14 years old; (3) diseases were controlled during follow-up; (4) complete follow-up data. Exclusion criteria were (1) complicated with diabetes, cardiovascular and cerebrovascular diseases, liver and spleen dysfunction, infectious diseases, blood, or immune system diseases; (2) have taken drugs that affect platelets within two weeks, such as ticlopidine, heparin aspirin, and dipyridamole. There were 47 cases of CD and 41 cases of UC in the children. There were 56 males and 32 females. The onset age was (9.25 ± 2.41) years.

Guardian inclusion criteria were (1) age 18–70; (2) the education level was junior high school or above; (3) be the immediate relative of the child and the main caregiver and understand the general situation of the child; (4) in good health and to be able to complete the relevant evaluation of this study normally. Exclusion criteria were (1) the presence of serious physical diseases or mental disorders. A total of 146 guardians were aged from 26 to 66, with an average of (45.23 ± 13.15) years.

2.2. Evaluative Methods. During the outpatient visit or hospitalization, the guardian was evaluated with scales. One gastroenterology nurse was assigned to administer the scales. Before the test, the guardian should be explained to the purpose and basic methods of the test. Unified instructions were used for each scale, and the contents of the test that the guardian does not fully understand could be further analyzed. After the guardian fully understands the measurement content, the guardian would independently complete the evaluation of all scales according to their own actual situation, and the evaluation time was 30 min. The form would be returned on the spot after being filled in by the guardian. A total of 146 scales were issued, and 146 were recovered with a recovery rate of 100%. The method flow chart of this study is shown in Figure 1.

2.3. Assessment Content and Tools. Sense of disease uncertainty: the Chinese version of the scale Mishel uncertainty in illness scale-family member (MUIS-FM) [11] was used for evaluation, which was applied to measure the status of the guardian's sense of disease uncertainty. The content of the scale included 4 dimensions such as complexity, uncertainty, unpredictability, and lack of information. It included 33 items in total. The lowest score was 33 points, and the highest score was 165 points. The higher the score was, the stronger the uncertainty of the disease was. Dimension scores = (average score of dimension/highest score of dimension) × 100%.

Family strength: the family hardiness index (FHI) [12] was used for evaluating the internal strengths of family members. The scale included three dimensions of commitment, challenge, and control, with a total of 20 items. The Likert 4-level scoring method was adopted. A score of 1 was assessed as strongly disagree. A score of 2 was assessed as disagree. A score of 3 was assessed as agree. A score of 4 was assessed as strongly agree. Reverse scoring questions included the items 1, 2, 3, 8, 10, 14, 16, 19, and 20, and the remaining items were positive scoring questions. The higher the total score was, the better the family resilience was. Cronbach's coefficient of this scale was 0.80.

Mental resilience: assessed by the Connor–Davidson resilience scale(CD-RISC) [13], jointly developed by Connor KM and Davidson JR, it contained 25 items in total. Domestic scholar Liu et al. [14] introduced and sinicized it, including three dimensions of tenacity, strength, and optimism. The total score was the sum of the scores of all items. Cronbach's coefficient and retest validity of the scale were 0.89 and 0.87, respectively, which were used to measure the positive psychological characteristics conducive to the individual's adaptation to adversity such as disease and adverse events. The 4-level scoring method was adopted, and the total score was 0–100. The higher the cumulative score of each item, the better the mental resilience.

2.4. Statistical Methods. SPSS 21.0 was used for statistical analysis of all data. The measurement data conforming to normal distribution was represented by the mean ± standard deviation, the measurement data not conforming to normal distribution was represented by the median (P25, P75), count data were represented by the number of cases or percentage, and correlation was the Spearman correlation analysis method. The test level was bilateral $\alpha = 0.05$.

3. Results

3.1. General Information of the Guardian. In the general information of 146 guardians, female (52.74%), 45–59 years old (43.15%), college education or above (62.33%), unemployed or retired (58.90%), full understanding of the disease (49.32%), mother of the child (35.62%), and family monthly

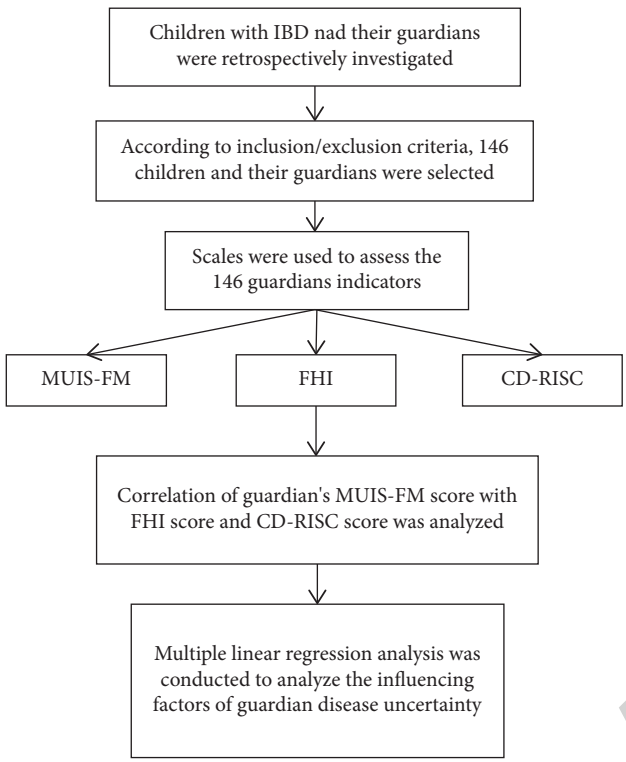

Figure 1: Method flow chart. IBD: inflammatory bowel disease, MUIS-FM: Mishel uncertainty in illness scale-family member, FHI: family hardiness index, CD-RISC: Connor–Davidson resilience scale. A total of 146 guardians of children with inflammatory bowel disease were investigated. The guardians' sense of disease uncertainty, family strength, and mental resilience were evaluated by MUIS-FM, FHI, and CD-RISC, respectively. These analyzed the correlation of MUIS-FM between FHI and CD-RISC, and the influencing factors of uncertainty in illness were analysed by multiple linear regression.

income 2001–3000 (43.15%) accounted for a high proportion, as shown in Table 1.

3.2. Guardian's MUIS-FM Rating. The MUIS-FM scores of 146 guardians in this study ranged from low to high in order of complexity, unpredictability, lack of information, and uncertainty, as shown in Table 2.

3.3. Guardian's FHI Rating. FHI averaged an overall score of 42.68, as shown in Table 3.

3.4. Guardian's CD-RISC Rating. The average score of CD-RISC was 61.55, lower than the average score of CD-RISC of the general community in China 65.4 ($t = -4.36$, $P < 0.05$), as shown in Table 4.

3.5. Correlation of the Guardian's MUIS-FM Score with the FHI Score and CD-RISC Score. The total score of MUIS-FM was significantly correlated with the total score of FHI and its dimensions, and the total score of MUIS-FM was significantly correlated with the total score of CD-RISC and its dimensions, as shown in Table 5.

Table 1: General information of the guardian.

Items	Number of people	Percentage
Gender		
Male	69	47.26
Female	77	52.74
Age (years)		
<45	51	34.93
45–59	63	43.15
≥60	32	21.92
Marital status		
Married	126	86.30
Unmarried, divorced, or widowed	20	13.70
Schooling		
Junior and senior secondary	55	37.67
College degree or above	91	62.33
Employment status		
Be on the job	60	41.10
Unemployed or retired	86	58.90
Knowledge of the disease		
Know thoroughly	72	49.32
Know	69	47.26
Know nothing	5	3.42
Relationship with children		
Father	48	32.88
Mother	52	35.62
Grandfather	12	8.22
Grandmother	13	8.90
Maternal grandfather	12	8.22
Maternal grandmother	9	6.16
Average monthly family income (yuan)		
<1000	8	5.48
1000–2000	51	34.93
2001–3000	63	43.15
>3000	24	16.44

3.6. Multiple Linear Regression of Factors Influencing Guardian's Sense of Disease Uncertainty in Children with IBD Analysis Results ($n = 130$). Multiple linear regression analysis was conducted with the total score of sense of disease uncertainty as the dependent variable and general information, family resilience, and psychological resilience as independent variables. The results showed that the challenge score in the FHI scale and the fortitude score and the strength score in the CD-RISC scale were the main influencing factors of guardians' sense of disease uncertainty in children with IBD ($P < 0.05$). The results of multiple linear regression analysis are shown in Table 6.

4. Discussion

According to the data analysis of this study, the MUIS-FM score of the guardians of IBD in children was higher than the domestic norm ($P < 0.05$), indicating that the guardians of IBD in children had a strong sense of disease uncertainty and lacked the ability to determine the etiology, pathogenesis,

Table 2: Guardian's MUIS-FM rating.

Items	Number of entries	Divide entries	Dimension scores	Average Score	Score ranges	Score index (%)
Unpredictability	5	3.43 (3,3.8)	17 (15,2)	17.17	6–25	68.68
Lack of information	7	3.27 (2.9,3.6)	23 (20,3)	22.86	13–32	71.44
Complexity	13	1.39 (1.2,1.5)	18 (16,2)	18.04	13–29	62.21
Uncertainty	8	3.88 (3.3,4.5)	31 (26,36)	31.24	13–40	78.10
Total points	33	2.7 (2.6,2.9)	89.5 (84,95)	89.32	66–112	79.75

Table 3: Guardian's FHI rating.

Items	Number of entries	Divide entries	Dimension scores	Average Score	Score ranges
Commitment	9	2.1 (1.9,2.3)	19 (17,2)	19.15	9–27
Control	6	2.0 (1.7,2.3)	12 (10,14)	12.34	6–21
Commitment	5	2.2 (1.8,2.6)	11 (9,13)	11.19	5–20
Total points	20	2.2 (1.9,2.3)	43 (38.75,46)	42.68	27–59

Table 4: Guardian's CD-RISC rating.

Items	Number of entries	Divide entries	Dimension scores	Average Score	Score ranges
Tenacity	13	2.3 (1.9,2.6)	30 (25,34.3)	30.12	12–50
Strength	8	2.6 (2.1,3.2)	21 (17,25.3)	21.03	8–32
Optimism	4	2.6 (2,3.3)	10.5 (8,13)	10.40	1–16
Total points	25	2.4 (2.2,2.7)	61 (54,68)	61.55	41–87

Table 5: Correlation of the guardian's MUIS-FM score with the FHI score and CD-RISC score.

Items		FHI				CD-RISC			
		Commitment	Control	Commitment	Total points	Tenacity	Strength	Optimism	Total points
MUIS-FM	r	−0.276	−0.230	−0.406	−0.462	−0.433	−0.438	−0.325	−0.386
	P	0.001	0.005	<0.001	<0.001	<0.001	<0.001	<0.001	0.027

Table 6: Multiple linear regression of factors influencing the guardian's sense of disease uncertainty in children with IBD analysis results.

Items	B	SE	β	t	P
Constant	123.676	4.822	—	25.650	<0.001
Commitment	−0.186	0.190	−0.074	−0.977	0.330
Control	−0.213	0.207	−0.075	−1.029	0.305
Commitment	−0.570	0.200	−0.211	−2.855	0.005
Tenacity	−0.324	0.086	−0.279	−3.772	<0.001
Strength	−0.367	0.115	−0.234	−3.191	0.002
Optimism	−0.240	0.216	−0.086	−1.109	0.269
Average monthly family income	0.000	0.001	−0.073	−1.043	0.299

treatment plan, nursing measures, prognosis, and other information of IBD. This result was similar to that of Kang et al. [9]. According to relevant literature [9], guardians of children with IBD were uncertain about the diagnosis, symptoms, treatment, and prognosis of the disease. It was concluded that guardians' cognition was mainly affected by the following four factors: (1) the symptoms of the disease were not clear; (2) lack of information and knowledge about disease diagnosis; (3) complex nursing and treatment; (4) the disease process and prognosis were unpredictable. In this study, the average total score of guardian uncertainty was 89.32, which was in the middle level. Through the observation of the scores of each dimension, the highest score index was uncertainty, while the lowest score was complexity, which indicated that the guardian disease of inflammatory bowel disease in children had a sense of uncertainty on the change of illness, prognosis, and treatment measures [8, 15]. Inflammatory bowel disease (IBD) was a chronic nonspecific inflammation of the intestine, characterized by repeated attacks and difficult radical cure, and had the risk of cancer [16]. In addition, the disease would cause abdominal pain, diarrhea, bloody stools, weight loss and other symptoms, causing malnutrition, fever, conjunctivitis, arthritis, and other systemic reactions. If complications occur in children, the condition of IBD will be rapidly aggravated, affecting the recovery of the disease, which is not conducive to the prediction of IBD. At the same time, the aggravation of the illness will cause the guardian to worry and cause anxiety and other negative emotions, resulting in a sense of disease uncertainty [17]. Since the treatment period of IBD was long and there were many adverse reactions of drugs (such as purine preparations and glucocorticoids), the guardian was concerned that the adverse reactions of drugs would affect the normal growth and development of the children and make the guardian feel uncertain about the treatment of the disease. In addition, it was a common phenomenon that children's drug tolerance and compliance were reduced in the treatment process.

Parents did not understand this and mistakenly believed that the treatment was ineffective or aggravated the condition, which would further aggravate the uncertainty of the disease and affected the disease control and treatment [18]. In this study, most parents came from rural areas with a low education level, limited access to disease information and ability, and lack of disease treatment and nursing knowledge, resulting in a sense of uncertainty [19].

Correlation analysis of this study showed that the MUIS-FM score was negatively correlated with the FHI total score and MUIS-FM dimensions (commitment, control, challenge) and the CD-RISC total score and CD-RISC dimensions (tenacity, strength, optimism) ($P < 0.05$), and multiple linear regression analysis showed that the challenge score in the FHI scale and the fortitude score and the strength score in the CD-RISC scale were the main influencing factors of guardian disease uncertainty in children with IBD. It was suggested that the stronger the guardian's disease uncertainty was, the weaker the family challenge ability was and the lower the psychological fortitude and strength were; on the contrary, the weaker the guardian's disease uncertainty was, the stronger the family challenge ability and the guardian's psychological fortitude and strength were, which was consistent with the relevant research results. Family resilience refers to the family characteristics and attributes that family members use internal resources to adapt to the stressful environment and successfully overcome the crisis under pressure. The challenge dimension is one of the key components of family resilience. Studies had shown that family resilience had a protective effect on families [20, 21]. Therefore, when the guardian faced the long-term ill children in repeated treatment, the psycology of guardians would have a strong sense of crisis and be severely hit. This situation may cause family instability, especially for families with poor family resilience [22].

The guardian could not correctly view the disease of the children, and there were phenomena such as mutual shirking of responsibility, distrust, and disagreement among family members. The lack of family's ability to challenge the disease affected the treatment of the children, resulting in a high sense of uncertainty about the disease. Mental resilience was the ability to rebound in the face of difficulties and setbacks. When the mental resilience of guardians was poor, their psychological and coping ability, tenacity, and stress resistance would also be reduced, and they were unwilling to face a series of pains brought by the disease and adopted negative coping methods so that their disease uncertainty would increase [23, 24]. Nursing staff should give guardians of children with disease-related knowledge education, improve the confidence of cure, improve the level of mental resilience, and reduce the sense of uncertainty of disease.

5. Strengths and Limitations

The significance of this study was that the results shown that the illness uncertainty of the guardians of children with inflammatory bowel disease was more serious, which was related to the resilience and psychological resilience of their families. This conclusion suggested that there was a strong sense of illness uncertainty in the guardians of children with inflammatory bowel disease, and attention to the overall family harmony and psychological tolerance of the guardians of children with inflammatory bowel disease should not be ignored. Therefore, this study had certain guiding significance for the treatment of children with inflammatory bowel disease. However, the small number of subjects included in this study may lead to bias in the study results. Therefore, future studies should increase the sample size to further verify the results of this study.

6. Conclusions

In conclusion, the guardians of children with IBD had a more serious sense of disease uncertainty, which was related to family resilience and psychological resilience. The guardians of inflammatory bowel disease in children had a strong sense of disease uncertainty, so it was important to pay attention to the overall family harmony and psychological tolerance of the guardians of IBD in children.

Data Availability

The data used for this study have been included within the manuscript.

Conflicts of Interest

The authors declare no conflicts of interest.

References

[1] S. S. Seyedian, F. Nokhostin, and M. D. Malamir, "A review of the diagnosis, prevention, and treatment methods of inflammatory bowel disease," *Journal of Medicine and Life*, vol. 2, no. 2, pp. 113–122, 2019.

[2] Q. Guan, "A comprehensive review and update on the pathogenesis of inflammatory bowel disease," *Journal of Immunology Research*, vol. 2019, Article ID 7247238, 16 pages, 2019.

[3] M. A. Aardoom, G. Veereman, and L. de Ridder, "A review on the use of anti-TNF in children and adolescents with inflammatory bowel disease," *International Journal of Molecular Sciences*, vol. 20, no. 10, p. 2529, 2019.

[4] P. F. van Rheenen, "Managing abnormal liver tests in children with inflammatory bowel disease," *Current Opinion in Pediatrics*, vol. 33, no. 5, pp. 521–529, 2021.

[5] H. K. Michel, N. Siripong, R. B. Noll, and S. C. Kim, "Caregiver and adolescent patient perspectives on comprehensive care for inflammatory bowel diseases: building a family-centered care delivery model," *Crohn's & colitis 360*, vol. 2, no. 3, otaa055, Article ID otaa055, 2020.

[6] A. Yue, X. Pu, W. Zheng, B. Wang, Z. Yang, and Y. Shi, "Relation of social-emotional development of infants to depressive symptom and positive parenting behavior of caregivers in poor rural areas," *Chinese Mental Health Journal*, vol. 36, no. 1, pp. 30–36, 2022.

[7] Z. T. Han, H. M. Zhang, Y. M. Wang, S. S. Zhu, and D. Y. Wang, "Uncertainty in illness and coping styles: moderating and mediating effects of resilience in stroke patients," *World Journal of Clinical Cases*, vol. 9, no. 30, pp. 8999–9010, 2021.

Hindawi
Emergency Medicine International
Volume 2023, Article ID 9870169, 1 page
https://doi.org/10.1155/2023/9870169

Retraction

Retracted: Analysis of the Effectiveness of Transradial Access Puncture in the Application of Complications and Comfort after Cerebral Angiography

Emergency Medicine International

Received 28 November 2023; Accepted 28 November 2023; Published 29 November 2023

This article has been retracted by Hindawi, as publisher, following an investigation undertaken by the publisher [1]. This investigation has uncovered evidence of systematic manipulation of the publication and peer-review process. We cannot, therefore, vouch for the reliability or integrity of this article.

Please note that this notice is intended solely to alert readers that the peer-review process of this article has been compromised.

Wiley and Hindawi regret that the usual quality checks did not identify these issues before publication and have since put additional measures in place to safeguard research integrity.

We wish to credit our Research Integrity and Research Publishing teams and anonymous and named external researchers and research integrity experts for contributing to this investigation.

The corresponding author, as the representative of all authors, has been given the opportunity to register their agreement or disagreement to this retraction. We have kept a record of any response received.

References

[1] H. Wan, L. Gao, and D. Huang, "Analysis of the Effectiveness of Transradial Access Puncture in the Application of Complications and Comfort after Cerebral Angiography," *Emergency Medicine International*, vol. 2022, Article ID 3457034, 6 pages, 2022.

Hindawi
Emergency Medicine International
Volume 2022, Article ID 3457034, 6 pages
https://doi.org/10.1155/2022/3457034

Research Article

Analysis of the Effectiveness of Transradial Access Puncture in the Application of Complications and Comfort after Cerebral Angiography

Hongyan Wan,[1] Lan Gao,[1] and Daohua Huang [2]

[1]*Zhongda Hospital Southeast University, Department of Interventional Radiology and Vascular Surgery, Nanjing 210009, China*
[2]*Zhongda Hospital Southeast University, Department of Nursing, Nanjing 210009, China*

Correspondence should be addressed to Daohua Huang; daohuahuang2022@sina.com

Received 12 July 2022; Revised 9 August 2022; Accepted 24 September 2022; Published 11 October 2022

Academic Editor: Hang Chen

Objective. To investigate the analysis of the effectiveness of transradial access puncture in the application of complications and comfort after cerebral angiography. *Methods*. Retrospectively analyzed 80 patients who met the inclusion and exclusion criteria and were randomly divided into the control group (femoral artery group $n = 40$) and test group (radial artery group $n = 40$) using a random number table from January 2021 to January 2022 admitted to the department of neurology and department of vascular interventions in our hospital and compared the incidence of postoperative puncture site bleeding, time to first postoperative urination, and incidence of postoperative urinary retention and postoperative changes in comfort level. *Results*. There was 1 case of postoperative puncture site bleeding in the test group and 6 cases of postoperative puncture site bleeding in the control group, with statistically significant differences ($P < 0.05$); the time to first urination in the test group (62.47) was significantly better than that in the control group (85.97), with statistically significant differences ($P < 0.05$); there were 0 cases of urinary retention in the test group and 6 cases in the control group, with statistically significant differences ($P < 0.05$). The GCQ scores of patients in the test group were significantly higher than those in the control group, and the difference was statistically significant ($P < 0.05$). *Conclusion*. Transradial access puncture has a good clinical effect and can effectively reduce the complication rate of patients, which is worth promoting.

1. Introduction

In recent years, the incidence of various cerebrovascular diseases has shown a significant increase as the aging population in China continues to increase, and the main clinical symptoms of these diseases are distorted eyes and mouth and speech dysfunction, which seriously threaten the physical and mental health and quality of life of the elderly population due to the high disability and mortality rates [1]. Digital silhouette whole brain angiography and interventional therapy have been widely used in clinical medicine because of the advantages of convenient and simple operation and significant effect [2]. However, in the process of patient treatment, postoperative complications are likely to occur, which not only affect the effectiveness of treatment but also threaten the physical health of patients [3]. Therefore, effective measures must be taken to deal with the complications that occur in patients promptly.

The femoral artery itself has the advantages of coarse vessel diameter, relatively superficial location, clearer body projection, and high success rate of cannulation and is often used as the preferred channel for puncturing cerebral angiography, but is prone to puncture-related complications [4]. A study [5] counted 100 DSA inpatients and found that the incidence of vascular complications in patients with transfemoral access was 9.6%. The study [6] found that compression of the puncture site for 6 h was often required after transfemoral access puncture, and the operated limb also required 6–8 h of braking and 24 hours of bed rest. The study [7] found that prolonged postoperative bed rest is

prone to many adverse effects, such as lumbar pain and discomfort, urinary retention, insomnia, and anxiety, which affect the postoperative recovery of patients to a greater extent.

The radial artery is relatively shallowly located, and the percutaneous radial artery vascular access test was first applied to coronary angiography in 1989 and first applied to interventional treatment in 1993 [8]. After years of practice, improvement, and refinement, transradial artery puncture has been gradually applied to cerebrovascular interventions [9]. The study [10] reported that the success rate of neurointerventional procedures with transradial access reached 94.5%, and the complication rate was also lower compared with transfemoral access puncture, which was only 2.9%. After transradial artery puncture, the puncture site requires compression bandaging, except for the wrist joint on the punctured side, which requires 6–8 hours of braking. The rest of the limb joints are not restricted in postoperative activities and have a high level of safety and comfort [11]. The study [12] showed that patients with transradial access usually had significantly less time in bed relative to 24 h after femoral artery surgery by 1.9.

Based on this, 80 patients who were admitted to the department of neurology and interventional vascular surgery from January 2021 to January 2022 and met the inclusion and exclusion criteria were selected for this study and randomly divided into a control group (femoral artery group $n = 40$) and a test group (radial artery group $n = 40$) using a random number table to compare the incidence of postoperative puncture site bleeding, time to first postoperative urination, and incidence of postoperative urinary retention in both groups. The results of the study were presented. The aim was to investigate the effectiveness of transfemoral and transradial arteries in terms of postoperative complications and comfort after cerebral angiography.

2. Objects and Methods

2.1. Object. Eighty patients who were hospitalized in our neurology and interventional vascular surgery departments from January 2021 to January 2022 and met the inclusion and exclusion criteria were selected, and the patients were randomly divided into a control group (femoral artery group, $n = 40$ cases) and a test group (radial artery group, $n = 40$ cases) using a random number table, with 16 females and 24 males in the control group, with a mean age of 62.679.44 years; in the test group, there were 20 female and 20 male cases with a mean age of 63.758.51 years. The study protocol was reported to and approved by the ethics department of our hospital before the trial, and the patients or their families were informed of the detailed study protocol and signed an informed consent form before the trial began.

2.1.1. Inclusion Criteria. The inclusion criteria were as follows: history of cerebral ischemic or hemorrhagic cerebrovascular disease, cerebral aneurysm; suspicion of intracranial and extracranial arterial occlusion or stenosis, cerebral aneurysm by relevant MRA, CTA, carotid ultrasound, TCD, and other auxiliary examinations; negative Allen test results; good pulsation of the distal radial artery by transvascular ultrasound; conscious patients who can express themselves correctly; and patients who are unwilling to undergo femoral artery puncture.

2.1.2. Exclusion Criteria. The exclusion criteria were as follows: patients who have used the radial artery for hemodialysis or other purposes; patients with arterial stenosis or lesions at the end of the hand; trauma to the hand or history of previous surgery; abnormalities in the vessels of the arm; and unwillingness to participate in this study.

2.2. Research Methodology

2.2.1. Control Group. Patients underwent cerebral angiography with femoral artery access, and postoperative puncture sites were given inguinal pressure bandages (manufacturing license number: Su Food and Drug Administration Machinery Manufacturing Xu 20160050) for cross-row bandaging, and all patients were bandaged by the same physician. After the operation, the doctor and nurse in charge of the patient gave bedside instructions, instructed precautions and physical activities, applied local pressure and bandages to the puncture site of the operated limb for 6 h, and applied brakes for 6–8 h to keep the patient's hip joint straight. At the same time, the patient was instructed to perform an ankle pump exercise or massage the punctured side of the limb once every 2 hours.

2.2.2. Test Group. Patients underwent cerebral angiography via radial artery access (TRA) puncture, and postoperative puncture sites were given elastic bandages (manufacturing license number: State Armament No. 20170241) for circumferential bandaging, and all patients were bandaged by the same physician. After returning to the ward after the operation, the doctor and nurse in charge of this patient performed bedside preaching, instructed precautions and physical activity patterns, local pressure bandaging of the punctured limb on the operation side for 6–8 hours, wrist braking for 6 hours, and unrestricted joints of the other limbs for 2 hours in bed.

2.2.3. Postoperative Care Measures for Appropriate Complications. (1) Subcutaneous hematoma: The most common postoperative complication is mainly due to factors such as improper hemostatic methods or the patient's coagulation dysfunction. In addition to closely monitoring the patient's heart rate and blood pressure, the patient should be promptly and effectively treated for the tightness of the dressing, and the patient should be instructed to do effective care in daily life to avoid unnecessary bleeding. (2) Arterial thrombosis: Once the patient has a lower extremity temperature drop, numbness, pain, and other conditions, the possibility of arterial thrombosis is higher. Therefore, care should be taken to maintain the appropriate tightness of the bandage and closely monitor the color and temperature of

the patient's limbs to effectively avoid the appearance of arterial thrombosis. (3) Urinary retention: A common complication is mainly caused by factors such as sudden changes in living habits or changes in emotions. Should pay attention to helping patients relieve bad psychological emotions in a timely manner and guide patients to carry out effective measures such as bed urination to help them deal with urinary retention in a timely manner.

2.3. Evaluation Indexes

2.3.1. Incidence of Postoperative Puncture Site Bleeding. Incidence of postoperative puncture point bleeding = total number of cases of postoperative puncture point bleeding/total number of postoperative cases $(40) \times 100\%$. Postoperative puncture site bleeding can be divided into the following four conditions: (1) local bruising at the puncture site, mainly manifested as skin bruising with or without hard nodules around the puncture site; (2) local bleeding at the puncture site, manifested as blood oozing from the puncture site, around the balloon compression pad or on the dressing; (3) local hematoma at the puncture site, visible to the naked eye or local palpable hard nodules at the puncture site with a diameter >5 cm; (4) DSA and ultrasound imaging data in the presence of pseudoaneurysm are preferable.

2.3.2. Time to First Postoperative Voiding and Incidence of Urinary Retention. Time of first urination refers to the time of first urination starting after the patient returns to the ward after surgery; urinary retention refers to the accumulation of a large amount of urine in the bladder that cannot be excreted by itself, which is mainly based on the patient's complaints and the doctor's percussion to initially determine whether urinary retention has occurred, and then determined by bedside ultrasonography.

2.3.3. Changes in Postoperative Comfort. The General Comfort Questionnaire (GCQ) was developed by Kolcabas, an American comfort care specialist, to assess patients' comfort in postoperative bed rest, and consists of 4 physical, psychospiritual, environmental, and sociocultural dimensions and 28 items. The scale uses a Likert scale from 1 to 4, with 1 being "strongly disagree" and 4 being "strongly agree." The higher the total score obtained, the higher the comfort level obtained by the patient. In 2006, the study [13] translated the scale into Chinese and tested its reliability, adding 2 items to the sociocultural dimensions to form a 30-item Chinese version of the GCQ. The Cronbach content of the Chinese version of the GCQ was also validated, with a validity of 0.86 and a coefficient of 0.92, which has high reliability and validity [14].

2.4. Efficacy Criteria. Use the homemade nursing satisfaction questionnaire to investigate the patient's satisfaction with nursing care using a self-made nursing satisfaction questionnaire, and the score is a percentage system. The higher the score, the higher the degree of satisfaction.

2.5. Data Collection. In accordance with the study design and process, study-trained, permanent staff conducted an informed script with patients who met the criteria and collected the required information after obtaining consent.

2.6. Statistical Methods. The collected data were entered into Excel by the double entry method, and then, the data in Excel were imported into SAS version 9.4 software for statistical analysis. The measurement data in this study were expressed as mean ± standard deviation, and the comparison of relevant data between groups was analyzed by the t-test, and the $P < 0.05$ between the two groups was statistically significant.

3. Results

3.1. Comparison of General Information between the Two Groups. During the implementation of this study, there were no lost cases or dropped cases in both groups, and there was no statistically significant comparison between the two groups in terms of general information ($P > 0.05$) (Table 1).

3.2. Comparison of Each Other Evaluation Index between the Two Groups

3.2.1. Comparison of Postoperative Puncture Site Bleeding, Time to First Voiding, Urinary Retention, and GCQ. The (Table 2) incidence of complications in the two groups was significantly lower in the observation group than in the control group, and the data comparison was statistically significant ($P < 0.05$), as given in Table 2.

3.3. Nursing Satisfaction Statistics of Patients in Both Groups. The nursing satisfaction statistics of patients in the control group was 70.00% (28/40), which was much lower than the nursing satisfaction of 95.00% (38/40) of patients in the observation group, and the empirical evidence was statistically significant ($\chi^2 = 9.680$, $P < 0.05$).

4. Discussion

Cerebrovascular diseases, including cerebral atherosclerosis, cerebral artery injury, cerebral aneurysm, and cerebral arteriovenous fistula, account for 25–50% of neurological hospitalizations. DSA is the gold standard for the diagnosis of cerebrovascular disease and the basis for neurointerventional treatment, and specialized care with evidence-based medicine is increasingly important [15]. In this retrospective case-control study, the compliance rate of patients in the control group with high procedural compliance was lower than that in the intervention group, and the compliance rate of patients with low compliance was higher than that in the intervention group. The differences were statistically significant.

4.1. TRA Performed Cerebral Angiography Reduces the Rate of Bleeding at the Puncture Site. The study [15] reported that "radial artery occlusion and spasm, bleeding and hematoma, and vagal reflexes may occur after neurointerventional

Table 1: Comparison of general information between the two groups' cases (percentage, %).

Projects	Test group ($n = 40$)	Control group ($n = 40$)	Statistical values	P
Gender			0.808^{2}	0.369
Male	20 (50)	24 (60)		
Female	20 (50)	16 (40)		
Age (years)	63.75 ± 8.51	62.67 ± 9.44	0.53^{1}	0.594
Education level	—	—	0.115^{2}	0.990
Elementary school and below	5 (12.5)	6 (15)		
Middle school				
High school or junior college	21 (52.5)	20 (50)		
College and above	6 (15)	6 (15)		
Marital status				
Unmarried	8 (20)	8 (20)		
Married			1.753^{2}	0.416
Divorced or widowed	0 (0)	1 (2.5)		
Prothrombin time (sec)	32 (80)	34 (85)		
Platelets (10^{9}/L)	8 (20)	5 (12.5)		
Duration of surgery (minutes)				
1-hour postoperative intake (ml)	11.56 ± 1.15	11.45 ± 1.28	-0.38^{1}	0.702
	229.2 ± 41.67	241.3 ± 53.51	-1.13^{1}	0.263
2-hour postoperative intake (ml)	38.47 ± 7.69	38.27 ± 7.50	0.12^{1}	0.906
	243.8 ± 93.6	260 ± 103.7	-0.74^{1}	0.464
4-hour postoperative intake (ml)	520.8 ± 132.2	504.3 ± 144.1	0.53^{1}	0.595
	953.5 ± 198.6	965 ± 194.2	$-0.26^{1)}$	0.794

Note. 1): t-value; 2)χ^2-value.

Table 2: Comparison of postoperative puncture site bleeding, urinary retention, and GCQ scores between the two groups.

Group	Number of examples	Bleeding from puncture site with or without		First urination Time (minutes)	Urinary retention with or without		GCQ score
Test group	40	1 (2.5)	39 (97.5)	62.47 ± 15.24	0	40	70.65 ± 7.66
Control group	40	6 (15)	34 (85)	85.97 ± 32.88	6	34	61.45 ± 8.72
χ^2		3.914		-4.1^{1}	6.486[2]		5.01^{1}
P		0.048		0.0001	0.011		<0.0001

Note. 1): t-value; 2)χ^2-value.

treatment of TRA." The results of this study showed that the incidence of bleeding at the puncture site via TRA in the test group was 2.5% (1 case), but there were no complications such as radial artery spasm and occlusion and vagal reflexes, which is similar to the low incidence of complications (2.9%) of neurointerventional treatment via TRA in the study of the literature [7]. The incidence of puncture site bleeding was 12.5% lower in the trial group compared to the control group, and the difference between the two groups was statistically significant, with P values < 0.05 in both groups. However, P values > 0.05 for prothrombin time, platelets, and procedure time were not statistically significant in both groups. In addition, the TRA route has requirements for the surgeon and needs to be performed by a physician with some experience in the intervention and mastery of the technique.

4.2. TRA Cerebral Angiography Can Reduce the Incidence of Postoperative Urinary Retention. After transcatheter femoral artery puncture, patients are required to lie flat and the surgical limb is braked. A large proportion of patients have urinary retention due to various reasons such as long-term bed rest without changing position, pain at the puncture site, fear of bleeding from the puncture site, more unaccustomed to urination in bed, and anxiety and tension. After transcatheter radial artery puncture, local pressure dressing for 6–8 h, wrist braking for 6 h, and other limb joints of the extremities are not restricted, the time to get out of bed is 2 h later. This is similar to the results of the literature [16, 17] in which cerebral angiography through TRA was performed with a time to get out of the bed of 1.9. The shortened bedtime eliminated patients' concerns about bleeding at the puncture site and relieved their anxiety and tension, thus shortening the time to first postoperative urination and reducing the occurrence of urinary retention to a greater extent. In this study, the time to first postoperative urination was significantly better in the test group patients (62.47) than in the control group patients (85.97), with $P < 0.05$ for the two groups; there were 0 cases of urinary retention in the test group patients and 6 cases in the control group patients, with a statistically significant difference between the two groups, with P value < 0.05.

4.3. TRA Performed Cerebral Angiography Can Improve Patients' Comfort. Studies [2, 18] have shown that shortening bed rest and surgical limb braking time after total cerebral angiography helps improve patients' discomfort status and improve their postoperative hospital comfort, which greatly facilitates their recovery. The results of this pilot study showed that the test group was better than the control group in terms of GCQ scores (P value < 0.05), and the difference between the two groups was statistically significant.

Compared with the traditional transfemoral route, the success rate of puncture is relatively low, but it has the advantages of high safety, low postoperative bleeding complications, no combined application of active anticoagulation therapy, no bed rest, and shortened hospital stay, which are gradually being implemented in major hospitals [19, 20]. With the improvement of puncture technique and the popularization of medical devices, it has become one of the main ways of coronary angiography and interventional procedures [21, 22].

The main reasons for unsuccessful procedures are puncture failure and radial artery spasms. Multiple punctures can cause a loss of operator confidence and also lead to radial artery spasms [23, 24]. The highest failure rate of transradial artery surgery in small elderly women has been reported in the literature, which may be related to the small size of the radial artery and its susceptibility to spasms [25, 26]. Therefore, it is proposed that small elderly women are a relative contraindication to transradial artery surgery. In addition, the absence of radial artery pulsation, positive Allen's test, arteriovenous fistulae on renal dialysis, and treatment with sheaths of 8F or more are absolute contraindications. Patients with good radial artery pulsation and a negative Allen test should be selected.

Most of the operations are performed on the right side of the patient, using the right radial artery for puncture. In our department, the left pedal vein is mostly chosen as the venous access, and after two years of practice, it has been proved that the left pedal vein is superior to other parts of the venous access. The left pedal vein is far away from the surgical area, so changing the infusion does not affect the surgical operation. Intraoperative blood pressure monitoring also does not affect the infusion rate of the left foot vein.

Improving puncture technique and preventing radial artery spasms can improve the success rate of surgery. Preoperative elimination of patient tension, selection of patient-appropriate instruments, improvement of the first puncture success rate, injection of vasodilators via the radial artery, selection of small-sized catheters whenever possible, and gentle handling are all keys to successful surgery.

5. Conclusions

The rate of bleeding and urinary retention at the puncture site of transradial access puncture is lower than that of femoral access puncture during cerebral angiography, and the time to first urination of the patient after the procedure is significantly shorter, while the comfort of the patient after the procedure is improved to a greater extent, with excellent clinical results.

Data Availability

The experimental data used to support the findings of this study are available from the corresponding author upon request.

Conflicts of Interest

The authors declare that they have no conflicts of interest.

References

[1] T. W. Rooke, A. T. Hirsch, S. Misra et al., "2011 ACCF/AHA focused update of the guideline for the management of patients with peripheral artery disease (updating the 2005 guideline) a report of the American college of cardiology foundation/American heart association task force on practice guidelines," *Journal of the American College of Cardiology*, vol. 58, no. 19, pp. 2020–2045, 2011.

[2] A. A. Kolkailah, R. S. Alreshq, A. M. Muhammed, M. E. Zahran, M. A. El-Wegoud, and A. F. Nabhan, "Transradial versus transfemoral approach for diagnostic coronary angiography and percutaneous coronary intervention in people with coronary artery disease," *Cochrane Database of Systematic Reviews*, vol. 4, Article ID D12318, 2018.

[3] B. D. Braithwaite and W. J. Quiñones-Baldrich, "Lower limb intraarterial thrombolysis as an adjunct to the management of arterial and graft occlusions," *World Journal of Surgery*, vol. 20, no. 6, pp. 649–654, 1996.

[4] M. Hamon, C. Pristipino, C. Di Mario et al., "Consensus document on the radial approach in percutaneous cardiovascular interventions: position paper by the European Association of Percutaneous Cardiovascular Interventions and Working Groups on Acute Cardiac Care and Thrombosis of the European Society of Cardiology," *EuroIntervention*, vol. 8, no. 11, pp. 1242–51, 2013.

[5] L. You and L. Zhang, "Nursing study on wound management after transradial coronary intervention," *Electronic Journal of Practical Clinical Nursing*, vol. 2, no. 37, pp. 116-117, 2017.

[6] W. Yoon, H. Kim, Y. W. Kim, S. R. Kim, and I. S. Park, "Usefulness and stability of intraoperative digital subtraction angiography using the transradial route in arteriovenous malformation surgery," *World Neurosurgery*, vol. 111, pp. e799–e805, 2018.

[7] K. C. Joshi, A. Beer-Furlan, R. W. Crowley, M. Chen, and S. A. Munich, "Transradial approach for neurointerventions: a systematic review of the literature," *Journal of Neurointerventional Surgery*, vol. 12, no. 9, pp. 886–892, 2020.

[8] Z. B. She, S. H. Wang, and Z. Q. Qu, "Clinical analysis of whole brain angiography via distal radial artery route," *Chinese Journal of Practical Neurological Diseases*, vol. 23, no. 10, pp. 863–866, 2020.

[9] C. H. Li, C. C. Li, C. L. Lu, J. S. Wu, L. J. E. Ku, and C. Y. Li, "Urban-rural disparity in lower extremities amputation in patients with diabetes after nearly two decades of universal health Insurance in Taiwan," *BMC Public Health*, vol. 20, no. 1, pp. 212–215, 2020.

[10] I. Dato, F. Burzotta, C. Trani, F. Crea, and G. P. Ussia, "Percutaneous management of vascular access in transfemoral

Hindawi
Emergency Medicine International
Volume 2023, Article ID 9786387, 1 page
https://doi.org/10.1155/2023/9786387

Retraction

Retracted: Application Value of Management Model Based on "Zero Tolerance" Concept in Pressure Ulcer Management

Emergency Medicine International

Received 28 November 2023; Accepted 28 November 2023; Published 29 November 2023

This article has been retracted by Hindawi, as publisher, following an investigation undertaken by the publisher [1]. This investigation has uncovered evidence of systematic manipulation of the publication and peer-review process. We cannot, therefore, vouch for the reliability or integrity of this article.

Please note that this notice is intended solely to alert readers that the peer-review process of this article has been compromised.

Wiley and Hindawi regret that the usual quality checks did not identify these issues before publication and have since put additional measures in place to safeguard research integrity.

We wish to credit our Research Integrity and Research Publishing teams and anonymous and named external researchers and research integrity experts for contributing to this investigation.

The corresponding author, as the representative of all authors, has been given the opportunity to register their agreement or disagreement to this retraction. We have kept a record of any response received.

References

[1] Y. Liu, C. Zhou, N. Li, and X. Gong, "Application Value of Management Model Based on "Zero Tolerance" Concept in Pressure Ulcer Management," *Emergency Medicine International*, vol. 2022, Article ID 6792584, 6 pages, 2022.

Hindawi
Emergency Medicine International
Volume 2022, Article ID 6792584, 6 pages
https://doi.org/10.1155/2022/6792584

Research Article

Application Value of Management Model Based on "Zero Tolerance" Concept in Pressure Ulcer Management

Yufei Liu,[1] Changming Zhou,[1] Nan Li,[2] and Xiaoxue Gong[2]

[1]*Department of Emergency Intensive Care, The Second Hospital of Dalian Medical University, Dalian 116023, Liaoning, China*
[2]*Department of Invasive Technology, The Second Hospital of Dalian Medical University, Dalian 116023, Liaoning, China*

Correspondence should be addressed to Xiaoxue Gong; sunny367@126.com

Received 8 August 2022; Revised 14 September 2022; Accepted 28 September 2022; Published 10 October 2022

Academic Editor: Hang Chen

Background. Pressure injuries are the most prevalent health problem worldwide. Improving the quality of hospital pressure injury management is an important indicator to improve the quality of hospital management. *Objective*. To explore the application value of the management model centered on the concept of "zero tolerance" in the management of pressure ulcers (PU). *Methods*. The effects of conventional management mode and management mode centered on the concept of "zero tolerance" on PU patients and nursing staff were retrospectively analyzed. The patients were evaluated by the general comfort questionnaire (GCQ), Generic Quality of Life Inventory 74 (GQOL-74), and pressure ulcer healing scale (PUSH). At the same time, the satisfaction of PU patients and nursing staff with different management modes was investigated. *Results*. When comparing the conditions of patients under different management modes, it was found that the "zero tolerance" management mode can improve the comfort and quality of life of patients during hospitalization. Compared with the conventional management mode, the "zero tolerance" management mode can significantly improve the degree of pressure ulcer healing in patients. In addition, the "zero tolerance" management model can not only improve the satisfaction of patients with management but also improve the satisfaction of nursing staff with management. *Conclusion*. Standardized management of PU patients with the concept of "zero tolerance" as the core can improve the health status and quality of life of patients, promote wound healing, and improve the satisfaction of patients and nurses with the management plan.

1. Introduction

Pressure ulcers (PUs), formerly known as pressure injury (PI), refer to localized damage to the skin or subcutaneous tissue caused by pressure combined with shearing force, usually occurring at the bony prominence [1–3]. PU is the most prevalent health problem worldwide and has been designated by several countries as one of the most important sentinel events in healthcare [4, 5]. The place where PU occurs is uncertain, and it can occur outside the hospital, after admission, or even during transport. Pressure injury has the characteristics of long cycle, high cost and serious consequences, and has caused adverse effects on patients, patient families, medical institutions, and society [6–8].

From the patient's perspective, PU can cause pain, both during dressing changes and at rest. It has been reported that more than 65 percent of patients with PU report that pain from pressure injury has had a severe adverse effect on their daily living, mobility, and sleep [9, 10]. In addition, about 30% of PU patients have experienced emotional problems such as self-isolation, social fear, and low self-esteem due to the disordered image of patients caused by PU [11, 12]. If the pressure injury is not taken timely and effective care measures, it will lead to a series of complications such as bacterial infection and osteomyelitis. This is not only detrimental to wound healing but also can cause sepsis or cancer due to secondary infection, which is life-threatening [13, 14]. From the perspective of the patient's family, most pressure injury patients lack self-care ability due to limited activities, and their wound healing cycle is long. In addition, a patient's pressure injury imposes a significant financial cost on the family, including moist healing dressings, stress reduction

equipment, new technologies and therapies, and nutritional supplements. From the perspective of medical institutions and society, stress injuries not only increase the workload of nurses in medical institutions by nearly 50% but also bring enormous economic pressure to the health care system and society [15]. In view of this, the prevention of pressure injury has become the focus of clinical nursing work, and the management of PU has also become an important part of contemporary hospital management.

"Zero tolerance" means zero and no tolerance for errors or potential pitfalls. It is the essence of the "Broken Window Theory" proposed by American political scientist James Wilson and criminologist George Kaelin [16]. The "zero tolerance" management concept tells us that small incidents and small details that are easily overlooked may lead to some major problems and should be prevented at the beginning of the incident to avoid bad hinting effects or blind obedience [17]. When implementing "zero tolerance," it is necessary to effectively unify "prevention" and "governance," nip the signs of violations in the bud, and improve the quality of management. The "zero tolerance" management concept is often used in the management of large industrial enterprises and is less used in medicine. This study aims to explore the application effect of the concept of "zero tolerance" in pressure injury management and provides guidance for improving the quality of pressure injury management in hospitals.

2. Materials and Methods

2.1. General Information. The clinical data of patients hospitalized in our hospital from January 2018 to December 2021 were retrospectively analyzed. Among them, our hospital implemented the conventional management model from January 2018 to December 2019 and implemented the "zero tolerance" management model from January 2020 to December 2021. The inclusion criteria of the PU patients are as follows: (1) should meet the relevant diagnostic criteria for pressure injury; (2) be awake and have the ability to communicate and communicate independently; and (3) should have complete clinical data required for this study. Exclusion criteria are as follows: (1) with contraindications to turning over; (2) transferred to hospital during treatment; (3) with mental illness; and (4) with severe skin disease or extensive skin ulceration.

Among the final included research subjects, 175 cases received the conventional management mode (referred to as the conventional group), and 180 cases received the "zero tolerance" management mode (referred to as the innovative group). The general data of patients under different management modes are shown in Table 1. After statistical analysis, it was found that the data of the two groups were balanced and comparable. In addition, the basic situation of nursing staff under different management modes was counted, including 68 nursing staff in the period of implementing the conventional management mode and 72 nursing staff in the period of implementing the "zero tolerance" management mode. After comparative analysis, it was found that the baseline data of nurses under different management modes were also balanced and comparable, as shown in Table 2. It is worth noting that the sample size of the conventional group and the innovative group in this study is slightly different because this study is a retrospective analysis and collected actual patients and nursing staff in our hospital. Although the sample sizes of the two groups were slightly different, the differences were small, and the baseline data of the two groups were balanced and comparable (Tables 1 and 2). Therefore, small differences in sample size do not affect the experimental results.

2.2. Management Plan. Routine management mode is as follows: (1) nursing staff inform patients and their families about pressure injury; (2) patients follow doctor's orders to cooperate with physicians in pressure injury treatment and care; (3) pay attention to changes in patients' physical signs and wound healing; (4) keep the ward environment clean and the beds clean and tidy, and regularly assist patients to turn over and change their clothes; (5) instruct patients to eat scientifically, and inform their family members of daily nursing precautions.

Management model based on the concept of "zero tolerance." The specific contents of the "zero tolerance" management model are as follows: (1) to train the nurses in the department on the "zero tolerance" management concept and to evaluate the participants. Promote the training staff to pay attention to the management of stress injury and enhance the initiative of management. (2) Through regular inspections and special personnel responsibility system, we can timely find out the bad phenomena in the management. Medical staff should formulate measures and intervene in time for potential risk factors, and never let go of any adverse phenomena that may cause management problems. Hospital managers should also pay enough attention to accidental adverse phenomena and minor faults to ensure timely elimination of potential hidden dangers. (3) The problems in nursing work should be recorded and analyzed in time, and relevant meetings should be organized to discuss the reasons for the problems. Based on the results of the analysis, we will improve the management of pressure injury, scientifically optimize the management process, and constantly update the management standards. (4) For possible serious situations, an emergency response plan should be formulated in advance, and the emergency response plan should be exercised in advance to ensure the nursing staff's ability to deal with emergencies. (5) Strengthen the effective management of pressure injury through continuous improvement of management measures, improve the management awareness of relevant nursing staff, and ensure the quality of nursing.

2.3. Observation Indicators. (1) The comfort state of the patients was assessed by the general comfort questionnaire [18] (GCQ). The GCQ includes 4 dimensions of physiology, psychology, spirit, social culture, and environment, with a total of 28 items (10 positive rating items and 18 negative rating items). All items were scored using a 4-level scoring method, with a total score ranging from 4 to 112, with higher scores indicating higher comfort. (2) Generic Quality of Life Inventory 74 [19] (GQOL-74) was used to assess the quality of life of patients. GQOL-74 has a total of 74 items, and it

Table 1: Comparison of general data of patients under different management modes.

Factor	Conventional ($n = 175$)	Innovative ($n = 180$)	χ^2/t	P
Gender			0.168	0.682
Male	101 (57.71)	100 (55.56)		
Female	74 (42.29)	80 (44.44)		
Age (years)	64.28 ± 5.16	65.31 ± 5.49	1.820	0.069
BMI (kg/m^2)	25.26 ± 1.12	25.09 ± 1.08	1.456	0.146
Staging of pressure injuries			1.725	0.631
I	58 (33.14)	66 (36.67)		
II	41 (23.43)	35 (19.44)		
III	39 (22.29)	46 (25.56)		
IV	37 (21.14)	33 (18.33)		

Table 2: Comparison of general data of nursing staff under different management modes.

Factor	Conventional ($n = 68$)	Innovative ($n = 72$)	χ^2/t	P
Gender			0.501	0.419
Male	7 (10.29)	5 (6.94)		
Female	61 (34.86)	67 (93.06)		
Age (years)	28.16 ± 3.19	27.62 ± 3.47	0.957	0.340
Education level			0.654	0.419
College	36 (52.94)	43 (59.72)		
Undergraduate and above	32 (18.29)	29 (40.28)		
Job title			0.914	0.339
Primary	45 (66.18)	42 (58.33)		
Intermediate and above	23 (13.14)	30 (41.67)		

evaluates the health-related quality of life of the respondents from four dimensions: physical function, psychological function, social function, and material life status. Each functional dimension score and total score of GQOL-74 were converted into a range of 0 to 100, with higher scores indicating better quality of life. (3) The pressure ulcer healing score scale [20] (PUSH) was used to evaluate and compare the management effect of the two groups of patients. The PUSH scale can comprehensively evaluate the pressure injury of PU patients from the area of pressure ulcer, the amount of exudate, and the type of wound tissue. The total score of PUSH scale ranges from 0 to 17, with lower scores indicating better wound healing in PU patients. (4) Self-made satisfaction scale was used to evaluate the satisfaction of patients and nurses with the management plan. The satisfaction level is divided into four levels: very satisfied, relatively satisfied, basically satisfied, and not very satisfied.

2.4. Statistical Analysis. The data of this study were analyzed using SPSS 25 and GraphPad 8.3 statistical software. Quantitative data conforming to a normal distribution were expressed as ($\overline{x} \pm s$), and differences between groups were tested by t-test. Categorical data were represented by n (%), χ^2 test was used for comparison between two groups, and rank sum test was used for rank data. The comparison of all data indicated that the difference was significant at $P < 0.05$.

3. Results

3.1. Comparison of GCQ Scores. When comparing the GCQ scores of patients under different management modes, it was found that after the intervention, the GCQ scores of patients who received different management modes were improved compared with those at the time of admission. Also, the GCQ scores of patients who received "zero tolerance" management were greatly higher than those of patients who received the conventional management ($P < 0.05$). The detailed data are shown in Table 3, and these results suggest that a management model based on the concept of "zero tolerance" can help improve the comfort of PU patients during hospitalization.

3.2. Comparison of GQOL-74 Scores. When comparing the GQOL-74 scores of patients under different management modes, it was found that after intervention, the GQOL-74 scores of patients who received different management modes were improved compared with those at admission. Also, the GQOL-74 scores of patients who received the "zero tolerance" management were greatly higher than those of patients who received routine management ($P < 0.05$). Detailed data are shown in Table 4, and these results suggest that a management model based on the concept of "zero tolerance" can help improve the quality of life of PU patients.

3.3. Comparing the Management Effects of Different Management Modes on Patients. The management effect of different management modes on PU patients was evaluated by the pressure ulcer healing score scale. As shown in Table 5 and Figure 1, after one week of intervention, the PUSH scores of patients who received the "zero tolerance" concept management were greatly lower than those who received conventional management ($P < 0.05$). After 2 weeks of intervention, the PUSH scores of the two groups of patients continued to decline, and the change trend was the same as that after 1 week of intervention.

Table 3: Comparison of GCQ scores.

Group	n	Before intervention	After intervention	t	P
Conventional	175	65.15 ± 9.16	76.92 ± 8.33	12.580	<0.001
Innovative	180	64.33 ± 10.09	85.17 ± 7.79	21.930	<0.001
t		0.801	9.641		
P		0.424	<0.001		

Table 4: Comparison of GQOL-74 scores.

Group	n	Before intervention	After intervention	t	P
Conventional	175	57.61 ± 5.17	66.90 ± 6.31	15.070	<0.001
Innovative	180	56.92 ± 5.63	72.65 ± 6.99	23.510	<0.001
t		1.202	8.128		
P		0.230	<0.001		

Table 5: Comparison of management effects.

Group	n	Before intervention	After 1 week of intervention	After 2 weeks of intervention
Conventional	175	11.67 ± 2.48	10.16 ± 2.16	9.42 ± 1.86
Innovative	180	11.32 ± 2.51	9.58 ± 2.08	8.13 ± 1.65
t		1.321	2.577	6.917
P		0.187	0.010	<0.001

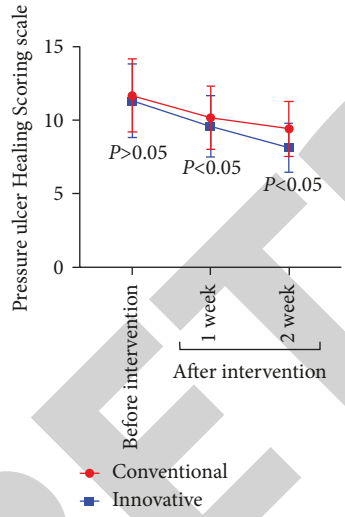

Figure 1: Comparison of management effects.

3.4. Patient and Caregiver Satisfaction with the Management Program. Investigate the degree of satisfaction of patients with the management plan under different management modes. After comparison, the satisfaction of the two groups of patients with the management plan under different management modes was evaluated ($Z = -2.501$, $P = 0.012$). Among them, "zero tolerance" management patients had greatly higher rates of very high satisfaction than those who received conventional management, as shown in Table 6.

Investigate the satisfaction degree of nursing staff to the management scheme under different management modes. After comparison, the satisfaction of the two groups of nursing staff with the management scheme under different management modes was evaluated ($Z = -1.987$, $P = 0.047$). Nurses under the "zero tolerance" management mode were greatly more satisfied with the management scheme than those under the conventional management mode, see Table 7.

4. Discussion

The multiple hazards brought about by pressure injuries alert clinical medical workers to prevent the occurrence of pressure injuries. However, in clinical practice, most patients bring pressure injuries outside the hospital [21]. Patients with prehospital pressure injuries were more likely to have their condition worsened due to lower levels of self-management. Therefore, effective management of patients with existing pressure injuries on admission has become the focus of clinicians. In the management of PU patients, there are many factors that lead to the deterioration of the patient's condition or poor treatment effect, and it is necessary to explore and optimize the entire management process [22]. In the process of improper management, there is not only a lack of staff's sense of responsibility and management awareness but also a lack of patients' own awareness of the disease. These are the hidden dangers of effective management of PU patients and also the reasons for the poor treatment effect of patients. In the management of PU patients, a little management negligence may bring about huge problems in management. If the management process optimization and details are not strengthened, it is easy to cause the patient's condition to deteriorate and cause unnecessary doctor-patient disputes.

In this study, the "zero tolerance" management concept was introduced into the management of PU patients, and the management process of "nursing staff training, hidden danger inspection, cause analysis, development of plans, and improvement plans" was strictly implemented. Adhering to the concept of "zero tolerance" in the implementation

Table 6: Comparison of patient satisfaction with different management programs.

Group	n	Very satisfied	Relatively satisfied	Basically satisfied	Not so satisfied
Conventional	175	81 (46.29)	53 (30.29)	33 (18.86)	8 (4.57)
Innovative	180	101 (56.11)	59 (32.78)	15 (8.33)	5 (2.78)
Z			−2.501		
P			0.012		

Table 7: Comparison of nursing staff's satisfaction with different management programs.

Group	n	Very satisfied	Relatively satisfied	Basically satisfied	Not so satisfied
Conventional	68	33 (48.53)	14 (20.59)	12 (17.65)	9 (13.24)
Innovative	72	45 (62.50)	16 (22.22)	6 (8.33)	5 (6.94)
Z			−1.987		
P			0.047		

process, on the one hand, it can improve the self-discipline of nursing staff and avoid adverse events caused by the negligence of nursing staff. On the other hand, it can also enhance the responsibility of the nursing staff and improve the quality of care for PU patients. This study found that under the management model based on the "zero tolerance" concept, the health status, quality of life, and wound healing of PU patients were significantly improved. As a new management model, the management model based on the concept of "zero tolerance" is an extension and optimization of traditional management. It can find out the problems in the nursing process in time, and through discussion and analysis, so as to obtain the solution to the problem. In addition, the management model based on the concept of "zero tolerance" emphasizes continuous improvement of nursing management. That is, from problem finding to problem solving, a periodic method of finding and solving problems is formed, thereby improving the quality of care.

The results of this study showed that after the implementation of the management model based on the "zero tolerance" concept, the satisfaction of both patients and nurses was significantly improved. This study believes that nursing satisfaction is an important content in the evaluation of nursing quality and hospital management quality. Scholars such as Alıcı [23] also indicated in their studies that individualized nursing satisfaction affects the quality of life of patients with the same results. In addition, scholars such as Gniadek [24] also believe that satisfaction with nursing can check the quality of medical services. It is worth noting that after the implementation of the management model based on the concept of "zero tolerance," not only the satisfaction of patients with management has been significantly improved but also the satisfaction of nursing staff with the management plan. Nursing staff has high satisfaction with the management plan, which not only helps to improve the quality of nursing care for patients but also helps to improve the service quality of the whole hospital.

5. Conclusion

In this study, the application of "zero tolerance" management concept in the management of PU patients can significantly improve the health status of PU patients and promote the healing of patients' wounds. In addition, management programs based on the concept of "zero tolerance" can also improve the satisfaction of patients and caregivers with management work. Therefore, we believe that standardized management of patients with pressure injury based on the concept of "zero tolerance" can improve the health status and quality of life of patients, promote wound healing, and improve the satisfaction of patients and nursing staff with the management program.

Data Availability

The data used to support the findings of this study are available from the corresponding author upon request.

Conflicts of Interest

The authors declare that there are no conflicts of interest.

References

[1] A. S. Sumarno, "Pressure ulcers: the core, care and cure approach," *British Journal of Community Nursing*, vol. 24, no. Sup12, pp. S38–S42, 2019.

[2] A. Mitchell, "Adult pressure area care: preventing pressure ulcers," *British Journal of Nursing*, vol. 27, no. 18, pp. 1050–1052, 2018.

[3] P. Avsar, Z. Moore, D. Patton, T. O'Connor, A. M. Budri, and L. Nugent, "Repositioning for preventing pressure ulcers: a systematic review and meta-analysis," *Journal of Wound Care*, vol. 29, no. 9, pp. 496–508, 2020.

[4] X. Zhang, N. Zhu, Z. Li, X. Xie, T. Liu, and G. Ouyang, "The global burden of decubitus ulcers from 1990 to 2019," *Scientific Reports*, vol. 11, no. 1, Article ID 21750, 2021.

[5] U. Anaba-Wright and J. Kefas, "Reducing pressure ulcers in care homes in Barnet: a quality improvement project," *British Journal of Community Nursing*, vol. 25, no. Sup9, pp. S33–S37, 2020.

[6] E. Jaul, J. Barron, J. P. Rosenzweig, and J. Menczel, "An overview of co-morbidities and the development of pressure ulcers among older adults," *BMC Geriatrics*, vol. 18, no. 1, p. 305, 2018.

[7] J. S. Mervis and T. J. Phillips, "Pressure ulcers: pathophysiology, epidemiology, risk factors, and presentation," *Journal of the American Academy of Dermatology*, vol. 81, no. 4, pp. 881–890, 2019.

Hindawi
Emergency Medicine International
Volume 2023, Article ID 9840485, 1 page
https://doi.org/10.1155/2023/9840485

Retraction

Retracted: *C*-Reactive Protein, Procalcitonin, and a Novel Pathogenesis and Therapeutic Target of Thrombocytopenia in Sepsis

Emergency Medicine International

Received 28 November 2023; Accepted 28 November 2023; Published 29 November 2023

This article has been retracted by Hindawi, as publisher, following an investigation undertaken by the publisher [1]. This investigation has uncovered evidence of systematic manipulation of the publication and peer-review process. We cannot, therefore, vouch for the reliability or integrity of this article.

Please note that this notice is intended solely to alert readers that the peer-review process of this article has been compromised.

Wiley and Hindawi regret that the usual quality checks did not identify these issues before publication and have since put additional measures in place to safeguard research integrity.

We wish to credit our Research Integrity and Research Publishing teams and anonymous and named external researchers and research integrity experts for contributing to this investigation.

The corresponding author, as the representative of all authors, has been given the opportunity to register their agreement or disagreement to this retraction. We have kept a record of any response received.

References

[1] J. Li, L. Hu, and L. Li, "*C*-Reactive Protein, Procalcitonin, and a Novel Pathogenesis and Therapeutic Target of Thrombocytopenia in Sepsis," *Emergency Medicine International*, vol. 2022, Article ID 2498435, 9 pages, 2022.

Hindawi
Emergency Medicine International
Volume 2022, Article ID 2498435, 9 pages
https://doi.org/10.1155/2022/2498435

Research Article

C-Reactive Protein, Procalcitonin, and a Novel Pathogenesis and Therapeutic Target of Thrombocytopenia in Sepsis

Jing Li, Lijuan Hu, and Lei Li

Department of Emergency, Shanxi Bethune Hospital, Taiyuan, China

Correspondence should be addressed to Lei Li; 100380@yzpc.edu.cn

Received 3 September 2022; Revised 23 September 2022; Accepted 29 September 2022; Published 8 October 2022

Academic Editor: Hang Chen

Objective. The aim of the study is to analyze the clinical characteristics, pathogen distribution, and drug sensitivity information of adult sepsis, and to provide reference for empirical clinical use; to explore the relationship between *C*-reactive protein (CRP) and calcitonin (PCT) The clinical value in the diagnosis of adult sepsis. *Methods*. We collected 455 cases of hospitalized patients with positive blood culture, including 352 cases with sepsis and 103 cases without sepsis; 1609 cases of hospitalized patients with suspected infection and negative blood culture, including 287 cases of sepsis, and 518 cases of non-infectious systemic inflammatory response syndrome (SIRS) and 804 cases of local infection. Age, gender, route of admission, admission status, CRP, PCT, and white blood cell (WBC) levels were collected from the patients. The differences between the factors were statistically analyzed, and the receiver operating characteristic curve (ROC curve) was plotted to obtain the optimal cut-off values of CRP and PCT and their area under the curve (AUC), and to compare the CRP, PCT and PCT, and the CRP + PCT tandem to diagnose sepsis sensitivity and specificity. *Results*. (1) 387 pathogenic strains were isolated from blood cultures of patients with sepsis, 71.06% Gram-negative, 26.87% Gram-positive and 2.07% fungi. (2) Among Gram-positive bacteria, *Staphylococcus aureus* was 87.5% resistant to penicillin and sensitive to vancomycin, milantropine, and teicoplanin; among Gram-negative bacteria, *Escherichia coli* was resistant to piracillin The resistance rate was 73.1%, fully susceptible to viraemia (100%) and resistant to imipenem, amikacin, and lacillin/tazole. (3) Among patients with positive blood cultures, CRP and PCT levels were higher in patients with sepsis than in those without sepsis. Pairwise comparison of ROC curves showed that the diagnostic value of PCT was greater than that of CRP ($P = 0.016$). *Conclusion*. CRP and PCT have a good reference value for diagnosis of sepsis patients and determination of the degree of infection in septic patients, especially PCT is more valuable for diagnosis of sepsis.

1. Introduction

Bacterial sepsis is an infectious disease that, if not controlled and treated in a timely manner, can develop into severe sepsis, posing a serious threat to the life and health of patients [1]. In recent years, the incidence of this disease has not only increased gradually but also the morbidity and mortality rate has become high, with 500,000 bacterial sepsis patients losing their lives worldwide every year [2]. A study [3] showed that the morbidity rate of sepsis patients in ICU was 8.68%, mortality rate was 44.7%, and the per capita medical cost was about $502/day. A study [4] found that mortality in patients with sepsis in the ICU has surpassed myocardial infarction as the leading cause. Although much research and progress has been made in recent years on its mechanisms and treatment, the mortality rate of sepsis remains high, reaching 20%–50% [5, 6]. Therefore, early and correct diagnosis and assessment of the severity of the disease, how to prevent the misuse of antibiotics and improve the prognosis of patients through individualized treatment are the focus of clinical research.

PCT, first proposed in 1984, is a pro-peptide substance of calcitonin, which is mainly produced by thyroid *C* cells under physiological conditions; it contains a protein of 116 amino acids with a molecular mass of 14.5 kD, and PCT has a half-life of 25–30 h in the blood [7, 8]. The study [9] found that the level of PCT correlates well with the severity of the infection, and the more severe the infection, the higher its level. It is generally considered that PCT levels less than 0.5 ug/L are within the normal range; PCT levels are greater

than 2 ug/L. Serum PCT levels are slightly higher when the body has a fungal infection or a parasitic infection, but are significantly higher in the case of non-bacterial infections. When the body is invaded by a virus, serum PCT levels generally do not increase. Therefore, PCT can be used for the differential diagnosis of bacterial or viral infections and provide some help in clinical treatment, but it cannot effectively identify bacterial infections or sepsis caused by nonbacterial infections [10].

CRP is a plasma protein produced by the liver and is considered to be a marker of inflammatory response. Studies [11, 12] first identified CRP as a substance that precipitates with C polysaccharide (CPS), a nonspecific bacterial polysaccharide component of *Streptococcus pneumoniae*, in the serum of patients with *Streptococcus pneumoniae*. Studies [13, 14] showed that its biological function may be to clear pathological substances or pathogens from the body by binding to phospholipid components of apoptotic and necrotic cells or invading bacteria, fungi, parasites and other pathogens and activating the complement and mononuclear phagocyte systems. Studies [15, 16] have shown that serum concentrations are below 10 mg/L in normal subjects, but in patients with severe infections or sepsis, CRP concentrations rise rapidly 6 hours after the onset of stimulation and reach a maximum within approximately 48 hours, with concentrations decreasing rapidly and returning to normal within 1 week, whereas concentrations do not increase in virally infected individuals, but this also provides an extremely important basis for determining the type of early infection The basis for this study was the following.

In this study, we included patients with negative and positive blood cultures, analyzed clinical data from patients with sepsis, compared the differences in CRP and PCT levels between patients, and investigated the role of these two indicators in the diagnosis of sepsis. Optimal threshold values were obtained, and the sensitivity and specificity of the indicators for the diagnosis of sepsis at the threshold values and the relationship between CRP and PCT levels and the severity of sepsis were analyzed.

2. Materials and Methods

2.1. Study Subjects and Groupings. Cases of blood culture-positive inpatients and suspected infectious, blood culture-negative inpatients admitted to our hospital from January 2015 to July 2021 were collected for retrospective analysis. The study population was divided into blood culture-positive sepsis, blood culture-positive non-septic, blood culture-negative sepsis, blood culture-negative non-infectious SIRS, and blood culture-negative localized infection (Table 1), according to the diagnostic criteria for sepsis established by the American Thoracic Society/American Academy of Critical Care Medicine consensus conference, and the diagnostic criteria for SIRS (Table 2).

2.2. Inclusion Criteria. The inclusion criteria were as follows:

(1) Hospitalized patients over 18 years old.

(2) The etiological data are complete.

(3) The disease course information recorded in medical records is complete.

2.3. Exclusion Criteria. The exclusion criteria were as follows:

(1) Have a hospitalization record and have used antibiotics 2 weeks before admission.

(2) Patients who have been included in study cohort with repeated admissions.

(3) Died or discharged within 24 hours after admission.

(4) Emergency biochemical and procalcitonin examinations were not performed.

2.4. Pathogen Detection and Drug Resistance Detection. 5 mL of fasting elbow venous blood was collected from all patients within 24 h after admission, placed in EDTA-Na anticoagulated EP tubes, centrifuged at 3 500 r/min for 10 min, and the serum was separated and placed at −70°C for measurement. The PCT level was measured by electrochemiluminescence with a Roche e411; the CRP level was measured by immunoturbidimetric method, and platelet-related parameters including platelet count (PLT), mean platelet volume (MPV), platelet distribution width (PDW), and large platelet ratio (P-LC) were measured by hematocrit analyzer in all patients after the onset of disease. *R*). All operations were performed in strict accordance with the standard instructions. After identification of the samples, drug sensitivity analysis was performed using the Beidou Phoenix IM-100 fully automated microbiological analysis system; some drug sensitivity tests were performed using the *K-B* method or MIC broth dilution method, and the results were judged according to the American Clinical Laboratory Standardization Institute (CLSI) standards, and the specific instruments and manufacturers are shown in Table 3.

2.5. Detection of CRP, PCT, and WBC. Samples for CRP, PCT, and WBC testing were obtained from fresh or during hospitalization of patients. CRP was detected by automatic biochemical analyzer Cobas C501-2; PCT was detected by automatic electrochemiluminescence immunoassay analyzer Cobas e601; WBC was detected by Sysmex XN-3000 automatic blood analyzer. The specific instruments and manufacturers are shown in Table 3.

3. Results

A total of 387 strains of pathogenic bacteria were isolated from blood culture of 352 patients, including 275 strains (71.06%) of gram-negative bacteria, 104 strains (26.87%) of gram-positive bacteria, and 8 strains of fungi (2.07%). The top three pathogenic bacteria with composition ratio are as follows: 134 strains (34.63%) of *Escherichia coli*, 79 strains (20.41%) of *Klebsiella pneumoniae* and 40 strains (10.34%) of *Staphylococcus aureus*. The distribution of pathogenic bacteria detected in blood cultures of 387 adult septic patients is shown in Table 4 and Figure 1.

Table 1: Grouping of study subjects and diagnostic criteria.

Grouping	Diagnostic criteria
Blood culture positive sepsis	Determination of SIRS caused by pathogen infection
Blood culture positive non sepsis	It was determined that pathogen infection did not cause SIRS
Blood culture negative sepsis	Sirs caused by suspected infection or local infection
Blood culture negative non infected SIRS	No evidence of infection and SIRS
Blood culture negative local infection	Etiology showed that local infection did not cause SIRS

Table 2: Diagnostic criteria for SIRS.

SIRS	At least 2 symptoms are met
Symptom 1	Body temperature >38°C or <36°C for two consecutive times
Symptom 2	Heart rate >90 beats per minute
Symptom 3	Respiratory rate >20 times/min or P_aCO_2 <32 mmhg
Symptom 4	WBC $>12\times10^9$/L or $<4\times10^9$/L or immature cells >10%

Table 3: Main instruments and manufacturers used in test process.

Main instruments	Manufacturer
BD Phoenix-100 Automatic Microbial Identification Instrument	Becton Dickinson
BD Bactec™ FX Blood Culture System	Becton Dickinson
BD Bruker Mass Spectrometer Microflex Lt/Sh System Electrothermal Incubator	Brooke Dalton company
Electric constant temperature incubator	Shanghai Xinmiao
Ultralow temperature freezer	Fuzhou Keze
Biological safety cabinet	Shanghai Lixin
Clean workbench	Suzhou Antai Air Technology Co., Ltd
Micropipette	Eppendorf, Germany
High-speed cryogenic centrifuge	Eppendorf, Germany
Automatic biochemical analyzer cobas C501-2	Roche
Automatic electrochemiluminescence immunoassay analyzer cobas e601	Roche
Sysmex XN-3000 automatic blood cell analyzer	Sisen Meikang medical electronics (Shanghai) Co., Ltd
SLAN-96S real-time PCR system	Zhishan biotechnology Co., Ltd

During the study period, 40, 5, 4, 2, 2, 2, and 1 cases were infected with *Staphylococcus aureus*, *Staphylococcus epidermidis*, *Staphylococcus haemolyticus*, *Staphylococcus cephalosporus*, *Staphylococcus* humanus, and *Staphylococcus* saprophyticus, respectively. Among the Gram-positive bacteria, *S. aureus* was 87.5% resistant to penicillin and sensitive to vancomycin, mirantolimus, and teicoplanin; other types of staphylococci were more resistant to penicillin, benzocillin, and erythromycin and sensitive to rifampicin, linezolid, vancomycin, mirantolimus, and teicoplanin, as shown in Table 5; streptococci were up to 80% resistant to erythromycin and clindamycin. The resistance rate to penicillin, cephalosporin, linezolid, and vancomycin was low, and the sensitivity rate was over 90%, as shown in Table 6. Among Gram-negative bacteria, *E. coli* had a resistance rate of 73.1% to piracillin, complete susceptibility (100%) to viraemia, and resistance to imipenem, amikacin, and laracillin/tazole. The susceptibility rate of bactam was above 95%; *Klebsiella pneumoniae* was 24.1% resistant to piroxicillin and relatively sensitive to amikacin with a sensitivity of 96.2%; *Pseudomonas aeruginosa* was resistant to amikacin, fully sensitive to gentamicin (100%) and had a relatively low antibiotic resistance rate; *Acinetobacter baumannii* had a relatively high antibiotic resistance rate and was 53.3% sensitive to amikacin, as Table 7 shows.

A total of 455 hospitalized patients were included, including 352 patients with sepsis and 103 patients without sepsis. There was no difference in gender and age between sepsis and nonseptic patients ($P>0.05$), but there was a statistical difference in admission route. Patients with toxemia had a higher proportion of emergency admissions and were relatively critically ill on admission, while nonseptic patients had relatively average admissions. In addition, levels of CRP (146.4, 115.9) mg/L in sepsis were higher than nonseptic CRP (58.9, 65.1) mg/L ($P<0.001$), and levels of PCT in sepsis (12.6,45.0) ng/mL level was higher than PCT in non-septic (0.4, 0.8) ng/mL ($P<0.001$), WBC in κ toxemia (10.7, 9.2) $\times10^9$/L and non-septic WBC (10.7, 9.2) $\times10^9$/L There was a statistical difference between WBC (8.2, 6.2) $\times10^9$/L in toxemia ($P<0.001$), and WBC was converted into a categorical variable for analysis, see Table 8 and Figure 2 for details.

In patients with positive blood cultures, CRP and PCT levels were higher in sepsis than in non-sepsis. ROC curve analysis showed that the ACC for CRP, PCT and CRP + PCT tandem for the diagnosis of sepsis were 0.85 (95% CI, 0.80–0.89), 0.90 (95% CI, 0.88–0.94) and 0.92 (95% CI 0.89~0.94). When the critical value of CRP was 97.05 mg/L, the sensitivity and specificity were 77.8% and

Table 4: Distribution of pathogenic bacteria detected in 387 adult blood cultures.

Pathogenic bacteria	Number of cases ($n = 387$)	Composition ratio (%)
Total G^- bacteria	275	71.06
Escherichia colibacillus	134	34.63
Klebsiella pneumoniae	79	20.41
Pseudomonas aeruginosa	23	5.94
Acinetobacter baumannii	15	3.88
Burkholderia	5	1.29
Citrobacter	4	1.03
Enterobacter spp.	2	0.52
Myxobacteria	2	0.52
Klebsiella oxytoca	2	0.52
Proteus mirabilis	2	0.52
Aeromonas hydrophila	2	0.52
Salmonella typhi	2	0.52
Corynebacterium striatum	1	0.26
Salmonella enteritis	1	0.26
Pseudomonas putida	1	0.26
Total G^+ bacteria	104	26.87
Staphylococcus spp.	54	13.95
Staphylococcus aureus	40	10.34
Staphylococcus epidermidis	5	1.29
Staphylococcus haemolyticus	4	1.03
Staphylococcus capitis	2	0.52
Staphylococcus hominis	2	0.52
Staphylococcus saprophyticus	1	0.26
Streptococcus spp.	31	8.01
Streptococcus pneumoniae	11	2.84
Streptococcus sanguis	4	1.03
Streptococcus viridans	3	0.78
Group *G Streptococcus*	3	0.78
Streptococcus constellatus	3	0.78
Streptococcus oralis	2	0.52
Streptococcus anginosus	2	0.52
Streptococcus bovis	1	0.26
Streptococcus salivarius	1	0.26
Streptococcus anoxy	1	0.26
Enterococcus spp.	18	4.65
Enterococcus faecium	10	2.58
Enterococcus faecalis	6	1.55
Enterococcus gallinarum	1	0.26
Enterococcus caseliflavus	1	0.26
Arcanobacterium pyogenes	1	0.26
Fungus	8	2.07
Candida spp.	7	1.81
Cryptococcus neoformans	1	0.26

80.7%, respectively; when the critical value of PCT was 1.34 ng/mL, the sensitivity and specificity were 86.5% and 79.5%, respectively; the sensitivity and specificity of CRP + PCT tandem diagnosis were 84.3% and 87.5%, respectively. Pairwise comparison of ROC curves indicated that the diagnostic value of PCT was greater than that of CRP ($P = 0.016$). CRP and PCT levels were higher in patients with severe sepsis/septic shock. When CRP and PCT were 197.01 mg/L and 28.55 ng/mL, respectively, the AUC was 0.67 (95% CI, 0.62–0.73) and 0.98 (95% CI, 0.96–1.00), and the diagnostic sensitivity and specificity of CRP was 50.5% and 79.7%, respectively, and that of PCT was 92.8% and 96.1%, respectively as shown in Figure 3 and Table 9.

4. Discussion

Sepsis is a relatively common infectious disease that poses a serious threat to the quality of daily life and the health of patients. If timely diagnosis can be made at an early stage in patients with sepsis and early effective treatment can be taken for them, the treatment effect can be significantly improved and the morbidity and mortality rate of patients with sepsis can be reduced [17]. In the medical clinical tests for sepsis patients, the results of biological methods such as blood culture and urine culture are slow and therefore the degree of application is relatively low. Diagnostic assessment of diseases by detecting changes in the level of biomarkers is the result of recent discoveries in molecular biology, and this diagnostic

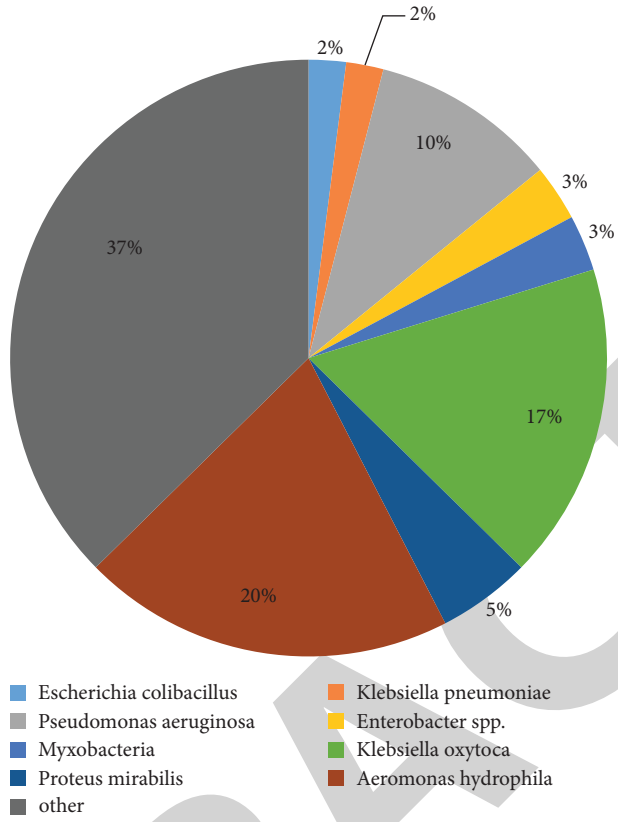

Figure 1: Distribution of pathogenic bacteria detected in blood culture of 387 adult sepsis patients.

Table 5: Resistance rate of Gram-positive *Staphylococcus aureus* (%).

Antimicrobial agents	*Staphylococcus aureus* ($n = 40$)		Drug resistance
	Sensitive	Intermediary	
Penicillin	10.0	2.5	87.5
Erythromycin	50.0	7.5	42.5
Ciprofloxacin	77.5	2.5	20.0
Clindamycin	80.0	2.5	17.5
Gentamicin	82.5	0	17.5
Oxacillin	85.0	0	15.0
Compound xinruoming	95.0	0	5.0
Li Fuping	92.5	2.5	5.0
Linezolid	97.5	0	2.5
Vancomycin	100	0	0
Furantoin	100	0	0
Teicoplanin	100	0	0

Table 6: Resistance rate of Gram-positive other staphylococci (%).

Antimicrobial agents	*Other staphylococci* ($n = 14$)		Drug resistance
	Sensitive	Intermediary	
Penicillin	21.4	0	78.6
Erythromycin	28.6	0	71.4
Oxacillin	28.6	0	71.4
Ciprofloxacin	42.9	0	57.1
Gentamicin	64.3	0	35.7
Compound xinruoming	78.6	0	21.4
Clindamycin	85.7	0	14.3
Li Fuping	100	0	0
Linezolid	100	0	0
Vancomycin	100	0	0
Furantoin	100	0	0
Teicoplanin	100	0	0

method allows not only to explore the occurrence and development of diseases from a molecular point of view but also to make effective and accurate judgments in the early stages of disease development. Sepsis is a systemic inflammatory response caused by inflammatory infection, and the morbidity and mortality rate can be as high as 40%; early and effective diagnosis is the key to improving patient prognosis and reducing morbidity and mortality [18]. Currently, PCT and CRP are the most widely used diagnostic biomarkers for sepsis.

In this study, there were records in the hospital's electronic medical record system confirming that patients with pathogenic bacteria detected in clinical blood cultures were blood culture-positive patients. Studies [19, 20] have shown that SCT levels can be used to predict blood culture results and that a high SCT level increases the likelihood that a patient will have a positive blood culture. In systematic case studies, some patients had significant sepsis based on diagnostic criteria, but the diagnosis at discharge was usually recorded as a bloodstream infection or bacteremia, and the clinical diagnosis of sepsis was low. According to the study, a

Table 7: Gram-positive *Streptococcus* drug resistance rate (%).

Antimicrobial agents	*Streptococcus* ($n = 31$)		Drug resistance
	Sensitive	Intermediary	
Erythromycin	19.4	0	80.6
Clindamycin	19.4	0	80.6
Levofloxacin	87.1	0	12.9
Chloramphenicol	87.1	0	12.9
Cefotaxime	90.3	0	9.7
Penicillin	93.5	0	6.5
Linezolid	96.8	0	3.2
Vancomycin	96.8	0	3.2

Table 8: Comparison of clinical data between sepsis and nonsepsis patients.

	Total	Sepsis	Non sepsis	*P*
Number of cases	455	352	103	—
Gender				
Male	249	192 (54.3%)	57 (55.5%)	—
Female	206	160 (45.3%)	46 (44.5%)	0.888
Age	63.4 ± 17.6	64.4 ± 17.3	59.9 ± 18.4	0.732
Admission route				
Emergency treatment	195	173 (49.3%)	22 (21.6%)	—
Outpatient department	260	179 (50.7%)	81 (78.8%)	<0.001
Admission				
Critical	76	70 (19.7%)	6 (5.9%)	—
Urgent	131	119 (33.6%)	12 (11.5%)	—
Commonly	248	163 (46.5%)	85 (82.3%)	<0.001
CRP (IQR) mg/L	124.3 (119.5)	146.6 (115.7)	58.7 (65.3)	<0.001
PCT (IQR) ng/mL	6.4 (37.7)	12.5 (45.2)	0.6 (0.7)	<0.001
WBC[a] (IQR) $\times 10^9$/L	10.7 (9.4)	11.5 (10.4)	8.4 (8.4)	<0.001
WBC[b]	—	—	—	—
$>12 \times 10^9$/L or $<4 \times 10^9$/L	253	218 (61.7%)	35 (34.2%)	—
4×10^9/L~12×10^9/L	202	134 (38.2%)	68 (66.2%)	<0.001

higher proportion of septic patients and a higher proportion of critically ill patients were admitted to the emergency department compared with non-septic patients. Because white blood cell counts are an indicator of SIRS, the results of this analysis also confirmed that a higher proportion of patients with sepsis had abnormal white blood cell counts compared with patients without sepsis. Studies [21, 22] reported that the best diagnosis was obtained when the white blood cell threshold was 1.49 ng/mL, which is similar to the threshold obtained in this study. When CRP and PCT were 97.05 ng/L and 1.34 ng/L, respectively, the diagnostic sensitivity and specificity of PCT levels were higher than CRP, and PCT had a better diagnostic value. The specificity of tandem CRP + PCT was 87.5%, which was higher than that of CRP (80.7%) and PCT (79.5%). A study [23] presented epidemiologic data and clinical outcomes of severe sepsis and septic shock, and studies [24, 25] showed that among patients with confirmed severe sepsis/septic shock, overall morbidity and mortality in intensive care units and hospitals reached 28.7% and 33.5% respectively, indicating severe clinical outcomes. In addition, severe sepsis/septic shock imposes a significant financial burden on patients, which is a serious problem for specialists.

In this study, sepsis was divided into a sepsis group, a severe sepsis group, and a septic shock group according to the severity of sepsis. When CRP and PCT levels were compared, sepsis was found to be associated with severe sepsis and septic shock. A statistical difference was observed in septic shock: CRP and PCT levels were higher in severe sepsis/septic shock than in sepsis. A level of 28.55 ng/mL had a better diagnostic value. PCT performed better than CRP in the diagnosis of sepsis compared to the area under the ROC curve.

In conclusion, the detection of serum PCT and CRP can effectively assess the development of sepsis patients, which has certain value for early diagnosis and prognosis, and the prognosis of patients is closely related to platelet count and related parameters, which has certain guiding significance for prognosis prediction. This study can provide some reference for the diagnosis of clinical sepsis, but there are some shortcomings in the study design. First, this part of the study was retrospective and failed to continuously monitor the dynamic changes of CRP and PCT and to follow up patients discharged from the hospital; therefore, the risk factors for sepsis-related mortality could not be analyzed. Second, because we did not have real access to the patients and the data came from information recorded in the electronic medical

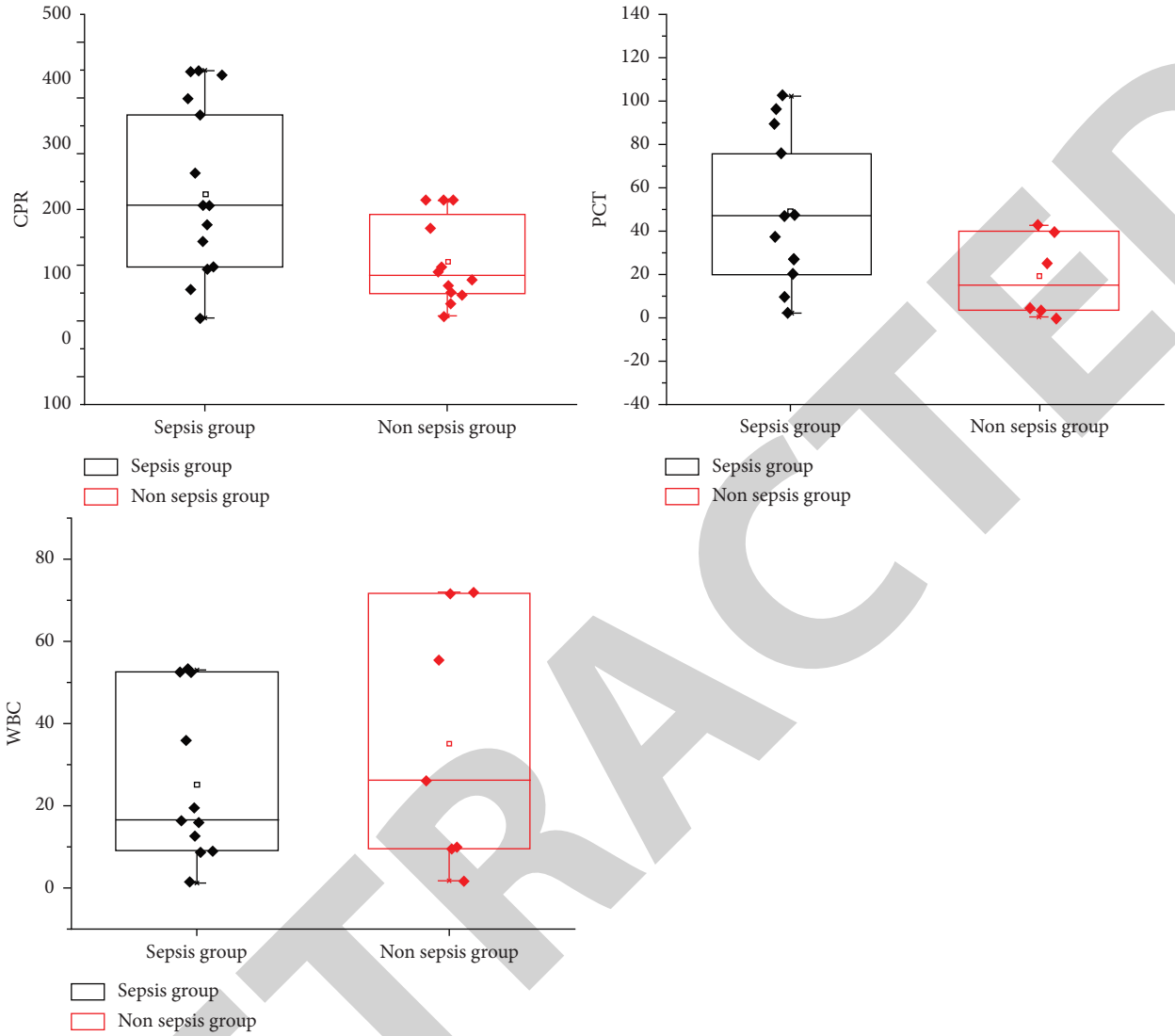

Figure 2: Comparison of CRP, PCT, and WBC levels between blood culture-positive sepsis and non-sepsis. Note: CRP: C-reactive protein; PCT: procalcitonin; WBC: white blood cell count; ***: $P < 0.001$. CRP, PCT and WBC levels were compared using Wilcoxon rank sum test for two independent samples.

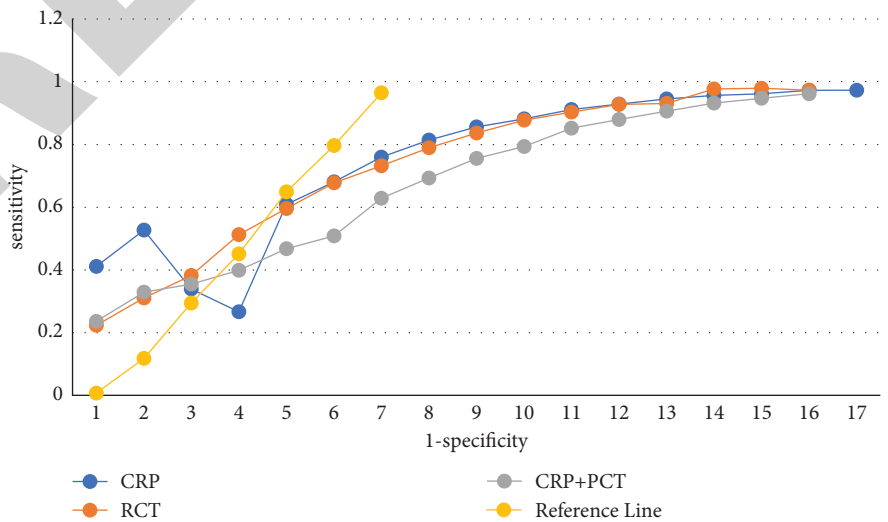

Figure 3: ROC curves of CRP, PCT, and CRP + PCT in diagnosis of sepsis. Note: CRP: C-reactive protein; Pct: procalcitonin. Statistical method: ROC curve analysis.

Table 9: Diagnostic value of CRP, PCT and CRP + PCT tandem for sepsis.

Variable	Cutoff value	AUC (95% CI)	Standard error	Poor sensitivity (%)	Specificity (%)	*P*
CRP	97.07 mg/	0.87 (0.82~0.88)	0.023	77.8	80.7	<0.001
PCT	1.35 ng/mL	0.92 (0.87~0.95)	0.014	86.6	79.7	<0.001
PCT + CRP	—	0.93 (0.88~0.96)	0.016	84.5	87.7	<0.001

record system, data were missing for some patients, and a follow-up rigorous prospective study could be designed to compensate for the shortcomings of this study.

Data Availability

The experimental data used to support the findings of this study are available from the corresponding author upon request.

Conflicts of Interest

The authors declare that they have no conflicts of interest regarding this work.

References

[1] S. Sharma and N. Duggal, "Role of procalcitonin, Il-6 and *C*-reactive protein in suspected cases of sepsis," *Indian Journal of Pathology & Microbiology*, vol. 62, no. 4, p. 578, 2019.

[2] Y. Zhou, Z. Liu, J. Huang et al., "Usefulness of the heparin-binding protein level to diagnose sepsis and septic shock according to sepsis-3 compared with procalcitonin and C reactive protein: a prospective cohort study in China," *BMJ Open*, vol. 9, no. 4, Article ID e026527, 2019.

[3] E. Sadeghi, A. Nasimfar, M. Karamyyar, and L. J. Manesh, "Comparison of serum procalcitonin level with erythrocytes sedimentation rate, *C*-reactive protein, white blood cell count, and blood culture in the diagnosis of bacterial infections in patients hospitalized in motahhari hospital of urmia (2016)," *Journal of Advanced Pharmaceutical Technology & Research*, vol. 9, no. 4, p. 147, 2018.

[4] Z. Bakhshiani, S. Fouladi, S. Mohammadzadeh, and N. Eskandari, "Correlation of sPD1 with procalcitonin and *C*-reactive protein levels in patients with sepsis," *Cell Journal (Yakhteh)*, vol. 23, no. 1, pp. 14–20, 2021.

[5] Y. X. Shang, Z. Zheng, M. Wang et al., "Diagnostic performance of Neutrophil CD64 index, procalcitonin, and *C*-reactive protein for early sepsis in hematological patients," *World Journal of Clinical Cases*, vol. 10, no. 7, pp. 2127–2137, 2022.

[6] A. Molinero-Fernandez, M. Moreno-Guzman, L. Arruza, M. Á. López, and A. Escarpa, "Toward early diagnosis of late-onset sepsis in preterm neonates: dual magneto immunosensor for simultaneous procalcitonin and C-reactive protein determination in diagnosed clinical samples," *ACS Sensors*, vol. 4, no. 8, pp. 2117–2123, 2019.

[7] L. Ruan, G. Y. Chen, Z. Liu et al., "The combination of procalcitonin and *C*-reactive protein or presepsin alone improves the accuracy of diagnosis of neonatal sepsis: a meta-analysis and systematic review," *Critical Care*, vol. 22, no. 1, pp. 316–319, 2018.

[8] M. Stocker, W. van Herk, S. El Helou et al., "*C*-reactive protein, procalcitonin, and white blood count to rule out neonatal early-onset sepsis within 36 hours: a secondary analysis of the neonatal procalcitonin intervention study," *Clinical Infectious Diseases*, vol. 73, no. 2, pp. e383–e390, 2021.

[9] V. Patil, A. Avhad, A. Kulkarni, and K. Pandere, "High-sensitive *C*-reactive protein in patients with coronary artery disease," *Journal of Natural Science, Biology and Medicine*, vol. 11, no. 1, p. 39, 2020.

[10] S. Eschborn and J. H. Weitkamp, "Procalcitonin versus *C*-reactive protein: review of kinetics and performance for diagnosis of neonatal sepsis," *Journal of Perinatology*, vol. 39, no. 7, pp. 893–903, 2019.

[11] P. Chaftari, A. Qdaisat, A. M. Chaftari et al., "Prognostic value of procalcitonin, c-reactive protein, and lactate levels in emergency evaluation of cancer patients with suspected infection," *Cancers*, vol. 13, no. 16, p. 4087, 2021.

[12] M. Vassallo, C. Michelangeli, R. Fabre et al., "Procalcitonin and C-reactive protein/procalcitonin ratio as markers of infection in patients with solid tumors," *Frontiers of Medicine*, vol. 8, Article ID 627967, 2021.

[13] R. M. El Shabrawy, A. Gawish, R. Elgabry, F. M. Nasr, M. Diab, and D. Gamal, "Presepsin, procalcitonin and *C* reactive protein as diagnostic biomarkers of sepsis in intensive care unit patients," *Microbes and Infectious Diseases*, vol. 2, 2021.

[14] R. D. Güleç, F. D. Arslan, T. Çalışkan et al., "Could presepsin be an alternative marker in the early diagnosis of sepsis in COVID-19?" *Scandinavian Journal of Clinical and Laboratory Investigation*, vol. 82, no. 2, pp. 108–114, 2022.

[15] B. Ritchie, K. Porritt, T. Marin, and N. Williams, "Diagnostic test accuracy of serum measurement of procalcitonin and *C*-reactive protein for bone and joint infection in children and adolescents: a systematic review protocol," *JBI Evidence Synthesis*, vol. 18, no. 3, pp. 564–570, 2020.

[16] S. Li, J. Gu, W. Nan et al., "Procalcitonin and C-reactive protein predict infection in hematopoietic stem cell transplantation patients," *Leukemia Research*, vol. 105, Article ID 106574, 2021.

[17] S. Walker, I. Harding, K. Soomro et al., "An evaluation into the use of procalcitonin levels as a biomarker of bacterial sepsis to aid the management of intrapartum pyrexia and chorioamnionitis," *AJOG Global Reports*, vol. 2, no. 3, Article ID 100064, 2022.

[18] C. Liu, C. Fang, and L. Xie, "Diagnostic utility of procalcitonin as a biomarker for late-onset neonatal sepsis," *Translational Pediatrics*, vol. 9, no. 3, pp. 237–242, 2020.

[19] M. Beltempo, I. Viel-Thériault, R. Thibeault, A. S. Julien, and B. Piedboeuf, "C-reactive protein for late-onset sepsis diagnosis in very low birth weight infants," *BMC Pediatrics*, vol. 18, no. 1, pp. 16–18, 2018.

[20] R. Mr Umran, J. M Hashim, and H. Jameel, "Significance of serum procalcitonin level in the early diagnosis of neonatal sepsis," *Iranian Journal of Neonatology IJN*, vol. 11, no. 3, pp. 1–6, 2020.

[21] I. Demir and M. Yücel, "Investigation of relation between mortality of geriatric patients with sepsis and C-reactive protein, procalcitonin and neutrophil/lymphocyte ratio in

Hindawi
Emergency Medicine International
Volume 2023, Article ID 9794070, 1 page
https://doi.org/10.1155/2023/9794070

Retraction

Retracted: Analysis of the Effect of Quality Nursing on Recovery after Thoracic Surgery

Emergency Medicine International

Received 8 August 2023; Accepted 8 August 2023; Published 9 August 2023

This article has been retracted by Hindawi following an investigation undertaken by the publisher [1]. This investigation has uncovered evidence of one or more of the following indicators of systematic manipulation of the publication process:

(1) Discrepancies in scope
(2) Discrepancies in the description of the research reported
(3) Discrepancies between the availability of data and the research described
(4) Inappropriate citations
(5) Incoherent, meaningless and/or irrelevant content included in the article
(6) Peer-review manipulation

The presence of these indicators undermines our confidence in the integrity of the article's content and we cannot, therefore, vouch for its reliability. Please note that this notice is intended solely to alert readers that the content of this article is unreliable. We have not investigated whether authors were aware of or involved in the systematic manipulation of the publication process.

In addition, our investigation has also shown that one or more of the following human-subject reporting requirements has not been met in this article: ethical approval by an Institutional Review Board (IRB) committee or equivalent, patient/participant consent to participate, and/or agreement to publish patient/participant details (where relevant).

Wiley and Hindawi regrets that the usual quality checks did not identify these issues before publication and have since put additional measures in place to safeguard research integrity.

We wish to credit our own Research Integrity and Research Publishing teams and anonymous and named external researchers and research integrity experts for contributing to this investigation.

The corresponding author, as the representative of all authors, has been given the opportunity to register their agreement or disagreement to this retraction. We have kept a record of any response received.

References

[1] Y. Zhou and M. Xu, "Analysis of the Effect of Quality Nursing on Recovery after Thoracic Surgery," *Emergency Medicine International*, vol. 2022, Article ID 6204832, 10 pages, 2022.

Hindawi
Emergency Medicine International
Volume 2022, Article ID 6204832, 10 pages
https://doi.org/10.1155/2022/6204832

Research Article

Analysis of the Effect of Quality Nursing on Recovery after Thoracic Surgery

Yujing Zhou and Ming Xu

Department of Thoracic Surgery, Shanghai Pulmonary Hospital Affiliated to Tongji University, Shanghai, China

Correspondence should be addressed to Yujing Zhou; 18017537515@163.com

Received 22 August 2022; Revised 8 September 2022; Accepted 14 September 2022; Published 7 October 2022

Academic Editor: Hang Chen

Objective. To observe the feasibility and safety of rapid rehabilitation nursing in the perioperative period of thoracoscopic treatment of lung cancer patients. Rapid rehabilitation nursing was compared with conventional perioperative nursing to explore its clinical efficacy, i.e., its advantages in improving postoperative comfort, postoperative rehabilitation efficiency, and hospitalization cost of patients undergoing thoracoscopic lung cancer resection. *Methods*. We carried out a retrospective analysis of 337 lung cancer patients who underwent lobectomy in our thoracic surgery department from July 2019 to June 2021, of which 168 lung cancer patients whose perioperative care method was traditional rehabilitation care were classified as *A* and 169 lung cancer patients who started to implement the intelligent medical intervention method in the department in September were classified as intelligent medical *B*. By reviewing patient cases and departmental statistics, general information, length of stay, hospitalization cost, complication rate, pain score, bowel movement recovery time, and pulmonary function index of the two groups *A* and *B* were compared. Nursing satisfaction was investigated by using a questionnaire. All the data in the study were processed and analyzed using SPSS 17.0 software. *Results*. There were no differences in preoperative general data, pathological findings, preoperative underlying diseases, lesion involvement sites, and postoperative TNM stages ($P > 0.05$), which were comparable; the incidence of postoperative pulmonary infection and atelectasis complications, postoperative hospitalization time, and hospitalization cost were lower in group *B* than in group *A*; the postoperative chest tube drain placement time was shorter in group *B* than in group *A*, and the difference between the two groups was statistically significant ($P < 0.05$). The incidence of postoperative pain and discomfort in group *B* was lower than that in group *A*, and the difference between the two groups was statistically significant ($P < 0.05$); the incidence of postoperative chest pain, bleeding, pneumothorax, pulmonary infection, and atelectasis in group *B* was lower than that in group *A*, and the difference between the two groups was statistically significant ($P < 0.05$). *Conclusion*. Intelligent medical rehabilitation nursing has good application value in thoracoscopic lung cancer surgery. Applying the concept of intelligent medical rehabilitation nursing provides an important experimental basis and theoretical basis for improving the postoperative survival quality and clinical symptoms of patients undergoing thoracoscopic lung cancer resection, which helps to promote the postoperative recovery of patients with thoracoscopic lung cancer, improves the recovery efficiency of patients and their overall quality of life, and is superior to the conventional nursing group.

1. Introduction

The incidence of lung cancer is increasing year by year due to the rapid development of society and the increasing and younger population of smokers. In western developed countries and industrialized cities in China, lung cancer accounts for the first place in malignant tumor incidence in men and the second or third place in women [1, 2], which has seriously threatened the health of all human beings. The histological types of lung cancer are generally divided into two categories: small cell carcinoma and non-small-cell carcinoma, of which non-small-cell lung cancer accounts for 80%, which also includes adenocarcinoma, squamous cell carcinoma, large cell carcinoma, and squamous adenocarcinoma [3, 4]. The clinical manifestations of lung cancer mainly include [5, 6] cough, bloody sputum, chest pain,

fever, and symptoms of metastatic lung cancer foci. Most of the patients with intermediate- and late-stage cancer are exhibit severe cachexia and cancer pain in combination. Studies have shown that 35%–45% of patients with early and intermediate malignancy experience moderate or severe cancer pain, while 75% of patients in the progressive stage of the disease experience cancer pain of different degrees, of which 25%–30% suffer from severe cancer pain, especially for patients with advanced malignancy; nearly 80% of patients with intermediate and advanced lung cancer have obvious pain, so cancerous pain is a serious problem for tumor patients and medical workers [7, 8]. Cancer pain caused by lung cancer is one of the most important factors affecting the quality of life of lung cancer patients, most of who suffer from negative psychology, especially palliative care patients. Therefore, effective control of lung cancer pain is clinically important to improve patients' quality of life, which can make the last days of a patient's quality of life more dignified.

Lung cancer is one of the most common malignant tumor diseases in clinical thoracic surgery, and the most ideal treatment mode now is a comprehensive treatment mode based on surgery combined with radiotherapy and other treatment modalities [9, 10]. Among these, surgical treatment plays a leading role. At present, the main surgical methods for lung cancer are (1) wedge resection or partial resection; (2) lobectomy; (3) segmental resection; and (4) total pneumonectomy. The most common procedure performed at our hospital is lobectomy combined with lymph node dissection. Since the scope of surgical resection and trauma of lung cancer is much larger than that of ordinary pneumonectomy, lung function is often severely damaged and there are more postoperative complications. As surgery leads to loss of respiratory muscle, the proliferation of the elastic fiber layer of lung tissue, narrowing of the airway, and gradual reduction in the function of the airway mucosa result in a weakened endocrine elimination of the airway. Patients often develop respiratory dysfunction and other related complications after surgery. Patients are prone to postoperative complications such as bleeding, pneumothorax, pulmonary infection, and pulmonary atelectasis due to surgical trauma and anesthesia. Helping postoperative patients with lung cancer to effectively remove endocrine secretions from the airways is of positive significance to reducing the occurrence of postoperative complications and alleviating patients' postoperative pain, so effective perioperative nursing interventions are crucial to reduce the occurrence of postoperative complications in patients.

Intelligent medical is a concept that uses a series of optimized measures proven effective by evidence-based medicine in the perioperative period to accelerate patients' postoperative recovery. It focuses on the entire perioperative period, through a number of effective interventions for patients before, during, and after surgery, in order to shorten the patient's hospital stay, reduce hospital costs, reduce postoperative complications, and improve the efficiency of recovery. Perioperative care is an integral part of the intelligent medical concept and an important measure to improve patients' comfort. Studies have shown that active and effective intelligent medical rehabilitation care for lung cancer patients can effectively improve patients' respiratory function and reduce the incidence of postoperative complications in lung cancer patients [11], and nursing interventions play a key role in this treatment process [12]. However, the development of the nursing concept guided by the concept of intelligent medical rehabilitation surgery is relatively slow in its application in pulmonary surgery compared with other disciplines, and most clinical departments are still using traditional conventional nursing methods, which restricts the development and progress of intelligent medical rehabilitation surgery [13, 14]. In order to improve the understanding of the concept of intelligent medical rehabilitation nursing in the perioperative period of lung cancer, it is hoped that nursing staff can actively adopt this advanced nursing concept.

In this paper, we conducted a study on the application of intelligent medical rehabilitation nursing in the perioperative period of lung cancer patients and retrospectively analyzed 337 lung cancer patients who underwent lobectomy in our thoracic surgery department from July 2019 to June 2021, among which 168 perioperative lung cancer patients were treated with traditional rehabilitation and 169 lung cancer patients who started to adopt intelligent medical intervention methods in the department were classified as intelligent medical. The results found that intelligent medical rehabilitation care has good application value in thoracoscopic lung cancer surgery, and the application of the intelligent medical rehabilitation care concept provides an important experimental basis and theoretical basis for improving the postoperative survival quality and clinical symptoms of patients undergoing thoracoscopic lung cancer resection, which helps to promote the postoperative recovery of thoracoscopic lung cancer patients and improve the recovery efficiency of patients and their overall quality of life and is better than the conventional care group.

2. Materials and Methods

2.1. Sampling Method. A total of 337 lung cancer patients who underwent lobectomy at the Thoracic Surgery Department of Shanghai Pulmonary Hospital Affiliated with Tongji University from July 2019 to June 2021 were selected. 168 lung cancer patients who used traditional nursing methods in the perioperative period were selected as *A*, and 169 lung cancer patients who received intelligent medical nursing intervention methods after September 2020 were selected as intelligent medical as *B*.

2.2. Inclusion Criteria

(1) According to the pathological staging criteria of lung cancer, all patients belonged to stage I–III patients with resectable lung cancer

(2) None of them received radiotherapy or chemotherapy before surgery, and preoperative assessment could tolerate unilobe lobectomy

(3) Preoperative CT examination showed that the patient had no hilar or mediastinal lymph node metastasis and no other malignant tumors

(4) The patient has no functional lesions of important organs and no liver and kidney system diseases

2.3. Exclusion Criteria

(1) Those with exploratory surgery or multilobectomy

(2) Those with benign lung lesions

(3) Those suffering from autoimmune diseases

(4) Those who cannot cooperate with nursing intervention and observers due to cognitive impairment

2.4. Sample Size. Multivariate analysis in statistics generally requires that the sample size be 5 to 10 times that of the independent variable. This study expects up to 33 independent variables, so the required sample size is 165–330 cases. In this study, 300 cases were collected, and the sample size was increased by 10% to expand it to 337 cases.

2.5. Perioperative Management of Traditional Rehabilitation. According to the traditional nursing routine standards of thoracic surgery, perioperative management methods of traditional rehabilitation were as follows:

(1) Admission education included medical history inquiry, ward environment introduction, safety knowledge (such as preventing falling from bed) related education, the introduction of a competent physician and nurse in charge, ward visiting time and visiting system introduction, diet-related knowledge education, and operation-related knowledge introduction.

(2) Respiratory function exercise: the nurse in charge demonstrates and instructs the patient to perform respiratory function training, mainly with pursed lip abdominal breathing and balloon blowing. ① Pursed lip abdominal breathing: a combination of abdominal breathing and pursed lip breathing. The specific method is to assist the patient to take a sitting or semirecumbent position, close the mouth and inhale deeply through the nose, then hold breath for 2–3 seconds, then slightly tilt chest forward, reduce the lips to a whistle-like shape, and breathe out through the mouth slowly, take a deep breath, and breathe out slowly. ② The blowing balloon method: the patient takes a deep breath, blows the balloon hard, stops for 1–2 seconds, and then removes the balloon.

(3) Analgesic management: influenced by traditional concepts, patients do not use analgesics preventively after surgery. When the patient's NRS score is >4 points, 75–100 mg of laryngeal hydrochloride is administered intramuscularly for analgesia.

(4) Early postoperative ambulation: according to traditional nursing routine, patients in the traditional rehabilitation lay flat on the first day after operation, take bedside X-rays, remove catheter on the second day, and assist in percussion on the back and expectoration, on the second day after operation. Three days later, according to the chest X-ray results, the chest drainage tube was removed and then patients could gradually get out of bed.

2.6. The Operation Method of Intelligent Medical Circle. Referring to "Guidelines for Intelligent Medical Surgery for Gastrectomy" by the European Association of Intelligent Medical Surgery, "Chinese Expert Consensus on Application of Intelligent Medical Surgery in Colorectal Surgery (2015 Edition)" by the Chinese Medical Association, and "China Intelligent Medical Surgery Periphery" issued by China Intelligent Medical Surgery Expert According to Expert Consensus on Operational Management (2016), combined with the characteristics of our department, we have made improvements in the following aspects of perioperative nursing interventions for lung cancer.

2.6.1. On the Basis of Traditional Education for Patients in Intelligent Medical, Concept of Intelligent Medical Surgery and Pain Education Are Added. The specific method is as follows:

(1) Outpatient consultation: during the outpatient consultation, the receiving physician will issue a publicity and education sheet for the introduction of perioperative knowledge. After entering the ward, a nurse in charge will introduce the basic content of the implementation of the concept of intelligent medical surgery and carry out publicity and education on lung cancer prevention. The hazards of smoking, inducing factors, pathogenesis, treatment methods, and prognosis of disease and key points of perioperative nursing and cooperation are explained to patients so that patients and their families have sufficient psychological preparation.

(2) Missionary time: two focused missionary classes are held every Tuesday and Friday afternoon, and each class lasts two hours. Participants include patients and their families who are preparing for surgery. The lecturers are responsible nurses and head nurses, and the method is the slide show.

(3) Propaganda and education content: in addition to the admission education content of *A*, perioperative knowledge of the concept of intelligent medical surgery will be introduced, and the advantages and importance of intelligent medical procedures will be explained through multimedia pictures and texts, so as to gain patients' understanding of intelligent medical care. The role of surgery and the current treatment level of hospitals and departments, pain-related knowledge, including pain score and pain medication, key points of cooperation before and after surgery, preoperative respiratory function training, and how to get out of bed early after surgery

are explained, so that patients can get out of bed early. A good communication is established, and there is an exchange relationships with medical staff, and at the same time, through intensive publicity and education, they let patients get to know each other and understand each other, which is more conducive to patients to maintain a relaxed and comfortable psychological state. After propaganda class, responsible nurses with qualifications of psychological counselors in the department communicate inwards to find out the stressors of patients' nervousness and anxiety. By listing typical rehabilitation cases, patients are encouraged to enhance their confidence, eliminate doubts, actively cooperate with treatment, and focus on handover.

2.6.2. Respiratory Function Training. The patients in intelligent medical were given a three-ball respiratory function trainer after admission and performed respiratory function training 4–6 times a day for 10 minutes each time. The main operation method is connecting the threaded connection tube of the lung function trainer to the interface and mouthpiece of the shell:

(1) Inspiratory function training: first, place the base marked with the "Inhalation" mark, place it below, and place it vertically. Hold a mouthpiece and inhale deeply at a uniform and deep inspiratory flow rate to raise the float, while holding your breath for as long as possible, and then relax. Each inhalation training time is 10 to 15 minutes, and then return to normal breathing.

(2) Exhalation function training: place the base marked with "Blowing" mark below, place it vertically, hold the mouthpiece, exhale evenly and deeply, raise the float, and do it for as long as possible. Hold, then relax, exhale for 10 to 15 minutes, and then resume normal breathing. After training, clean the trainer and put it away. At the same time, it is instructed to test tidal volume before the operation, record maximum inhalation and intake before the operation, and continue to use a respiratory function trainer to exercise respiratory function after operation. On the first day after operation, the patient began to practice using a respiratory function trainer, frequency was the same as that before operation, and the patient's physical strength was limited to the limit. The responsible nurse encouraged and supervised the patient to perform respiratory function training and assisted the patient to tap back and expel sputum.

In training of respiratory function, following points should be paid attention to the following:

(1) All medical staff in the department should be proficient in using respiratory training devices. Before using it, they must explain to patients and their families that respiratory function training is very important to the success of the operation, strive for patients to understand the importance of respiratory function training for the operation and cooperate with medical staff to complete training. Medical staff should often go to ward off to encourage and urge patients to complete training, to ensure that each patient can use a respiratory function trainer proficiently and to ensure the time and frequency of daily exercise.

(2) For preoperative patients with cardiovascular and cerebrovascular diseases, heart failure, and other diseases, it is necessary to observe the clinical manifestations of patients during respiratory function exercise. During the exercise of respiratory function, nurses gave corresponding guidance and supervision according to the specific situation of the patients and the training process was gradual to avoid adverse reactions such as respiratory muscle fatigue.

After one week of respiratory function exercise according to the above method, lung function was re-examined before the operation. It was found that values of MVV, FVC, and FEV1 were improved to different degrees after respiratory exercise and the difference was statistically significant (see Table 1 for specific values).

2.6.3. Analgesic Management. The patients in intelligent medical were given preventive analgesics; that is, 5 mg of Tylenin was given orally TID on the first day after operation, and patients were observed for dizziness, constipation, nausea, and vomiting, and other reactions to other medicines.

Pain-related knowledge education is carried out before surgery, and pain assessment scales are posted in wards and corridors to teach patients to use pain scales correctly, including the following:

(1) Definition of pain.

(2) Causes of pain such as surgical injury and influence of disease itself.

(3) Complications that may be caused by pain. For example, pain will affect postoperative coughing and deep breathing and may cause complications such as pneumonia and atelectasis.

(4) Criteria and methods for pain assessment.

(5) Common clinical analgesics, drug use methods and possible adverse reactions.

(6) Teaching patients and their families to perform pain self-score. Postoperative chest pain was evaluated by pain numbers.

The NRS was used to fill in the pain nursing assessment sheet every day to evaluate the location, nature, and score of pain, the impact of pain on sleep, life, and mood, changes in the patient's treatment compliance, and whether there was constipation, nausea, and vomiting, skin itching, and other adverse reactions. Pain assessment sheets were written at 15 :

Table 1: Comparison of pulmonary function indexes of patients in accelerated rehabilitation before admission and operation.

Project	Company	Admission ($n = 169$)	Preoperative ($n = 169$)	P value
MVV (maximum minute ventilation)	L/min	111.15 ± 12.72	131.02 ± 10.87	<0.001
FVC (forced vital capacity)	L	3.52 ± 0.53	3.68 ± 0.42	0.003
FEV1 (forced expiratory volume in first second)	L	2.86 ± 0.37	2.96 ± 0.35	0.001

00 every day, identified by the patient's description of the most severe pain numerical score in the past 24 hours and linked to the previous day's pain score. The pain score is expressed in a digital form of 0–10 points, with 0 points indicating no pain, 1–3 points indicating mild pain (basically no pain when lying down quietly and not affecting sleep), 4–6 points indicating moderate pain severe pain (pain when lying down quietly, affecting sleep), and 7–9 points indicating severe pain (pain intolerable). Scores were continued 6 hours after surgery, on the 1st and 5th days after surgery, and the pain score scale was continued for 3 consecutive days after oral administration of Tylenine was stopped.

2.6.4. Early Postoperative Ambulation. The patients in intelligent medical started to breathe deeply and coughed after waking up the day after operation. They changed their body positions in bed 6 hours after the operation. They started to sit by the bed in the morning on the first day after the operation, and then stood up (i.e., get out of bed trilogy).

Activity steps: assess the patient's general condition at the bedside, and if the condition is stable, assist in properly fixing the patient's chest closed drainage tube, subcutaneous negative pressure drainage tube, and other pipelines to avoid the drainage tube being folded, compressed, or prolapsed. Sit and lay down, encourage the patient verbally, assist him to slowly move his body to the bedside to sit and stand, first drop his legs for about 5 minutes, and observe whether the patient had symptoms such as dizziness, chest tightness, palpitations, sweating, and other symptoms, and the patient's response, if there is no discomfort, nurses and family members supported patient's bilateral armpits with both hands to assist him to stand up and stand firmly for 2-3 minutes. If there is no discomfort, assist the patient with bedside activities. After the patient gradually adapts, the patient can be supported to walk around the hospital bed for 3 to 5 minutes and gradually increase the amount of activity based on the general condition of the patient. It is not recommended to leave the ward during activities on the same day. If the patient can tolerate activity on the second day, it is recommended that family members and nurses are accompanied by the ward corridor andthe patient is prohibited from going downstairs. The amount of daily activity should be gradually increased according to the patient's physical strength. At the same time, strengthen the observation of the patient's condition to prevent falls.

2.7. Observation Indicators. The postoperative hospitalization days, hospitalization expenses, postoperative complication rate, bowel sound recovery time, postoperative pain numerical scale (NRS) score, and nursing satisfaction survey were observed. The changes in MVV, FVC, and FEV1 in intelligent medical at admission and the main indexes of pulmonary function were observed. The incidence of postoperative complications in patients was determined according to criteria for postoperative complications established by the US Centers for Disease Control and Prevention (CDC).

2.8. Data Collection Methods. General information, hospitalization time, hospitalization expenses, complication rate, pain score, bowel movement recovery time, and pulmonary function indexes were obtained by consulting the patient medical record system and department statistics. Questionnaire surveys and statistical analysis were performed.

3. Results

This study selected 337 lung cancer patients who underwent lobectomy in the Department of Thoracic Surgery, Shanghai Pulmonary Hospital, Tongji University, from July 2019 to June 2021. There were 168 lung cancer patients with traditional care methods during the perioperative period, including 100 adenocarcinomas and 68 squamous carcinomas, in 109 males and 59 females, aged 40–81 years, with a mean age of (57.22 ± 8.95) years. Smart medical (B) included 169 lung cancer patients who received a new rapid rehabilitation care intervention method after September 2019, including 113 adenocarcinomas and 56 squamous carcinomas, in 110 men and 59 women, aged 37–80 years, with a mean age (57.60 ± 10.23) years. There were no differences in general information such as gender, age, preoperative underlying disease, surgical site and method, postoperative pathology, and clinical TNM stage ($P > 0.05$), as shown in Table 2.

Patients in both conventional rehabilitation group A and smart medical group B successfully completed the corresponding single lobe resection and lymph node dissection. There were no cases of surgical death and no cases of secondary surgery within 30 days. The postoperative recovery time of bowel sounds was $(26.12\,\mathrm{V} \pm 3.34)$ hours for conventional rehabilitation A and (21.40 ± 2.60) hours for smart medical B. It was seen that the recovery time of bowel sounds shortened for smart medical patients. The postoperative hospitalization time was (11.98 ± 4.00) days for conventional rehabilitation A and smart medical B. The hospitalization cost of conventional rehabilitation A was (4.96 ± 1.22) thousand yuan and that of intelligent medical B was (4.36 ± 0.76) thousand yuan. The overall satisfaction score of nursing care for conventional rehabilitation A was (141.30 ± 2.62) points and that of intelligent medical B was (143.08 ± 2.03) points, which showed that the patient satisfaction improved with the adoption of intelligent medical

Table 2: Comparison of general data of patients.

Project	Content	A ($n = 168$)	B ($n = 169$)	P
Age	Year	57.23 ± 8.96	51.61 ± 10.24	0.718
Gender	Male	109 (64.8%)	110 (65.3%)	0.969
	Female	59 (35.2%)	59 (34.8%)	—
Pathology	Adenocarcinoma	100 (59.6%)	113 (66.7%)	0.164
	Squamous cell carcinoma	68 (41.4%)	56 (33.3%)	
Basic diseases	Hypertension	34 (20.5%)	28 (18.5%)	0.836
	Coronary heart disease	16 (9.3%)	21 (13.5%)	
	Diabetes	21 (12.3%)	18 (11.4%)	
Lesion location	Upper lobe of the right lung	45 (26.5%)	61 (36.3%)	0.055
	Middle lobe of the right lung	12 (7.3%)	11 (6.6%)	
	Right inferior lobe of the lung	45 (26.5%)	34 (20.2%)	
	Upper lobe of the left lung	32 (19.1%)	43 (25.5%)	
	Left inferior lobe of the lung	34 (20.3%)	20 (11.9%)	
Pathological stage	IA	36 (21.2%)	34 (20.3%)	0.882
	IB	43 (25.3%)	39 (23.3%)	
	IIA	30 (17.6%)	37 (21.7%)	
	IIB	32 (19.3%)	30 (17.8%)	
	IIIA	27 (16.3%)	29 (17.3%)	

care measures and the difference was statistically significant ($P < 0.05$) (Table 3).

The incidences of postoperative atelectasis and pulmonary infection in traditional rehabilitation A were 6.59% and 8.92%, respectively, while the incidences of postoperative atelectasis and pulmonary infection in intelligent medical B were 1.78% and 2.96%, which were lower. Compared with traditional rehabilitation, the incidence of arrhythmia in traditional rehabilitation A was 3.57% and the incidence of arrhythmia in intelligent medical B was 1.78%, which was lower than that in traditional rehabilitation, but there was no statistical significance ($P > 0.05$), as shown in Table 4.

The NRS scores of patients in traditional rehabilitation A were (6.02 ± 0.71) points and (5.88 ± 0.63) points 6 hours after operation and on the 1st day after operation, respectively. The NRS scores of patients in intelligent medical B were 6 hours after operation and on the first day after operation were (5.92 ± 0.70) and (5.72 ± 0.64) points, respectively. Due to the effect of the analgesic pump on the first day after operation, the NRS scores of patients in traditional rehabilitation A on the 2nd, 3rd, 4^{th}, and 5th days after the operation were (4.92 ± 0.86), (3.81 ± 0.65), (3.29 ± 0.75), and (2.75 ± 0.67) points. The NRS scores of patients in intelligent medical B on the 2nd, 3rd, 4^{th}, and 5th days after operation were (3.64 ± 0.78), (2.73 ± 0.72), (2.37 ± 0.59), and (1.87 ± 0.59) points, indicating that after scientific analgesia measures given after surgery, NRS scores of patients were lower than those of traditional rehabilitation, as shown in Table 5.

The patients in intelligent medical used a three-ball breathing trainer for respiratory function exercise after admission. The MVV, FVC, and FEV1 at admission were (111.13 ± 12.71) L/min, (3.51 ± 0.51) L, and (2.85 ± 0.39) L, respectively. The pulmonary function indexes MVV, FVC, and FEV1 of preoperative remeasurement were (131 ± 10.85) L/min, (3.66 ± 0.40) L, and (2.98 ± 0.33) L, respectively, which were improved compared with admission, indicating that the respiratory function trainer is of great significance to improve lung function of patients, as shown in Table 1.

4. Discussion

Lung cancer is the most common malignant tumor disease in clinical thoracic surgery, and thoracoscopic surgery is now the common means of treating lung cancer. Single port video-assisted thoracic surgery (SP-VATS) has the advantages of less surgical trauma, shorter hospital stay, and faster postoperative recovery, its surgical safety and 5-year survival rate are comparable to those of traditional thoracotomy, and it has been adopted by the National Comprehensive Cancer Network (NCCN) clinical treatment guidelines as a standard procedure for the treatment of early-stage lung cancer [15]. Because the extent of surgical resection and trauma for lung cancer is much greater than that of ordinary lobectomy, lung function is often severely impaired and postoperative complications are more frequent. Surgery leads to damage to respiratory muscles, proliferation of the elastic fibrous layer of lung tissue, narrowing of the airway, and progressive reduction in the function of the airway mucosa, resulting in reduced endocrine elimination of the airway, and respiratory dysfunction and other related complications usually occur in patients after surgery [16]. Some studies have demonstrated that giving lung cancer patients active and effective rapid rehabilitation nursing measures can effectively improve patients' respiratory function and reduce the incidence of postoperative complications in lung cancer patients. Active and effective rapid rehabilitation nursing interventions can effectively improve the respiratory function of lung cancer patients and have a positive effect on reducing complications and promoting recovery [17].

Currently, as an emerging concept, smart medicine has been applied in many surgical fields, especially in gastrointestinal surgery, with desirable results. The new nursing

Table 3: Comparison of bowel sounds recovery time, postoperative hospitalization time, hospitalization expenses, and nursing satisfaction.

Project	Company	A ($n = 168$)	B ($n = 169$)	P value
Bowel sound recovery time	Hours/h	26.15 ± 3.31	21.41 ± 2.61	<0.001
Postoperative hospital stay	Days/d	11.99 ± 4.01	8.92 ± 2.44	<0.001
Hospitalization expenses	Ten thousand	4.95 ± 1.24	4.34 ± 0.77	<0.001
Nursing satisfaction Comprehensive score	Minute	141.33 ± 2.61	143.05 ± 2.05	<0.001

Table 4: Comparison of postoperative complications.

Postoperative complications	A ($n = 168$)		B ($n = 169$)		P value
	Number of cases	Incidence rate (%)	Number of cases	Incidence rate (%)	
Atelectasis	10	6.58	4	1.77	0.031
Pulmonary infection	15	8.93	5	2.95	0.021
Arrhythmia	7	3.55	3	1.79	0.247
Total	32	19.05	10	6.50	0.009

Table 5: Comparison of postoperative pain scores.

Category	A ($n = 168$)	B ($n = 169$)	P value
6 hours after surgery	6.03 ± 0.72	5.94 ± 0.72	0.215
Day 1 after surgery	5.87 ± 0.61	5.71 ± 0.65	0.026
Day 2 after surgery	4.94 ± 0.85	3.65 ± 0.77	<0.001
Day 3 after surgery	3.82 ± 0.66	2.71 ± 0.74	<0.001
Day 4 after surgery	3.27 ± 0.77	2.35 ± 0.61	<0.001
Day 5 after surgery	2.77 ± 0.66	1.89 ± 0.57	<0.001

interventions guided by the theory of intelligent medicine mainly include a series of procedures, such as effective preoperative education and psychological care, new respiratory function training, effective analgesia, and early bed removal. The application of the smart medical concept in thoracic surgery lobectomy has proven to effectively reduce postoperative stress and shorten the hospital stay [18]. The hospitalization cost, postoperative pain score, and nursing satisfaction of patients guided by the smart medical concept were better than those of traditional rehabilitation, which is consistent with the results of the literature [19]. A study [20] found that active and effective preoperative mental health education can alleviate patients' anxiety and fears and enable them to receive surgical treatment in a good psychological state. A study [21] reported that the use of an intelligent medical rehabilitation surgical care model to intervene in the preoperative preparation of colon cancer patients could lead to voluntary medical care and reduce surgical complications. Clinical practice confirms that anxious and nervous psychological states may affect the effective implementation of the rapid rehabilitation model, that a good psychological state is an important factor in maintaining an individual's health, and that a patient's psychological state affects the speed of an individual's recovery. The model plays an important role [22]. Based on this theory, we have made the following improvements to the department's preoperative education and psychological intervention:

(1) In terms of the time of education, traditional preoperative education starts with the patient's admission to the hospital, while the intelligent medical team's education time starts with the outpatient diagnosis so that patients and their families have a sufficient psychological preparation.

(2) In terms of the content of education, the intelligent medical team began explaining the cause of the disease, treatment methods, the level of surgery in the department, the prognosis of the disease, and the current status and achievements of ERAS in the department in the form of slides and leaflets so that patients and their families can understand the disease. They have a correct understanding of the prognosis and gain support and cooperation.

(3) In terms of psychological support, in addition to paying close attention to the psychological conditions of patients and their families, the smart medical team also identifies abnormal psychological conditions of patients in a timely manner and is guided by nurses in the department who are qualified as psychological counselors.

The incidence of postoperative pulmonary atelectasis and infection in smart medicine was 1.78% and 2.96%, respectively, which was lower than that of T-shaped radiation rehabilitation. Meanwhile, the comparison of various lung function indexes between patients' admission and preoperative lung function in smart medicine showed that patients' MVV, FVC, and FEV1 improved, suggesting that respiratory function trainers can improve patients' lung function and reduce postoperative lung function complications significantly. According to the basic principles of respiratory mechanics, there are fast breathing zones and slow breathing piers in human lung tissue. Due to postoperative pain and other reasons, patients have improper breathing patterns that allow gas to enter only the fast breathing zone of the lungs. After open heart surgery, the patient breathes less tidal volume, and at the same time, due to increased sputum secretion, fine bronchial constriction, or sputum not cleared in time, it is easy to cause complications such as pneumonia and pulmonary atelectasis. Therefore, effective respiratory function training in the perioperative period is important for the prevention of postoperative complications.

The NRS scores on postoperative days 2, 3, 4, and 5 were (3.64 ± 0.78), (2.73 ± 0.72), (2.37 ± 0.78). 0.59), and (1.87 ± 0.59) for the patients in smart medical *B*, respectively, which were lower than those of conventional rehabilitation, and the differences were statistically significant. This is consistent with the findings of [23] that postoperative multimodal analgesia can reduce postoperative pain scores. Open heart surgery is the most traumatic surgical procedure, and severe pain caused by surgical trauma and postoperative indwelling chest drains is the main cause of patients' stress reactions. Due to postoperative pain, patients have difficulty with sputum evacuation, restricted activities, depressed mood, and decreased immunity. Therefore, effective postoperative analgesia is especially important to accelerate patients' postoperative recovery. While the traditional concept of postoperative analgesia is to administer medication while the patient is in pain, the concept of smart medical surgery is multimodal analgesia and timed and scheduled medication. Due to the misunderstanding of traditional pain medication, some patients are reluctant to receive oral pain medication after surgery because they fear that taking pain medication will become addictive and affect postoperative wound healing. Pain education guided by the concept of smart medicine should focus on explaining to patients and families that short-term use of analgesics is not carcinogenic and is beneficial to postoperative recovery. Equipped with a portable pain scale, the content of pain education should be displayed with slides to ensure accurate and comprehensive understanding and acceptance by patients and their families.

The recovery time of postoperative bowel sounds in smart medicine was (21.40 ± 2.60) hours, which was shorter than the conventional rehabilitation, and the difference was statistically significant. One of the concepts of smart medicine is to get patients out of bed as early as possible after surgery, which can provide multiple psychological benefits to patients. A study [24] found that early postoperative bedtime activity improved splanchnic neuromodulation, promoted the recovery of gastrointestinal function, and prevented abdominal distension. A prospective randomized controlled study concluded that rapid postoperative rehabilitation of colorectal cancer patients to get out of bed and move around with exhaustion and defecation earlier than traditional rehabilitation methods promoted postoperative rehabilitation and recovery. However, in clinical work, medical staff and patients' families often consider the risk of postoperative complications, such as patients' weakness and early bed activity. Meanwhile, this study showed that the implementation of the trilogy did not increase the incidence of arrhythmias by getting out of bed, and the difference was not statistically significant. A study of 384 patients by foreign scholars found that early bed activity after gastrointestinal surgery did not increase the incidence of arrhythmias. There was a significant increase in the incidence of arrhythmias, falls, and other accidents. A study [25] of patients with resected bowel cancer also confirmed this idea. Getting out of bed as early as possible can accelerate blood circulation in the lower extremities, which can well prevent the occurrence of venous thrombosis in the lower extremities while maintaining the patient's good local skin and functional status. Early bed activity can also increase respiratory frequency, make secretions in the respiratory tract easier to discharge, reduce the occurrence of incisional infection, pulmonary atelectasis, and pleural effusion, promote lung recruitment, and improve patients' lung function.

In nursing interventions guided by the concept of smart medicine, emphasis is placed on helping patients get up early after surgery. Early waking up emphasizes that changing position as soon as possible on the day of surgery can effectively prevent the occurrence of upright hypotension, improve the patient's respiratory status, and promote the drainage of disease fluid if the patient's condition permits. From the first postoperative day, patients can sit and get up, thus promoting the recovery of peristalsis, reducing the occurrence of bloating and constipation, promoting blood return to the lower extremities, and reducing the risk of venous thrombosis of the lower extremities. With the increase in activity, the patient's bowel movement increases and the patient's appetite increases, which helps improve the nutritional status of the deceased, facilitate tissue repair and incision healing, enhance the patient's own self-care ability, and make the patient recover better after surgery. Optimistic awareness can accelerate the recovery process of patients, minimize the number of escorts, and reduce the burden and pressure on patients' families and is also important for shortening the number of treatment days and reducing hospitalization costs.

5. Conclusion

First, intelligent medical rehabilitation nursing has good application value in the postoperative recovery of thoracoscopic lung cancer surgery patients, and the application of its concept is safe and feasible.

Second, the intelligent medical rehabilitation nursing model in the postoperative recovery of patients undergoing thoracoscopic lung cancer surgery reduces patients' pain, decreases the incidence of postoperative complications, shortens the retention time of chest drains, improves patients' comfort during the perioperative period, and reduces the number of hospital days and hospitalization costs, and this nursing intervention is better than conventional nursing.

Third, the implementation of the intelligent medical rehabilitation care model can help promote the postoperative recovery of patients undergoing thoracoscopic lung cancer surgery and improve the overall quality of life of patients.

6. Prospects and Shortcomings

First, in the context of the current postoperative management of lung cancer, the development of the intelligent medical rehabilitation nursing model improves the efficiency of patient recovery, gives patients more effective measures for perioperative nursing interventions, helps improve their survival quality, and provides an important experimental basis and theoretical basis for improving the postoperative survival quality or clinical symptoms of patients undergoing thoracoscopic lung cancer resection,

which is worthy of further clinical application and promotion.

Secondly, the shortcomings of this study are that the research method is retrospective, with large bias, rough, and often inaccurate due to incomplete records, increased errors, subjective factors, and other shortcomings such as the inability to compare the observation group with the control group simultaneously and perform random sampling for the sample source. So the next study should also screen and include more cases that meet the criteria for more in-depth analysis and fully incorporate consideration of post-radiotherapy treatment to draw more meaningful conclusions and provide an important reference for intelligent medical rehabilitation care treatment of lung cancer.

Data Availability

The simulation experiment data used to support the findings of this study are available from the corresponding author upon request.

Conflicts of Interest

The authors declare that they have no conflicts of interest regarding the publication of this paper.

Authors' Contributions

Yujing Zhou and Ming Xu are contributed equally to this work.

References

[1] Y. H. Hou, W. C. Shi, S. Cai et al., "Effect of intravenous lidocaine on serum interleukin-17 after video-assisted thoracic surgery for non-small-cell lung cancer: a randomized, double-blind, placebo-controlled trial," *Drug Design, Development and Therapy*, vol. 15, pp. 3379–3390, 2021.

[2] X. Li, K. Chen, F. Yang, and J. Wang, "Perspectives on early-stage lung cancer identification and challenges to thoracic surgery," *Chronic Diseases and Translational Medicine*, vol. 8, no. 2, pp. 79–82, 2022.

[3] T. R. Grenda, S. Whang, and N. R. Evans, "Transitioning a surgery practice to telehealth during COVID-19," *Annals of Surgery*, vol. 272, no. 2, pp. e168–e169, 2020.

[4] A. H. Sadeghi, A. P. M. Maat, Y. J. J. Taverne et al., "Virtual reality and artificial intelligence for 3-dimensional planning of lung segmentectomies," *JTCVS Techniques*, vol. 7, pp. 309–321, 2021.

[5] T. J. Batchelor and O. Ljungqvist, "A surgical perspective of ERAS guidelines in thoracic surgery," *Current Opinion in Anaesthesiology*, vol. 32, no. 1, pp. 17–22, 2019.

[6] X. Wei, H. Yu, W. Dai et al., "Discrepancy in the perception of symptoms among patients and healthcare providers after lung cancer surgery," *Supportive Care in Cancer*, vol. 30, no. 2, pp. 1169–1179, 2022.

[7] D. Sanchez-Lorente, R. Guzman, M. Boada, N. Carriel, A. Guirao, and L. Molins, "Is it appropriate to perform video-assisted thoracoscopic surgery for advanced lung cancer?" *Future Oncology*, vol. 14, pp. 29–31, 2018.

[8] J. Burel, M. El Ayoubi, J. M. Baste et al., "Surgery for lung cancer: postoperative changes and complications—what the radiologist needs to know," *Insights into Imaging*, vol. 12, no. 1, pp. 116–213, 2021.

[9] R. Prieto, B. Ferrell, J. Y. Kim, and V. Sun, "Self-management coaching: promoting postoperative recovery and caregiving preparedness for patients with lung cancer and their family caregivers," *Clinical Journal of Oncology Nursing*, vol. 25, no. 3, pp. 290–296, 2021.

[10] J. C. R. Alcantud, G. Varela, B. Santos-Buitrago, G. Santos-García, and M. F. Jiménez, "Analysis of survival for lung cancer resections cases with fuzzy and soft set theory in surgical decision making," *PLoS One*, vol. 14, no. 6, Article ID e0218283, 2019.

[11] H. Yu, Q. Yu, Y. Nie et al., "Data quality of longitudinally collected patient-reported outcomes after thoracic surgery: comparison of paper-and web-based assessments," *Journal of Medical Internet Research*, vol. 23, no. 11, Article ID e28915, 2021.

[12] C. Pompili, M. Koller, G. Velikova et al., "EORTC QLQ-C30 summary score reliably detects changes in QoL three months after anatomic lung resection for non-small cell lung cancer (NSCLC)," *Lung Cancer*, vol. 123, pp. 149–154, 2018.

[13] L. V. Klotz, C. Gruenewald, E. L. Bulut et al., "Cytoreductive thoracic surgery combined with hyperthermic chemoperfusion for pleural malignancies: a single-center experience," *Respiration*, vol. 100, no. 12, pp. 1165–1173, 2021.

[14] M. L. L. Madariaga, F. M. Troschel, T. D. Best, S. J. Knoll, H. A. Gaissert, and F. J. Fintelmann, "Low thoracic skeletal muscle area predicts morbidity after pneumonectomy for lung cancer," *The Annals of Thoracic Surgery*, vol. 109, no. 3, pp. 907–913, 2020.

[15] Y. Yasuura, H. Konno, T. Hayakawa et al., "Chylothorax after pulmonary resection and lymph node dissection for primary lung cancer; retrospective observational study," *Journal of Cardiothoracic Surgery*, vol. 17, no. 1, pp. 11–16, 2022.

[16] W. Dai, S. Chang, C. Pompili et al., "Early postoperative patient-reported outcomes after thoracoscopic segmentectomy versus lobectomy for small-sized peripheral non-small-cell lung cancer," *Annals of Surgical Oncology*, vol. 29, no. 1, pp. 547–556, 2022.

[17] Z. Xiang, B. Wu, X. Zhang et al., "Preoperative three-dimensional lung simulation before thoracoscopic anatomical segmentectomy for lung cancer: a systematic review and meta-analysis," *Frontiers in surgery*, vol. 9, Article ID 856293, 2022.

[18] A. E. Abbas, "Surgical management of lung cancer: history, evolution, and modern advances," *Current Oncology Reports*, vol. 20, no. 12, pp. 98–107, 2018.

[19] Y. J. Chang, K. C. Hung, L. K. Wang et al., "A real-time artificial intelligence-assisted system to predict weaning from ventilator immediately after lung resection surgery," *International Journal of Environmental Research and Public Health*, vol. 18, no. 5, p. 2713, 2021.

[20] J. Smelt, F. Martin, M. Al-Sahaf et al., "Retrospective observational study into the early causes of death following surgery for NSCLC," *The Thoracic and Cardiovascular Surgeon*, vol. 68, no. 7, pp. 633–638, 2020.

[21] Z. Wu, Q. Wang, C. Wu et al., "Three-port single-intercostal versus multiple-intercostal thoracoscopic lobectomy for the treatment of lung cancer: a propensity-matched analysis," *BMC Cancer*, vol. 19, no. 1, p. 8, 2019.

[22] H. Begum, A. Swaminath, Y. Lee et al., "The histologic effects of neoadjuvant stereotactic body radiation therapy (SBRT) followed by pulmonary metastasectomy—rationale and protocol design for the post SBRT pulmonary metastasectomy

Hindawi
Emergency Medicine International
Volume 2023, Article ID 9816329, 1 page
https://doi.org/10.1155/2023/9816329

Retraction

Retracted: Effect of Zhuyun I Recipe Capsule Enema on the Immune Microenvironment of the Endometrium during Implantation Window in Rats

Emergency Medicine International

Received 8 August 2023; Accepted 8 August 2023; Published 9 August 2023

This article has been retracted by Hindawi following an investigation undertaken by the publisher [1]. This investigation has uncovered evidence of one or more of the following indicators of systematic manipulation of the publication process:

(1) Discrepancies in scope
(2) Discrepancies in the description of the research reported
(3) Discrepancies between the availability of data and the research described
(4) Inappropriate citations
(5) Incoherent, meaningless and/or irrelevant content included in the article
(6) Peer-review manipulation

The presence of these indicators undermines our confidence in the integrity of the article's content and we cannot, therefore, vouch for its reliability. Please note that this notice is intended solely to alert readers that the content of this article is unreliable. We have not investigated whether authors were aware of or involved in the systematic manipulation of the publication process.

Wiley and Hindawi regrets that the usual quality checks did not identify these issues before publication and have since put additional measures in place to safeguard research integrity.

We wish to credit our own Research Integrity and Research Publishing teams and anonymous and named external researchers and research integrity experts for contributing to this investigation.

The corresponding author, as the representative of all authors, has been given the opportunity to register their agreement or disagreement to this retraction. We have kept a record of any response received.

References

[1] H. Zhou, P. Guo, P. Zeng et al., "Effect of Zhuyun I Recipe Capsule Enema on the Immune Microenvironment of the Endometrium during Implantation Window in Rats," *Emergency Medicine International*, vol. 2022, Article ID 4746121, 11 pages, 2022.

Hindawi
Emergency Medicine International
Volume 2022, Article ID 4746121, 11 pages
https://doi.org/10.1155/2022/4746121

Research Article

Effect of Zhuyun I Recipe Capsule Enema on the Immune Microenvironment of the Endometrium during Implantation Window in Rats

Hang Zhou,[1] Pei Guo,[1] Pengfei Zeng,[1] Zhixing Yin,[1] Li Yan,[1] Jinzhu Huang,[1] Yi Wang,[2] Juan Li,[2] Wanting Xia,[3] Yang Wang,[4] Chang Liu,[5] and Qian Zeng [3]

[1]*Department of Gynecology, Chengdu University of Traditional Chinese Medicine, Chengdu, Sichuan, China*
[2]*Department of Pathology, Hospital of Chengdu University of Traditional Chinese Medicine, Chengdu, Sichuan, China*
[3]*Department of Gynecology, Hospital of Chengdu University of Traditional Chinese Medicine, Chengdu, Sichuan, China*
[4]*Department of Gynecology, Xinan Gynecological Hospital, Chengdu, Sichuan, China*
[5]*Department of Gynecology, Zhengzhou Third People's Hospital, Chengdu, Sichuan, China*

Correspondence should be addressed to Qian Zeng; zqian666d@126.com

Received 30 July 2022; Revised 31 August 2022; Accepted 8 September 2022; Published 7 October 2022

Academic Editor: Hang Chen

Background. Preterm birth is the leading cause of neonatal death, and there are no effective clinical means for the prevention and treatment of spontaneous preterm birth, mainly because the mechanism for labor initiation has not been fully elucidated. *Objective*. The effect of enucleation with Zhuyun I Recipe Capsule enema (ZRC) on the maternal-fetal interface microenvironment in SD rats with kidney deficiency and blood stasis. *Methods*. In this study, poor endometrial tolerance was induced by hydroxyurea and epinephrine in SD rats with kidney deficiency and blood stasis type of endometrium, and gavage with norethindrone (estradiol) or Bamboo Rhythm No.1 formula. HOXA10 mRNA levels were measured by qPCR. In addition, the expression of IL-6, VEGF, TGF–β, and IGFBP-1 in the uterus was detected by IHC and ELISA. *Results*. Hydroxyurea- and epinephrine-induced PER was associated with low levels of HOXA10 in the endometrium and reduced levels of IL-6, TGF-β, VEGF, and IGFBP-1 in the endometrium. These were abolished by ZRC and Progynova treatment compared to PER rats, resulting in a dramatic increase in the levels of HOXA10 mRNA, IL-6, TGF-β, VEGF, and IGFBP-1 proteins. *Conclusions*. ZRC improves metaplasticization of endometrial stromal cells and promotes angiogenesis in rats with kidney deficiency and blood stasis. The moderate dose of kidney tonic to promote blood circulation method is superior in promoting angiogenesis, facilitating the establishment and maintenance of pregnancy, limiting trophoblast invasion of metaplasia, reducing miscarriage, and improving pregnancy rate.

1. Introduction

The World Health Organization (WHO) estimated in 2013, based on globally available health data, that one in four (25%) couples living in developing countries with a normal desire to have children fail to meet their fertility needs, with female infertility accounting for about one in two of these cases [1, 2]. The latest 2015 guidelines of the American Society for Reproductive Medicine (ASRM) define infertility as the failure of a couple of reproductive age to conceive successfully when they have lived together for more than 1 year, have normal sexual intercourse, and do not use any contraception [3, 4]. For women unilaterally, infertility is the inability to conceive and absence of a full-term delivery despite a pregnancy [5]. From pregnancy to childbirth, women bear more responsibility and stress, both in terms of the vertical line of time spanning the length and the horizontal line of physical burden. With the rise of equal rights for men and women, women are increasingly involved in social production activities and share the cost of living of the

family, which inevitably generates more interest, psychological and environmental pressures, plus the fact that Chinese traditional culture is born from Confucianism, which emphasizes the idea of peace as the most important thing, and preaches that "if you don't tolerate a small amount, you will make a big mistake." The traditional Chinese culture is based on Confucianism, which emphasizes the idea of harmony and promotes the virtues of "if you don't tolerate a little, you'll make a big mistake," "if you tolerate, you'll get help," and "a gentleman doesn't argue," and the two schools of Buddhism and Taoism, which have a common influence on the cultural foundation. There are also related theories such as "the way of heaven is not contentious but good at winning, not saying anything but good at responding" and "of the six degrees and ten thousand actions, patience is the first" [6, 7]. These ideas and statements may have rarely been systematically studied or passively inculcated, but in the trajectory of an individual's growth from childhood to adulthood, there were moments and scenes where he or she was imbued with these ideas, such as the example of elders who taught by themselves. The strong cultural factors may lead Chinese women to have difficult thoughts such as "not good enough to say, afraid to say, unwilling to say" after stress arises, and no effective stress relief mechanism is formed [8]. As a result, gynecological diseases such as infertility occur.

If we think about infertility from a woman's perspective, we should divide the problem into two stages: one is the inability to conceive normally, and the other is the inability to deliver a healthy, viable fetus after pregnancy. Specifically, there are a series of complex, precise, and coordinated physiological processes, including the delivery of good-quality oocytes from the dominant follicle, the movement of the egg in the pelvis and fallopian tube, the swimming of sperm in the reproductive tract, the meeting of sperm and egg to exchange chromatin to form a fertilized egg, the coordination of the embryonic oogenesis progress with the endometrial tolerance, the positioning of the embryonic follicle for adhesion and implantation, the invasion of trophoblast cells, and the normal development of the blastocyst and fetus. The key intersection separating infertility from infertility is at the stage of blastocyst implantation (localized adhesive implantation), or the window of implantation [9, 10]. The endometrial implantation window is a relatively short period of time when the embryo and the intrauterine microenvironment are highly coordinated, synchronized, and unified, partially overlapping with the concept of endometrial tolerance, which simultaneously emphasizes that the role of the embryo cannot be ignored [10].

Kidney deficiency and blood stasis are common syndrome types of infertility [11]. Clinically, the prescription of the effect of Zhuyun I Recipe Capsule enema can achieve ideal results in patients with failed in vitro fertilization-embryo transfer (IVF-ET), kidney deficiency, and blood stasis. Although there are studies on the correlation between laminin and infertility, abnormal expression of adhesion molecules based on kidney deficiency and blood stasis models has not been observed and explained. Although the rectal route has higher bioavailability and reduced hepatic metabolic burden than the oral and force-feeding routes, it has rarely been used in infertility-related animal studies. Therefore, this paper focuses on the effects of the Zhuyun I Recipe Capsule enema prescription on endometrial metaplasia in rats with kidney deficiency and blood stasis models on day 8 of pregnancy and factors related to TGF-β, IL-6, and VEGF at the gestational-fetal interface, and explores the possible mechanisms of its role in theoretical support for pregnancy.

2. Material and Method

2.1. Ethics Statement. The scheme of the animal experiment was approved by the institutional and local animal care and use committees from the Hospital of the Chengdu University of TCM (#2019DL006).

2.2. Animal Study. SPF female SD rats ($n = 36$, 5-week-old, 220–240g) from Kunming Laboratory Animal Center were kept in polypropylene cages with sawdust bedding at room temperature with 50% humidity, 12/12 light/dark cycle, and free access to food or water.

After acclimatization, 36 rats were randomly separated into six groups ($n = 6$)[3]. Control rats received 0.9% saline. Rats of H-A (hydroxyurea-adrenaline)-treated group received hydroxyurea (9CO63D05) at a dose of 400 mg/kg daily orally for 9 days, and adrenaline (1710201) at a dose of 0.3 mg/Kg subcutaneously at day 4 to establish the poor endometrial receptivity (PER). Positive control rats (Progynova group) received Progynova (512306042) at a dose of 0.02 mg/kg daily orally for 9 days[4]. In this experiment, the drug dose of SD rats was compared with that of adults (weight: 50 kg). According to the conversion method of drug use dose between rats and humans in "pharmacological experimental methods," the equivalent dose ratio of the two was 0.018[3]. The formula was as follows: the clinical dose of humans was set as χ mg/kg, and the dose conversion of SD rats was as follows:

$$\text{Dosage for } rats \frac{\chi mg/kg * 50kg}{0.2Kg} * 0.018 = 4.5 \div \frac{mg}{kg}. \quad (1)$$

In ZRC treatment groups, increasing concentrations of TCM were enema (Patent No: ZL20141039113.7) to rats for 10 days at low, middle, and high doses at 8.21, 16.43, and 32.86 g/kg·BW, respectively, each day in the morning (Figure 1). Zhuyun No.1 prescription's composition, proportion, origin, and preparation of the drug are shown in Table 1. Distilled water was used for preparing drugs. Zhuyun No.1 prescription was provided by our hospital. The enema fixator and enema procedure of rats are shown in Figures 1(a) and 1(b).

On day 10, female and male rats (2 : 1) were put together. The day seeing vaginal plugs was set as pregnancy day 1 and drugs were provided until day 5. Then, rats were killed for ELISA assay and checking implantation status[5]. Both implantation rate and average number of embryos were sharply decreased in PER rats compared to controls,

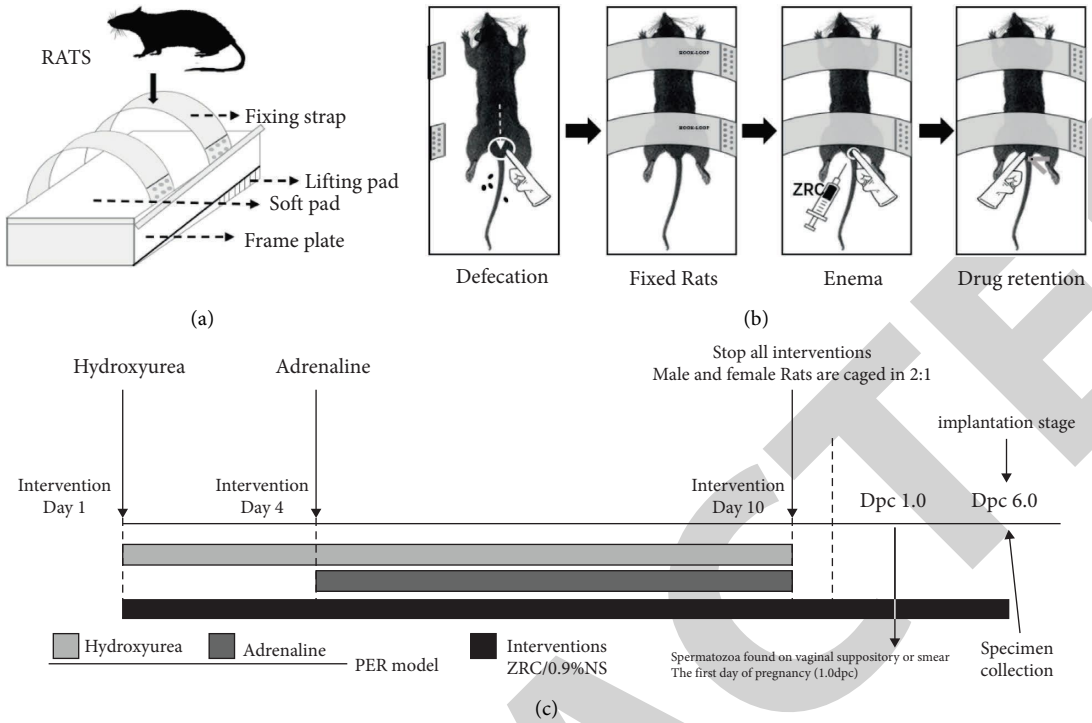

Figure 1: Note: (a) Rat enema fixator: it is composed of a fixing strap, soft pad, and frame plate. (b) Rat enema administration process: the rats were placed in the prone position and bound to the fixator by hook loop; and the operator stroked the abdomen of rats along the colon and stimulated the anus of rats so that the rats could discharge the feces of the lower intestinal tract as much as possible and make them empty, which is conducive to the retention and absorption of liquid medicine. Next, it was confirmed that the feces were no longer excreted, the operator raised the sacrococcygeal region of rats about 40° and injected the liquid into the anus of rats about 8 cm with a 5 ml enema syringe, and pushed it slowly and evenly. After pushing, one hand was used to take out the syringe, while the other hand immediately used the sterilized wooden clip to clamp the anus, keeping it for 20 minutes, and putting it into the cage; (c) Experimental intervention flowchart.

Table 1: Composition and source of Zhuyun I prescription.

Product name	Scientific name	Production unit	B.N.	Place of production	Proportion of weight
TuSizi	*Cuscuta chinensis lam.*	Sichuan Guoqiang Herbal Pieces Co., Ltd	19030104	Sichuan	3
FuPenzi	*Rubus idaeus* L.	Sichuan BaiCaoYuan Pharmaceutical Co., Ltd	190401	Zhejiang	2
GouQizi	*Lycium chinense Mill.*	Sichuan Qianyuan Herbal Pieces Co., Ltd	191201	NingXia	2
DanShen	*Salvia miltiorrhiza Bunge.*	Sichuan Jiuweige Herbal Pieces Co., Ltd	191901	Sichuan	2
XuDuan	Dipsacales	Sichuan Heyi Natural Pharmaceutical Co., Ltd	19071704	Sichuan	4
Shanzha	*Crataegus pinnatifida Bunge*	Sichuan Hengkangyuan Pharmaceutical Co., Ltd	191001	Shanxi	3
ShanYao	*Dioscorea oppositifolia* L.	Sichuan Guoqiang Herbal Pieces Co., Ltd	19080105	Henan	3
SiGualuo	*Luffa cylindrica*	Sichuan Herbal Pieces Co., Ltd	190614	Sichuan	3

indicating the successful PER establishment. The intervention flow chart of the whole experiment is shown in Figure 1(c).

2.3. Procedure of Rat Enema Drug Administration. After 1 week of acclimatization and observation of the vital status and general signs of the adult female rats of SPF class SD, the rats were weighed and numbered after confirmation of no obvious pathology. Pull up vertically (avoid lifting from the end to cause damage); place in the supine position, exposing the lower abdomen; assistant No. 2 synchronous preparation: raise the sacrococcygeal area of the rat about 40°, use a 5ml enema syringe to inject the liquid into the rat's anus about 8cm. After pushing, take out the syringe with one hand, and immediately clamp the anus with a sterilized wooden clip with the other hand, keep it for 20 minutes, and put it into the cage, as shown in Figure 1.

2.4. Procedure of Smear Operation to Monitor Morphological Changes in Endometrium. Operate in the following acid-base staining sequence: 95% alcohol fixation ⟶ hematoxylin staining ⟶ tap water wash ⟶ 1% hydrochloric acid differentiation ⟶ tap water wash ⟶ 1% eosin staining ⟶ tap water wash ⟶ xylene solution. The operation time of each step was as follows: 5 min, 7 min, 5–10s, 5s, 5–10s, 1 min, 5–10s, and 5 min; and remove the

slide to control the excess liquid. Then, place the slide in a position with good air convection to dry naturally and place it under the microscope for observation. (Points to note: when the cotton swab is applied to the slide, firstly, the front and back of the slide should be distinguished, and the frosted side, which is convenient for writing the number in the hand, should be the front side, which is conducive to the last step of microscopic observation (reducing the time for distinguishing the front and back sides); secondly, the force should be appropriate so that the secretion is transferred to the slide without destroying the cells, and the overlap of the different spreads on the same slide should be minimized to reduce the stacking of cells. Because the nuclear staining solution has certain volatility and the degree of cell density and sparseness varies, the specific staining time can be adjusted according to the specific situation. The staining time can be adjusted according to the specific situation).

2.5. Scanning Electron Microscopy Observation. Acicular cells (number and morphology): SEM preparation procedure: fixation with osmic acid for 2 hours at 4°C; rinse with distilled water twice (8 minutes each); stepwise dehydration twice in 50%, 70% and 90% ethanol (each 8 minutes); 100% alcohol dehydration at room temperature for 10 minutes; isoamyl acetate = 1 : 1, 3 : 7, 1 : 9, each dehydration for 10 minutes; pure isovaleric acid dehydration for 10 minutes; hexamethyldimethylamine drying 10 minutes". Ultrathin sections were made; acinar cell count: 12 fields of view were randomly selected from each sample to observe acinar cells according to the Rebecca method, and the lumen surface of endometrial epithelial cells was selected according to the range of acinar cells for scoring: 0 Score: no acinar cells; 1 score: < 25%; 2 score: 25%-50%; 3 score > 50%, then the scores were statistically analyzed.

2.6. Enzyme-Linked Immunosorbent Assay (ELISA). The uterine tissue was homogenized with five volume lysis buffer and centrifuged at 800 g for 15 min. The supernatant containing the cytoplasmic part was stored in a refrigerator at −80°C for the detection of indicator proteins. IL-6 kit (ab9324, Abcam, USA), TGF-β ELISA kit, VEGF ELISA kit, and IGFBP1 ELISA kit (F16921, F171720, and F15791, WESTING Co. Ltd, CHN) were used to detect the protein of uterine homogenate.

Preparation of standard solution: take eight 1.5 ml centrifuge tubes, add 900 μl sample diluent into the first tube, and add 500 μ l sample diluent into the second-to-eighth tubes. Add 100 μl of a standard solution of 10 μg/ml into the first tube, place it on the vortex mixer, and then suck out 500 μl with the sampler and move it to the second tube. In this way, repeated double dilution was performed, and 500 μl was aspirated from the seventh tube and discarded. The eighth tube was blank control. Dilute with 1 : 20 double distilled water, add 100 μl of plasma to each well, mix well, wash 4–6 times at 37°C for 40 min, dry on filter paper, add 50 μl double distilled water and primary antibody to each well except blank, mix well, wash plate at 37°C for 20 min, add 100 μl enzyme-labeled antibody, wash plate at 37°C for 10 min, and add 100 ul substrate working solution at 37°C in dark light. After 15 min, 100 UL of the solution was added to stop mixing, and OD450 was recorded. Taking 1000, 500, 250, 125, 62.5, 31.2, 15.6, and 0 ng/ml as abscissa and OD value as ordinate, the standard curve was drawn with software. The content of each index was calculated according to the OD value of the sample.

2.7. Immunohistochemical (IHC) Staining. Uteri were fixed in paraformaldehyde. After slicing, dewaxed sections were put into the dyeing vat, 3% methanol H2O2 was used for 15 min, and PBS was used for washing three times (8 min each). The slices were immersed in 0.01 M citrate buffer solution, boiled in the microwave oven, and then the power was cut off. The procedure was repeated one time 5 min later. After cooling, PBS was washed twice for 5 min each time. The blocking liquid of goat serum was dripped and kept at room temperature for 20 minutes. Rabbit anti-rat IL-6 polyclonal antibody (ab9324, Abcam, USA), rabbit anti-rat TGF-β polyclonal antibody (abs15221, Absin, CHN), rabbit anti-rat VEGF polyclonal antibody (abs131208, Absin, CHN), and rabbit anti-rat IGFBP-1 polyclonal antibody (abs136650, Absin, CHN) were added to the groups with different indexes. Add biotinylated second antibody at 37°C for 30 min; wash three times with PBS water for 5 min each time; use DAB color reagent kit, mix the reagent, drop it on the slice, develop color at room temperature, control the reaction time under the microscope, generally about 2 min, and wash with distilled water. The specimens were lightly counterstained with hematoxylin, dehydrated, transparent, mounting slides with neutral gum for light microscope examination. A Ba200 digital trinocular camera system (McCurdy Industrial Group Co., Ltd.) was used to capture 3 fields of view for the processes of dehydration, trimming, embedding, sectioning, staining, and sealing.

2.8. Relative Real-Time PCR (qRT-PCR) Assay. After thawing the tissue on ice, pour out the preservation solution, add 1 ml Trizol into the EP tube to extract DNA from uterine tissue, confirm the quality of nucleic acid, reverse transcription, add 90 μl referee water to dilute, add corresponding primers, using GAPDH as an internal reference, and the annealing temperature is 54°C. Amplification conditions as follows: 94°C 3 min, 30 cycles, and extension at 72°C for 10 min. Levels of Ang-1, Ang-2, and Tie-2 were measured by SYBR green method: HOXA10 F5′-TGCATATTTGGAATGCGCCG-3'and R5′-CCAAGAATCTCGCTGGGGTT-3′.

2.9. Statistical Analyses. SPSS 22.0 was applied for data analysis. If data not only meet the normal distribution but also conform to the homogeneity of variance, the one-way ANOVA and LSD test are used to compare the data among groups. If the data conform to the normal distribution but the variance is not uniform, thanes' T2 test is used for

comparison among groups after ANOVA analysis. The data in the following table are all expressed by means ± standard deviation ($x \pm s$). If data are not normally distributed, Mann–Whitney U test was adopted to analyze the comparison between the groups.

3. Results

3.1. Condition of Uterus and Endometrium. The wet weight of the uterus and the index of uterine organs of model rats were sharply decreased compared to normal controls (Figure 2). However, compared to model rats, the uterus wet weight and uterine organ index of low-, heavy-, and high-dose ZRC groups and the control group were significantly higher, especially in ZRC medium-dose group ($P < 0.05$). Under the light microscope, the endometrium of the blank group was covered with intact epithelium, well-developed, sufficient epithelial cells, abundant blood vessels, regular glands, large glandular cavity, and loose interstitial arrangement, showing spindle shape; in the model group, the endometrium was covered with thin, poorly developed, less epithelial cells, fewer glands, narrowed glandular space, not rich blood vessels, dense stroma, and some stromata were compact. The development was not synchronized. In ZRC low-, medium-, and high-dose groups, the endometrial epithelia showed an increasing trend. The epithelial cells were evenly arranged in a long columnar shape, with abundant glands. The glandular cavity was round or oval, with abundant blood vessels and even and loose stroma. The normal group had abundant villi, with mononuclear cells on the surface of the villi, round and full, as mature pinopodes; and the model group had few villi on the surface of the endometrium, with serious destruction, and a small amount of pinopodes expression in the developing stage. The level of pinopodes in the ZrC group was higher than that in the model rats, especially in the middle- and high-dose groups, and the pinopode expression in the middle-dose group tended to be mature. The number of pinopodes in the positive group was also more than that in the model rats, but slightly less than the drug group, for the developing pinhole, which tended to be mature.

3.2. IL-6 Expression in Endometrial Tissue in Treated Rat. The IL-6 expression in uterine tissue in PER H-A rats was sharply downregulated compared to normal controls (Figure 3). Compared to PER H-A rats, Progynova or TCM drastically upregulated IL-6 levels in uterine tissue ($P < 0.05$).

The TGF-β expression in endometrial PER H-A rats was sharply downregulated compared to controls (Figure 4). Compared to PER H-A rats, Progynova or ZRC at middle or high doses drastically upregulated TGF-β in endometrial. No significant difference was found between low-dose ZRC and model rats.

3.3. VEGF Levels. Compared to controls, PER H–A rats have lower uterine VEGF levels (Figure 5), which were sharply upregulated by Progynova or ZRC. Compared to PER-Progynova, high-dose ZRC drastically upregulated uterine VEGF.

3.4. IGFBP-1 Levels. PER H-A rats exhibited significantly lower uterine IGFBP-1 than controls (Figure 6), which were sharply upregulated by Progynova or ZRC treatment.

3.5. HOXA10 Levels. Compared to controls, PER H-A rats had a significantly low HOXA10 mRNA, which was sharply upregulated by Progynova. However, ZRC (8.21 g/kg) drastically upregulated HOXA10 mRNA, compared to Progynova treatment (Figure 7).

4. Discussion

The specific pathogenesis of endometriosis (EM) is still unclear and has been inconsistently understood by researchers over the years, including the implantation theory, the somatic epithelial metaplasia theory, and the induction theory [12]. The classical implantation theory proposed by Sampson has been accepted by many researchers, and the main routes of transmission include retrograde flow, lymphatic and venous dissemination, and medical implantation, among which the most recognized route of transmission is retrograde flow [13]. With a deeper understanding of EM, it was found that the explanation of the mechanism of EM pathogenesis by menstrual reflux seems to be one sided because it cannot explain multiple as well as extrapelvic EM, and fails to explain why only 10%–15% of so many women with common menstrual reflux develop EM [14].

In recent years, it has been proposed that EM is an immune disorder [15, 16]. The ectopic endometrial tissue in normal women acts as a foreign body that induces immune cells in the peritoneal fluid and stimulates an immune response, which results in the removal of endometrial tissue or cells that reflux with menstrual blood. In contrast, EM patients develop immune tolerance to their own organism, resulting in ectopic endothelial tissue or cells failing to be removed by evading surveillance by the immune system and thus implanting and growing in the pelvic abdomen, forming ectopic lesions.

It is increasingly recognized that angiogenesis is an important link in the development of EM, endometrial angiogenesis disorders may be an important pathological basis for EM pathogenesis and an important feature of EM, and the survival and growth of EM lesions are dependent on abundant blood supply [17]. The presence of a large number of blood vessels in the peritoneal and ectopic endothelial tissues surrounding EM was seen by laparoscopy and histopathology, respectively [18]. It was found that the in situ endothelium of EM patients was rich in vascular growth factors, and their vascular growth potential was stronger than that of the in situ endothelium of healthy women [19].This result is consistent with the "in situ endothelium" determinism proposed by Academician Lang Jinghe, who believes that ectopic endothelium can only become a lesion in the pelvic and abdominal cavity after the "three-part process" of adhesion, invasion, and blood vessels [20].

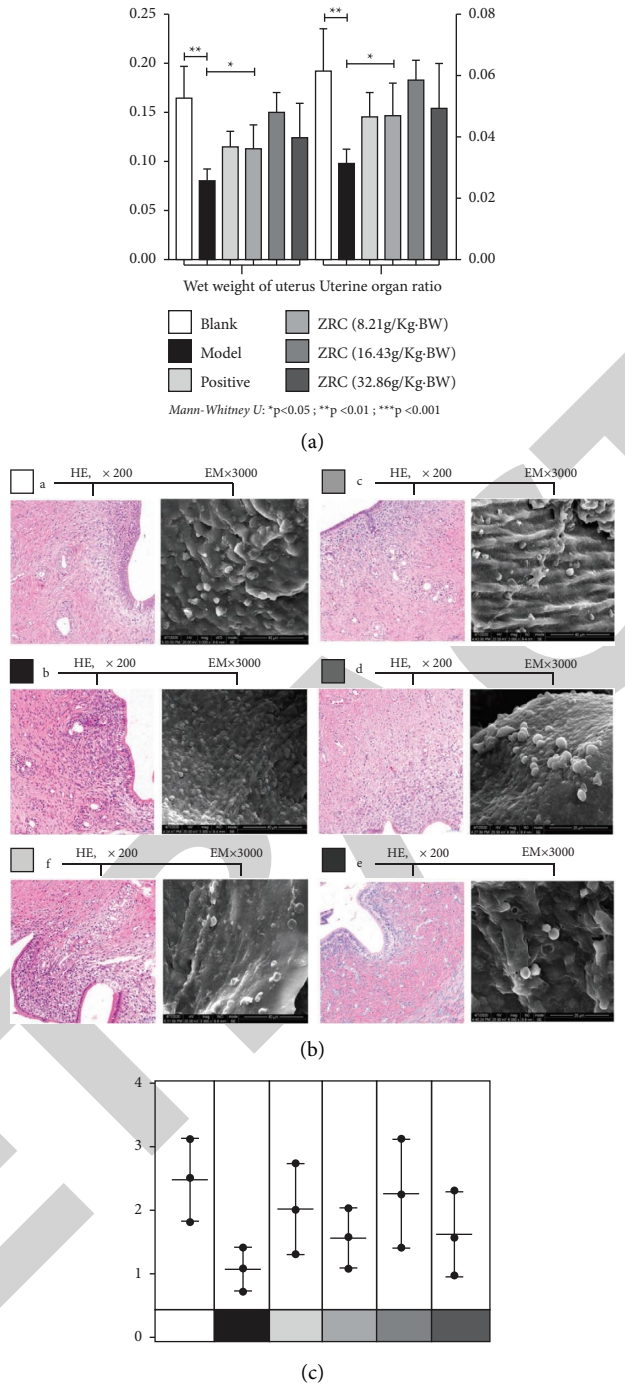

Figure 2: Note (a) wet weight of the uterus and the index of the uterine organs. (b) Expression of endometrial morphology (HE,×200) and pinocytosis morphology (SEM,×3000) in treated rats: (a) Controls; (b) Hydroxyurea + Adrenaline; (c) Progynova; (d) ZRC (8.21 g/kg·BW); (e) ZRC (16.43 g/kgv·BW); and (f) ZRC (32.86 g/kg·BW). (c) There were significant differences in the mean ± standard deviation of the endocytosis score under the electron microscope among the groups.

Enema is a traditional method of treating diseases by inserting drugs into the anus or intestines, and it has unique advantages in treating infertility. Firstly, the location of the uterus (womb and adnexa) is adjacent to the rectum, and the drug can act directly on the uterus and the ramus; secondly, the drug is warm but not hot, which can warm up the blood vessels; meanwhile, "the lung and the large intestine are adjacent to each other," and the drug can be delivered to the whole body through the action of "all the veins converge in the lung." According to this study, the formula of "activating the blood circulation around the rectum" avoids blood stagnation in the kidneys and clinical efficacy is better. Rectal administration can reduce the stimulation of drugs to the gastrointestinal tract and

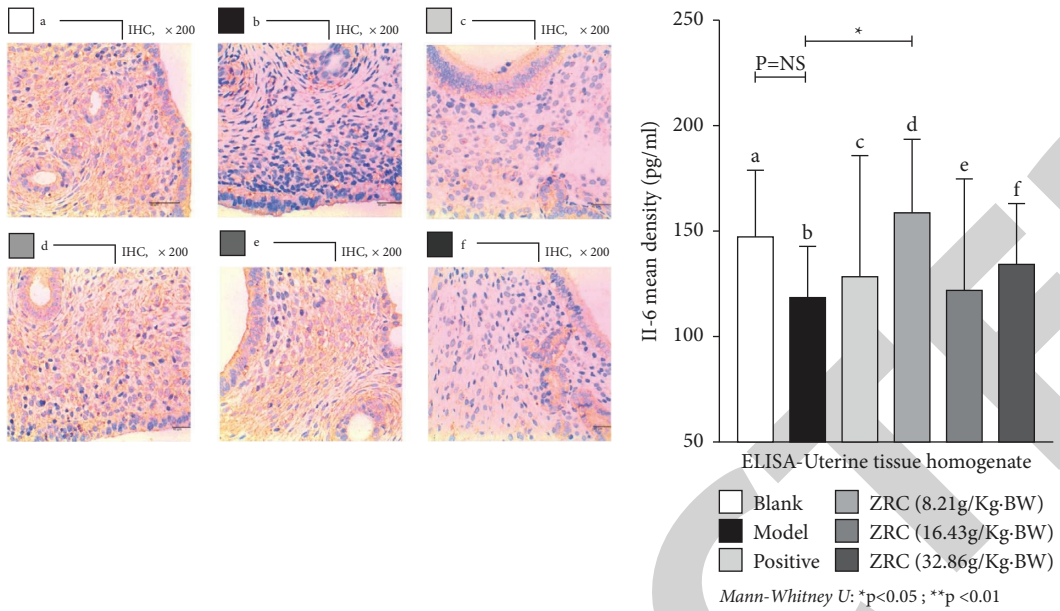

Figure 3: IL-6 levels in endometrial tissue. Note: (A) IHC staining of IL-6: (a) Normal controls; (b) H-A; (c) Progynova; (d) ZRC (8.21 g/kg·BW); (e) ZRC (16.43 g/kgv·BW); and (f) ZRC (32.86 g/kg·BW). (B) Levels of IL-6 by ELISA. TGF-β expression in endometrial tissue in treated rat.

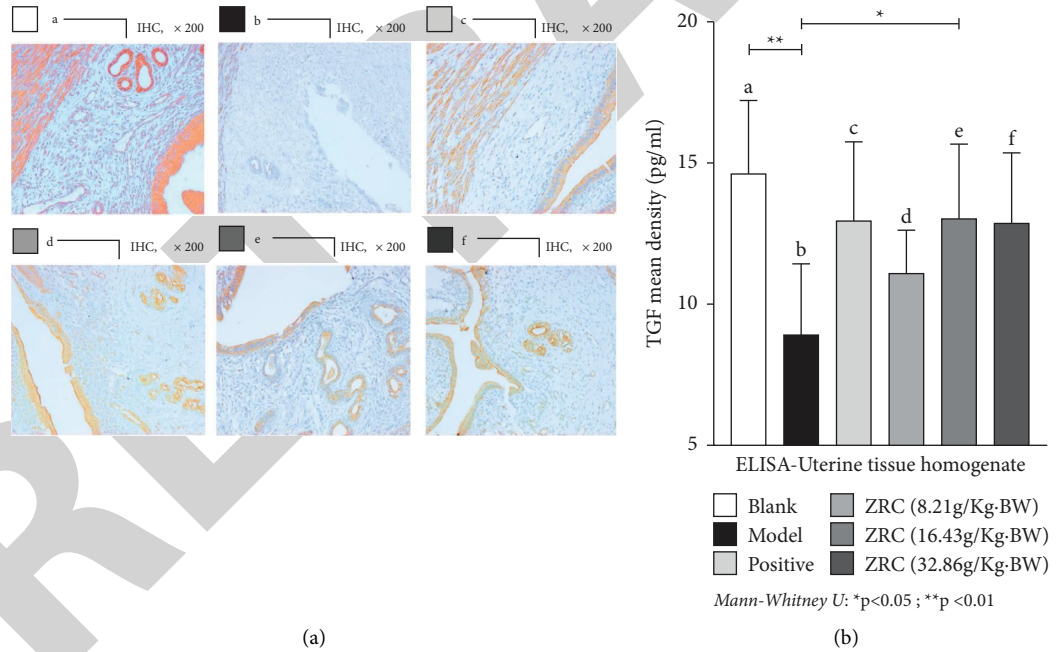

Figure 4: Levels of TGF-β. Note: (A) TGF-β levels in rat endometrial tissues: (a) Normal control; (b) H-A; (c) Progynova; (d) ZRC (8.21 g/kg); (e) ZRC (16.43 g/kg); and (f) ZRC (32.86 g/kg). (B) TGF-β in rat endometrial tissues is shown by ELISA.

improve the bioavailability of drugs; the absorption pathway is mainly absorbed by the middle rectal vein, inferior vein, and anal vein, accounting for 50%–70% of drug absorption; rectal administration significantly reduces the first-pass elimination effect of the liver and increases the local blood concentration; meanwhile, a small amount of drugs enter the liver from the superior rectal vein and participate in the general circulation after metabolism. Many clinical reports have shown that enemas can improve blood concentration, viscosity, and coagulability, improve endometrial blood supply, promote pelvic circulation, and increase clinical pregnancy rates in patients with infertility/IVF-ET failure [20]. See Figure 8.

Currently, an increasing number of studies have found that growth factors and cytokines play an important role in maternal-fetal interactions during embryo implantation [21]. On

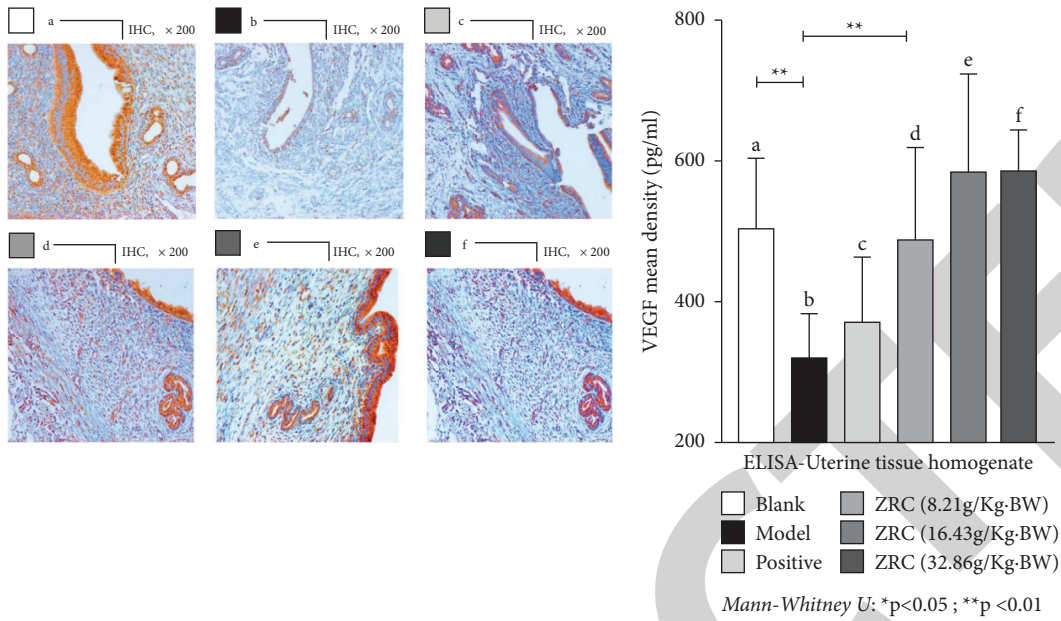

Figure 5: Levels of VEGF. Note: (A) VEGF levels in rat endometrial tissue: (a) Normal control; (b) H-A; (c) Progynova; (d) ZRC (8.21 g/kg BW); (e) ZRC (16.43 g/kg·BW); and (f) ZRC (32.86 g/kg·BW). (B) VEGF levels shown by ELISA.

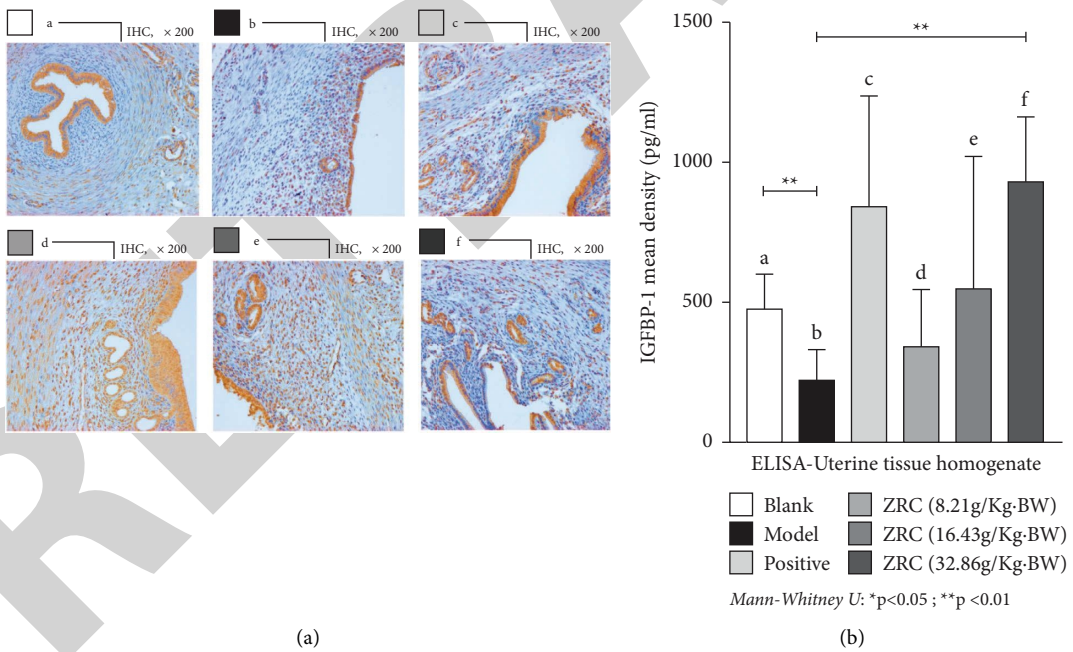

Figure 6: Levels of IGFBP-1. Note: (A) Endometrial GFBP-1 levels: (a) Normal control; (b) H-A; (c) Progynova; (d) ZRC (8.21 g/kg); (e) ZRC (16.43 g/kg); and (f) ZRC (32.86 g/kg). (B) IGFBP-1 levels are shown by ELISA.

the one hand, it is known that the endometrium makes inflammatory cytokines. On the other hand, cyclic changes in inflammatory cytokine expression in the uterus are associated with the proliferative and secretory phases, especially during the implantation window. Although some studies have shown that cytokines are regulated by steroid hormones such as estradiol and progesterone, some experimental studies have shown that autocrine and paracrine cytokines regulate local steroid hormones [22]. Thus, the balance of the inflammatory immune microenvironment at the embryo-maternal interface is indispensable for successful embryo positioning, adhesion, and implantation.

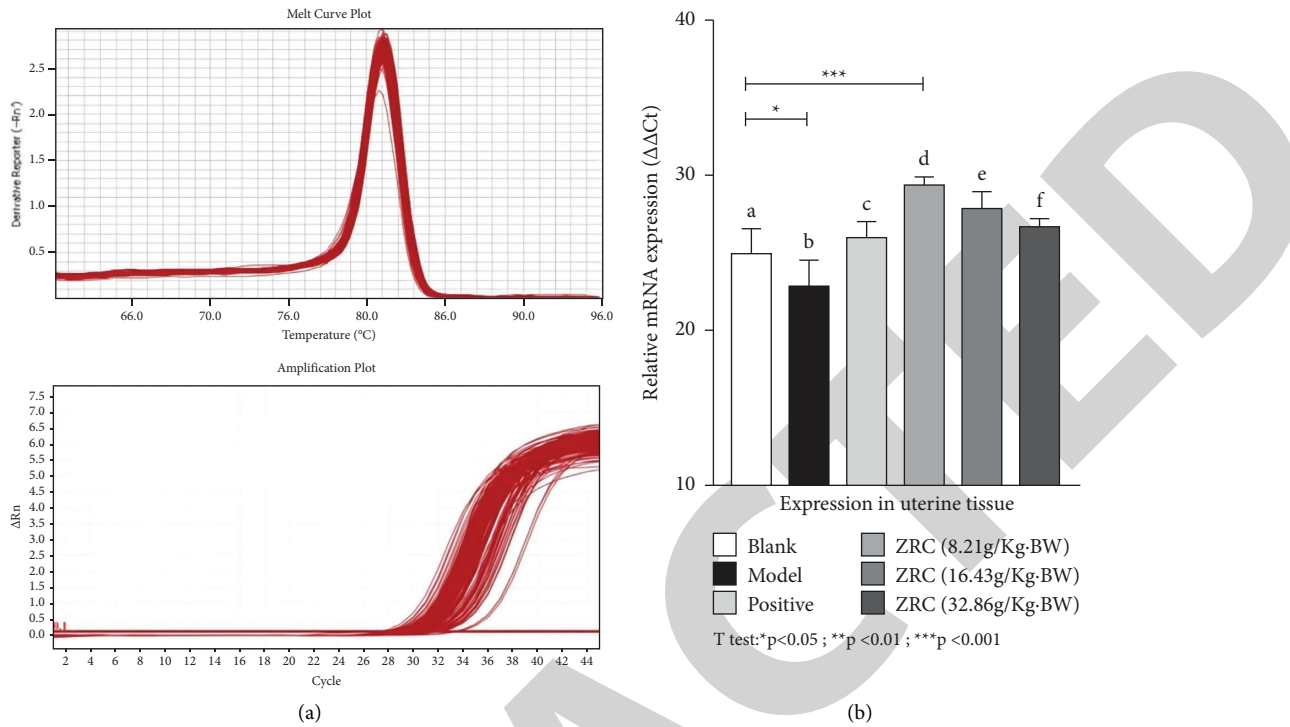

Figure 7: (a) HOXA10 concentration curve and initial concentration curve. Note: (B) Relative mRNA expression in endometrium: (a) Normal control; (b) H-A; (c) Progynova; (d) ZRC (8.21 g/kg BW); (e) ZRC (16.43 g/kg·BW); and (f) ZRC (32.86 g/kg·BW).

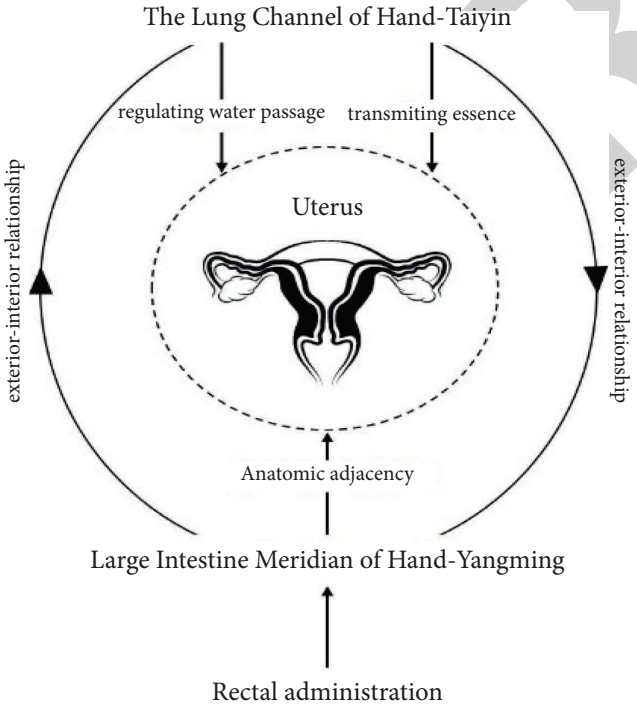

Figure 8: Mechanism of enema in TCM.

During the early stages of embryonic development, angiogenesis is the most essential condition for meconium and embryo implantation. The vascular endothelial growth factor is the most potent mitogenic factor that promotes blood vessel growth, stimulates angiogenesis, and maintains vessel wall permeability and integrity. A study [23] has shown that reduced or no expression of VEGF in localized areas can lead to poor angiogenesis, abnormal differentiation, and infiltration of trophoblast cells, resulting in miscarriage or implantation failure.

By comparing the morphology of metaphase on the 8th day of pregnancy, it was found that kidney deficiency and blood stasis could inhibit endometrial metaphase. Low, medium, and high doses of Zhuyun I Recipe Capsule improved methylation of endometrial stromal cells and promoted angiogenesis in rats with kidney deficiency and blood stasis. The middle dose of Zhuyun I Recipe Capsule was better than other groups in promoting angiogenesis, which was beneficial to the establishment and maintenance of pregnancy, limiting the invasion of trophoblast into the metaplasia, reducing abortion, and improving the pregnancy rate. It has a bidirectional regulating effect on ovulation, reduces the increase in blood viscosity caused by cold stimulation and blood clotting, can regulate reproductive endocrine, improve ovarian function, regulate analgesia and vasodilatory function of patients, and restore normal ovarian function. Study [24]showed that the warming and activating effect of Zhuyun I Recipe Capsule can promote the growth of endometrium and follicles and facilitate the discharge of follicles. The study [25] concluded that Bamboo Zhuyun I Recipe Capsule can promote ovulation and transport sperm, thus achieving the purpose of treating infertility.

Thus, from the analysis of the formula and modern pharmacology, as well as from the experimental and clinical efficacy of Zhuyun I Recipe Capsule for EM, it can effectively

treat EM by enhancing immunity (tonifying the kidney) and improving hemodynamics (resolving blood stasis).

4.1. Problems and Prospects. The shortcomings of this experimental study: firstly, the estrogen level of rats is much lower than that of humans, and there may be some limitations when extrapolating the results from animal models to humans; secondly, in the rat autologous endograft mapping over, considering the large workload, different personnel were involved in the suturing, which caused some errors in the experiment. In combination with this experiment, we will conduct clinical and in vitro cellular experiments in the future to further explore the specific mechanism of action of Zhuyun I Recipe Capsule on EM with kidney deficiency and blood stasis. Second, in the future EM modeling process, we will learn from the experience of this experiment and adopt a clear division of labor to achieve uniformity and minimize avoidable errors due to handling factors.

Data Availability

The data used to support the findings of this study can be obtained from the corresponding author upon reasonable request.

Conflicts of Interest

The authors declared that they have no conflicts of interest regarding this work.

Acknowledgments

The project was funded by the National Natural science foundation of China (no. 81973901), Key R&D projects in Sichuan Province (no. 2020YFS0043), and Chengdu Science and technology benefiting people project (no. 2016-HM01-00343-SF).

References

[1] H. Achache and A. Revel, "Endometrial receptivity markers, the journey to successful embryo implantation," *Human Reproduction Update*, vol. 12, pp. 731–746, 2006.

[2] Li Ying and R. Zhu, "Studies on the expression of integrin β1 and laminin in endometrium of infertile patients and normal early pregnancy decidual tissue," *Journal of Mathematical Medicine*, vol. 20, no. 5, pp. 640–642, 2007.

[3] J. Sun, *Animal Experiment Method*, pp. 422–435, People's Medical Publishing House, Beijing China, 2001.

[4] F. Qianyi, D. He, and L. Xu, "Establishment of a rat model of kidney deficiency, blood stasis and endometrial receptivity," *Henan Traditional Chinese Medicine*, vol. 34, no. 4, pp. 618–621, 2014.

[5] Z. Peng, K. Hai-Bin, and D. O. Physiology, *Endometrial Decidualization Model and its Application Research Progress*, Journal of Nanchang University(Medical ences), 2013.

[6] X. Wanting, Z. Yanmei, Z. Ying et al., "Curative effect of assisted reproduction technology by Traditional Chinese Medicine multi-channel interventional therapy on 95 cases of in vitro fertilization and embryo transfer failure," *Journal of Traditional Chinese Medicine*, vol. 37, no. 5, pp. 681–687, 2017.

[7] X. Hongxiang, "Clinical observation on endometriosis-induced infertility treated by herbal enema," *Journal of Practical Traditional Chinese Medicine*, 2011.

[8] M. Salker, G. Teklenburg, M. Molokhia et al., "Natural selection of human embryos:impaired decidualization of endometrium disables embryo-maternal interactions and causes recurrentpregnancy loss," *PLoS One*, vol. 5, no. 4, Article ID e10287, 2010.

[9] S. Li, F. Zhao, and R. Liu, "Expression of matrix metalloproteinase-9 and laminin and pregnancy outcome in abortion model," *Shanxi Medical Journal*, vol. 36, no. 2, pp. 99–102, 2007.

[10] Y. Shi, L. Wu, and G. Mu, "Effects of erjianyu decoction and modified Recipe on the expression of integrin $\alpha v\beta 3$, SCF mRNA and HOA-10 mRNA in mouse endometrium," *Chinese Journal of Traditional Chinese Medicine*, vol. 32, no. 5, pp. 1997–2000, 2017.

[11] S. Tabibzadeh, Q. F. Kong, A. Babaknia, and L May, "Progressive rise in the expression of interleukin-6 in human endometrium during menstrual cycle is initiated during the implantation window," *Human Reproduction*, vol. 10, no. 10, pp. 2793–2799, 1995.

[12] M. Dziekoński, A. Zmijewska, A. Franczak, G. Kotwica, W. Czelejewska, and S. Okrasa, "The expression of mRNAs for opioid precursors in endometrium of cyclic and early pregnant pigs; effects of IL-1β, IL-6 and TNFα," *Journal of Animal and Feed Sciences*, vol. 24, no. 2, pp. 118–126, 2015.

[13] J. D. Godkin and J. J. Doré, "Transforming growth factor beta and the endometrium," *Reviews of Reproduction*, vol. 3, pp. 1–6, 1998.

[14] S. N. Lennard, F. Stewart, and W. R. Allen, "Transforming growth factor-β1 expression in the endometrium of the mare during placentation," *Molecular Reproduction and Development*, vol. 42, no. 2, pp. 131–140, 1995.

[15] M. R. Kim, D. W. Park, J. H. Lee et al., "Progesterone-dependent release of transforming growth factor-beta1 from epithelial cells enhances the endometrial decidualization by turning on the Smad signalling in stromal cells," *MHR: Basic science of reproductive medicine*, vol. 11, pp. 801–808, 2005.

[16] X. J. Yi, H. Y. Jiang, K. K. H. Lee, W. S. O, P. L. Tang, and P. H. Chow, "Expression of vascular endothelial growth factor (VEGF) and its receptors during embryonic implantation in the golden hamster (*Mesocricetus auratus*)," *Cell and Tissue Research*, vol. 296, no. 2, pp. 339–349, 1999.

[17] M. M. Kaczmarek, J. Kiewisz, D. Schams, and A. Ziecik, "Expression of VEGF-receptor system in conceptus during peri-implantation period and endometrial and luteal expression of soluble VEGFR-1 in the pig," *Theriogenology*, vol. 71, no. 8, pp. 1298–1306, 2009.

[18] L. Shangwei, T. Zongjian, and H. Ziyan, *Expression of IGFBP-1 and IGFBP-2 in Endometrium and Their Relationships with Serum Progesteron during Peri-Implantation in Rat*, Journal of West China University of Medical ences, 2002.

[19] L. H. Zhu, L. H. Sun, Y. L. Hu et al., "βPCAF impairs endometrial receptivity and embryo implantation by down-regulating β3-integrin expression via HOXA10 acetylation," *Journal of Clinical Endocrinology and Metabolism*, vol. 98, no. 11, pp. 4417–4428, 2013.

[20] J. A. R. Gordon, M. Q. Hassan, S. Saini et al., "Pbx1 represses osteoblas togenesis by blocking HOXA10-mediated recruitment of chromatin remodeling factors," *Molecular and Cellular Biology*, vol. 30, no. 14, pp. 3531–3541, 2010.

[21] H. P. Gaide Chevronnay, C. Selvais, H. Emonard, C. Galant, E. Marbaix, and P. Henriet, "Regulation of matrix

Hindawi
Emergency Medicine International
Volume 2023, Article ID 9835949, 1 page
https://doi.org/10.1155/2023/9835949

Retraction

Retracted: Systematic Review and Meta-Analysis of the Evaluation of the Efficacy of Manipulation and Cervical Traction in the Treatment of Radical Cervical Spondylosis

Emergency Medicine International

Received 8 August 2023; Accepted 8 August 2023; Published 9 August 2023

This article has been retracted by Hindawi following an investigation undertaken by the publisher [1]. This investigation has uncovered evidence of one or more of the following indicators of systematic manipulation of the publication process:

(1) Discrepancies in scope
(2) Discrepancies in the description of the research reported
(3) Discrepancies between the availability of data and the research described
(4) Inappropriate citations
(5) Incoherent, meaningless and/or irrelevant content included in the article
(6) Peer-review manipulation

The presence of these indicators undermines our confidence in the integrity of the article's content and we cannot, therefore, vouch for its reliability. Please note that this notice is intended solely to alert readers that the content of this article is unreliable. We have not investigated whether authors were aware of or involved in the systematic manipulation of the publication process.

Wiley and Hindawi regrets that the usual quality checks did not identify these issues before publication and have since put additional measures in place to safeguard research integrity.

We wish to credit our own Research Integrity and Research Publishing teams and anonymous and named external researchers and research integrity experts for contributing to this investigation.

The corresponding author, as the representative of all authors, has been given the opportunity to register their agreement or disagreement to this retraction. We have kept a record of any response received.

References

[1] J. Chen, R. Chen, Y. Li et al., "Systematic Review and Meta-Analysis of the Evaluation of the Efficacy of Manipulation and Cervical Traction in the Treatment of Radical Cervical Spondylosis," *Emergency Medicine International*, vol. 2022, Article ID 3837995, 10 pages, 2022.

Hindawi
Emergency Medicine International
Volume 2022, Article ID 3837995, 10 pages
https://doi.org/10.1155/2022/3837995

Research Article

Systematic Review and Meta-Analysis of the Evaluation of the Efficacy of Manipulation and Cervical Traction in the Treatment of Radical Cervical Spondylosis

Jianquan Chen,[1,2] Rongbin Chen,[1,2] Yong Li,[2] Maoshui Chen,[2] Zhouming Lv,[2] Haobin Zeng,[2] and Qiang Lian [2]

[1]*The Second Clinical Medicine College, Guangzhou University of Chinese Medicine, Guangzhou, China*
[2]*Department of Orthopaedics, Guang Dong Province Hospital of Traditional Chinese Medicine Zhuhai Branch, Zhuhai, Guangdong, China*

Correspondence should be addressed to Qiang Lian; lianqiangdr@163.com

Received 2 August 2022; Revised 6 September 2022; Accepted 13 September 2022; Published 6 October 2022

Academic Editor: Hang Chen

Background. With the accelerated pace of life in modern society, changes in work style, and the popularity of computers, the prevalence of cervical spondylosis (CSR) is increasing, and the age of onset is advancing. Once suffering from this disease, it is often difficult to cure and recurring, with complex clinical symptoms, causing a serious impact on human health. *Objective*. To evaluate the efficacy of manipulation and cervical traction in the treatment of radical cervical spondylosis. *Methods*. The PubMed, CNKI, and Wanfang databases were searched for literature. The literature related to this study was included according to selective criteria and inhibitory elimination criteria, and valuable information was selected for statistical analysis, resulting in a total of 11 randomized controlled trials with 994 subjects. *Results*. The short-term efficacy of manual treatment for CSR was superior to that of cervical traction alone ($P < 0.05$); subgroup analysis showed that the short-term efficacy of pulling or rotational manipulation was superior to that of cervical traction ($P < 0.05$). The mean difference between symptoms and manipulation VAS scores was higher before and after treatment when compared with cervical traction for CSR ($P < 0.05$); the subgroup analysis showed that VAS scores, upper extremity anesthesia scores, and survivorship scores were lower for pulling or rotating manipulation than for cervical traction ($P < 0.05$). *Conclusion*. The advantages of manual therapy in terms of short-term efficacy, VAS pain scores, neck pain, upper extremity anesthesia, and survivorship improvement provide a theoretical basis for its clinical impact.

1. Introduction

The cervical spine is the smallest, but the most flexible and the most frequently active joint in the spine, and it is located below the skull and above the thoracic vertebrae. In order to accommodate visual, auditory, and olfactory stimulus responses, the cervical spine needs to have greater and sharper mobility, so its range of motion is much greater than that of the thoracic and lumbar spine [1, 2]. Therefore, the cervical spine is not only one of the most important parts of the human body but also the most susceptible part of the human body, and cervical spondylosis is currently a common and frequent clinical disease. Cervical spondylosis, also known as cervical spine syndrome, is a disorder based on degenerative pathological changes, mainly manifested as neck and shoulder pain, dizziness and headache, numbness of the upper limbs, muscle atrophy, spasm of both lower limbs in severe cases, difficulty in walking, and even paralysis of the extremities, urinary, and fecal disorders [3, 4].

Since entering the new century, the incidence of cervical spondylosis has shown a significant trend of increase in recent years due to the increasing busyness of work, increasing competitive pressure, the widespread use of food additives, pesticides, and fertilizers, environmental pollution, and the increasing trend of aging as the average life expectancy of our people increases, and the disease has

become one of the extremely common diseases in the departments of orthopedic injury, neurology, acupuncture, massage, and physical therapy [5, 6]. As electronic products such as smartphones and computers are widely used in all areas of people's lives, as well as the increase in study and work pressure and irregular living habits of teenagers and middle-aged people, cervical spondylosis is no longer the "patent" of the elderly, but the number of people suffering from cervical spondylosis, such as college students and white-collar workers, is increasing year by year. After a survey, it was found that the rate of cervical spondylosis among college students in some universities is as high as 79% [7, 8]. According to the relevant literature, the rate of cervical spondylosis in white-collar workers in some areas is 34%, but the symptoms of neck pain or numbness are as high as 54% [9, 10].

Currently, both surgical and nonsurgical treatment options are mainly used to treat cervical spondylosis at home and abroad. Many traumas of the cervical spine and the early treatment of cervical spondylosis can be treated nonoperatively, while in those cases with neurological impairment and spinal instability, surgical treatment should be adopted when nonoperative treatment has no significant effect. As medical devices become more and more advanced and medical technology becomes more and more developed, the effect of surgical treatment becomes more and more obvious. For cervical spondylosis with poor self-healing ability at the injury site (e.g., soft tissue injury), surgical treatment should be preferred. The main purpose of surgical treatment is to address the following: (1) decompress the spinal cord and nerve tissue, (2) stabilize the cervical spine of the involved segment, (3) restore the vertebral space to a normal height, and (4) obtain a spinal canal volume compatible with the spinal cord. At present, the main surgical treatment methods for cervical spondylosis at home and abroad are decompression, fusion, and internal fixation. Nonsurgical treatments are important for the treatment of all types of cervical spondylosis. Although nonsurgical treatment has no obvious effect on the more acute spinal cord type of cervical spondylosis (cervical spondylosis that must be treated surgically), nonsurgical treatment has the following roles: (1) stabilizing the disease or slowing down the development of the disease, (2) providing time for preoperative preparation, and (3) determining that nonsurgical procedures are ineffective and providing a basis for doctors to choose surgical treatment. Not only that, nonsurgical treatment plays a vital role in the postoperative rehabilitation of cervical spondylosis and in reducing the occurrence of postoperative complications. The main methods of nonsurgical treatment are Western medicine, traction therapy, braking method therapy, sinus nerve block therapy, physical therapy, and hyperoxia therapy. Traction therapy must be taken before surgery. Cervical traction can relax the neck muscles, open the intervertebral foramen, facilitate the retraction of protrusions, relieve and correct the folding state of the vertebral artery, correct the disorder of the small vertebral joints, break and fix the head, and reduce the local traumatic reaction. For the two treatments of cervical spondylosis, cervical traction is an indispensable part, and it has an obvious effect on the treatment of various types of cervical spondylosis in clinical treatment, especially for early cases, so this treatment method is widely used in the treatment of cervical spondylosis.

However, there are relatively few evidence-based studies on the effectiveness of manipulation and cervical traction in the treatment of CSR. Therefore, the purpose of this meta-analysis was to evaluate the literature on the efficacy of the use of manipulation and cervical traction in the treatment of CSR.

2. Materials and Methods

2.1. Inclusion and Exclusion Criteria

2.1.1. Inclusion Criteria. The inclusion criteria were as follows: systematic reviews and randomized controlled trials (RCTs), subjects with symptomatic cervical spondylosis radiculopathy and diagnosed by CT or MRI, and the area and race are not limited.

2.1.2. Exclusion Criteria. The exclusion criteria were as follows: literature reviews, case reports, convention abstracts, retrospective or cross-sectional studies, and meta-analysis; literature lacking original information, and literature included less than the above two endpoints.

2.2. Intervention. The treatment group was given manipulation, and the type of manipulation was limited to pulling manipulation and rotation manipulation. The control group was assigned cervical traction.

2.3. Primary Endpoint. Short-term efficacy: According to the "Diagnosis and Curative Effect Standards of Traditional Chinese Medicine Diseases," "Guiding Principles for Clinical Research of New Chinese Medicines," "Cervical Spondylopathy Treatment Scores," and "22 Specialties 95 Disease Types of Chinese Medicine Diagnosis and Treatment Plan," a method developed by Tanaka Yasuji, short-term efficacy is classified as valid and invalid.

2.4. Secondary Endpoints. The secondary endpoints were as follows: mean difference scores before and after treatment of the Visual Analogue Scale (VAS) scores and the mean difference scores of symptom scores before and after treatment: neck pain, upper extremity anesthesia, and survivorship were calculated according to the evaluation method of "95 diseases in 22 specialties of Chinese medicine consultation and treatment program" developed by the study [11] and the pain distribution and proportion method published by a study [12].

2.5. Literature Retrieval. Keywords including massage, orthopedic manipulation, spinal manipulation, cervical traction, cervical radical treatment, and randomized controlled trials were searched in databases such as PubMed, Embase, The Cochrane Library (Issue 8, 2020), Web of Science,

Table 1: Basic characteristics.

Study	Year	Cases (n =)		Gender (M/F)		Age, mean ± SD (years)		Type of manipulation	Endpoints
—	—	—		—		—		—	—
—	—	T1	T2	T1	T2	T1	T2	—	—
Deng [5]	2020	57	55	36/21	32/23	46.31 ± 10.21	44.18 ± 13.62	Rotation manipulation	AB
Zhang [6]	2015	36	36	24/12	26/10	43.42 ± 13.31	46.52 ± 14.52	Rotation manipulation	AB
Zhan [7]	2006	154	117	—	—	—	—	Pulling manipulation	AC
Qin [8]	2012	30	30	17/13	16/14	—	—	Rotation manipulation	AC
Liu [9]	2007	40	38	22/18	18/20	46.51 ± 6.24	43.3 ± 8.97	Rotation manipulation	AC
Fan [10]	2011	40	40	18/22	16/24	46.71 ± 10.67	44.75 ± 13.17	Rotation manipulation	AB
Jiang [11]	2012	41	38	—	—	51.82 ± 10.37	48.93 ± 10.11	Pulling manipulation	BC
Zhao [12]	2012	36	36	10/26	15/21	41.08 ± 10.48	44.17 ± 9.12	Rotation manipulation	AB
Li [13]	2012	30	30	14/16	12/18	44.82 ± 10.89	45.26 ± 9.64	Rotation manipulation	ABC
Zhang [14]	2008	31	19	—	—	54.23 ± 5.3	55.68 ± 4.63	Pulling manipulation	AB
Li [15]	2010	30	30	17/13	15/15	—	—	Pulling manipulation	AC

Note. T1: treatment group; T2: control group; A: short-term efficacy; B: mean differential VAS scores before and after treatment; C: mean differential symptom scores before and after treatment (neck pain, upper limb anesthesia, or viability).

CNKI, and Wanfang between January 2000 and August 2020. Studies in other databases, such as Google Scholar, and Baidu Library, were also included as supplements.

2.6. Literature Selection and Data Collection. Following the predetermined specific criteria, two reviewers independently read the titles and abstracts of the publications and independently excluded articles that did not meet the criteria while conducting a full-text reading and data removal on articles that did meet the requirements. Conflicts were resolved through discussion, and a third reviewer was brought in when necessary. Data extraction included: (1) general information: title, publisher, and date of reporting; (2) basic characteristics of the included publications: study population, treatment method, number of cases, and basic patient information; (3) primary endpoint: short-term efficacy; (4) secondary endpoints: mean difference scores in visual analog scale (VAS) scores before and after treatment and mean difference scores in symptom scores (neck pain, upper extremity anesthesia, and survivorship) before and after treatment difference scores.

2.7. Quality Assessment. The tool for assessing the risk of bias for Systematic Reviews of Interventions 6.0, developed by the Cochrane Collaboration, was carried out to evaluate RCTs.

2.8. Statistical Analysis. RevMan 5.3 software was used to perform all data analysis. As for effect sizes, binary data used odds ratio (OR), and continuous data used mean difference (MD), both with 95% confidence intervals (CI). For heterogeneity analysis, the chi-square test was performed (I^2 values of 25% are regarded as low heterogeneity, 25% to 50% are regarded as moderate heterogeneity, and >50% are regarded as high heterogeneity). If $P > 0.10$, I^2 <50%, the heterogeneity degree used to be low, and fixed-effects mannequin evaluation used to be adopted, whereas $P \leq 0.10$, $I^2 \geq 50\%$ suggested an excessive heterogeneity degree and a random-effects mannequin used to be utilized to verify sources of heterogeneity. Aside from research studies with evident heterogeneity, a fixed-effects mannequin evaluation was applied. Small study consequences and guide bias were once evaluated via visible inspection of respective funnel plots. Funnel plots are plots of the general error (SE (log (OR)) of the estimated effect size (OR) on log-transformed estimates for the trials, which can also be shown to be skewed and asymmetric in the presence of guidelines or differential bias. In addition, we performed a subgroup analysis according to the type of manipulation, and $\alpha = 0.05$ was statistically significant.

3. Results

3.1. RCT Selection and Description. There were 11 RCTs with a total of 994 patients included, and the general patient profile is shown in Table 1. Although a total of 58 publications were searched for in this meta-analysis. However, 47 were irrelevant, incomplete, or described duplicate data and were excluded from further analysis, and a total of 11 RCTs were eligible. Figure 1 presents the process of literature selection. 525 and 469 patients were in the treatment and control groups, respectively. Basically, the exceptionality of proof was once low with an excessive chance of bias. Most studies are not blind in nature, a loss is generally underreported or unclear, and there is usually a lack of hidden information about allocation. The risk of bias summary and graph are shown in Figures 2 and 3.

3.2. Publication Bias. Visual detection of each funnel plot verified a positive degree of asymmetry, indicating publication bias for short-term effects with 10 RCTs (Figure 4).

3.3. Meta-Analysis Results

3.3.1. Short-Term Efficacy. After analysis, 10 studies reported short-term efficacy. The Chi-square test showed $P = 0.78$ and $I^2 = 0\%$. As shown in Figure 5, the fixed-effects method of assessment showed OR = 0.38, 95% CI (2.21, 5.41), $P < 0.00001$, and the short-term efficacy of

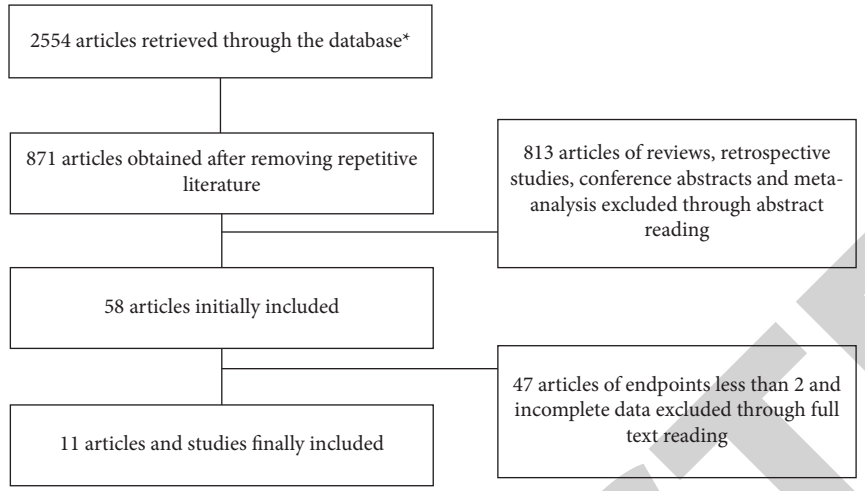

*Literature search results: PubMed (340) , Embase (49) , Web of Science (24) , The Cochrane Library (23) , CNKI (1269) , Wanfang Data (849)

Figure 1: Literature selection process.

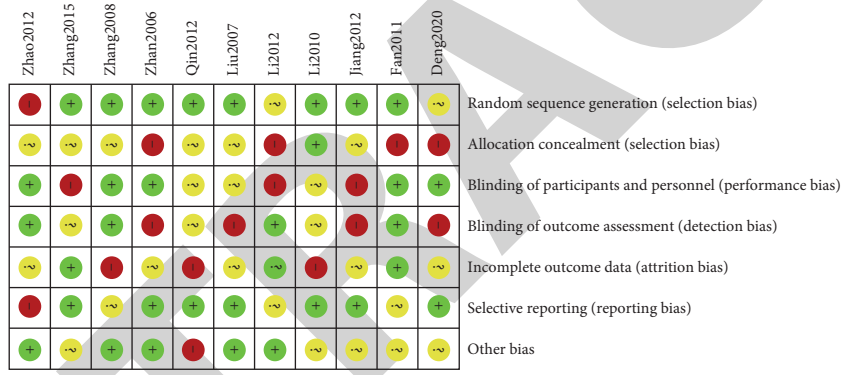

Figure 2: Risk of bias summary.

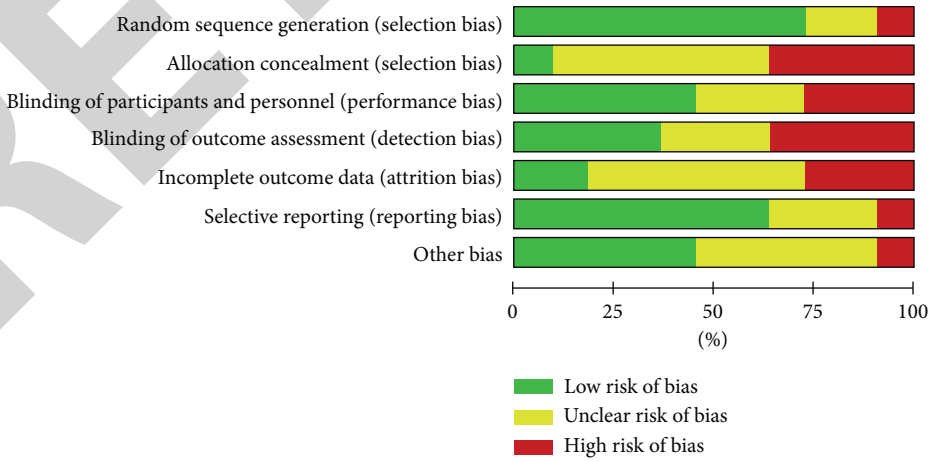

Figure 3: Risk of bias graph.

manipulation for CSR was superior to cervical traction treatment in all cases, with a statistically significant difference; subgroup analysis showed that the short-term efficacy of distraction manipulation for CSR was superior to cervical traction treatment alone, with no statistically significant difference (OR = 1.51.95% CI (0.68, 3.36), $P = 0.32$, $I^2 = 0\%$);

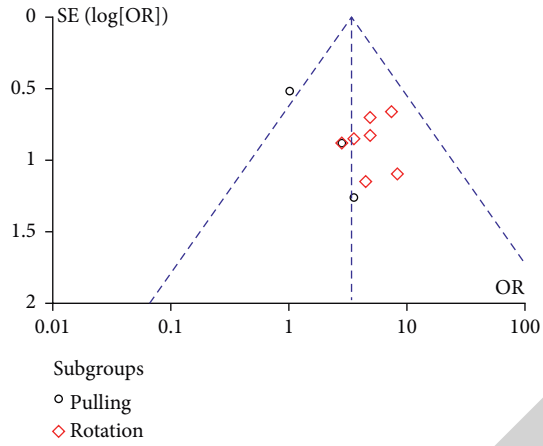

Figure 4: Funnel plots of short-term efficacy with 10 RCTs.

Study or Subgroup	Experimental Events	Experimental Total	Control Events	Control Total	Weight (%)	Odds Ratio M-H,Fixed, 95% CI
1.2.1 Pulling						
Zhang2008	30	31	17	19	3.3	3.53 [0.30, 41.86]
Zhan2006	145	154	110	117	35.8	1.03 [0.37, 2.84]
Li2010	28	30	25	30	8.2	2.80 [0.50, 15.73]
Subtotal (95% CI)		*215*		*166*	*47.4*	*1.51 [0.68, 3.36]*
Total events	203		152			
Heterogeneity: $Chi^2 = 1.50$, df = 2 (P = 0.47); $I^2 = 0\%$						
Test for overall effect: Z = 1.00 (P = 0.32)						
1.2.2 Rotation						
Zhao2012	34	36	28	36	7.6	4.86 [0.95, 24.75]
Zhang2015	33	36	25	36	10.2	4.84 [1.22, 19.21]
Qin2012	29	30	26	30	4.3	4.46 [0.47, 42.51]
Liu2007	38	40	32	38	8.1	3.56 [0.67, 18.89]
Li2012	28	30	25	30	8.2	2.80 [0.50, 15.73]
Fan2011	39	40	33	40	4.0	8.27 [0.97, 70.73]
Deng2020	54	57	39	55	10.3	7.38 [2.01, 27.10]
Subtotal (95% CI)		*269*		*265*	*52.6*	*5.06 [2.74, 9.36]*
Total events	255		208			
Heterogeneity: $Chi^2 = 1.17$, df = 6 (P = 0.98); $I^2 = 0\%$						
Test for overall effect: Z = 5.17 (P < 0.00001)						
Total (95% CI)		*484*		*431*	*100.0*	
Total events	458		360			
Heterogeneity: $Chi^2 = 7.93$, df = 9 (P = 0.54); $I^2 = 0\%$						
Test for overall effect: Z = 5.05 (P < 0.00001)						
Test for subgroup differences: $Chi^2 = 5.51$, df = 1 (P = 0.02), $I^2 = 81.8\%$						

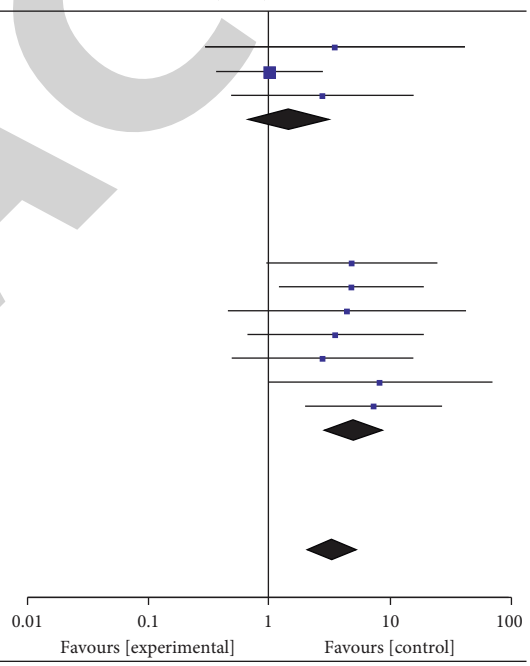

Figure 5: Comparison between the short-term efficacy of manipulation and cervical traction in the treatment of CSR.

rotational manipulation was superior to cervical traction alone, with a statistically significant difference (OR = 5.06, 95% CI (2.74, 9.36), $P < 0.00001$, $I^2 = 0\%$).

3.3.2. Mean Difference Scores before and after Treatment of VAS Scores. Six studies covered the mean difference scores in VAS scores before and after treatment. The Chi-square test resulted in $P = 0.26$, $I^2 = 23\%$. As shown in Figure 6, the fixed-effects Mannix assessment indicated SMD = 1.23, 95% CI (1.02, 1.45), $P < 0.00001$, a statistically significant difference, and the analysis showed that the mean difference manipulated VAS scores before and after CSR treatment were higher than those of cervical traction treatment alone, with a statistically significant difference; the subgroup analysis showed that the mean difference in distraction manipulation in CSR treatment score was higher than that of cervical traction treatment alone, with a statistically significant difference (SMD = 1.58, 95% CI (1.18, 1.98), $P < 0.0001$, $I^2 = 0\%$); the rotation manipulation was higher than that of cervical traction treatment alone, with a statistically significant difference (SMD = 1.10, 95% CI (0.85, 1.35), $P < 0.00001$, $I^2 = 0\%$).

3.3.3. Mean Difference Scores before and after Treatment of Symptom Scores (Neck Pain). Mean difference symptom scores (neck pain) before and after treatment were mentioned in 5 studies.The Chi-square test resulted in $P = 0.27$ and $I^2 = 22\%$. Fixed-effects human model evaluation showed MD = 0.28, 95% CI (0.15, 0.41), $P < 0.0001$ (Figure 7). The mean difference scores of manipulation in the treatment of

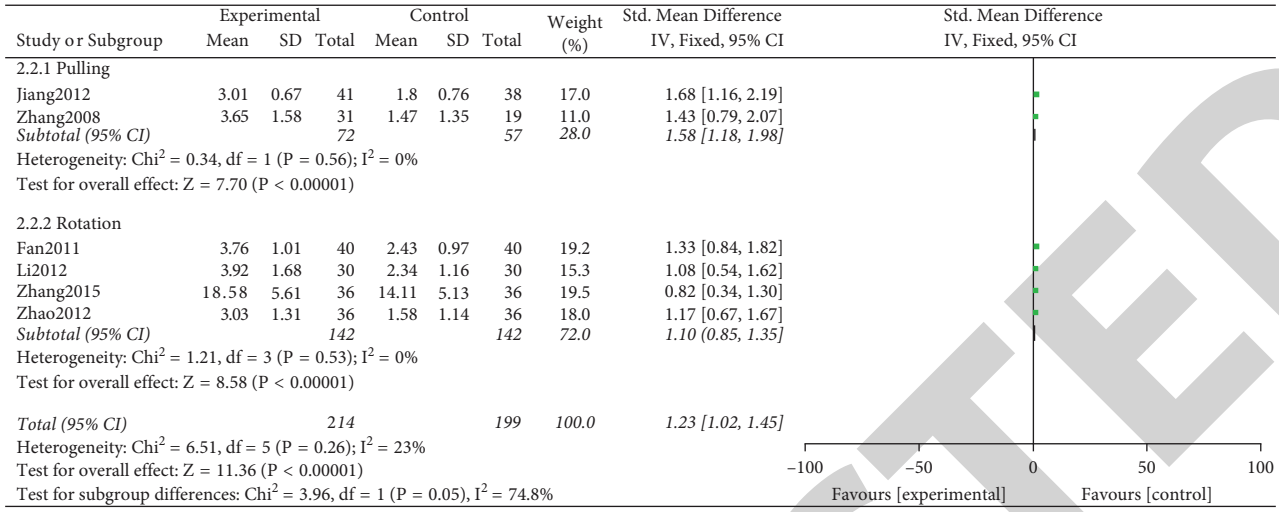

Figure 6: Comparison between the mean difference scores before and after treatment of VAS scores of manipulation and cervical traction in the treatment of CSR.

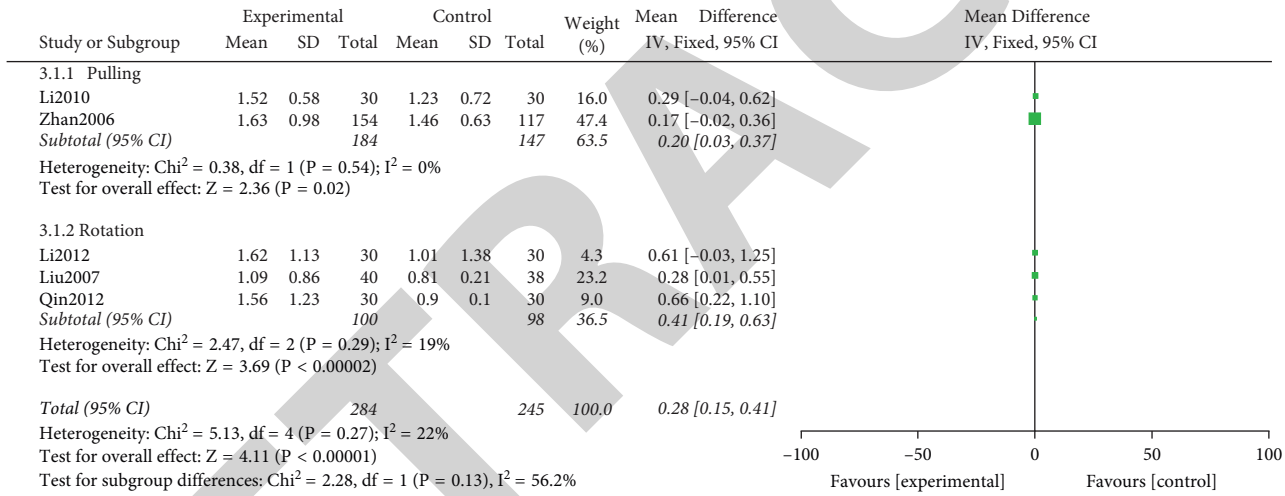

Figure 7: Comparison between the mean difference scores before and after treatment of symptom scores (neck pain) of manipulation and cervical traction in the treatment of CSR.

CSR were higher than those of cervical traction treatment alone. The difference was statistically significant. Subgroup analysis showed that the mean difference scores of pulling manipulation in the treatment of CSR were higher than that of cervical traction treatment alone. The difference was statistically significant (MD = 0.20, 95% CI (0.03, 0.37), $P < 0.0001$, $I^2 = 0\%$), and rotation manipulation was higher than that of cervical traction treatment alone. The difference was statistically significant (MD = 0.41, 95% CI (0.19, 0.63), $P < 0.0002$, $I^2 = 19\%$).

3.3.4. Mean Difference Scores before and after Treatment of Symptom Scores (Upper Limb Anesthesia). Six studies reported mean differential symptom scores (upper extremity anesthesia) before and after treatment. Chi-square test results: $P = 0.26$, $I^2 = 23\%$. A fixed-effects mannequin evaluation indicated MD = 0.11, 95% CI (0.08, 0.14), $P < 0.0001$ (Figure 8). The mean difference scores of manipulation in the treatment of CSR were higher than those of cervical traction treatment alone, the difference was statistically significant. Subgroup analysis showed that the mean difference scores of pulling manipulation in the treatment of CSR were higher than that of cervical traction treatment alone. The difference was statistically significant (MD = 0.10, 95% CI (0.07, 0.14), $P < 0.0001$, $I^2 = 0\%$), and rotation manipulation was higher than that of cervical traction treatment alone. The difference was statistically significant (MD = 0.25, 95% CI (0.10, 0.41), $P = 0.002$, $I^2 = 10\%$).

3.3.5. Mean Difference Scores before and after Treatment of Symptom Scores (Viability). Two studies reported mean differential symptom scores (Viability) before and after treatment. The Chi-square test showed $P = 0.77$, $I^2 = 0\%$. A fixed-effects mannequin evaluation indicated MD = 0.42, 95%CI (0.25, 0.59), $P < 0.00001$ (Figure 9). The viability mean difference scores of manipulation in the treatment of

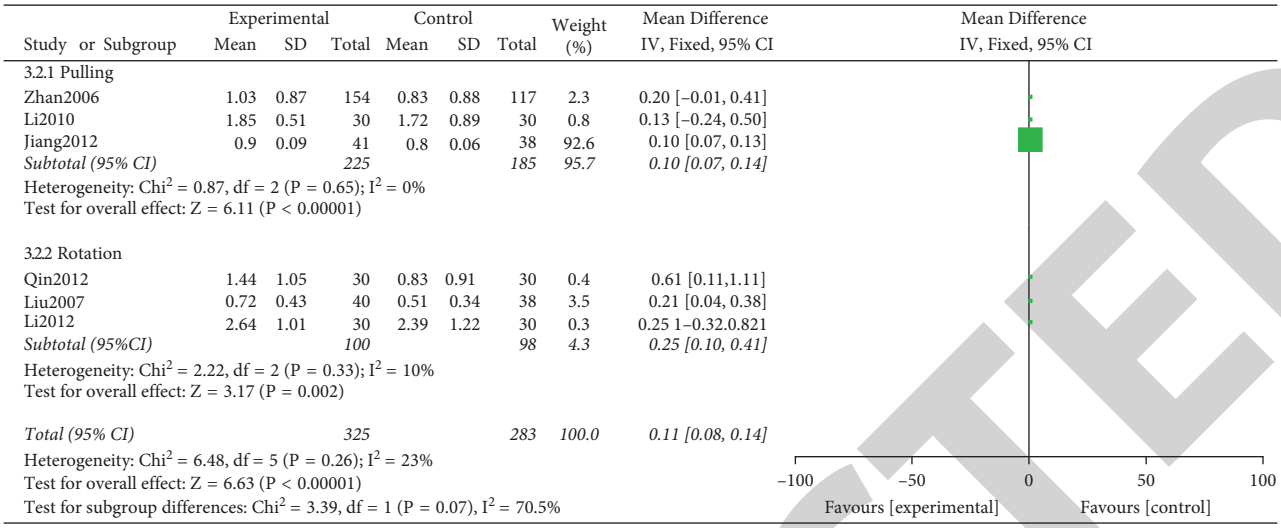

Figure 8: Comparison between the mean difference scores before and after treatment of symptom scores (upper limb anesthesia) of manipulation and cervical traction in the treatment of CSR.

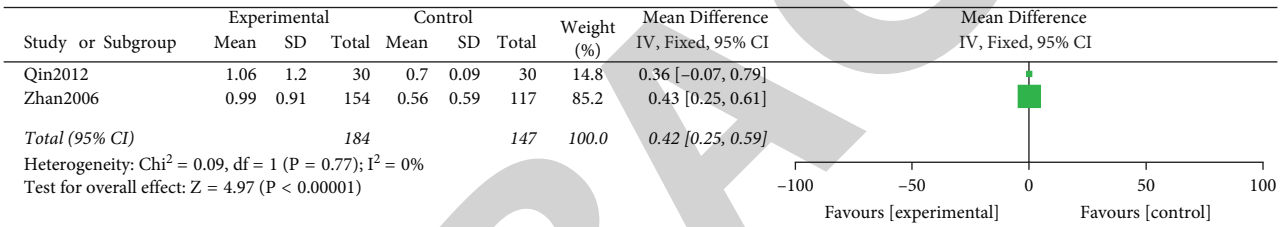

Figure 9: Comparison between the mean difference scores before and after treatment of symptom scores (viability) of manipulation and cervical traction in the treatment of CSR.

CSR were higher than those of cervical traction treatment alone. The difference was statistically significant.

4. Discussion

The onset of cervical spondylosis is becoming younger and younger and occurs early when the normal biomechanical equilibrium is disrupted, with the earlier manifestation being a change in physiological curvature [13, 14]. Changes in the physiological curvature of the cervical spine (referred to as cervical curvature) are a manifestation of degenerative changes in the overall function of the cervical spine, which include disc degeneration and biomechanical and pathophysiological changes. The cervical spine and the surrounding tissues work together to maintain stability, and they are susceptible to static or dynamic damage, as a large movable ball is placed on top of a thin column in a chain relationship between the head and the neck. The biomechanical significance of cervical flexion lies in its function of increasing the resistance to longitudinal pressure to support head elevation. Cervical spine manipulative rotation therapy has been found to be clinically effective in the treatment of cervical spondylosis, drop pillow, and muscle strain, but inappropriate use of rotation techniques has been reported to decrease the mechanical properties of vascular stretch [15, 16].

Abnormal changes in cervical curvature are very closely related to the disruption of the normal biomechanical balance of the cervical spine [17, 18]. The degeneration of cervical curvature is pathologically based on long-term abnormal stress in the cervical spine and its development is in addition to the previously thought causes of disc degeneration [19]. Current studies have shown that vertical hyperplasia (congenital or developmental) of the cervical articular processes are the cause of the posterior concavity and straightening of the cervical curve [20]. In daily work, the neck is often in a flexed position, the posterior wall joints are stretched and subjected to greater tensile stress, and the paravertebral muscle tissue plays a significant role in maintaining stability. The degeneration of the intervertebral disc, the proliferation of the articular processes, and the destruction of the muscle tissue may be the root causes of the physiological curvature of the cervical spine.

In adolescence, the cervical spine curve is round and smooth, but later, as age increases, early degeneration of the intervertebral discs occurs, affecting the cervical curve profile. Adverse stress stimuli (e.g., posture, external force) exacerbate the compensatory mechanical response of the cervical curve. The compensatory mechanical response of the cervical curve is dual in nature, i.e., stable and compressive, and manifests itself primarily through changes in the cervical curve, which can maintain internal and external

balance by altering the stress state of the cervical spine while paying a price in the indeterminate transition to stability, and is more likely to stimulate a sensitive structure when the damage accumulates to produce the associated symptoms. Clinical X-ray observations of low-age cervical spondylosis are mainly changes in cervical A-degree values with little relationship to dorsal stromal hyperplasia [21, 22]. Even in degeneration-related cervical spondylosis, abnormalities such as straightening, reversion, S-shape, and interruption of cervical curvature are widely observed in about 52%–97%, with straightening of cervical curvature being particularly predominant [23]. The change of cervical curvature is an early sign and objective indication of cervical spondylosis, and the change of physiological curvature occurs before the formation of bone spurs. Therefore, restoring the normal curve of the cervical spine is becoming more and more of a consensus in the treatment of cervical spondylosis, and restoring the cervical curvature should be an important treatment in the early treatment of cervical spondylosis in young and middle-aged patients. The trend of cervical flexion and flexion-extension activity of traction as the most commonly used treatment method is gradually decreasing with age, while the performance of mobility is more obvious [24]. The cervical disc begins to degenerate after adulthood, and the degeneration process can induce nonspecific inflammatory reactions in the local soft tissue, synovial membrane, articular cartilage and ligaments, and other tissues, resulting in clinical symptoms [25]. Due to the stress relationship, the posterior part of the cervical spine is more reactive, and compensatory straightening of the cervical spine is required to relieve symptoms. Cervical degeneration causes narrowing of the intervertebral space, and a sharp decrease in the height of the anterior edge of the intervertebral space in the narrowed segment can cause a reduction in physiological pronation. Due to biological stress, the intervertebral joint mainly holds weight at the posterior part; especially at the posterior edge of the vertebral body, there is an imbalance in the long-term stress, and osteophytes occur at the weight-bearing part of the joint. The osteophytes of the cervical spine hook protrude mainly upward, resulting in an increase in the posterior height of the vertebral body. It has been reported that the anterior-posterior height difference of the degenerated cervical spine is higher than normal. As the height of the posterior edge of the vertebral body increases, the bones of the adjacent vertebral body protruding from the hyperplasia are close to each other and resist each other, so that the height of the posterior edge of the cervical vertebrae also increases and the physiological anterior convexity becomes smaller and disappears. The osteophytes of the small joints in the posterior part of the cervical spine can also increase the height of the posterior part of the cervical spine and have a certain influence on the change of curvature. When the cervical spine degenerates, the elastic tissue of the ligaments decreases, the laxity and tension of the collar ligaments decrease, and the ability to maintain physiological pronation decreases [26]. Due to the degeneration of the intervertebral junction structure, the elasticity of the fibrous ring and ligaments decreases, the osteophytes of the vertebral body edge and small joints, and the obstruction of the joint space narrows, resulting in the reduction of cervical spine mobility. Therefore, cervical degeneration is related to intervertebral mobility. Cervical spine degeneration can reduce cervical flexion and cervical flexion and extension mobility.

According to the traditional Chinese medicine "tendon-bone" theory, "tendons are also the eastern joints and bones, and they are the gateway to the whole body and facilitate the movement of the whole body. It can be seen that the tendons are described by the theory of Chinese medicine as "a complex and balanced movement system structure of the general term. Modern medicine believes that the main body of the tendons contains muscles, tendons, fascia, ligaments, joint capsule, synovial membrane, and other systems, which is the general name of the human tendon system. The connotation of the tendon system is not only the sum of different parts of the tendon tissue but also the unity of the tendon in structure and function. In the human body, the force generated by muscle contraction acts on the bone through the tendons, and the biological force is effectively integrated by the tendons of different parts through the bone. Ultimately, the tendons act on the bone to produce a coordinated and unified movement pattern. Therefore, tendons and bones are structurally inseparable and functionally coordinated with each other. The realization of the function of the cervical spine mainly depends on the balance between tendons and bones. The balance between the cervical vertebrae is based on the normal cervical curvature. In the normal cervical degree, the cervical spine is in a state of balance in motion, and in the abnormal cervical curvature, the cervical spine must also reach a state of balance in motion, so when the balance of maintaining the cervical spine pyloric degree is out of balance, its stability is bound to change. The physiological curvature will not be maintained. In order to maintain the stability of the cervical spine, the forces between the tissues of the neck must be redistributed. This means that the self-function is compensated and a new balance is established. This compensation and the establishment of a new equilibrium are mainly accomplished by the muscle tissue. When the compensatory demand exceeds the compensatory capacity of the cervical spine itself, it will cause a muscle spasm, congestion and edema, which will lead to a series of cervical spondylosis symptoms. It can be seen that the biomechanical balance of cervical spondylosis is disrupted at the beginning of the disease, especially the further contraction of the cervical curvature, which changes the degree between the anterior and posterior parts of the intervertebral disc, i.e., the anterior and posterior angles of the intervertebral disc, as well as the change in the activity of the small joints regulating the intervertebral disc's pinchability. Through this pathological state of the cervical spine, we have realized through research that cervical flexion is closely related to the occurrence, development, rehabilitation, and prevention of cervical spondylosis. Pillows are commonly used in our daily lives, so it is an effective way to treat cervical spondylosis by using pillows to play their traction role and restore the physiological curvature and cervical flatness of the cervical spine. In addition, the pillow can work for a long time to improve the symptoms of the

cervical spine for the use of cervical spine Li lead pillow can pass the external balance, pull the narrowed intervertebral space, and disc internal pressure, so that the fibrous tissue reset, the nerve root stimulation forced to relieve, limit the cervical spine activities, conducive to neuromuscular tissue edema and nerve root and surrounding tissue adhesion, so as to play a therapeutic role.

5. Conclusion

This study started from the monotherapy point of view, using manipulation to compare with cervical traction, and focused on evaluating the short-term efficacy and pain improvement of the two therapies in the treatment of cervical spondylosis radiculopathy. The results show that manipulation has advantages in short-term efficacy, VAS pain scores, neck pain, upper limb anesthesia, and viability improvement. Consequently, appropriate remedy strategies need to be chosen in accordance with the particular stipulations of patients. Nevertheless, the conclusion mentioned above should be verified by extra multicenter RCTs with a massive pattern variety and excessive quality.

Data Availability

The data used to support the findings of this study are available from the corresponding author upon request.

Conflicts of Interest

The authors declare that they have no conflicts of interest.

Acknowledgments

This study was funded by the Traditional Chinese Medicine Bureau of Guangdong Province of China (No. 20183008).

References

[1] N. Theodore, "Degenerative cervical spondylosis," *New England Journal of Medicine*, vol. 383, no. 2, pp. 159–168, 2020.

[2] J. M. Caridi, M. Pumberger, and A. P. Hughes, "Cervical radiculopathy: a review," *HSS Journal: The Musculoskeletal Journal of Hospital for Special Surgery*, vol. 7, no. 3, pp. 265–272, 2011.

[3] Z. Deng, K. Wang, H. Wang, T. Lan, H. Zhan, and W. Niu, "A finite element study of traditional Chinese cervical manipulation," *European Spine Journal*, vol. 26, no. 9, pp. 2308–2317, 2017.

[4] T. Ando, "Diagnosis and management of cervical spondylosis," *Rinsho Shinkeigaku*, vol. 52, no. 7, pp. 469–479, 2012.

[5] D. Zhen, S. Zhipi, and Z. H. Sheng, "Therapeutic effect of shi's rotation manipulation treatment for cervical spondylotic radiculopathy," *China Journal Traditional Medical Traumatic and Orthopedics*, vol. 28, pp. 5–9, 2020.

[6] Z. Ruichun, M. Xinwen, and S. Mingqiu, "Cervical three steps nine manuevers in treatment of cervicalspondylosis radiculopathy by randomized controlled clinical trial," *Journal Liaoning University Traditional China Medicine*, vol. 17, pp. 81–83, 2015.

[7] Z. Hong-sheng, N. Shou-guo, W. Jian-kang et al., "Pulling-manipulation in dorsal position for the treatment of cervicalspondylotic radiculopathy: a randomized, multicenter controlled trial," *Chinese Journal of Traumatology*, vol. 19, no. 5, pp. 257–260, 2006.

[8] Q. Yi, L. Zhenyu, and L. Yao, "Randomized controlled clinical study of the clinical efficacy of the sun manipulation of rotating treatment to cervical spondylotic radiculopathy," *China Journal Traditional Medical Traumatic and Orthopedics*, vol. 20, pp. 3–5, 2012.

[9] L. Zhi-kun, S. Cheng-zhi, W. Zhu-han, L. Guo-wen, and K. Jimin, "Treatment of cervical spondylotic radiculopathy with vertebral adjusting and promotion of blood circulation coordination improved reduction manipulation," *Chinese Journal of Traumatology*, vol. 20, no. 8, pp. 571-572, 2007.

[10] F. Jingqing, G. Chengxiang, and C. Bolai, "Clinical observation of "guo-style changqi tongluo" in the treatment of cervical spondylotic radiculopathy," *Practice and Clinical Medicine*, vol. 27, pp. 2267–2269, 2011.

[11] C. B. Jiang, J. Wang, Z. X. Zheng, J. S. Hou, L. Ma, and T. Sun, "Efficacy of cervical fixed-point traction manipulation for cervical spondylotic radiculopathy: a randomized controlled trial," *Journal of Chinese Integrative Medicine*, vol. 10, no. 1, pp. 54–58, 2012.

[12] Z. Yan and S. Xiaolin, "Clinical observation on "three steps and nine methods" for treatment of the cervical spondylotic radiculopathy," *Journal of Zhejiang China Medicine University*, vol. 36, pp. 1225–1227, 2012.

[13] L. Ruitao, *The Clinical Study of Treatment of Cervical Spondylotic Radiculopathy by "Long Shi" Manipulation*, Guangzhou University of Chinese Medicine, Guangzhou, China, 2012.

[14] Z. Jinxin, *Clinical Observation of the Sun's Rotatory Manipulation about the Treatment of the Spondylotic Radiculopathy*, Guangzhou University of Chinese Medicine, Guangzhou, China, 2008.

[15] L. Yubin, *The Clinical Research of Buckling Neck and ZhengGu Gimmick to Treat Cervical Spondylotic Radiculopathy*, Hubei University of Chinese Medicine, Hubei, China, 2010.

[16] C. M. W. Goedmakers, T. Janssen, X. Yang, M. P. Arts, R. H. M. A. Bartels, and C. L. A. Vleggeert-Lankamp, "Cervical radiculopathy: is a prosthesis preferred over fusion surgery? a systematic review," *European Spine Journal*, vol. 29, no. 11, pp. 2640–2654, 2019.

[17] A. Goel, R. Vutha, A. Shah, A. Patil, A. Dhar, and A. Prasad, "Cervical spondylosis in patients presenting with "severe" myelopathy: analysis of treatment by multisegmental spinal fixation—a case series," *Journal of Craniovertebral Junction and Spine*, vol. 10, no. 3, pp. 144–151, 2019.

[18] A. Goel, P. Dharurkar, A. Shah, S. Gore, N. Bakale, and T. Vaja, "Facetal fixation arthrodesis as treatment of cervical radiculopathy," *World Neurosurgery*, vol. 121, pp. e875–e881, 2019.

[19] Y. L. Chang, X. Mu, and J. M. Wen, "Case-control study on bone-setting manipulation for the treatment of isolated systolic hypertension combined with cervical spondylosis," *Zhong Guo Gu Shang*, vol. 28, no. 12, pp. 1086–1090, 2015.

[20] M. C. Zhang, Y. Y. Shi, and D. Y. Chen, "(Study on the clinical value of cervical spondylosis with articulatio atlantoepistrophica sublaxation)," *Zhong Guo Gu Shang*, vol. 29, pp. 898–902, 2016.

[21] R. Qin, X. Chen, P. Zhou, M. Li, J. Hao, and F. Zhang, "Anterior cervical corpectomy and fusion versus posterior laminoplasty for the treatment of oppressive myelopathy owing to cervical ossification of posterior longitudinal

Hindawi
Emergency Medicine International
Volume 2023, Article ID 9798523, 1 page
https://doi.org/10.1155/2023/9798523

Retraction

Retracted: Diagnostic Predictive Value of Tryptase, Serum Amyloid A and Lipoprotein-Associated Phospholipase A2 Biomarker Groups for Large Atherosclerotic Cerebral Infarction

Emergency Medicine International

Received 28 November 2023; Accepted 28 November 2023; Published 29 November 2023

This article has been retracted by Hindawi, as publisher, following an investigation undertaken by the publisher [1]. This investigation has uncovered evidence of systematic manipulation of the publication and peer-review process. We cannot, therefore, vouch for the reliability or integrity of this article.

Please note that this notice is intended solely to alert readers that the peer-review process of this article has been compromised.

Wiley and Hindawi regret that the usual quality checks did not identify these issues before publication and have since put additional measures in place to safeguard research integrity.

We wish to credit our Research Integrity and Research Publishing teams and anonymous and named external researchers and research integrity experts for contributing to this investigation.

The corresponding author, as the representative of all authors, has been given the opportunity to register their agreement or disagreement to this retraction. We have kept a record of any response received.

References

[1] W. Jia, X. Li, F. Lei et al., "Diagnostic Predictive Value of Tryptase, Serum Amyloid A and Lipoprotein-Associated Phospholipase A2 Biomarker Groups for Large Atherosclerotic Cerebral Infarction," *Emergency Medicine International*, vol. 2022, Article ID 5784909, 7 pages, 2022.

Hindawi
Emergency Medicine International
Volume 2022, Article ID 5784909, 7 pages
https://doi.org/10.1155/2022/5784909

Research Article

Diagnostic Predictive Value of Tryptase, Serum Amyloid A and Lipoprotein-Associated Phospholipase A2 Biomarker Groups for Large Atherosclerotic Cerebral Infarction

Wenhui Jia,[1] Xia Li,[1] Fang Lei,[2] Fengyun Hu,[1] Fenglian Li,[3] Xueying Zhang,[3] Siyu Liu,[1] Feifei Huang,[1] and Changxin Li[4]

[1]*The Fifth Clinical Medical College of Shanxi Medical University, Department of Neurology, Shanxi Provincial People's Hospital, Taiyuan 030000, China*
[2]*Dalian Medical University, Dalian 116000, China*
[3]*College of Information and Computer,, Taiyuan University of Technology, Jinzhong 030600, China*
[4]*The First Clinical Medical College of Shanxi Medical University, Department of Neurology, Taiyuan 030000, China*

Correspondence should be addressed to Changxin Li; lichangxin0351@stu.cpu.edu.cn

Received 8 August 2022; Revised 14 September 2022; Accepted 19 September 2022; Published 3 October 2022

Academic Editor: Hang Chen

Background. There has been a gradual trend towards younger ageing of acute cerebral infarction in recent years. Atherosclerotic plaque rupture followed by dislodgement of emboli and resulting arterial embolism is an important mechanism for the development of acute cerebral infarction. Traditional independent risk factors for cerebral infarction have received attention from clinicians, but the risk factors for large artery atherosclerotic cerebral infarction are still unclear. Various blood biomarkers have an important role in the early diagnosis of large artery atherosclerotic cerebral infarction. *Objective*. To assess the diagnostic predictive value of a group of biomarkers for large artery atherosclerotic cerebral infarction. *Methods*. Lipoprotein-associated phospholipase A2 (LP-PLA2), trypsin-like protein (TPS), serum amyloid A (SAA), and supersensitive C-reactive protein (hs-CRP) levels were measured in the case group (30 cases) and control group (54 cases), respectively. *Results*. The differences in the general data between the two groups were not statistically significant ($P > 0.05$). Logistic regression and ROC curve analysis showed that Lp-PLA2, TPS, and SAA were positively associated with the diagnosis of large atherosclerotic cerebral infarction ($P < 0.05$). The area under the ROC curve of the multivariate model for the biomarker group reached 0.995. *Conclusion*. Biomarkers are closely associated with the occurrence of large atherosclerotic cerebral infarction and can be used as clinical adjuncts for diagnosis and assessment of prognosis.

1. Introduction

Stroke has a high recurrence, disability, and mortality rate, and places a heavy economic and psychological burden on society and the patient's family. Ischemic strokes account for approximately 80% of all strokes. The treatment of ischemic strokes is not limited to symptomatic treatment (salvage of ischemic brain tissue), but also to the diagnosis and treatment of the cause, which has been unanimously accepted by neurologists [1]. The diagnosis of ischemic stroke based on TOAST etiological staging [2], followed by treatment planning and recurrence prevention, plays an important role in the management of stroke. With the widespread use of TOAST etiology in clinical practice, the incidence of LAAS in each subtype has been found to be increasing in recent years. A study by Chen et al. [3] found that the incidence of LAAS accounted for 16.5% of patients in the Yonsei Stroke Registry in Korea when examining the risk factors and subtypes of 1000 patients with acute cerebral infarction. The study by Dobrocky et al. [4] found that LAAS accounted for 25.3% of all TOAST subtypes, second only to cardiogenic embolism (46.2%); the study by Zhou et al. [5] found that

small artery occlusion and LAAS were the most common (44.2% and 37.6%, respectively) when reporting the relationship between acute cerebral infarction TOAST staging and risk factors. Although the results of domestic and international studies vary, the prevalence of LAAS among TOAST subtypes is relatively high in China. Because patients with LAAS have severe intracranial and extracranial large artery stenosis or occlusion, the potential for disability, death, and recurrence of stroke remains high with aggressive pharmacological and nonpharmacological interventions, and should therefore be studied with emphasis [6].

At present, the diagnosis of acute cerebral infarction (ACI) relies mainly on imaging, but many primary care institutions lack equipment such as head MRI and CT and do not have the capacity to complete relevant examinations in a timely manner. In contrast, early identification, etiological typing, disease assessment, risk stratification, and prognostic assessment of ACI, as well as personalised treatment plans, are of great clinical and social importance. In cardiology and respiratory emergency cases, such as troponin for acute myocardial infarction and D-dimer for early diagnosis of pulmonary embolism are of great value [7]. We lack a widely used, rapid, and sensitive blood biomarker for the clinical diagnosis of ACI, so finding a blood biomarker that can rapidly diagnose ACI is a clinical imperative. However, not much research has been done in this area.

Previous studies have shown that the levels of several blood biomarkers (ultrasensitive C-reactive protein, lipoprotein-associated phospholipase A2, and metalloproteinase-9) are elevated to varying degrees during the acute phase of ischemic stroke, but changes in a single marker have limitations for the diagnosis of ischemic stroke [8, 9]. Therefore, we screened four indicators widely reported in the literature, hs-CRP, TPS, Lp-PLA2, and SAA, all of which have been shown in several studies to be atherosclerotic inflammatory factors [10, 11].

Based on this, 84 patients with large atherosclerotic cerebral infarction were selected for this study, and the levels of TPS, Lp-PLA2, SAA, and hs-CRP were measured in patients with LAA, and the diagnostic predictive value of the four biomarkers for LAA was further evaluated to provide the reference value for clinical application.

2. Materials and Methods

2.1. General Information. Select 100 consecutive cases of acute cerebral infarction diagnosed in the Department of Neurology of Shanxi Provincial People's Hospital from January 2021 to January 2022, of which 30 inpatients with large atherosclerotic cerebral infarction (LAA) by TOAST etiology typing were selected, including 20 males and 10 females with an average age of (62.37 ± 14.11) years, and another age-sex matched fifty-four cases were selected as the control group with age- and sex-matched healthy physical examiners.

2.2. Diagnostic Criteria. All cases of cerebral infarction met the diagnostic criteria for cerebral infarction established by the Chinese guidelines for the diagnosis and treatment of acute ischemic stroke 2018 [12], were confirmed by cranial magnetic resonance imaging (MRI); patients with first-onset cerebral infarction were hospitalized within 72 hours of onset, and the 100 patients with acute cerebral infarction enrolled were classified as large atherosclerotic cerebral infarction according to the TOAST etiological typing in the Org 10172 trial of acute stroke treatment.

2.3. Inclusion and Exclusion Criteria. All met the following inclusion criteria: (1) the diagnostic criteria established by the 4th National Cerebrovascular Disease Conference [13] and confirmed by cranial CT/MRI; (2) could cooperate with the completion of routine blood and serum biomarker tests; (3) gave informed consent to the study and voluntarily signed the informed consent form. The exclusion criteria include the following: (1) those who are unable to complete serum biomarker tests; (2) those with major organ diseases such as heart, liver, or kidney; (3) those with previous cerebral haemorrhage, subarachnoid haemorrhage, traumatic brain injury, or haematological disorders; (4) those with a clear history of tuberculosis, syphilis, connective tissue disease, or other diseases that can cause vascular damage; (5) those who are unable to cooperate with the completion of this study.

2.4. Experimental Method. General information including gender, age, previous medical history (hypertension, hyperlipidaemia, and, diabetes), smoking and alcohol consumption was recorded. Blood specimens were collected on the morning of the second day of admission and biomarkers were measured. High-sensitivity C-reactive protein (hs-CRP) was measured by reflectance turbidimetry, brain natriuretic peptide (BNP) by immunofluorescence, and fibrinogen (FIB) by immunoturbidimetry, all measured on a Beckman coulter AU5800 fully automated biochemistry analyser. Lipoprotein-associated phospholipase A2 (Lp-PLA2), myelin basic protein (MBP), and glial fibrillary acidic protein (GFAP) were measured by ELISA, the kits were purchased from eBioscience, and the enzyme standard was a GO full wavelength enzyme standard from Thermo Fisher, USA. Normal reference values were as follows: hs-CRP 0.1–10 mg/L, BNP 0–38 pg/ml, FIB 2–4 g/L, Lp-PLA2 ≤ 175 ng/ml, MBP ≤ 80 ng/L, and GFAP ≤ 1.0 ng/L.

2.5. Statistical Methods. All data were statistically analysed using SPSS 22.0 software, measures were expressed as mean ± standard deviation ($x \pm s$), the t-test was used for the measurement data and the χ^2-test was used for the count data, binomial classification logistic regression was used to screen the variables and establish the regression equation to generate a new set of variables. ROC curve analysis was performed for the new variables and each individual index, and $P < 0.05$ was considered statistically different.

3. Results

3.1. Comparison of General Clinical Information between the Case Group and the Control Group. The differences in gender, age, smoking history, drinking history, and BMI

between the case group and the control group were not statistically significant ($P > 0.05$), indicating an equal distribution of general information between the two groups (Table 1).

3.2. Comparison of Lipids, Fasting Glucose, Uric Acid, and White Blood Cell Count between the Case Group and the Control Group. The differences in CHO, HDL-C, LDL, UA, and blood WBC levels between the case group and the control group were not statistically significant ($P > 0.05$), and the differences in TG and fasting glucose levels were statistically significant ($P < 0.05$) (Table 2).

3.3. Comparison of Biomarkers between Case and Control Groups. The levels of serum hs-CRP, LP-PLA2, SAA, and TPS in the case group were significantly higher than those in the control group, and the differences were statistically significant by the *t*-test ($P < 0.05$). HCY and FIB were not statistically significant between the two groups ($P > 0.05$) (Table 3).

3.4. Logistic Regression Analysis of the Three Biomarkers. Logistic regression analysis showed that among the three biomarkers, TPS, Lp-PLA2, and SAA were positively correlated with the diagnosis of the acute phase of atherosclerotic cerebral infarction ($P < 0.05$), while the correlation of hs-CRP was not significant ($P > 0.05$) (Table 4).

3.5. ROC Curve Analysis of the Diagnostic Value of Three Biomarkers Alone and in Combination for the Acute Phase of Atherosclerotic Cerebral Infarction. Logistic regression analysis in this study showed that the area under the curve (AUC) of the three biomarkers was TPS > SAA > Lp-PLA2 with a maximum value of 0.935, and SAA was positively correlated with the acute phase diagnosis of LAA ($P < 0.05$) with an area under the curve (AUC) of 0.916, suggesting a high clinical value for ACI diagnosis and prediction (Table 5 and Figure 1).

4. Discussion

A widely used, rapid and sensitive diagnostic test is still lacking in the acute phase of ischemic stroke. In some other medical emergencies, diagnostic tests based on blood biomarkers have become a routine. For example, troponin, creatine kinase, brain natriuretic peptide, and D-dimer play an important role in the early diagnosis of acute myocardial infarction, heart failure, and pulmonary embolism. Previous studies have shown that the levels of several blood biological markers (ultrasensitive C-reactive protein, lipoprotein-associated phospholipase A2, and metalloproteinase-9) are increased to varying degrees during the acute phase of ischemic stroke [14], but changes in a single marker have limitations for the diagnosis of ischemic stroke. In China, atherosclerotic cerebral infarction is an important subtype of TOAST etiology, so in this study, six blood biomarkers associated with atherosclerotic cerebral infarction were screened to form a biomarker panel (lipoprotein-associated phospholipase A2 (Lp-PLA2) A2 (Lp-PLA2), myeloperoxidase (MPO), matrix metalloproteinase-9 (MMP-9), myeloperoxidase (MPO), matrix metalloproteinase-9 (MMP-9), hypersensitive C-reactive protein (Hs-CRP), fibrinogen (FIB), and brain natriuretic peptide (BNP)). Logistic regression analysis and ROC curves were used to investigate the diagnostic value of biomarker groups in the acute phase of atherosclerotic cerebral infarction.

LP-PLA2 is a novel inflammatory marker that has been extensively studied both nationally and internationally as a key enzyme mediating the inflammatory effects of ox-LDL and promoting AS formation [15]. The Rotterdam study [16] (Rotterdam Study and TRS Study), a prospective case-cohort study, confirmed for the first time that serum Lp-PLA2 is a new independent predictor of cerebral infarction. Numerous domestic and international studies have shown that LP-PLA2 is closely associated with AS and cerebral infarction, is a risk factor for ACI, predicts the prognosis of ACI, and is a predictor of ACI recurrence [17]. A study by Luo et al. [18] found that elevated Lp-PLA2 levels in patients with atherosclerotic cerebral infarction were positively correlated with NIHSS scores, which has an important clinical value for the diagnosis and treatment of atherosclerotic cerebral infarction. Related studies have further shown that Lp-PLA2 is closely associated with large vessel stenosis and may even serve as a potential biomarker for predicting the degree of cerebrovascular stenosis in patients with ACI [19]. The results of this study showed that serum LP-PLA2 levels were significantly higher in LAA patients than in controls and were positively correlated with the diagnosis of the acute phase of LAA. ROC curve analysis showed that the area under the curve was 0.822, indicating that LP-PLA2 was closely associated with the occurrence of LAA and had diagnostic predictive value for the acute phase of LAA.

The study by Kang et al. [20] reported for the first time that it is synthesized by hepatocytes, secreted and involved in the formation and development of AS, promoting the formation of AS plaques, leading to plaque rupture and thrombosis. The study by Lee et al. [21] confirmed that SAA accelerates atherosclerotic plaque progression in apolipoprotein *E* knockout mice. In recent years, several domestic and international studies have shown that SAA can initiate and develop atherosclerosis through a series of proinflammatory and proatherogenic activities that have been clearly shown to influence the progression of atherosclerosis and may be a candidate target for clinical trials in cardiovascular disease [22]. SAA is not only a marker of cardiovascular disease but also an early atherosclerotic process participant [23]. The study by Leng et al. [24] concluded that SAA is a useful biomarker for the diagnosis of atherosclerotic thrombotic ischemic stroke. In addition, several studies confirmed that SAA is one of the most sensitive markers of inflammation in the acute phase of cerebral infarction [25]. Several foreign studies have concluded that SAA levels can assess the severity of acute cerebral infarction and determine the prognosis [26]. The study by Sun et al. [27] found that SAA levels

Table 1: Comparison of general clinical information between the case and control groups.

–	–	Case group	Control group	χ^2	P
Gender	Male	20	36	0.0	1.0
	Female	10	18		
Smoking	Yes	16	19	2.613	0.106
	No	14	35		
Drinking	Yes	9	12	0.622	0.430
–	No	21	42		
–	–	*Number of cases*	$\overline{x} \pm s$	t	P
Age	Case group	30	62.37 ± 14.11	1.952	0.054
–	Control group	54	55.96 ± 14.57	–	–
BMI	Case group	30	24.86 ± 2.28	0.731	0.467
–	Control group	54	24.40 ± 3.40	–	–

Table 2: Comparison of blood lipids, fasting glucose, uric acid, and white blood cell count between the case group and the control group.

-	–	Number of cases	$\overline{x} \pm s$	t	P
CHO	Case group	30	4.24 ± 1.15	0.609	0.544
(mmol/L)	Control group	54	4.39 ± 1.01	–	–
TG	Case group	30	1.27 ± 0.46	2.37	0.02
(mmol/L)	Control group	54	1.63 ± 0.93	–	–
HDL-C	Case group	30	1.13 ± 0.45	1.379	0.172
(mmol/L)	Control group	54	1.29 ± 0.54	–	–
LDL	Case group	30	2.78 ± 0.91	0.678	0.5
(mmol/L)	Control group	54	2.65 ± 0.81	–	–
Blood sugar	Case group	30	6.06 ± 1.97	3.149	0.002
(mmol/L)	Control group	54	5.07 ± 0.84	–	–
UA	Case group	30	285.91 ± 68.08	0.151	0.881
(μmol/L)	Control group	54	288.83 ± 91.36	–	–
WBC	Case group	30	6.84 ± 1.86	1.759	0.086
($\times 10^9$/L)	Control group	54	6.07 ± 1.88	–	–

Table 3: Comparison of each biomarker index between the case group and the control group.

–	–	Number of cases	$\overline{x} \pm s$	t	P
Hs-CRP	Case group	30	8.81 ± 10.82	3.503	0.001
(mg/L)	Control group	54	2.37 ± 5.04	–	–
LP-PLA_2	Case group	30	396.60 ± 233.34	3.191	0.003
(ng/L)	Control group	54	251.94 ± 110.71	–	–
SAA	Case group	30	1589.23 ± 788.28	6.389	<0.001
(ng/L)	Control group	54	646.78 ± 231.32	–	–
TPS	Case group	30	11.80 ± 6.37	6.848	<0.001
(ng/ml)	Control group	54	3.81 ± 0.73	–	–
HCY	Case group	30	26.93 ± 18.11	0.986	0.331
(μmol/L)	Control group	54	21.79 ± 11.77	–	–
FIB	Case group	30	3.23 ± 0.61	0.243	0.809
(g/L)	Control group	54	3.26 ± 0.49	–	–

Table 4: Logistic regression analysis of large artery atherosclerotic cerebral infarction.

Biomarkers	Regression coefficient	Standard error	OR	P
Constants	−26.811	11.798	0.000	0.023
TPS	1.441	0.680	4.226	0.034
SAA	0.012	0.006	1.012	0.045
LP-PLA2	0.023	0.012	1.023	0.045

were significantly and positively correlated with ACI and were a risk factor for ACI. Logistic regression analysis in this study showed that SAA was positively correlated with the diagnosis of acute phase of LAA ($P < 0.05$) with an area under the curve (AUC) of 0.916, suggesting a high clinical value for ACI diagnosis and prediction.

Table 5: AUC of single biomarker and combined assay for predicting probability of new variable *Y*.

Test items	AUC	Standard error	*P*	95%CI	
				Lower limit	Upper limit
TPS	0.935	0.037	<0.001	0.863	1.000
SAA	0.916	0.037	<0.001	0.843	0.988
Lp-PLA2	0.822	0.046	<0.001	0.731	0.912
Y	0.995	0.004	<0.001	0.987	1.000

Y-value = TPS + SAA + Lp-PLA2.

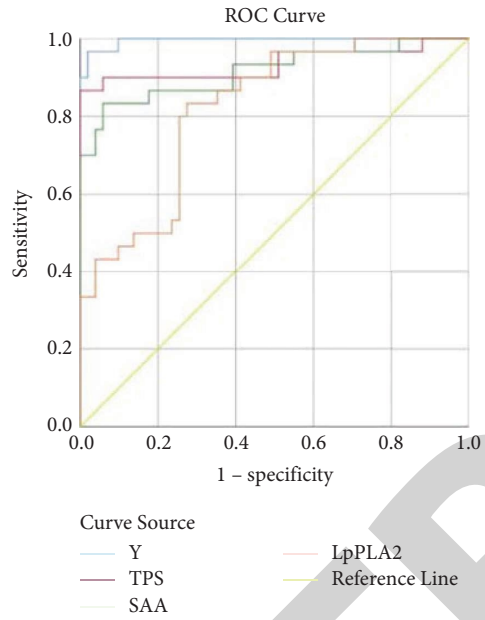

Figure 1: ROC curves for the new variable *Y* and the three biomarkers.

TPS is a natural protease with multiple biological activities that may be involved in the development and progression of AS by preventing reverse HDL cholesterol transport, aggregating inflammatory cells, and other mechanisms leading to atherosclerotic plaque formation and rupture. In recent years, the relationship between TPS and AS has been increasingly studied, with TPS emerging as a new inflammatory marker for AS. The study by Tsang et al. [28] concluded that TPS levels significantly correlated with carotid intima-media thickness were higher in patients with carotid plaque and independently predicted changes in subclinical atherosclerosis. An experimental study in monkeys and hamsters found that TPS inhibition blocked macrophage foam cell formation and reduced atherosclerotic plaque formation [29]. It was found [30] that TPS inhibited LXRα activation through the PAR-2/LXRα/LXRα target gene signaling pathway, which promoted macrophage lipid accumulation and foam cell formation, further promoting AS formation. However, there are few studies on the correlation between TPS and large atherosclerotic cerebral infarction, and the present study found that after studying LAA patients and normal controls, TPS levels in the case group were significantly different from those in the control group, and logistic regression analysis showed that TPS was positively correlated with the diagnosis of acute phase of LAA, and TPS was further associated with LAA, with an area under the curve (AUC) of 0.935, suggesting that the diagnosis and prediction of ACI has a high clinical value.

In this study, the inflammatory markers LP-PLA2, SAA, and TPS associated with LAA were selected, and the levels of each inflammatory marker were found to be elevated during the acute phase of cerebral infarction. Logistic regression analysis showed that LP-PLA2, SAA, and TPS were positively correlated with LAA ($P < 0.05$), and all were independent risk factors for LAA. Analysis of these three biomarkers used to diagnose LAA using ROC curves showed that TPS had the highest AUC value of 0.935 if a single indicator was used to diagnose LAA. A new variable *Y* was generated by multiple logistic regression analysis combining the three biomarkers, and the area under the ROC curve used to diagnose the new variable *Y* was obtained by plotting the ROC curve at 0.995 and the value of the new variable *Y* was higher than the area of any individual indicator. It can be seen that by detecting the TPS biomarker set, SAA and Lp-PLA2 are more valuable than one alone, increasing the specificity and sensitivity of LAA diagnosis to more than 99%, which is valuable for rapid diagnosis and pathogen typing of LAA.

5. Conclusions

The results of this study suggest that the combined detection of multiple biomarkers is an effective means to improve the clinical value of ischemic stroke diagnostic tests. It is although the complexity of the stroke process and the specificity of the brain tissue structure, the sensitivity and specificity of stroke biomarkers have been the main problems faced by stroke biomarker research. However, we found that TPS, Lp-PLA2, and SAA were significantly higher, and the area under the ROC curve of the multivariate model LP-PLA2, SAA, and TPS combined reached 0.995. The sensitivity and specificity of the combined prediction group for the diagnosis of LAA was extremely high, which has a high clinical value for the diagnosis of LAA and can provide a reference value for clinical application, and is worthy of further promotion in our clinical practice.

Data Availability

The experimental data used to support the findings of this study are available from the corresponding author upon request.

Conflicts of Interest

The authors declare that they have no conflicts of interest regarding this work.

Acknowledgments

This work was supported by grants from the National Natural Science Foundation of China (62171307), the Youth Foundation of Shanxi Provincial Health Commission (201301029), and the provincial special supporting foundation for Shanxi Provincial People's Hospital (136).

References

[1] H. Zhang, X. Zhao, C. Wang et al., "A preliminary study of the association between apolipoprotein E promoter methylation and atherosclerotic cerebral infarction," *Journal of Stroke and Cerebrovascular Diseases*, vol. 28, no. 4, pp. 1056–1061, 2019.

[2] Q. Li, M. Liu, R. Fu et al., "Alteration of circulating innate lymphoid cells in patients with atherosclerotic cerebral infarction," *American Journal of Tourism Research*, vol. 10, no. 12, 2018.

[3] L. Chen, Q. Yang, R. Ding, D. Liu, and Z. Chen, "Carotid thickness and atherosclerotic plaque stability, serum inflammation, serum MMP-2 and MMP-9 were associated with acute cerebral infarction," *Experimental and Therapeutic Medicine*, vol. 16, no. 6, pp. 5253–5257, 2018.

[4] T. Dobrocky, J. Kaesmacher, S. Bellwald et al., "Stent-retriever thrombectomy and rescue treatment of M1 occlusions due to underlying intracranial atherosclerotic stenosis: cohort analysis and review of the literature," *Cardiovascular and Interventional Radiology*, vol. 42, no. 6, pp. 863–872, 2019.

[5] D. Zhou, J. Li, D. Liu et al., "Irregular surface of carotid atherosclerotic plaque is associated with ischemic stroke: a magnetic resonance imaging study," *Journal of Geriatric Cardiology: JGC*, vol. 16, no. 12, pp. 872–879, 2019.

[6] T. Ni, Y. Fu, W. Zhou et al., "Carotid plaques and neurological impairment in patients with acute cerebral infarction," *PLoS One*, vol. 15, no. 1, Article ID e0226961, 2020.

[7] Y. Wang, S. Xu, S. Pan, H. Ouyang, Z. Zang, and J. Tan, "Association of serum neuron-specific enolase and bilirubin levels with cerebral dysfunction and prognosis in large-artery atherosclerotic strokes," *Journal of Cellular Biochemistry*, vol. 119, no. 12, pp. 9685–9693, 2018.

[8] Z. Yan, B. Fu, D. He, Y. Zhang, J. Liu, and X. Zhang, "The relationship between oxidized low-density lipoprotein and related ratio and acute cerebral infarction," *Medicine*, vol. 97, no. 39, Article ID e12642, 2018.

[9] J. Anniwaer, M. Z. Liu, K. D. Xue, A. Maimaiti, and A. Xiamixiding, "Homocysteine might increase the risk of recurrence in patients presenting with primary cerebral infarction," *International Journal of Neuroscience*, vol. 129, no. 7, pp. 654–659, 2019.

[10] L. Wu, L. Qian, L. Zhang et al., "Fibroblast growth factor 21 is related to atherosclerosis independent of nonalcoholic fatty liver disease and predicts atherosclerotic cardiovascular events," *Journal of American Heart Association*, vol. 9, no. 11, Article ID e015226, 2020.

[11] G. J. Wang, X. Dong, and Y. Li, "Cluster of Differentiation 147 (CD147) serves as a promoter of atherosclerosis in patients with cerebral infarction," *European Review for Medical and Pharmacological Sciences*, vol. 26, no. 16, pp. 5710–5717, 2022.

[12] D. H. Kang, W. Yoon, S. K. Kim et al., "Endovascular treatment for emergent large vessel occlusion due to severe intracranial atherosclerotic stenosis," *Journal of Neurosurgery*, vol. 130, no. 6, pp. 1949–1956, 2019.

[13] H. Kim, S. Kim, S. Han et al., "Prevalence and incidence of atherosclerotic cardiovascular disease and its risk factors in Korea: a nationwide population-based study," *BMC Public Health*, vol. 19, no. 1, pp. 1112–1211, 2019.

[14] W. B. Zhang, Y. Y. Zeng, F. Wang, L. Cheng, W. J. Tang, and X. Q. Wang, "A high neutrophil-to-lymphocyte ratio predicts hemorrhagic transformation of large atherosclerotic infarction in patients with acute ischemic stroke," *Aging (Albany NY)*, vol. 12, no. 3, pp. 2428–2439, 2020.

[15] Y. Ouchi, J. Sasaki, H. Arai et al., "Ezetimibe lipid-lowering trial on prevention of atherosclerotic cardiovascular disease in 75 or older (ewtopia 75) A randomized, controlled trial," *Circulation*, vol. 140, no. 12, pp. 992–1003, 2019.

[16] D. Yang, M. Lin, S. Wang et al., "Primary angioplasty and stenting may be superior to thrombectomy for acute atherosclerotic large-artery occlusion," *Interventional Neuroradiology*, vol. 24, no. 4, pp. 412–420, 2018.

[17] A. E. Hassan, V. M. Ringheanu, L. Preston, W. G. Tekle, and A. I. Qureshi, "Acute intracranial stenting with mechanical thrombectomy is safe and efficacious in patients diagnosed with underlying intracranial atherosclerotic disease," *Interventional Neuroradiology*, vol. 28, 2022.

[18] J. Luo, T. Wang, P. Gao, T. Krings, and L. Jiao, "Endovascular treatment of intracranial atherosclerotic stenosis: current debates and future prospects," *Frontiers in Neurology*, vol. 9, 2018.

[19] X. Feng, K. L. Chan, L. Lan et al., "Stroke mechanisms in symptomatic intracranial atherosclerotic disease: classification and clinical implications," *Stroke*, vol. 50, no. 10, pp. 2692–2699, 2019.

[20] D. H. Kang and W. Yoon, "Current opinion on endovascular therapy for emergent large vessel occlusion due to underlying intracranial atherosclerotic stenosis," *Korean Journal of Radiology*, vol. 20, no. 5, pp. 739–748, 2019.

[21] H. N. Lee, C. W. Ryu, and S. J. Yun, "Vessel-wall magnetic resonance imaging of intracranial atherosclerotic plaque and ischemic stroke: a systematic review and meta-analysis," *Frontiers in Neurology*, vol. 9, 2018.

[22] B. A. Gross, S. M. Desai, G. Walker, B. T. Jankowitz, A. Jadhav, and T. G. Jovin, "Balloon-mounted stents for acute intracranial large vessel occlusion secondary to presumed atherosclerotic disease: evolution in an era of supple intermediate catheters," *Journal of Neurointerventional Surgery*, vol. 11, no. 10, pp. 975–978, 2019.

[23] Y. U. Liu, J. Cheng, X. Guo et al., "The roles of PAI-1 gene polymorphisms in atherosclerotic diseases: a systematic review and meta-analysis involving 149, 908 subjects," *Gene*, vol. 673, pp. 167–173, 2018.

[24] X. Leng, L. Lan, H. L. Ip et al., "Hemodynamics and stroke risk in intracranial atherosclerotic disease," *Annals of Neurology*, vol. 85, no. 5, pp. 752–764, 2019.

[25] Y. Liu, M. Wang, B. Zhang et al., "Size of carotid artery intraplaque hemorrhage and acute ischemic stroke: a cardiovascular magnetic resonance Chinese atherosclerosis risk evaluation study," *Journal of Cardiovascular Magnetic Resonance*, vol. 21, no. 1, pp. 36–39, 2019.

[26] M. Ghuman, A. C. O. Tsang, J. M. Klostranec, and T. Krings, "Sentinel angiographic signs of cerebral hyperperfusion after angioplasty and stenting of intracranial atherosclerotic stenosis: a technical note," *AJNR. American journal of neuroradiology*, vol. 40, no. 9, pp. 1523–1525, 2019.

[27] R. Sun, L. Wang, C. Guan, W. Cao, and B. Tian, "Carotid atherosclerotic plaque features in patients with acute ischemic stroke," *World Neurosurgery*, vol. 112, pp. e223–e228, 2018.

[28] A. C. O. Tsang, E. Orru, J. M. Klostranec et al., "Thrombectomy outcomes of intracranial atherosclerosis-related occlusions: a systematic review and meta-analysis," *Stroke*, vol. 50, no. 6, pp. 1460–1466, 2019.

Hindawi
Emergency Medicine International
Volume 2023, Article ID 9849537, 1 page
https://doi.org/10.1155/2023/9849537

Retraction

Retracted: A Meta-Analysis of How Nonalcoholic Fatty Liver Disease Affect Antiviral Treatment of Patients with e Antigen-Positive Chronic Hepatitis B

Emergency Medicine International

Received 8 August 2023; Accepted 8 August 2023; Published 9 August 2023

This article has been retracted by Hindawi following an investigation undertaken by the publisher [1]. This investigation has uncovered evidence of one or more of the following indicators of systematic manipulation of the publication process:

(1) Discrepancies in scope
(2) Discrepancies in the description of the research reported
(3) Discrepancies between the availability of data and the research described
(4) Inappropriate citations
(5) Incoherent, meaningless and/or irrelevant content included in the article
(6) Peer-review manipulation

The presence of these indicators undermines our confidence in the integrity of the article's content and we cannot, therefore, vouch for its reliability. Please note that this notice is intended solely to alert readers that the content of this article is unreliable. We have not investigated whether authors were aware of or involved in the systematic manipulation of the publication process.

Wiley and Hindawi regrets that the usual quality checks did not identify these issues before publication and have since put additional measures in place to safeguard research integrity.

We wish to credit our own Research Integrity and Research Publishing teams and anonymous and named external researchers and research integrity experts for contributing to this investigation.

The corresponding author, as the representative of all authors, has been given the opportunity to register their agreement or disagreement to this retraction. We have kept a record of any response received.

References

[1] Y. Chen, Q. Liu, J. Han et al., "A Meta-Analysis of How Nonalcoholic Fatty Liver Disease Affect Antiviral Treatment of Patients with e Antigen-Positive Chronic Hepatitis B," *Emergency Medicine International*, vol. 2022, Article ID 4774195, 7 pages, 2022.

Hindawi
Emergency Medicine International
Volume 2022, Article ID 4774195, 7 pages
https://doi.org/10.1155/2022/4774195

Research Article

A Meta-Analysis of How Nonalcoholic Fatty Liver Disease Affect Antiviral Treatment of Patients with e Antigen-Positive Chronic Hepatitis B

Yandong Chen, Qiang Liu, Jing Han, Siyu Gao, Qian Xiao, Xiaoli Huang, Lu Lu, and xiaolin Zhou

Yichang Central People's Hospital, The First College of Clinical Medical Science, China Three Gorges University, Yichang, Hubei, China

Correspondence should be addressed to xiaolin Zhou; yczhouxl@163.com

Received 13 August 2022; Revised 12 September 2022; Accepted 21 September 2022; Published 3 October 2022

Academic Editor: Hang Chen

Background. Nonalcoholic fatty liver disease (NAFLD) and chronic hepatitis B (CHB) are both the most common underlying diseases leading to cirrhosis and hepatocellular carcinoma, and NAFLD and HBV infection are the first and second leading causes of chronic liver disease in China. However, there are still a lot of controversies about whether the combined presence of CHB and NAFLD will affect the course or outcome of liver disease together with HBV, and how the two affect each other. *Objective*. To investigate the effect of nonalcoholic fatty liver disease (NAFLD) on antiviral therapy in patients with chronic hepatitis B (CHB). *Methods*. Computer searches of databases such as PubMed, CNKI, VIP.com, and Wanfang Data Knowledge Service Platform were used. The time frame was from the creation of the database to June 2022. The search subject terms were hepatitis B, CHB, or NAFLD. The observation group consisted of patients with e antigen-positive CHB with NAFLD, and the control group consisted of patients with e-antigen + CHB. Extracts including title, name, date of publication, number of samples, antiviral drugs, and outcome indicators were used for Meta-analysis. Funnel plots were drawn to analyze literature bias. *Results*. Seven papers including 1348 patients with HBeAg + CHB (observation group: $n = 547$, control group: $n = 801$) were finally included. *Results*. Meta-analysis showed that CHB patients with NAFLD had lower efficacy than CHB patients after 48 weeks of antiviral treatment with nucleotide analogs, as measured by three outcome indicators HBV DNA conversion rate, ALT-normalization, and HBeAg conversion rate. *Conclusion*. NAFLD reduces the effect of antiviral therapy in CHB patients, and the clinicopathological features of patients with NAFLD combined with chronic hepatitis B are different from those of patients with chronic hepatitis B alone, so early diagnosis by liver histological examination should be actively performed and reasonable antiviral therapy should be administered.

1. Introduction

NAFLD is one of the chronic liver diseases that has become one of the major chronic liver diseases in China and the most common chronic liver disease in the world, which is associated with insulin resistance and also with genetic susceptibility to liver damage when metabolic stress is produced, characterized by hepatic steatosis, and its disease spectrum includes from simple steatosis, nonalcoholic steatohepatitis, cirrhosis and cryptogenic cirrhosis [1, 2]. When NAFLD progresses to NASH, the risk of death increases, as it can develop cirrhosis and even liver cancer. In China, the main cause of cirrhosis is chronic hepatitis B, and more than 50 million people die each year from hepatitis B and from its complications, mainly liver failure and or hepatocellular carcinoma [3, 4]. Chronic hepatitis B is the most common chronic liver disease in China, but over the 30 years of reform and opening up, the standard of living has been improving, so people's lifestyles are changing, and NAFLD has become the leading cause of chronic liver disease in China, and the number of patients with the combination of both has increased [5].

In Western countries, the prevalence of NAFLD in the general population is about 30%, and the prevalence is even higher in obesity. The prevalence of NAFLD has been reported to affect 80–100 million people in the United States, of which 10–22% may develop NASH [6, 7]. The prevalence of NAFLD is increasing especially in Asian countries such as China and Japan, and the age is getting younger. One study showed that the rate of CHB combined with NAFLD was 18% to 62% in Europe and the Middle East and 14% to 17% in the Asia-Pacific region[8]. A study of 1309 patients with CHB in rural China with follow-up showed that the prevalence of combined NAFLD in patients with CHB increased from 6.40% in the year 2008 to 21.54% in the year 2012 in a 4-year period from 2008 to 2012, showing an increasing trend year by year [9].

Antiviral therapy is crucial for disease progression in CHB patients, and in recent years, antiviral therapies have been widely used in the clinic, and this modality has achieved notable success in the treatment of chronic hepatitis B. Data [10] showed that hepatic degeneration, hepatocellular neoplasm, positive hepatocellular neoplasm, and serum hepatitis B virus DNA levels were significantly reduced in steatosis patients, suggesting a protective effect of steatosis against lipofuscinosis. The study [11] demonstrated that NAFLD inhibits HBV without affecting host lipid homeostasis. However, the study [12] reported that antiviral therapy was ineffective in CHB patients with high CAP (controlled attenuation parameter). Therefore, there is controversy about how NAFLD affects CHB.

Based on this, in order to investigate the clinical effect of a simple antiviral method for chronic hepatitis B, computerized searches of PubMed, CNKI, VIP.com, and Wanfang Data Knowledge Service Platform databases were used in conjunction with the actual situation. The time range was from the establishment of the database to June 6, 2022. The keywords were Chinese search subject headings: hepatitis B, CHB, or NAFLD. English subject headings: Chinese and Red Cross, NAFLD. The observation group consisted of patients with *e* antigen-positive CHB, and the control group consisted of patients with *e*-antigen + CHB. Extracts including title, name, publication date, sample number, antiviral drug, and outcome index were used for Meta-analysis. Funnel plots were drawn to analyze literature bias. It is reported below.

2. Materials and Methods

2.1. Literature Search. Databases such as PubMed, CNKI, VIP.com, and Wanfang Data Knowledge Service Platform were searched using computers. The time range was from database creation to June 6, 2022. The keywords were Chinese search subject headings: hepatitis B, CHB, or NAFLD. English subject headings: Chinese and Red Cross, NAFLD. The observation group consisted of patients with *e* antigen-positive CHB, and the control group consisted of patients with *e* antigen + CHB. Extracts including title, name, publication date, sample number, antiviral drug, and outcome index were used for Meta-analysis. Funnel plots were drawn to analyze literature bias.

2.2. Inclusion Criteria. Inclusion criteria were as follows: the observation group of the research objects is the CHB patients with NAFLD who are positive for e antigen. The control group was CHB patients with positive e-antigen; study type: cohort study or case-control study; outcome indicators: serum HBV DNA level decreased to below 3 lg IU/mL, ALT normalized, and HBeAg negative conversion.

2.3. Exclusion Criteria. Exclusion criteria were as follows: (1) full text not available; (2) incomplete data; (3) duplication in the literature; (4) conclusion that the indicators do not match.

2.4. Data Extraction. The extracted content includes the title, first author, publication year, subject numbers, antiviral drugs, and outcome indicators.

2.5. Statistical Analysis. Statistical software 5.3 was used and $P < 0.05$ was considered statistically significant. RR and its 95% CI were chosen as statistical data. Heterogeneity between the literature was tested by the P test and the I^2 test. $P < 0.05$ and $I^2 < 50\%$ indicated that the literature was homogeneous (no heterogeneity) and a fixed-effects model was used, otherwise a random-effects model was used.

3. Results

3.1. Publication Screening. A computer search of databases such as PubMed, CNKI, VIP.com, and Wanfang Data Knowledge Service Platform. The time range was from the establishment of the database to June 6, 2022. Keywords: hepatitis B, nonalcoholic hepatitis. A total of 7 articles were included, including 1348 HBeAg + CHB patients, 547 observation cases, and 801 controls. The screening flow chart is shown in Figure 1, the characteristics of the literature are listed (Table 1), and the evaluation quality is shown in Table 2.

3.2. HBV DNA Negative Conversion. As shown in Figure 2, all 7 publications had the data of HBV- conversion after 48-week of antivirus. Statistical analysis found that 7 publications had a very small heterogeneity, so a fixed-effect model was adopted. Data indicated that HBV- conversion in CHB patients with NAFLD after 48-week of antiviral treatment was significantly decreased than in CHB patients.

3.3. ALT Normalization. As shown in Figure 3, all 7 studies provided data on the normalization of ALT after 48 weeks of antiviral treatment. Statistical analysis found a small heterogeneity among publications, so a fixed-effect model was adopted. Data demonstrated that the ALT-normalization rate in CHB patients with NAFLD after 48-week of antiviral treatment was lower than that in CHB patients.

3.4. HBeAg Negative Conversion. As shown in Figure 4, all 7 studies provided the data of HBeAg negative conversion after 48 weeks of antiviral treatment. Statistical analysis

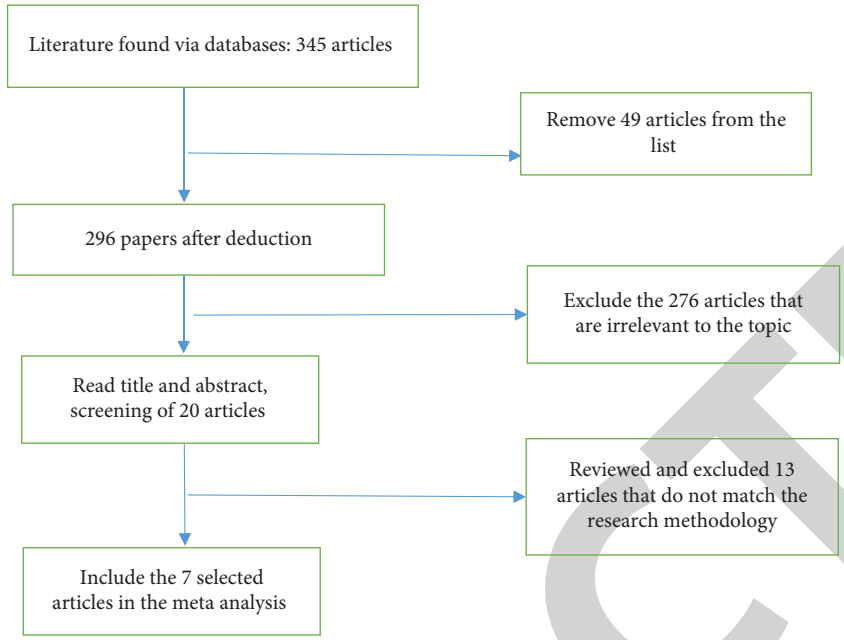

Figure 1: Literature screening process.

Table 1: Literature's Basic characteristics.

First author	Issuing time (year)	Antiviral drugs	Total number of n	Observation group/control group	HBV DNA Yin turn (observation group/ control group)	ALT return to normal (observation group/ control group	HBeAg negative conversion (observation group/ control group)
XI Jin [13]	2012	ETV	213	65/148	35/100	38/105	12/33
Li-Yao Zhu [14]	2016	ETV	125	61/64	38/48	40/52	13/15
Sun Jianmin [8]	2015	ETV	62	32/30	24/26	20/26	11/13
Wang Yanling [9]	2016	ADV	204	82/122	56/97	58/102	15/32
Wang Hao [10]	2019	ETV	273	123/150	113/141	100/135	24/44
Chen Xi [11]	2021	ETV	289	102/187	81/157	71/150	8/10
Wang Hao [12]	2018	TDF	182	82/100	75/94	65/90	14/29

Note. ETV: entecavir; TDF: tenofovir; ADV: adefovir dipivoxil.

found that 7 publications had a very small heterogeneity, so a fixed-effect model was adopted. Data indicated that the HBeAg rate of CHB patients with NAFLD after 48-week of antiviral treatment was lower than CHB patients.

3.5. Literature Bias Analysis. A funnel plot analysis was performed on the rate of HBV conversion in the included literature (Figure 5).

4. Discussion

Chronic hepatitis B refers to a chronic disease characterized by the degree of hepatocellular damage after infection with hepatitis B [3]. Chronic disease is characterized by the degree of hepatocellular damage as the main pathological change after the infection [15, 16]. The disease is characterized by the degree of damage to liver cells. When the regulation of the body's immune

Table 2: Literature quality NOS scale.

First author	Time of publication	Research object selection				Comparability between groups	Exposure factor measurement			Total score
		1	2	3	4		a	b	c	
XI Jin	2012	*	*	*	*	**	*	*		8
Li-Yao Zhu	2016	*	*	*	*	*	*	*		7
Sun Jianmin [8]	2015	*	*	*	*	**	*	*		8
Wang Yanling [9]	2015	*	*	*	*	**	*	*		8
Wang Hao [10]	2019	*	*	*	*	**	*	*		8
Chen Xi [11]	2021	*	*	*	*	*	*	*		7
Wang Hao [12]	2018	*	*	*	*	**	*	*		8

Note. a determination of exposure factors; *b* use the same method to determine exposure factors of cases and control groups; *c* nonresponse rate; 1 Whether the determination of cases is appropriate; 2 Representation of cases; 3 Selection of control groups 4. Controls Sure.

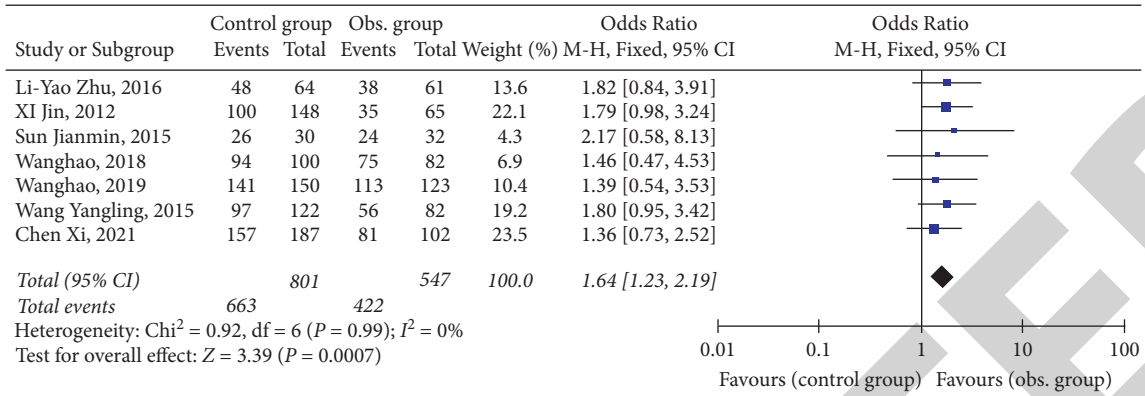

Figure 2: Data of HBV DNA negative conversion after 48-week antivirus.

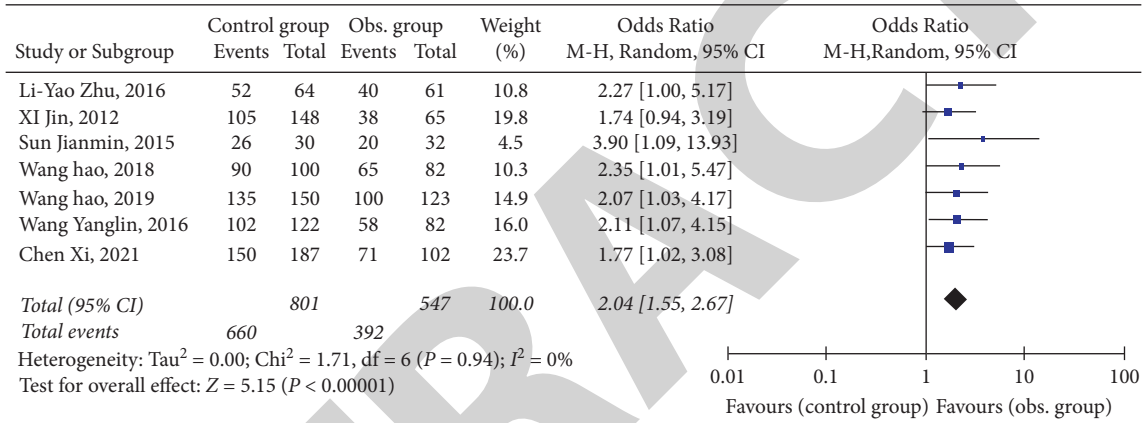

Figure 3: Data of ALT normalization after 48-week antivirus.

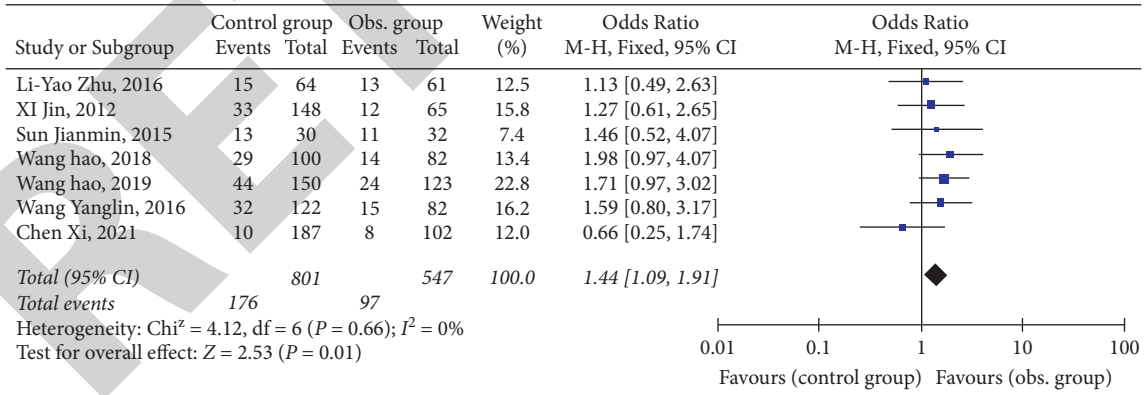

Figure 4: Data of HBeAg negative conversion after 48-week antivirus.

system is disturbed, the patient's liver cells are damaged, resulting in liver damage. In the case of NAFLD, the liver cells are damaged, resulting in abnormal liver function and liver fibrosis. NAFLD is a liver disease caused by genetic predisposition and insulin resistance. NAFLD is a disease of liver parenchyma caused by excessive fat content in the liver cells due to genetic predisposition and insulin resistance. To some extent chronic hepatitis B and NAFLD are two separate diseases [17, 18], they often appear in a combined form and have a more pronounced effect on each other, leading to liver fibrosis. The two diseases are often combined and have a significant impact on each other, leading to liver fibrosis, which can accelerate cirrhosis if the patient does not receive the relevant treatment in the first place. If the patient does not receive the relevant treatment in the first place, the transformation process of

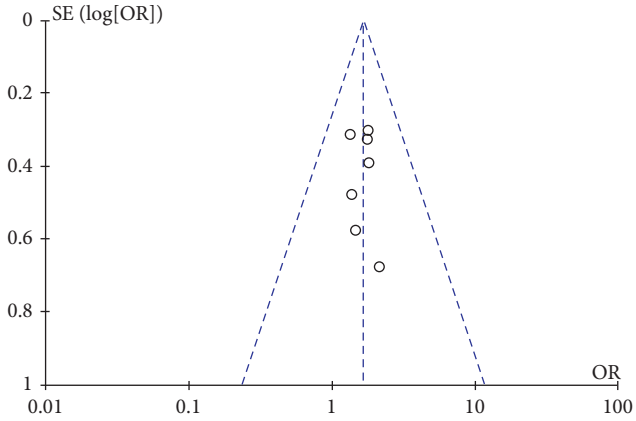

Figure 5: Funnel plot analysis of the negative conversion rate of HBV DNA in the included literature.

cirrhosis will be accelerated, which is undoubtedly a great difficulty for clinical treatment. This is undoubtedly a great difficulty for clinical treatment.

The results of this study showed that the patients' AST, TG, TC, and ALT improved more significantly when they were treated with hepatoprotective therapy and the observation group was treated with antiviral therapy alone. Although the basic hepatoprotective therapy could improve liver function, fibrosis level, and ballooning changes to some extent, the effect was more significant with the addition of the antiviral method, and the patients were able to achieve 89% and 100% of the liver function level and HBV DNA conversion rate after the treatment [19].

It has been noted in the literature that there is also variability in the effectiveness of the use of antiviral treatment in patients with different NAFLD scores. Here among them the biochemical parameters of the 7 and 8 subgroups improved significantly compared to the pretreatment period, while the effect of antiviral therapy was more significant in patients with scores of 5–6. This fundamentally confirms that there is a correlation between the severity of fatty liver disease and the effectiveness of antiviral treatment for hepatitis B. The NAFLD score has a significant impact on the effectiveness of antiviral treatment for chronic hepatitis B disease. It is recommended that for this group of patients, intensive NAFLD treatment is used, which includes specific measures such as medications and exercise.

Treatment of CHB includes antiviral therapy with interferon and nucleoside analogs. Due to different mechanisms, we included only patients receiving antiviral therapy with nucleoside analogs. A total of 7 publications, including 1348 HBeAg + CHB patients with NOS score $\geq$ 7, were included and were of high quality. The meta-analysis finally concluded from the perspective of three outcome indicators, HBV-conversion, ALT-normalization, and HBeAg conversion, that CHB patients with NAFLD had lower efficacy than CHB patients after 48 weeks of antiviral therapy with nucleoside analogs. This is consistent with the results observed in most of the literature.

However, this meta-analysis has some drawbacks and limitations.

(1) Antiviral treatment with nucleoside analogs is a long-term process. Due to the different follow-up time points of the included studies, this meta-analysis only examined the virological and biochemical responses after 48 weeks of antiviral therapy. However, there was a significant correlation between the duration of antiviral treatment and its response. Therefore, other experiments are needed to observe the efficacy at other time points.

(2) Through a literature search, we retrieved 16 relevant studies, but because 9 of them did not specify the e-antigens of the included patients, no comprehensive analysis was performed. Only 6 papers were included for analysis, which is not a large enough sample size and may be potentially biased.

In patients with more severe fatty liver disease, the implementation of antiviral therapy can improve the overall liver function of the patient; thus, enabling the demonstration that the combination of antiviral therapy for those with poor hepatoprotective therapy alone can promote disease regression. For NAFLD scores of 5 to 6, patients with liver function ALT greater than 3NLN are recommended to be treated with simple antiviral therapy. This can reduce the liver load to some extent.

In conclusion, our study suggests that NAFLD inhibits antiviral therapy in patients with CHB. More experiments with larger samples are still needed to draw more accurate conclusions.

5. Conclusion

In conclusion, in patients with chronic hepatitis B combined with NAFLD, the use of hepatoprotective therapy along with antiviral therapy can improve the overall HBV DNA and HBsAg conversion rate, as well as liver function, improve NAFLD classification, better repair the degree of liver damage, and improve liver function, which is worth further promotion in clinical treatment. It is worth to further promote its use in clinical treatment.

Data Availability

The data used to support the findings of this study are available from the corresponding author upon reasonable request.

Conflicts of Interest

The authors declare that there are no conflicts of interest regarding the publication of this paper.

Acknowledgments

This study was supported by the Yichang City Medical and Health Scientific Research Project(No.B22-2-002).

Hindawi
Emergency Medicine International
Volume 2023, Article ID 9836710, 1 page
https://doi.org/10.1155/2023/9836710

Retraction

Retracted: Clinical Evaluation of Unilateral Vertebroplasty for OVCF

Emergency Medicine International

Received 8 August 2023; Accepted 8 August 2023; Published 9 August 2023

This article has been retracted by Hindawi following an investigation undertaken by the publisher [1]. This investigation has uncovered evidence of one or more of the following indicators of systematic manipulation of the publication process:

(1) Discrepancies in scope
(2) Discrepancies in the description of the research reported
(3) Discrepancies between the availability of data and the research described
(4) Inappropriate citations
(5) Incoherent, meaningless and/or irrelevant content included in the article
(6) Peer-review manipulation

The presence of these indicators undermines our confidence in the integrity of the article's content and we cannot, therefore, vouch for its reliability. Please note that this notice is intended solely to alert readers that the content of this article is unreliable. We have not investigated whether authors were aware of or involved in the systematic manipulation of the publication process.

In addition, our investigation has also shown that one or more of the following human-subject reporting requirements has not been met in this article: ethical approval by an Institutional Review Board (IRB) committee or equivalent, patient/participant consent to participate, and/or agreement to publish patient/participant details (where relevant).

Wiley and Hindawi regrets that the usual quality checks did not identify these issues before publication and have since put additional measures in place to safeguard research integrity.

We wish to credit our own Research Integrity and Research Publishing teams and anonymous and named external researchers and research integrity experts for contributing to this investigation.

The corresponding author, as the representative of all authors, has been given the opportunity to register their agreement or disagreement to this retraction. We have kept a record of any response received.

References

[1] X. Wen, Y. Zhang, W. Jiang, W. An, B. Zhang, and J. Liu, "Clinical Evaluation of Unilateral Vertebroplasty for OVCF," *Emergency Medicine International*, vol. 2022, Article ID 2037185, 6 pages, 2022.

Hindawi
Emergency Medicine International
Volume 2022, Article ID 2037185, 6 pages
https://doi.org/10.1155/2022/2037185

Research Article

Clinical Evaluation of Unilateral Vertebroplasty for OVCF

Xiaoming Wen, Yan Zhang, Wei Jiang, Wenbo An, Binggang Zhang, and Jianjun Liu

Department of Orthopedics, West Hospital, Affiliated Hospital of Gansu University of Traditional Chinese Medicine, Lanzhou 730060, China

Correspondence should be addressed to Jianjun Liu; liujj200607@163.com

Received 28 June 2022; Revised 2 August 2022; Accepted 18 August 2022; Published 30 September 2022

Academic Editor: Hang Chen

Objective. To investigate the clinical evaluation of unilateral vertebroplasty for OVCF. *Methods*. A retrospective analysis was performed on 60 patients treated with PVP from January 2020 to December 2021. Patients were divided into two groups according to the treatment method, 30 patients in the PVP group received PVP and 30 patients in the PCVP group received PCVP. The VAS score, ODI score, bone cement dosage, and leakage were compared between the two groups preoperatively, immediately postoperatively, and 7 and 30 days postoperatively. *Results*. VAS scores in the PCVP and PVP groups before, immediately after, and 7 days after surgery were $P > 0.05$, and the difference was not statistically significant; ODI score in group 1 before surgery was not statistically significant ($P > 0.05$); bone cement injection volume in the PVP group was significantly higher than that in the PCVP group ($P < 0.05$), and the difference was statistically significant; the difference in bone cement leakage between the two groups was not statistically significant ($P > 0.05$). *Conclusion*. Under the same puncture conditions, the PCVP group used the method of injection while retreating to achieve a better bone cement dispersion effect by using less bone cement and achieving uniform dispersion of bone cement. It can relieve the patients' back pain and improve the back function.

1. Research Methodology

1.1. General Information. A retrospective analysis was conducted on 30 OVCF patients (30 vertebral bodies) treated with PVP from January 2020 to December 2021 (PVP group) and 30 OVCF patients (30 vertebral bodies) treated with PCVP (PCVP group). All patients underwent preoperative bone mineral density examination to indicate severe osteoporosis. MR examination or ECT examination was performed to determine the fracture site and identify whether it was a fresh fracture.

1.2. Surgical Methods. All patients were prone on the hospital bed, and the operation area was anesthetized (5 ml, 0.1% lidocaine), routinely disinfected, and covered.

In the PVP group, unilateral needling is performed under c-arm guidance, usually with severe symptoms. If there was no significant difference in symptoms on both sides, the left side was selected for puncture. Fluoroscopy confirmed that the needle insertion position was good. The working sleeve was removed, and the wound was covered with a sterile dressing at the end of the drawing period and 2-3 minutes after injection. About 10 to 15 minutes after the injection, after confirming that the residual bone cement in vitro is completely solidified, the patient is turned to the supine position on the flat car with the cooperation of the nurse, then returned to the ward, and the operation is completed.

In the PCVP group, the PCVP operation was the same as that of the PVP. Usually, the side with severe symptoms was selected for puncture. A working cannulation with a diameter of 3.7 mm was selected for puncture and the needle position was confirmed by using fluoroscopy. In the responsible vertebral body, take out the angle syringe when necessary and inject bone cement. Pull out the angle syringe 1~2 minutes after injection and then rotate and pull out the working sleeve. Cover the wound. About 10 to 15 minutes after the injection, after confirming that the residual bone cement in vitro is completely solidified, the patient is turned

to the supine position on the flat car with the cooperation of the nurse, then returned to the ward, and the operation is completed.

1.3. Postoperative Treatment. After returning to the ward, the patient was instructed to stay in bed for 2 hours, asked to take a supine position, pain relief and symptomatic treatment according to the patient's pain condition was provided, and was routinely given antiosteoporosis treatment. 2 hours after surgery, patients were instructed to walk moderately while wearing the waist circumference. According to the patient's postoperative recovery, we planned to discharge the patient after DR examination and explained the preventive measures, postoperative follow-up, and regular anti-osteoporosis matters. All patients successfully underwent the operation.

1.4. Observation Indicators. VAS score, ODI score, and bone cement injection volume were observed before surgery, immediately after surgery, and 7 days and 30 days after surgery.

Bone cement leakage rate: high-resolution CT plain scan was performed after operation, and cement leakage manifests beyond the vertebral body margins. Bone cement distribution and diffusion: select the layer with the largest bone cement distribution area in the CT image for plane division. On the cross section, the vertebral body was divided into two areas, left and right, in the middle, and each area was divided into 3 subareas, the front, middle, and rear, and each area was divided into 4 equal parts, for a total of 24 subareas. If bone cement covers the eight regions, then the distribution of bone cement can theoretically be considered ideal [1].

Pain evaluation [2]: pain was assessed on the Visual Analog Scale (VAS) from 0 to 10 at each time point. The higher the OVCF score, the higher the pain.

OSS Disability Index (ODI) [3]: the degree of disability increases with the OVCF score, which ranges from 0 to 100 according to the ODI score.

1.5. Statistical Processing. SPSS 22.0 software is used for data statistical analysis. The data of normal distribution were expressed as ($\overline{x} \pm s$), and the independent sample T test was used for intergroup comparison. The count data is represented by %, and the test method is χ^2. $P < 0.05$ indicates statistically significant difference between groups.

2. Results

2.1. General Data. There was no statistical significance in the general data ($P > 0.05$, Table 1).

2.2. VAS Scores of Pain in Both Groups. As shown in Table 2, the VAS scores of pain in the PCVP and PVP groups preoperatively, postoperatively, and 1 week postoperatively were $P > 0.05$.

Table 1: General data of patients ($\overline{x} \pm s$)/[cases (%)].

Group	Age range	Duration of disease (days)	Sex	
			M	F
PCVP group ($n = 30$)	68.4 ± 2.3	4.8 ± 0.5	8	22
PVP group ($n = 30$)	69.2 ± 2.4	5.0 ± 0.6	10	20
t/c^2	1.318	1.403	0.318	
P	0.193	0.166	0.573	

Table 2: Pain VAS scores of patients presurgery, postsurgery, and 1 week and 1 month ($\overline{x} \pm s$, points).

Group	Presurgery	Postsurgery	1 week after surgery
PCVP group	8.10 ± 0.67	3.03 ± 0.69	1.54 ± 0.12
PVP group	7.97 ± 0.78	3.07 ± 0.80	1.63 ± 0.22
P	0.832	0.837	0.054

Note. $P < 0.05$ difference is statistically significant.

2.3. ODI Functional Index and Bone Cement Injection Volume before and after Surgery in Both Groups. The results of the data in Table 3 show that the ODI score before and after surgery in both groups ($P > 0.05$) and the amount of bone cement injection in the PVP group were significantly higher than that in the PCVP group ($P < 0.05$).

2.4. Bone Cement Leakage and Dispersion in the Two Groups. As shown in Table 4, there was no significant difference in bone cement leakage between the two groups, $P > 0.05$.

3. A Typical Surgical Case

As shown in Figure 1, in the patient's unilateral vertebroplasty, the curved puncture cannula was successfully punctured with satisfactory puncture results (Figures 1(a) and 1(b)). The angle of inclusion in the coronal plane was 27° (Figures 1(c) and 1(d)), and the injection of bone cement was successfully completed while retraction was taking place (Figures 1(e) and 1(f)). The postoperative CT images showed that the bone cement injection was symmetrically dispersed and evenly diffused (Figures 1(g) and 1(h)), and the surgical result was good.

4. Discussion

Some researchers believe [4] that the bilateral arch root approach is more advantageous for relieving patients' postoperative low back pain because the relief of patients' postoperative pain depends largely on the symmetrical distribution of bone cement in the injured vertebrae, which equalizes the stress in the injured vertebrae, which is one of the important mechanisms for pain relief. However, some studies [5] have shown that the use of unilateral pedicle approach with cement injection has been effective in restoring the height of the injured vertebral body, and the use of bilateral approach will undoubtedly increase the risk of surgery, prolong the operation time, and increase the X-ray exposure time of the patient, which may not be beneficial to

Table 3: Preoperative and postoperative ODI score and bone cement injection volume ($\overline{x} \pm s$).

Group	ODI functional index		Bone cement injection volume (ml)
	Presurgery	Postsurgery	
PCVP group	38.13 ± 3.22	21.45 ± 2.21	3.92 ± 1.41
PVP group	37.94 ± 3.18	22.23 ± 2.30	4.86 ± 1.21
P	0.819	0.186	0.007

Table 4: Bone cement leakage and bone cement dispersion [cases (%)].

Group	Bone cement leakage	Degree of bone cement dispersion
PCVP group	2/6.67%	27/90.00%
PVP group	5/40.00%	18/60.00%
X^2/P	1.456/0.228	7.2/0.007

Note. $P < 0.05$ difference is statistically significant.

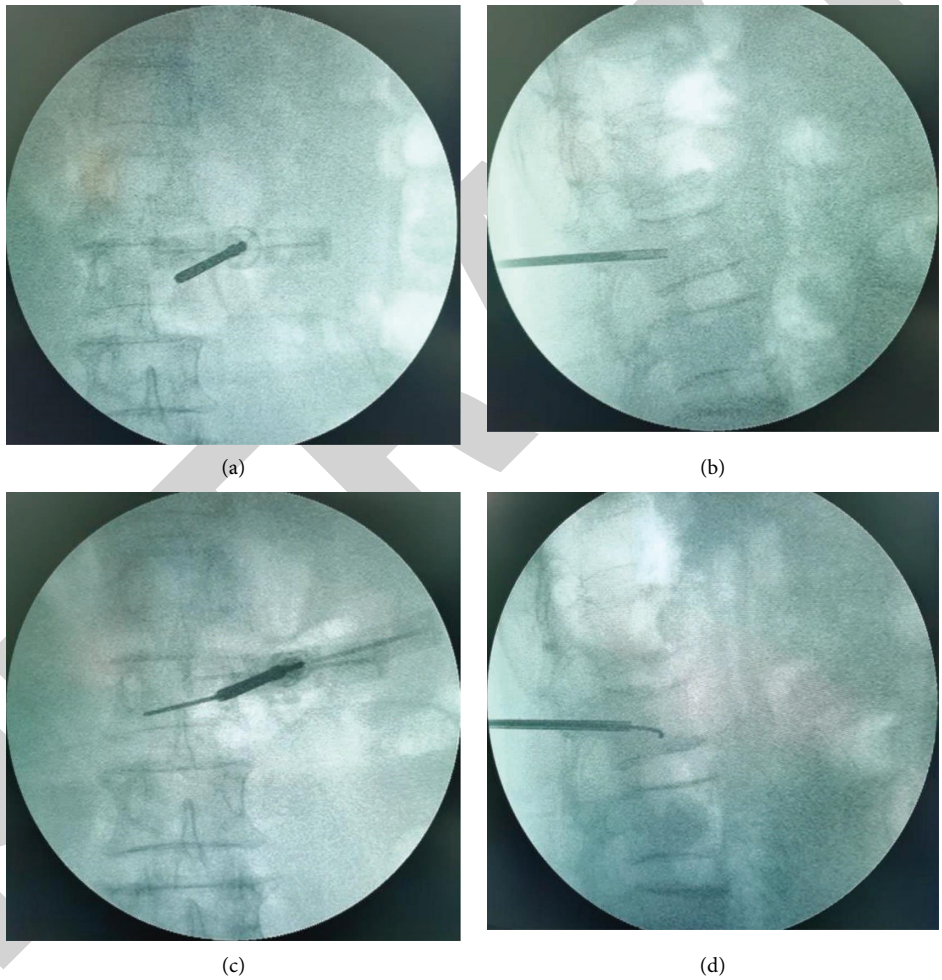

(a) (b)

(c) (d)

Figure 1: Continued.

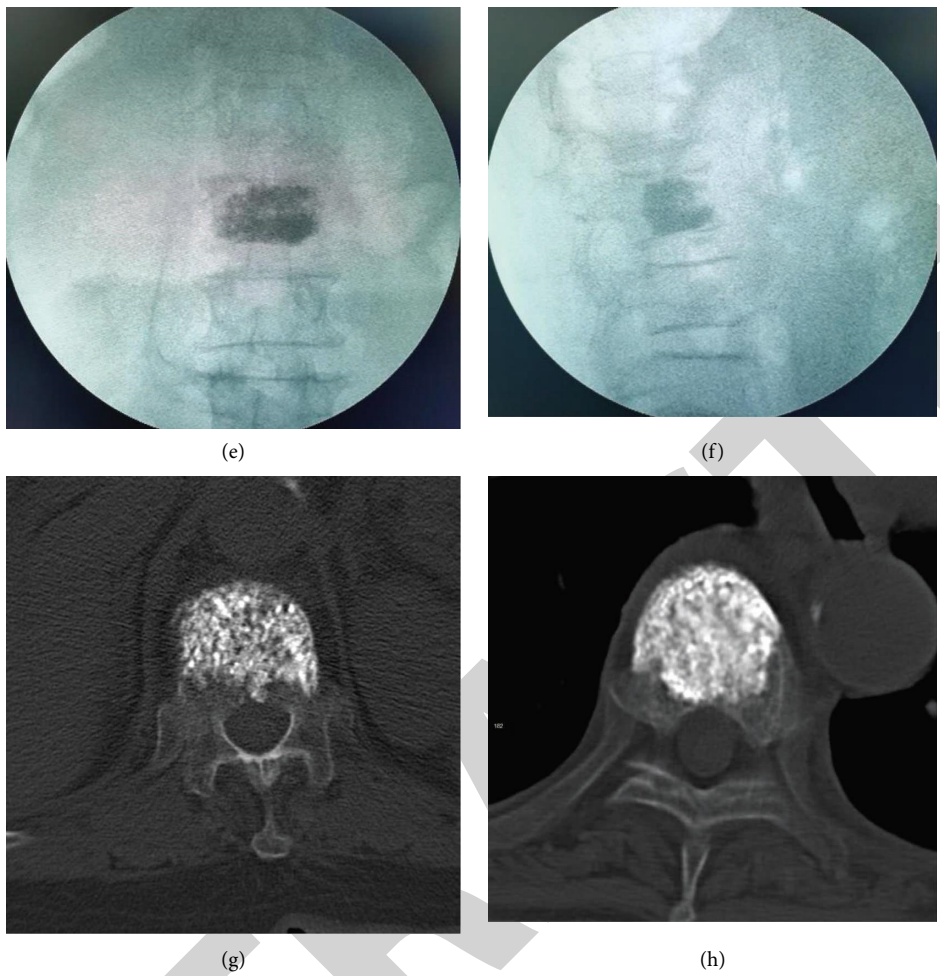

Figure 1: Intraoperative and postoperative CT images of unilateral arcuate vertebroplasty. (a, b) show the front and side views after successful puncture of the arcuate puncture cannula; (c, d) show the front and side views of the arcuate guide needle placed in the vertebral body; (e, f) show the front and side views after bone cement injection; (g, h) show the CT images after bone cement injection.

the patient. The results of this study also confirm that the operative time and the number of X-ray exposures (time) were significantly higher in the bilateral group than in the unilateral group. Reference [6] suggests that there is no significant difference in recent clinical outcomes between bilateral and unilateral pedicle approaches for the treatment of osteoporotic vertebral compression fractures, and the question has mostly focused on which approach is more effective in terms of clinical outcomes (especially pain relief) for patients. Angled vertebroplasty is based on a unilateral puncture in which a nickel-titanium alloy guide pin with ultra-high elasticity and good metallic mechanical strength is delivered through a puncture cannula to the other side of the vertebral body, creating a lateral space to facilitate delivery of the cannula [7]. The anterior edge of the vertebral body midline is the outlet of the anterior cement, and the bone cement can diffuse laterally without resistance. The arc-shaped diffusion distribution ensures symmetrical distribution of the bone cement, allowing it to be evenly distributed on both sides of the vertebral body, with the same advantages as bilateral puncture. It is important to pay attention to the depth and direction of the puncture cannula to avoid puncturing the anterior edge of the vertebral body or the anterior part of the upper and lower end plates; thus, increasing the risk of bone cement leakage [8]. This study focuses on the application of PCVP in the treatment of OVCF.

Based on the PVP-modified PCVP, the bone cement can spread through the anterior part of the spine to the middle of the spine without increasing the puncture angle, and the injection site is highly mobile and symmetrically and uniformly distributed, which balances the strength of both sides of the vertebral body and solves the problem of uneven distribution of bone cement in traditional treatment, resulting in poor pain [9]. The comparison of pain scores between the two groups after surgery showed that there was no significant difference in visual scores between the PCVP and PVP groups preoperatively, postoperatively, and 7 days after surgery, indicating that PCVP and PVP can be very effective. Our results showed no statistically significant differences in ODI score, VAS scores, and PVP at 1 day, 2 months, and 6 months after PCVP. In addition, References [10, 11] and others have confirmed that PCVP has no significant advantage in relieving pain and improving spinal cord function.

Traditional OVCF vertebroplasty mainly consists of PVP and PKP. PVP usually requires increased cement injection to achieve diffusion, but also increases the risk of cement leakage as a result. If the PKP procedure is performed with balloon expansion, it can better restore the height of the injured vertebral body and compact the cancellous bone around the left cavity, forming an artificial barrier to prevent cement leakage. If PKP is performed by balloon expansion, the height of the injured vertebral body can be better restored, and the cancellous bone around the left cavity can be compacted to form an artificial barrier to prevent cement leakage and reduce the injection of bone cement. However, from a biomechanical point of view, References [12, 13] found that cement-induced increase in vertebral stiffness increases the risk of fracture of adjacent vertebrae. In addition, vertebral bone cement increases the likelihood of secondary Kummell's disease [14, 15].

In angled vertebroplasty, an angled needle creates a small gap between the vertebral fractures and is injected posteriorly, and better spreading of the vertebrae and the same therapeutic results can be achieved with a small amount of bone cement [16]. Some studies even suggest that a large amount of bone cement filling should be limited to less than 5 ml, which can greatly reduce the leakage rate of bone cement [17]. In the early stage of injection, the bone cement had relatively good mobility and high dispersion in the vertebral body but with a high infiltration rate; in the late stage of injection, the bone cement had poor relative mobility, low dispersion in the vertebral body, uneven distribution, and low leakage rate [18]. In this study, we found that the amount of bone cement injected in the PVP group was significantly higher than that in the PCVP group, and the difference was statistically significant. References [19, 20] also confirmed that there was also no significant difference in bone cement leakage between the two groups, which is consistent with the present study. This is related to the fact that the surgeons in the surgical group may have a long history of PVP and have extensive clinical experience in reducing bone cement leakage.

5. Conclusion

In patients with OVCF, the injection was performed by the method of injection while retreating under the same puncture conditions, and the use of less bone cement can achieve uniform dispersion of bone cement, which can achieve better dispersion of bone cement, relieve patients' back pain, and improve back function. However, this study has disadvantages such as small sample size, no long-term follow-up, and only patients with newly occurred vertebral compression fractures were included, and the evaluation of postoperative vertebral stability and whether fractures occurred need further improvement, and the results may be biased, and more in-depth studies will be conducted in the next step.

Data Availability

The simulation experiment data used to support the findings of this study are available from the corresponding author upon request.

Conflicts of Interest

The authors declare that there are no conflicts of interest regarding the publication of this paper.

Authors' Contributions

Xiaoming Wen and Yan Zhang contributed equally to this work.

References

[1] Q. Zhou, H. Liu, H. Kou et al., "Early efficacy evaluation of curved vertebroplasty device and its influence on bone cement distribution," *Chinese Journal of Orthopaedic Surgery*, vol. 25, no. 10, pp. 892–897, 2017.

[2] Anonymity, "Visual analog scoring method," *Journal of Clinical and Experimental Medicine*, vol. 12, no. 23, p. 1925, 2013.

[3] G. Tang, Q. Yang, J. Hou, Z. He, X. Sun, and Y. Song, "Comparison of unilateral and bilateral kyphoplasty for osteoporotic vertebral fractures," *Chinese Journal of Orthopaedic Surgery*, vol. 29, no. 10, pp. 939–942, 2021.

[4] Z. D. Cui, G. Yang, and D. P. Zhang, "[Clinical efficacy and radiation exposure analysis of vertebroplasty and curved vertebroplasty in the treatment of osteoporotic vertebral compression fracture]," *Zhong Guo Gu Shang*, vol. 34, no. 8, pp. 725–731, 2021.

[5] G. Yao, Y. X. Shen, M. Li, and B. Cai, "[Biomechanical effects of different bone cement diffusion patterns after vertebroplasty: finite element analysis]," *Zhongguo Gu Shang*, vol. 34, no. 8, pp. 732–737, 2021.

[6] S. Marcia, M. Muto, J. A. Hirsch et al., "What is the role of vertebral augmentation for osteoporotic fractures? a review of the recent literature," *Neuroradiology*, vol. 60, no. 8, pp. 777–783, 2018.

[7] L. Wen, Y. Liu, C. Guang et al., "Comparison of the efficacy of modified PVP and PCVP techniques through unilateral puncture at the root of the transverse process in the treatment of lumbar osteoporotic fractures," *Journal of Neck and Low Back Pain*, vol. 41, no. 2, p. 4, 2020.

[8] Q. Cao, M. Duan, L. Zhang, Y. Feng, Y. Zhou, and J. Wang, "Analysis of the effect of manual reduction of PCVP and unilateral PKP in the treatment of osteoporotic vertebral compression fractures," *Clinical Misdiagnosis and Mistreatment*, vol. 34, no. 2, p. 5, 2021.

[9] S. Fang, J. Min, Z. Zeng et al., "Analysis of risk factors for refracture of adjacent vertebral bodies after percutaneous vertebral dilatation and balloon kyphoplasty," *China Orthopedics*, vol. 34, no. 8, pp. 705–709, 2021.

[10] Q. Deng, X. Qiao, Z. Li et al., "Investigation of risk factors for non-operative vertebral refracture after osteoporotic vertebral compression fracture," *Chinese Journal of Osteoporosis*, vol. 27, no. 4, pp. 613–617, 2021.

[11] Y. Li, J. Shu, Z. Wang et al., "Effect of teriparatide on residual low backpain after percutaneous kyphoplasty for osteoporotic vertebral compression fractures," *Chinese Journal of Traumatology*, vol. 38, no. 3, pp. 198–204, 2022.

[12] X. Y. Xu, D. M. Luo, S. L. Liu, X. T. Shen, Z. Y. Zhou, and G. D. Yuan, "[Treatment of severely osteoporotic vertebral compression fractures with the vertebral body stent system and percutanous kyphoplasty combined with zoledronic acid]," *Zhongguo Gu Shang*, vol. 33, no. 9, pp. 827–830, 2020.

Hindawi
Emergency Medicine International
Volume 2023, Article ID 9814961, 1 page
https://doi.org/10.1155/2023/9814961

Retraction

Retracted: Efficacy and Safety of Glycosides of Tripterygium wilfordii Combined with Renin-Angiotensin System in the Treatment of IgA Nephropathy: A Systematic Review and Meta-Analysis

Emergency Medicine International

Received 8 August 2023; Accepted 8 August 2023; Published 9 August 2023

This article has been retracted by Hindawi following an investigation undertaken by the publisher [1]. This investigation has uncovered evidence of one or more of the following indicators of systematic manipulation of the publication process:

(1) Discrepancies in scope
(2) Discrepancies in the description of the research reported
(3) Discrepancies between the availability of data and the research described
(4) Inappropriate citations
(5) Incoherent, meaningless and/or irrelevant content included in the article
(6) Peer-review manipulation

The presence of these indicators undermines our confidence in the integrity of the article's content and we cannot, therefore, vouch for its reliability. Please note that this notice is intended solely to alert readers that the content of this article is unreliable. We have not investigated whether authors were aware of or involved in the systematic manipulation of the publication process.

Wiley and Hindawi regrets that the usual quality checks did not identify these issues before publication and have since put additional measures in place to safeguard research integrity.

We wish to credit our own Research Integrity and Research Publishing teams and anonymous and named external researchers and research integrity experts for contributing to this investigation.

The corresponding author, as the representative of all authors, has been given the opportunity to register their agreement or disagreement to this retraction. We have kept a record of any response received.

References

[1] M. Chen, P. Zhang, L. Li, Z. Yu, N. Liu, and L. Wang, "Efficacy and Safety of Glycosides of Tripterygium wilfordii Combined with Renin-Angiotensin System in the Treatment of IgA Nephropathy: A Systematic Review and Meta-Analysis," *Emergency Medicine International*, vol. 2022, Article ID 5314105, 12 pages, 2022.

Hindawi
Emergency Medicine International
Volume 2022, Article ID 5314105, 12 pages
https://doi.org/10.1155/2022/5314105

Research Article

Efficacy and Safety of Glycosides of Tripterygium wilfordii Combined with Renin-Angiotensin System in the Treatment of IgA Nephropathy: A Systematic Review and Meta-Analysis

Ming Chen, Peiqing Zhang, Lianhua Li, Zhuo Yu, Na Liu, and Lifan Wang

Heilongjiang Academy of Traditional Chinese Medicine, Department of Nephropathy, Heilongjiang 150036, China

Correspondence should be addressed to Lifan Wang; wlf4648374@126.com

Received 17 August 2022; Revised 9 September 2022; Accepted 16 September 2022; Published 30 September 2022

Academic Editor: Hang Chen

Background. IgA nephropathy (IgAN) is currently the most common primary glomerular disease, accounting for approximately 36.7% to 58.2% of primary glomerular disease in kidney biopsies in China. Definitive diagnosis depends on immunopathological examination of the kidney. The prognosis of this disease was generally considered to be good, but recent studies have found that about half of patients can progress to end-stage renal disease within 30 years of onset. Because the pathogenesis is unknown, there is no specific treatment. *Objective*. To evaluate the efficacy and safety of glycosides of Tripterygium wilfordii (GTW) in combination with renin-angiotensin system (RAS) inhibitors for the treatment of IgAN. *Methods*. Search Embase, Pubmed, Cochrane, CNKI, Web of Science, Wanfang, and VIP for all randomized controlled trials (RCTs) on treating IgAN with RASI from the self-built database to December 2021. Relevant data were searched and collected separately by two reviewers. The Cochrane risk of bias model was used for quality assessment, and RevMan 5.3 was used for data analysis. *Results*. Thirteen Chinese publications with a total of 958 patients were finally included. There was no statistically significant difference in baseline information (including laboratory data and clinical parameters) between the two groups of patients. The urine protein quantification in both groups showed a significant decreasing trend as the treatment duration increased. At 3, 6, 9, and 12 months after treatment, urine protein was significantly lower than the baseline value in both the observation and control groups ($P < 0.05$). During the follow-up period, there was no statistical difference in blood creatinine (Scr) and eGFR values between the two groups compared with the baseline values ($P > 0.05$). Patients with CKD stage 2 achieved a higher remission rate compared with patients with CKD stage 3, with a statistically significant difference ($P < 0.05$), and the difference between the two groups was not significant for patients in the same stage. There was no statistically significant difference in the total effective rate between the two groups ($P > 0.05$). During the follow-up period, there was no statistically significant difference in urine protein quantification, Scr, and eGFR between the two groups. In terms of the incidence of adverse reactions, the observation group was less than the control group, and there was a significant difference between the two groups ($P < 0.05$). *Conclusion*. GTW combined with RASI is one of the safe and effective treatment modes for IgAN nephropathy. It can not only effectively reduce the excretion of urinary protein in patients and delay the progression of chronic kidney disease but also has less serious side effects and is well tolerated by patients, so it can be a new choice of therapeutic drugs for this group of patients.

1. Introduction

IgA nephropathy (IgAN), also known as Berger's disease, is divided into two categories: primary and secondary. Primary IgA nephropathy is more common, accounting for about 36.7% to 58.2% of primary glomerular diseases diagnosed by renal pathology in China, and its incidence has been gradually increasing in recent years [1, 2]. It can be seen at any age, and patients aged 16–35 years account for about 80% of the total number of patients with the disease [3, 4]. The main pathological manifestation is the deposition of IgA-based immune complexes with or without IgG and IgM in the glomerular thylakoid region or capillary loops.

In terms of clinical manifestations, IgA nephropathy is characterized by varying degrees of hematuria, proteinuria, edema, hypertension, renal insufficiency, and, in a small

number of patients, acute kidney injury (AKI) [5, 6]. The prognosis of this disease was generally considered to be good, but recent studies have shown that IgA nephropathy has a poor long-term prognosis and is one of the more important primary causes of end-stage renal disease (ESRD) in China. About 50% of patients progress to ESRD within 30 years and require renal replacement therapy to maintain life [7, 8]. The specific pathogenic effects and causative targets of IgA nephropathy remain unclear, and because its clinical manifestations vary and the severity of the disease varies, there are no uniform and standardized therapeutic measures, and most existing treatment regimens are centered on controlling risk factors [9, 10]. Persistent proteinuria >1 g/d, persistent severe hypertension, and renal impairment are the more important risk factors in the clinical manifestations of IgA nephropathy [11, 12]. The current treatment focuses on reducing proteinuria, controlling blood pressure levels, and slowing the progression of renal function.

The renin-angiotensin system (RAS) blockers are the most widely used drugs with proven efficacy in the treatment of IgA nephropathy, mainly including angiotensin-converting enzyme inhibitors (ACEI) and angiotensin II receptor antagonists (ARB). The 2012 KDIGO guidelines recommend long-term treatment with RAS blockers for patients with urine protein >1 g/d; RAS blockers are recommended for patients with urine protein between 0.5 and 1 g/d [13, 14].

Glycosides of Tripterygium wilfordii (GTW), an active ingredient extracted from the peeled root of Tripterygium wilfordii, is the most widely used Chinese patent immunosuppressant with powerful anti-inflammatory and immunosuppressive effects and is used more frequently in diabetic nephropathy and rheumatic diseases. Studies have shown [15, 16] that the most important active component of rehmannia polysaccharide, rehmannia lactone alcohol, significantly reduced serum IgA levels and improved abnormal IgA glycosylation in rats with IgA nephropathy. It has been shown to be effective in IgA nephropathy with normal renal function and moderate proteinuria, but its use in the treatment of IgA nephropathy with decompensated renal function has been less studied. Patients with abnormal renal function at the time of renal biopsy have more severe pathological damage and higher pathological grade, and they often show insensitivity to hormones. Therefore, in this study, we investigated the clinical efficacy of tretinoin combined with the RAS blocker by comparing it with glucocorticoid combined with the RAS blocker and explored the effectiveness and safety of tretinoin in reducing urinary protein and delaying the progression of chronic kidney disease so as to provide a theoretical basis for the clinical treatment of patients with IgA nephropathy.

2. Materials and Methods

2.1. Inclusion and Exclusion Criteria

2.1.1. Inclusion Criteria

(1) Studies should be published RCTs of GTWplus RASI in treating IgAN

(2) Follow-up time is more than 3 months

(3) IgAN diagnosis by renal biopsy

(4) Complete data

(5) The language of literature is limited to Chinese and English

2.1.2. Exclusion Criteria

(1) Non-RCT studies

(2) Incomplete data

(3) Failure to exclude patients with systemic diseases

2.2. Literature Search. By searching Embase, PubMed, Cochrane, CNKI, Web of Science, Wanfang, and VIP, the search interval was from the creation of the database to December 2021. Search terms were as follows: ("IgA nephropathy" or "glomerulonephritis, IgA") and ("Tripterygium," "Glycosides of Tripterygium wilfordii," or "GTW") and ("ACEI," or "ARB," "Puri," or "Sartan," or "RAS inhibitor"). Search for possible study titles, abstracts, and full text has been conducted.

2.3. Quality Assessment. Publication quality was evaluated according to the Cochrane risk of bias method. Two reviewers independently extracted data, evaluated the search results, and evaluated the full text when necessary, using standard data extraction methods for extraction. A third evaluator was asked to help resolve disagreement.

2.4. Data Collection and Analysis. Data such as participant characteristics, study baseline, and intervention characteristics for each group were extracted from all the included studies. The main results included complete remission (CR), partial remission (PR), and total remission (TR); UTP, Scr, and ALB were used as observation metrics; adverse events (AEs) were used as safety metrics. At least one of the above indicators is satisfying. Statistical analysis was performed using Cochrane RevMan 5.3. The heterogeneity between the literature is low ($P \geq 0.10$; $I^2 \leq 50\%$), and the heterogeneity is good; the fixed-effects model is used; the heterogeneity between the literature is poor ($P < 0.10$; $I^2 > 50\%$); a random-effects model is adopted; categorical variables choose odds ratio (OR) as the effect size, and continuous variables choose mean difference (MD) as the effect size, and the results are represented by forest plots. $P < 0.05$ is designated as significant.

2.5. Statistical Methods. SPSS 18.0 was used for analysis. The measurement data were described as the mean ± standard deviation ($\overline{x} \pm s$) (normal data) or M (1/4, 3/4) (non-normal data); the count data were expressed as a number of cases and percentages. Quantitative data were compared using a t-test, and repeated measures data were analyzed by ANOVA for repeated measures; count data were compared using the χ^2 test or rank sum test. Differences were considered statistically significant at $P < 0.05$.

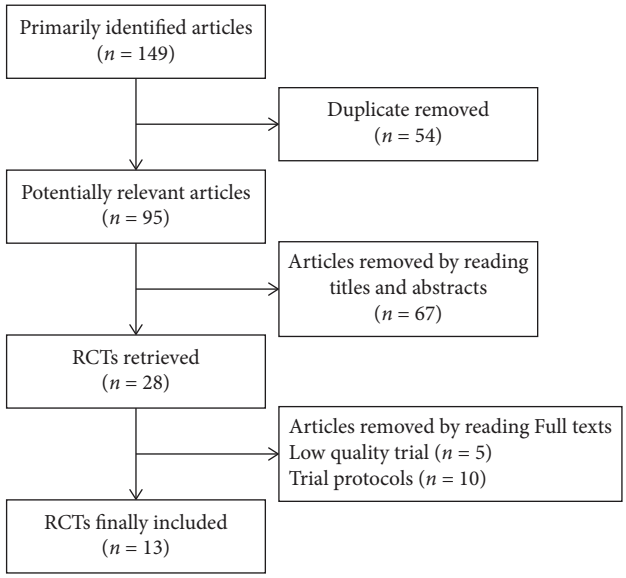

Figure 1: Flowchart of the process for selecting studies for the systematic review.

3. Results

3.1. Literature Search and Screening Results. According to our criteria, we retrieved a total of 149 pieces of literature that met the requirements, all of them in Chinese; 54 pieces of literature were deleted, 67 pieces of literature were excluded from reading titles and abstracts, and 15 pieces of literature were excluded after reading the full text and finally included in this research literature 13 Article [10–22]; a total of 958 cases were included in this systematic review, including 431 cases in the treatment group and 527 cases in the control group. The retrieval process is shown in Figure 1, and the clinical data included in the literature are shown in Table 1.

3.2. Risk of Bias Assessment. Seven studies [12–14, 16, 18, 20, 21] mentioned a randomized design, one study [12] described allocation concealment, and one study [22] described a blinded design. None of the studies mentioned detection bias, except for 3 studies [14, 20, 21] that described complete outcome data, and 4 studies [14, 18, 20, 21] published incomplete outcome data. We performed a Cochrane risk of bias assessment, "+" low risk of bias, "–" high risk of bias, and "?" risk of bias is unknown. See Figures 2 and 3 for details.

3.3. TR. Among the 13 included studies, the definitions of TR, CR, and PR are different, as detailed in Table 2. The 5 studies [12–14, 17, 18] (the control group selected RASI as the treatment drug) compared the TR after 3 months of treatment, and the differences between the study groups were of little statistical heterogeneity ($P = 0.97$, $I^2 = 0\%$); a fixed-effects model was adopted. Data indicated that treatment TR was significantly better than control TR (OR = 4.3, 95% CI: 2.59, 7.16, $P < 0.00001$). 6 studies [10, 11, 15, 16, 21, 22] compared the TR after 6 months of treatment, and the statistical heterogeneity among the study groups was less ($P = 0.97$, $I^2 = 0\%$), and a fixed-effects model was adopted. Data indicated that treatment TR was significantly better than control TR (OR = 4.7, 95% CI: 2.77, 7.98, $P < 0.00001$). The subgroup analysis of the TR of the 3-month and 6-month treatment revealed less heterogeneity ($P = 1.0$, $I^2 = 0\%$), and a fixed-effects model was adopted. Data indicated no difference in the TR (OR = 4.49, 95% CI: 3.11, 6.48, $P = 0.81$) as shown in Figure 4. 3 studies [12, 14, 17] (the control group selected GTW as the treatment drug) with the TR after 3 months of treatment, and there was very little heterogeneity ($P = 0.65$, $I^2 = 0\%$), and a fixed-effects model was adopted. Data indicated that the treatment TR group was significantly better than the control TR group (OR = 3.85, 95% CI: 2.13, 6.97, $P < 0.00001$) as shown in Figure 5.

3.4. UTP. 6 studies [12–14, 17–20] compared the quantitative changes of UTP in patients after 3 months of treatment. There was statistical heterogeneity ($P < 0.0001$, $I^2 = 83\%$), and no source accounting for it was found. Random effect model analysis revealed that treatments were significantly better controls (MD = −258.21, 95% CI: −358.67, −157.75, $P < 0.00001$). 5 studies [10, 11, 15, 16, 21] compared the quantitative changes of UTP after 6 months of treatment, and very little heterogeneity was found ($P = 0.59$, $I^2 = 0\%$), and fixed-effect model analysis revealed that treatments were significantly better controls(MD = −338.55, 95% CI: −431.63, −245.48, $P < 0.00001$). The UTP changes in the 3-month and 6-month treatment groups were analyzed by subgroup, and there was statistical heterogeneity among the study groups (MD = −338.55, 95% CI: −431.63, −245.48, $P < 0.00001$), and no source of heterogeneity was found. The random-effects model analysis revealed no difference (MD = −284.28, 95% CI: −365.94, −202.61, $P = 0.25$) as shown in Figure 6.

3.5. ALB. 3 studies [13, 17, 18] compared the changes in ALB after 3 months of treatment and found heterogeneity among groups ($P < 0.00001$, $I^2 = 93\%$), and no source of heterogeneity was found. Random-effect model analysis revealed that ALB improvement in treatments was better than controls (MD = 5.04, 95% CI: 0.58, 9.5, $P = 0.03$). 4 studies [10, 11, 15, 16] compared the changes in ALB of patients after 6 months of treatment and found no heterogeneity ($P = 0.0004$, $I^2 = 83\%$), and the random-effect model analysis revealed no difference in ALB (MD = 1.26, 95% CI: 1.05, 3.57, $P = 0.29$). Subgroup analysis was performed on the ALB in the 3-month and 6-month treatment groups. There was statistical heterogeneity among the study groups ($P < 0.00001$, $I^2 = 93\%$), and random-effects model analysis demonstrated no difference in ALB (MD = 2.96, 95% CI: 0.29, 5.64, $P = 0.14$) as shown in Figure 7.

Table 1: Characteristics of the studies included in this systematic review.

Studies	Baseline characteristics of participants	Interventions/Controls
Shen 2009	*N*: 52 Gender: M26 F26; Age: 32 .48 ± 10.12 (18–60); UTP: 1.0–3.5 g/d; Ccr > 60 ml/min; Pathology: WHO II (12), III (30), IV (10).	*I* (*n* = 26): GTW (1 mg/kg/d), Benazepril (10 mg/d). C (*n* = 26): benazepril (10 mg/d). Follow-up period: 6 months
Yu 2012	*N*42; Age: 37.10 ± 10.70; UTP: 1.0–3.5 g/d; Normal renal function.	*I* (*n* = 20): GTW (60 mg/d), fosinopril (10–20 mg/d). *C* (*n* = 22): fosinopril (10–20 mg/d). Follow-up period: 6 months.
Yang 2014	*N*96; Gender: *A*: M17 F14; *B*: M19 F14; C: M17 F15; Age: *A*: 49.3 ± 10.6; *B*: 51.1 ± 12.3; *C*: 50.01 ± 10.12; UTP: <1.0 g/d.	*A* (*n* = 31): benazepril (10 mg/d). *B* (*n* = 33): GTW (60 mg/d). *C* (*n* = 32): GTW (60 mg/d), benazepril (10 mg/d). Follow-up period: 3 months.
Xiang 2014	*N*60; Gender: *I*: M18 F12; *C*: M19 F11 Age: *I*: 50.3 ± 9.6; *C*: 51.3 ± 8.2; UTP: <3.5 g/d; normal renal function. Pathology: Lee II ~ III.	*I* (*n* = 30): GTW (1 mg/kg/d), telmisartan (80 mg/d). *C* (*n* = 31): telmisartan (80 mg/d). Follow-up period: 3 months.
Yu 2016	*N*90; Gender: *I*: M15 F15; C1: M16 F14; C2: M14 F16; Age: *I*: 46.1 ± 9.4; *C*1: 45.2 ± 5.7; *C2*: 45.9 ± 4.1;	*I* (*n* = 30): GTW (60 mg/d), benazepril (10 mg/d). *C*1 (*n* = 30): benazepril (10 mg/d). *C*2 (*n* = 30): GTW (60 mg/d). Follow-up period: 3 months.
Zhu 2017	*N*60; Gender: *I*: M15 F15; *C*: M17 F13; Age: *I*: 39.5 ± 12.5; *C*: 34.9 ± 11.5; UTP: 1.0–3.5 g/d; Normal renal function.	*I* (*n* = 30): GTW (60 mg/d), ARB. *C* (*n* = 30): ARB. Follow-up period: 6 months.
Cai 2018 [16]	*N*68; Gender: *I*: M19 F15; *C*: M18 F16; Age: *I*: 46.12 ± 9.05; C: 45.78 ± 8.83; UTP: 1.0–3.5 g/d.	*I* (*n* = 34): GTW (60 mg/d), telmisartan (40–80 mg/d). *C* (*n* = 34): telmisartan (40–80 mg/d). Follow-up period: 6 months.
Liang et al. 2019 [17]	*N*128; Gender: M66 F62; Age: 46.0 ± 12.1; UTP: 1.0–3.0 g/d.	*I* (*n* = 46): GTW (60 mg/d), irbesartan (300 mg/d). *C*1 (*n* = 42): GTW (60 mg/d). *C*2 (*n* = 40): irbesartan (300 mg/d). Follow-up period: 3 months.
Wei 2019 [18]	*N*70; Gender: *I*: M19 F16; *C*: M21 F14; Age: *I*: 39.57 ± 5.16; *C*: 37.65 ± 5.58.	*I* (*n* = 35): GTW (60 mg/d), irbesartan (150 mg/d). *C* (*n* = 35): irbesartan (150 mg/d). Follow-up period: 3 months.
Xu 2020 [19]	*N*58; Gender: *I*: M17 F12; *C*: M16 F13; Age: *I*: 39.65 ± 2.81; *C*: 40.03 ± 2.49	*I* (*n* = 29): GTW (30 mg/d), benazepril (10 mg/d). *C* (*n* = 29): benazepril (10 mg/d). Follow-up period: 3 months.
Feng 2020	*N*90; Gender: M57 F33; Age: 53.53 ± 9.52.	*I* (*n* = 45): GTW (60 mg/d), telmisartan (80 mg/d). *C* (*n* = 45): GTW (60 mg/d). Follow-up period: 3 months.
Wang, 2020 [21]	*N*34; Gender: *I*: M10 F7; *C*: M11 F6; Age: *I*: 42.61 ± 4.22; *C*: 43.75 ± 3.92.	*I* (*n* = 17): GTW (60 mg/d), olmesartan (20 mg/d). *C* (*n* = 17): olmesartan (20 mg/d). Follow-up period: 6 months.
Li and Huang, 2021 [22]	*N*110; Gender: *I*: M26 F29; *C*: M27 F28; Age: *I*: 41.52 ± 12.33; *C*: 41.47 ± 12.51.	*I* (*n* = 17): GTW (60 mg/d), telmisartan (40 mg/d). *C* (*n* = 17): telmisartan (40 mg/d). Follow-up period: 6 months

Note. N: number, M: male, F: female, *I*: intervention group, and *C*: comparison group.

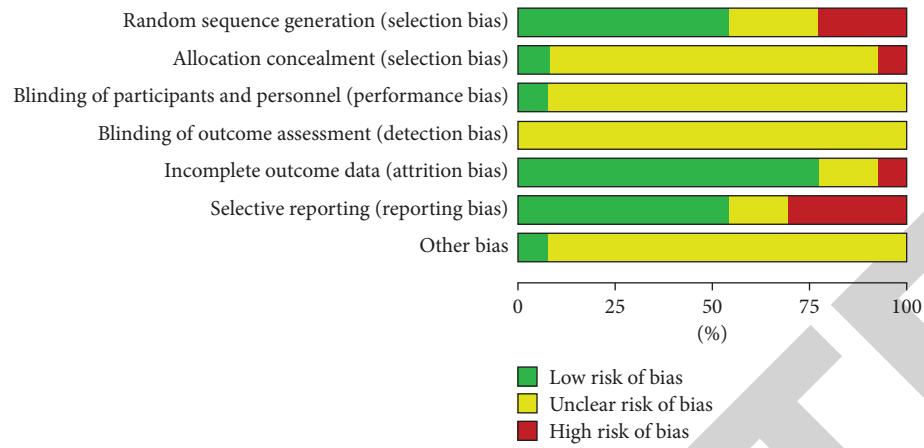

Figure 2: Risk of bias graph.

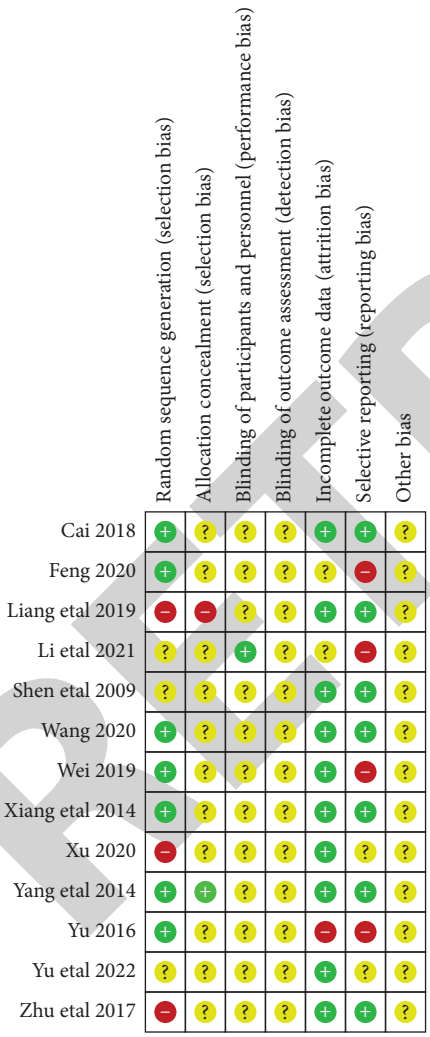

Figure 3: Risk of bias summary. "+" low risk of bias, "−" high risk of bias, and "?" unclear risk of bias.

3.6. Scr. 5 studies [13, 17–20] compared the changes in Scr of patients after 3 months of treatment and found heterogeneity among groups ($P = 0.0003$, $I^2 = 80\%$). Random-effect model analysis found that treatments improved Scr (MD = −5.07, 95% CI: −9.12, −1.01, $P = 0.01$); 4 studies [10, 11, 16, 21] compared the change in Scr after 6 months of the treatment. Results indicated heterogeneity among groups ($P = 0.0009$, $I^2 = 74\%$). Random effect model analysis found that treatments improved Scr (MD = −6.92, 95% CI: −10.73, −3.10, $P = 0.02$). Subgroup analysis was performed on Scr in the monthly group. There was statistical heterogeneity among the study groups ($P < 0.00001$, $I^2 = 79\%$). Random effect model analysis found no difference in Scr (MD = −6.92, 95% CI: −10.73, −3.10, $P = 0.3$) as shown in Figure 8.

3.7. AE. Among the included studies, 5 studies did not mention the occurrence of AE, and AEs were reported in the other 8 studies (Table 3), all of which described that the AEs were relieved and controlled after effective treatment, and there were no withdrawals due to AE. We compared the incidence of AE among the 8 included studies, of which 4 studies [12, 13, 17, 18] compared the incidence of AE after 3 months of treatment and found little heterogeneity ($P = 0.20$, $I^2 = 35\%$); fixed-effect model analysis revealed a significant difference in AE incidence between the groups (OR = 2.01, 95% CI: 0.79, 5.11, $P = 0.14$). 4 studies [10, 11, 15, 22] compared the occurrence of AE after 6 months of treatment, and there was little statistical heterogeneity among the groups($P = 0.48$, $I^2 = 0\%$); the fixed-effect model analysis revealed that 6-month treatment drastically increased AE (OR = 2.31, 95% CI: 1.15, 4.66, $P = 0.02$). The subgroup analysis of AE in the 3-month and 6-month treatment groups showed very little heterogeneity ($P = 0.48$, $I^2 = 0\%$), and the fixed-effect model analysis revealed no difference in AE (OR = 2.20, 95% CI: 1.26, 3.85, $P = 0.82$) (Figure 9).

3.8. Publication Bias Assessment. Taking the TR as an example, a funnel plot was drawn to detect whether there was a small sample size publication bias. The results indicated that the studies were basically distributed on two sides of the funnel plot line. It can be clearly observed that the included literature has a certain degree of skewed distribution. The risk of publication bias is low (Figure 10).

Table 2: Definition of clinical outcomes in each study.

Studies	Complete remission (CR)	Partial remission (PR)	Total remission (TR)
Shen 2009 [10]	UTP < 0.3 g/d, ALB>35.0 g/L, Scr normal	UTP > 0.3 g/d, but reduced by more than 50% of the baseline value, renal function is stable (Scr < 25% baseline value)	CR and PR
Yu 2012 [11]	UTP reduced by ≥ 75%	UTP reduced by ≥ 50%, but ≤ 75%	CR and PR
Yang 2014 [12]	UTP reduced by ≥ 75%	UTP reduced by 50% ~ 75%	CR and PR
Xiang 2014 [13]	UTP < 0.4 g/d, Scr normal	UTP is reduced by more than 50% of the baseline value, Scr rises by less than 50% of the base value	CR and PR
Yu 2016 [14]	UTP reduced by ≥ 75%	UTP reduced by 50% ~ 75%	CR and PR
Zhu 2017 [15]	No introduction	No introduction	UTP reduced by ≥ 50%
Cai 2018 [16]	Macroscopic or microscopic hematuria basically disappear, and UTP is reduced by ≥ 80%	Macroscopic or microscopic hematuria improved significantly, and UTP was reduced by50%~79%	CR and PR
Liang et al., 2019 [17]	UTP ≤ 0.3 g/d	UTP > 0.3 g/d, reduced by ≥ 50%	CR and PR
Wei 2019 [18]	UTP < 0.5 g/d, ALB > 30.0 g/L, clinical symptoms disappeared	UTP < 1.5 g/d, ALB: 25 ~ 30.0 g/L, improvement of clinical symptoms	CR and PR
Xu 2020 [19]	No introduction	No introduction	No introduction
Feng 2020 [20]	No introduction	No introduction	No introduction
Wang 2020 [21]	Complete disappearance of hematuria and proteinuria	Alleviation of hematuria and proteinuria symptoms	CR and PR
Li and Huang 2021 [22]	Symptoms disappear, no microscopic hematuria, UTP < 0.2 g/d	Symptoms improved significantly, with no microscopic hematuria, UTP < 0.2 g/d, reduced by >50%	CR and PR

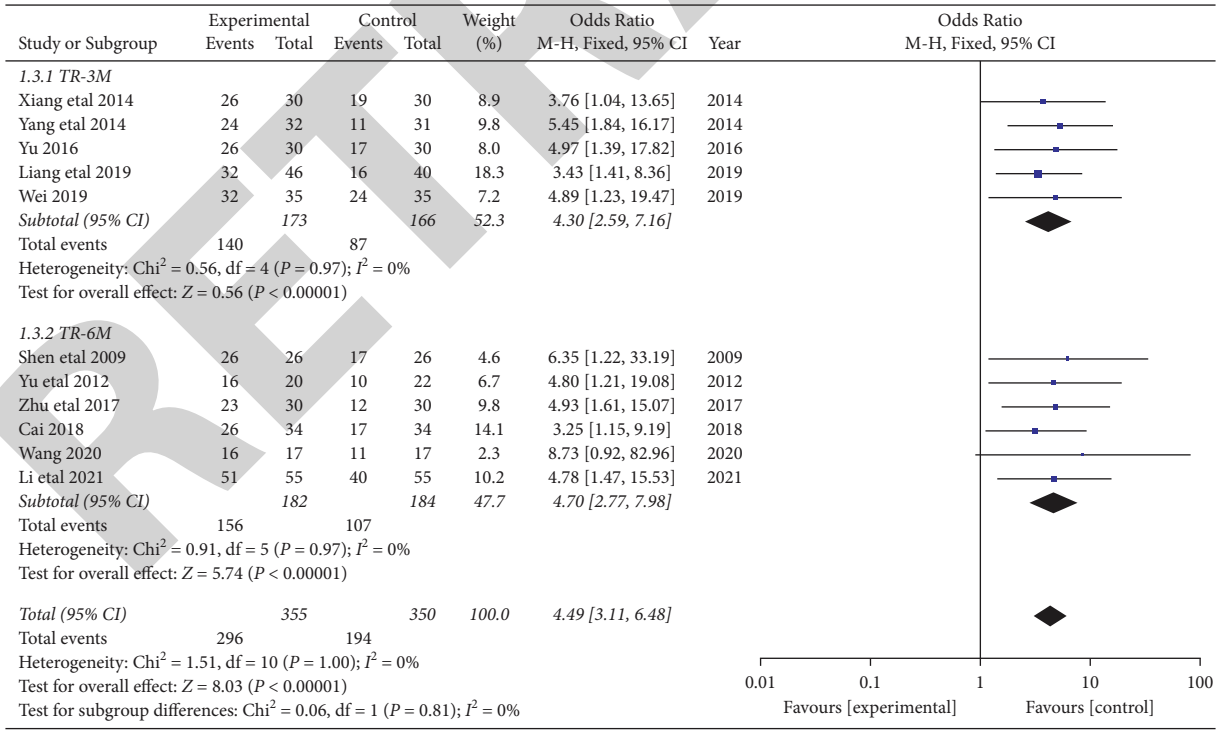

Figure 4: Comparison of GTW combined with RASI versus RASI TR-3 months versus 6 months.

4. Discussion

IgA nephropathy is currently the most prevalent primary glomerular disease in China [17, 18]. Patients with ESRD can only rely on hemodialysis, peritoneal dialysis, or renal transplantation to maintain their lives, and the quality of life of patients and their families is significantly reduced. Therefore, it is necessary to treat IgA nephropathy through

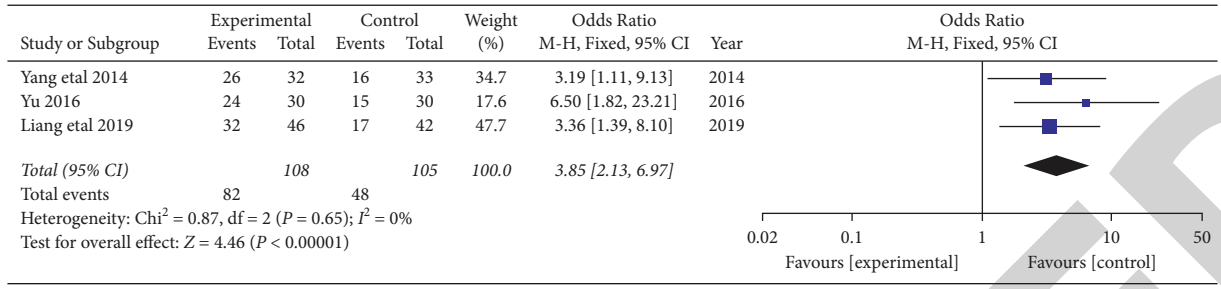

Figure 5: Comparison of GTW combined with RASI versus GTWTR-3 months.

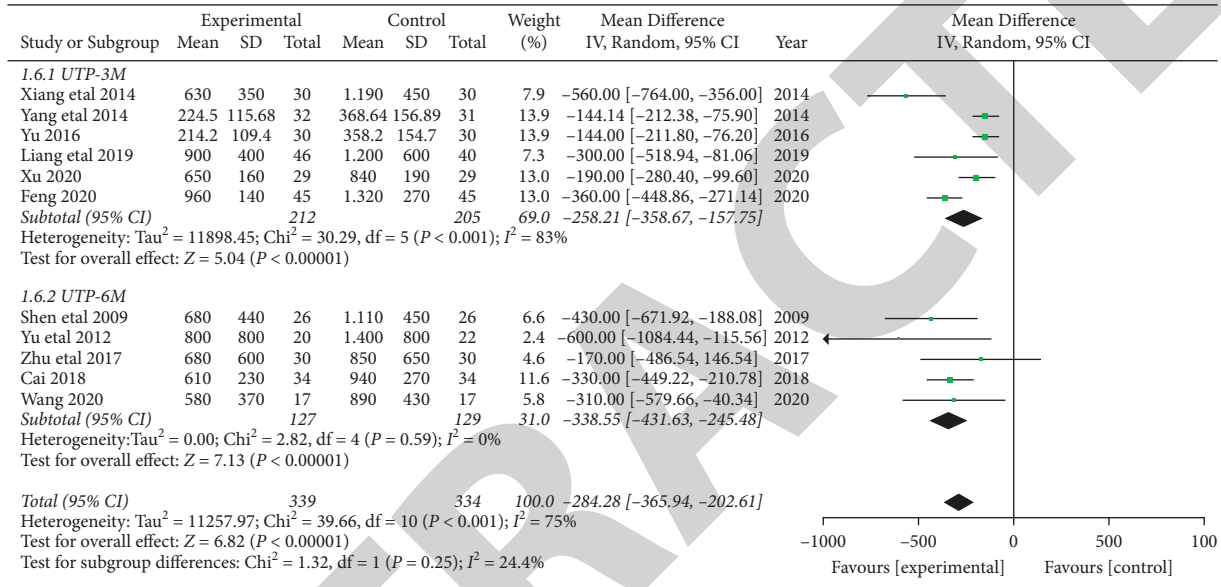

Figure 6: GTW combined with RASI versus control UTP-3 months versus 6 months.

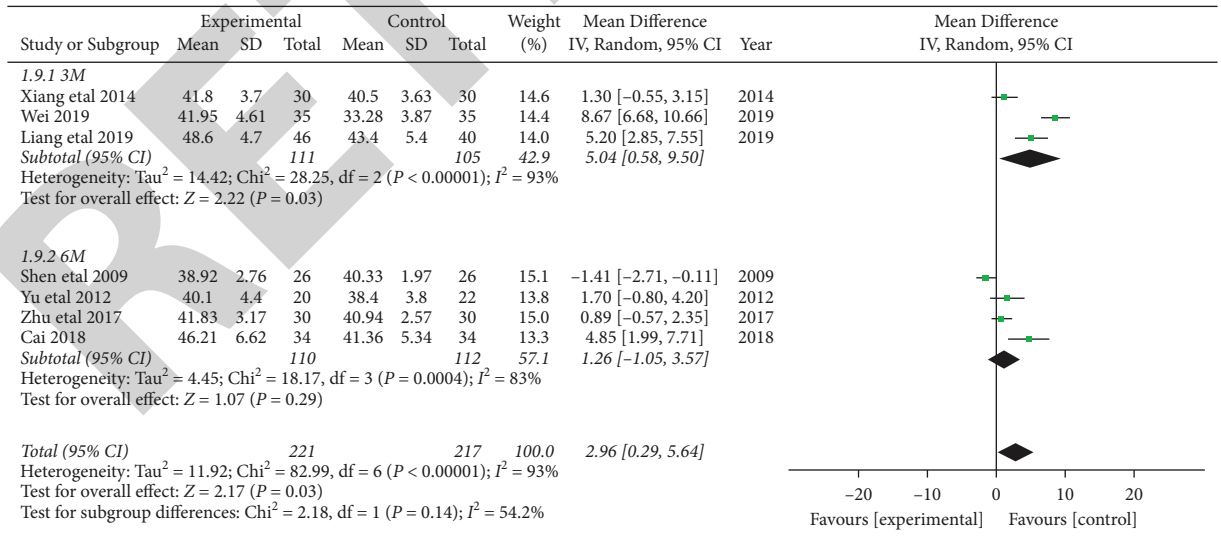

Figure 7: Comparison of GTW combined with RASI versus control group ALB-3 months versus 6 months.

active and effective measures to reduce urinary protein and slow down the progression of renal function. A number of studies have been conducted to investigate the factors affecting the prognosis of IgA nephropathy. Analyses have shown that patients with persistent large amounts of proteinuria, persistent uncontrolled hypertension, and renal

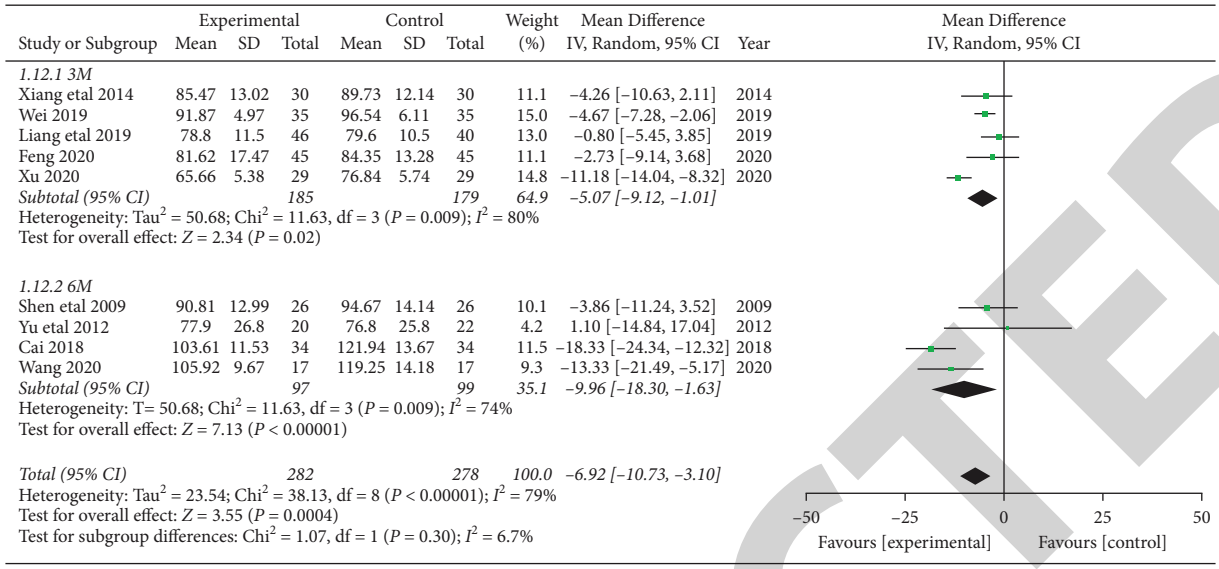

Figure 8: GTW combined with RASI versus control Scr-3 months versus 6 months.

impairment at the onset of disease have relatively severe renal pathology, poor long-term prognosis, and relatively poorer response to medications [21–23].

The duration of urinary protein has a greater impact on renal prognosis than the amount of urinary protein. Studies [24, 25] found that patients with urine protein >3 g/d had 25 times faster decline in renal function compared to patients with urine protein quantification <1 g/d. When urine protein decreased to less than 1 g/d in patients with massive proteinuria, the rate of decline in renal function slowed, and the natural course of the disease was similar to that of patients with low urine protein. Patients with urine protein less than 0.5 g/d have a better long-term prognosis than those with urine protein between 0.5 and 1 g/d. Studies [7, 26] have observed the natural course of IgA nephropathy and found that GFR decreases at an average rate of 1 to 3 ml/min per year in patients with normal renal function at presentation, while it increases rapidly to 9 ml/min per year in those presenting with nephrotic syndrome. The state of renal function at presentation also reflects the severity of pathological damage. Patients with renal insufficiency have a relatively high degree of thylakoid hyperplasia, a higher proportion of glomerulosclerosis, and often a higher Lee's classification [27, 28]. As the eGFR decreases and the residual glomeruli decrease, the rate of eGFR decline is accelerated, and once the blood creatinine exceeds 265.2 umol/L, the rate of GFR decline can reach 20 ml/min per year [29, 30]. Therefore, although the blood creatinine of patients in CKD2-3 is relatively not high, the renal impairment will be further aggravated if timely treatment is not carried out, and the CKD2-3 stage is also the last time for effective intervention before patients enter ESRD [31, 32].

Although the pathogenesis of immune complex deposition in glomeruli due to abnormal body immunity is widely recognized, opinions differ on whether immunosuppressive agents should be used alone or in combination in the treatment of IgA nephropathy [33, 34]. The 2012 KDIGO guidelines recommend 6 months of glucocorticoid therapy for patients with GFR >50 ml/min and persistent urinary protein >1 g/d despite 3–6 months of supportive therapy [35, 36]. However, no treatment recommendations are available for patients with proteinuria, GFR <50 ml/min, and not in ESRD. The incidence of autoimmune diseases has been increasing in recent years, and with it, the use of glucocorticoids has become more widespread [37]. The abuse of glucocorticoids has been accompanied by adverse effects of hormones such as femoral head necrosis, diabetes mellitus, and severe fatal infections, making the overall cost of the disease higher, and some patients are unable to tolerate them, refusing to take them, and easily giving up treatment and increasing the risk of disease progression.

Since the 1970s, when the effectiveness of tretinoin application in nephritis was demonstrated, various tretinoin products have been gradually and widely used in the treatment of chronic glomerulonephritis [38]. With the improvement of the pharmaceutical process, the initial tretinoin tonics have been replaced by preparations such as tretinoin polysaccharide tablets, with a significant reduction in adverse effects. In previous studies, tretinoin polysaccharide was mainly used in patients with IgA nephropathy with normal renal function and related treatment regimens such as tretinoin alone or in double doses, tretinoin combined with RAS blockers, tretinoin combined with hormones, and mortification of mortification, all of which showed good effects in reducing urinary protein and delaying the progression of renal function [39]. The results of this study also confirmed the significant efficacy of raglan polysaccharide combined with RAS blockers with fewer adverse effects in patients with IgA nephropathy in CKD stages 2-3.

The mechanism of raglan polysaccharide in IgA nephropathy is (1) inhibition of proliferation of thylakoid cells and stroma: the basic change of IgA nephropathy is the proliferation of glomerular thylakoid cells and stroma due to

Table 3: Reports of adverse events included in the study.

Studies	Therapeutic regimen	Sample size	Cough	Gastrointestinal symptoms	Elevated liver enzymes	Scr rise	WBC decline	Irregular menstruation	Dizziness headache	Skin allergies	Total
Shen 2009 [10]	GTW + Benazepril	26	4	0	2	0	3	0	0	0	9
	Benazepril	26	4	0	0	0	0	0	0	0	4
Yu 2012 [11]	GTW + Fosinopril	20	2	0	2	2	2	1	0	0	9
	Fosinopril	22	2	0	0	3	0	0	0	0	5
Yang 2014 [12]	GTW + Benazepril	32	0	2	0	0	1	0	0	0	3
	Benazepril	31	0	0	0	0	0	0	0	0	0
	TWM	33	0	2	0	0	0	0	0	0	2
Xiang 2014 [13]	GTW + Telmisartan	30	0	0	2	0	0	3	0	0	5
	Telmisartan	30	0	0	0	0	0	0	0	0	0
Yu 2016 [14]	GTW + Benazepril	30	?	?	?	?	?	?	?	?	?
	Benazepril	30	?	?	?	?	?	?	?	?	?
	GTW	30	?	?	?	?	?	?	?	?	?
Zhu 2017 [15]	GTW + ARB	30	0	0	5	0	0	0	0	0	5
	ARB	30	0	0	1	0	0	0	0	0	1
Cai 2018 [16]	GTW + Telmisartan	34	?	?	?	?	?	?	?	?	?
	Telmisartan	34	?	?	?	?	?	?	?	?	?
Liang et al., 2019 [17]	GTW + Irbesartan	46	0	2	0	0	0	0	0	0	2
	Irbesartan	40	0	2	0	0	0	0	0	0	2
	GTW	42	0	1	0	0	0	0	0	0	1
Wei 2019 [18]	GTW + Irbesartan	35	0	1	0	0	1	0	1	0	3
	Irbesartan	35	0	2	0	0	0	0	1	0	4
Xu 2020 [19]	GTW + Benazepril	29	?	?	?	?	?	?	?	?	?
	Benazepril	29	?	?	?	?	?	?	?	?	?
Feng 2020	GTW + Telmisartan	45	?	?	?	?	?	?	?	?	?
	GTW	45	?	?	?	?	?	?	?	?	?
Wang 2020 [21]	GTW + Olmesartan	17	?	?	?	?	?	?	?	?	?
	Olmesartan	17	?	?	?	?	?	?	?	?	?
Li and Huang 2021 [22]	GTW + Telmisartan	55	0	5	0	0	0	0	0	1	6
	Telmisartan	55	0	3	0	0	0	0	1	1	5

the stimulation of immune complexes in the thylakoid region. Previous animal studies have shown that the most important monomer of tretinoin that exerts immunosuppressive and anti-inflammatory effects is tretinoin lactone alcohol. This component can significantly reduce the level of serum IgA in rats with IgA nephropathy and improve the degree of abnormal glycosylation, as well as downregulate the level of the CD71 molecule, the main receptor of IgA1 in the glomerular thylakoid region, and reduce the deposition of IgA1 in the thylakoid region, thus inhibiting the proliferation of glomerular thylakoid cells and the increase of stroma [40]; (2) protection of podocytes: raffinose polysaccharide can stabilize the podocyte skeleton, reduce the damage to the podocytes, and protect the podocytes. Protection of podocytes: raglan polysaccharide can stabilize the podocyte skeleton, reduce podocyte damage, and increase the expression of nephrin and podocin, the key molecules of podocyte surface lytic membrane; (3) improvement of the glomerular filtration barrier: it mainly includes the repair of mechanical and charge barriers, thus reducing the loss of urinary protein in patients; (4) anti-inflammation, inhibition of immune response, and reduction of glomerular damage by cytokines. Thus, raglan polysaccharide has a clinical and basic test-proven effect on repairing and ameliorating the pathological damage of IgA nephropathy, which can effectively slow down the natural course of the disease.

The stability of the renin-angiotensin system, or RAS system, is essential for maintaining normal renal physiological function. Abnormally glycosylated IgA1 deposited in the glomerular thylakoid region can specifically activate the local RAS system in the kidney, which is one of the important causes of the development of IgA nephropathy.

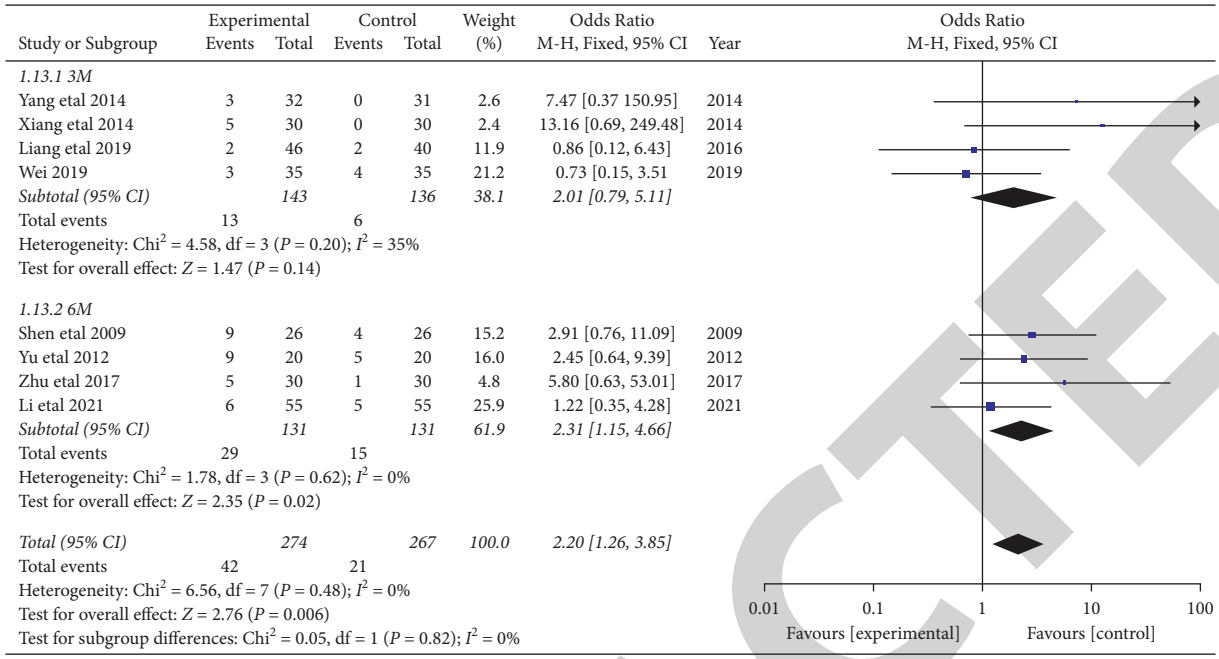

Figure 9: GTW combined with RASI versus control AE-3 months versus 6 months.

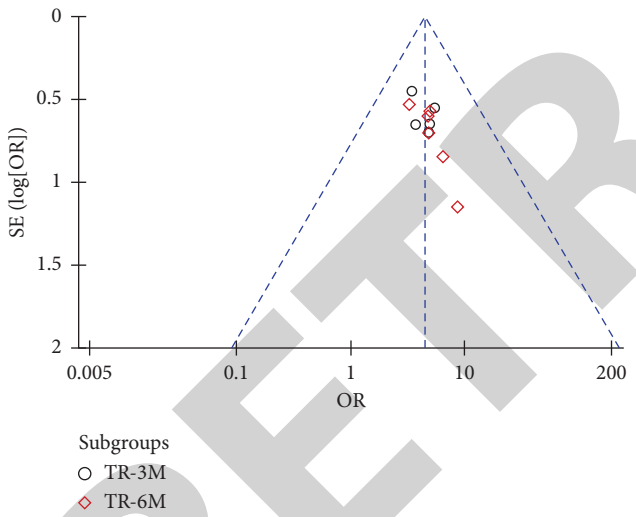

Figure 10: Funnel plots of TR published bias.

Therefore, RAS blockers are well-proven effective drugs for the treatment of IgA nephropathy. In particular, RAS blockers are recommended for patients with urinary protein >0.5 g/d, regardless of whether blood pressure is elevated or not, when blood pressure is tolerated.

It can be seen that the feasibility and practicality of combining RAS blockers with raglan polysaccharides are high. Therefore, this study included patients with IgA nephropathy with eGFR between 30 and 90 ml/(min-1.73 m^2) and investigated the efficacy and side effects of a regimen of regimen polysaccharide combined with RAS blocker in the treatment of IgA nephropathy patients with CKD stage 2 to 3 by comparing the commonly used classical drugs, i.e., hormones combined with RAS blockers so as to clarify the superiority of the regimen of regimen polysaccharide combined with the RAS blocker. The superiority of the regimen of regioidoside combined with the RAS blocker in treating these patients was clarified.

Based on the above, the effect of GTW combined with RASI on IgAN was evaluated, hoping to provide a scientific basis for IgAN treatment. This study conducted a meta-analysis by screening existing randomized controlled trial studies and found that GTW plus RASI for IgAN improved the TR of treatment, decreased the quantification of double colic, increased ALB, and improved renal function. Specific findings showed that GTW combined with RASI was superior to GTW or RASI alone after 3 months of treatment in terms of total clinical efficacy. After 6 months of GTW in combination with RASI, it had an advantage over RASI alone. There was no significant advantage compared to 3 months of treatment. In terms of double stranding, GTW combined with RASI for 3 and 6 months had an advantage compared to the RASI group alone, but there was no significant advantage in reducing double stranding compared to treatment for 6 and 3 months; in terms of alcoholic gonadal function antipulmonary function anti-inflammatory patients, GTW combined with RASI for 3 months had an advantage in improving ALB compared to the RASI group alone. There was no significant advantage of GTW combined with RASI treatment for 6 months in terms of improvement in ALB compared to RASI alone. There was no significant advantage compared to treatment at 6 months and 3 months. In terms of Scr, GTW combined with RASI at 3 and 6 months of treatment had an advantage in improving renal function compared with RASI alone, but there was no significant advantage in reducing renal function at 6 months of treatment and after 3 months of treatment; in terms of AE, there was no difference between GTW plus RASI at 3

months and RASI alone, but the incidence of adverse reactions at 6 months of treatment was higher than with RASI alone.

The results of this clinical trial showed that raglan polysaccharide combined with the RAS blocker not only reduced urinary protein but also delayed the progression of renal function and was a safe and effective treatment option for CKD stage 2 to 3 IgA nephropathy. The abnormal menstrual events that occurred during treatment mostly improved after discontinuation of the drug and had less impact on older patients. For the possible events of hematocrit and abnormal liver function, they can be avoided by only closely monitoring the changes in routine blood and liver function of patients.

5. Conclusion

(1) For patients with chronic kidney disease IgA nephropathy, tretinoin polysaccharide combined with the RAS blocker can not only effectively control urinary protein but also delay the progression of renal function

(2) The efficacy of tretinoin combined with the RAS blocker is remarkable, with few adverse effects and no serious side effects such as abnormal glucose and osteoporosis of glucocorticoids, which is significantly superior compared with hormones

(3) Patients with different stages of chronic kidney disease respond differently to treatment, and those in lower stages have better responsiveness to treatment and are more likely to achieve clinical remission [41]

Data Availability

The experimental data used to support the findings of this study are available from the corresponding author upon request.

Ethical Approval

Ethical issues have been completely observed.

Conflicts of Interest

The authors declare that they have no conflicts of interest.

Acknowledgments

The study received funds from "Heilongjiang Natural Science Fund (LH2021H070)."

References

[1] F. P. Schena and I. Nistor, "Epidemiology of IgA nephropathy: a global perspective," *Seminars in Nephrology*, vol. 38, no. 5, pp. 435–442, 2018.

[2] J. C. Stanley and H. Deng, "Progress in pathogenesis of immunoglobin A nephropathy," *Cureus*, vol. 12, no. 6, p. e8789, 2020 Jun 23.

[3] C. C. Lim, S. Baikunje, J. C. J. Choo, P. H. Tan, M. Foo, and K. T. Woo, "Clinical course of Immunoglobulin A nephropathy with crescents in a multi-ethnic Southeast Asian cohort," *Nephrology*, vol. 25, no. 9, pp. 708–713, 2020.

[4] J. W. He, X. J. Zhou, J. C. Lv, and H. Zhang, "Perspectives on how mucosal immune responses, infections and gut microbiome shape IgA nephropathy and future therapies," *Theranostics*, vol. 10, no. 25, pp. 11462–11478, 2020.

[5] J. Barratt and J. Floege, "SGLT-2 inhibition in IgA nephropathy: the new standard of care?" *Kidney International*, vol. 100, no. 1, pp. 24–26, 2021.

[6] J. Floege, S. J. Barbour, D. C. Cattran et al., "Management and treatment of glomerular diseases (part 1): conclusions from a kidney disease: improving global outcomes (KDIGO) controversies conference," *Kidney International*, vol. 95, no. 2, pp. 268–280, 2019.

[7] Y. Ji, K. Yang, B. Xiao et al., "Efficacy and safety of angiotensin-converting enzyme inhibitors/angiotensin receptor blocker therapy for IgA nephropathy: a meta-analysis of randomized controlled trials," *Journal of Cellular Biochemistry*, vol. 120, no. 3, pp. 3689–3695, 2019.

[8] C. Y. Song, Y. G. Xu, and Y. Q. Lu, "Use of Tripterygium wilfordii Hook F for immune-mediated inflammatory diseases: progress and future prospects," *Journal of Zhejiang University-Science B*, vol. 21, no. 4, pp. 280–290, 2020 Apr.

[9] H. Y. Wang, J. Yuan, and X. Q. Wang, "A systematic review and meta-analysis of Tripterygium wilfordii polyglycosides in the treatment of adult IgA nephropathy," *China Medical Herald*, vol. 17, no. 23, pp. 122–129, 2020.

[10] P. Pattrapornpisut, C. Avila-Casado, and H. N. Reich, "IgA nephropathy: core curriculum 2021," *American Journal of Kidney Diseases*, vol. 78, no. 3, pp. 429–441, 2021.

[11] D. C. Wheeler, R. D. Toto, B. V. Stefansson et al., "A prespecified analysis of the DAPA-CKD trial demonstrates the effects of dapagliflozin on major adverse kidney events in patients with IgA nephropathy," *Kidney International*, vol. 100, no. 1, pp. 215–224, 2021.

[12] M. Abramson, S. Mon-Wei Yu, K. N. Campbell, M. Chung, and F. Salem, "IgA nephropathy after SARS-CoV-2 vaccination," *Kidney Medicine*, vol. 3, no. 5, pp. 860–863, 2021.

[13] D. Xie, H. Zhao, X. Xu et al., "T of macrophage infiltration in glomeruli predicts response to immunosuppressive therapy in patients with IgA nephropathy," *Journal of the American Society of Nephrology*, vol. 32, no. 12, pp. 3187–3196, 2021.

[14] V. Dotz, A. Visconti, H. J. Lomax-Browne et al., "O-and N-glycosylation of serum immunoglobulin A is associated with IgA nephropathy and glomerular function," *Journal of the American Society of Nephrology*, vol. 32, no. 10, pp. 2455–2465, 2021.

[15] J. Rehnberg, A. Symreng, J. F. Ludvigsson, and L. Emilsson, "Inflammatory bowel disease is more common in patients with IgA nephropathy and predicts progression of ESKD: a Swedish population-based cohort study," *Journal of the American Society of Nephrology*, vol. 32, no. 2, pp. 411–423, 2021.

[16] Y. P. Cai, "Analysis of the effect of tripterygium wilfordii polyglycosides combined with telmisartan in the treatment of patients with primary IgA nephropathy with moderate proteinuria [J]," *Henan Medical Research*, vol. 27, no. 20, pp. 3726–3728, 2018.

Hindawi
Emergency Medicine International
Volume 2023, Article ID 9780649, 1 page
https://doi.org/10.1155/2023/9780649

Retraction

Retracted: Effect of Risk-Focused Diversified Safety Management Mode in Patients with Major Artery Stent Implantation

Emergency Medicine International

Received 28 November 2023; Accepted 28 November 2023; Published 29 November 2023

This article has been retracted by Hindawi, as publisher, following an investigation undertaken by the publisher [1]. This investigation has uncovered evidence of systematic manipulation of the publication and peer-review process. We cannot, therefore, vouch for the reliability or integrity of this article.

Please note that this notice is intended solely to alert readers that the peer-review process of this article has been compromised.

Wiley and Hindawi regret that the usual quality checks did not identify these issues before publication and have since put additional measures in place to safeguard research integrity.

We wish to credit our Research Integrity and Research Publishing teams and anonymous and named external researchers and research integrity experts for contributing to this investigation.

The corresponding author, as the representative of all authors, has been given the opportunity to register their agreement or disagreement to this retraction. We have kept a record of any response received.

References

[1] Y. Shao, C. Wu, Y. Mao, D. Li, Y. Wang, and K. Zhu, "Effect of Risk-Focused Diversified Safety Management Mode in Patients with Major Artery Stent Implantation," *Emergency Medicine International*, vol. 2022, Article ID 1284254, 9 pages, 2022.

Hindawi
Emergency Medicine International
Volume 2022, Article ID 1284254, 9 pages
https://doi.org/10.1155/2022/1284254

Research Article

Effect of Risk-Focused Diversified Safety Management Mode in Patients with Major Artery Stent Implantation

Yan Shao, Cai-Juan Wu, Youjun Mao, Dong-Mei Li, Yun-Zhou Wang, and Kang Zhu

Changzhou 2nd Hospital, Vascular Surgery, Changzhou 213164, China

Correspondence should be addressed to Cai-Juan Wu; 41804019@xs.ustb.edu.cn

Received 3 August 2022; Revised 28 August 2022; Accepted 2 September 2022; Published 30 September 2022

Academic Editor: Hang Chen

Background. Intracranial atherosclerotic stenosis (ICAS) causes a series of neurological symptoms, such as vertigo, impaired consciousness, limb weakness, ataxia, dysphagia, ocular motility disorders, and visual impairment. With the improvement of people's living standards, there are higher requirements for nursing care. Nursing, as an indispensable part of medical care, is closely related to achieving the goal of patient's safety and the overall quality of nurses, quality of care, and nursing management methods. *Objective*. To explore the effect of risk-centered diversified safety management in patients undergoing aortic stenting. *Methods*. Eighty patients with cerebral infarction were selected and treated with percutaneous transluminal angioplasty and stent implantation (PTAS). Then they were divided into a control group (40 cases) with routine monitoring and an experimental group (40 cases) with risk-focused intervention of a diversified safety management model according to the mode of care. Patient satisfaction and blood index test results were compared after the intervention. *Results*. Patients in the experimental group had 6 falls, 3 bed falls, 3 phlebitis, 4 tube slips, and 10 deep vein thrombosis, all significantly fewer than those in the control group. Thirty-eight patients in the experimental group expressed satisfaction with safe management, which was substantially better than the control group ($P < 0.05$). The levels of tissue plasminogen activator (tPA), plasminogen activator inhibitor-1 (PA1-1), and von Willebrand factor (vWF) in the experimental group were (13.5 ± 1.3) ng/mL, (60.1 ± 9.9) ng/mL, and (2.1 ± 0.2), respectively, which were substantially lower than those in the control group ((14.6 ± 2.4) ng/mL, (64.2 ± 10.7) ng/mL, and (2.8 ± 0.3)), respectively ($P < 0.05$). *Conclusion*. The risk-centered diversified safety management model can effectively reduce the probability of adverse events in patients, improve patient satisfaction with nursing services, and promote faster postoperative recovery, which has clinical application value.

1. Introduction

The primary cause of ischemic cerebrovascular disease and transient ischemic attack (TIA) in China is intracranial atherosclerotic stenosis (ICAS) [1, 2]. The results of the 2014 CICAS study showed that 46.6% of patients with ischemic stroke and TIA in China had atherosclerosis and that patients with combined ICAS had severe symptoms and a high recurrence rate during the follow-up period [3, 4]. Therefore, effective treatment of ICAS has received a lot of attention from neurologists in China.

Currently, the main treatments for ICAS include pharmacological therapy, endovascular therapy, and intracranial and extracranial arterial bypass grafting. In recent years, endovascular treatment has gained attention because of its minimally invasive and rapid recovery characteristics, but the results of the SAMMPRIS study and the VISSIT study suggest that the incidence of the primary endpoint event (stroke and death within 30 d of enrollment) in the endovascular treatment group was 14.7%, which far exceeded the incidence of 5.8% in the drug group [5, 6]. As the SAMMPRIS study has been questioned in various aspects regarding operator experience and enrolled cases, it has been explored accordingly in China. The results of a multicenter registry study of stenting for symptomatic intracranial artery stenosis in China, led by Tiantan Hospital, showed that the perioperative endpoint event rate for endovascular treatment of patients with symptomatic ICAS after rigorous

screening was 4.3% [7, 8], which was much lower than the complication rate in the stent group of the SAMMPRIS study. The results of the CASSISS study, led by Xuanwu Hospital, will be available in 2015, which also excluded complex lesions >14 mm in length [9, 10]. With the continuous improvement of modern medical imaging techniques and adjuvant treatment materials, percutaneous transluminal angioplasty and stenting (PTAS) has gradually become available to the general public. It has now been developed as a new method for the treatment of sclerotic stenosis of large intracranial arteries. Relevant clinical studies have shown that patients with asymptomatic intracranial large artery stenosis treated with PTAS of the intracranial arteries have a significantly lower probability of postoperative stroke and better long-term outcomes, which is conducive to improving the prognosis of patients [11, 12].

Nursing, as an indispensable part of medical care, is closely related to the overall quality of nurses, nursing quality, and nursing management methods and is related to the achievement of patient safety goals [13, 14]. In recent years, the safety of patients during hospital treatment has become an important issue of general concern at home and abroad. Foreign research on this issue started earlier and is more in-depth, with many relevant studies and relatively perfect research results. The important research directions of nursing risk management abroad mainly include the incidence of nursing risk accidents, the concept of patient safety, and relevant safety measures. According to the prevalence and seriousness of patient safety problems, foreign scholars actively analyze and explore their causes and propose targeted measures. At this stage, some developed countries have begun to pay attention to the training of medical staff in patient safety education knowledge and have constructed a content system for patient safety education [15, 16]. Diversity management is a human resource management activity, the basic principle of which is to recognize different problems in the work and adopt different methods to help solve them [17, 18]. It can reach all aspects of the work and continuously improve the hidden problems in each of them, helping to improve the effectiveness of care.

Therefore, 80 patients with cerebral infarction were selected for PTAS of the intracranial artery, and routine care and diverse risk-focused safety management were given during the procedure. The intervention lasted for one month, and the changes in the indicators after the intervention were recorded. The effects of the risk-focused diversified safety management in patients undergoing PTAS surgery of large arteries were compared and analyzed, hoping to provide reference values for its future clinical application.

2. Materials and Methods

2.1. The Research Object. A total of 80 patients with cerebral infarction aged 18-75 years who received treatment in our hospital from January 2020 to May 2022 were selected. The two groups were divided according to whether the diversified risk-focused safety management mode intervention was carried out after PTAS. The control group (40 cases) received routine monitoring, and the experimental group (40 cases) received the risk-focused diversified safety management mode intervention. Inclusion criteria are as follows: I. Patients with cerebral infarction confirmed by CT or MRI diagnosis on admission; II. No serious heart, liver, or renal insufficiency; III. No rheumatic heart disease, atrial fibrillation, blood system, or autoimmune diseases; IV. No drugs affecting coagulation function within one month; V. No history of major brain injury or surgery and no history of active hemorrhagic disease; VI. Cerebrovascular DSA confirmed intracranial arterial stenosis ≥50%. Exclusion criteria are as follows: I. Patients with transient cerebral ischemia; II. Chronic complete occlusion or severe calcification of intracranial arteries; III. Stenosis or occlusion of the middle cerebral artery, distal anterior cerebral artery, and posterior cerebral artery; IV. Neurological dysfunction after severe stroke (NIHSS score [19, 20] more than 4 or consciousness disorder); V. People allergic to contrast agent.

The experimental procedure was approved by our ethics committee, and written informed consent was obtained from all subjects included in the study.

2.2. Treatment Measures. DSA examination was as follows: most subjects underwent routine preoperative examination after admission. Food was forbidden four hours before surgery, and the patient was sent to the Cath lab for total cerebral angiography under local anesthesia. After a successful femoral artery puncture by the Seldinger method, a 6F arterial sheath was inserted, and angiography was performed on the aortic arch, internal carotid artery, bilateral common carotid artery, subclavian artery, and vertebral artery. At the same time, the front and side positions were continuously exposed until the veins were empty. For suspicious vascular lesions that could not be identified by conventional projection, multiangle angiography was continued. The WASID equation [21] was used to calculate the degree of intracranial arterial stenosis: stenosis rate % = $[1 - (D_{\text{stenosis}}/D_{\text{constant}})] \times 100\%$. D_{stenosis} refers to the diameter of the smallest vessel in the stenosis segment, and D_{constant} refers to the diameter of the proximal artery in the stenosis segment. The measured rates of arterial stenosis were determined by two experienced neurointerventionists who read the films independently.

All patients underwent percutaneous endovascular stent implantation (PTAS). Postoperative blood pressure management was that the systolic blood pressure was maintained for severe stenosis between 100 and 130 mmHg, and systolic pressure was maintained in patients with nonsevere stenosis between 110 and 140 mmHg. Clopidogrel 75 mg/d and aspirin 100 mg/d were given orally for 12-16 weeks, followed by aspirin 100 mg/d for continuous treatment.

2.3. Risk Management Methods

(I) Recognition period. The cases of falling/falling in bed, deep vein thrombosis, accidental burns, medication errors, phlebitis, and qualified rate of transport and handover were recorded. All risk

factors related to objective patient safety management during treatment were sorted, and inspection tables were constructed. The number of cases of projects related to objective patient safety management that occurred in each clinical department was noted in detail. Indicators related to the management of patient safety objectives were screened. The nursing risk management projects in technology, service, business, and management were comprehensively counted from the perspectives of human, machine, material, environment, and law.

(II) Evaluation Period. Questionnaires were issued, and statistical analysis was conducted on all risk management projects. The risk index (number of occurrences × severity × discovery) was determined. A score of more than 350 was classified as unacceptable risk, 100-349 as major risk, 35-99 as moderate risk, 10-34 as permissible risk, and 1-9 as negligible risk. According to the statistical results, the checklist and Plato were formulated, and the patient safety objective risk management items were determined according to rules 20 and 80.

(III) Coping period. From the management aspect, the first is to run the nursing risk assessment scale comprehensively. Four nursing risk assessment scales were constructed and improved, including the risk factor assessment record for preventing patients from falling/falling in bed, the risk factor assessment scale for preventing catheter slip, the risk factor assessment scale for preventing phlebitis, and the risk factor assessment scale for preventing deep vein thrombosis. Through trial, revision, training, pilot, comprehensive rollout, and other management means, a comprehensive assessment of patients was implemented, which aimed to reduce or eliminate the incidence of falling/falling in bed, catheter shedding, phlebitis, and other items that affect the patient safety objectives and effectively ensure patient safety. Second, all relevant systems, processes, standards, and plans were enhanced for the implementation of patient safety objectives, such as the establishment of management systems, processes, standards, and plans for preventing patients from falling/falling in bed, preventing patients from phlebitis, and preventing pipeline slippage and deep vein thrombosis standard operation instructions (SOPs). A patient safety management system and assessment standards were established, as did the core monitoring index and key department management monitoring index of the whole hospital inpatient safety management. The nursing work notification system and health education system of various patient safety objectives were optimized and implemented. The third is to strengthen and implement oversight. The system and standard for verification, supervision, guidance, and evaluation of special risk projects of nursing management departments at all levels were established. Continuous improvement of care quality was carried out through PDCA quality management tools. A hospital-level comprehensive CQI nursing quality management project was established to strengthen the implementation and implementation of patient safety objectives and ensure effective management. From the aspect of personnel management, the implementation of training work was strengthened, and training plans were improved. Systematic and comprehensive training and assessment of the newly built specifications were conducted to ensure unified mastery and consistent execution of the working standards. In terms of facilities and environment, various warning labels should be established and improved to ensure patient safety, such as antifall/falling in bed, careful sliding, careful stepping, careful breaking of road, careful use of sugar, turning over card, antiscald, anticatheter falling off, careful electric shock, high-risk drugs, easily confused drugs, and other safety management labels. In terms of articles, all kinds of safe and qualified articles were provided, including all kinds of disposable articles, sterile articles, and implanted articles. In terms of equipment, operation procedures, troubleshooting, and emergency plans were established for various instruments and equipment, and training was implemented in a planned way to ensure that the efficiency of all staff was 100%.

(IV) Monitoring period. Risk project quality inspection standards and evaluation standards were developed, and comprehensive organizational inspection, supervision, and evaluation of nursing work were planned to carry out the risk management and implementation effect. A comprehensive summary of project risk management achievements was made. The existing deficiencies should be carefully analyzed, improved, and implemented to make continuous quality progress and ensure the unification of standards. The implementation of specific norms as well as the realization of key projects, important standards, key norms, homogeneous management, and implementation were also important.

(V) Filing Period. Through comprehensive implementation, patients' safety objectives were fully collected and sorted out, and successful measures and methods were consolidated. A series of nursing risk management project case collections and standard operation protocols (SOPs) were set up to solidify and implement the project. All nursing colleagues in the hospital were educated and warned to prevent risks and learn and improve together.

2.4. Observation Indicators

(I) Management effectiveness evaluation. A questionnaire survey was used to evaluate the satisfaction with safety management and other contents of inpatients one month after the intervention. The Inpatient Safety Management Satisfaction Scale was mainly developed according to the Inpatient Satisfaction Scale, relevant literature, and specific work practice and has good reliability and validity.

(II) Blood index test. Two-milliliter venous blood samples were collected on an empty stomach at 7:00 am before the intervention and after the intervention experiment. Plasma was separated by centrifugation within 1 h (3000 RPM, 10 min, 20°C), and the upper plasma was divided into a 0.5 mL EP tube, which was numbered according to the collection date and stored in a low-temperature refrigerator at −70°C for examination.

The detection principle was as follows: quantitative determination of target antigen levels was conducted by the ELISA double antibody sandwich method. The coated antitarget antigen-antibody was combined with the target antigen in the plasma to be tested, and the enzyme-conjugated antibody was added to form a complex, which reacted with the substrate to display color. The A value measured at 490 nm was proportional to the plasma antigen content to be measured. According to the corresponding standard point data, the standard curve was drawn in Excel, and the standard curve equation was established. The concentrations of tissue plasminogen activator (tPA), plasminogen activator inhibitor-1 (PA1-1), and von Willebrand factor (vWF) in the samples to be tested were calculated by the standard curve equation. Normal plasma concentrations of tPA and PAI-1 are 1.0-12.0 ng/mL and L5~45 ng/mL, respectively. The plasma vWF level was measured as its ratio to the standard plasma content, and the normal range was 60%-150% or 0.6-1.5.

2.5. Postoperative Care

2.5.1. Close Observation of Vital Signs. Patients were admitted to the intensive care unit directly after surgery and were given intensive care with continuous monitoring of several parameters and close observation of changes in vital signs. Blood pressure was measured every 5-10 min during the 24 hours after surgery, and once an hour after the blood pressure stabilized for 24 h. The patient's consciousness, pupils, speech and body movement, and the presence of severe headache were observed at any time, and the doctor was notified of any abnormalities to prevent complications.

2.5.2. Prevention of Arterial Embolism and Bleeding in the Lower Extremity. After Wingspan stenting, the puncture site is usually sutured intravascularly with a vascular suture, but the suture may fail due to the influence of the technique, and the arterial pulsation and color of the punctured limb should be noted. Therefore, the pulsation and skin color of the dorsalis pedis artery on the operated side should be closely observed, and the dorsalis pedis artery should be measured every 30 min for 6 consecutive times. If the pulsation of the dorsalis pedis artery is significantly weaker than that of the opposite side and the pain of the lower limb is obvious after the operation, and the skin color is cyanotic, it indicates the possibility of arterial embolism of the lower limb. No lower limb artery embolism occurred in this group, but there were two cases of bleeding at the puncture site.

2.5.3. Application of Postoperative Anticoagulant Drugs. The application of postoperative anticoagulant drugs is directly related to the success or failure of surgery. The most dangerous postoperative complication is acute arterial occlusion, which is mainly caused by subplaque bleeding or secondary thrombosis after plaque rupture. Therefore, postoperative treatment with low-molecular weight heparin is routinely administered, and patients are given warfarin 0.4 mLq 12 h subcutaneously for 1 week, aspirin 100 mg, and plavix 75 mg orally according to the doctor's prescription after returning to the ward. During the period of anticoagulation, the clotting situation was closely observed, and the clotting time and prothrombin time were monitored after the operation. The skin mucosa was closely observed for bleeding spots or purpura, the color of urine and stool, and other organs for signs of bleeding.

2.6. Statistical Methods. Data were processed and analyzed by SPSS 22.0. The counting data were expressed as the rate (%), while measurement data were expressed as the mean ± standard deviation ($\overline{x} \pm s$). The differences between the two groups were compared by T test, and continuous indicator groups were compared by analysis of variance. $P < 0.05$ was considered statistically significant.

3. Results

3.1. Basic Information of the Research Subjects. Eighty patients with cerebral infarction were randomly divided into the experimental group and the control group, with 40 in each group. In the experimental group, there were 16 males and 24 females, with an average age of 55.3 ± 2.7 years. After preoperative examination, there were 18 cases of severe stenosis and 21 cases of nonsevere stenosis, while in the control group, there were 15 males and 25 females, with an average age of 56.4 ± 3.1 years. There were 22 cases of severe stenosis and 19 cases of nonsevere stenosis. There was no considerable difference in basic data between the two groups ($P > 0.05$) (Table 1).

3.2. The Incidence of Adverse Events in the Two Groups. Statistically, there was no remarkable difference in unsafe events in postoperative transport between the two groups

Table 1: General patient information.

Group	Cases	Male cases	Female cases	Age (years old)	Severe stenosis (case)	Nonsevere stenosis (case)
Experimental group	40	16	24	55.3 ± 2.7	18	21
Control group	40	15	25	56.4 ± 3.1	22	19

($P > 0.05$). In the experimental group, there were 6 falls, 3 bed falls, 3 phlebitis, 4 pipeline slippage, and 10 deep vein thrombosis. In the control group, there were 28 falls, 22 bed falls, 14 phlebitis, 10 pipeline slippage, and 24 deep venous thrombosis. The experimental group had remarkably fewer unsafe events than the control group, and the difference between the two groups was considerable ($P < 0.05$) (Figure 1).

3.3. Survey Results of Patients' Satisfaction with Nursing Services. The results in Figure 2 showed that there was no statistically significant difference between the groups in the satisfaction of nursing staff with the service attitude, dress code, and operation technique ($P > 0.05$). In the experimental group, 36 patients were satisfied with the hand hygiene of nursing staff and 35 patients were satisfied with the operation standard, while in the control group, 29 patients were satisfied with the hand hygiene of nursing staff and 27 patients were satisfied with the operation standard ($P < 0.05$).

3.4. Investigation Results of Patients' Satisfaction with Safety Management. According to the investigation shown in Figure 3, there was no statistical significance between the two groups in terms of checking patients' information and respecting patients' privacy during nurses' operations ($P > 0.05$). Thirty-eight, 35, and 37 patients in the experimental group were satisfied with safety education, medication safety, and safety reminders, respectively, while 30, 24, and 28 patients in the control group were satisfied with safety education, medication safety, and safety reminders, respectively, with considerable differences ($P < 0.05$).

3.5. Overall Evaluation of Patient Satisfaction. According to the survey results, there was no great difference between the two groups in satisfaction with the nursing service arrangement ($P > 0.05$). There were 38 patients in the experimental group who were satisfied with safety management, while there were only 27 patients in the control group who were satisfied with safety management, and the difference between the two groups was considerable ($P < 0.05$) (Figure 4).

3.6. Results of Blood-Related Indicators of Patients. Blood test results showed no notable differences in blood tPA, PA1-1, or vWF between the two groups before postoperative intervention (Figures 5–7). After intervention, the levels of tPA, PA1-1, and vWF in the experimental group were 13.5 ± 1.3 ng/mL, 60.1 ± 9.9 ng/mL, and 2.1 ± 0.2 ng/mL, respectively. When compared with those of the control group ((14.6 ± 2.4) ng/mL, (64.2 ± 10.7) ng/mL, and (2.8 ± 0.3)), the difference was considerable ($P < 0.05$).

4. Discussion

Intracranial atherosclerotic stenosis (ICAS) is one of the major causes of ischemic stroke [22, 23], accounting for more than 10% of all ischemic strokes. In Asian countries, the proportion can be as high as 30% to 67%; in China, ICAS is the most common cause of ischemic stroke, and it causes more severe stroke, longer hospitalization, and a higher recurrence rate than that of other causes [24, 25]. Patients with symptomatic intracranial atherosclerotic stenosis (symptomatic ICAS, sICAS) refer to patients with ICAS who have symptoms of cerebral ischemia and have stroke recurrence and mortality rates of 12.2%-23% within 1 year [26, 27]. Randomized clinical trial Stenting versus Aggressive Medical Therapy for Intracranial Arterial Stenosis (SAMMPRIS) and CarotidOcclusion SurgeryStudy (COSS) showed that stents were given to patients with acute ischemic stroke (AIS) caused by sICAS. stroke (AIS) is not superior to intensive medical management (IMM) alone [28, 29]. By IMM, we mean controlling patients' lipids, blood pressure, and blood glucose; regulating patients' lifestyles; enforcing smoking cessation; and encouraging exercise on the top of antiplatelet therapy [30]. However, even if IMM is strictly implemented in patients with sICAS, their 1-year stroke recurrence and mortality rates are maintained at more than 10% [31].

PTAS of intracranial arteries can directly dilate the narrowed intracranial stenotic arteries and rapidly improve the blood supply to the brain tissue in the ischemic area, which has advantages that cannot be replaced by previous pharmacological antithrombotic therapy. In addition, many relevant clinical application studies have shown that it has good therapeutic effects and safety [32]. With the introduction of relevant laws and regulations and the improvement of patients' awareness of their rights, ensuring patient safety and improving patient satisfaction are the gold standards for measuring hospital quality at this stage [33]. At present, it is important to establish a perfect risk management system, comprehensively improve the awareness and ability of risk management, and enhance the safety management of risk events. In this study, risk management items were identified and a relatively standardized and reasonable risk management pathway was explored and established.

Preoperatively, we understood the detailed condition of the patient and took the initiative to introduce the advantages and purposes of this treatment to the patient and family members to reduce the pressure on the patient. After the operation, we closely observed the vital signs, paid attention to the arterial pulsation and skin color of the punctured limb, and prevented the occurrence of arterial embolism and bleeding in the lower limb. All are for routine anticoagulation drug therapy, including close monitoring of

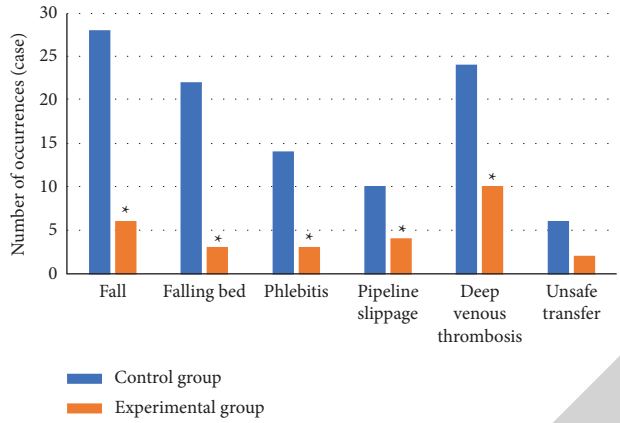

Figure 1: Comparison of occurrence of risk events. (*Note.* * represents a considerable difference vs. control group, $P < 0.05$).

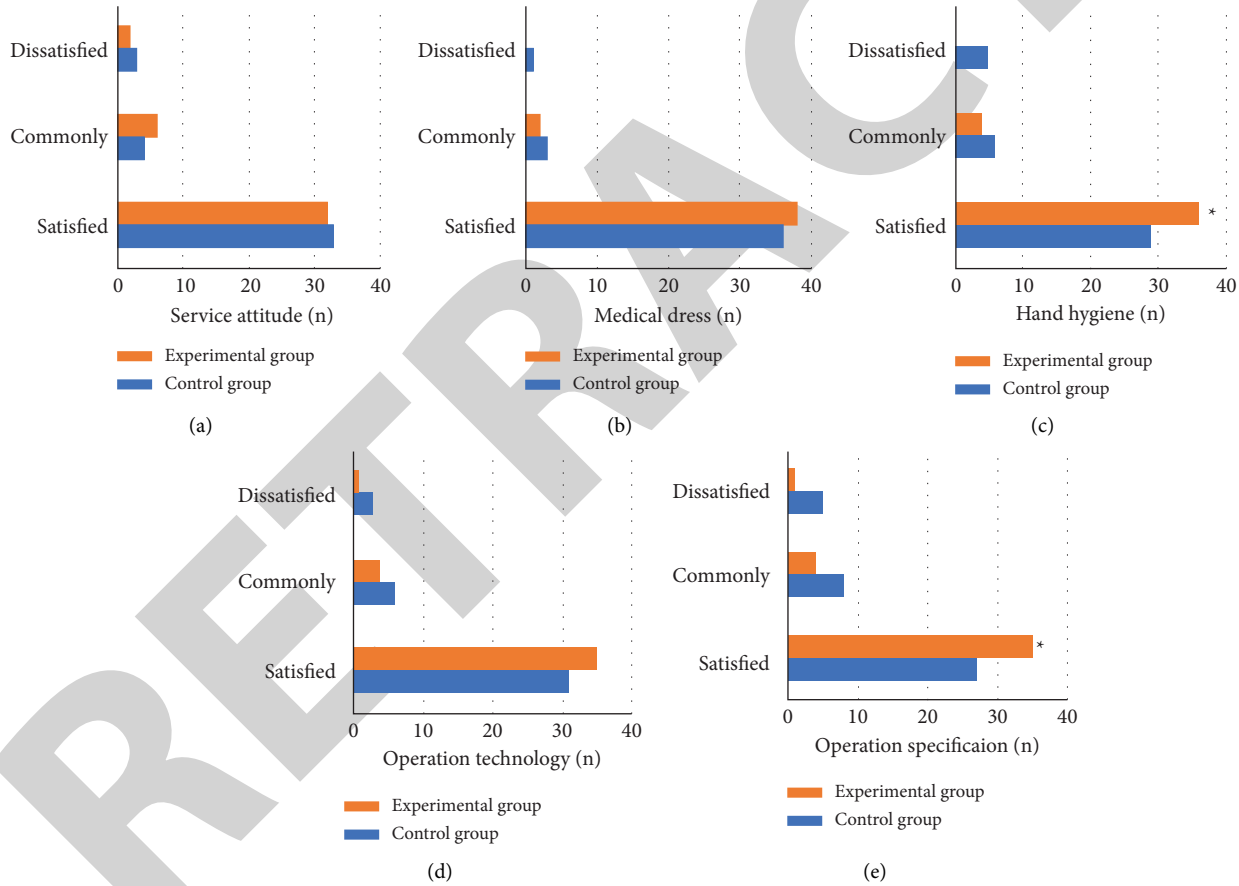

Figure 2: Results of patients' satisfaction with nursing services. (*Note.* * represents a considerable difference vs. control group, $P < 0.05$).

blood clotting, observation of blood pressure changes, adjustment of the speed of antihypertensive drugs at any time, observation of the patient's consciousness, pupils' speech, and limb movement; it is the use of prophylactic drugs to prevent the occurrence of cerebral vasospasm. In conclusion, early detection of changes in condition and notification to physicians for timely treatment are the keys to reducing complications and improving the success rate of surgery. In medical activities, nurses have the most opportunities to communicate and contact with patients, and the triviality and complexity of nursing operations increase the incidence of nursing risk events. After one month of safety management intervention, the probability of adverse events in the experimental group was much lower than that in the control group, and the difference between the two groups was considerable ($P < 0.05$), effectively reducing the risk of

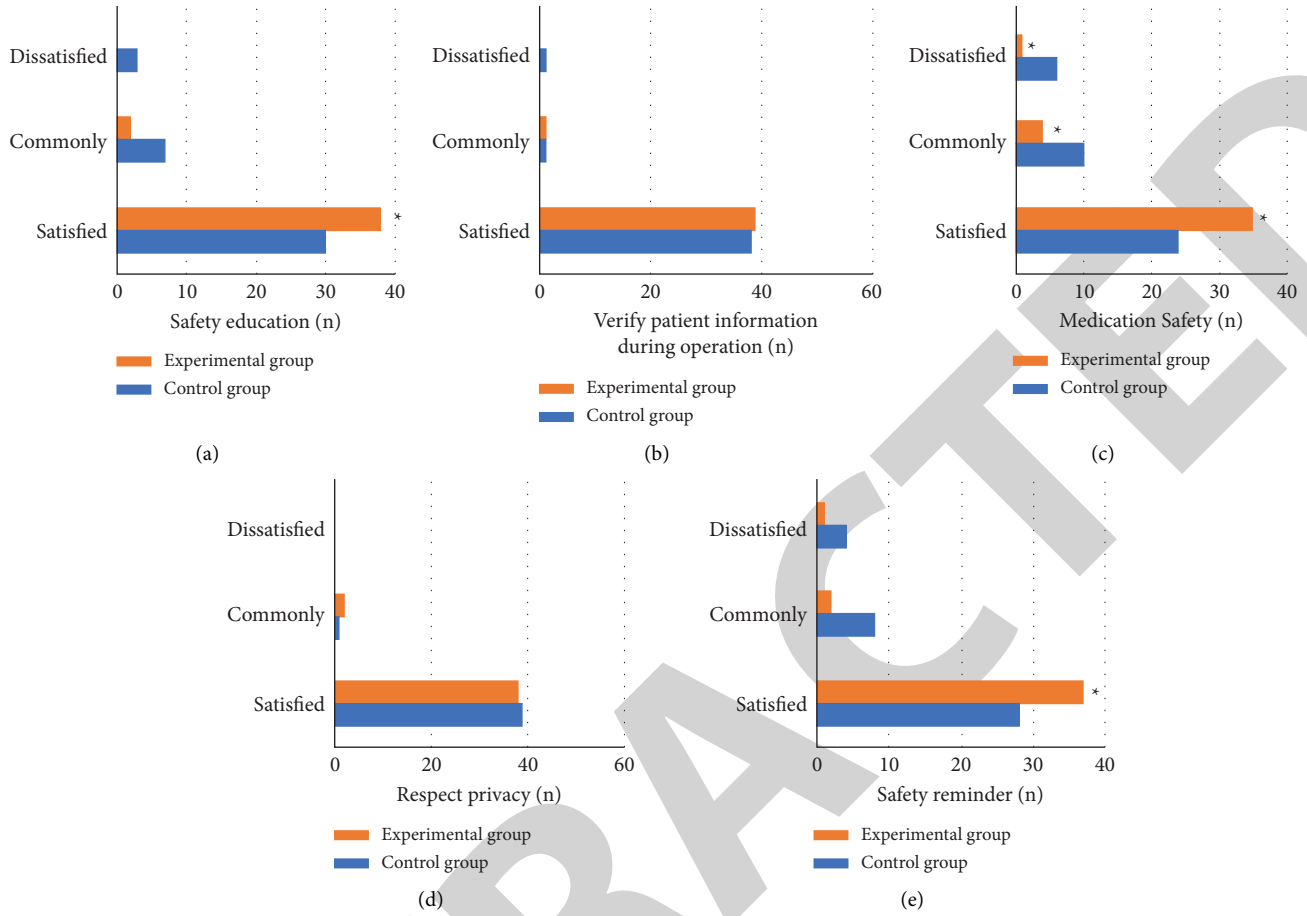

Figure 3: Results of patient satisfaction with safety management. (*Note.* *represents a considerable difference vs. control group, $P < 0.05$).

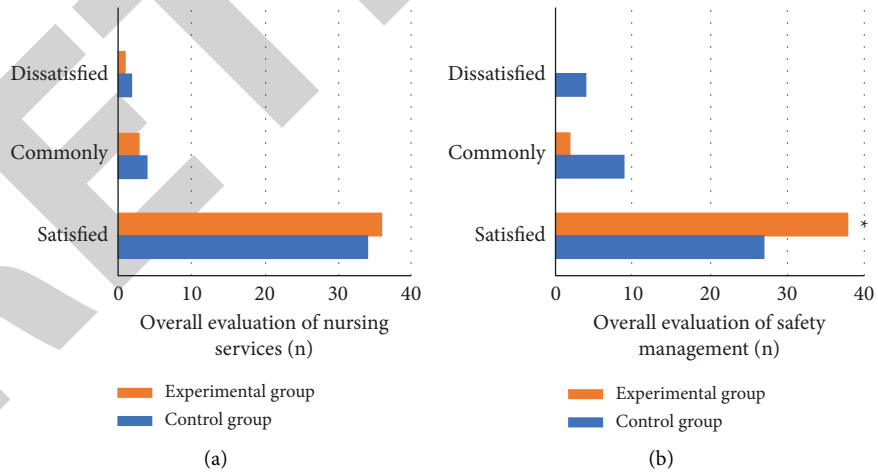

Figure 4: Results of overall patient satisfaction (*Note.* *represents a considerable difference vs. control group, $P < 0.05$).

adverse events. In the process of contact with patients, etiquette service provided an effective way to express, and nurses' considerate and meticulous service was an effective way to improve service quality. The results showed that the experimental group was significantly better than the control group ($P < 0.05$). In addition, the overall satisfaction of patients in the experimental group with safety management was also much better than that of the control group, indicating that our risk-focused safety management measures were indeed effective.

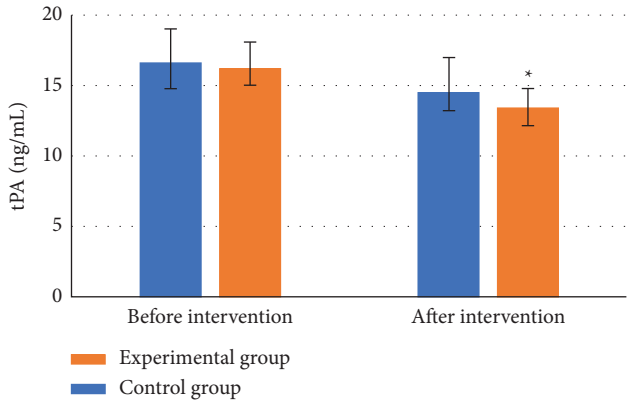

Figure 5: Comparison of tPA levels in patients' blood. (*Note.*-*represents a considerable difference vs. control group, $P < 0.05$).

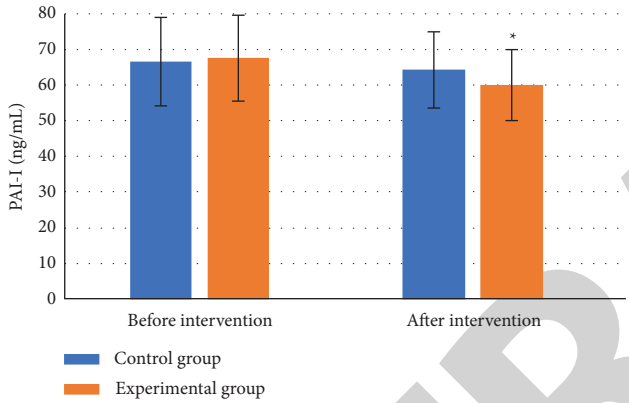

Figure 6: Comparison of blood PA1-1 levels of patients. (*Note.*-*represents a considerable difference vs. control group, $P < 0.05$).

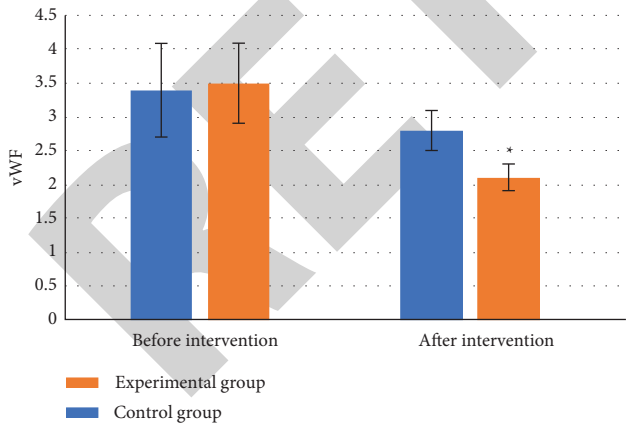

Figure 7: Comparison of vWF levels in patients' blood. (*Note.* * represents a considerable difference vs. control group, $P < 0.05$).

5. Conclusion

The results show that the risk-focused diversified safety management mode can effectively reduce the incidence of adverse events in patients, improve patients' satisfaction with nursing services, and promote faster postoperative recovery of patients. However, due to limited conditions, the sample size included in this study was small, and there was no great difference in some indicators. In addition, due to the limited research time, long-term safety management intervention for patients cannot be achieved. Further research is needed. In conclusion, the risk-focused diversified safety management model can effectively improve the quality of nursing, promote patient rehabilitation, and has clinical application value.

Data Availability

The experimental data used to support the findings of this study are available from the corresponding author upon request.

Conflicts of Interest

The authors declare that they have no conflicts of interest regarding this work.

References

[1] G. Zhang, Y. Ling, S. Zhu et al., "Direct angioplasty for acute ischemic stroke due to intracranial atherosclerotic stenosis-related large vessel occlusion," *Interventional Neuroradiology*, vol. 26, no. 5, pp. 602–607, 2020.

[2] T. H. Lee, "Management of carotid artery stenosis," *Acta Neurol Taiwan*, vol. 30, no. 4, pp. 123–127, 2021.

[3] T. Gu, R. I. Aviv, A. J. Fox, and E. Johansson, "Symptomatic carotid near-occlusion causes a high risk of recurrent ipsilateral ischemic stroke," *Journal of Neurology*, vol. 267, no. 2, pp. 522–530, 2020.

[4] A. A. Ballout, R. B. Libman, J. R. Schneider et al., "Hypoperfusion intensity ratio is associated with stroke mechanism in patients undergoing mechanical thrombectomy," *Journal of Stroke and Cerebrovascular Diseases*, vol. 31, no. 7, Article ID 106539, 2022.

[5] S. Uchiyama, K. Toyoda, K. Kitagawa et al., "Branch atheromatous disease diagnosed as embolic stroke of undetermined source: a sub-analysis of NAVIGATE ESUS," *International Journal of Stroke*, vol. 14, no. 9, pp. 915–922, 2019.

[6] H. Nordmeyer, R. Chapot, and P. Haage, "Endovascular treatment of intracranial atherosclerotic stenosis," *Röfo: Fortschritte auf dem Gebiete der Rontgenstrahlen und der Nuklearmedizin*, vol. 191, no. 7, pp. 643–652, 2019.

[7] B. H. Baek, W. Yoon, Y. Y. Lee, S. K. Kim, J. T. Kim, and M. S. Park, "Intravenous tirofiban infusion after angioplasty and stenting in intracranial atherosclerotic stenosis-related stroke," *Stroke*, vol. 52, no. 5, pp. 1601–1608, 2021.

[8] A. J. Hessels, M. Paliwal, S. H. Weaver, D. Siddiqui, and T. A. Wurmser, "Impact of patient safety culture on missed nursing care and adverse patient events," *Journal of Nursing Care Quality*, vol. 34, no. 4, pp. 287–294, 2019.

[9] B. McCarthy, S. Fitzgerald, M. O'Shea et al., "Electronic nursing documentation interventions to promote or improve patient safety and quality care: a systematic review," *Journal of Nursing Management*, vol. 27, no. 3, pp. 491–501, 2019.

[10] Z. Wang, X. Liu, Q. Cui, Z. Wang, and X. Li, "Application of diversified nursing mode in clinical nursing of patients with gestational diabetes mellitus," *Minerva Medica*, vol. 112, no. 6, pp. 832–834, 2021.

Hindawi
Emergency Medicine International
Volume 2023, Article ID 9864247, 1 page
https://doi.org/10.1155/2023/9864247

Retraction

Retracted: Clinical Efficacy and Safety Analysis of Levofloxacin for the Prevention of Infection after Traumatic Osteoarthrosis and Internal Fixation: Systematic Review and Meta-Analysis

Emergency Medicine International

Received 28 November 2023; Accepted 28 November 2023; Published 29 November 2023

This article has been retracted by Hindawi, as publisher, following an investigation undertaken by the publisher [1]. This investigation has uncovered evidence of systematic manipulation of the publication and peer-review process. We cannot, therefore, vouch for the reliability or integrity of this article.

Please note that this notice is intended solely to alert readers that the peer-review process of this article has been compromised.

Wiley and Hindawi regret that the usual quality checks did not identify these issues before publication and have since put additional measures in place to safeguard research integrity.

We wish to credit our Research Integrity and Research Publishing teams and anonymous and named external researchers and research integrity experts for contributing to this investigation.

The corresponding author, as the representative of all authors, has been given the opportunity to register their agreement or disagreement to this retraction. We have kept a record of any response received.

References

[1] W. Wang, C. Zou, and J. Zhang, "Clinical Efficacy and Safety Analysis of Levofloxacin for the Prevention of Infection after Traumatic Osteoarthrosis and Internal Fixation: Systematic Review and Meta-Analysis," *Emergency Medicine International*, vol. 2022, Article ID 8788365, 9 pages, 2022.

Hindawi
Emergency Medicine International
Volume 2022, Article ID 8788365, 9 pages
https://doi.org/10.1155/2022/8788365

Research Article

Clinical Efficacy and Safety Analysis of Levofloxacin for the Prevention of Infection after Traumatic Osteoarthrosis and Internal Fixation: Systematic Review and Meta-Analysis

Weiliang Wang,[1] ChuanQi Zou,[2] and Jie Zhang [3]

[1]*Department of Traumatology, Beijing Daxing District People's Hospital, Beijing 102600, China*
[2]*Department of Orthopedics, Banan Hospital of Chongqing Medical University, Chongqing 400000, China*
[3]*Department of Pharmacy, The First Affiliated Hospital of Nanchang University, Nanchang, Jiangxi 330001, China*

Correspondence should be addressed to Jie Zhang; drzhangjie0301@sina.com

Received 19 July 2022; Revised 28 August 2022; Accepted 13 September 2022; Published 29 September 2022

Academic Editor: Hang Chen

Objective. Levofloxacin has been widely used in clinical anti-infection treatment; however, its adverse reactions to levofloxacin were also obvious in patients. Herein we aimed to systematically evaluate the clinical efficacy and safety of systemic administration of levofloxacin in the prevention of postoperative infection after traumatic osteoarthrosis and internal fixation. *Methods*. PubMed, Cochrane Library, OVID, EBSCO, CNKI, VIP database, and Wanfang Database were searched from December 1993 to December 2021. Meanwhile, China ADR Information Bulletin and WHO Pharmaceutical were searched manually. Newsletter and FDA Drug Safety Newsletter, also to retrieve the Websites of Chinese, Chinese, and drug regulatory authorities; To obtain data on adverse events in children with systemic administration of levofloxacin. The literature was screened according to inclusion and exclusion criteria. The risk of bias was evaluated for the included RCT literature. *Results*. There was a statistical difference in the comparison of the incidence of fever between the experimental group and the control group (OR = 2.29, 95% CI (1.75,2.98),$P < 0.00001$, $I^2 = 0\%$, $Z = 6.11$); elevated white blood cell count (OR = 1.82, 95% CI (1.31,2.52),$P = 0.0003$, $I^2 = 0\%$, $Z = 3.60$); incidence of wound infection (OR = 2.11, 95% CI (1.54,2.90),$P < 0.00001$, $I^2 = 0\%$, $Z = 4.64$); adverse drug reaction (OR = 1.82, 95% CI (1.21,2.74),$P = 0.004$, $I^2 = 0\%$, $Z = 2.86$). *Conclusion*. In the clinical use of levofloxacin, adverse drug reactions including fever, elevated white blood cell count, and wound infection should be concerned.

1. Introduction

With the development of modern medical science, the types of orthopedic trauma treatment and internal fixation are also increasing, and actively dealing with the prognosis of postoperative infection has become a question that orthopedic surgeons need to pay attention [1–3]. According to statistics, the infection rate of orthopedic surgery is as high as 11.41% and the incision classification of class i, ii, and iii is 1.89%, 7.63%, and 13.08%, respectively [4]. The fluoroquinolone synthetic antibiotic levofloxacin has been widely used in the clinical control of systemic infection due to its advantages of the broad antibacterial spectrum, strong activity, no skin test before use, and no cross-resistance with other antibacterial drugs [5]. At the same time, the adverse reactions of levofloxacin were also more obvious, and unreasonable drug use was an important cause of adverse reactions in patients [6].

Levofloxacin has been widely used in clinical anti-infection treatment because of its wide antibacterial spectrum, high antibacterial activity, and good tissue permeability [7]. However, animal experiments have shown that quinolones can induce irreversible joint damage in young animals, suggesting that quinolones may also have the same toxicity in children, so the application of quinolones in the pediatric field is strictly limited. The drug instructions in the United States and China clearly stipulate that levofloxacin can only be used for the treatment of anthrax in children <18 years

old [8]. Levofloxacin has a certain therapeutic value for children with drug-resistant *Mycobacterium tuberculosis* and drug-resistant mycoplasma infection, and relevant clinical studies have also been carried out. Therefore, it is off-label to clarify the occurrence of cartilage damage of levofloxacin.

Levofloxacin is a broad-spectrum fungicide. Its bactericidal mechanism includes acting on dividing cells to inhibit the activity of bacterial DNA rotation, inhibiting the synthesis of RNA and protein, and promoting the phagocytic function of white blood cells. Meanwhile, it also acts on nondividing cells to make them lose viability and thus can cure infection radically. It has the advantages of rapid absorption, high peak concentration, and relatively stable activity. The safety of levofloxacin was improved because of its selective inhibition of topoisomerase ii in bacteria and mammals; the difference between the two was up to 1400 times. Levofloxacin (LVLX) is a new generation of fluoroquinolone drug, which was marketed in 1993. It belongs to the monofouroxacin containing a fluorine group. The structure of levofloxacin is levofloxacin optical isomer, which has stronger antibacterial activity than dextral isomer 8~128 times is 2 times ofloxacin the clinical dosage of ofloxacin is 1/2. Compared with the first generation of fluoroquinolones, the antibacterial spectrum expanded to Gram-negative cordyceps, Gram-positive chlamydia mycoplasma, and *Legionella* have good antibacterial activity. Good tissue distribution has no cross-infection with other antibacterial drugs, such as drug resistance and other advantages adverse reactions are also greatly reduced, which makes the comprehensive clinical efficacy reach a new level.

Levofloxacin (LVLXDR-3355) is a fluoroquinolone drug developed in Japan in 1986. The active isomer of ofloxacin. It is widely used in clinical practice because of its higher efficacy better tissue distribution lower adverse reactions than ofloxacin. In general, if osteoarthritis is caused by infectious factors, levofloxacin is the drug of choice for treatment, which usually has anti-inflammatory and analgesic effects. However, at present, most osteoarthritis is a disease caused by degenerative changes in the joints, so the use of levofloxacin is not able to achieve a good therapeutic effect. At present, osteoarthritis (OA) is still one of the most common musculoskeletal diseases in the world. OA progresses rapidly, with joint destruction occurring within three to seven years. The pathogenesis of OA is still unclear. Age, infection or inflammation, injury, extra-articular malformation, joint instability, environmental factors, estrogen, excessive weight bearing, obesity, excessive exercise, genetics, diet, and so on the pathogenesis factors. Although infection is not the main factor in the pathogenesis of OA, the discovery of inflammatory cytokines and the current unsatisfactory treatment results inspire us to rethink the role of infection in the pathogenesis and pathogenesis of OA. OA is an inflammatory disease in which a variety of cytokines and inflammatory chemokines are involved in its pathogenesis, among which interleukin plays a major role. At present, it is still controversial whether an infection is the cause of OA, and the role of infection in the occurrence and development of OA is not well understood. Traditional research methods have certain limitations in this respect. With the continuous development of molecular biology technology and means, we can have a deeper understanding of the relationship between infection and OA, thus providing broad prospects for the treatment of OA.

As a common complication of orthopedic patients, the infection has aroused high attention of clinical medical staff, and perioperative prophylactic medication is becoming more and more important. To understand the distribution and drug resistance of common pathogens in bone and joint infection sites of orthopedic patients in our hospital, and to provide an etiological basis for the prevention and treatment of infection [9]. The study showed that there were significant differences in surgical site infection rate among different incisions, underlying diseases, advanced age, long preoperative hospital stay, paralysis and bed rest, use of adrenal glucocorticoids, and implants were risk factors for postoperative infection. At the same time, strengthening the cleaning and disinfection of the ward and the surgical environment, as well as the disinfection and sterilization of instruments and other nondrug prevention strategies are also important links in the control of postoperative infection. In addition, the development of single-tube closed drainage and absorbable artificial bone loaded with antibiotics can also reduce the risk of infection to a certain extent [10].

There are research orifices. It was found that levofloxacin had certain damage to rat, rabbit, and human chondrocytes, but there was a difference in species, rat > rabbit > human. Some studies have found that quinolones can cause reversible damage to the bone joint. Therefore, this study comprehensively collected safety studies and related information on levofloxacin, and evaluated the occurrence of bone and joint adverse events, in order to provide a reference for the off-label use of levofloxacin.

2. Materials and Methods

2.1. Literature Retrieval. Literature databases: PubMed, Cochrane Library, OVID, EBSCO; Chinese database: CNKI, China Weipu Science and Technology Periodical database, and Wanfang Database. The retrieval time was from January 1993 to 2022 January. Databases under development: WHO clinical trial registration platform (http://apps.whe.int/trialsearch/), American clinical trial registration platform (http://clinieahfials.gov/). Gray literature: proceedings of special conferences, etc., and references of related literature retrospection (Figure 1).

2.2. Literature Inclusion Criteria. Inclusion criteria were as follows: (1) subjects were > 18 years old; (2) levofloxacin oral or intravenous infusion, dosage, and course of treatment are not limited; (3) description of any adverse events related to bone and joint, including clinical manifestations and signs (joint swelling, pain, claudication, etc.). Auxiliary examination: X-ray, MRI, and histopathological examination to determine bone and joint changes.

2.3. Exclusion Criteria. Exclusion criteria were as follows: (1) the experimental design was nonrandomized controlled literature; (2) for the two literature with the same data, the

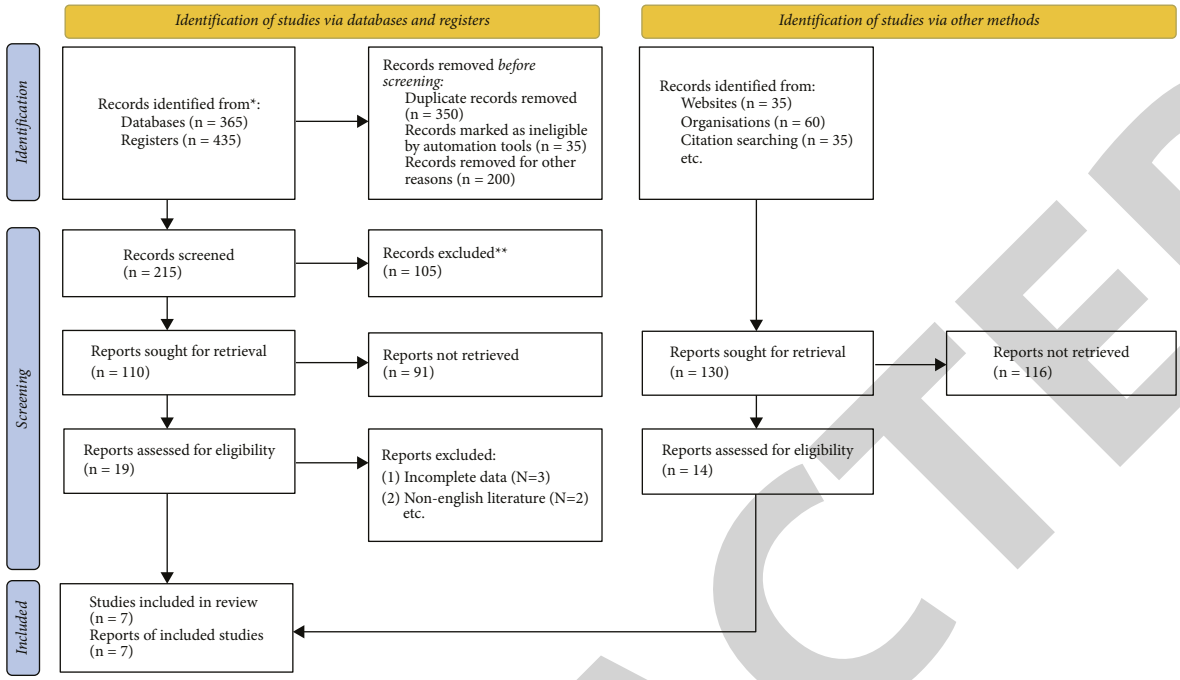

Figure 1: Flow chart of the literature screening.

one published for the first time was regarded; (3) literature that cannot provide valid data for analysis; (4) the second published literature shall be subject to the highest level of the journal; (5) study of combined drug therapy; (6) repeated publications.

2.4. Literature Screening. Preliminary screening was conducted through reading articles, and then further screening was conducted after reading abstracts or full texts of literature that might meet the inclusion criteria. If necessary, contact the authors for more research information before making a judgment.

2.5. Data Extraction. The main contents include the following: (1) basic information of included literature: author, publication date, country of study implementation, type of study design and sample size, number of lost follow-ups; (2) subjects: age, diagnosis; (3) intervention: drug name, said, dosage and course of treatment, combined medication, and other circumstances; (4) related contents of literature bias risk assessment; (5) outcome indicators. WHO-UMC causality assessment was used to evaluate the association between adverse events and levofloxacin.

2.6. Literature Bias Risk Assessment. RCT was conducted in accordance with the risk assessment method of bias recommended in the Cochrane System Evaluator's Manual 5.1.0, which included 6 items randomization, assignment hiding, blinds, the integrity of outcome data, selective reporting of results, and other possible sources of bias, see Figures 2(a) and 2(b)) and Figures 3(a)–3)(d).

2.7. Statistical Analysis. For the data of levofloxacin adverse events reported in the literature, OR and 95% CI were used as the effect size for meta-analysis. Descriptive analysis was used when quantitative synthesis was not possible, and $P < 0.05$ was considered statistically significant.

3. Result

3.1. Literature Retrieval Results and Included Research Characteristics. In this study, PubMed, Cochrane, Web of Knowledge, Embase, CBM, CNKI, CECDB, and CQVIP were searched. A total of relevant literature was retrieved during the initial screening. Repeated publications and RCTs were excluded by reading titles and abstracts, and 19 literature were left. 19 full papers were reviewed, different reports of the same clinical study and literature inconsistent with the content of this study were excluded, and references of relevant literature were searched to prevent literature omission. Finally, a total of 12 RCTs were included in the study [11–24]. All the retrieval and screening processes were completed by two evaluators independently, and any different opinions were unified through internal discussion (Table 1).

3.2. Incidence of Fever. Among the 14 RCTs' literature included in the incidence of fever, a heterogeneity test was carried out and it was found that the heterogeneity of the selected studies was small, so a meta-analysis with fixed

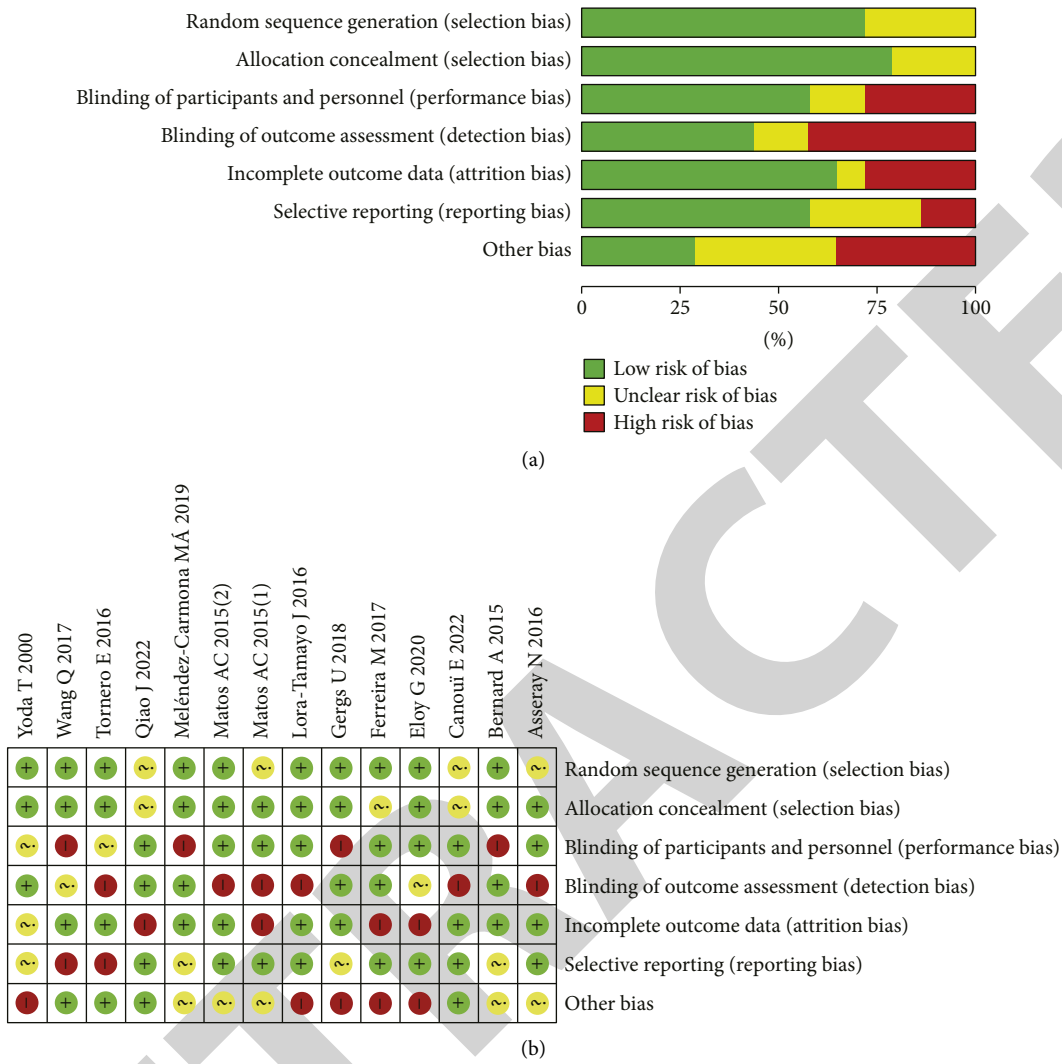

Figure 2: Literature quality evaluation chart. (a) Risk of bias graph. (b) Risk of bias summary.

models could be performed. The results of the meta-analysis showed that the rhombus plot and vertical line no intersected in the forest map of incidence of fever for 4 included literature, so there was a statistical difference in the comparison of the incidence of fever between the experimental group and the control group (OR = 2.29, 95% CI (1.75, 2.98), $P < 0.00001$, $I^2 = 0\%$, $Z = 6.11$) (Figure 4).

3.3. Elevated White Blood Cell Count. Among the 14 RCTs' literature included in elevated white blood cell count, a heterogeneity test was carried out and it was found that the heterogeneity of the selected studies was small, so a meta-analysis with fixed models could be performed. The results of the meta-analysis showed that the rhombus plot and vertical line no intersected in the forest map of elevated white blood cell count for 4 included literature, so there was a statistical difference in the comparison of elevated white blood cell count between the experimental group and the control group (OR = 1.82, 95% CI (1.31,2.52), $P = 0.0003$, $I^2 = 0\%$, $Z = 3.60$) (Figure 5).

3.4. Incidence of Wound Infection. Among the 14 RCTs' literature included in the incidence of wound infection, a heterogeneity test was carried out and it was found that the heterogeneity of the selected studies was small, so a meta-analysis with fixed models could be performed. The results of the meta-analysis showed that the rhombus plot and vertical line no intersected in the forest map of incidence of wound infection for 4 included literature, so there was a statistical difference in the comparison of the incidence of wound infection between the experimental group and the control group (OR = 2.11, 95% CI (1.54,2.90), $P < 0.00001$, $I^2 = 0\%$, $Z = 4.64$) (Figure 6).

3.5. Adverse Drug Reaction. Among the 14 RCTs' literature included in adverse drug reactions, a heterogeneity test was carried out and it was found that the heterogeneity of the selected studies was small, so a meta-analysis with fixed models could be performed. The results of the meta-analysis showed that the rhombus plot and vertical line no intersected in the forest map of adverse drug reactions for 4

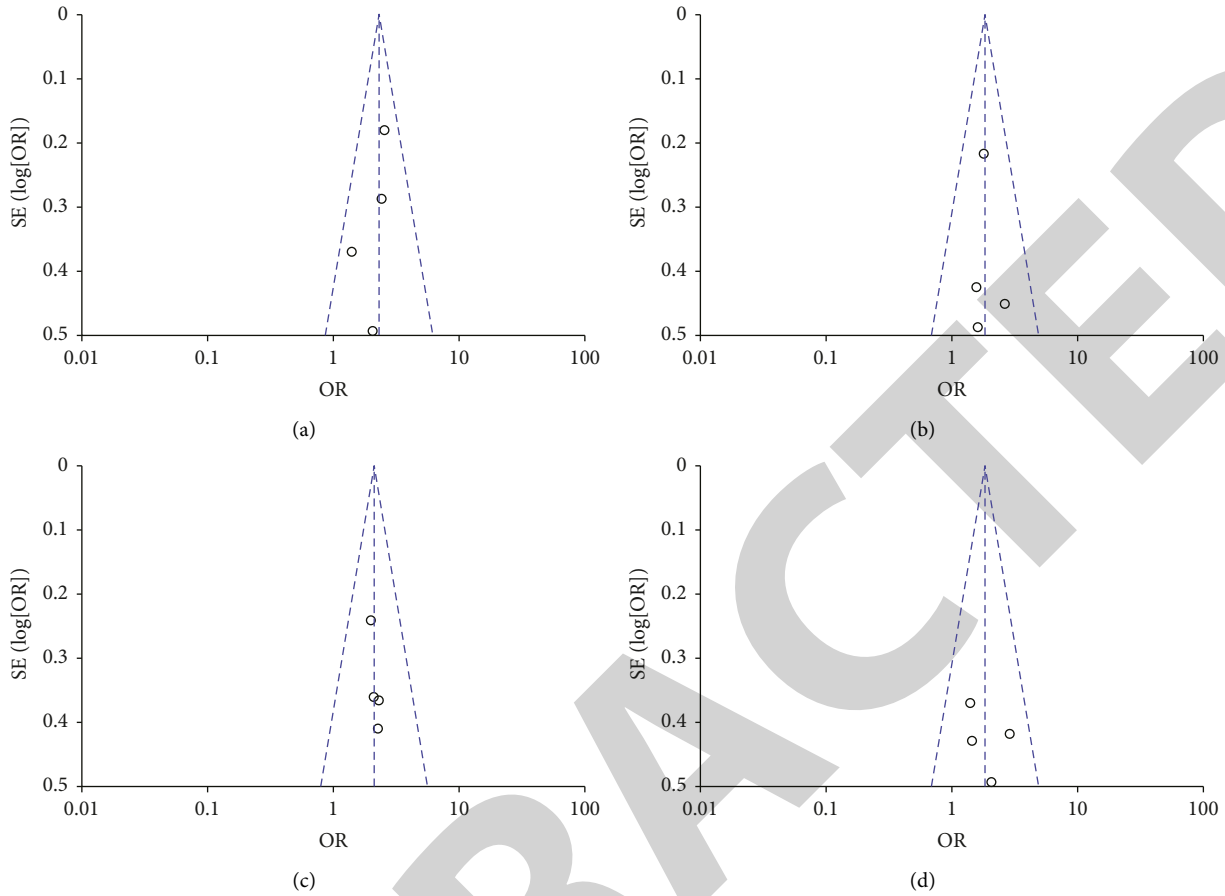

Figure 3: a-d: Funnel plot of literature publication bias.

Table 1: Basic clinical features of 14 literature were included in our study.

Study	Age	Gender (Male)	(%) Experimental group (N)	Control group (N)	NOS score
Meléndez-Carmona MÁ 2019	53.71 ± 12.2	41.25	42/65	30/65	8
Asseray N 2016	55.65 ± 13.4	69.12	160/260	100/260	7
Tornero E 2016	63.12 ± 14.5	45.72	78/143	54/143	8
Lora-Tamayo J 2016	67.15 ± 14.5	44.12	100/175	75/100	8
Bernard A 2015	52.85 ± 8.4	51.89	20/34	14/34	8
Yoda T 2000	64.36 ± 10.2	63.45	24/44	20/44	7
Qiao J 2022	62.62 ± 12.2	78.10	30/50	20/50	9
Gergs U 2018	62.61 ± 13.0	48.75	26/42	16/42	9
Canouï E 2022	57.25 ± 14.5	59.23	62/102	40/102	7
Eloy G 2020	66.22 ± 15.2	56.22	32/59	27/59	8
Ferreira M 2017	61.35 ± 8.1	53.16	25/45	20/45	8
Matos AC 2015(1)	57.25 ± 16.0	66.34	22/35	18/35	8
Matos AC 2015(2)	58.51 ± 8.6	48.34	48/67	35/67	9
Wang Q 2017	66.34 ± 6.5	53.12	55/66	42/66	9

included literature, so there was a statistical difference in the comparison of adverse drug reactions between the experimental group and the control group (OR = 1.82, 95% CI (1.21,2.74), $P = 0.004$, $I^2 = 0\%$, $Z = 2.86$) (Figure 7).

4. Discussion

The efficacy of perioperative antibiotics in preventing surgical infection has been widely verified in clinics [25]. Levofloxacin has been widely used in the prevention of postoperative infection due to its wide antibacterial spectrum, strong antibacterial activity, and low drug resistance rate, as well as its unique pharmacokinetic characteristics, such as 5.8 h half-life, high tissue concentration, and no skin test [26]. However, in the clinical application of levofloxacin as a broad-spectrum antibiotic, adverse drug reactions also occur from time to time. In addition to the influence of individual differences and other objective factors, in order to

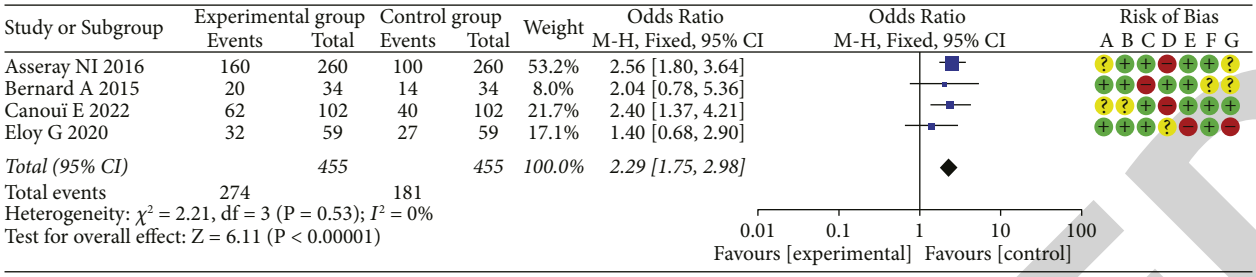

Risk of bias legend

(A) Random sequence generation (selection bias)
(B) Allocation concealment (selection bias)
(C) Blinding of participants and personnel (performance bias)
(D) Blinding of outcome assessment (detection bias)
(E) Incomplete outcome data (attrition bias)
(F) Selective reporting (reporting bias)
(G) Other bias

Figure 4: Meta-analysis of incidence of fever between two groups.

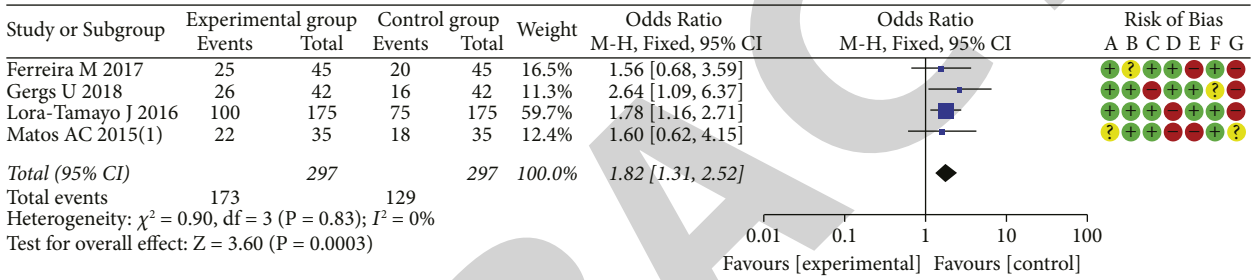

Risk of bias legend

(A) Random sequence generation (selection bias)
(B) Allocation concealment (selection bias)
(C) Blinding of participants and personnel (performance bias)
(D) Blinding of outcome assessment (detection bias)
(E) Incomplete outcome data (attrition bias)
(F) Selective reporting (reporting bias)
(G) Other bias

Figure 5: Meta-analysis of elevated white blood cell count between two groups.

effectively reduce the incidence of ADR, ensure the health of patients and minimize the pain of patients, clinicians need to make a comprehensive analysis of the clinical data of patients [27–30].

Surgical site infection is one of the most common postoperative complications, surgical site infection, particularly surgical site infection of the incision, the most direct impact is delayed healing of the incision, appear even incision split, more serious may lead to the surgical site physical disability and corresponding organ dysfunction or failure, there is also a cause of deaths; therefore, we must pay attention to the occurrence of surgical site infection complications, and adopt effective prevention and treatment measures. Surgical site infection complications occurred more influencing factors, such as the surface of the operating room environment and air quality, skin disinfection of operation, quality of equipment, the performer such as hand hygiene can cause late complications, surgical site infection in patients with surgical site infection and disease occurrence is necessary to real-time monitoring, and adopt specific measures to prevent complications of infection, Through the implementation of "whole-process quality management" measures to reduce the incidence of surgical site infection complications. In order to better understand the incidence of surgical site infection in patients with bone and joint surgery, and to obtain effective prevention and treatment measures for complications. The overall results showed that the complications of bone and joint surgery site infection were mainly in type I incisions, accounting for 83.33% of all infected patients. The results also showed that there was a certain correlation between surgical risk index and the incidence of surgical site infection complications, that is, the higher the surgical risk index, the higher the incidence of surgical site infection complications; It is suggested that the prevention of infection complications should be prepared before determining the risk index of surgery and performing surgery, so as to reduce the probability of complications of surgical site infection. We also see the importance of implementing whole-process quality management. In terms of perioperative medication, this study believes that the proportion of patients taking drugs should be reduced and targeted medication should be

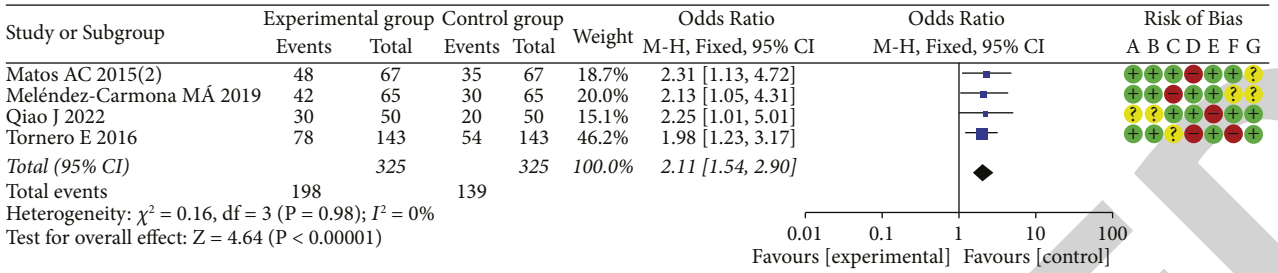

Risk of bias legend

(A) Random sequence generation (selection bias)
(B) Allocation concealment (selection bias)
(C) Blinding of participants and personnel (performance bias)
(D) Blinding of outcome assessment (detection bias)
(E) Incomplete outcome data (attrition bias)
(F) Selective reporting (reporting bias)
(G) Other bias

Figure 6: Meta-analysis of incidence of wound infection between two groups.

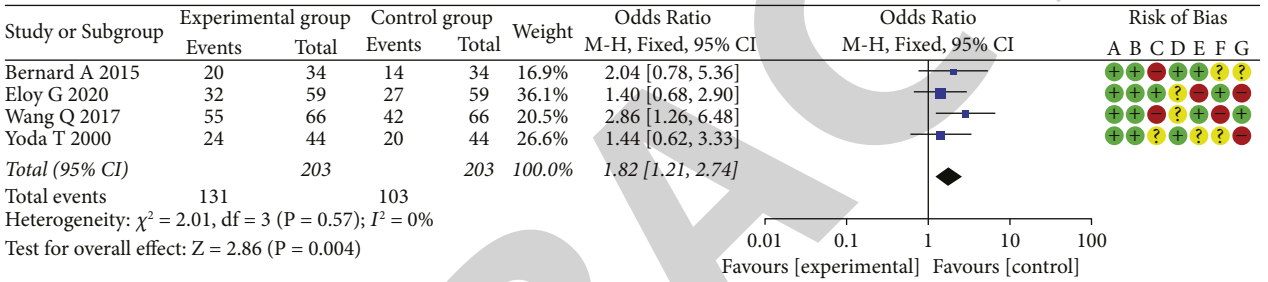

Risk of bias legend

(A) Random sequence generation (selection bias)
(B) Allocation concealment (selection bias)
(C) Blinding of participants and personnel (performance bias)
(D) Blinding of outcome assessment (detection bias)
(E) Incomplete outcome data (attrition bias)
(F) Selective reporting (reporting bias)
(G) Other bias

Figure 7: Meta-analysis of adverse drug reaction between two groups.

increased. Moreover, antibacterial drugs of the first generation cephalosporin should be the main drug, and antibacterial drugs of the third generation cephalosporin should not be directly used.

Over 60 years old in patients receiving levofloxacin there was a higher incidence of adverse reactions to prevent infection treatment mainly includes: the main reasons for elderly patients with viscera function decline, easily complicated by a variety of disease, and levofloxacin by kidney metabolism, effects on kidney burden, clinical applications in the old people should take into consideration the reduction and regular monitoring of kidney function [31]. In addition, from the animal experiments on quinolone antibiotics, it was found that young animals taking quinolone antibiotics would produce cartilage damage to joint tissue, so children, pregnant and lactating women should be forbidden levofloxacin [32–35]. At the same time, because levofloxacin belongs to quinolones antibiotic effect, from this group of cases cure effect and ADRs of reaction after taking levofloxacin, static drop 1- or 2-times daily fee sand star of left oxygen drugs for prevention of postoperative infection, there was no significant difference, and oxygen cost effect of medication to reduce the incidence of ADR is safer and more effective [36–39].

To sum up, levofloxacin should be paid attention to the following points in preventing infection after bone joint and internal fixation: (1) when prescribing levofloxacin, the patient's physical condition should be consulted in detail. If the patient is allergic, it should be avoided as far as possible; (2) the storage temperature of levofloxacin and other drugs should be controlled within 20°C and stored away from light to prevent improper storage and degradation of drugs, reduce pharmacological effect and cause adverse reactions; (3) patients should eat before infusion, to avoid drug reaction to aggravate the stimulation of empty abdomen, so that gastrointestinal discomfort magnify; (4) pay attention to keep the infusion speed slow, 100 ml infusion time is not less than 1 h; (5) pay attention to the patients with liver and kidney function decline, especially the elderly patients, for the weak patients with levofloxacin in vivo clearance rate reduced, the half-life prolonged, in order to prevent drug accumulation caused toxicity, doctors must reduce the drug dosage; (6)

levofloxacin can pass through the blood-brain barrier, into the brain tissue and may cause central nervous system reaction, for patients with cerebrovascular disease, epilepsy or family history of mental illness and other basic diseases of the central nervous system, should pay attention to control or prohibit the use. As a common complication of orthopedic patients, the infection has aroused high attention of clinical medical staff, and perioperative prophylactic medication is becoming more and more important. In order to understand the distribution and drug resistance of common pathogens in bone and joint infection sites of orthopedic patients, and to provide an etiological basis for the prevention and treatment of infection. The risk factors for postoperative infection were underlying diseases, advanced age, long hospital stay, paralyzed bed, use of adrenal glucocorticoids, and implants. At the same time, strengthening the cleaning and disinfection of the ward and surgical environment, as well as the disinfection and sterilization of instruments and other nondrug prevention strategies are also important links in the control of postoperative infection. In addition, single-tube closed drainage and absorbable artificial bone technologies can also reduce the risk of infection to a certain extent.

Available evidence shows that the incidence of osteoarticular adverse events with levofloxacin is low and most of them are resolved during follow-up. It can provide a basis for the off-label use of levofloxacin after fully evaluating the risks and benefits.

Data Availability

The data used to support this study are available from the corresponding author upon request.

Conflicts of Interest

The authors declare that they have no conflicts of interest.

Authors' Contributions

Weiliang Wang and ChuanQi Zou contributed equally to this work.

References

[1] T. Toros and K. Ozaksar, "Reconstruction of traumatic tubular bone defects using vascularized fibular graft," *Injury*, vol. 52, no. 10, pp. 2926–2934, 2021 Oct.

[2] D. Musu and E. Cotti, "Traumatic bone cyst of the jaws: an overview," *Journal of Biological Regulators & Homeostatic Agents*, vol. 33, no. 4, pp. 1261–1263, 2019 Jul-Aug.

[3] M. Izadi, B. Dadsetan, Z. Najafi et al., "Levofloxacin versus ceftriaxone and azithromycin combination in the treatment of community acquired pneumonia in hospitalized patients," *Recent Patents on Anti-infective Drug Discovery*, vol. 13, no. 3, pp. 228–239, 2019.

[4] D. Deshpande, J. G. Pasipanodya, S. G. Mpagama et al., "Levofloxacin pharmacokinetics/pharmacodynamics, dosing, susceptibility breakpoints, and artificial intelligence in the treatment of multidrug-resistant tuberculosis," *Clinical Infectious Diseases*, vol. 67, no. suppl_3, pp. S293–S302, 2018 Nov 28.

[5] E. Shtaniuk, T. Kovalenko, L. Krasnikova, M. Mishyna, and O. Vovk, "[Characteristics of levofloxacin and its clinical application (review)]," *Georgian Medical News*, vol. 307, pp. 173–180, 2020 Oct.

[6] I. Karampela and M. Dalamaga, "Could respiratory fluoroquinolones, levofloxacin and moxifloxacin, prove to be beneficial as an adjunct treatment in COVID-19?" *Archives of Medical Research*, vol. 51, no. 7, pp. 741-742, 2020 Oct.

[7] M. T. Drayson, S. Bowcock, T. Planche et al., "Levofloxacin prophylaxis in patients with newly diagnosed myeloma (TEAMM): a multicentre, double-blind, placebo-controlled, randomised, phase 3 trial," *The Lancet Oncology*, vol. 20, no. 12, pp. 1760–1772, 2019 Dec.

[8] M. Biagi, X. Tan, T. Wu et al., "Activity of potential alternative treatment agents for stenotrophomonas maltophilia isolates nonsusceptible to levofloxacin and/or trimethoprim-sulfamethoxazole," *Journal of Clinical Microbiology*, vol. 58, no. 2, 2020 Jan 28.

[9] A. C. Bennett, C. L. Bennett, B. J. Witherspoon, and K. B. Knopf, "An evaluation of reports of ciprofloxacin, levofloxacin, and moxifloxacin-association neuropsychiatric toxicities, long-term disability, and aortic aneurysms/dissections disseminated by the Food and Drug Administration and the European Medicines Agency," *Expert Opinion on Drug Safety*, vol. 18, no. 11, pp. 1055–1063, 2019 Nov.

[10] J. Yuan, B. Mo, Z. Ma et al., "Safety and efficacy of oral nemonoxacin versus levofloxacin in treatment of community-acquired pneumonia: a phase 3, multicenter, randomized, double-blind, double-dummy, active-controlled, non-inferiority trial," *Journal of Microbiology, Immunology, and Infection*, vol. 52, no. 1, pp. 35–44, 2019 Feb.

[11] M. Á Meléndez-Carmona, I. Muñoz-Gallego, E. Viedma, J. Lora-Tamayo, and F. Chaves, "Intraosteoblastic activity of levofloxacin and rifampin alone and in combination against clinical isolates of meticillin-susceptible *Staphylococcus aureus* causing prosthetic joint infection," *International Journal of Antimicrobial Agents*, vol. 54, no. 3, pp. 356–360, 2019 Sep.

[12] N. Asseray, C. Bourigault, D. Boutoille et al., "Levofloxacin at the usual dosage to treat bone and joint infections: a cohort analysis," *International Journal of Antimicrobial Agents*, vol. 47, no. 6, pp. 478–481, 2016 Jun.

[13] E. Tornero, L. Morata, J. C. Martínez-Pastor et al., "Importance of selection and duration of antibiotic regimen in prosthetic joint infections treated with debridement and implant retention," *Journal of Antimicrobial Chemotherapy*, vol. 71, no. 5, pp. 1395–1401, 2016 May.

[14] J. Lora-Tamayo, G. Euba, J. Cobo et al., "Short- versus long-duration levofloxacin plus rifampicin for acute staphylococcal prosthetic joint infection managed with implant retention: a randomised clinical trial," *International Journal of Antimicrobial Agents*, vol. 48, no. 3, pp. 310–316, 2016 Sep.

[15] A. Bernard, G. Kermarrec, P. Parize et al., "Dramatic reduction of clindamycin serum concentration in staphylococcal osteoarticular infection patients treated with the oral clindamycin-rifampicin combination," *Journal of Infection*, vol. 71, no. 2, pp. 200–206, 2015 Aug.

[16] T. Yoda, E. Sakai, K. Harada, M. Mori, I. Sakamoto, and S. Enomoto, "A randomized prospective study of oral versus intravenous antibiotic prophylaxis against postoperative infection after sagittal split ramus osteotomy of the mandible," *Chemotherapy*, vol. 46, no. 6, pp. 438–444, 2000 Nov-Dec.

Hindawi
Emergency Medicine International
Volume 2023, Article ID 9805374, 1 page
https://doi.org/10.1155/2023/9805374

Retraction

Retracted: Risk Factors of Catheter-Related Infection in Unplanned Extubation of Totally Implantable Venous-Accessportsin Tumor Patients

Emergency Medicine International

Received 28 November 2023; Accepted 28 November 2023; Published 29 November 2023

This article has been retracted by Hindawi, as publisher, following an investigation undertaken by the publisher [1]. This investigation has uncovered evidence of systematic manipulation of the publication and peer-review process. We cannot, therefore, vouch for the reliability or integrity of this article.

Please note that this notice is intended solely to alert readers that the peer-review process of this article has been compromised.

Wiley and Hindawi regret that the usual quality checks did not identify these issues before publication and have since put additional measures in place to safeguard research integrity.

We wish to credit our Research Integrity and Research Publishing teams and anonymous and named external researchers and research integrity experts for contributing to this investigation.

The corresponding author, as the representative of all authors, has been given the opportunity to register their agreement or disagreement to this retraction. We have kept a record of any response received.

References

[1] M. Xu, L. Deng, Y. Zhu et al., "Risk Factors of Catheter-Related Infection in Unplanned Extubation of Totally Implantable Venous-Accessportsin Tumor Patients," *Emergency Medicine International*, vol. 2022, Article ID 4235316, 7 pages, 2022.

Hindawi
Emergency Medicine International
Volume 2022, Article ID 4235316, 7 pages
https://doi.org/10.1155/2022/4235316

Research Article

Risk Factors of Catheter-Related Infection in Unplanned Extubation of Totally Implantable Venous-Accessportsin Tumor Patients

Min Xu,[1] Lie Deng,[1] Yanyi Zhu,[2] Yuanfang Li,[3] Fan Wang,[3] Hui Li,[3] and Ying Zhou[3]

[1]*Breast Surgery Affiliated Cancer Hospital, Institute of Guangzhou Medical University, Guangzhou 510000, China*
[2]*Radiotherapy Area 5, Affiliated Cancer Hospital, Institute of Guangzhou Medical University, Guangzhou 510000, China*
[3]*Nursing Department Affiliated Cancer Hospital, Institute of Guangzhou Medical University, Guangzhou 510000, China*

Correspondence should be addressed to Ying Zhou; zh_ying2021@163.com

Received 10 August 2022; Revised 8 September 2022; Accepted 17 September 2022; Published 27 September 2022

Academic Editor: Hang Chen

Background. Totally implantable intravenous ports (TIVAPs) are mostly used for long-term intravenous infusion therapy in cancer patients and can be left in the body for long periods of time for easy management, making them a simple and safe infusion device. Although the risks associated with long-term retention of fully implantable IV ports are less than those associated with other intravenous catheters, various complications may still occur at the time of implantation or during long-term use. *Purpose*. To provide a scientific basis for clinical reduction of implantable intravenous port-associated infection complications by studying the risk factors for catheter-associated infection complications in patients applying implantable intravenous ports. *Methods*. A retrospective study was conducted on oncology patients treated with TIVAP at our hospital between January 2017 and November 2021, with a review of patients who were unplanned for extubation. Their demographic data, underlying disease status, and surgery-related data were counted to summarize and analyze the complications and related influencing factors of implantation and postimplantation. *Results*. A total of 70 individuals with a mean age of 56.49 ± 12.19 years were included in the study. Among them, 39 were male and 64 had the highest percentage of epithelial tumors, followed by tumors of the lymphopoiesis system and mesenchymal tumors with 4 and 2 cases, respectively. Forty-eight of these patients did not have their ports removed as planned due to the occurrence of catheter-related hematogenous infections. In univariate analysis, BMI and neutropenia were risk factors for catheter-associated infections. In the multivariate analysis, BMI (OR = 1.38, 95% CI: 1.07–1.78, $p = 0.013$) was an independent risk factor for catheter-associated infections. *Conclusions*. The overall complication rate of fully implanted intravenous ports was high, but most complications improved with symptomatic management, and no deaths due to port complications were identified. Infection was the most common complication, with catheter-associated bloodstream infection being the most common cause of unplanned port extraction. Patients with a higher BMI were at high risk of developing implantable IV port-associated infections, which may be an independent risk factor for implantable IV port-associated infections.

1. Introduction

According to the data released by China's tumor registry in 2012, the incidence and mortality of tumors in China have been increasing at an accelerated rate, with about 3.5 million new cancer cases and 2.5 million deaths due to cancer each year [1, 2]. Malignant tumors not only seriously threaten the life safety of patients but also bring a heavy economic burden and great psychological pressure to patients' families, while the long treatment period of malignant tumors and the frequent need for repeated chemotherapy bring serious inconvenience and disturbance to patients' life. Patients with malignant tumors, especially those with advanced malignant tumors, need to rely on intravenous supply for various therapeutic drugs and nutrition, and repeated venipuncture can bring a series of side effects such as damage to the venous wall; meanwhile, chemotherapy drugs and hypertonic drugs can easily cause phlebitis, and if the operation is not proper,

once the chemotherapy drugs leak out, it may cause local tissue necrosis and increase patients' pain. Therefore, it is especially important to establish a long-term, safe, and convenient infusion channel.

Since its clinical application, intravenous catheterization has shown its advantages in several ways, especially in obese, edematous, and cachectic patients, and in patients where superficial veins are difficult to find, it is extremely important to establish reliable deep venous access. Most of the central venous catheters terminate at the junction of the superior vena cava and right atrium, thus, during drug infusion, irritating drugs such as hypertonic drugs and chemotherapeutic drugs can be rapidly diluted by a high flow rate and high flow of blood, rapidly reducing the damage of irritating drugs to the vessel wall. When intravenous cannulation is applied to tumor patients as the route of infusion of irritant drugs and chemotherapy drugs, it obviously solves the damage of irritant drugs and chemotherapy drugs to peripheral veins and at the same time provides a good way for patients' treatment. There are 3 major types of central venous catheter placement techniques commonly used in clinical practice, namely: central venous catheter (CVC), peripherally inserted central catheter (PICC), and implantable venous access port (IVAP). [3, 4]. The disadvantages of peripherally inserted central catheters and IVAPs have been reported in the literature because a portion of the catheter interface is exposed to the body surface, increasing the risk of catheter-related infections and interfering with patients' daily activities [5, 6].

The implantable intravenous port, also known as the implantable central venous port access system (CVPAS), is a deep vein placement technique, the most important feature of which is that it can be implanted subcutaneously for long-term retention in the body [7]. It establishes an ideal long-term intravenous access, consisting of an injection seat for puncture and an intravenous catheter system, suitable for infusion of chemotherapy drugs, hypertonic drugs, parenteral nutrition fluids, and blood products, as well as for blood sample collection, among others. IV access is established by simply puncturing the noninvasive needle vertically through the base of the infusion port, which reduces the pain caused to the patient by repeated punctures of the peripheral veins while protecting the vessels. Since its first application by Chang et al. in 1983 [8], it has been gradually promoted for its convenience of portability, simplicity of daily care, low maintenance cost, reduction of the number of punctured vessels, improvement of patients' quality of life, and long service life, and is adapted to patients requiring long-term, repeated intravenous infusion therapy and chemotherapy. In China, the implantable intravenous infusion port technology was introduced in 1988 and was first reported in 1998 [9], and with the promotion of the use of the IVAP technology and the growth of patient demand, this technology was gradually accepted and applied in many hospitals in China. The occurrence of IVAP-related complications not only prolongs patients' hospital stays and shortens the use of infusion ports, but also increases the economic burden on patients. Therefore, it is important to understand and be familiar with IVAP-related complications in order to prevent, detect, and manage them in a timely manner.

Complications of IVAP are classified as early and late complications. Early complications refer to complications that occur during the period from intraoperative or postimplantation to the first use of the implantable IVAP, which mainly include vascular and nerve injury, hematoma formation, hemothorax, hemopneumothorax, air embolism, pericardial tamponade, arrhythmia, etc.; late complications refer to complications that occur after the first use of the implantable IVAP, which mainly include catheter-related infections, thrombosis, catheter occlusion, and cardiac arrhythmia. It mainly includes catheter-related infections, thrombosis, catheter occlusion, drug extravasation, catheter displacement or fracture, catheter entrapment syndrome, superior vena cava ulceration or perforation, and infusion seat overturning [10, 11], and catheter-related infections are the most common among them. Studies [12, 13] reported that 46.2% of patients who had their infusion port removed during use did so because of catheter-associated infections, a rate much higher than complications such as thrombosis or other dysfunctions. According to relevant data, despite the fact that infusion ports reduce the chance of bacterial infection, 3–10% of infusion ports are removed once complications of infusion port-associated infections occur [14]. A study [15] analyzed complications associated with IVAP treatment and found that IVAP-associated bacteremia was the most expensive to treat. Risk factors for IVAP complications have been reported differently in the literature and include operative technique, patient age, gender, choice of puncture route, type of tumor (parenchymal organ tumor, hematologic tumor), the patient's own physical condition, type of chemotherapeutic agent, and IVAP-related care. It has been reported in the literature [16] that malignant hematologic disease is the most significant risk factor for catheter-associated infections. Studies [17] have found that catheter-associated infections are common in young patients with the malignant hematologic disease, and it has been hypothesized that this may be due to intense chemotherapy and neutropenia. In contrast, other literature in recent years has reported a lower rate of infection in outpatients using IVAP. In this study, we analyzed which factors increase the occurrence of infectious complications in patients with IVAP to provide some valid and scientific references for reducing the incidence of IVAP infections in future clinical work.

2. Methods

2.1. Participants. A retrospective survey was conducted of patients who received TIVAP for cancer at our institution between January 2017 and November 2021 and patients who were unplanned for extubation. Approval was obtained from our hospital ethics committee, and informed consent was obtained from each patient.

Inclusion criteria: ① patients with a preliminary clinical diagnosis of malignancy by cytology, histopathology, or bone marrow pathology, or preoperatively by imaging and relevant tumor indicators, and who were clearly diagnosed by pathology after surgery, and who underwent IVAP placement and maintenance in our hospital; ② patients who

required long-term and repeated infusion therapy; ③ patients with IVAP implanted through the subclavian and internal jugular veins.

Exclusion criteria: ① combined systemic infection; ② uncontrolled infection in the tissue surrounding the IVAP implantation site; ③ abnormal coagulation function (PLT < 50/nl, PT < 50%, or INR > 1.5); ④ history of acute thrombosis and occlusion of the subclavian and superior vena cava.

2.2. Data Collection. The collected data included demographic information (age, sex, BMI, education, smoking, alcohol, surgical history, history of central vein catheterization, comorbidities, medication history, and tumor type), laboratory reports (erythrocytes, leukocytes, platelets, C-reactive, international normalized ratio (INR), activated partial thromboplastin time (APTT), D-Dimer, and neutrophils), and TIVAP-related information (operation duration, postoperative infusion port interval, secondary adjustment of the infusion port position, implantation method, catheter placement site, conduit material, infection occurred ten days after catheterization, iatrogenic skin injury, missing extraction of the infusion needle, irregular catheter care, home catheter, surgery during indwelling TIVAP, radiotherapy at the indwelling site, and catheter retention time). In the present study, the first outcome was TIVAP-related infection. TIVAP-related infection was defined as documented bacteremia and colonization of the catheter tip with the same microorganisms (significant microbial growth), signs of infection (fever, chills, and/or hypotension), and no obvious source of bacteremia other than the catheter [16]. Tumor types are classified as epithelial tumors, lymphopoietic system tumors, and mesenchymal tumors.

2.3. TIVAP Procedure. All TIVAP procedures are performed by the surgeon under local anesthesia in the operating room under sterile conditions. The surgical access can be through the subclavian or internal jugular veins on both sides or arm veins on both sides, depending on the patient's vascularity at the puncture site, skin condition, and treatment modality. Internal jugular vein implantation is used as an example. The patient is placed in a supine position with the head tilted back and turned to the opposite side. After routine anesthesia and disinfection, the puncture site is determined, the puncture is performed under ultrasound guidance, and blood is drawn back to determine whether the puncture was successful. After a successful puncture, a guide wire is introduced in the direction of the puncture needle, and the skin and subcutaneous tissue are dilated using a skin dilator, after which a catheter is introduced, a capsule bag is bluntly separated, an infusion port holder is implanted in the capsule bag, the catheter is connected to the syringe, and a noninvasive butterfly needle is used. The injection seat was punctured, and the infusion port and catheter were then checked for patency with sodium heparin saline. Finally, the skin was sutured. After the puncture was completed, the chest X-ray was determined to be free of twisting and knotting of the catheter before use.

2.4. Catheter Care. Maintenance care of the CVC was performed by experienced nurses according to Infusion Nursing Standards of Practice, including daily inspection of the skin around the port of infusion for pressure, swelling, hematoma, and infection. The use of 10–20 ml of saline to flush the tube at the beginning and end of the infusion and every 4 h during continuous infusion or between infusions of two drugs with contraindications. At the same time, 3–5 ml of heparin-saline solution at a concentration of 100 μ/mL is used to seal the tube under positive pressure at the end of the infusion and after the flush. If the tube is not used for a long time, the CVC will be maintained every 4 weeks, including the flush and seal.

2.5. Statistical Analysis. For baseline characteristics, variables were expressed as mean ± standard deviation (SD) or proportions. Differences in baseline characteristics between the catheter-associated infection group and other reason groups were assessed using Student's *t*-tests, the chi-square test for continuous variables, and Fisher's exact test for categorical variables. Risk factors associated with catheter-associated infections were analyzed univariately using logistic regression analysis, and those with p values < 0.10 were included in multivariate analysis. The results were expressed as the ratio (OR), with a ratio of 95%.

3. Results

3.1. Patient Characteristics. A retrospective study of oncology patients treated with TIVAP in our hospital between January 2017 and November 2021 and unplanned extubation was conducted. Their demographic data, underlying disease status, and procedure-related data were counted to summarize and analyze implantation and postimplantation complications and related influencing factors. A total of 70 individuals, with a mean age of 56.49 ± 12.19 years, were finally included in the study. Among them, 39 were male and 64 had the highest percentage of epithelial tumors, followed by tumors of the lymphopoietic system and mesenchymal tumors with 4 and 2 cases, respectively. Forty-eight of these patients did not have their ports removed as planned due to the occurrence of catheter-related hematogenous infections. Forty-eight of these patients had unscheduled port removal due to the occurrence of catheter-associated hematogenous infection, 12 were removed due to catheter obstruction or thrombosis formation, 6 were removed due to port exposure and extravasation, and 4 were removed due to puncture port infection. Catheter-associated bloodstream infections occurred in 48 patients, 23 of whom were male, aged 30–90 years, with a procedure length of 0.5–1.5 hours, a mean catheter retention time of 245.08 ± 418.50 days, and catheter use of mostly 3–7 days per month (Table 1).

3.2. Comparison between Catheter-Associated Infections Group and Other Reason Group. The clinical presentation of catheter-associated bloodstream infections often includes chills, fever, chills, or erythema, swelling, and pain at the site of catheter placement, nodules, and/or pus exudation.

Table 1: Univariate analysis of catheter blood flow infection leading to infusion portpullout.

Characteristics	Catheter-associated infections ($n = 48$)	Other reason ($n = 22$)	p
Age (years)	57.65 ± 11.58	53.95 ± 13.36	0.242[a]
Male	23 (47.9%)	16 (72.7%)	0.052[b]
BMI (kg/m^2)	23.55 ± 3.41	21.74 ± 2.85	**0.034**
Bi index (points)	96.04 ± 15.16	97.27 ± 11.72	0.737
Educational level	—	—	0.454
Primary school and below	18 (37.5%)	5 (22.7%)	—
Middle school	24 (50.0%)	13 (59.1%)	—
University and above	6 (12.5%)	4 (18.2%)	—
Tumor classification	—	—	0.808[b]
Epithelial tumor	20 (90.9%)	44 (91.7%)	—
Lymphohematopoietic system tumor	1 (4.5%)	3 (6.3%)	—
Mesenchymal tumor	1 (4.5%)	1 (2.1%)	—
Surgical history	13 (27.1%)	5 (22.7%)	0.699
Smoking history	16 (33.3%)	8 (36.4%)	0.804
History of central venous catheterization	4 (8.3%)	0 (0%)	0.401
Anticoagulant drug use history	4 (8.3%)	0 (0%)	0.401
Hypertension	13 (27.1%)	2 (9.1%)	0.089
Diabetes	9 (18.8%)	2 (9.1%)	0.303
Erythrocyte abnormality	16 (33.3%)	5 (22.7%)	0.369
Leukocyte abnormality	13 (27.1%)	2 (9.1%)	0.089
Platelet abnormality	13 (27.1%)	3 (13.6%)	0.214
Abnormal C-reactive protein	22 (45.8%)	9 (40.9%)	0.700
INR abnormality	7 (14.6%)	5 (22.7%)	0.401
APTT abnormality	14 (29.2%)	2 (9.1%)	0.063
D-dimer abnormality	15 (31.3%)	11 (50%)	0.132
Neutropenia	22 (45.8%)	4 (18.2%)	**0.026**
Operation duration (h)	0.89 ± 0.27	0.85 ± 0.27	0.616
Postoperative infusion port interval		—	0.916
<24°h	41 (85.4%)	19 (86.4%)	—
≥24°h	7 (14.6%)	3 (13.6%)	—
Secondary adjustment of infusion port position	1 (2.1%)	1 (4.5%)	0.566
Implantation method	—	—	0.329
Ultrasonic guidance	14 (29.2%)	4 (18.2%)	—
Blind puncture	34 (70.8%)	18 (81.8%)	—
Catheter placement site	—	—	0.584
Internal jugular vein	18 (37.5%)	8 (36.4%)	—
Subclavian vein	27 (56.3%)	11 (50.0%)	—
Vein of arm	3 (6.3%)	3 (13.6%)	—
Conduit material	—	—	0.566
Polyurethane	47 (97.9%)	21 (95.5%)	—
Silica gel	1 (2.1%)	1 (4.5%)	—
Infection occurred ten days after catheterization	1 (2.1%)	3 (13.6%)	**0.053**
Iatrogenic skin injury	4 (8.3%)	4 (18.2%)	0.229
Missing extraction of infusion needle	2 (4.2%)	0 (0%)	0.331
Irregular catheter care	7 (14.6%)	2 (9.1%)	0.524
Home catheter maintenance	6 (12.5%)	2 (9.1%)	0.677
Surgery during indwelling TIVAP	4 (8.3%)	2 (9.1%)	0.916
Radiotherapy at the indwelling site	6 (12.5%)	2 (9.1%)	0.677
Catheter retention time (days)	245.08 ± 418.50	127.18 ± 87.70	0.068

[a]ANOVA; [b]chi square test.

Because of the lack of specificity and sensitivity, the diagnosis of CRBSI should not be based solely on this basis, and care should be taken to distinguish between catheter-associated bloodstream infections that originate from the catheter and those that arise from other sites because some catheter-associated bloodstream infections are secondary to surgical incisional infections, nosocomial pneumonia, gastrointestinal infections, and urinary tract infections. Therefore, catheter-associated bloodstream infections are only considered to be bloodstream infections caused by catheter infections and can exclude other sources. Also, the culture of the head end of the catheter is the same pathogenic organism as the blood culture, but it is difficult to distinguish between the two in the current clinical practice. In addition, some studies have shown that local inflammatory manifestations are uncommon in the presence of catheter-

Table 2: Analysis of influencing factors for catheter-related blood source infection.

Variable	*B*	*S.E.* (*B*)	Wald	*p*	OR (95%CI)
BMI	0.321	0.129	6.235	**0.013**	1.38 (1.07–1.78)
Catheter retention time (days)	0.001	0.002	0.340	0.560	1.00 (0.99–1.01)
Female	1.175	0.828	2.011	0.156	3.24 (0.64–16.42)
Hypertension	1.619	0.935	3.001	0.083	5.05 (0.81–31.55)
Neutropenia	1.663	0.920	3.263	0.071	5.27 (0.87–32.04)
Infection occurred ten days after catheterization	−3.872	2.024	3.659	**0.056**	0.02 (0–1.10)
Abnormal leukocyte level	1.742	1.282	1.846	0.174	5.71 (0.46–70.48)
APTT level abnormality	1.464	1.311	1.248	0.264	4.32 (0.33–56.42)

associated infections, with Gram-positive bacteria being the main pathogenic organism in CRBSI, and it is rare for this organism to cause local or systemic signs of infection. CRBSI should be considered to be caused by an *aureus* or Gram-negative bacillus infection if there is a clear manifestation of inflammation at the placement site along with fever, chills, or obvious clinical signs of systemic infection [18]. In the absence of laboratory results, in patients with clinical manifestations of bloodstream infection such as chills and fever, if the body temperature returns to normal after removal of the suspected catheter, it can only be used as indirect evidence of catheter-associated infection but not definitively as CRBSI. Therefore, when a catheter-associated infection is suspected, catheter specimen culture and blood culture results should be obtained to further clarify the diagnosis.

There were no significant differences between the catheter-associated infections group and the other reason group in terms of age, sex, educational level, tumor classification, surgical history, smoking history, history of central venous catheterization, anticoagulant drug use history, hypertension, diabetes, erythrocyte abnormality, leukocyte abnormality, platelet abnormality, abnormal C-reactive protein, INR abnormality, APTT abnormality, D-Dimer abnormality, operation duration, postoperative infusion port interval, secondary adjustment of infusion port position, implantation method, catheter placement site, conduit material, infection occurred ten days during catheterization, Iatrogenic skin injury, missing extraction of infusion needle, irregular catheter care, home catheter maintenance, surgery during indwelling TIVAP, radiotherapy at the indwelling site, and catheter retention time. Patients with the catheter-associated infections group had a higher BMI (23.55 ± 3.41 vs. 21.74 ± 2.85, $p = 0.034$), and a higher rate of neutropenia (45.8% vs. 18.2%, $p = 0.026$) than the other reason group (Table 1).

3.3. Risk Factors. The risk factors for catheter-related infection in unplanned extubation of totally implantable venous-access ports in tumor patients were reported in Tables 1 and 2. According to the univariable analysis, BMI and neutropenia were risk factors for catheter-related infection. According to the multivariable analysis, BMI (OR = 1.38,95%CI:1.07–1.78, $p = 0.013$) was an independent risk factor for catheter-related infection (Table 2).

4. Discussion

The purpose of treatment of advanced malignant tumors is usually to reduce 'patients' pain, prolong 'patients' survival, and improve patients' quality of life. Intravenous chemotherapy and nutritional support are one of the important means for the clinical treatment of advanced malignant tumors, and because of long-term repeated infusions of chemotherapy drugs and multiple punctures, patients' extravasation of chemotherapy drugs leads to an increased incidence of peripheral local tissue necrosis and peripheral phlebitis, which seriously affects the treatment of patients and aggravates their pain. The implantable intravenous infusion port began to be used for clinical intravenous infusion in the 1980s [19], and IVAP technology has been successfully applied in recent years for postoperative chemotherapy of malignant tumors such as lung cancer, breast cancer, and cervical cancer and for patients who repeatedly require intravenous infusion multiple times and have difficulty in peripheral infusion, all of which have achieved outstanding results [20]. Implantable intravenous ports have been compared with external infusion devices in much literature, and the conclusions reached are that implantable intravenous ports are relatively less risky. Studies [21] have shown that implantable intravenous ports are better than PICCs in reducing the occurrence of infections in patients with hematologic malignancies, not only by greatly reducing the number of punctured veins but also by smoothly delivering drugs directly to the central vein. Also, it can not only greatly reduce the number of punctured veins, but also smoothly deliver drugs to the central vein, greatly reduce the damage of chemotherapy drugs and hypertonic drugs to peripheral veins, and reduce the occurrence of phlebitis. Studies in the literature [22] have shown that the IVAP technique, as one of the permanent intravenous infusion routes for oncology patients, shows a reduced incidence of infection compared with other infusion techniques and improves the quality of life in patients with malignant tumors.

The TIVAP consists of two parts: an internal catheter and an infusion seat, including a subcutaneous implant port (or reservoir) connected to a central venous catheter, most often inserted into the internal jugular, subclavian, or cephalic veins. As the preferred intravenous access for oncology chemotherapy patients, TIVAP not only reduces the pain associated with repeated punctures but also avoids damage to the peripheral vasculature from highly

concentrated and highly irritating chemotherapeutic agents. Also, because the TIVAP load is buried in the body, it has little impact on the patient's image and normal life, resulting in greater patient acceptance and satisfaction. However, factors affecting unplanned TIVAP removal, such as catheter-associated infections, remain a current concern. Therefore, it remains important to explore the risk factors for catheter-associated infections and to investigate how to prevent them. In this study, based on the unplanned extraction population, 48 patients developed catheter-associated bloodstream infections, and the rate of catheter-associated infections was 67.6%, which was much higher than in other studies. The rate of neutropenia in patients in the catheter-associated infection group (45.8% vs. 18.2%, $p = 0.026$) was higher than in the other causes group, similar to previous studies that reported that cancer patients are more susceptible to bacterial infections due to immunocompromise [23]. Interestingly, we calculated the interval between postoperative TIVAP use and found no difference in catheter-associated infections caused by TIVAP use within 24 hours versus 24 hours later, implying that delayed postoperative TIVAP use does not increase the incidence of catheter-associated infections. This has some guiding value for the use of clinical TIVAP but, of course, still requires subsequent confirmation with a larger sample size. In addition, we found that BMI was an independent risk factor for catheter-associated infections by multifactor regression analysis. This suggests that the more obese people are, the higher the incidence of catheter-associated infections. This may be because the accumulation of adipocytes promotes inflammation and alters hormonal secretion patterns, and these changes tend to alter the immune system, making obese individuals more susceptible to bacterial infections. In addition, BMI as a risk factor for infection has been demonstrated in other studies [24]. Although BMI cannot be changed to a great extent during hospitalization, early prevention in patients with a higher BMI is of greater clinical importance.

Before considering how to prevent TIVAP catheter-associated infections, it is important to understand the mechanisms of bacterial infection. First, the lack of proper disinfection procedures during TIVAP catheter implantation allows microorganisms to migrate along the catheter surface and is a major cause of catheter-associated infections. Second, inappropriate disinfection measures during TIVAP maintenance can also lead to bacterial infections. In addition, intraluminal infections caused by microbial migration into the catheter lumen are a common route of infection. Another possible but uncommon cause is distant blood-borne bacterial infections. Therefore, prevention of TIVAP catheter-associated infections should begin with insertion, which should be performed with strict sterilization guidelines. In addition, real-time ultrasound-guided intravenous cannulation and proper skin preparation are key to preventing catheter-associated infections. In addition, strict asepsis should be implemented during dressing changes and maintenance. Numerous studies have shown that the use of chlorhexidine gluconate with alcohol disinfection is effective in reducing the rate of catheter microbial colonization [25]. In addition, the skin around the TIVAP should be carefully assessed daily for signs of infection, such as pressure pain and swelling. More importantly, enhanced psychological care and related health education for patients also play an important role in the prevention of TIVAP catheter-associated infections, and we believe that good prevention can effectively reduce the incidence of TIVAP catheter-associated infections.

There are some limitations to this study. First, this study is a single-center retrospective study. Secondly, the sample size of this study was small. However, this study concludes that BMI is an independent risk factor for TIVAP catheter-associated infections and is the first one reported to date, which has some guiding value for clinical practice. This can be validated in subsequent studies using a large sample of data.

5. Conclusion

The overall complication rate of fully implanted intravenous ports was high, but most of the complications improved with symptomatic management, and no deaths due to port complications were identified. Infection was the most common complication, with catheter-associated bloodstream infection being the most common cause of unplanned port extraction. BMI (OR = 1.38, 95% CI: 1.07 to 1.78, $p = 0.013$) was an independent risk factor for catheter-associated infection. In patients with a higher BMI, we should enhance care to prevent the development of catheter-associated infections.

Data Availability

The experimental data used to support the findings of this study are available from the corresponding author upon request.

Conflicts of Interest

The authors declare that they have no conflicts of interest.

Authors' Contributions

Min Xu, Lie Deng, and Yanyi Zhu, all three authors, have contributed equally to this work.

References

[1] G. Wei, Y. Wang, G. Yang, Y. Wang, and R. Ju, "Recent progress in nanomedicine for enhanced cancer chemotherapy," *Theranostics*, vol. 11, no. 13, pp. 6370–6392, 2021.

[2] D. Lebeaux, N. Fernández-Hidalgo, A. Chauhan et al., "Management of infections related to totally implantable venous-access ports: challenges and perspectives," *The Lancet Infectious Diseases*, vol. 14, no. 2, pp. 146–159, 2014.

[3] C. C. T. Hsu, G. N. C. Kwan, H. Evans-Barns, J. A. Rophael, and M. L. van Driel, "Venous cutdown versus the seldinger technique for placement of totally implantable venous access ports," *Cochrane Database of Systematic Reviews*, vol. 2016, no. 8, Article ID Cd008942, 2016.

Hindawi
Emergency Medicine International
Volume 2023, Article ID 9826874, 1 page
https://doi.org/10.1155/2023/9826874

Retraction

Retracted: Total Thoracoscopic versus Robotic Surgery for Repair of Atrial Septum Defect: A Propensity Matching Score Analysis

Emergency Medicine International

Received 28 November 2023; Accepted 28 November 2023; Published 29 November 2023

This article has been retracted by Hindawi, as publisher, following an investigation undertaken by the publisher [1]. This investigation has uncovered evidence of systematic manipulation of the publication and peer-review process. We cannot, therefore, vouch for the reliability or integrity of this article.

Please note that this notice is intended solely to alert readers that the peer-review process of this article has been compromised.

Wiley and Hindawi regret that the usual quality checks did not identify these issues before publication and have since put additional measures in place to safeguard research integrity.

We wish to credit our Research Integrity and Research Publishing teams and anonymous and named external researchers and research integrity experts for contributing to this investigation.

The corresponding author, as the representative of all authors, has been given the opportunity to register their agreement or disagreement to this retraction. We have kept a record of any response received.

References

[1] Y. Liu, Z. Liu, X. Li et al., "Total Thoracoscopic versus Robotic Surgery for Repair of Atrial Septum Defect: A Propensity Matching Score Analysis," *Emergency Medicine International*, vol. 2022, Article ID 5371493, 6 pages, 2022.

Hindawi
Emergency Medicine International
Volume 2022, Article ID 5371493, 6 pages
https://doi.org/10.1155/2022/5371493

Research Article

Total Thoracoscopic versus Robotic Surgery for Repair of Atrial Septum Defect: A Propensity Matching Score Analysis

Yanyi Liu,[1] **Zhuang Liu**,[1] **Xin Li**,[1] **Ning Li**,[1] **Ruirui Kong**,[1] **Yiyao Jiang**,[2] **Shenglin Ge**,[1] **and Chengxin Zhang**[1]

[1]*Department of Cardiac Surgery, The First Affiliated Hospital of Anhui Medical University, Hefei 230022, Anhui, China*
[2]*Department of Cardiac Surgery, The First Affiliated Hospital of Bengbu Medical College, Bengbu 233000, Anhui, China*

Correspondence should be addressed to Shenglin Ge; ahydgsl@163.com and Chengxin Zhang; zcxayfy@126.com

Received 2 August 2022; Revised 28 August 2022; Accepted 2 September 2022; Published 23 September 2022

Academic Editor: Hang Chen

Robotic surgery can provide less surgical trauma than conventional surgery, but differences between robotic and thoracoscopic surgery for atrial septal defect (ASD) repair are not well documented. To explore whether ASD can be repaired by thoracoscopic surgery or robotic surgery, which procedure is less invasive, and the difference in outcomes between these two procedures, this article studies 160 patients undergoing ASD repair at our institution. Sixty-five patients underwent total thoracoscopic surgery and 95 patients underwent total endoscopic robotic surgery. Propensity score matching yielded 64 well-matched patient pairs. Surgical data and early postoperative outcomes between the two matched groups were analyzed and compared. The results show that thoracoscopic and robotic surgery to repair ASD are both safe and reliable, and the early curative effect is good. However, regardless of similar complication rates, robotic surgery has a shorter time, less postoperative drainage, and faster recovery than thoracoscopic surgery.

1. Introduction

Atrial septal defect (ASD) is the most common congenital heart disease (CHD) of adulthood [1], accounting for about 30–40% of adult CHD [2, 3]. The 2008 ACC/AHA and 2010 ESC guidelines for the management of adult CHD recommended that atrial septal defect repair should be performed either surgically or percutaneously if right atrial and ventricular enlargement occur, regardless of symptoms [4, 5]. Compared to conventional sternotomy, minimally invasive cardiac surgeries for closure of ASD have been proven to be safe and effective with less surgical trauma and faster recovery [3, 6, 7]. The last five years have seen a dramatic growth in the adoption of thoracoscopic and robotic technology, with the publication of several large series showing satisfactory early outcomes [8–10]. Some studies have reported the similar early outcomes when comparing thoracoscopic surgeries with open surgeries [7, 11]. However, research comparing total thoracoscopic ASD closure with totally endoscopic robotic surgery is relatively scarce. Therefore, in this study, we sought to compare the outcomes of ASD patients treated with total thoracoscopic surgeries and totally endoscopic robotic surgeries.

Conventional ASD repair via median sternotomy has been recognized as the standard approach with low morbidity and mortality since the 1950s [11]. However, conventional surgeries have the shortcomings of large incision, unaesthetic scar, and damaging the integrity of the sternum [12]. With the advancement of minimally invasive technology, total thoracoscopic ASD repair is being performed increasingly over the past decade, owing to its advantages in minimizing surgical trauma [13]. Ma reported 96 cases of total thoracoscopic ASD repair without robotic assistance and concluded that the procedure was associated with faster recovery and superior quality of life compared to conventional surgeries [14]. Robotic surgery system was first used in cardiac surgery in the late 1990s [8]. Since then, the safety and efficacy of robotic surgeries have also been demonstrated by many studies [6], with a mean 30-day mortality of 0.7% (0%–0.8%) reported by Doulamis et al. in 2019 [15].

Robotic surgeries have gradually become another effective alternative to conventional sternotomy. Thus far, only a few reports comparing robotic surgery to thoracoscopy for mitral disease have been published [16, 17]. However, for ASD repair, the comparison between the two techniques has rarely been reported. In this study, to minimize the selection bias, we closely matched patients' baseline characteristics between the two groups using the propensity-score matching method. To the best of our knowledge, this study is the first of its kind reported in the literature.

2. Materials and Methods

2.1. Patient Selection. A retrospective analysis was performed for 160 patients undergoing closure of secundum-type ASD through minimally invasive approach from November 2015 to January 2022. The average age of patients was 38.62 ± 15.58 years (range: 7–73 years). Of the 160 patients, 105 were female and 55 were male. Patients' baseline characteristics were listed in Table 1. The preoperative diagnosis, including size, anatomic type of the ASD, and some other associated anomalies were confirmed by transthoracic echocardiography (TTE). The selection criteria for both robotic and thoracoscopic surgeries were listed as follows: (1) confirmed secundum ASD with left-to-right shunt in the atrial level, age >5 years, body weight ≥15 kg; (2) without severe valvular, aortic, or congenital heart diseases that require concomitant repair; (3) without severe coronary artery disease requiring concomitant CABG; (4) without conditions unsuitable for endoscopic visualization (history of right thoracotomy, severe pleural adhesion, severe pericarditis, deformities of the thorax, and morbid obesity); (5) without severe asthma, emphysema, or COPD; (6) without severe peripheral vascular disease which may restricts femoral cannulation; and (7) without significant hepatic compromise, dialysis dependent renal failure, untreated cerebrovascular disease, and severe bleeding disorder.

2.2. Anesthesia and Position. After successful induction of general anesthesia, all the patients received double lumen tube intubation for left single-lung ventilation. A transesophageal echocardiography (TEE) probe was routinely placed to confirm the diagnosis of ASD and examine the repair quality intraoperatively. Patients were maintained at supine position with right hemithorax elevated to 20°–30°.

2.3. Robotic Surgery. After systemic heparinization, the right internal jugular vein was cannulated percutaneously (14–16F, Kangxin Medical, China) for superior vena cava drainage under the guidance of TEE. The right femoral artery was surgically cannulated for arterial return (14–20F, Kangxin Medical, China) and inferior vena cava drainage was from the femoral vein (16–24F, Kangxin Medical, China). After the initiation of left single-lung ventilation, a 3–4 cm thoracotomy was made through the fourth intercostal space on the anterior axillary line to place a 0-degree endoscope. On the right anterior axillary line, two 8-mm endoscopic trocars were placed through the third and sixth intercostal spaces for the left and right arms of the robot, respectively. The atrial retractor arm was placed through the fifth intercostal space on the midclavicular line.

The pericardium was incised about 2 cm anteriorly to the phrenic nerve. After the initiation of cardiopulmonary bypass (CPB), superior and inferior vena cava were blocked. Ascending aorta clamping was not performed and the operation was performed on the beating heart. Depending on the size of the defect, ASD was closed by primary suturing or using a bovine pericardial patch. At the end of closing ASD, left atrial deairing was completed by holding positive pressure of the lungs to expel blood from the left atrium. The right atrium was closed using two layers of running 4–0 polypropylene suture. After the patient weaned from CPB, the effect of repairing was confirmed by TEE. A chest tube was inserted through the right arm port site following decannulation of the femoral vessels and meticulous hemostasis.

2.4. Thoracoscopic Surgery. The location of the three ports: port1 (1.5 cm) was made parasternally in the third intercostal space for entries of left-hand surgical instruments; port 2 (1.5 cm) was made in the fifth intercostal space between the midclavicular line and anterior axillary line for entries of right-hand surgical instruments; A thoracoscope was inserted through a small incision (port 3, 2 cm) in the fourth intercostal space on the right anterior axillary line. The establishment of the peripheral CPB and intrathoracic part of operation was the same as those of the robotic group.

2.5. Study Endpoints. The primary endpoint of this study was in-hospital mortality. The secondary endpoints included operation time, CPB time, ICU stay time, mechanical ventilation time, postoperative hospital stay time, postoperative drainage, total RBC usage, in-hospital complications, and 6-month MACCE. MACCE was defined as major cardiovascular and cerebrovascular events during 6-month follow-up since the day of operation, including events of death, new-onset arrhythmia, myocardial infarction, stroke, and peripheral vascular embolism.

2.6. Statistical Analysis. Quantitative variables were expressed as mean ± standard deviation if normally distributed; otherwise, as the median and 25–75 percentile. Categorical variables were expressed as frequencies and percentages. To compare the two groups before matching, we use the independent-sample T test for continuous data with normal distribution, nonparametric test (the Mann–Whitney U test) for continuous data with skewed distribution, and χ^2 analysis or Fisher's exact tests for categorical variables. After matching, continuous variables with normal distribution were compared by paired T test and continuous variables with skewed distribution by the Wilcoxon rank-sum test. Categorical variables were compared by McNemar's test between two matched groups. The survival data were analyzed using the Kaplan–Meier method and compared by the log-rank test.

Table 1: Patient baseline characteristics before propensity matching.

Characteristics	Thoracoscopic group ($N = 65$)	Robotic group ($N = 95$)	P value
Male (n (%))	23(35.4)	3233.7	0.824
Age (y, mean ± SD)	39.69 ± 14.82	37.88 ± 16.12	0.473
Weight (kg, mean ± SD)	59.33 ± 10.77	58.06 ± 10.79	0.464
Diabetes (n (%))	0(0.0)	8(8.4)	0.042
Hypertension (n (%))	5(7.7)	5(5.3)	0.771
Current smoke (n (%))	2(3.1)	5(5.3)	0.787
Congestive heart failure (n (%))	1(1.5)	6(6.3)	0.290
Atrial fibrillation (n (%))	4(6.2)	5(5.3)	1.000
Systemic embolism (n (%))	0(0.0)	0(0.0)	NA
Defect diameter (cm, mean ± SD)	2.88 ± 0.77	2.67 ± 0.89	0.128
Defect type (n (%))			0.945
Fossa ovalis type	38(58.5)	54(56.8)	
SVC type	3(4.6)	5(5.3)	
IVC type	21(32.3)	29(30.5)	
Mixed type	3(4.6)	7(7.4)	
LVEF (%, mean ± SD)	62.45 ± 4.66	61.74 ± 4.36	0.328
PASP (mmHg, mean ± SD)	51.02 ± 10.98	52.41 ± 11.82	0.452
Creatinine (μmol/L, mean ± SD)	63.69 ± 15.37	62.86 ± 11.90	0.714
With PAPVC (n (%))	2(3.1)	7(7.4)	0.419

SVC type: superior vena cava type; IVC type: inferior vena cava type; LVEF: left ventricular ejection fraction; PASP: pulmonary artery systolic pressure; and PAPVC: partial anomalous pulmonary venous connection.

The matching criteria included eleven fixed-effect variables (gender, age, weight, defect size, diabetes, hypertension, history of atrial fibrillation, history of congestive heart failure, left ventricular ejection fraction, pulmonary artery systolic pressure, and blood creatinine). Patients in the thoracoscopic group were then matched in a 1 : 1 nearest neighbour fashion to patients in the robotic group with similar propensity scores; a propensity score difference of less than 0.1 was required for each match. All statistical tests above were two sided, with significance set at $P < 0.05$. Statistical analysis was performed using SPSS Statistics, version 25.0 (IBM, Chicago, Illinois).

3. Results

Baseline characteristics of the two groups before matching were summarized in Table 1. Table 1 demonstrates the baseline characteristics of the two groups were not entirely balanced before PSM. Patients who were in the robotic group were more likely to have a higher rate of diabetes (8.4% vs. 0.0%, $P < 0.05$). During the process of PSM, 64 patients in the thoracoscopic group were successfully matched with 64 patients of the robotic group in a 1 : 1 fashion. After propensity matching, all the baseline characteristics were balanced between the two groups. Baseline characteristics after matching are summarized in Table 2.

Perioperative data for two matched groups were presented in Table 3. After propensity matching, the robotic surgery had shorter operation time ($P < 0.001$), shorter CPB time ($P < 0.001$), shorter length of ICU stay ($P = 0.001$), shorter mechanical ventilation time ($P = 0.02$), and shorter postoperative hospital stay time ($P = 0.025$). In addition, the robotic group had statistically significant less thoracic drainage ($P = 0.001$) and less total RBC usage ($P < 0.001$). The total hospital costs showed no significant difference between the groups ($P = 0.097$).

The results of in-hospital complications showed that delayed mechanical ventilation (DMV), new-onset arrhythmia, and systemic embolism were the most common postoperative complications in this study. 4 cases with early new-onset arrhythmia (<14 days) were observed in the thoracoscopic group, all of which were atrial fibrillation; whereas in the robotic group, there was 2 patients with early new-onset arrhythmia (<14 days), including 1 case of atrial fibrillation and 1 case of supraventricular tachycardia. Early systemic embolism (<14 days) includes stroke and peripheral embolism. Before discharge, two patients (3.1%) of the thoracoscopic group and one patient (1.6%) of the robotic group presented with a stroke, while two patients (3.1%) of the thoracoscopic group had peripheral arterial embolism. In addition, there was no significant difference between the two groups on in-hospital mortality, new-onset arrhythmia (<14 days), systemic embolism (<14 days), delayed mechanical ventilation, renal failure, residual shunt, reoperation for bleeding, pneumonia, and pneumothorax (Table 4).

During the 6-month follow-up after operation, 24 patients were lost, and the follow-up rate was 81.25%. 1 patient of the thoracoscopic group and 1 patient of the robotic group presented with new-onset atrial fibrillation 5 months and 4 months after operation, respectively. In addition, 1 patient of the thoracoscopic group presented with a stroke 2 months after operation, and he was rehospitalized and cured. There was no significant difference in the incidence of 6-month MACCE between the two groups (log-rank $\chi^2 = 2.822$, $P = 0.093$, Figure 1). There was no in-hospital death or follow-up death in both the matched groups, and the survival rate within 6 months were both 100%.

Table 2: Patient baseline characteristics after propensity matching.

Characteristics	Thoracoscopic group ($N = 64$)	Robotic group ($N = 64$)	P value
Male (n (%))	23(35.9)	21(32.8)	0.710
Age (y, mean ± SD)	39.64 ± 14.93	36.86 ± 15.91	0.310
Weight (kg, mean ± SD)	59.40 ± 10.84	57.91 ± 9.42	0.407
Diabetes (n (%))	0 (0.0)	0 (0.0)	NA
Hypertension (n (%))	5 (7.8)	3 (4.0)	0.715
Current smoke (n (%))	2 (3.1)	4 (6.3)	0.676
Congestive heart failure (n (%))	1 (1.6)	2 (3.1)	1.000
Atrial fibrillation (n (%))	4 (6.3)	2 (3.1)	0.676
Systemic embolism (n (%))	0 (0.0)	0 (0.0)	NA
Defect diameter (cm, mean ± SD)	2.87 ± 0.77	2.65 ± 0.80	0.111
Defect type (n (%))			0.780
Fossa ovalis type	38 (59.4)	39 (60.9)	
SVC type	3 (4.7)	4 (6.3)	
IVC type	20 (31.3)	16 (25.0)	
Mixed type	3 (4.7)	5 (7.8)	
LVEF (%, mean ± SD)	62.17 ± 4.13	62.06 ± 4.55	0.889
PASP (mmHg,mean ± SD)	50.95 ± 11.05	50.81 ± 10.82	0.942
Creatinine (μmol/L, mean ± SD)	63.92 ± 15.38	62.83 ± 11.32	0.650
With PAPVC (n (%))	2 (3.1)	5 (7.8)	0.437

SVC type: superior vena cava type; IVC type: inferior vena cava type; LVEF: left ventricular ejection fraction; PASP: pulmonary artery systolic pressure; and PAPVC: partial anomalous pulmonary venous connection.

Table 3: Perioperative details (propensity-matched groups).

	Thoracoscopic group ($N = 64$)	Robotic group ($N = 64$)	P value
Operation time (min, median (IQR))	300.00 (250.00, 373.75)	210.00(180.00, 240.00)	<0.001
CPB time (min, median (IQR))	123.50 (95.25, 164.50)	74.50 (64.25, 92.00)	<0.001
Surgical closure technique			0.244
Pericardial patch	61 (95.3)	64 (100.0)	
Primary suturing	3 (4.7)	0 (0.0)	
Concomitant PAPVC repair	2 (3.1)	5 (7.8)	0.453
ICU stay (h, median (IQR))	22.00 (20.00, 46.00)	19.00 (18.00, 24.00)	0.001
Mechanical ventilation time (h, median (IQR))	6.75 (4.50, 15.00)	4.00 (3.00, 6.75)	0.02
Postoperative hospital-stay (d, median (IQR))	9.00 (7.00, 13.00)	8.00 (7.00, 9.00)	0.025
Thoracic drainage[a] (ml, median (IQR))	277.50 (151.25, 460.75)	207.50 (101.25, 300.00)	0.001
Total RBC usage (U, median (IQR))	3.00 (0.00, 4.00)	0.00 (0.00, 0.00)	<0.001
Total hospital costs ($\times 10^4$\$, median (IQR))	1.33 (1.13, 1.76)	1.49 (1.34, 1.69)	0.097

[a]:the volume of thoracic drainage in the first 24 hours after operation; CPB: cardiopulmonary bypass; ICU: intensive care unit; and PAPVC: partial anomalous pulmonary venous connection.

Table 4: In-hospital complications (propensity-matched groups).

	Thoracoscopic group ($N = 64$)	Robotic group ($N = 64$)	P value
In-hospital mortality (n (%))	0 (0.0)	0 (0.0)	NA
New-onset arrhythmia (n (%))	4 (6.3)	2 (3.1)	0.687
Atrial fibrillation	4 (6.3)	1 (1.6)	
Supraventricular tachycardia	0 (0.0)	1 (1.6)	
Systemic embolism (n (%))	4 (6.3)	1 (1.6)	0.375
Stroke	2 (3.1)	1 (1.6)	
Peripheral embolism	2 (3.1)	0 (0.0)	
Reoperation for bleeding (n (%))	1 (1.6)	0 (0.0)	NA
DMV (n (%))	7 (10.9)	3 (4.7)	0.344
Residual shunt	1 (1.6)	1 (1.6)	1.000
Intraoperative (TEE)	0 (0.0)	0 (0.0)	NA
Before discharge (TTE)	1 (1.6)	1 (1.6)	1.000
Pneumonia (n (%))	3 (4.7)	1 (1.6)	0.625
Renal failure (n (%))	0 (0.0)	1 (1.6)	NA
Pneumothorax (n (%))	1 (1.6)	1 (1.6)	1.000

DMV: delayed mechanical ventilation (>24 h).

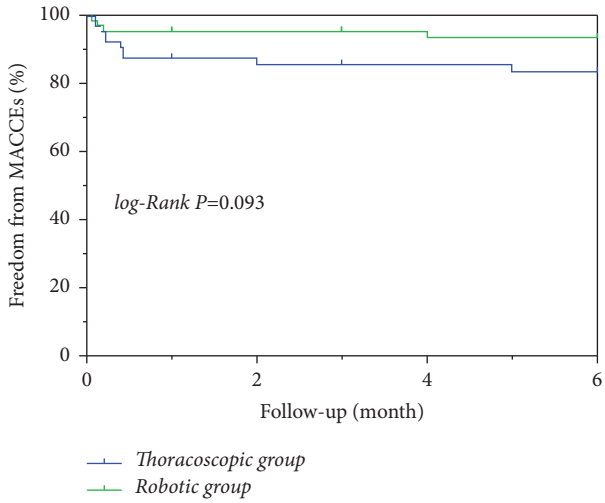

Figure 1: The Kaplan–Meier survival curve. Over 6 months of follow-up, freedom from MACCEs for matched thoracoscopic group and robotic group were 83.6% and 93.4%, respectively ($P = 0.093$).

4. Discussion

In this study, we found the operation time and CPB time of the robotic group were both significantly shorter than the thoracoscopic group. To analyze the reason, we believe it is just because that robotic devices have many advantages over thoracoscopy, such as wrist-like articulated instruments that can move at six degrees of freedom and lack of tremors. This helps improve the speed and accuracy of suturing, thus shortening the operation and CPB time. On the contrary, the long-shafted instrument of thoracoscopy, to some extent, limited the surgeon's mobility and caused fatigue easily. Besides, robotic surgeries allowed maximum visualization of intracardiac structures and bleeding point by three-dimension (3D) high-definition imaging [6], which facilitate the process of surgical hemostasis intraoperatively. Accordingly, the 24-hour thoracic drainage volume of the robotic group decreased significantly in this study, reflecting less tissue damage and better hemostatic effect of robotic surgery. This is slightly different from the results reported by Wei et al. in 2020 [17]. In Wei's study, 24-hour drainage was higher in the robotic MVP group when compared to the thoracoscopic MVP group despite no statistical difference ($P > 0.05$).

There is a paucity of data comparing postoperative outcomes between robotic and thoracoscopic surgery for ASD repair in previous studies. In this study, we observed that the length of ICU-stay, postoperative mechanical ventilation time, and the length of postoperative hospital decreased significantly in the robotic group. This result suggests that patients in the robotic group recovered faster than their counterparts in the thoracoscopic group. In addition, our study also indicated robotic surgeries significantly reduced the usage of RBC. In this study, there was no significant difference between the two groups in the total hospital cost. However, cost-benefit analysis of the robotic surgeries was beyond the scope of this study. Thus, the factors such as the institutional cost of the robot, the inflation rate, and per capita income increase were not taken into account. Further studies are still necessary to weigh the benefit of patients and the real economic cost.

In this study, none of the patients who underwent robotic surgery had mortality, as done in thoracoscopic surgery. This indicates that both of the two techniques are safe approaches for ASD repair. Balkhy et al. reported a single-center experience of 1103 patients who underwent robotic surgeries over 7 years and found that atrial fibrillation was the most common early postoperative complications, with the incidence of 12% [8]. In robotic surgeries, new-onset atrial fibrillation is thought to result from the atriotomy incision [1]. However, the incidence of new-onset atrial fibrillation in this study (1.6% for the robotic group, 6.3% for thoracoscopic group) was lower than that reported by Balkhy et al. Embolism events can be seen after both robotic and thoracoscopic surgeries in this study. Cerny et al. conducted a multicenter registry of 2563 robotic cardiac surgeries and reported a perioperative stroke rate of 0.2% in 2021 [18]. However, in this study, of the 4 patients (3 before discharge and 1 in follow-up) who experienced stroke, 2(50.0%) patients had underlying atrial fibrillation. In addition, in terms of early postoperative embolism events (<14 days), no statistically significant difference was found between the two groups. Besides, there was also no significant difference in the incidence of 6-months MACCEs after operation. However, longer follow-up time and greater sample sizes are warranted for validation of these findings.

5. Limitations

This study has several limitations. First, our study is a single-centered, nonrandomized study. The lack of a prospective and randomized nature is a limitation. Observed indicators can be influenced by some subjective factors. Limited sample size may reduce the power to detect significant difference. Furthermore, we only compared the in-hospital and early follow-up outcomes. However, midterm and long-term follow-up results need to be further investigated. In addition, the hospital cost in this study cannot be expected to be reproduced in other centers due to the factors such as the inflation rate and different economic level.

6. Conclusion

This study indicates the early outcomes in totally endoscopic robotic surgery for ASD repair are similar to the total thoracoscopic surgery. Both these two procedures are proven to be safe and reliable for ASD closure. However, robotic surgery can provide shorter operation time, less postoperative drainage, and quicker recovery than thoracoscopic surgery.

Data Availability

The experimental data used to support the findings of this study are available from the corresponding authors upon request.

Hindawi
Emergency Medicine International
Volume 2023, Article ID 9863185, 1 page
https://doi.org/10.1155/2023/9863185

Retraction

Retracted: The Impact of 3S2E Nursing Management on the Psychological Status of Respiratory Function and Quality of Life of Patients with Severe Pneumonia in the ICU

Emergency Medicine International

Received 28 November 2023; Accepted 28 November 2023; Published 29 November 2023

This article has been retracted by Hindawi, as publisher, following an investigation undertaken by the publisher [1]. This investigation has uncovered evidence of systematic manipulation of the publication and peer-review process. We cannot, therefore, vouch for the reliability or integrity of this article.

Please note that this notice is intended solely to alert readers that the peer-review process of this article has been compromised.

Wiley and Hindawi regret that the usual quality checks did not identify these issues before publicationand have since put additional measures in place to safeguard research integrity.

We wish to credit our Research Integrity and Research Publishing teams and anonymous and named external researchers and research integrity experts for contributing to this investigation.

The corresponding author, as the representative of all authors, has been given the opportunity to register their agreement or disagreement to this retraction. We have kept a record of any response received.

References

[1] Y. Xu, X. Li, Q. Yang, and X. Ma, "The Impact of 3S2E Nursing Management on the Psychological Status of Respiratory Function and Quality of Life of Patients with Severe Pneumonia in the ICU," *Emergency Medicine International*, vol. 2022, Article ID 4949498, 5 pages, 2022.

Hindawi
Emergency Medicine International
Volume 2022, Article ID 4949498, 5 pages
https://doi.org/10.1155/2022/4949498

Research Article

The Impact of 3S2E Nursing Management on the Psychological Status of Respiratory Function and Quality of Life of Patients with Severe Pneumonia in the ICU

Yaoyao Xu, Xia Li, Qin Yang, and Xiuxian Ma

Department of Critical Care Medicine, Traditional Chinese Medicine, Wenzhou Municipal Hospital of Traditional Chinese Medicine, Wenzhou 325000, China

Correspondence should be addressed to Xiuxian Ma; mxx15058708229@163.com

Received 23 August 2022; Revised 6 September 2022; Accepted 9 September 2022; Published 23 September 2022

Academic Editor: Hang Chen

Objective. This study examines the effects of the 3S2E nursing management mode on patients with severe pneumonia in the intensive care unit's respiratory function, psychological status, and quality of life (ICU). *Methods*. According to a random number table, 82 ICU patients with severe pneumonia who were admitted between March 2021 and March 2022 were enrolled and assigned to the control and observation class ($n = 41$, respectively) in a 1 : 1 ratio. The observation class added 3S2E manner in addition to ordinary breastfeeding, whereas the control class received treatment in the usual nursing mode. The two groups' preintervention and postintervention times for mechanical ventilation, white blood cell count (WBC) recovery, duration of hospital stay, problems, respiratory function, psychological state, and living quality were compared. *Results*. Fever time abatement, mechanical ventilation time, WBC recovery time, and length of hospital stay in the observation category were found to be shorter in comparison with the control class ($P < 0.05$). In contrast to the other group, the observation group had fewer issues ($P < 0.05$). Both teams' oxygenation indices and SaO_2 were higher after the intervention ($P < 0.05$), with the observation team's index being higher than the control group's index. The total SAS and SDS scores of the two groups were less in the postintervention period than in the preintervention period, with the observational class having lower postintervention SAS and SDS ratings than the comparison group ($P < 0.05$). The postintervention ratings in the observation class were higher than those in the control, and the World Health Organization Quality of Life (WHOQOL) scale scores in the 2 categories were greater after the intervention than they were before ($P < 0.05$). *Conclusion*. 3S2E nursing management model improves respiratory function, alleviates negative emotions, and improves living quality in ICU patients with severe pneumonia.

1. Introduction

Pneumonia is one of the commonest infections in elderly patients. The major cause of mortality in pneumonia is lower respiratory tract infection. Pneumonia in the elderly is mostly correlated with age-dependent and pathologic changes in the immune system and the lungs. 3S2E nursing management is a new nursing management model based on nursing safety systems and clinical practices, which has achieved a good effect on severe diseases in recent years.

A common respiratory condition that requires special treatment is severe pneumonia. The patient's lung tissue develops from acidosis, hypoxia, and viral and bacterial attack, which usually affects multiple organs [1–3]. Severe pneumonia may progress to multiple organ dysfunction syndromes and septic shock, and the disease is life-threatening with high mortality, which requires timely and effective treatment [4, 5]. At present, the treatment plan and nursing intervention for severe pneumonia still need to be improved, and effective nursing intervention is particularly critical for the rehabilitation of patients [2, 6]. The intervention of "3S2E" nursing management model in patients with severe pneumonia can improve the patient's respiratory function and reduce their anxiety and depression [1, 7]. Therefore, this study focused on 3S2E on respiratory function, psychological health, and standard of living of ICU patients with severe pneumonia.

This study aimed to demonstrate the role of 3S2E nursing management model in respiratory function living quality in ICU patients with severe pneumonia.

2. Data and Methods

2.1. Objects and Groups. According to a random number table, 82 ICU individuals with severe pneumonia who were admitted between June 2021 and June 2022 were enrolled and assigned to the control class and observation class ($n = 41$, respectively) in 1 : 1 ratio. In the control group, there were 25 men and 16 women, respectively, and the weight ranged from 43 to 82 kg, with an average of 62.34 ± 8.85 kg; the average age was 71.64 6.94 years. The observation group consisted of 24 men and 17 women. The average age was 72.02 ± 7.94, with a range of 60 to 86 years. Between 41 and 87 kg, the average weight was 63.42 ± 9.29 kg. The baseline data did not significantly differ between both categories ($P > 0.05$).

2.2. Inclusion and Exclusion Criteria

2.2.1. Inclusion Criteria. (1) It was built on 2007 [6] Infectious Diseases Society of America/American Thoracic Society diagnostic criteria for severe pneumonia; (2) the patient has normal cognitive function and communication abilities; (3) the form of informed consent was signed by the patient.

2.2.2. Exclusion Criteria. (1) Those having autoimmune diseases/tumors; (2) pulmonary diseases other than severe pneumonia; (3) the liver and kidney function of the patient was severely impaired; (4) those with cognitive dysfunction or severe mental illness; (5) patients with other severe infections.

2.3. Participants. The control group applied routine nursing management, which included the following (1) psychological intervention: medical staff communicate with sufferers to understand their psychological status, carried out individualized psychological intervention according to the psychological characteristics of patients, and told successful cases for fearful and pessimistic patients. Patients with anxiety and depression can be adjusted by listening to music for relief to improve their confidence in treatment. (2) Respiratory care: for patients with mechanical ventilation, the humidification of their airway should be ensured to avoid pipe blockage. For patients who were unable to expectorate, the sputum should be discharged through postural drainage. The patients with thick sputum were treated by atomization inhalation to expel the sputum. (3) Oxygen therapy care: patients with carbon dioxide retention should carry out low-flow uninterrupted oxygen inhalation, and the oxygen concentration needs to be kept at 30%–35%. For patients with hypoxic symptoms, their blood oxygen saturation should be closely monitored, and appropriate oxygen inhalation methods should be used to keep the patient's oxygen flow at 5 L/min. (4) Management of complications: as severe pneumonia is prone to multiple complications, the complications should be reported and handled in time.

Our study was approved by the institutional review board of the hospital and was conducted in accordance with the ethical principles of Helsinki. Written informed consent was obtained from each participant.

Based on the usual nursing care provided to the control group, the observational class was given care using the 3S2E nursing management method. A 3S2E nursing team consisting of a leading physician, a leading nurse, a head nurse, and a nurse was set up, and the detailed management methods were as follows: (1) S1 (improvement of nursing skills): provided standardized training for nurses, including how to dynamically observe the patient's condition, detect abnormalities in time, and maintain effective venous access. All nurses learned the latest disease-related knowledge, nursing progress, and surgical knowledge and carried out nursing skills assessment, and for those who fail the assessment, multiple pieces of training were required to improve their nursing skills. (2) S2 (optimization of nursing services): the basic services should be consolidated, and basic nursing measures should be implemented accordingly. The nursing staff should provide humanistic care to patients and meet their reasonable needs as far as possible in order to provide patients with a good inpatient environment. More communication should be conducted with patients to relieve their negative emotions. The changes of blood oxygen saturation, blood pressure, and inflammatory factors of patients were recorded and evaluated to formulate targeted monitoring and rehabilitation programs. (3) S3 (ensuring safe nursing care): medical staff should prepare risk prevention plans and receive training in advance, especially guidance on key procedures such as catheterization, intubation, and sputum aspiration, so as to ensure the safe transfer and transfer of patients and standardize the rational use of drugs. (4) E1 (evaluation): the medical staff assessed the patient's respiratory function such as oxygenation index and SaO2. (5) E2 (health education): following patient's hospitalization, the responsible nurse introduced the ward and hospital environment to his family members and distributed disease knowledge brochures. Health education was conducted according to patients' different personalities and education levels, including knowledge related to severe pneumonia, treatment methods, family care, and successful case analysis. At least 15 minutes of mental health education should be given to enhance their confidence.

2.4. Observation of Indicators. (1) The antipyretic time, mechanical ventilation time, WBC recovery time, and hospital stay of the two groups were observed. (2) The two groups' complications were noticed. (3) Before and following the intervention, alterations in the respiratory function indices, including the oxidation index and SaO_2, were seen in the two groups. (4) Monitoring the two groups' psychological states before and after the intervention. To assess anxiety and depression, respectively, the Self-Rating Anxiety Scale (SAS) and Self-rating Depression Scale (SDS) were employed. The more severe the patients' anxiety or

Table 1: Comparison of the two groups' hospital stays, WBC recovery times, mechanical ventilation times, and times for fever abatement ($\overline{x} \pm s$, d).

Group	Number of cases	Time of fever abatement	Mechanical ventilation	WBC recovery	Length of hospital stay
Observation group	41	5.45 ± 1.42	6.23 ± 1.46	6.54 ± 1.38	20.47 ± 5.46
Control group	41	8.37 ± 1.71	9.28 ± 2.35	9.74 ± 1.64	29.38 ± 4.58
t		8.412	7.059	9.560	8.006
P		<0.05	<0.05	<0.05	<0.05

Table 2: Complications comparison.

Group	Number of cases	Bronchiectasis	Pulmonary edema	Septic shock	Incidence (%)
Observation group	41	1	1	1	7.32
Control group	41	5	3	3	26.83
t					5.513
P					<0.05

Table 3: Comparison of respiratory function ($\overline{x} \pm s$).

Group	Number of cases	Oxygenation index (mmHg)		SaO_2 (%)	
		Pre-intervention	Post-intervention	Pre-intervention	Post-intervention
Observation group	41	217.95 ± 14.32	285.32 ± 22.41*	83.24 ± 2.51	96.87 ± 2.18*
Control group	41	215.62 ± 18.85	250.87 ± 17.89*	83.61 ± 2.37	92.17 ± 2.43*
t		0.630	7.693	0.686	9.219
P		>0.05	<0.05	>0.05	<0.05

Note. compared with pre-intervention $^*P < 0.05$.

sadness, the higher the score. (5) Pre- and postintervention observations revealed changes in four different aspects of quality of life, including the environment, social relationships, psychology, and physiology. Each factor was translated to a scale of 100, with higher scores indicating better life quality.

2.5. Statistical Treatment. Data processing was conducted by SPSS 26.0. The counting data were expressed as n (%) and were subjected to a t-test analysis for the measuring data. When $P < 0.05$, the difference was significant.

3. Results

3.1. Comparison of the Length of Hospital Stay, Mechanical Ventilation, WBC Recovery, and Time for Fever Abatement. In comparison with the control group, the observation group's length of hospital stay, length of mechanical ventilation, recovery of WBC, and time from fever were all shorter ($P < 0.05$) (Table 1).

3.2. Comparison of Complications. Fewer complications occurred in the observation group compared to the control group ($P < 0.05$) (Table 2).

3.3. Comparison of Respiratory Function. Following the intervention, both groups' oxygenation index and SaO_2 levels were higher than they had been previously ($P < 0.05$); the monitoring unit had greater indications than the control ($P < 0.05$) (Table 3).

3.4. Psychological Status Comparison. The two groups postintervention SAS and SDS scores were lower than their preintervention scores (P0.05); the observation group's postintervention SAS and SDS scores were lower than those of the control group's ($P < 0.05$) (Table 4 and Figure 1).

3.5. WHOQOL-BREF Comparison. The postintervention World Health Organization Quality of Life (WHOQOL) scores in the observation group were greater than those in the control group ($P < 0.05$), and the scores in the two groups after the intervention were better than those before the intervention (Table 5).

4. Discussion

Atypical pneumonia is caused by atypical pathogens that are not detectable with Gram stain and cannot be cultured using standard methods. Severe pneumonia has an acute onset and rapid progress and is often accompanied by varying degrees of respiratory failure, septic shock, and decreased blood pressure. Excitation of the sympathetic adrenal concomitant system results in decreased intestinal perfusion pressure and vasoconstriction of the intestinal mucosa, which then leads to ischemia and hypoxia of intestinal mucosal tissues [7, 8]. In addition, severe pneumonia is in a negative nitrogen balance, which leads to a decline in the patient's immune status. The increased permeability of the intestinal mucosa and the impaired barrier function will aggravate the systemic inflammatory response, thus forming a vicious circle and leading to the occurrence of multiple organ dysfunction syndromes [9–11]. Prompt and effective treatment and

Table 4: Psychological status comparison ($\overline{x} \pm s$, points).

Group	Number of cases	SAS		SDS	
		Pre-intervention	Post-intervention	Pre-intervention	Post-intervention
Observation group	41	64.35 ± 4.51	44.52 ± 4.17*	61.48 ± 3.47	43.61 ± 3.27*
Control group	41	62.79 ± 5.12	49.87 ± 3.68*	62.08 ± 3.65	48.42 ± 4.56*
t		1.464	6.160	0.763	5.489
P		>0.05	<0.05	>0.05	<0.05

Note. compared with pre-intervention $^{*}P < 0.05$.

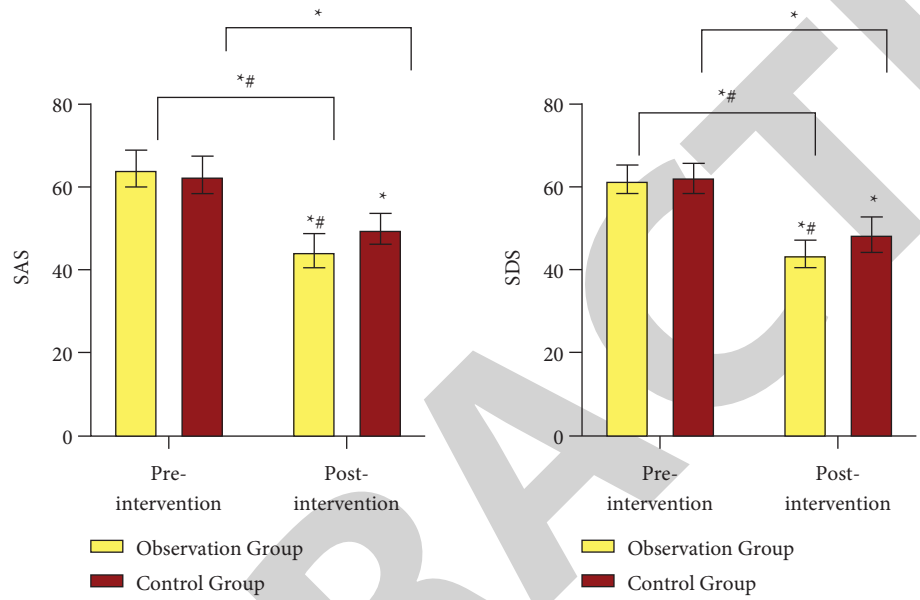

Figure 1: Comparison of psychological status (a): SAS scores of the two groups in post-intervention were less than in pre-intervention, the observation group had lower post-intervention SAS than the control group; (b): SDS scores of the two groups in post-intervention were less than in pre-intervention, the observation group had lower post-intervention SDS than the control group. compared with pre-intervention $^{*}P < 0.05$. compared with the control group, $^{\#}P < 0.05$.

Table 5: WHOQOL-BREF comparison ($\overline{x} \pm s$, points).

Group	Number of cases	Environment		Social		Psychological field		Physical field	
		Pre-intervention	Post-intervention	Pre-intervention	Post-intervention	Pre-intervention	Post-intervention	Pre-intervention	Post-intervention
Observation group	41	52.35 ± 5.35	73.24 ± 3.56*	70.64 ± 4.26	87.87 ± 4.49*	44.52 ± 5.41	70.25 ± 5.67*	47.42 ± 5.67	76.52 ± 4.58*
Control group	41	53.24 ± 4.26	64.51 ± 4.78*	72.01 ± 3.89	81.02 ± 5.45*	43.78 ± 3.54	61.98 ± 4.72*	48.18 ± 5.25	63.37 ± 5.07*
t		0.833	9.379	1.521	6.212	0.733	7.178	0.630	12.324
P		> 0.05	< 0.05	> 0.05	< 0.05	> 0.05	< 0.05	> 0.05	< 0.05

Note. compared with pre-intervention $^{*}P < 0.05$.

nursing are of great significance to severe pneumonia. With the ceaseless changes in medical models and the gradual increase in patients' demand for nursing care, traditional routine care has been unable to meet the needs of patients [12–15]. Therefore, a new nursing model that is promoted for people with severe pneumonia is quite significant.

3S2E nursing management mode is a new nursing mode. It primary enhances nursing service awareness, improves nursing skills, ensures nursing safety, evaluates patients' conditions, and provides health education for them [16–19]. In the 3S2E nursing management mode, nursing staff provide high-quality nursing services for patients, focus on the changes in patient's vital signs, and inform physicians in time when abnormal conditions are found, to facilitate timely treatment by physicians and ameliorate patients' prognosis. This study put forward the fever abatement time and mechanical ventilation. Patients in the observation category had shorter hospital stays and WBC recovery than those in the control category. It considered that the 3S2E nursing management mode can speed up the patient's fever reduction and WBC recovery and can shorten mechanical ventilation time and hospitalization. The nurse management

Hindawi
Emergency Medicine International
Volume 2023, Article ID 9803698, 1 page
https://doi.org/10.1155/2023/9803698

Retraction

Retracted: Related Factor Analysis and Nursing Strategies of Diarrhea in Critically Ill Patients with Enteral Nutrition

Emergency Medicine International

Received 28 November 2023; Accepted 28 November 2023; Published 29 November 2023

This article has been retracted by Hindawi, as publisher, following an investigation undertaken by the publisher [1]. This investigation has uncovered evidence of systematic manipulation of the publication and peer-review process. We cannot, therefore, vouch for the reliability or integrity of this article.

Please note that this notice is intended solely to alert readers that the peer-review process of this article has been compromised.

Wiley and Hindawi regret that the usual quality checks did not identify these issues before publication and have since put additional measures in place to safeguard research integrity.

We wish to credit our Research Integrity and Research Publishing teams and anonymous and named external researchers and research integrity experts for contributing to this investigation.

The corresponding author, as the representative of all authors, has been given the opportunity to register their agreement or disagreement to this retraction. We have kept a record of any response received.

References

[1] D. Liu, Q. Liu, and X. Wen, "Related Factor Analysis and Nursing Strategies of Diarrhea in Critically Ill Patients with Enteral Nutrition," *Emergency Medicine International*, vol. 2022, Article ID 8423048, 8 pages, 2022.

Hindawi
Emergency Medicine International
Volume 2022, Article ID 8423048, 8 pages
https://doi.org/10.1155/2022/8423048

Research Article

Related Factor Analysis and Nursing Strategies of Diarrhea in Critically Ill Patients with Enteral Nutrition

Donglian Liu,[1] Qinghong Liu,[1] and Xiansong Wen[2]

[1]*Department of Emergency, Ganzhou People's Hospital, Ganzhou341000, Jiangxi, China*
[2]*Department of Nursing, Ganzhou People's Hospital, Ganzhou341000, Jiangxi, China*

Correspondence should be addressed to Xiansong Wen; gzsrmyyebh@163.com

Received 25 July 2022; Revised 2 September 2022; Accepted 9 September 2022; Published 21 September 2022

Academic Editor: Hang Chen

Objective. To explore the related factors of diarrhea in critically ill patients with enteral nutrition (EN) in the intensive care unit (ICU). *Methods*. This single-center retrospective study analyzed the occurrence of intolerant diarrhea in ICU patients receiving EN treatment in our hospital. By collecting clinical data, univariate and multivariate logistic regression analysis was used to screen the risk factors for diarrhea. *Results*. Among 120 patients included in the study, 68 (48.33%) had diarrhea. Age (OR = 2.599, $P = 0.027$), use of antibiotics (OR = 3.496, $P = 0.007$), ICU hospitalization time (OR = 1.311, $P = 0.001$), and mechanical ventilation time (OR = 1.273, $P = 0.035$) were all independent risk factors for diarrhea in EN. *Conclusion*. Older age, frequent use of antibiotics, long ICU stay, and mechanical ventilation time can lead to diarrhea in ICU patients receiving EN treatment. It is necessary to effectively analyze the above independent factors and implement targeted interventions to improve the incidence of diarrhea in patients.

1. Introduction

Intensive care unit (ICU) is a specialized department for intensive care and treatment of critically ill patients in hospitals. Studies have shown that the incidence of malnutrition in ICU is 38%–78% [1] and is associated with poor prognosis. Critically ill patients in the intensive care unit (ICU) have high metabolism, high consumption, and stress state. Therefore, the demand for nutrition increases, but such patients often due to chewing, swallowing, consciousness and other factors lead to abnormal eating and need nutritional support treatment. Enteral nutrition (EN) is an important means of nutritional support for ICU patients [2]. Compared with parenteral nutrition (PN), early application of EN can promote the recovery of gastrointestinal mucosal integrity [3] and is also found to be related to the reduction of infection rate, mortality, and hospitalization time [4]. EN is also a treatment recommended by the European Society for European Society for Clinical Nutrition and Metabolism (ESPEN) [5]. EN in a broad sense refers to the way in which nutrients required by patients are provided orally or through tubes (nasogastric tube, nasointestinal tube, and fistula tube) [6]. However, in the ICU, patients who take food orally have certainty in food composition and time frequency. Therefore, EN mentioned in this study is limited to obtaining nutrients through pipelines, excluding oral or semiautonomous eating. Although EN is beneficial for critically ill patients, it often causes complications during treatment, which can aggravate the patient' s condition and even threaten life. Diarrhea is one of the common manifestations of treatment intolerance. Kozeniecki studies have shown that the incidence of diarrhea in critically ill patients during enteral nutrition can reach 66% [7]. Diarrhea in enteral nutrition may lead to loss of nutrients, acid-base imbalance of water electrolyte, perianal skin rupture, and increase hospitalization time and mortality [8]. Therefore, understanding the related factors of diarrhea in enteral nutrition and implementing corresponding measures can effectively improve the prognosis of severe patients.

Due to the latest medical development, the cure rate and survival rate of ICU patients have improved. People have higher requirements for the prognosis of such patients and

the quality of life after discharge. Therefore, reducing the risk of diarrhea in EN treatment to ensure the quality of treatment is critical for ICU patients. At present, the causes of diarrhea after enteral nutrition therapy in ICU patients are not clear. Most of the epidemiological data on diarrhea in critically ill patients in ICU come from countries other than China, which may not reflect the actual situation in China. Regrettably, this issue has rarely attracted the attention of researchers in China. Based on this, we explored the related factors of diarrhea in ICU patients during EN treatment. The research results are of great significance to guide clinicians to take effective intervention measures and reduce the risk of diarrhea.

2. Materials and Methods

2.1. Design. This single-center, retrospective study collected data of 120 patients who received EN treatment in ICU of our hospital from November 2020 to November 2021. This study was approved by the institutional ethics committee and carried out with the informed consent of patients.

2.2. Patients. Patients receive EN in ICU of our hospital. The inclusion criteria are as follows: the patient's age is ≥18 years old, ICU stay is ≥2 days, in line with EN treatment indications, and complete basic clinical data. Exclusion criteria are as follows: at the end stage of malignant tumor, patients had suffered from diseases with diarrhea symptoms such as irritable bowel syndrome and inflammatory bowel disease, acute gastrointestinal bleeding, intestinal polypectomy, radical resection of esophageal cancer, and other gastrointestinal surgery histories.

2.3. Method of EN. All patients in the ICU stay within 24~48 h, immediately began to nasal feeding tube enteral nutrition support treatment. The daily calorie intake of patients in this study was 30 kcal/kg d. Enteral nutrient solution was continuously input through a thermostatic heater, and the speed and dose were reasonably adjusted according to the patient's intestinal tolerance. Gastric contents were withdrawn at q6h, and gastric contents greater than 150 ml should be suspended and evaluated again after 2 h.

2.4. Precautions for EN Feeding

(1) EN implementation process: the bed head raised 30°to 45°
(2) Before feeding implementation, ensure that the gastrointestinal tube in place and fixed properly
(3) q4h feed 20 ml warm water to wash the pipeline to ensure smooth pipeline
(4) Daily oral care to prevent oral infection (ordinary patients: 2 times/day; mechanical ventilation patients: 3 times/day)

2.5. Collection of Materials. Collect relevant information through the hospital electronic medical record system. It mainly includes gender, age, BMI, EN treatment days, feeding methods, ICU admission diagnosis, mechanical ventilation use, EN preparation type, hypoproteinemia occurrence, antimicrobial use, acute physiology and chronic health evaluation II (APACHE II), ICU hospitalization time, mechanical ventilation time, EN use, and potassium (K), sodium (Na), chlorine (CI), calcium (Ca), and magnesium (Mg) electrolyte levels.

2.6. Grouping. Diagnostic criteria: defecation frequency ≥3 times/d; feces volume ≥200 g/d. According to the Bristol stool classification method, feces were paste or water samples. Nurses and doctors are responsible for the mobile phones of the above information. Before that, they received unified training, including disease definition and data entry. Finally, 58 patients with diarrhea were included in the diarrhea group, and 62 patients without diarrhea were included in the nondiarrhea group.

2.7. Statistical Analysis. Statistical Package for Social Sciences software for Windows, version 23.0 (SPSS Inc, Chicago, IL, USA) was used to analyze the data. Quantitative data were expressed as mean ± standard deviation, and *t*-test was performed. The enumeration data are described by various cases and percentages, chi-square test, when 1 ≤ theoretical frequency <5 chi-square values need to be corrected, when the theoretical frequency <1 using the exact probability method. Single-factor and multifactor conditional logistic regression models were used to screen the independent factors affecting diarrhea, OR value and 95% confidence interval of risk were calculated, and P values <0.05 was considered statistically significant.

3. Results

3.1. Baseline Information. Originally, 124 patients met the criteria, but 5 patients were excluded (Figure 1). Finally, 120 patients were included in the study, including 58 cases of diarrhea, 73 males, 67 patients with hypoproteinemia, 79 patients with antimicrobial drugs, 110 patients with nasogastric tube feeding, and 95 patients with mechanical ventilation. The ventilation time was 7.46 ± 1.95 days, 71 patients aged ≥60 years old, 105 patients with EN treatment for 4 days, and the EN usage for 4 days was (1033.49 ± 206.64) ml. 61.67% of the patients entered ICU for EN treatment due to respiratory diseases (Table 1).

3.2. Single Factor Analysis of Diarrhea in ICU Patients with EN Treatment. There were statistically significant differences in age, antibiotic use, ICU hospitalization time, and mechanical ventilation time between the diarrhea group and the nondiarrhea group ($P < 0.05$). In addition, the remaining indicators between the two groups are not statistically significant (Table 2). The number of patients aged ≥60 years who developed diarrhea after EN treatment was much larger than

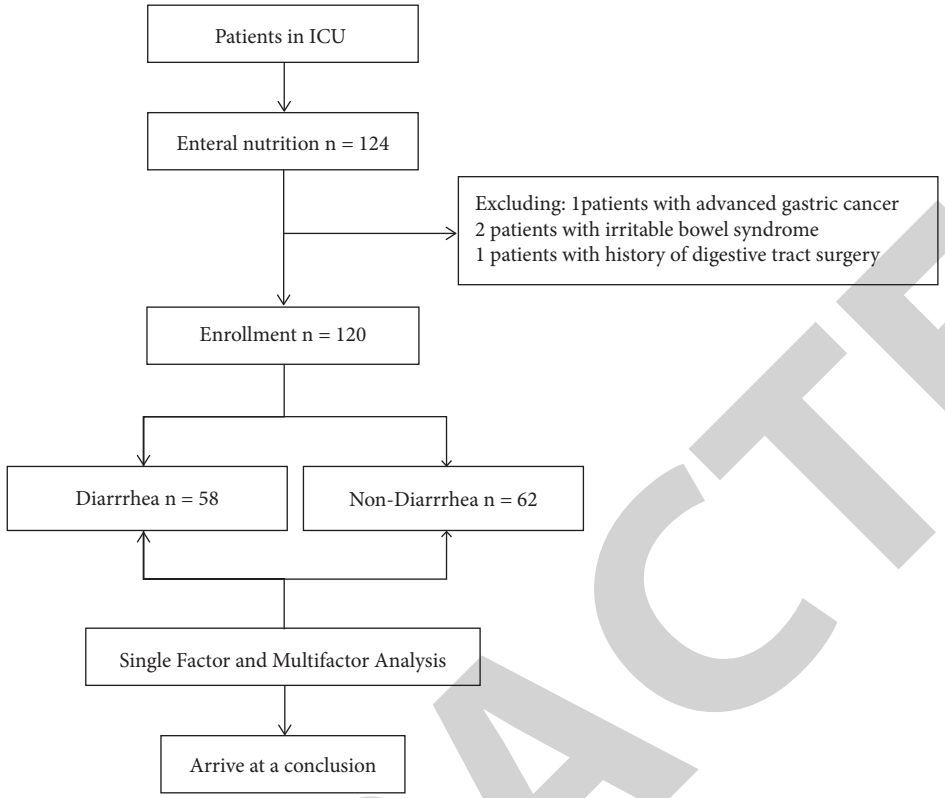

Figure 1: Flow chart for inclusion in the study.

that of those who did not (41 vs 30). Similarly, 58% (46/73) of patients who used antibiotics developed diarrhea (Figure 2). The ICU hospitalization time ($r = -0.367$, $P < 0.001$) and mechanical ventilation time ($r = -0.232$, $P < 0.011$) were negatively correlated with the risk of diarrhea (Figure 3).

3.3. Multivariate Analysis of Diarrhea in ICU Patients Undergoing EN Treatment. The results of single factor analysis were statistically significant indicators (age, use of antibiotics, ICU hospitalization time, and mechanical ventilation time) as independent variables, to ICU patients with diarrhea after EN treatment as the dependent variable, assignment (Table 3). Multivariate logistic regression analysis showed that age ≥60 years old (OR = 2.599 (1.112–6.074), $P = 0.027$), use of antibiotics (OR = 3.496 (1.416–8.632), $P = 0.007$), ICU hospitalization time (OR = 1.311 (1.113–1.544), $P = 0.001$), and mechanical ventilation time (OR = 1.273 (1.017–1.593), $P = 0.035$) were risk factors for diarrhea in ICU patients with EN, and the difference was statistically significant ($P < 0.05$) (Table 4). In addition, we also found that the cutoff values of ICU hospitalization time and mechanical ventilation time in distinguishing EN diarrhea were 9.5 days and 8.5 days, respectively, and their AUCs in distinguishing diarrhea were 0.710 and 0.632, respectively, $P < 0.05$ (Table 5 and Figure 4).

4. Discussion

EN intolerance can be manifested as gastrointestinal reactions such as gastric retention, nausea, vomiting, diarrhea, and aspiration. Diarrhea is one of the manifestations of early enteral nutrition intolerance, which will lead to treatment interruption. In severe cases, it will increase the duration of mechanical ventilation, prolong hospitalization time, even increase the mortality of patients, affect the psychology of patients, and greatly increase the workload of nursing [9]. The incidence of EN intolerance was significantly higher in ICU patients (35.6%) than in general patients [10]. Studying the related factors of diarrhea in ICU patients with enteral nutrition is of great significance to the treatment, prevention, and prognosis improvement of patients.

According to research reports, intensive care unit patients with diarrhea rate as high as 66% [7]. Weiting chen et al. [11] found that the early diarrhea rate of enteral nutrition in ICU patients was 30.8%. In this study, 120 severe patients were treated with enteral nutrition, and 58 cases had diarrhea, with the incidence of 48.33%. It may be that the definition of diarrhea was different, so the diarrhea rate was overestimated. Ferrie et al. [12] defined diarrhea as follows: continuous 2 days, the number of daily defecation ≥3 times, or the number of daily un shaping stool ≥3 times, or the number of daily defecation ≥3 times and the amount ≥300 ml/d. Diarrhea is defined by the World Health Organization as ≥ 3 times of unformed stools per day [13]. According to the 2018 British Adult Chronic Diarrhea Survey Guide, chronic diarrhea is defined as follows: unshaping stool ≥3 times a day for more than 4 weeks [14]. Diarrhea defined in this study meets the following three conditions: defecation frequency ≥3 times/d, fecal volume ≥200 g/d, fecal nature is paste or water sample (Bristol stool type 5–7). The study was a retrospective study. The treatment time of the included severe patients receiving enteral

Table 1: Clinical characteristic of patients.

Characteristics	Value
No. of diarrhea patients	58 (48.33)
Male sex, *n* (%)	73 (60.83)
Hypoproteinemia, *n* (%)	67 (55.83)
Use of antibiotics, *n* (%)	79 (65.83)
Mechanical ventilation, *n* (%)	95 (79.17)
BMI (kg/m^2, mean ± SD)	21.71 ± 3.01
APACHE II score (mean ± SD)	20.31 ± 6.24
ICU hospitalization time (d, mean ± SD)	9.22 ± 2.81
Duration of mechanical ventilation (d, mean ± SD)	7.46 ± 1.95
Age, years, *n* (%)	
≥60	71 (59.17)
<60	49 (40.83)
Feeding patterns, *n* (%)	
Nasogastric tube	110 (91.67)
Nasojejunal tube	10 (8.33)
EN preparation, *n* (%)	
Integral protein	105 (87.50)
Oligopeptide	15 (12.50)
Days of EN treatment, *n* (%)	
4 days	105 (87.50)
7 days	15 (12.50)
Amount of EN (mL, mean ± SD)	
4 days	1033.49 ± 206.64
7 days	1212.47 ± 240.31
ICU admission diagnosis, *n* (%)	
Central nervous system	12 (10.00)
Respiratory system	74 (61.67)
Cardiovascular system	16 (13.33)
Postoperation	11 (9.17)
Others	7 (5.83)
Electrolyte (mmol/L, mean ± SD)	
K	4.64 ± 1.20
Na	137.15 ± 8.72
CI	97.44 ± 9.86
Ca	2.22 ± 0.59
Mg	0.74 ± 0.19

nutrition was not limited, so the observation time was long and the sample size was small, which may be an important reason for the overestimation of diarrhea rate.

Analysis of influencing factors of diarrhea during EN in ICU patients: Single factor analysis showed that there were significant differences in age, antibiotic use, ICU hospitalization time, and mechanical ventilation time between patients with diarrhea and those without diarrhea. The above indicators were further analyzed by multivariate logistic regression analysis, and the results confirmed that age ≥60 years old, the use of antibiotics, ICU hospitalization time, and mechanical ventilation time were independent risk factors for diarrhea in ICU patients during EN intervention. The dynamic balance of gastrointestinal microorganisms maintains human health. Firmicutes and Bacteroidetes in the intestine can control the amount of carbohydrates in the human body through fermentation, and the short-chain fatty acids of the fermentation products can absorb more liquids and electrolytes in the body. Once this function is destroyed, the accumulated metabolites accumulate, leading to osmotic effect and diarrhea [15]. Clinically, patients with diarrhea showed a higher number of Clostridium and a lower number of Bifidobacterium, and the imbalance of these two flora may be related to its pathogenesis. The number of bifidobacteria is a beneficial bacterium in the intestine, and the decrease in this number will reduce the inhibitory ability of the gastrointestinal tract to pathogens to some extent, such as increasing the risk of *Clostridium difficile* infection [16]. Thibault et al. [17] pointed out that antibiotics were an independent risk factor for diarrhea in patients. The use of antibiotics can provide environmental support for the reproduction and infection of *Clostridium difficile*. It can also lead to the disorder of intestinal probiotics, cause intestinal allergy, release antimicrobial toxins, increase gastric motility, and lead to nutrient absorption disorders, thereby causing diarrhea [18]. Previous studies have shown that antibiotic use is an important risk factor for nosocomial diarrhea [19, 20]. A recent study has shown that the diversity of gut microbiome is affected by antibiotic administration, and gut microbiome composition changes over time [21]. Our study found that 58% (46/73) of the same patients who used antibiotics developed diarrhea. At present, there are still controversial results on the effect of age on EN treatment intolerance [10, 22]. Our results suggest that increased age may be a risk factor for diarrhea in critically ill patients. The higher the patient's age, the lower their own immunity, reactivity and reserve capacity, and the degenerative changes in organ physiological function. The intestinal villi and microvilli of elderly patients are sparse, thick and short, and the mucosa is thin. In addition, the mitochondria of elderly patients are prone to swelling, fracture, and dissolution [23]. Compared with young people, the proportion of beneficial bacteria in fecal samples of the elderly, such as thick-walled bacteria, Clostridium, and Lactobacillus, is reduced, and the number of pathogenic bacteria such as Streptococcus and Staphylococcus is increased [24]. In addition, the elderly are at high risk for antibiotic-associated diarrhea. Antibiotic treatment based on enteral nutrition support will also increase the risk of antibiotic-associated diarrhea. There is no report on the correlation between ICU hospitalization time and diarrhea in critically ill patients treated with EN. But it is certain that the longer the ICU hospitalization time, the more complex the condition, the higher the body consumption, the longer the EN treatment of gastrointestinal dysfunction, and the higher the risk of diarrhea. The gastrointestinal motility of ICU patients is weak, and mechanical ventilation will further reduce their gastric motility function. The longer the duration of mechanical ventilation, the greater the impact on gastric motility, and the higher the incidence of diarrhea. In addition, maintaining long-term intra-abdominal pressure in patients with long-term mechanical ventilation may also be an important cause of EN treatment intolerance [22]. Heyland et al. found that patients with diarrhea did not use mechanical ventilation for a shorter period of time and had a longer hospital stay than those who were resistant to enteral nutrition [25]. In general, it is necessary to be vigilant against the occurrence of diarrhea in elderly patients who have long been in ICU during EN treatment and take timely measures. In addition, patients receiving EN treatment during mechanical ventilation should also be paid more attention, and the use of antibiotics should be reduced as much as possible during treatment. There are still many limitations in this study. Firstly, this is a single-center retrospective study, so the sample size is small and the results may be biased.

Table 2: Single factor analysis of diarrhea condition.

Characteristics	Diarrhea group ($n = 58$)	Nondiarrhea group ($n = 62$)	P Value
Male sex, n (%)	38 (65.52)	35 (56.45)	0.309
BMI (kg/m^2, mean ± SD)	21.87 ± 2.93	21.55 ± 3.09	0.569
APACHE II score (mean ± SD)	20.38 ± 6.14	20.24 ± 6.39	0.905
ICU hospitalization time (d, mean ± SD)	10.24 ± 3.03	8.26 ± 2.21	<0.001
Duration of mechanical ventilation (d, mean ± SD)	7.86 ± 1.99	7.08 ± 1.85	0.028
Age, years, n (%)			0.013
≥60	41 (70.69)	30 (48.39)	
<60	17 (29.31)	32 (51.61)	
Hypoproteinemia, n (%)			0.888
Yes	32 (55.17)	35 (56.45)	
No	26 (44.83)	27 (43.55)	
Use of antibiotics, n (%)			0.003
Yes	46 (79.31)	33 (53.23)	
No	12 (20.69)	29 (46.77)	
Mechanical ventilation			0.078
Yes	16 (27.59)	9 (14.52)	
No	42 (72.41)	53 (85.48)	
Feeding patterns, n (%)			0.582
Nasogastric tube	54 (93.10)	56 (90.32)	
Nasojejunal tube	4 (6.90)	6 (9.68)	
EN preparation, n (%)			0.679
Integral protein	50 (86.21)	55 (88.71)	
Oligopeptide	8 (13.79)	7 (11.29)	
Days of EN treatment, n (%)			0.073
4 days	54 (93.10)	51 (82.26)	
7 days	4 (6.90)	11 (17.74)	
Amount of EN (mL, mean ± SD)			
4 days	1042.29 ± 203.22	1025.26 ± 211.11	0.654
7 days	1227.50 ± 225.48	1198.40 ± 254.42	0.510
ICU admission diagnosis, n (%)			0.754
Central nervous system	4 (6.90)	8 (12.90)	
Respiratory system	35 (60.34)	39 (62.90)	
Cardiovascular system	9 (15.52)	7 (11.29)	
Postoperation	6 (10.34)	5 (8.06)	
Others	4 (6.90)	3 (5.17)	
Electrolyte (mmol/L, mean ± SD)			
K	4.52 ± 1.03	4.76 ± 1.33	0.272
Na	135.75 ± 6.67	138.47 ± 10.16	0.087
CI	98.54 ± 6.24	96.42 ± 12.29	0.239
Ca	2.15 ± 0.54	2.28 ± 0.63	0.220
Mg	0.73 ± 0.22	0.75 ± 0.15	0.546

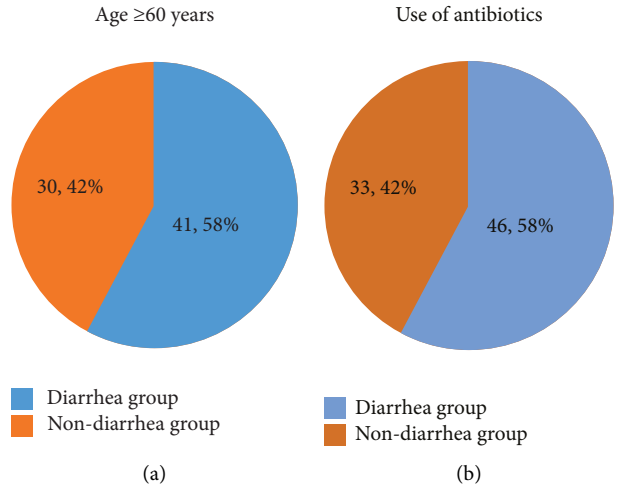

Figure 2: Proportion of diarrhoea cases in patients aged ≥60 years and on antimicrobials. (a) Proportion of diarrhea in patients aged ≥60 years old. (b) Proportion of diarrhea in patients using antibiotics.

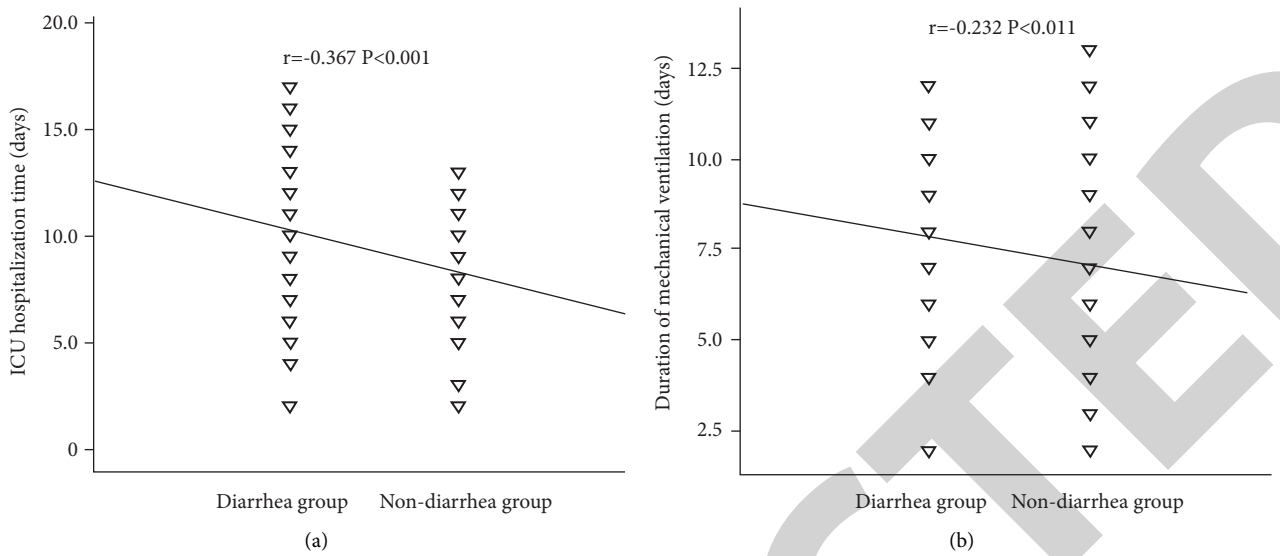

Figure 3: Correlation between ICU hospitalization time, mechanical ventilation time, and diarrhea risk. (a) The correlation between ICU hospitalization time and diarrhea condition. (b) The correlation between the duration of mechanical ventilation and diarrhea condition.

Table 3: Variable valuation.

Factors	Variables	Valuation
Age	X1	0 = <60 years, 1 = ≥60 years
Use of antibiotics	X2	0 = no, 1 = yes
ICU hospitalization time	X3	Actual values
Mechanical ventilation time	X4	Actual values

Table 4: Multivariate logistic regression analysis results.

Variable	β	Wald χ^2	P value	OR (95% CI)
Age (1 = ≥60 years)	0.955	4.861	0.027	2.599 (1.112~6.074)
Use of antibiotics (1 = Yes)	1.252	7.366	0.007	3.496 (1.416~8.632)
ICU hospitalization time	0.271	10.486	0.001	1.311 (1.113~1.544)
Mechanical ventilation time	0.241	4.442	0.035	1.273 (1.017~1.593)

Table 5: ROC curve parameters.

Factors	Cutoff (d)	AUC	Youden index	Sensitivity (%)	Specificity (%)	P value	95%CI
ICU hospitalization time	9.5	0.710	0.361	60.3	75.8	<0.001	0.616–0.804
Mechanical ventilation time	8.5	0.632	0.253	41.4	83.9	0.013	0.531–0.732

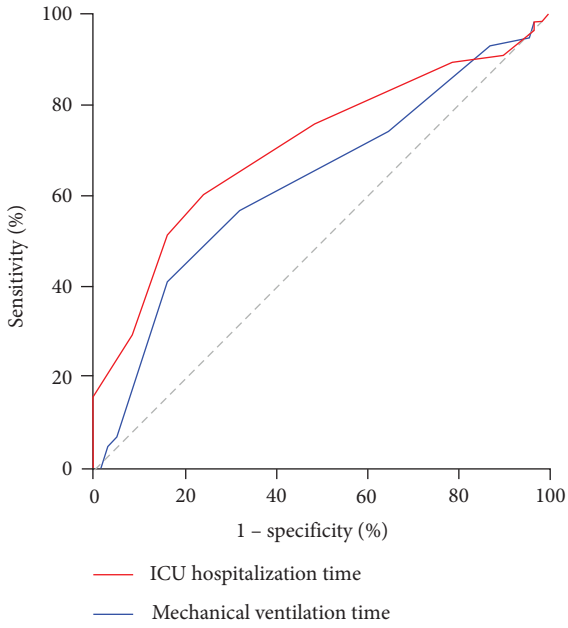

Figure 4: ROC curve for diagnosis of diarrhea.

Secondly, the data collected in the study were not comprehensive, and the relationship between diabetes history, enteral nutrition temperature, fasting before intervention, and diarrhea was not studied. Therefore, the risk factors may be small.

5. Conclusion

In summary, older age, frequent use of antibiotics, long ICU stay, and mechanical ventilation time can lead to diarrhea in ICU patients receiving EN treatment. It is necessary to effectively analyze the above independent factors and implement targeted interventions to improve the incidence of diarrhea in patients.

Data Availability

The data used to support the findings of this study are available from the corresponding author upon request.

Conflicts of Interest

The authors declare that they have no conflicts of interest.

References

[1] C. CH. Lew, R. Yandell, R. J. L. Fraser, A. P. Chua, M. F. F. Chong, and M. Miller, "Association between malnutrition and clinical outcomes in the intensive care unit: a systematic review," *JPEN - Journal of Parenteral and Enteral Nutrition*, vol. 41, no. 5, pp. 744–758, 2017.

[2] A. Reintam Blaser, J. Starkopf, W. Alhazzani et al., "ESICM Working Group on Gastrointestinal Function. Early enteral nutrition in critically ill patients: ESICM clinical practice guidelines," *Intensive Care Medicine*, vol. 43, no. 3, pp. 380–398, 2017.

[3] M. Braga, L. Gianotti, O. Gentilini, V. Parisi, C. Salis, and V. Di Carlo, "Early postoperative enteral nutrition improves gut oxygenation and reduces costs compared with total parenteral nutrition," *Critical Care Medicine*, vol. 29, no. 2, pp. 242–248, 2001.

[4] M. A. Silva, S. da Graça Freitas dos Santos, C. D. Tomasi et al., "Enteral nutrition discontinuation and outcomes in general critically ill patients," *Clinics*, vol. 68, no. 2, pp. 173–177, 2013.

[5] R. Rosen, Y. Vandenplas, M. Singendonk et al., "Pediatric gastroesophageal reflux clinical practice guidelines: joint recommendations of the north American society for pediatric gastroenterology, hepatology, and nutrition and the European society for pediatric gastroenterology, hepatology, and nutrition," *Journal of Pediatric Gastroenterology and Nutrition*, vol. 66, no. 3, pp. 516–554, 2018.

[6] J. I. Boullata, K. Gilbert, G. Sacks et al., "American Society for Parenteral and Enteral Nutrition. A.S.P.E.N. clinical guidelines: parenteral nutrition ordering, order review, compounding, labeling, and dispensing," *JPEN - Journal of Parenteral and Enteral Nutrition*, vol. 38, no. 3, pp. 334–377, 2014.

[7] M. Kozeniecki and R. Fritzshall, "Enteral nutrition for adults in the hospital setting," *Nutrition in Clinical Practice*, vol. 30, no. 5, pp. 634–651, 2015.

[8] G. Elke, M. Wang, N. Weiler, A. G. Day, and D. K. Heyland, "Close to recommended caloric and protein intake by enteral nutrition is associated with better clinical outcome of critically ill septic patients: secondary analysis of a large international nutrition database," *Critical Care*, vol. 18, no. 1, p. R29, 2014.

[9] A. Sedaghat, F. Yahyapoor, Z. Dehnavi et al., "The prevalence and possible causes of enteral tube feeding intolerance in critically ill patients: a cross-sectional study," *Journal of Research in Medical Sciences*, vol. 26, no. 1, 2021.

[10] K. Wang, K. McIlroy, L. D. Plank, M. S. Petrov, and J. A. Windsor, "Prevalence, outcomes, and management of enteral tube feeding intolerance: a retrospective cohort study in a tertiary center," *JPEN - Journal of Parenteral and Enteral Nutrition*, vol. 41, no. 6, pp. 959–967, 2017.

[11] W. Chen, H. Wang, Y. Chen, D. Yuan, and R. Chen, "The independent risk factors of early diarrhoea in enteral nutrition for ICU patients," *Journal of International Medical Research*, vol. 47, no. 10, pp. 4929–4939, 2019.

[12] S. Ferrie and V. East, "Managing diarrhoea in intensive care," *Australian Critical Care*, vol. 20, no. 1, pp. 7–13, 2007.

[13] World Health Organization, http://www.who.int/mediacentre/factsheets/fs330/en/, 2013.

[14] R. P. Arasaradnam, S. Brown, A. Forbes et al., "Guidelines for the investigation of chronic diarrhoea in adults: British Society of Gastroenterology, 3rd edition," *Gut*, vol. 67, no. 8, pp. 1380–1399, 2018.

[15] P. Pushpanathan, G. S. Mathew, S. Selvarajan, K. G. Seshadri, and P. Srikanth, "Gut microbiota and its mysteries," *Indian Journal of Medical Microbiology*, vol. 37, no. 2, pp. 268–277, 2019.

[16] R. L. Koretz, "Probiotics in gastroenterology: how pro is the evidence in adults?" *American Journal of Gastroenterology*, vol. 113, no. 8, pp. 1125–1136, 2018.

[17] R. Thibault, S. Graf, A. Clerc, N. Delieuvin, C. P. P. C. Heidegger, and C. Pichard, "Diarrhoea in the ICU: respective contribution of feeding and antibiotics," *Critical Care*, vol. 17, no. 4, p. R153, 2013.

[18] J. H. Song and Y. S. Kim, "Recurrent *Clostridium difficile* infection: risk factors, treatment, and prevention," *Gut and Liver*, vol. 13, no. 1, pp. 16–24, 2019.

Hindawi
Emergency Medicine International
Volume 2023, Article ID 9820756, 1 page
https://doi.org/10.1155/2023/9820756

Retraction

Retracted: Clinical Features and Surgical Strategies of Distal Radius Posttraumatic Deformity

Emergency Medicine International

Received 28 November 2023; Accepted 28 November 2023; Published 29 November 2023

This article has been retracted by Hindawi, as publisher, following an investigation undertaken by the publisher [1]. This investigation has uncovered evidence of systematic manipulation of the publication and peer-review process. We cannot, therefore, vouch for the reliability or integrity of this article.

Please note that this notice is intended solely to alert readers that the peer-review process of this article has been compromised.

Wiley and Hindawi regret that the usual quality checks did not identify these issues before publication and have since put additional measures in place to safeguard research integrity.

We wish to credit our Research Integrity and Research Publishing teams and anonymous and named external researchers and research integrity experts for contributing to this investigation.

The corresponding author, as the representative of all authors, has been given the opportunity to register their agreement or disagreement to this retraction. We have kept a record of any response received.

References

[1] N. Zhang and J. Fang, "Clinical Features and Surgical Strategies of Distal Radius Posttraumatic Deformity," *Emergency Medicine International*, vol. 2022, Article ID 5268822, 7 pages, 2022.

Hindawi
Emergency Medicine International
Volume 2022, Article ID 5268822, 7 pages
https://doi.org/10.1155/2022/5268822

Research Article

Clinical Features and Surgical Strategies of Distal Radius Posttraumatic Deformity

Ning Zhang [1] **and Jiahu Fang** [2]

[1]*Department of Orthopedics, Yixing People's Hospital, Yixing, Jiangsu 214200, China*
[2]*Department of Orthopedics, Jiangsu Province Hospital, Nanjing, Jiangsu 210000, China*

Correspondence should be addressed to Jiahu Fang; jiahu2020@126.com

Received 29 July 2022; Revised 12 August 2022; Accepted 16 August 2022; Published 19 September 2022

Academic Editor: Hang Chen

Objective. To investigate the clinical features and surgical strategies of distal radius posttraumatic deformity. *Methods*. A retrospective analysis was performed on the data of 30 patients with distal radius posttraumatic deformity treated by osteotomy and orthopedic surgery in the department of orthopedics, the First Affiliated Hospital of Nanjing Medical University, from February 2016 to November 2018. All the patients underwent preoperative anterior and lateral X-ray plain scanning of bilateral wrist joints, showing different degrees of radius shortening, inferior ulnar and radial mismatch, palmar angle, and ulnar deviation angle, among which 11 patients had an uneven joint surface. After a full evaluation, osteotomy and orthopedic surgery were performed to restore the original anatomical structure, plaster fixation was performed for two weeks after surgery, and regular outpatient follow-up was conducted. The function of the wrist was evaluated by the MMWS (wrist joint improvement) scoring scale before and after surgery, and the changes in the wrist joint-related treatment parameters were evaluated according to X-ray. *Results*. All 30 patients had no neurological symptoms after surgery, and all wounds healed within the first stage. All patients were followed up for 6–12 months, with an average healing time of 3.5 months. There was no reduction loss, internal fixation loosening, or fracture in the regular postoperative review. Postoperative MMWS (wrist joint improvement) score scale data were significantly higher than those before surgery, and there were differences between groups ($P < 0.05$). Postoperative treatment parameters of wrist joints such as palmar inclination angle, ulnar deviation angle, radius height, and lower ulnar and radial matching were significantly improved, and there were differences between groups ($P < 0.05$). *Conclusions*. The patients with distal radius posttraumatic deformity have the clinical characteristics of shortening of radius, mismatch of lower ulnar and radius, an abnormal inclination of palm, and ulnar declination. For patients with distal radius posttraumatic deformity, osteotomy and orthopedic surgery can effectively improve wrist function and improve patients' quality of life, which is worthy of clinical reference.

1. Introduction

A distal radius fracture is a common fracture type in orthopedic clinics. The incidence of this fracture is high, accounting for about 20% of total body fractures [1–3], and it is mostly bipolar in age. In the elderly, osteoporosis is mostly low-energy fractures, and in young people, it is mostly high-energy fractures and powdery. Most distal radius fractures can achieve satisfactory treatment results through appropriate treatment in the early stage, but there are still some patients who fail to get the correct treatment in the early stage, leading to the occurrence of posttraumatic deformity.

A distal radius posttraumatic deformity often leads to biomechanical changes of the wrist and functional damage to the hand and forearm, among which ulnar deviation, abnormal palm inclination, and loss of radius height are the most common [4–7]. The posttraumatic deformity is a common complication of distal radius fractures, which can occur in or out of the joint. There are many reasons that can lead to malunion in the process of fracture healing, such as incorrect force lines, joint deformation, insufficient radius height, etc. [7–9].

Biomechanical research shows that the shortening of the radius by 2.5 mm can increase the axial pressure of the ulnar

column by 42%. The increase in ulnar pressure often causes TFCC damage and changes the harmony of the lower ulnar and radial joints. At the same time, when the radius is shortened by 10 mm, the pronation and supination functions of the lower ulnar and radial are reduced by 50% and 30%, respectively [10, 11]. Previous studies have also proved that dorsal angulation also transfers the vertical stress of the radiovolar side to the dorsal ulnar side. A 20° angle of dorsal deformity will increase the stress on the ulnar side by 50%, while a 45° angle of dorsal angulation will increase it by 67%. At the same time, due to the mismatch of the lower radioulnar joint, a rotation obstacle and instability of the lower radioulnar joint are caused, resulting in the instability of the radiocarpal joint and the instability of the metacarpophalangeal joint [12]. Similarly, the reduction of the ulnar deflection angle also changes the mechanical distribution of the wrist joint. The mechanical stop of the tendon changes due to the structural changes of the carpal tunnel, which affect the flexion of the finger and reduce the grip strength. At the same time, it changes the distribution of axial force at the distal end of the radius, increasing the force through the lunate fossa [13]. For the elderly with low-energy fractures, the slight unevenness of the articular surface can be tolerated. However, for young people with high-energy fractures, joint steps larger than 1-2 mm will lead to osteoarthritis of the wrist, with very poor clinical results [14, 15].

Therefore, the aim of this study is to explore the clinical characteristics and surgical strategies of posttraumatic deformity of the distal radius, in order to provide guidance for the treatment of posttraumatic deformity of the distal radius in the future.

2. Methods

2.1. Clinical Data. In this retrospective study, 30 patients diagnosed with the distal radius posttraumatic deformity treated in the First Affiliated Hospital of Nanjing Medical University from February 2016 to November 2018 were selected as the research objects. A total of 30 patients were included in this study, including 21 males and 9 females; the age ranged from 16 to 68 years, with an average of 47.5 years. They were all patients with posttraumatic deformities of the distal radius. The time from fracture to operation was 35–95 days, with an average of 59 days.

The study was admitted by the medical ethics committee of Yixing People's Hospital and Jiangsu Province Hospital. All patients had informed consent and signed the informed consent form.

2.2. Inclusion and Exclusion Criteria. Inclusion criteria: (1) patients with posttraumatic deformities of the distal radius confirmed by preoperative imaging data, including radius shortening, lower ulnar radial mismatch, palmar angle, ulnar deviation angle abnormalities, and articular surface irregularities; (2) patients who have no wound infection or damage before operation and whose soft tissue conditions allow internal fixation; (3) patients who have no obvious preoperative contraindications and can tolerate surgery; and (4) complete clinical data.

Exclusion standard: (1) patients with bone tumors, osteogenesis imperfecta, and other diseases; (2) patients with severe osteoporosis; (3) patients who cannot cooperate with rehabilitation treatment after operation; (4) patients with other diseases that affected the postoperative wrist function score in the past; and (5) elderly patients over 70 years old.

2.3. Intervention. All patients were divided into groups of less than 50 days and more than 50 days according to the length of the posttraumatic period. For patients within 50 days after trauma, we give priority to osteotomies along the original fracture line. For patients more than 50 days after trauma, we divided them into simple metaphysis deformity without intra-articular deformity and complex deformity involving the articular surface. For patients with simple metaphyseal deformity without intra-articular deformity, on the basis of dorsal release, a simple arc osteotomy or linear osteotomy is performed at the proximal end of the lower radioulnar joint through the volar approach. The osteotomy line is as close to the articular surface as possible, and the distal bone block of the osteotomy line is enough to place the steel plate. For patients with articular surface deformity, more than two osteotomy lines are often required. Osteotomy is often performed along the original bone fracture line on the articular surface to correct the unevenness of the articular surface, and then the metaphyseal osteotomy is performed at the same time. Before surgery, patients are usually instructed to take necessary functional exercises for 7–10 days, and the softness of soft tissue has been restored.

All patients were placed in the supine position, under brachial plexus anesthesia, with the affected limb abducted on the lateral operating table convenient for fluoroscopy and the tourniquet on 1/3 of the upper arm. Take a longitudinal incision on the radial side of the flexor carpi radialis and cut the skin, subcutaneous tissue, and deep fascia in turn. Blunt separation and entry along the radial flexor carpi and radial artery space exposing the pronator muscle. Protect the radial artery and median nerve and preserve the pronator muscle. The dorsal additional incision is used for soft tissue release and auxiliary reduction, and the dorsal radial column is used for auxiliary fixation when necessary. For patients with a simple metaphyseal deformity without joint deformity, a simple arc osteotomy or linear osteotomy is performed at the proximal end of the lower radioulnar joint. The steel plate at the distal end of the radius is placed as close as possible to the watershed of the articular surface and parallel to the articular surface. The gram needle temporarily fixes the distal bone block of the osteotomy line through the steel plate hole, and the height of the radius and the ulnar deflection angle are adjusted with the help of the steel plate. Then, press the steel plate and stick it to the radial shaft to complete the correction of the palmar angle and bone grafting, if necessary. For patients with articular surface deformity, it is often necessary to perform articular surface osteotomy along the fracture line of the articular surface and then perform radial

Table 1: Clinical characteristics of patients.

	All patients ($n = 30$)
Age (years)	47.5 ± 7.37
Sex	
Male (n%)	21 (70%)
Female (n%)	9 (30%)
BMI (kg/m^2)	17.15 ± 2.03
Marital status	
Married	13 (43.3%)
Single	6 (20%)
Divorced or separated	6 (20%)
Widowed	3 (10%)
Unknown/missing	2 (6.7%)
Uneven articular surface	11 (36.7%)

metaphysis osteotomy to restore the height of the radius, ulnar deviation angle, and palmar inclination after the articular surface is restored. During the operation, fluoroscopy was used to confirm that the relevant measurement data of the patient's wrist joint had been recovered, and then the incision was washed, sutured layer by layer, and wrapped with sterile excipients. Functional exercise should be carried out properly after two weeks of plaster fixation on the affected limb.

2.4. Observation Index

(1) MMWs (wrist joint improvement) rating scale: the patients were followed up at 1 month, 3 months, 6 months, and 12 months after the operation, and the MMWs (wrist joint improvement) score scale data of the patients after treatment were compared, including function, grip strength, activity strength, and pain. Then calculate the total score. The total score is 0–100 points; below 60 points are considered poor, 61–79 points are good, and 80–100 points are excellent.

(2) The treatment parameters of the ulnar deviation angle, palmar inclination angle, lower ulnar radial matching degree, and radial height were observed.

2.5. Statistical Analysis. All data of patients were included in spss22.0 software for summary and processing. The chi-square test was used for the relevant basic data, and the t-test was used for the data of the MMWS (wrist joint improvement) rating scale and treatment parameters. The difference was statistically significant in ($X \pm s$) and $P < 0.05$.

3. Results

3.1. Clinical Data. A total of 30 patients were included in this study, including 21 males and 9 females; the age ranged from 16 to 68 years, with an average of 47.5 years. They were all patients with the posttraumatic deformity of the distal radius. The time from fracture to operation was 35–95 days, with an average of 59 days. All patients had clinical complaints such as pain and wrist dysfunction, and there was a strong need to improve function. There were various degrees of radial shortening, lower ulnar radial mismatch, palmar angle, ulnar deviation angle abnormalities, and other abnormalities, including 11 cases of joint surface irregularities (Table 1).

3.2. Comparison of MMWS before and after Surgery. All 30 patients had no loss of correction and no neurological symptoms. The wounds healed in one stage. All patients were followed up for 6–12 months, with an average healing time of 3.5 months. No correction loss, internal fixation loosening, or fractures were found in the regular follow-up after the operation. The scores of MMWs (wrist joint improvement) after the operation were significantly higher than those before the operation. There was a difference between the two groups, from 36.72 ± 5.89 before the operation to 83.41 ± 9.29 after the operation ($P < 0.05$) (Table 2).

3.3. Comparison of Wrist-Related Treatment Parameters before and after Surgery. The patients after surgery, compared with those before surgery, had a remarkable difference in improvement of palmar inclination, ruler deflection angle, lower ulnar radial matching degree, and radius height, from 1.62 ± 1.32 to 16.73 ± 3.76, 8.03 ± 2.56 to 19.52 ± 3.71, 8.16 ± 2.14 to 1.93 ± 0.91, and 1.52 ± 0.41 to 8.14 ± 3.32, respectively ($P < 0.05$) (Table 3).

3.4. Imaging Manifestation. As shown in Figure 1, the patient had malunion of the left distal radius, shortening of the radius, mismatching of the lower ulna and radius, and significantly abnormal ulnar declination and dorsal inclination. The operation plan was designed according to the contralateral wrist joint before the operation. The operation was performed through a dorsal approach, a volar approach, a simple arc osteotomy of the metaphysis, and a correction of radial height, ulnar deviation, and palmar inclination with the help of a distal radial plate. The wrist deformity and pain disappeared, and the function was significantly improved.

Furthermore, in the other patients, there was malunion of the right distal radius, shortening of the radius, mismatching of the lower ulna and radius, ulnar deviation, abnormal palmar inclination, and an uneven articular surface. The operation plan was designed according to the contralateral wrist joint before the operation. The combined volar-dorsal approach was selected for the operation. The osteotomy was performed from the volar approach through the articular surface along the original bone fracture line. The articular surface was first restored to be flat, and then the metaphyseal osteotomy was performed. The height of the radius was adjusted, the inclination of the palm and the deviation of the ulna were adjusted, and the plate and screw were fixed. Imaging examination showed that the relevant treatment parameters at the wrist were basically the same as those on the contralateral side. After follow-up, the wrist deformity and pain disappeared, and the wrist function basically returned to normal (Figure 2).

Table 2: MMWS (wrist joint improvement) rating scale before and after surgery.

	Function	Grip	Activity	Pain	Total score
Before surgery ($n = 30$)	8.03 ± 1.56	4.16 ± 0.64	6.38 ± 2.16	13.44 ± 3.25	36.72 ± 5.89
After surgery ($n = 30$)	$22.92 \pm 2.73^*$	$21.64 \pm 3.78^*$	$22.68 \pm 3.89^*$	$20.53 \pm 5.05^*$	$83.41 \pm 9.29^*$
t	25.94	24.97	20.07	6.47	23.25
P value	< 0.05	< 0.05	< 0.05	< 0.05	< 0.05

Table 3: Wrist related treatment parameters before and after surgery.

	Palmar inclination	Ruler deflection angle	Lower ulnar radial matching degree (mm)	Radius height (mm)
Before surgery ($n = 30$)	1.62 ± 1.32	8.03 ± 2.56	8.16 ± 2.14	1.52 ± 0.41
After surgery ($n = 30$)	$16.73 \pm 3.76^*$	$19.52 \pm 3.71^*$	$1.93 \pm 0.91^*$	$8.14 \pm 3.32^*$
t	20.77	13.97	14.68	10.84
P value	< 0.05	< 0.05	< 0.05	< 0.05

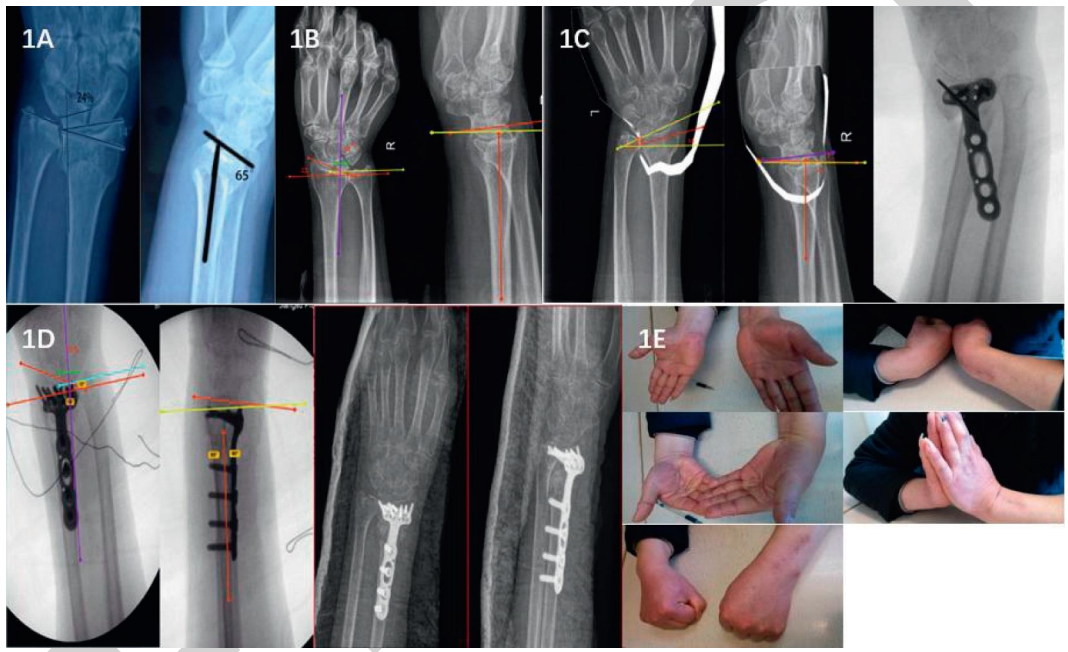

Figure 1: The imaging manifestation. (a) The deformity of the distal radius of the affected side before operation. (b) Anteroposterior and lateral radiographs of the contralateral distal radius joint of the patient. (c) Preoperative plan and intraoperative orthopedic diagram. (d) After deformity correction, the distal radius returned to normal metacarpal angle, ulnar deviation angle, radius height, and lower ulnar radial matching degree. (e) The wrist function of the patient recovered well after the operation.

4. Discussion

Most patients with posttraumatic deformities of the distal radius have obvious complaints of wrist deformity and wrist dysfunction and have strong surgical demands [7]. Patients with posttraumatic deformity of the distal radius often have complaints of wrist deformity, pain, and limited movement, and often have carpal tunnel syndrome caused by volar bone mass displacement and median nerve compression [9]. It is often seen in imaging that the characteristics of lower ulnar radial mismatch, radial shortening, abnormal ulnar declination/abnormal palmar inclination, and an uneven articular surface seriously affect the function of the wrist joint. Orthopedic surgery can significantly improve these conditions, restore wrist function, and improve the quality of life of patients with the above-mentioned posttraumatic joint deformity of the distal radius [16]. Once the diagnosis of deformity is made and the operation plan is determined, a reasonable osteotomy should be carried out as soon as possible to correct the deformity of the wrist and avoid or reduce the contracture of the soft tissue of the wrist [17]. A reasonable preoperative plan is very important for the correction of the deformity. In addition to the anteroposterior and lateral X-ray of the wrist joint of the affected limb before the operation, it is also necessary to take the anteroposterior and lateral X-ray of the wrist joint of the healthy side as the standard of orthopedics, which is crucial to the formulation of the preoperative plan [18].

In the course of our research, we found that for the malunion of simple fractures with few fracture lines,

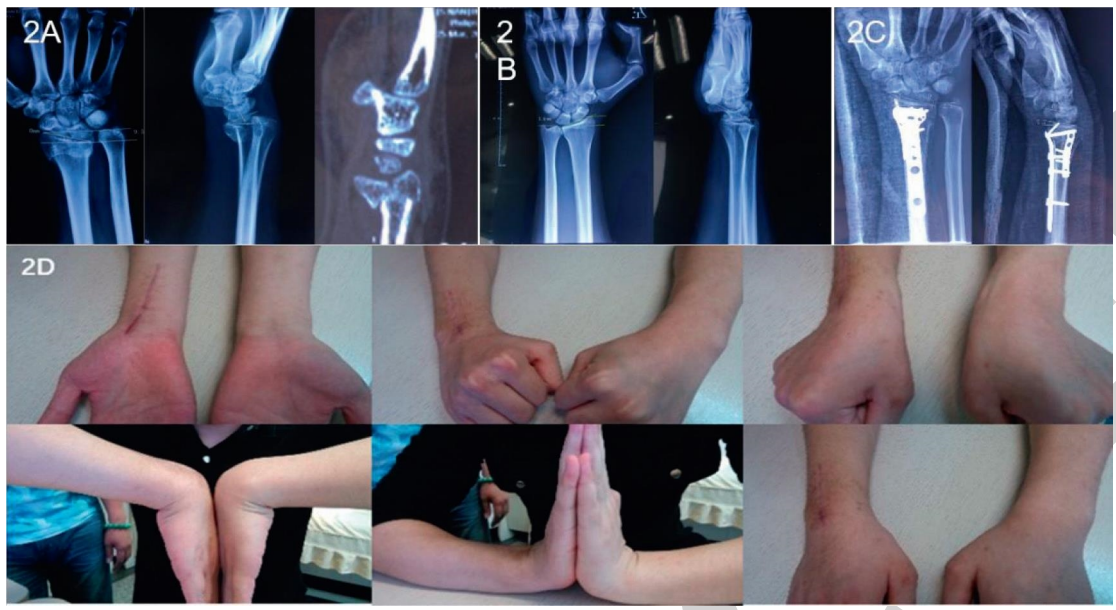

Figure 2: (a) The deformity parameters of the distal radius fracture before operation. (b) Preoperative contralateral normal parameters of patients. (c) Parameters after correction of postoperative deformity. (d) The wrist function after the operation.

osteotomy and orthopedic surgery should be performed as early as possible, and osteotomy should be performed along the original fracture line. Early intervention surgery is technically easier and reduces the overall time of disability. However, delayed surgery is also a suitable choice for some special cases, such as severely comminuted fractures. It is best to determine the final treatment plan after the fracture is completely healed, and for such complex fractures with many fracture lines, the restorative line is often the main focus rather than blindly pursuing anatomical repositioning. If there is an uneven articular surface, it is recommended to perform osteotomy and orthopedic surgery as soon as possible to restore the smoothness of the articular surface.

Previous studies have pointed out that correct osteotomy and orthopedics can improve the motion function of the wrist joint and forearm and relieve pain [19], and some studies have pointed out that the osteotomy should pass through the initial fracture line so that the most original fracture block can be reproduced [20]. During our research and observation, we found that for metaphyseal deformities that have not yet fully healed and unevenness caused by articular surface malunion, we give priority to osteotomy along the original fracture line, but for metaphyseal deformities that have been healed for a long time, we can perform arc or linear osteotomy near the articular surface at the proximal end of the lower radius and ulna to ensure that the distal bone block of the osteotomy line is enough to place the steel plate.

In the orthopedic process, the choice of fixation and surgical approach is equally important. With the development of technology, the volar approach for osteotomy and the placement of main plates have become mainstream [21, 22]. However, a dorsal incision is also indispensable. The dorsal approach for soft tissue release is necessary for orthopedic surgery. Patients with complex deformities and multiple osteotomy lines often need dorsal double columns for auxiliary fixation. During our operation, we choose the volar approach as the main approach, supplemented by the dorsal approach. The dorsal approach is mostly used to release soft tissue as the basis of osteotomy and orthopedics. During the operation, the steel plate can be used for auxiliary orthopedic reduction, such as the reduction of ulnar deflection with the help of the compression of the radial column steel plate, the reduction of palmar inclination with the help of the dorsal steel plate, etc.

Bone grafting is often needed to restore the relevant angle and further maintain joint stability during osteotomy and orthopedic surgery for posttraumatic deformities of the distal radius. The commonly used bone grafting method in clinics is structural bone grafting, mainly using iliac bone blocks, fibula, ribs, and allogeneic bone, of which the iliac bone block is the most commonly used. The iliac bone block is rich in cancellous bone, and studies have reported that its bone graft fusion rate is as high as 95%, which is the gold standard for bone defect repair [23]. However, there are still some deficiencies in the iliac bone graft, such as long-term pain and numbness in the bone donor area. Some studies have pointed out that the center of iliac bone mass often has the risk of bone necrosis, absorption, collapse, and displacement due to insufficient blood supply [24]. Nonstructural bone grafting refers to the use of granular bone blocks with a diameter of less than 5 mm for bone grafting, which is simple to prepare and implant and has a high fusion rate [25–27]. The fusion time of patients with nonstructural bone grafting is often shorter than that of structural bone grafting, but the granular bone is looser than the complete iliac bone block, and it is not as durable as the iliac bone block for the maintenance of articular surface and angle. The literature shows that there is no significant difference between structural bone grafting and nonstructural bone

grafting for osteotomy and correction of the distal radius deformity [28]. Our experience is similar to the literature. Nonstructural bone grafting has also achieved good clinical results.

A fracture of the styloid process of the ulna is a common injury related to the fracture of the distal radius. 53% of the distal radius fractures are accompanied by ulnar styloid process fractures, and 26% of them often have nonunion [29]. There has been a long debate about whether the fracture of the styloid process of the ulna has an impact on the healing of the fracture of the distal radius. The styloid process of the ulna plays an indispensable role in maintaining the biomechanical stability of the wrist, affecting the pronation and supination functions of the wrist. Found that whether the fracture of the styloid process of the ulna is anatomically reduced or whether it is completely healed has little effect on the improvement of the wrist function. Combined with recent research and our clinical experience, it is found that without affecting the stability of the radioulnar joint and the anatomical reduction of the distal radius, whether the fracture of the styloid process of the ulna is anatomically reduced or completely healed, the wrist function of the patient can recover to a good level after the operation. However, open reduction and internal fixation or reduction with the help of the radioulnar ligament should be used for those with an ulnar styloid process fracture displacement of more than 2 mm at the base and those with an extremely unstable distal radioulnar joint.

Although previous studies have carried out relatively complete research and a summary on the wrist deformity and wrist dysfunction of patients with posttraumatic deformity of the distal radius, there are still few clinical data on the treatment and correction of patients. Our study can supplement some samples and evidence for this field. Our study also has a series of deficiencies, such as too few samples and a follow-up time that is only controlled within one year. These deficiencies need to be corrected by expanding the sample and continuing the follow-up.

In summary, the posttraumatic deformity of the distal radius has its own unique clinical characteristics. Based on the full evaluation of the deformity of the patient combined with the demands of the patient, the deformity should be corrected using the contralateral limb as the template. There should be a detailed preoperative plan and a good osteotomy design. Sufficient soft tissue release is required during the operation. An anatomical steel plate is a powerful tool for intraoperative correction and reduction. Osteotomy and correction of the posttraumatic deformity of the distal radius can effectively improve the function of the wrist joint and significantly improve the quality of life of patients.

Data Availability

The data used to support the findings of this study are available from the corresponding author upon request.

Conflicts of Interest

The authors declare that they have no conflicts of interest.

References

[1] A. M. Ilyas and J. B. Jupiter, "Distal radius fractures–classification of treatment and indications for surgery," *Orthopedic Clinics of North America*, vol. 38, no. 2, pp. 167–173, 2007.

[2] F. T. Beil, F. Barvencik, M. Gebaur et al., "The distal radius, the most frequent fracture localization in humans: a histomorphometric analysis of the microarchitecture of 60 human distal radii and its changes in aging," *The Journal of Trauma*, vol. 70, pp. 154–158, 2011.

[3] E. Brogren, M. Hofer, M. Petranek, L. B. Dahlin, and I. Atroshi, "Fractures of the distal radius in women aged 50 to 75 years: natural course of patient-reported outcome, wrist motion and grip strength between 1 year and 2–4 years after fracture," *Journal of Hand Surgery*, vol. 36, no. 7, pp. 568–576, 2011.

[4] H. Hirahara, P. G. Neale, Y. T. Lin, W. P. Cooney III, and K. N. An, "Kinematic and torquerelated effects of dorsally angulated distal radius fractures and the distal radial ulnar joint," *The Journal of Hand Surgery*, vol. 28, no. 4, pp. 614–621, 2003.

[5] M. A. Mulders, P. N. d'Ailly, B. Cleffken, and N. W. Schep, "Corrective osteotomy is an effective method of treating distal radius malunions with good long-term functional results," *Injury*, vol. 48, no. 3, pp. 731–737, 2017.

[6] M. M. J. Walenkamp, S. Aydin, M. A. M. Mulders, J. C. Goslings, and N. W. L. Schep, "Predictors of unstable distal radius fractures: a systematic review and meta-analysis," *Journal of Hand Surgery*, vol. 41, no. 5, pp. 501–515, 2015.

[7] B. D. Bushnell and D. K. Bynum, "Malunion of the distal radius," *Journal of the American Academy of Orthopaedic Surgeons*, vol. 15, no. 1, pp. 27–40, 2007.

[8] K. J. Prommersberger, T. Pillukat, M. Mühldorfer, and J. van Schoonhoven, "Malunion of the distal radius," *Archives of Orthopaedic and Traumatic Surgery*, vol. 132, no. 5, pp. 693–702, 2012.

[9] S. C. Haase and K. C. Chung, "Management of malunions of the distal radius," *Hand Clinics*, vol. 28, no. 2, pp. 207–216, 2012.

[10] R. Hollingsworth and J. Morris, "The importance of the ulnar side of the wrist in fractures of the distal end of the radius," *Injury*, vol. 7, no. 4, pp. 263–266, 1975.

[11] F. W. Werner, A. K. Palmer, M. D. Fortino, and W. H. Short, "Force transmission through the distal ulna: effect of ulnar variance, lunate fossa angulation, and radial and palmar tilt of thedistal radius," *The Journal of Hand Surgery*, vol. 17, no. 3, pp. 423–428, 1992.

[12] F. Verhaegen, I. Degreef, and L. De Smet, "Evaluation of corrective osteotomy of the malunited distal radius on midcarpal and radiocarpal malalignment," *The Journal of Hand Surgery*, vol. 35, no. 1, pp. 57–61, 2010.

[13] D. L. Fernandez, J. T. Capo, and E. Gonzalez, "Corrective osteotomy for symptomatic increased ulnar tilt of the distal end of the radius," *The Journal of Hand Surgery*, vol. 26, no. 4, pp. 722–732, 2001.

[14] D. D. Anderson, B. R. Deshpande, T. E. Daniel, and M. E. Baratz, "A three-dimensional finite element model of the radiocarpal joint: distal radius fracture step-off and stress transfer," *The Iowa Orthopaedic Journal*, vol. 25, pp. 108–117, 2005.

[15] C. A. Goldfarb, J. R. Rudzki, L. W. Catalano, M. Hughes, and J. J. Borrelli, "Fifteen-year outcome of displaced intra-

Hindawi
Emergency Medicine International
Volume 2023, Article ID 9847534, 1 page
https://doi.org/10.1155/2023/9847534

Retraction

Retracted: Study on the Influencing Factors of Osteoarthritis in Southern China

Emergency Medicine International

Received 8 August 2023; Accepted 8 August 2023; Published 9 August 2023

This article has been retracted by Hindawi following an investigation undertaken by the publisher [1]. This investigation has uncovered evidence of one or more of the following indicators of systematic manipulation of the publication process:

(1) Discrepancies in scope
(2) Discrepancies in the description of the research reported
(3) Discrepancies between the availability of data and the research described
(4) Inappropriate citations
(5) Incoherent, meaningless and/or irrelevant content included in the article
(6) Peer-review manipulation

The presence of these indicators undermines our confidence in the integrity of the article's content and we cannot, therefore, vouch for its reliability. Please note that this notice is intended solely to alert readers that the content of this article is unreliable. We have not investigated whether authors were aware of or involved in the systematic manipulation of the publication process.

Wiley and Hindawi regrets that the usual quality checks did not identify these issues before publication and have since put additional measures in place to safeguard research integrity.

We wish to credit our own Research Integrity and Research Publishing teams and anonymous and named external researchers and research integrity experts for contributing to this investigation.

The corresponding author, as the representative of all authors, has been given the opportunity to register their agreement or disagreement to this retraction. We have kept a record of any response received.

References

[1] D. Lu, X. Ding, and W. Lu, "Study on the Influencing Factors of Osteoarthritis in Southern China," *Emergency Medicine International*, vol. 2022, Article ID 2482728, 6 pages, 2022.

Hindawi
Emergency Medicine International
Volume 2022, Article ID 2482728, 6 pages
https://doi.org/10.1155/2022/2482728

Research Article

Study on the Influencing Factors of Osteoarthritis in Southern China

Danqing Lu,[1] Xiaomin Ding,[2] and Wenqing Lu [1]

[1]*Department of Orthopedics, The Second People's Hospital of Kunshan, Suzhou, Jiangsu, China*
[2]*Department of Orthopedics, The Second Affiliated Hospital of Nantong University, Nantong, Jiangsu, China*

Correspondence should be addressed to Wenqing Lu; wenqinglu5066@163.com

Received 3 August 2022; Revised 26 August 2022; Accepted 31 August 2022; Published 14 September 2022

Academic Editor: Hang Chen

Background. Osteoarthritis (OA) is a common chronic disease with numerous and interacting influencing factors, and current inadequate patient perceptions and behaviors in access to care contribute to the difficulties in the diagnosis, treatment, and management of osteoarthritis. *Objective*. The purpose of this study was to investigate the influencing factors of osteoarthritis (OA) in a southern Chinese population and to provide a scientific basis for the prevention and treatment of OA. *Methods*. A 1 : 2 matched case-control study was used to select 160 patients with OA from three hospitals in southern China as a case group. Three hundred and twenty cases of the same sex and similar age (within ± 2 years) were selected as the control group, and relevant data were collected for univariate and multivariate conditional logistic regression analysis. *Results*. There were no significant differences between the two groups of participants in terms of age, sex, and education ($P > 0.05$). Logistic regression statistical analysis showed that genetic factors (OR = 4.52, 95% CI = 1.56–7.83), body mass index (OR = 2.57, 95% CI = 1.16–5.84), alcohol consumption (OR = 3.81, 95% CI = 1.53–5.87), and a history of external joint limb injury (OR = 3.37, 95% CI = 1.67–5.24) would increase the risk of OA. In contrast, eating more fresh vegetables (OR = 0.08, 95% CI = 0.03–0.31), more fresh fruits (OR = 0.34, 95% CI = 0.12–0.96), more soy products (OR = 0.11, 95% CI = 0.04–0.45), and exposure to sunlight (OR = 0.31, 95% CI = 0.14–0.71) would reduce the OA risk of OA. *Conclusion*. Obesity, alcohol consumption, and a history of joint trauma all increase the risk of OA in a southern Chinese population, whereas a diet rich in fresh vegetables, fresh fruit, soy products, and sun exposure would reduce the risk of OA. In the future, we should focus on improving patients' awareness of medical care and developing their self-management skills, improving GPs' treatment skills, improving negative attitudes of both doctors and patients, and promoting positive patient care.

1. Introduction

On January 23, 2000, the World Health Organization (WHO) launched a worldwide campaign for the "Decade of Bones and Joints," which aims to draw the attention of governments, medical research institutions, public, and all sectors of society to bone diseases, including osteoarthritis [1]. On October 12, 2001, the Ministry of Health (MOH) of China also held an awareness campaign for World Arthritis Day and decided to establish the MOH Arthritis Prevention and Control Education Program Fund [2]. Osteoarthritis (OA), also known as osteoarthritis, degenerative osteoarthropathy or proliferative arthritis, is an inflammatory disease characterized by damage to joint cartilage and osteophytes [3]. The etiology and pathogenesis of osteoarthritis are still unclear, and its occurrence is related to age, obesity, inflammation, trauma, and genetic factors, among which age is the main factor [4]. Preliminary surveys at home and abroad have shown that the overall incidence of osteoarthritis is about 15%, 10%–17% in people over 40 years, and 50% in people over 60 years [5]. Currently, there are 16 million patients with osteoarthritis in the United States, and in China, the population over 60 years is over 100 million, and it is estimated that there are more than 50 million patients with osteoarthritis [6]. Osteoarthritis occurs in joints with high load and high activity, such as the knee, spine (cervical and lumbar spine), hip, ankle, hand, and other joints. In Asia, osteoarthritis of the knee is

predominant, which may be related to different living habits and living environments. The epidemiological findings show that the peak prevalence of osteoarthritis in men and women can reach 24.7% and 54.6%, respectively, which is one of the diseases that greatly endanger the health of the elderly and seriously affect their quality of life [7]. With the rapid development of social economy, people's social lifestyle has changed, and the concept of health and medical model is also changing. It is too one-sided to evaluate the health status and treatment effect of patients only by quantitative indicators such as morbidity, mortality, survival rate, and cure rate. Osteoarthritis, as a chronic disease, seriously affects patients' work, family, and social interactions, so we need to explore the factors influencing osteoarthritis (OA) in southern China more comprehensively to provide a scientific basis for the prevention and treatment of OA.

Age is an independent risk factor for the development of osteoarthritis, and the prevalence of osteoarthritis increases with age [8, 9]. The overall prevalence of osteoarthritis is about 15%, 10%–17% in middle-aged and elderly people aged ≥40 years, 50% in those aged ≥60 years, and 80% in those aged ≥75 years [10,11]. OA has become one of the major diseases among the elderly in China, and prevention and reduction of OA has special significance in our current national situation. The study by Farhadian et al. [12] found that with the rising level of population aging in China, the family and socioeconomic burden of osteoarthritis patients has further increased. A study of 195 countries over the past 27 years found that the prevalence, incidence, and years of disability survival (YLDs) of osteoarthritis varied among countries, but with increasing life expectancy and an aging global population, all of these indicators are on the rise, posing a serious challenge to the world public health [13,14]. A study Jin et al. [15] found that nearly 2/3 of patients had poor understanding of the clinical manifestations of the osteoarthritis disease. There is a general lack of disease knowledge related to osteoarthritis basics, risk factors, diagnosis and treatment, and prevention in the middle-aged and elderly population in China [16, 17]. In this study, we selected orthopaedic and general practitioners in general hospitals and community general practitioners and patients to conduct a mixed-method study to understand the current status of patients' perceptions and behaviors of osteoarthritis, analyze the problems and barriers affecting patients' access to care and disease management, and provide optimal strategies for improving the access to care and disease prognosis of patients with osteoarthritis.

2. Materials and Methods

2.1. Participants

2.1.1. Case Group. A total of 160 patients with OA were recruited and investigated from June to December 2019, visits from orthopaedic specialists at 3 hospitals in southern China of OA. The inclusion criteria are as follows: X-ray-diagnosed patients with positive OA. There are typical clinical manifestations of OA. Patients diagnosed with OA by an orthopaedic specialist. The above 3 standards must be met at the same time. All procedures performed in studies involving human participants were in accordance with the ethical standards of the institutional or national research committee and with the 1964 Helsinki declaration and its later amendments are comparable ethical standards. This study is approved by the Ethics Committee of The Second People's Hospital of Kunshan.

2.1.2. Control Group. A hospital-based 1 : 2 paired case-control study was used. Patients who did not have OA in other outpatient clinics of the same hospital during the same period were used as a control. The matching conditions are the same sex and the age difference is less than 2 years.

2.2. Research Methods and Quality Control. After the written informed consent of the study subjects, a questionnaire survey was conducted in the same way for the case group and the control group. Self-designed questionnaires, including general conditions, living habits, genetic factors, past history, and specialties. Investigate the investigators uniformly before the investigation, and investigate the cases and controls in a unified way. Logically check the data before entering it, and correct any errors in a timely manner.

2.3. Statistical Analysis. After the data were collected and sorted, EpiData 3.2 software was used to establish the database. SPSS 23.0 statistical software was used to perform single-factor and multifactor conditional logistic regression analysis. Count data is described by n (%), and measurement data is expressed by mean ± standard deviation. $P < 0.05$ was considered statistically significant.

3. Results

3.1. General Demographics. A total of 501 questionnaires were returned, excluding 21 incomplete questionnaires, and a total of 480 valid questionnaires were obtained. There were 160 cases in the case group and 320 cases in the control group, of which 204 were male and 276 were female, with a sex ratio of 1 : 1.35. The age of the case group was 78 years, the youngest was 26 years, and the mean age was (57.36 ± 6.58) years. The age of the control group was 79 years, the youngest was 26 years, and the mean age was (58.06 ± 5.99) years. There was no significant difference between the two groups in terms of age and gender ($P > 0.05$). The education level of the case group was as follows: 39.79% were elementary school and below, 26.04% were junior high school, 22.50% were high school or secondary school, and 11.67% were college and above. The educational level of the control group was 40.31% for elementary school and below, 25.63% for middle school, 23.12% for high school or secondary school, and 10.94% for college and above. There was no significant difference between the two groups in terms of education ($P > 0.05$). The results are shown in Table 1.

Table 1: The assignment of each study variable.

Variables	Assignments
Living environment	Quiet = 0 and noisy = 1
Genetic factors(family with or without a history of OA)	None = 0, 1 person = 1, 2 persons = 2, 3 and above = 3
Staple food	Mainly coarse and coarse grains = 0 and mainly polished rice and flour = 1
BMI (kg/m^2)	<23 = 0, 23~25 = 1, and >25 = 2
Family per capita monthly income (RMB)	<2000 = 0, 2000~5000 = 1, and >5000 = 2
Consumption of fresh vegetables	Rarely = 0, <400 g/d = 1, and ≥400 g/d = 2
Consumption of fresh fruits	Rarely = 0, <100 g/d = 1, and ≥100 g/d = 2
Egg consumption	Rarely = 0, 1~3 eggs/week = 1, 4~6 eggs/week = 2, and ≥7 eggs/week = 3
Consumption of soy products	Rarely = 0, <100 g/d = 1, and ≥100 g/d = 2
Smoking	None = 0 and smoking = 1
Drinking	None = 0 and drinking = 1
Difficulty in falling asleep, awakening during sleep, or dreaming often	None = 0 and yeah = 1
Have a nap habit	None = 0 and yeah = 1
Sunshine duration (h/d)	<4 = 0 and ≥4 = 1
Take part in the physical exercise	None = 0 and yeah = 1
History of joint trauma	None = 0 and yeah = 1

3.2. Prevalence of OA and Univariate Analysis. The OA patients were mainly affected by the knee joint, accounting for 60.42%, followed by the low and middle lumbar joints (20.21%). The disease involved 54 patients with one joint, 66 with two, 23 with three, and 17 with more than three. Logistic analysis showed that there were statistically significant differences in 16 indicators between the case and the control group ($P < 0.05$). The statistical analysis results are shown in Table 2.

The noisy living environment, the consumption of polished rice and noodles, overweight or obesity, smoking, and drinking are the risk factors for OA. Regular consumption of fresh vegetables, fruits, eggs, soy products, the habit of taking a nap, long sunshine hours, and regular physical exercises are the protective factors.

3.3. Multivariate Stepwise Conditional Logistic Regression Analysis. The proposed variables were included in the standard α in = 0.05 and the standard α out = 0.05. The multifactor conditional logistic regression analysis was performed on the above factors. The 16 factors with statistical significance were screened for variables using the backward stepwise method. The factors that were finally selected in the regression equation included genetic factors, body mass index (BMI), consumption of fresh vegetables, consumption of fresh fruits, consumption of soy products, sunshine duration, drinking, and history of joint trauma. Logistic regression statistical analysis results suggest that genetic factors (OR = 4.52, 95% CI = 1.56–7.83), body mass index (OR = 2.57, 95% CI = 1.16–5.84), alcohol consumption (OR = 3.81, 95% CI = 1.53–5.87), and a history of external injury of the joint limb (OR = 3.37, 95% CI = 1.67–5.24) will increase the risk of OA. While taking more fresh vegetables (OR = 0.08, 95% CI = 0.03–0.31), taking more fresh fruits (OR = 0.34, 95% CI = 0.12–0.96), taking more soy products (OR = 0.11, 95% CI = 0.04–0.45), and exposure to the sun (OR = 0.31, 95% CI = 0.14–0.71) will reduce the risk of OA. The results of statistical analysis are shown in Table 3.

4. Discussion

The degradation of cartilage is a hallmark of osteoarthritis, a joint condition brought on by mechanical, metabolic, inflammatory, and immunological mechanisms [18, 19]. Reduced force absorption caused by damaged articular cartilage and increased wear on the ends of joints contributes to the disease's etiology, which can lead to progressive joint injury and degeneration. Clinical studies have shown that patients with osteoarthritis are commonly found in the joints that bear large amounts of weight, such as the ankle, knee, and hip. Once suffering from osteoarthritis, patients suffer from joint pain and functional impairment in going up and down the stairs, walking or getting off and getting into a car, and the quality of daily life is significantly reduced, and the physical and mental health of patients are compromised [20,21]. With the continuous improvement of the medical level, more and more patients with osteoarthritis choose to perform total knee arthroplasty, however, related studies have concluded that human work and life pressures are increasing, and this situation also causes some people to have psychological disorders, which, together with osteoarthritis disease, is not conducive to the physical recovery of the patients after total knee arthroplasty, and the clinical treatment effect is not good [22,23].

The results of this study suggest that long-term consumption of high amounts of vegetables and fresh fruits can reduce the risk of OA, mainly because of the high levels of vitamin C. Studies Janssens et al. [24,25] have shown that the risk of knee OA is three times higher in people with low vitamin C intake than in the high intake group because vitamin C promotes the proliferation of chondrocytes and the synthesis of collagen fibers in the body. In addition,

Table 2: Logistic analysis of univariate conditions affecting OA.

Variables	*B*	Sex	Wald	*P*	OR (95% CI)
Living environment	1.385	0.265	13.57	<0.001	4.09 (1.99, 8.47)
Genetic factors	1.962	0.588	10.92	0.001	7.96 (2.38, 25.43)
Staple food	0.896	0.316	9.32	0.002	2.65 (1.38, 5.06)
BMI	0.795	0.263	9.41	0.001	2.28 (1.31, 3.97)
Family per capita monthly income (RMB)	0.341	0.142	7.42	0.006	1.42 (1.12, 1.86)
Consumption of fresh vegetables	−1.658	0.322	25.12	0.001	0.19 (0.10, 0.32)
Consumption of fresh fruits	−0.688	0.219	11.16	<0.001	0.45 (0.29, 0.71)
Egg consumption	−0.515	0.151	9.18	0.002	0.65 (0.49, 0.86)
Consumption of soy products	−1.102	0.248	17.11	<0.001	0.34 (0.21, 0.56)
Smoking	0.718	0.335	4.25	0.041	1.95 (1.04, 3.82)
Drinking	1.207	0.372	9.38	0.001	3.16 (1.56, 6.72)
Difficulty in falling asleep, awakening during sleep, or dreaming often	1.055	0.317	12.14	0.001	2.74 (1.54, 4.85)
Have a nap habit	−0.851	0.259	10.65	<0.001	0.45 (0.27, 0.73)
Sunshine duration	−0.614	0.138	16.91	<0.001	0.57 (0.43, 0.76)
Take part in the physical exercise	−0.729	0.279	7.41	0.006	0.49 (0.27, 0.83)
History of joint trauma	1.209	0.398	7.94	0.005	3.11 (1.39, 6.87)

Table 3: Logistic regression analysis of multivariate conditions influencing factors of OA.

Variables	*β*	Sex	Wald	*P*	OR (95% CI)
Genetic factors	1.795	0.699	6.69	0.011	4.52 (1.56, 7.83)
BMI	0.974	0.429	4.79	0.025	2.57 (1.16, 5.84)
Drinking	2.518	0.855	8.46	0.021	3.81 (1.53, 5.87)
Consumption of fresh vegetables	−2.647	0.715	12.81	0.001	0.08 (0.03, 0.31)
Consumption of fresh fruits	−1.039	0.516	3.92	0.043	0.34 (0.12, 0.96)
Consumption of soy products	−2.271	0.762	8.65	0.003	0.11 (0.04, 0.45)
Sunshine duration	−1.205	0.425	7.92	0.004	0.31 (0.14, 0.71)
History of joint trauma	2.816	0.904	6.96	0.015	3.37 (1.67, 5.24)

studies Sherwood et al. [26,27] reported that the intake of soy products is a protective factor for OA, which is related to the relatively high amount of calcium and protein in soy products. Studies by Das Gupta et al. [28,29] reported that alcohol consumption is a risk factor for OA, so in daily life, it is recommended to drink less alcohol and eat more fresh vegetables, fruits, and soy products. Studies by McAlindon et al. [30,31] reported that prolonged sunlight exposure is a protective factor for OA, because vitamin D has the activity of regulating bone metabolism in the body, it is mainly synthesized in the skin through sunlight, and prolonged sun exposure results in high levels of active vitamin D synthesized in the body, and active vitamin D can promote bone growth and metabolism, which protects the body from OA.

The results of this study suggest that body mass index increases the risk of OA. Studies by Haq et al. [32,33] confirmed that obesity is a risk factor for OA, and that for every 2 units (i.e., 5 kg) an increase in the body mass index, the risk of OA increases by 36%. On the one hand, obesity acts to cause OA by increasing the bioburden; on the other hand, intermediate metabolites produced during lipid metabolism (e.g., arachidonic acid) aggravate local inflammation and accelerate the development of OA. In some specific cases, such as ligament injuries, overweight individuals, and age-related muscle weakening, the subchondral bone undergoes potential changes and eventually the overlying articular cartilage is affected [34].

The results of this study suggest that a history of bone trauma is a risk factor for OA, possibly due to degeneration of articular cartilage caused by bone trauma, which induces arthritis through a chronic mechanism of injury. Genetic factors are a risk factor for the development of OA. Studies by Jacobsen et al. [35,36] have identified an inherited, early-onset, polyarticular OA associated with abnormalities in the COL2A1 gene. In the hip joint, congenital developmental malformations are a risk factor for hip osteoarthritis. Studies by Bijlsma et al. [37] have shown that SNP loci increase the risk of knee and hip osteoarthritis in Asians and that OA is the result of a combination of the systemic and local factors. Although the occurrence of OA cannot be completely prevented at present, it can be reduced or delayed by some measures.

5. Conclusion

In summary, obesity, alcohol consumption, and a history of joint trauma all increase the risk of OA in southern Chinese population, whereas a diet rich in fresh vegetables, fresh fruits, soy products, and sun exposure reduces the risk of OA. Understanding the sociodemographic characteristics, disease and treatment, community health services, and quality of life of patients with osteoarthritis will further explore possible influencing factors and provide a basis for more comprehensive and targeted interventions for osteoarthritis in the future.

6. Outlook

First, due to time and capacity constraints, the sample size collected in this study was small, and the representativeness of patients' quality of life and each dimension may be insufficient.

Second, in the regression analysis, the mean scores of the dimensions of quality of life were classified as good and bad, the rationality of which needs to be further investigated; meanwhile, in the follow-up study, the influence of the three factors on the quality of life of patients with osteoarthritis: sociodemographic characteristics, disease and treatment, and access to health services and preventive care needs to be further analyzed.

Third, due to time and capacity constraints, nonosteoarthritis patients were not selected for further comparative analysis in this study. In future studies, nonosteoarthritis patients in the surveyed community could be randomly selected for quality of life assessment to investigate the differences in quality of life between osteoarthritis patients and nonosteoarthritis patients in the same setting.

Data Availability

The simulation experiment data used to support the findings of this study are available from the corresponding author upon request.

Conflicts of Interest

The authors declare that there are no conflicts of interest regarding the publication of this paper.

Authors' Contributions

Danqing Lu and Xiaomin Ding contributed equally to this work.

References

[1] D. Pinkaew, K. Kiattisin, K. Wonglangka, and P. Awoot, "Phonophoresis of phyllanthus amarus nanoparticle gel improves functional capacity in individuals with knee osteoarthritis: a randomized controlled trial," *Journal of Bodywork and Movement Therapies*, vol. 24, no. 1, pp. 15–18, 2020.

[2] F. Vilchez-Cavazos, J. M. Millan-Alanis, J. Blazquez-Saldana et al., "Comparison of the clinical effectiveness of single versus multiple injections of platelet-rich plasma in the treatment of knee osteoarthritis: a systematic review and meta-analysis," *Orthopaedic Journal of Sports Medicine*, vol. 7, no. 12, 2019.

[3] S. M. Goodman, B. Y. Mehta, L. A. Mandl et al., "Validation of the hip disability and osteoarthritis outcome score and knee injury and osteoarthritis outcome score pain and function subscales for use in total hip replacement and total knee replacement clinical trials," *The Journal of Arthroplasty*, vol. 35, no. 5, pp. 1200.e4–1207.e4, 2020.

[4] A. J. Buckland, L. Steinmetz, P. Zhou et al., "Spinopelvic compensatory mechanisms for reduced hip motion (ROM) in the setting of hip osteoarthritis," *Spine Deformity*, vol. 7, no. 6, pp. 923–928, 2019.

[5] M. Ukita, K. Matsushita, M. Tamura, and T. Yamaguchi, "Histone H3K9 methylation is involved in temporomandibular joint osteoarthritis," *International Journal of Molecular Medicine*, vol. 45, no. 2, pp. 607–614, 2020.

[6] M. Kenmochi, "Clinical outcomes following injections of leukocyte-rich platelet-rich plasma in osteoarthritis patients," *Journal of Orthopaedics*, vol. 18, pp. 143–149, 2020.

[7] M. S. Matada, M. S. Holi, R. Raman, and S. T. Jayaramu Suvarna, "Visualization of cartilage from knee joint magnetic resonance images and quantitative assessment to study the effect of age, gender and body mass index (BMI) in progressive osteoarthritis (OA)," *Current Medical Imaging Formerly Current Medical Imaging Reviews*, vol. 15, no. 6, pp. 565–572, 2019.

[8] F. M. Alfieri, M. C. C. Barros, K. C. d. Carvalho, I. Toral, C. F. D. Silva, and N. C. d. O. Vargas e Silva, "Geotherapy combined with kinesiotherapy is efficient in reducing pain in patients with osteoarthritis," *Journal of Bodywork and Movement Therapies*, vol. 24, no. 1, pp. 77–81, 2020.

[9] S. Parisi, M. C. Ditto, M. Priora et al., "Ultrasound-guided intra-articular injection: efficacy of hyaluronic acid compared to glucocorticoid in the treatment of knee osteoarthritis," *Minerva Medica*, vol. 110, no. 6, pp. 515–523, 2019.

[10] M. Khosravi, M. Arazpour, H. Saeedi, and M. Rezaei, "Design evaluation in novel orthoses for patients with medial knee osteoarthritis," *Journal of Biomedical Physics & Engineering*, vol. 9, no. 6, pp. 719–732, 2019.

[11] T. Ikeda, T. Jinno, T. Masuda et al., "Effect of exercise therapy combined with branched-chain amino acid supplementation on muscle strengthening in persons with osteoarthritis," *Hong Kong Physiotherapy Journal*, vol. 38, no. 01, pp. 23–31, 2018.

[12] M. Farhadian, Z. Morovati, and A. Shamsoddini, "Effect of kinesio taping on pain, range of motion, hand strength, and functional abilities in patients with hand osteoarthritis: a pilot randomized clinical trial," *The Archives of Bone and Joint Surgery*, vol. 7, no. 6, pp. 551–560, 2019.

[13] J. Yuan, W. Ding, N. Wu, S. Jiang, and W. Li, "Protective effect of genistein on condylar cartilage through downregulating NF-κB expression in experimentally created osteoarthritis rats," *BioMed Research International*, vol. 2019, Article ID 2629791, 2019.

[14] Y. Gu, K. Ren, L. Wang, and Q. Yao, "Loss of klotho contributes to cartilage damage by derepression of canonical Wnt/β-catenin signaling in osteoarthritis mice," *Aging*, vol. 11, no. 24, pp. 12793–12809, 2019.

[15] C. Jin, E. K. Song, A. Santoso, P. S. Ingale, I. S. Choi, and J. K. Seon, "Survival and risk factor analysis of medial open wedge high tibial osteotomy for unicompartment knee osteoarthritis," *Arthroscopy: The Journal of Arthroscopic & Related Surgery*, vol. 36, no. 2, pp. 535–543, 2020.

[16] D. Ma, T. Yu, L. Peng, L. Wang, Z. Liao, and W. Xu, "PIM1, CYP1B1, and HSPA2 targeted by quercetin play important roles in osteoarthritis treatment by achyranthes bidentata," *Evidence-Based Complementary and Alternative Medicine*, vol. 2019, Article ID 1205942, 10 pages, 2019.

[17] Y. Gu, K. Ren, C. Jiang, L. Wang, and Q. Yao, "Regulation of cartilage damage caused by lack of klotho with thioredoxin/peroxiredoxin (Trx/Prx) system and succedent NLRP3 activation in osteoarthritis mice," *American Journal of Translational Research*, vol. 11, no. 12, pp. 7338–7350, 2019.

[18] L. C. Garbin and C. S. Olver, "Platelet-rich products and their application to osteoarthritis," *Journal of Equine Veterinary Science*, vol. 86, Article ID 102820, 2020.

Hindawi
Emergency Medicine International
Volume 2023, Article ID 9874658, 1 page
https://doi.org/10.1155/2023/9874658

Retraction

Retracted: Association of β2-Agonist Receptor Gene Polymorphisms with Acute Exacerbations of COPD: A Prospective Observational Study

Emergency Medicine International

Received 8 August 2023; Accepted 8 August 2023; Published 9 August 2023

This article has been retracted by Hindawi following an investigation undertaken by the publisher [1]. This investigation has uncovered evidence of one or more of the following indicators of systematic manipulation of the publication process:

(1) Discrepancies in scope
(2) Discrepancies in the description of the research reported
(3) Discrepancies between the availability of data and the research described
(4) Inappropriate citations
(5) Incoherent, meaningless and/or irrelevant content included in the article
(6) Peer-review manipulation

The presence of these indicators undermines our confidence in the integrity of the article's content and we cannot, therefore, vouch for its reliability. Please note that this notice is intended solely to alert readers that the content of this article is unreliable. We have not investigated whether authors were aware of or involved in the systematic manipulation of the publication process.

Wiley and Hindawi regrets that the usual quality checks did not identify these issues before publication and have since put additional measures in place to safeguard research integrity.

We wish to credit our own Research Integrity and Research Publishing teams and anonymous and named external researchers and research integrity experts for contributing to this investigation.

The corresponding author, as the representative of all authors, has been given the opportunity to register their agreement or disagreement to this retraction. We have kept a record of any response received.

References

[1] F. Lu, N. Xu, and J. Zheng, "Association of β2-Agonist Receptor Gene Polymorphisms with Acute Exacerbations of COPD: A Prospective Observational Study," *Emergency Medicine International*, vol. 2022, Article ID 2711489, 5 pages, 2022.

Hindawi
Emergency Medicine International
Volume 2022, Article ID 2711489, 5 pages
https://doi.org/10.1155/2022/2711489

Research Article

Association of β2-Agonist Receptor Gene Polymorphisms with Acute Exacerbations of COPD: A Prospective Observational Study

Fengfeng Lu, Nengluan Xu, and Jianshi Zheng

Department of Pulmonary and Critical Care Medicine, Fujian Provincial Hospital, Fuzhou 350000, China

Correspondence should be addressed to Nengluan Xu; xnlldc@163.com

Received 20 June 2022; Revised 13 August 2022; Accepted 22 August 2022; Published 12 September 2022

Academic Editor: Hang Chen

Objective. To investigate the relationship between β2-agonist receptor gene polymorphisms and acute exacerbations of chronic obstructive pulmonary disease (COPD). *Methods*. Retrospective analysis of 99 patients in the respiratory and critical care unit of Fujian Provincial Hospital from 2018 to 2020. The clinical characteristics of different genotypes were compared, and the treatments of different genotypes and the analysis of factors associated with acute exacerbations of COPD were compared. *Results*. During the 12-month follow-up period, 53 patients developed acute exacerbations, with the 16Arg/Arg homozygous requiring significantly more antibiotics and hormones than the other two genotypes; when agonist receptor 16 gene polymorphism was associated with the risk of acute exacerbation, 16Arg/Gly patients had a 5.286-fold increased risk of acute exacerbation (OR = 6.286, 95% CI. 1.476–26.759, $P = 0.013$). 16Arg/Arg patients had a 5.060-fold increased risk of acute exacerbation (OR = 6.060, 95% confidence interval: 1.407–26.161, $P = 0.016$). *Conclusion*. Acute exacerbation of 16Arg/Arg COPD is very serious; 16Arg/Gly increases the risk of acute exacerbation in COPD patients; and provides help for future treatment and management options of the disease.

1. Introduction

Chronic obstructive pulmonary disease (COPD) is one of the most common chronic diseases of the respiratory system and is a global public health problem [1]. Chronic obstructive pulmonary disease (COPD) is a dynamic chronic disease characterized by persistent respiratory symptoms and or airflow limitation, which can be prevented and treated [2]. In China, the prevalence of COPD in people over 40 years of age is 13.7% [3] and is expected to be the 3rd leading cause of death worldwide by 2020 [4]. Acute exacerbation of chronic obstructive pulmonary disease (AECOPD) is an acute worsening of a patient's existing respiratory symptoms (mainly manifested as worsening dyspnea and increased cough and sputum) beyond the patient's daily variation and causes the patient to require additional medication [5]. Acute exacerbations account for 70% of the disease in clinical practice, so it is generally accepted that acute exacerbations of COPD are key events in the development and progression of the disease, and are important indicators for assessing patients' future health status and disease prognosis [6]. The total annual per capita cost accounts for 40% of the average total household income in China in that year (for urban patients associated with COPD), and the economic burden is more severe in rural areas [7]. Patients with COPD experience 0.5–3.5 acute exacerbations per year, with some COPD patients having at least 2 acute exacerbations per year, which we usually define as frequent acute exacerbations [8]. Patients with frequent exacerbations have higher morbidity and mortality, poorer health status, and more severe economic impact than patients with infrequent exacerbations [9, 10]. In recent years, there has been increasing interest in the role of genetic factors in the pathogenesis and pharmacological efficacy of COPD.

Inhaled β-agonists are one of the main bronchodilators in the treatment of COPD [11]. β2-adrenergic receptor (ADRB2) is a G protein-coupled transmembrane receptor that is highly expressed in lung tissue, and activation of this receptor has the function of relaxing bronchial smooth

muscle, anti-inflammatory and improving airway epithelial mucus [12]. adrB2 is located on chromosome 5q31–32. It is an intronless, relatively small gene encoding 413 amino acids [13]. At least five single nucleotide polymorphisms (SNPs) have been identified so far, namely, +46A/G, 79C/G, +100G/A, +491C/T, and −47C/T, corresponding to nucleotide variant sites 16, 27, 34, 164, and 19. Most of the existing studies have focused on 16 [16Arg > Gly; rs 1042713] and 27 [27Gln > Glu; rs 1042714] variants.

Previous high-quality studies examining the clinical characteristics of patients with frequent acute exacerbations of COPD are not numerous, and some of the findings are still inconsistent. Studies [14] have shown that typing of chronic obstructive pulmonary disease (COPD) is an independent predictor to assess the frequency of their future acute exacerbations. In recent years, literature and foreign guidelines have pointed out that better outcomes have been obtained with targeted and individualized treatment after the phenotypic classification of COPD [15]. It is suggested that different COPD phenotypes have different characteristics, and more valuable findings may be obtained if the clinical characteristics of patients with frequent acute exacerbations (FE) of COPD are sought on the basis of phenotypes. The aim of this study is to analyze the clinical characteristics of different COPD patients, to find the possible risk factors for each COPD frequent acute exacerbation (FE), and to compare and generalize them, which can eventually provide targeted individualized treatment for patients, reduce the frequency of future acute exacerbations, and promote the development of precision medicine.

2. Research Methodology

2.1. Patient Data. Ninety-nine patients from the Department of Respiratory and Critical Care Medicine of Fujian Provincial Hospital from 2018 to 2020 were included in this study.

2.1.1. Inclusion Criteria

(1) Meet the diagnostic criteria for acute exacerbation of chronic obstructive pulmonary disease [16]. Acute deterioration of the patient's original respiratory symptoms (mainly manifested by increased dyspnea and cough and sputum) beyond the patient's daily variation and leading to the patient's need for additional medication.

(2) Patients aged 40–85 years.

2.1.2. Exclusion Criteria

(1) Combination of other serious lung diseases, such as active tuberculosis, lung cancer, diffuse interstitial pulmonary fibrosis, and bronchiectasis

(2) Combination of cardiovascular, cerebrovascular, hepatic and renal, hematopoietic systems and other serious primary diseases, psychiatric patients, such as cerebral hemorrhage and massive cerebral infarction, chronic cardiac insufficiency, acute myocardial infarction, uremia, lymphoma, and leukemia

(3) Recent use of immunosuppressive drugs, long-term glucocorticoid therapy, and the presence of serious immune system diseases

2.2. Clinical Information. Clinical data including demographic data, smoking status, blood gas analysis, baseline lung function, and bronchial dilation test results were obtained through the electronic medical record system. A questionnaire was used for all patients to obtain the number of hospitalizations due to acute exacerbations, systemic glucocorticoid use, and antibiotic use in the past 12 months. At the same time, venous blood samples were collected from each patient for ADRB2 gene polymorphism detection.

2.3. Gene Polymorphism Detection Process. DNA extraction kit (Guangzhou Meiji Bio, HiPure Universal DNA Kit) was used for DNA extraction, and gene amplification was performed on a Bio-rad T-100 PCR instrument. Primers: upstream: ACATAACGGGCAGAACGCAC, downstream: CGATGAGAGACATGACGATGC, select qualified PCR products were genotyped by next-generation sequencing on an ABI 3730 sequencer.

2.4. Statistical Methods. SPSS 17.0 software was used for analysis. Measurement data were expressed as mean ± standard deviation ($\overline{x} \pm s$), and differences between groups were analyzed by variance analysis; count data were expressed as rates, and differences between groups were analyzed by chi-square test. Binary Logistic was used to analyze the association between gene polymorphisms and acute exacerbation. Two-sided $P < 0.05$ was considered statistically significant.

3. Statistical Results

3.1. Clinical Features. A total of 99 patients with the chronic obstructive pulmonary disease were included in this analysis, with an average age of (69.38 ± 6.69) years, (52–83) years old, 96 males, 20 Arg/Arg, 61 Arg/Gly, and 18 Gly/Gly. There was no significant difference in the smoking index, FEV1, FEV1% and FEV1/FVC, CAT score, mMRC, number of acute exacerbations, and drug combination (all $P > 0.05$). The difference between the types was statistically significant ($P < 0.05$, Tables 1 and 2). Furthermore, binary logistic regression analysis showed that the risk of acute exacerbation increased by 5.286 times (OR = 6.286, 95% CI: 1.476~26.759, $P = 0.013$) in the heterozygous genotype Arg/Gly, and still increased by 5.060 times after adjusting for FEV1 OR = 6.060, 95% CI: 1.407~26.161, $P = 0.016$, Table 3).

4. Discussion

Chronic obstructive pulmonary disease (COPD) is a common disease typically characterized by incomplete reversible airflow limitation and persistent respiratory

Table 1: Comparison of clinical characteristics of different genotypes.

	Arg/Arg ($n = 20$)	Arg/Gly ($n = 61$)	Gly/Gly ($n = 18$)	F value/chi-square	P value
Age	70.60 ± 7.05	69.33 ± 6.52	68.22 ± 7.01	0.599	0.551
Male	20	58	18	1.927	0.382
Smoking index	49.68 ± 31.92	46.07 ± 30.28	45.69 ± 30.56	0.117	0.890
FEV1 (L)	0.84 ± 0.22	0.93 ± 0.31	0.97 ± 0.27	1.203	0.305
FEV1 (%)	32.71 ± 8.94	36.86 ± 11.86	36.02 ± 9.91	1.072	0.346
FEV1/FVC (%)	38.58 ± 10.72	39.12 ± 10.26	44.35 ± 9.08	2.070	0.132
CATscore	15.30 ± 4.89	15.23 ± 6.45	14.44 ± 6.30	0.127	0.881
mMRC	2.45 ± 1.00	2.25 ± 1.06	1.72 ± 1.13	2.439	0.093
Exacerbations	16 (80.0%)	30 (49.2%)	7 (38.9%)	7.649	0.022

Note. FEV1, FVC, CAT, mMRC.

Table 2: Comparison of treatment methods for different genotypes.

	Arg/Arg	Arg/Gly	Gly/Gly		
LAMA	0	5 (8.2%)	1 (5.6%)		
LABA + ICS	1 (5.0%)	9 (14.8%)	3 (16.7%)	1.511	0.825
ICS + LABA + LAMA	19 (95.0%)	47 (77.0%)	14 (77.8%)		
Antibiotics used					
0	8 (40.0%)	31 (50.8%)	12 (66.7%)		
1	2 (10.0%)	17 (27.9%)	6 (33.3%)		
2	6 (30.0%)	6 (9.8%)	0	14.944	0.021
≥3	4 (20.0%)	7 (11.5%)	0		
Number of hormones					
0	13 (65.0%)	40 (65.6%)	14 (77.8%)		
1	1 (5.0%)	17 (27.9%)	4 (22.2%)		
2	4 (20.0%)	2 (3.3%)	0	14.732	0.022
≥3	2 (10.0%)	2 (3.3%)	0		
Number of acute exacerbations					
0	5 (25.0%)	31 (50.8%)	11 (61.1%)		
1	6 (30.0%)	12 (19.7%)	7 (38.9%)		
2	5 (25.0%)	10 (16.4%)	0	12.558	0.051
≥3	4 (20.0%)	8 (13.1%)	0		

Note. LAMA, LABA, LAMA.

Table 3: Correlation between rs 1042713 and acute exacerbation of the chronic obstructive pulmonary disease.

	B	S.E,	Wals	P	Exp (B)	95% of EXP (B) C.I.	
						Lower limit	Higher limit
Arg/Arg			6.864	0.032	Ref		
Arg/Gly	1.838	0.739	6.186	0.013	6.286	1.476	26.759
Gly/Gly	0.419	0.547	0.587	0.444	1.521	0.520	4.444
Arg/Arg[1]			6.498	0.039	Ref		
Arg/Gly	1.802	0.745	5.848	0.016	6.060	1.407	26.101
Gly/Gly	0.408	0.548	0.553	0.457	1.504	0.513	4.404

Note.[1]Adjustment factor is FEV1.

symptoms. As the disease progresses, lung function declines progressively, leading to a reduced workforce and, in severe cases, respiratory failure, pulmonary heart disease, and even death. According to the results of a recent large epidemiological cross-sectional survey in China, the prevalence of COPD defined by spirometry reached 8.6%, and there are nearly 100 million COPD patients nationwide, second only to hypertension and diabetes, and this data is on the rise, which urgently needs the attention of the whole society [17]. The active search for clinical factors or biomarkers that predict the future risk of frequent acute exacerbations in COPD patients is an important clinical event at present.

It was found [18] that among the 16 focal polymorphisms of the ADRB2 gene, those carrying the Arg/Arg isoform required antibiotics and systemic hormones in the event of an acute exacerbation, indicating a more severe condition; those with the 16Arg/Gly isoform had a higher risk of acute exacerbation. Studies [19,20] found that 16Arg/Gly and 27Gln/Glu polymorphisms by themselves did not affect airflow limitation. Our study found no significant differences in pulmonary function indicators between ADRB2 genotypes, but they may lead to an increased risk of exacerbations, as well as to different severity of the disease. Currently, only a few studies have analyzed the role of ADRB2 gene polymorphisms in COPD and the application of antibiotics and systemic hormones. The study [21] found a significant increase in the use of antibiotics and hormones in patients with 16Arg/Arg COPD during acute exacerbations, but did not affect the number of hospitalizations associated with acute exacerbations consistent with the results of this study. Similarly, the study [22] found no relationship between ADRB2 polymorphism and the number of hospitalizations associated with COPD exacerbations. At present, the mechanism by which ADRB2 gene polymorphisms are associated with the severity of COPD exacerbations remains unclear. According to Ligert's theory, ADRB2 containing the glycine 16 position may be downregulated by exposure to endogenous catecholamines [23]. All of the patients we included had severe to very severe COPD. Most of the

patients were treated with beta-agonists and the receptors were more significantly downregulated. As a result, they were more prone to respiratory infections and required more hormones.

Most of the current studies on the association of ADRB2 gene polymorphisms with exacerbations of COPD are on the risk of acute exacerbations when inhaling β-agonists with different genotypes [24]. In a subgroup analysis of the POET-COPD trial, patients inhaling salmeterol with genotype Arg/Arg had a significantly lower risk of acute exacerbations than Arg/Gly and Gly/Gly, although we did not specifically include patients who received beta-agonists. These patients were treated with β-agonists, but they all received β-agonists because of the severity of their disease. Therefore, it can be stated that the above findings are consistent with ours. However, in other clinical trials, the ADRB2 gene polymorphism was not associated with acute exacerbations in COPD patients who inhaled long-acting beta-agonists. Therefore, the study [25] was systematically reviewed after including all the above-mentioned trials and found no statistical differences.

The relationship between ADRB2 gene polymorphisms and acute exacerbations of inhaled beta-agonists in COPD patients remains unclear. The study [26] found that airway smooth muscle cells expressing the Arg allele had less receptor downregulation when exposed to β-receptor agonists compared to airway smooth muscle cells expressing the Gly allele in an in vitro study.

5. Conclusion

Patients with different phenotypes of frequent acute exacerbations (FE) of chronic obstructive pulmonary disease (COPD) may have their own distinct clinical manifestations. Our study found that 16Arg/Arg COPD worsens severely; 16Arg/Gly increases the risk of acute exacerbations in COPD patients, which may help identify risk factors for COPD that are more likely to lead to increased frequency of hospitalization, and provide assistance for future disease diagnosis and management programs.

Data Availability

The simulation experiment data used to support the findings of this study are available from the corresponding author upon request.

Conflicts of Interest

The authors declare that there are no conflicts of interest regarding the publication of this paper.

Acknowledgments

This study was supported by the Fujian Science and Technology Program Project (NO. 2018Y0010) and Medical Innovation Project of the National Health and Family Planning Commission (NO. 2017-CX-5).

References

[1] A. Agustí and J. C. Hogg, "Update on the pathogenesis of chronic obstructive pulmonary disease," *New England Journal of Medicine*, vol. 381, no. 13, pp. 1248–1256, 2019.

[2] B. R. Celli and J. A. Wedzicha, "Update on clinical aspects of chronic obstructive pulmonary disease," *New England Journal of Medicine*, vol. 381, no. 13, pp. 1257–1266, 2019.

[3] R. Pranata, A. Y. Soeroto, I. Huang et al., "Effect of chronic obstructive pulmonary disease and smoking on the outcome of COVID-19," *International Journal of Tuberculosis & Lung Disease*, vol. 24, no. 8, pp. 838–843, 2020.

[4] K. E. Lowe, E. A. Regan, A. Anzueto et al., "COPDGene® 2019: redefining the diagnosis of chronic obstructive pulmonary disease," *Chronic Obstructive Pulmonary Diseases (Miami, Fla.)*, vol. 6, no. 5, pp. 384–399, 2019.

[5] C. Wang, J. Xu, L. Yang et al., "Prevalence and risk factors of chronic obstructive pulmonary disease in China (the China Pulmonary Health [CPH] study): a national cross-sectional study," *The Lancet*, vol. 391, no. 10131, pp. 1706–1717, 2018.

[6] A. I. Ritchie and J. A. Wedzicha, "Definition, causes, pathogenesis, and consequences of chronic obstructive pulmonary disease exacerbations," *Clinics in Chest Medicine*, vol. 41, no. 3, pp. 421–438, 2020.

[7] C. M. Riley and F. C. Sciurba, "Diagnosis and outpatient management of chronic obstructive pulmonary disease: a review," *JAMA*, vol. 321, no. 8, pp. 786–797, 2019.

[8] I. Iheanacho, S. Zhang, D. King, M. Rizzo, and A. S. Ismaila, "Economic burden of chronic obstructive pulmonary disease (COPD): a systematic literature review," *International Journal of Chronic Obstructive Pulmonary Disease*, vol. 15, pp. 439–460, 2020.

[9] B. M. Smith, M. Kirby, E. A. Hoffman et al., "Association of dysanapsis with chronic obstructive pulmonary disease among older adults," *Journal of the American Medical Association*, vol. 323, no. 22, pp. 2268–2280, 2020.

[10] E. Scoditti, M. Massaro, S. Garbarino, and D. M. Toraldo, "Role of diet in chronic obstructive pulmonary disease prevention and treatment," *Nutrients*, vol. 11, no. 6, p. 1357, 2019.

[11] L. Fang, P. Gao, H. Bao et al., "Chronic obstructive pulmonary disease in China: a nationwide prevalence study," *The Lancet Respiratory Medicine*, vol. 6, no. 6, pp. 421–430, 2018.

[12] C. A. Brandsma, M. Van den Berge, T. L. Hackett, G. Brusselle, and W. Timens, "Recent advances in chronic obstructive pulmonary disease pathogenesis: from disease mechanisms to precision medicine," *The Journal of Pathology*, vol. 250, no. 5, pp. 624–635, 2020.

[13] S. P. Duffy and G. J. Criner, "Chronic obstructive pulmonary disease: evaluation and management," *Medical Clinics of North America*, vol. 103, no. 3, pp. 453–461, 2019.

[14] D. M. G. Halpin, G. J. Criner, A. Papi et al., "Global initiative for the diagnosis, management, and prevention of chronic obstructive lung disease. The 2020 GOLD science committee report on COVID-19 and chronic obstructive pulmonary disease," *American Journal of Respiratory and Critical Care Medicine*, vol. 203, no. 1, pp. 24–36, 2021.

[15] R. R. Duan, K. Hao, and T. Yang, "Air pollution and chronic obstructive pulmonary disease," *Chronic Diseases and Translational Medicine*, vol. 6, no. 4, pp. 260–269, 2020.

[16] A. Corlateanu, Y. Mendez, Y. Wang, R. D. J. A. Garnica, V. Botnaru, and N. Siafakas, "Chronic obstructive pulmonary disease and phenotypes: a state-of-the-art," *Pulmonology*, vol. 26, no. 2, pp. 95–100, 2020.

Hindawi
Emergency Medicine International
Volume 2023, Article ID 9763530, 1 page
https://doi.org/10.1155/2023/9763530

Retraction

Retracted: Application of Computer-Based Simulation Teaching Combined with PBL in Colorectal Tumor Hemorrhage

Emergency Medicine International

Received 8 August 2023; Accepted 8 August 2023; Published 9 August 2023

This article has been retracted by Hindawi following an investigation undertaken by the publisher [1]. This investigation has uncovered evidence of one or more of the following indicators of systematic manipulation of the publication process:

(1) Discrepancies in scope
(2) Discrepancies in the description of the research reported
(3) Discrepancies between the availability of data and the research described
(4) Inappropriate citations
(5) Incoherent, meaningless and/or irrelevant content included in the article
(6) Peer-review manipulation

The presence of these indicators undermines our confidence in the integrity of the article's content and we cannot, therefore, vouch for its reliability. Please note that this notice is intended solely to alert readers that the content of this article is unreliable. We have not investigated whether authors were aware of or involved in the systematic manipulation of the publication process.

Wiley and Hindawi regrets that the usual quality checks did not identify these issues before publication and have since put additional measures in place to safeguard research integrity.

We wish to credit our own Research Integrity and Research Publishing teams and anonymous and named external researchers and research integrity experts for contributing to this investigation.

The corresponding author, as the representative of all authors, has been given the opportunity to register their agreement or disagreement to this retraction. We have kept a record of any response received.

References

[1] Y. Zhang, J. Hu, L. Li, and Y. Zhao, "Application of Computer-Based Simulation Teaching Combined with PBL in Colorectal Tumor Hemorrhage," *Emergency Medicine International*, vol. 2022, Article ID 1251388, 10 pages, 2022.

Hindawi
Emergency Medicine International
Volume 2022, Article ID 1251388, 10 pages
https://doi.org/10.1155/2022/1251388

Research Article

Application of Computer-Based Simulation Teaching Combined with PBL in Colorectal Tumor Hemorrhage

Yanling Zhang,[1] **Jinyan Hu**,[2] **Lingling Li**,[1] **and Yunpeng Zhao**[1]

[1]*Medical Oncology Department of Thoracic Cancer, Cancer Hospital of China Medical University, Liaoning Cancer Hospital and Institute, Shenyang 110042, China*
[2]*Nursing Department, Chifeng Municipal Hospital, Chifeng 024000, China*

Correspondence should be addressed to Yanling Zhang; zhangyanling@cancerhosp-ln-cmu.com

Received 1 July 2022; Revised 8 August 2022; Accepted 18 August 2022; Published 9 September 2022

Academic Editor: Hang Chen

Objective. This paper aims to explore the use of computer-based simulation teaching combined with PBL in colorectal tumor bleeding. *Methods*. The outpatient department organized 21 nursing staffs to conduct computer simulation combined with PBL teaching, compared emergency theory and skill scores, and investigated the recognition of computer simulation teaching combined with PBL. *Results*. The scores of theoretical knowledge examination before training were (84.31 ± 6.39) and (92.59 ± 2.93) after training; the scores of treatment skills examination were (85.69 ± 6.15) and (95.43 ± 2.88) after training; the scores of comprehensive treatment skills before training were (76.6 ± 6.31) and (91.43 ± 2.3) after training. The results of the questionnaires showed that the nurses were more agreeable to the new teaching methods and were able to complete the tasks in strict accordance with the requirements, ultimately achieving a level of satisfaction with their progress. *Conclusion*. Computer simulation teaching combined with PBL can deepen general practitioners' understanding of knowledge, improve practical ability, and provide a clinical basis for improving patient resuscitation in specialized oncology hospitals.

1. Introduction

First-aid skills are the most important means of rescuing patients with acute illnesses, and every medical personnel should be proficient in them, but for general practitioners, they usually resuscitate less and do not have enough clinical experience [1], and training is difficult. Patients in our department are usually admitted due to sudden illness or accident, and these patients are in serious condition and develop rapidly. In order to improve the ability of our physicians to solve emergencies, our department is generally used as the focus of medical internship. Problem-based learning (PBL) is a teaching activity innovatively applied by Barrows, a professor of neurology in the United States, at McMaster University in Canada in 1967 [2]. This teaching activity is guided by constructivist theory and is centered on the person being taught, and this teaching concept has become a more popular teaching program internationally [3, 4]. Compared with the traditional lecture-based teaching model, the PBL teaching model uses the teacher as the center of the classroom and clinical problems as the motivation for nurses to learn, so that nurses can better grasp the learning content and help nurses solve various problems in learning, so that nurses can develop more advanced skills and thinking when receiving instruction, which is extremely important for the optimization of teaching activities.

It has been more than 20 years since PBL was launched in Shanghai Second Medical University and Xi'an Medical University in 1986, and some higher medical schools in China have also started to try PBL teaching.

1.1. Narrow Learning Community. The learning community in traditional PBL has only nurses in the classroom, so the homogeneity of group members' thinking is high, and the overall thinking level of the learning group can hardly reach a high level, which makes the design of problem solutions

lack high innovation; the group of teachers is also limited to the lecturers of the course, who lack the necessary skills and motivation to participate.

1.2. Single Form of Problem Situation Presentation. The problems in PBL come from real, complex, and ill-structured problems in life. However, teachers in traditional PBL still use text and video to represent problem situations, which cannot give nurses an immersive feeling and make it difficult to empathize with the environment emotionally and psychologically to achieve effective transfer of knowledge.

1.3. High Teaching Cost. Traditional PBL requires a large number of small classrooms for group discussions, and each small classroom must be equipped with sufficient teaching tools, learning resources, and instructors. However, with the continuous expansion of Chinese universities, schools are faced with the contradiction of more nurses and fewer instructors, shortage of teaching resources such as classrooms and libraries, and tight education funding. This has led to schools implementing PBL in the form of large class discussions, where over 100 nurses are divided into small groups in a large classroom and a lead teacher leads the discussion, which is not true PBL in the true sense.

1.4. Simple Communication and Collaboration Channels. In traditional PBL, nurses' problem-solving process is mainly accomplished by consulting relevant textual materials and having face-to-face discussions, exchanges, and consultations with group members. Communication among nurses and between nurses and teachers is mainly focused on the classroom, but since they are at the same level of learning and have basically similar levels of thinking, there may be some difficulties in not developing nurses' critical thinking and creative thinking skills.

1.5. Lack of Depth and Systematic Knowledge. In teaching, if PBL is used alone, the knowledge gained gives a feeling of lack of depth and systematization, and a lot of time is wasted in group discussions. The knowledge acquired by nurses in traditional PBL teaching is sufficient for solving a selected clinical problem, but it is not broad and deep enough for mastering the systematic knowledge of a discipline, especially in some basic medical courses, because PBL breaks the integrity of basic theoretical knowledge, some contents may be missed, so it is not as deep and systematic as the theoretical learning emphasized in the traditional teaching mode, which will cause nurses to accumulate insufficient knowledge thickness of a discipline.

1.6. Lack of Suitable Teaching Materials. One reason for the resistance to the implementation of PBL cannot be overlooked: the lack of appropriate textbooks. Many schools implementing PBL have found that existing textbooks for basic medicine and clinical phases are not suitable for PBL and need to be rewritten, which is a challenge for both teachers and nurses with poor clinical reasoning and self-learning skills. The continuous cross-pollination between disciplines and the deepening of medical teaching reform, medical PBL is bound to change accordingly. We believe that the online virtual classroom and online virtual clinical skills center constructed by computer technology will provide a teaching platform for remote PBL and develop nurses' problem-solving skills and that telemedicine PBL will become an important development direction of PBL.

Our medical theoretical knowledge and the extensive use of high-tech top our instruments require nurses to have a more comprehensive knowledge structure and be able to skillfully apply our commonly used technologies. In recent years, the number of outpatients in our hospital has increased rapidly, and there are often difficult and critical patients from overseas. In addition to the 13 busy nursing work, inpatient nurses undertake the task of our care for outpatients. Although the number of emergency cases is small compared to that of general hospitals, the condition is aggressive, with many comorbidities, poor predictability, and serious consequences. In order to ensure the medical safety of outpatients, the outpatient department regularly organizes standardized training for nursing staff on theoretical knowledge of treatment and treatment skills and other comprehensive abilities of our care and has achieved remarkable results.

2. Related Work

PBL states that medical education should study not only the biological process of disease but also its connection with social groups, psychology, environment, and behavioral patterns; the purpose of education is to promote nurses to become self-motivated lifelong learners who can continuously update their knowledge.

PBL is a learning method for acquiring and synthesizing new knowledge through problem orientation [5, 6]. It uses "real problems" as a starting point for active, independent, and collaborative learning in small groups, seeking and using multiple learning resources, discovering answers to questions, and developing nurses' critical and analytical thinking skills [7, 8]. However, research has confirmed that there are special features of PBL teaching method in the practical teaching of basic clinical skills: (1) teaching of basic clinical skills contains a large amount of practical skills training, and if simple PBL teaching focuses only on theoretical problem solving, it is inevitably suspected that the theory is out of practice and cannot meet the high requirements of modern medical education standards for medical nurses' practical skills; (2) PBL teaching of basic clinical skills needs the assistance of more teaching equipment, in addition to network tools to help nurses access information, it also needs a practical teaching platform reflecting the real clinical environment; (3) the PBL teaching method for basic clinical skills has high requirements for the design of case problems, which should reflect both the basic theory and its cutting-edge advances and include clinical skills practical training projects; otherwise, it will play the role of putting the cart before the horse [9]. The PBL teaching method of basic clinical skills has higher

requirements for the design of case problems, which should reflect both the basic theory and its cutting-edge advances and include clinical skills practical training items; otherwise, it will play the role of putting the cart before the horse.

Traditional PBL (or classroom PBL) emphasizes that the teacher distributes the problem (or case) to be learned to the nurses before or during the class, and the nurses collect information related to the problem through various means around the problem or (case) and analyze and organize the collected information. In the first discussion, the instructor divides the learners into learning groups, one for every five to six nurses, and gives the nurses a certain amount of time in class to discuss and divide their learning. Nurses can then look up the information again with the questions that arose from the discussion session. In the second discussion, nurses participate in the study group again with the knowledge they have developed and the problems they have identified during the learning process. For problems that exist, the nurse needs to again continue to search in depth for information about the problem, analyze, organize, and synthesize new information with old information to form a hypothesis for the final solution. At the group discussion, the whole class submits the final problem solution reached through the discussion, and finally, the teacher gives a summary and feedback.

PBL is a new teaching method that has been rapidly developing worldwide. Since its introduction by McMaster University in Canada in 1969, PBL has been used mainly in medical and vocational schools and certain other educational fields, such as life sciences, nursing, dentistry, pharmacy, veterinary medicine, public health, architecture, business, law, engineering, forestry, and sociology [10, 11].

In just a few decades, PBL has been continuously explored and introduced into practice teaching all over the world, which must have its own indelible advantages. The main manifestations are. The PBL approach is consistent with today's philosophical view of education. PBL is based on some of today's learning theories, such as constructivist theory, contextual cognitive theory, and so on. And it is also consistent with the idea of lifelong education.

Since PBL embodies certain learning principles, it (1) enhances the spontaneity of nurses' learning. The survey found that nurses who use PBL learning are more willing to participate in teaching and learning and have more positive attitudes than those in traditional teaching methods. Nurses find PBL to be a more interesting, stimulating, and enjoyable way to learn. In PBL, nurses are more likely to become spontaneous and independent learners because they are less restricted by the teacher and more independent, which provides a solid foundation for lifelong learning.

In real life, social skills are an important element in the workplace. PBL is done in a collaborative group format, which motivates group members to cooperate in solving relevant problems. Thus, the dynamic process of collaborative learning, evaluating peers, and presenting and defending one's plan to other members of the group led to significant improvements in the nurses' interpersonal skills. All nurses do not have to follow the same pattern of learning; nurses are able to learn in the way they prefer. Stimulates student autonomy in learning. Nurses must set their own learning goals and standards to test whether they are meeting expectations, which increases their sense of responsibility for their own learning and gives them a higher degree of autonomy than traditional nurses. Teachers can give timely feedback on nurses' questions and performance to help nurses plan their next steps in learning. Combining student self-assessment, peer assessment, and teacher assessment allows nurses to become more fully aware of what is wrong with their learning. We provide an environment where nurses feel competent to learn and encourage and support them to develop their own learning interests. This interactivity is not limited to the classroom but is achieved in various forms of interaction between nurses and teachers inside and outside the classroom.

Because the process from problem identification to problem-solving in PBL is a cognitive process, and the answer to the problem in PBL is not unique, there are multiple solutions, so the nurse can only find a feasible solution in various ways to achieve the set goal or the desired effect.

3. Methods

Nurses from Shanghai Second Medical University and Xi'an Medical University participated in the study. Before starting the medical internship in our oncology, theoretical and practical skills examinations were conducted for common diseases in our oncology such as superior vena cava compression syndrome, acute spinal cord compression, malignant pleural effusion, pericardial effusion, and malignant colorectal tumor combined with cardiopulmonary resuscitation cases, and then a case was designed by the instructor for each disease. The operation of the SimMan4000 integrated simulator from Laerdal, Norway, was used for training. The teacher created a case of superior vena cava compression syndrome, acute spinal cord compression, malignant pleural effusion, pericardial effusion, and malignant colorectal tumor combined with CPR according to the teaching content. Then, according to the problems raised by the nurses, summarized into a number of several focused problems, each student chooses a few or a problem to find information, self-study (including checking textbooks, Internet search, search library books, literature); a few days later, focused discussion, each student report what they have prepared, and then discussion, the first hypothesis to argue, when nurses encounter more difficult. When nurses encounter more difficult problems or discussions, the teacher provides the necessary guidance and conducts a mutual aid course with nurses, the last class is summarized by the teacher, and finally a theory exam is given. The computer simulation teaching uses SimMan4000 integrated simulator for CPR skills training and assessment, the problems encountered in the computer simulation training nurses can discuss again or consult the information, and get the answers and repeatedly verify on the computer simulator to come up with the correct answers. Questionnaires were distributed to nurses' evaluation of the PBL combined with computer simulation

teaching method. There were 89 questionnaires distributed and 89 questionnaires were collected, with a 100% recovery rate.

(1) Establish a training group with the head nurse as the leader and select senior nurses with rich experience in treatment and training as instructors. Each person undertakes several projects to organize training.

(2) Formulate training plan. ①The training team will formulate outpatient treatment skills training plan and corresponding our treatment plan according to the annual nurse training plan of nursing department, combined with the characteristics of oncology outpatients and our situations that are prone to occur, such as cardiac arrest, hemorrhage (vaginal hemorrhage in cervical cancer, nasopharyngeal hemorrhage in nasopharyngeal cancer, gastrointestinal hemorrhage in liver cancer, etc.), drug allergy events, and sudden syncope, fall and suicide, etc., our treatment plan and resuscitation workflow, etc. ②The training team develops training programs and content to be focused on according to the outpatient treatment skills training plan, such as oxygen inhalation method, electric suction method, indwelling gastric tube, urinary catheterization, use of cardiac monitor and simple respirator, as well as cardiopulmonary resuscitation, cardiac defibrillation. ③ Training for nurses' comprehensive treatment ability includes the ability to identify and solve problems, our operation skills and critical care record writing ability, etc., old. Conduct training.

(3) The implementation of training treatment skills training is arranged by the chief nurse, and the instructor conducts centralized training for all inpatient nurses. The training method adopts a combination of scenario simulation method and instructor operation demonstration method, and the scenario simulation method is used for key training contents, such as resuscitation of patients in cardiac arrest and hemorrhagic shock. After the training, the trainees are assessed, and the chief nurse randomly checks the assessment every month, and the assessment results are linked to the performance.

(4) Effectiveness evaluation assessment is divided into three parts: theoretical knowledge of our nursing, skill operation, and comprehensive our application ability of nurses. The theoretical examination questions combined with the theoretical knowledge learned, unified questions, ≥80 points to pass; skills operation reference 55 clinical nursing technical operation scoring standards for assessment, ≥90 points to pass; nurses comprehensive our ability assessment for resuscitation of patients after the end of the assessment, including the ability of nurses to identify and solve problems, resuscitation equipment operation proficiency, oral medical advice implementation, and critical care records The assessment of writing ability is conducted, and ≥80 is qualified.

The results of clinical medicine undergraduates before and after the internship were significantly better than those before the internship, with significant differences (about 0.05), see Table 1.

In total, 98.9% of the nurses liked the teaching method combining computer simulation and PBL, 97.6% of the nurses thought that this teaching method deepened their understanding and memory and improved their practical ability, and 96.6% of the nurses thought that the teaching method combining computer simulation and PBL could cultivate both team spirit and problem-solving ability.

Before training, 16 nurses passed the treatment theory knowledge examination, with a passing rate of 76.1%, and after training, 21 nurses passed, with a passing rate of 100%; before training, 15 nurses passed the treatment skills examination, with a passing rate of 71.5%, and after training, 20 nurses passed, with a passing rate of 95.1%; before training, 16 nurses passed the treatment comprehensive ability examination, with a passing rate of 76.3%, and after training, 20 nurses passed, with a passing rate of 95.3%. After the training, 20 nurses passed the comprehensive treatment ability test, with a pass rate of 76.3%, and the pass rate was 95.3%. After the training, the nurses' treatment theory knowledge, treatment skills assessment, and treatment comprehensive ability assessment scores are significantly improved (see Table 2.

The teaching content is the interpretation of our 2015 bleeding guidelines in oncology, causes of cardiac arrest, and recognition and management of cardiac arrhythmias. The number of teaching hours were all 12 hours. The control group used the traditional teaching method, and the teacher applied the lecture method to explain and demonstrate colorectal tumor bleeding in our hospital; the experimental group used a computer simulator combined with PBL for teaching, and the computer simulator applied the SimMan4000 integrated simulator produced by Laerdal, Norway, for simulation teaching. The specific approach was as follows: each experimental group was further divided into 3 groups of 5 members each, and the teacher created a cardiac arrest scenario case according to the teaching content, discussed the information based on this case, and proposed the most likely scenario, i.e., proposed a hypothesis. Each group member reviews the information and then summarizes it to come up with a possible answer and operates and practices on the SimMan 4000 integrated simulator. Each group member acts as a nurse, doctor, and patient's family. First, the nurse finds that the patient (SimMan integrated simulator) loses consciousness, determines whether it is cardiac arrest, starts our colorectal tumor hemorrhage, and at the same time notifies the doctor, cardiac monitoring, opens the venous. One person will direct the resuscitation, two people will be responsible for chest compressions and artificial ventilation, one person will be responsible for defibrillation and one person will be responsible for intravenous drug administration, and each person will rotate different roles after proficiency. Then, there is group discussion for the teacher to review. With the help of the video, the nurses and the instructor analyzed the resuscitation process and pointed out the merits of the nurses and the

Table 1: Theoretical and skill examination scores before and after the internship ($\overline{x} \pm s$).

Group	n	SVCS	Sec	Cardiopulmonary resuscitation	Practical skills
Post-apprenticeship	89	65.5 ± 8.9	71.2 ± 8.3	65.9 ± 9.6	70.5 ± 6.5
Pre-apprenticeship	89	82.3 ± 9.2	84.9 ± 7.1	82.3 ± 9.1	89.1 ± 7.9
P		0.018	0.027	0.012	0.008

Table 2: Comparison of assessment scores of 21 nurses' treatment ability before and after training (scores).

Measurement items	n	Treatment theory knowledge	Treatment skills assessment	Comprehensive ability of first aid
Pretraining	21	84.32 ± 6.38	85.69 ± 6.13	76.9 ± 6.28
After training	21	92.62 ± 2.90	95.42 ± 2.87	91.5 ± 2.3
t-value		5.408	6.590	10.096
P-value		<0.05	<0.05	<0.05

aspects that needed further improvement, such as theoretical knowledge, resuscitation techniques, communication skills, and psychological status.

The teaching effectiveness was evaluated as follows:

3.1. Comparison of Theoretical and Skill Test Scores. Nurses in both groups were given the same difficulty of theoretical closed-book test and applied SimMan4000 integrated simulator for skill examination with computer scoring. The theoretical test scores and operational skills test scores of nurses in the experimental group for our colorectal tumor hemorrhage were significantly higher (see Table 3).

3.2. The Results of Questionnaire Survey for Nurses in Both Groups. After the examination, questionnaires were distributed to the nurses of both groups, which included the evaluation of the responsibility of the instructors, the approval of the teaching methods of the instructors and the evaluation of whether their theoretical and l clinical levels were improved. The results of the questionnaire survey are shown in Table 4.

4. Results

Since no universities in China have adopted multiple computer technologies to reform traditional medical PBL methods, it is difficult for us to conduct an empirical investigation study on the effects of computer technologies on reforming traditional medical PBL at this stage. In 2002, a university medical school was the first in China to establish an advanced clinical skills center using multiple technologies, including simulation and virtual technologies. At the same time, a university medical school also applied the PBL method to teaching various disciplines and achieved certain experience and effectiveness.

In the following, we will analyze the results of the questionnaire of the 2003 undergraduate clinical skills training of a university medical school and the statistical table of the questionnaire of microbiology "PBL" of a university medical school to explore the expected effect of using various computer technologies to reform the traditional medical PBL method.

The results of the 2003 undergraduate clinical skills training questionnaire at a university medical school are as follows:

The survey was conducted mainly for the participation of 2003 undergraduate nurses in clinical skills training. 104 questionnaires were distributed, 64 in the 2003 undergraduate class, and 40 in the diagnostic class. A total of 85 questionnaires were returned, and the results are shown in Tables 5–7.

The comparison of the effectiveness of teaching with or without simulation is shown in Table 8.

Figures 1–3 show the case information provided, the organization of the class, and the takeaways for the nurses.

The experimental results showed that the practical and theoretical scores of interns in the experimental group were significantly higher than those in the control group ($P < 0.05$). During the experiment, the interns in the laboratory group were satisfied with the teaching work and performed differently ($P < 0.05$)(Tables 9 and 10.

A comparison of the changes in the condition of the two groups of patients after our 0 h and 12 h is shown in Table 11.

The comparison of mortality rates between the two groups of patients at 7 and 21 days after surgery is shown in Table 12.

5. Discussion

Computer simulation technology has created a fully functional clinical simulation teaching environment, providing medical students with a new practical experience. Compared with traditional medical education, simulated medical education has a better training effect and has been widely used in the medical field [11, 12]. Through a large number of teaching practices, it has been proved that simulated medical training has the following advantages: (1) Cultivate teamwork spirit. The success of CPR is not achieved by one medical personnel but requires the teamwork of several medical personnel who work together and are skilled in order to achieve successful CPR and save patients' lives. This study shows that in the simulation teaching, the students learned through the CPR exercises on the computer simulator that the spirit of collaboration is important in clinical work, and the whole process of resuscitation requires mutual cooperation and cooperation in order to achieve the highest

Table 3: Comparison of theoretical and skill examination scores of nurses in the experimental and control groups ($\overline{x} \pm s$, scores).

Group	n	Theoretical examination results	Practical skills
Experimental group	45	$84.36 \pm 7.25^{*}$	$86.20 \pm 7.31^{**}$
Control group	45	77.20 ± 5.24	$71.35 \pm 9.18^{**}$

Table 4: Results of the questionnaire survey of 90 nurses' evaluation of the two teaching methods n (%).

Questionnaire items	Experimental group ($n = 45$)				Control group ($n = 45$)			
	Very satisfied	Satisfactory	General	Poor	Very satisfied	Satisfactory	General	Poor
Evaluation of teachers**	24 (69.9)	9 (29.7)	0 (0)	0 (0)	9 (27.5)	22 (64.9)	5 (13.3)	0 (0)
Agreement with old and new teaching methods*	14 (44.3)	19 (55.2)	0 (0)	0 (0)	12 (35.2)	13 (41.1)	7 (23.9)	0 (0)
Satisfaction with their own progress**	17 (51.6)	16 (48.6)	0 (0)	0 (0)	5 (17.1)	14 (42.3)	13 (39.5)	0 (0)

Table 5: The way of gain clinical all techniques.

Evaluation content	Classroom learning and training (%)	Internet learning (%)	After-class learning, peer-to-peer practice (%)
Student evaluation results	92.93	25.89	42.36

Table 6: The ratio of theories study and techniques exercise.

Evaluation content	Rationality of theory and training proportion (%)	Theoretical study is less, which affects the understanding of learning content (%)	Less skill training, more optional (%)
Student evaluation results	45.89	20.00	34.11

Table 7: The content degree of clinical techniques training.

Evaluation content	Small class lectures, model practice (%)	SP training (%)	E-learning (%)	Other (can be specified)
Student evaluation results	74.13	27.05	2.34	

efficiency in the shortest time [13, 14]. (2) There is no risk to the patient. Due to the increasing awareness of patients' rights, the national law requires interns to inform and obtain patients' consent when treating patients, and patients are afraid that some medical operations will be harmful to them, so they oppose interns or junior doctors to perform medical operations on themselves, which makes junior doctors lack practical experience and affects the improvement of medical standards, and the medical simulation system has solved this problem well. (3) Allowing for errors and the ability to correct them quickly. When students use the simulation system, they can make mistakes, because there are no adverse consequences, they can be corrected by the instructor in a timely manner, which helps to enhance memory and avoid making similar mistakes again. (4) Can be repeatedly operated, repeated training, participants can be repeatedly operated on the medical simulation system until proficiency. (5) Can be recorded and played back, the use of video data to find their own errors in the actual operation and to discuss and evaluate. (6) Adjustable and controllable operation process. (7) Standardization of medical training and assessment.

PBL encourages students to learn actively, and the most obvious advantage of PBL compared with traditional lecture method is that it emphasizes and encourages students to learn actively, encourages students to broaden their ideas and learn creatively, and requires the integration and convergence of basic and clinical expertise in various medical disciplines [15, 16]. Students obtain and evaluate information in various ways, and in PBL, teachers can grasp the problems of students' learning by organizing students' discussion and analysis and can tailor teaching to each student's characteristics, so that the common problems can be solved more successfully [17, 18]. At the same time, after the students finish the problem-based learning, they return to the initial state of the problem, and the key contents of the teaching can be remembered and understood deeply after repeated cycles.

The combination of computer simulation teaching and PBL enhances the attractiveness of classroom teaching and students' learning ability, stimulates the enthusiasm of operation and practice, and deepens the understanding and memory of knowledge, thus completely changing the previous situation of emphasizing knowledge transfer but not ability cultivation, teacher teaching but not student participation in the teaching process [19, 20]. PBL creates "problem scenarios" and sets learning into complex and meaningful problem situations. The process of learning is to learn the scientific knowledge implied behind the problems and to develop problem-solving skills, i.e., to develop the ability to learn independently. At the same time, the ability

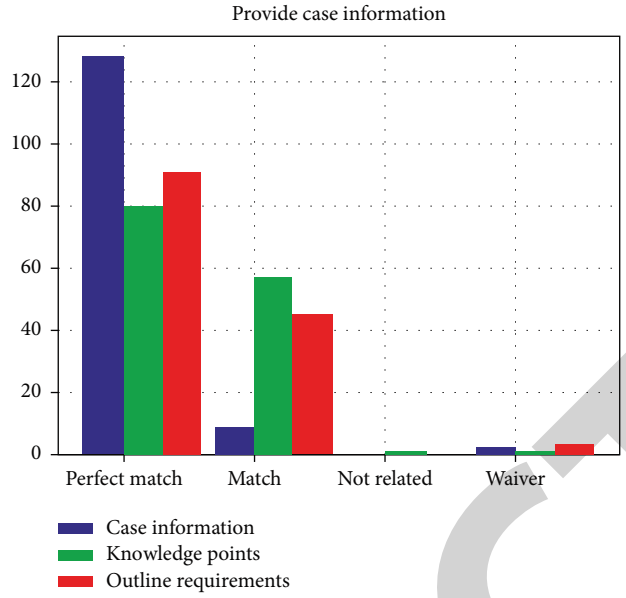

Figure 1: Availability of case information.

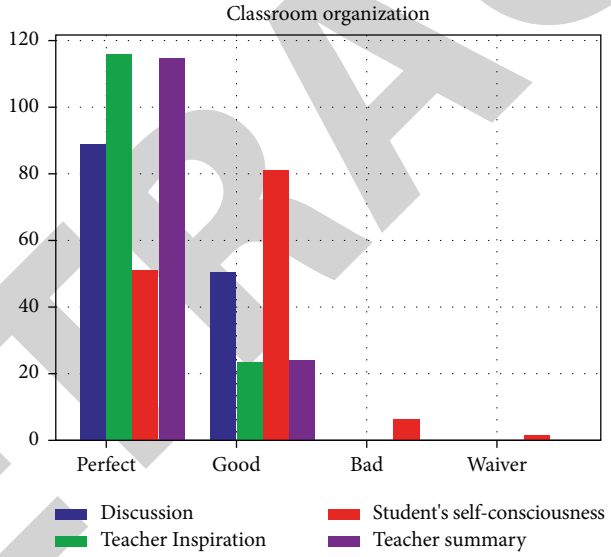

Figure 2: Classroom organization.

to acquire and evaluate information and the skill to disseminate information is improved [21, 22]. Computer simulation teaching combined with PBL can cultivate students' comprehensive quality, deepen their knowledge and understanding of the original theoretical knowledge in textbooks, and train both comprehensive analysis ability and knowledge application ability, so that students can really become the discoverer and applicator of knowledge and improve their comprehensive quality. In the specific computer simulation scenario, students can exercise their teamwork and social practice [23]. The students develop practical skills and good psychological quality. Focus on inducing students to think independently, enhance the cultivation of analytical skills, and give students more opportunities for independent thinking and self-development.

This study showed that the application of computer simulation combined with PBL in CPR teaching significantly improved students' performance, and 96.8% of students liked computer simulation combined with PBL, which fully demonstrated the advantages of this teaching method [24, 25]. Seven-year students with good English, strong learning ability and high overall quality can definitely improve their academic performance and clinical skills by applying computer simulation teaching combined with PBL in teaching, and prepare to serve patients better in the future.

With the development of new surgical procedures, improved surgeon techniques and the widespread use of broad-spectrum antibiotics, the incidence of fatal bleeding has become less common, but when this complication does occur, it is often critical, clinically difficult to treat, and

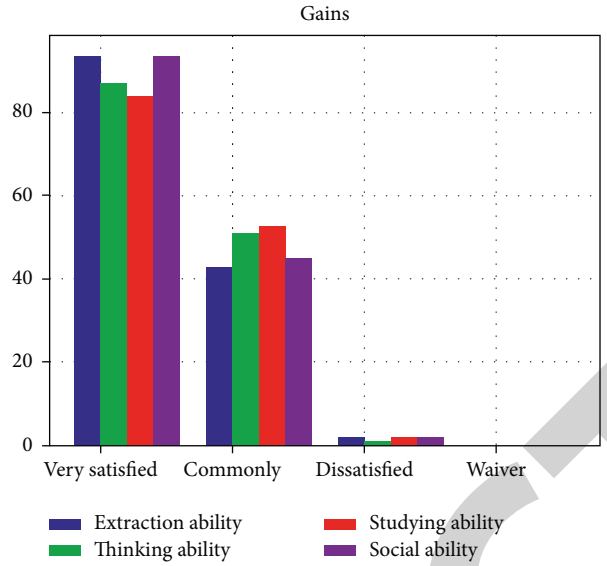

Figure 3: Gains of the nurses.

Table 8: The contrast of teaching effect on applying the simulated technology to teach or not.

	Trained	Untrained
Reached caecum	53%	18%
Time to caecum (min)	35	45
Pain (VAS)	6	7

Table 9: Comparison of assessment scores and satisfaction scores of teaching of clinical medicine interns in the two groups (points, $\overline{x} \pm s$).

Group	Theoretical knowledge	Hands-on
Experimental group ($n = 35$)	86.59 ± 5.64	77.68 ± 5.14
Control group ($n = 35$)	96.85 ± 5.38	93.46 ± 2.99
T	6.266	7.126
P	$P < 0.001$	$P < 0.001$

Table 10: Comparison of clinical medicine interns' satisfaction scores with medical teaching between the two groups.

Group	Very satisfied	Satisfactory	Dissatisfied	Total satisfaction
Experimental group ($n = 35$)	12	11	12	65.72%
Control group ($n = 35$)	14	16	5	88.56%
x^2				9.265
P				$P < 0.001$

Table 11: Comparison of changes in APACHE II scores between the two groups of patients after 0 h and 12 h of our care (score, $\overline{x} \pm s$).

Group	0 h	12 h
Experimental group	28.6 ± 5.5	17.4 ± 6.6
Control group	28.5 ± 5.3	23.9 ± 4.4
t	0.353	6.484
P	>0.05	<0.05

Table 12: Comparison of mortality rates between the two groups of patients at 7 and 21 days after surgery (cases (%)).

Group		
Experimental group	1 (1.8)	2 (3.4)
Control group	2 (3.6)	4 (6.8)
x^2	0.126	0.175
P	>0.05	>0.05

highly lethal. The first few minutes of treatment when bleeding occurs are critical, and correct and timely treatment by the first caregiver on the scene may save the patient's life. Therefore, it is critical for nursing staff to have the correct treatment measures in place to take accurate and effective measures to stop the bleeding and improve the success rate of resuscitation.

This study showed that the application of computer simulation teaching combined with PBL for colorectal tumor bleeding significantly improved the learning

performance of nurses, and the questionnaire results showed that nurses were more agreeable to the new teaching method and were able to complete the tasks strictly in accordance with the requirements, and eventually reached a level of satisfaction with their progress. This fully reflects the advantages of computer simulation teaching combined with PBL teaching method.

In summary, PBL teaching on computer simulation system can overcome the real problem of "few practice opportunities" for medical nurses by simulating real clinical scenes and expand their clinical thinking ability through "problem-centered" heuristic teaching. The problem of low practice opportunities for medical nurses can be overcome by simulating real clinical scenarios. Through the perfect combination of teaching methods and teaching methods, it provides an important guarantee for the overall improvement of clinical practice skills of medical and nursing staff.

Data Availability

The experimental data used to support the findings of this study can be obtained from the corresponding author upon request.

Conflicts of Interest

The authors declared that they have no conflicts of interest regarding this work.

References

[1] D. Wu, Y. Lei, M. He, C. Zhang, and L. Ji, "Deep reinforcement learning-based path control and optimization for unmanned ships," *Wireless Communications and Mobile Computing*, vol. 2022, Article ID 7135043, 8 pages, 2022.

[2] G. Cai, Y. Fang, J. Wen, S. Mumtaz, Y. Song, and V. Frascolla, "Multi-carrier M-ary DCSK system with code index modulation: an efficient solution for chaotic communications," *IEEE Journal of Selected Topics in Signal Processing*, vol. 13, no. 6, pp. 1375–1386, 2019.

[3] K. Chandra, A. S. Marcano, S. Mumtaz, R. V. Prasad, and H. L. Christiansen, "Unveiling capacity gains in ultradense networks: using mm-wave NOMA," *IEEE Vehicular Technology Magazine*, vol. 13, no. 2, pp. 75–83, 2018.

[4] F. B. Saghezchi, A. Radwan, J. Rodriguez, and T. Dagiuklas, "Coalition formation game toward green mobile terminals in heterogeneous wireless networks," *IEEE Wireless Communications*, vol. 20, no. 5, pp. 85–91, 2013.

[5] S. Palanisamy, B. Thangaraju, O. I. Khalaf, Y. Alotaibi, S. Alghamdi, and F. Alassery, "A novel approach of design and analysis of a hexagonal fractal antenna array (HFAA) for next-generation wireless communication," *Energies*, vol. 14, no. 19, p. 6204, 2021.

[6] S. Nagi Alsubari, S. N Deshmukh, A. Abdullah Alqarni et al., "Data analytics for the identification of fake reviews using supervised learning," *Computers, Materials & Continua*, vol. 70, no. 2, pp. 3189–3204, 2022.

[7] Q. Liu, C. Liu, and Y. Wang, "Integrating external dictionary knowledge in conference scenarios the field of personalized machine translation method," *Journal of Chinese Informatics*, vol. 33, no. 10, pp. 31–37, 2019.

[8] S. A. Bansode, V. R. More, S. P. Zambare, and M. Fahd, "Effect of constant temperature (20°C, 25°C, 30°C, 35°C, 40°C) on the development of the Calliphorid fly of forensic importance, *Chrysomya megacephala* (Fabricus, 1794)," *Journal of Entomology and Zoology Studies*, vol. 4, no. 3, pp. 193–197, 2016.

[9] F. A. Al-Mekhlafi, R. A. Alajmi, Z. Almusawi et al., "A study of insect succession of forensic importance: Dipteran flies (diptera) in two different habitats of small rodents in Riyadh City, Saudi Arabia," *Journal of King Saud University Science*, vol. 32, no. 7, pp. 3111–3118, 2020.

[10] A. Abd, A. Fahd Mohammed, and S. P. Zambare, "New species of flesh fly (Diptera: sarcophagidae) Sarcophaga (Liosarcophaga) geetai in India," *Journal of Entomology and Zoology Studies*, vol. 4, no. 3, pp. 314–318, 2016.

[11] A. M. Al-Azab, A. A. Zaituon, K. M. Al-Ghamdi, and F. M. A. Al-Galil, "Surveillance of dengue fever vector *Aedes aegypti* in different areas in Jeddah city Saudi Arabia," *Advances in Animal and Veterinary Sciences*, vol. 10, no. 2, pp. 348–353, 2022.

[12] A. R. Alqahtani, A. Badry, S. A. Amer, F. M. A. Al Galil, M. A. Ahmed, and Z. S. Amr, "ntraspecific molecular variation among *Androctonus crassicauda* (Olivier, 1807) populations collected from different regions in Saudi Arabia," *Journal of King Saud University Science*, vol. 34, no. 4, Article ID 101998, 2022.

[13] R. Ali, M. H. Siddiqi, and S. Lee, "Rough set-based approaches for discretization: a compact review," *Artificial Intelligence Review*, vol. 44, no. 2, pp. 235–263, 2015.

[14] A. L. Chetlen, M. Mendiratta-Lala, L. Probyn et al., "Conventional medical education and the history of simulation in radiology," *Academic Radiology*, vol. 22, no. 10, pp. 1252–1267, 2015.

[15] O. Chernikova, N. Heitzmann, M. Stadler, D. Holzberger, T. Seidel, and F. Fischer, "Simulation-based learning in higher education: a meta-analysis," *Review of Educational Research*, vol. 90, no. 4, pp. 499–541, 2020.

[16] S. Hartigan, M. Brooks, S. Hartley, R. E. Miller, S. A. Santen, and R. R. Hemphill, "Review of the basics of cognitive error in emergency medicine: still no easy answers," *Western Journal of Emergency Medicine*, vol. 21, no. 6, pp. 125–131, 2020.

[17] R. Hu, L. Daftari Besheli, J. Young et al., "Dual-energy head CT enables accurate distinction of intraparenchymal hemorrhage from calcification in emergency department patients," *Radiology*, vol. 280, no. 1, pp. 177–183, 2016.

[18] A. D. Uçar, E. Oymaci, E. B. Carti et al., "Characteristics of emergency gastrointestinal stromal tumor (GIST)," *Hepato-Gastroenterology*, vol. 62, no. 139, pp. 635–640, 2015.

[19] N. Chetta, G. Martines, A. Picciariello, and P. Capuano, "Successful laparoscopic sleeve gastrectomy in emergency for a gastric gastrointestinal stomal tumor (gist) with acute bleeding: a case report," *American Journal of Case Reports*, vol. 19, pp. 849–853, 2018.

[20] M. Maegele, O. Grottke, H. Schöchl, O. A. Sakowitz, M. Spannagl, and J. Koscielny, "Direct oral anticoagulants in our trauma admissions: perioperative management, and handling hemorrhage," *Deutsches Ärzteblatt International*, vol. 113, no. 35-36, pp. 575–582, 2016.

[21] F. Zandrino, S. M. Tettoni, I. Gallesio, and M. Summa, "Emergency arterial embolization of upper gastrointestinal and jejunal tumors: an analysis of 12 patients with severe bleeding," *Diagnostic and Interventional Imaging*, vol. 98, no. 1, pp. 51–56, 2017.

[22] K. H. Chu, T. E. Howell, G. Keijzers et al., "Acute headache presentations to the emergency department: a statewide cross-

Hindawi
Emergency Medicine International
Volume 2023, Article ID 9831045, 1 page
https://doi.org/10.1155/2023/9831045

Retraction

Retracted: Nursing of Vulvar Cancer Radical Operation Combined with Laparoscopic Inguinal Lymph Node Dissection

Emergency Medicine International

Received 28 November 2023; Accepted 28 November 2023; Published 29 November 2023

This article has been retracted by Hindawi, as publisher, following an investigation undertaken by the publisher [1]. This investigation has uncovered evidence of systematic manipulation of the publication and peer-review process. We cannot, therefore, vouch for the reliability or integrity of this article.

Please note that this notice is intended solely to alert readers that the peer-review process of this article has been compromised.

Wiley and Hindawi regret that the usual quality checks did not identify these issues before publication and have since put additional measures in place to safeguard research integrity.

We wish to credit our Research Integrity and Research Publishing teams and anonymous and named external researchers and research integrity experts for contributing to this investigation.

The corresponding author, as the representative of all authors, has been given the opportunity to register their agreement or disagreement to this retraction. We have kept a record of any response received.

References

[1] S. Huang and F. Qiu, "Nursing of Vulvar Cancer Radical Operation Combined with Laparoscopic Inguinal Lymph Node Dissection," *Emergency Medicine International*, vol. 2022, Article ID 8091114, 6 pages, 2022.

Hindawi
Emergency Medicine International
Volume 2022, Article ID 8091114, 6 pages
https://doi.org/10.1155/2022/8091114

Research Article

Nursing of Vulvar Cancer Radical Operation Combined with Laparoscopic Inguinal Lymph Node Dissection

Simei Huang and Feifei Qiu

Department of Anesthesiology, The Second Affiliated Hospital of Guangzhou University of Chinese Medicine, Guangzhou 510120, China

Correspondence should be addressed to Feifei Qiu; fcsss1984@163.com

Received 5 July 2022; Revised 23 July 2022; Accepted 29 July 2022; Published 5 September 2022

Academic Editor: Hang Chen

Purpose. The application, development, and care of radical surgery combined with laparoscopic inguinal lymph node dissection for vulvar cancer. *Methods*. We searched the PubMed, Web of Science, the Cochrane Library, and EMBASE databases for published literature on the care of radical surgery combined with laparoscopic inguinal lymph node dissection for vulvar cancer up to June 2022. We used the following search terms and terms: "vulvar cancer," "injury," "radical vulvar cancer surgery," "laparoscopic inguinal lymph node dissection," and "care." *Results*. Laparoscopic inguinal lymph node dissection has become a new surgical method for the treatment of vulvar cancer, and it effectively avoids all the problems associated with traditional surgery. In addition, radical vulvar cancer surgery and laparoscopic inguinal lymph node dissection combined with high-quality nursing interventions can promote patients' recovery and reduce the occurrence of complications, which has important clinical significance. *Conclusion*. This article reviews the application, development, and nursing care of radical vulvar cancer surgery combined with laparoscopic inguinal lymph node dissection.

1. Introduction

Vulvar cancer is a relatively rare malignant tumor of female genital organs, accounting for about 3%–5% of female genital tumors, and it occurs in people over 60 years old [1]. The pathogenesis of vulvar cancer is unclear [2]. Studies have shown that the occurrence of vulvar squamous carcinoma is associated with human papillomavirus (HP) infection, vulvar nonneoplastic epithelial lesions, such as vulvar sclerosing moss, and sexually transmitted diseases [3]. Lymph node metastasis is an important risk prognostic factor for vulvar cancer. Therefore, lymphadenectomy (IL) is an important part of the surgical procedure for vulvar cancer. Although this procedure can provide better tumor control, the traditional open inguinofemoral lymphadenectomy (OIL) has a large surgical area, bleeding, and is prone to surgical site infection and necrosis, and postoperative complications are quite high, mainly including skin infection, necrosis, and laceration in the inguinal area, lymphatic leakage, lymphatic cysts, and lymphoma of the lower extremities. Postoperative complications include skin infection, necrosis, laceration, lymphatic leakage, lymphatic cysts, and lymphedema of the lower extremities, which seriously affect the recovery and quality of life of patients, and even affect the subsequent treatment of patients and reduce their efficacy, with some literature reporting up to 50% or more [1, 2, 4].

Although a series of improvements in surgical approaches have led to a decrease in the incidence of postoperative complications, the results have not met expectations. With the increasing rise of minimally invasive concepts in cancer treatment, laparoscopic inguinal lymph node dissection has become a new surgical procedure applied in the treatment of vulvar cancer, which has been reported at home and abroad. Laparoscopic inguinal lymph node dissection has the advantages of less trauma, less bleeding, less interference with the physiological functions of tissues and organs, less postoperative pain, faster recovery,

less surgical scar, and less impact on immune function. It can effectively avoid the most common problems of skin necrosis in the inguinal region and poor long-term healing of the incision, reduce complications, and significantly improve patients' quality of life [5–7].

It is clinically important to carry out a quality nursing approach from the actual situation of patients to give them comprehensive rehabilitation care and promote their recovery. Preoperative psychological care, adequate preoperative preparation, postoperative incision observation and care, functional exercise, and prevention of complications are especially important for patients' recovery. Therefore, quality nursing interventions for radical vulvar cancer combined with laparoscopic inguinal lymph node dissection can promote patients' recovery, shorten the operation time, reduce the occurrence of complications, and improve the cure rate of patients, which is of great clinical significance (Figure1). This article reviews the application, development, and nursing modalities of radical vulvar cancer surgery combined with laparoscopic inguinal lymph node dissection. One hundred and twenty-one articles were read, of which 45 were RCTs and 11 were recommendations. Only 13 RCTs and 8 recommendations remained (Figure 2).

2. Overview of Vulvar Cancer

Vulvar cancer is a rare malignant tumor of the female reproductive system, accounting for only 2% to 5% of all malignant tumors of the female reproductive system. The incidence of vulvar cancer increases with age and is common in older women over the age of 75, especially postmenopausal women.

Vulvar cancer can be divided into two categories: vulvar cancer associated with HPV infection and vulvar cancer unrelated to HPV infection, the latter being mostly in young women and possibly combined with vulvar intraepithelial neoplasia (VIN). One study showed that high-risk HPV-DNA types were detected in approximately 40.1% of vulvar cancer patients, 80.4% of VIN-2, VIN-3, and 77.5% of VIN-1 patients, with HPV types 16, 18, 23, and 31 being the most common. In contrast, HPV-negative vulvar cancers are associated with intraepithelial nonneoplastic degeneration of the vulva (NNED), a group of chronic diseases characterized by degeneration of the mucosal tissue of the vulvar skin and pigmentary changes of vulvar pruritus, mainly including sclerosing lichen sclerosis (LS) and squamous epithelial hyperplasia of the vulva (SH). Patients with LS have a 4% to 6% risk of developing vulvar cancer. In addition, sexually transmitted diseases, herpes simplex virus infection, smoking, alcohol abuse, obesity, hypertension, diabetes, early sexual intercourse, and low social status may be associated with the development of vulvar cancer but are not independent risk factors [8, 9].

The most common pathological type of vulvar cancer is squamous cell carcinoma, which accounts for about 80%–90% of cases, followed by malignant melanoma, adenocarcinoma, basal cell carcinoma, verrucous carcinoma, and sarcoma. According to the degree of histological differentiation, they can be classified as hypodifferentiated,

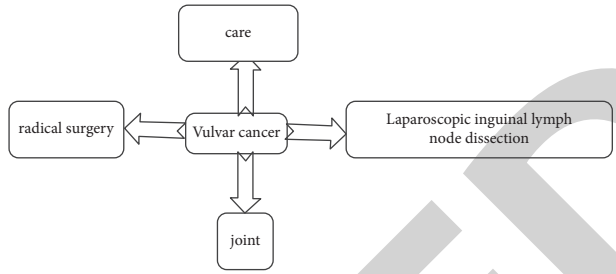

Figure 1: Nursing mechanism of vulvar cancer radical surgery combined with laparoscopic inguinal lymph node dissection.

intermediately differentiated, and highly differentiated. The earlier the stage, the higher the survival rate and the better the prognosis. Improving the early diagnosis rate of vulvar cancer is an important factor to improve its prognosis [10] (Table 1).

From Table 1, we can see that much evidence proves that the early diagnosis rate of vulvar cancer is an important factor in improving its prognosis, and the earlier the diagnosis, the earlier the treatment, the higher the survival rate, and the better the prognosis.

2.1. Treatment of Vulvar Cancer. The treatment of vulvar cancer is mainly surgical, and individualized surgical methods and radiotherapy plans are selected according to the disease, tumor stage, and physical condition [11, 12]. If it is an early-stage vulvar cancer, surgical treatment can be used, and the specific surgical method should be decided according to the stage. In the case of stage 1a vulvar cancer, local expanded vulvar excision can be used, and in the case of stage 1b vulvar cancer, the surgical approach should be decided according to the specific location of the cancer lesion. If it is a unilateral lesion, extensive local excision or modified extensive vulvectomy can be performed, and unilateral inguinal lymph node dissection is also required. If it is a midline vulvar cancer, local wide vulvectomy and bilateral inguinal lymph node dissection are required. In the case of locally advanced tumors, the extent of surgery should be evaluated on a case-by-case basis and may need to be combined with adjuvant therapy, such as radiotherapy, after surgery. In the case of advanced cancer with distant metastases, chemotherapy and targeted therapy may be required, depending on the patient's condition.

Radical vulvar cancer surgery is a surgical procedure to treat cancer of the vulva and inguinal lymph nodes and includes combined radical vulvar cancer surgery and radical vulvectomy. The Way radical vulvectomy, also known as the Way procedure, is a simultaneous extensive vulvectomy and bilateral inguinal resection with sequential pelvic-iliac fossa lymph node dissection if necessary. The Way procedure remains the classic standard procedure for the treatment of intermediate to advanced vulvar cancer. Inguinal lymph node dissection is a term published in urology in 2014. It is a procedure in which all lymph nodes and the surrounding fat pad in the inguinal region are removed. It is mainly used to treat inguinal lymph node metastases from malignant tumors, such as penile cancer [13, 14].

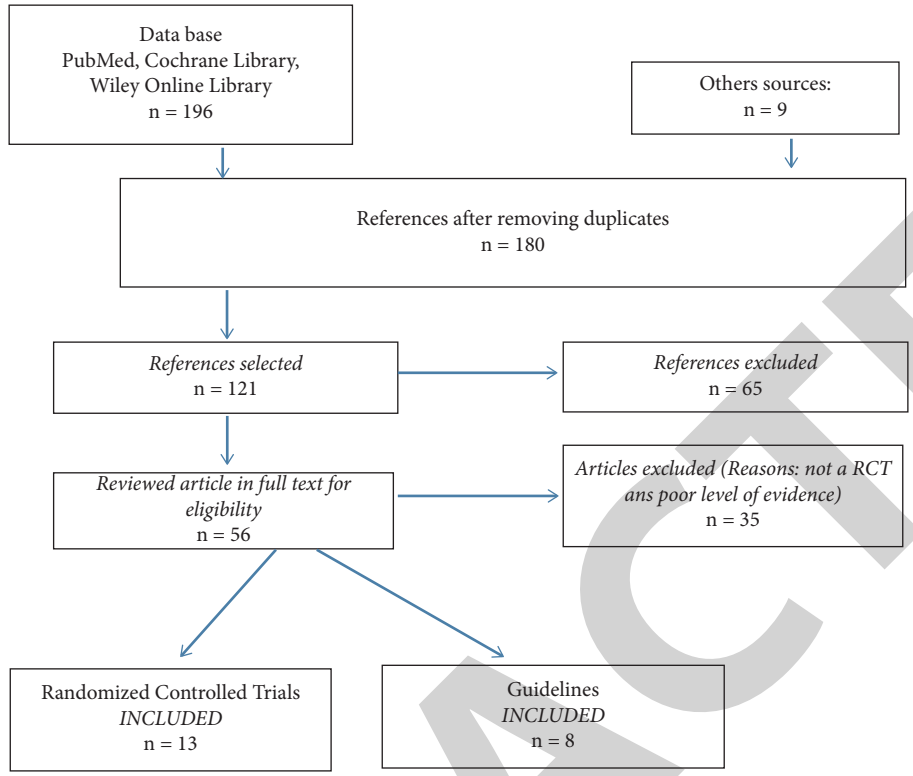

Figure 2: Read 121 articles, including 45 RCTs and 11 recommendations. Only 13 RCTs and 8 recommendations remained.

Table 1: Guidelines with high-level evidence and their impact size.

Organization	Guidelines with high standard of proof and effect size	
OARSI 2014 [22]	Exercise	Pain and function
	Weight loss	Pain and function
	Education	Pain
ESCEO 2014 [15]	Information/education	Treatment adherence
	Weight loss if overweight, exercise (strength training, aerobic training)	Function and pain
		Function and pain
NICE 2014 [18]	Education	Pain, function, and stiffness
	Exercise	Pain, function, and stiffness
	Weight loss	Pain, function, and stiffness
	Biomechanical interventions	Pain, function, and stiffness
AAOS 2013 [20]	Education	Pain
	Exercise	Function
	Weight loss	Disability
	Biomechanical interventions	Other symptoms
EULAR 2013 [14]	Education	Pain
	Exercise	Pain and function
	Weight loss	Pain and function
	Lifestyle changes	Pain and function
ACR 2012 [21]	Exercise	Pain and function
	Weight loss	Pain and function
RACGP NHMRC 2009 [19]	Weight loss	Pain and disability
	Exercise	Pain and function
	Education	Treatment adherence
		Pain and quality of life
SOFMER SFR SOFCOT 2008 [13]	Exercise	Pain and function
	Patient education and psychological support	Treatment adherence

Radiotherapy is often used as a preoperative or postoperative adjuvant treatment for vulvar cancer or as part of a comprehensive treatment for advanced vulvar cancer or advanced lesions to reduce the trauma of ultraextensive surgery and improve the prognosis of patients with vulvar cancer [15, 16]. Radiation therapy is not usually the first choice for vulvar cancer treatment, but it is an important part of the comprehensive treatment of vulvar cancer and is usually used in patients with lymph node metastases or in patients who are inoperable. Studies have shown that for patients with lymph node metastases, postoperative radiation therapy to the inguinal region and pelvis is beneficial in improving survival and reducing recurrence. Indications for radiation therapy include (1) patients with vulvar lesions that are too extensive to be surgically resected. Radiation therapy as preoperative treatment can reduce the extent of the lesion, decrease tumor cell activity, and increase the rate of surgical resection. (2) Patients who are too old and weak to tolerate surgery or have serious contraindications to surgery. (3) The surgical margin is not clean, or the surgical margin is too close to the tumor margin and postoperative radiotherapy. (4) Palliative radiotherapy for advanced and recurrent vulvar cancer can relieve symptoms and improve survival quality [1].

Due to the low incidence of vulvar cancer and the exact effect of initial surgical treatment, there are few clinical studies and a lack of evidence-based medical research on the application of chemotherapy alone for the treatment of vulvar cancer [17]. At present, clinically, chemotherapy is mostly used as adjuvant treatment to surgery or radiotherapy, for presurgical adjuvant treatment of locally progressive stages of vulvar cancer (such as stage III or IV) and for the combined application of chemotherapy and radiotherapy to patients who cannot be operated; or as postoperative adjuvant treatment, which can be used alone or combined with radiotherapy; or for treatment of recurrent vulvar cancer. Preoperative neoadjuvant chemotherapy is mainly used to control the primary tumor, reduce the size of the tumor, narrow the scope of surgical resection, or reduce surgery-related complications to facilitate subsequent treatment. At present, the commonly used chemotherapy regimens for vulvar cancer are mainly combination chemotherapy with cisplatin or 5-FU as the main drugs, including NF (HN2 + 5-FU) and PAB (DDP + ADM + BLM), which can be used in combination with radiotherapy and have good prospects for improving survival or life treatment of patients with moderately advanced or recurrent vulvar cancer. More clinical experience in chemotherapy of vulvar cancer still needs to be explored [18–20].

2.2. Laparoscopic Inguinal Lymph Node Dissection. Although laparoscopic inguinal lymph node dissection was first performed in vulvar cancer surgery, its safety and significant reduction of postoperative complications in the inguinal region were initially demonstrated by Mathevet et al. [21]. Since 2002, the subsequent use of laparoscopic inguinal lymph node dissection in vulvar cancer has rarely been reported. Some scholars have carried out laparoscopic inguinal lymph node dissection in patients with penile cancer and malignant melanoma of the lower extremities, drawing on the experience of laparoscopic techniques for lymph node dissection in breast cancer patients.

The low bleeding, low incidence of postoperative complications, and comparable number of lymph nodes resected with open surgery in laparoscopic surgery indicate that laparoscopic surgery is safe and feasible. Another index to evaluate the feasibility and safety of laparoscopic inguinal lymph node dissection is the postoperative tumor recurrence and 5-year survival of patients. Because laparoscopic inguinal lymph node dissection is an emerging technique, most of the current relevant studies are single-center studies with small sample sizes, and most of the articles are retrospective analyses without control groups and short follow-up times. Therefore, conducting prospective comparative studies with multicenter and larger samples will be under the direction of future research.

2.3. Nursing Method. Due to the special surgical site of vulvar cancer and the fact that the surgical incision is adjacent to the urethra and anus, it is very easy to be infected, easy to be moist locally, difficult to heal due to high tissue tension, and easy to form a cavity. The inguinal lymph node dissection under lumpectomy is less traumatic, has less bleeding, and is less painful, which avoids the problems of skin necrosis in the inguinal area, long-term poor healing of the incision, and the inability to carry out the subsequent treatment as scheduled and greatly shortens the hospital stay while reducing the damage. For the specificity of the surgical site, nursing care focuses on postoperative incision observation and care, guidance and feedback on patient activities, and appropriate psychological intervention, which are particularly important for patient recovery, and reasonable and effective treatment and care have important clinical significance [22, 23].

Psychological care: patients lack medical knowledge and are extremely concerned about the safety of surgery, incision pain, and prognosis. They are worried about the destruction of the vulva after surgery, which will seriously affect sexual life and the relationship between husband and wife. In order to reduce the patient's psychological burden, psychological care methods such as support and guidance are used to relieve the patient's psychological barriers, make him face reality correctly, and build up confidence.

Preoperative care: improve preoperative examination, exclude contraindications to surgery and anesthesia, and actively adjust blood pressure, blood sugar, and nutrition to improve the patient's tolerance to surgery. Keep the vulva clean and pay attention to prevent scratching the skin.

Intraoperative care: Keep the patient's thigh and abdomen on the same level, bend the knees, about 140° between the upper and lower legs, abduct the feet as much as possible to prevent the fibula capitulum from being in close contact with the leg support, the popliteal fossa is suspended, and the separation angle between the two legs is about 75°. This position is conducive to the exposure of the inguinal region and to keep the limbs in a functional position as much

as possible when laparoscopic inguinal lymphatic dissection is performed. When wide vulvectomy is performed, the legs are adjusted to 100°~120° apart, hip flexion 90°~100°, and knee flexion 90°~100°, which is conducive to exposing the vulva and facilitating the surgeon's operation; when closing the vulvar incision, the legs are adjusted to 70°~80° apart to reduce the tension of the incision and facilitate the healing of the incision after surgery. Small soft pillows are placed on the buttocks and lumbar area. After inguinal lymph node dissection, send the lymph nodes for pathological examination in a timely manner and establish pneumoperitoneum for pelvic lymph node dissection if the result is positive [24].

Postoperative care: first-level care, diet ban, stay with a companion, rehydration, and oxygenation were given as prescribed by the doctor after surgery. Due to the richness of nerve endings in the perineum, the postoperative incision was wrapped with a large number of cotton pads with pressure, and the patient often felt pain and discomfort. To ensure the patient's comfortable postoperative activities and rest, an anesthetic analgesic pump was used as prescribed by the doctor, and the patient's attention was distracted by communicating with the patient and listening to soft music, and the nursing operation was concentrated as much as possible with gentle movements to allow the patient to rest fully at night. Complications in the inguinal lymphatic drainage area are mainly skin flap infection and necrosis, resulting in delayed healing of the incision. The incision should be taken care of to prevent bleeding. To prevent vaginal adhesions, iodoform gauze is placed in the vagina, and the vulvar incision is cleaned and disinfected with iodophor solution daily. After inguinal lymph node dissection on both sides, lymphatic fluid, tissue fluid, and exudate will inevitably accumulate under the skin flap, so the drainage tube should be taken care of in a timely manner. When caring for the urinary catheter, it should be kept open. Take care of their bowel movements.

Functional exercise and rehabilitation guidance: patients are prone to vaginal opening stenosis caused by incision scar or contracture due to surgical removal of large amount of tissues. After 7~10 days postoperatively, functional exercises should be performed twice a day for 10~20 minutes each time, such as closing, separating, forward flexion, back extension, abduction, and adduction of the legs, with gentle and slow movements and a range of activities from small to large. According to the patient's age and condition, the patient should be instructed to perform pelvic floor muscle contraction training to reduce scar contracture and improve urinary and bowel function.

3. Discussion

Vulvar cancer is a malignant tumor that occurs mostly in women. The clinical cause of this disease is not clear but is thought to be mainly related to genetic predisposition, excessive alcohol consumption, and the use of exogenous estrogens. In recent years, the incidence of this disease has been on the rise. Vulvar cancer itself does not affect patients' life and health, but it can adversely affect vital organs and structures such as the liver, lungs, and bone due to cell shedding and metastasis, which can lead to various symptoms and threaten patients' life and health. Surgery is the main treatment method for vulvar cancer patients. In the past, modified radical surgery was usually used in clinical practice, which is effective in removing cancerous tissues, but it is more traumatic and has a slower recovery rate, which has a greater impact on patients' psychology and quality of life [25, 26].

With the further improvement of laparoscopic instruments and technical development, laparoscopy has been widely used in the treatment of gynecological malignancies. Care of vulvar cancer surgery is also an important part of the success of surgery. We should strengthen patient psychological care before surgery, fully improve preoperative examination and assessment preparation, closely observe the condition after surgery, and conduct a good job of observation and prevention of postoperative complications. Because of the large amount of subcutaneous tissue removed during open resection of inguinal lymph nodes, long-term poor healing of the inguinal incision is likely to occur after surgery, with an incidence of more than 50% reported in the literature. Laparoscopic inguinal lymphatic dissection can effectively avoid the common problems of skin necrosis and long-term poor healing of the inguinal incision after open surgery because the surgery is performed in the subcutaneous space, and there is no incision in the skin of the inguinal region, which is less traumatic, the postoperative recovery is fast, and the hospital stay is shortened [5, 27].

4. Conclusion

In conclusion, the combination of radical vulvar cancer surgery with laparoscopic inguinal lymph node dissection with quality nursing intervention can promote patients' recovery, shorten the operation time, and reduce the incidence of patients' complications, which has significant clinical significance.

Data Availability

The experimental data used to support the findings of this study are available from the corresponding author upon request.

Conflicts of Interest

The authors declare that they have no conflicts of interest.

References

[1] D. Weinberg and R. A. Gomez-Martinez, "Vulvar cancer," *Obstetrics & Gynecology Clinics of North America*, vol. 46, no. 1, pp. 125–135, 2019.

[2] A. Tan, A. K. Bieber, J. A. Stein, and M. K. Pomeranz, "Diagnosis and management of vulvar cancer: a review," *Journal of the American Academy of Dermatology*, vol. 81, no. 6, pp. 1387–1396, 2019.

[3] S. Merlo, "Modern treatment of vulvar cancer," *Radiology and Oncology*, vol. 54, no. 4, pp. 371–376, 2020.

Hindawi
Emergency Medicine International
Volume 2023, Article ID 9783815, 1 page
https://doi.org/10.1155/2023/9783815

Retraction

Retracted: Application of Melatonin with N-Acetylcysteine Exceeds Traditional Treatment for Acetaminophen-Induced Hepatotoxicity

Emergency Medicine International

Received 28 November 2023; Accepted 28 November 2023; Published 29 November 2023

This article has been retracted by Hindawi, as publisher, following an investigation undertaken by the publisher [1]. This investigation has uncovered evidence of systematic manipulation of the publication and peer-review process. We cannot, therefore, vouch for the reliability or integrity of this article.

Please note that this notice is intended solely to alert readers that the peer-review process of this article has been compromised.

Wiley and Hindawi regret that the usual quality checks did not identify these issues before publication and have since put additional measures in place to safeguard research integrity.

We wish to credit our Research Integrity and Research Publishing teams and anonymous and named external researchers and research integrity experts for contributing to this investigation.

The corresponding author, as the representative of all authors, has been given the opportunity to register their agreement or disagreement to this retraction. We have kept a record of any response received.

References

[1] M. Chen, J. Ke, S. Ma, H. Chai, L. Zhang, and L. Zhang, "Application of Melatonin with N-Acetylcysteine Exceeds Traditional Treatment for Acetaminophen-Induced Hepatotoxicity," *Emergency Medicine International*, vol. 2022, Article ID 2791743, 8 pages, 2022.

Hindawi
Emergency Medicine International
Volume 2022, Article ID 2791743, 8 pages
https://doi.org/10.1155/2022/2791743

Research Article

Application of Melatonin with N-Acetylcysteine Exceeds Traditional Treatment for Acetaminophen-Induced Hepatotoxicity

Mengfei Chen, Jinfang Ke, Shilan Ma, Hua Chai, Liang Zhang, and Ling Zhang

Department of Emergency, People's Hospital of Ningxia Hui Autonomous Region, Ningxia, China

Correspondence should be addressed to Ling Zhang; zhangling_7015@sina.com

Received 16 June 2022; Revised 6 July 2022; Accepted 14 July 2022; Published 2 September 2022

Academic Editor: Hang Chen

Acetaminophen (APAP) overdose is one of the leading causes of acute liver damage. Given N-acetylcysteine (NAC) and melatonin (MLT) both have an attenuated value for APAP-induced liver toxification, where an optimized integrated treatment has not been well deciphered. Here, by giving a single dose of APAP (500 mg/kg) to wild-type male mice, combined with a single dose of 500 mg/kg NAC or 100 mg/kg MLT separately as the therapeutic method, this study aimed to investigate the effects of NAC and melatonin (MLT) alone or combined on acetaminophen (APAP)-induced liver injury. In this study, NAC and MLT both partially have an alleviated function in APAP-challenged liver injury. However, MLT's add-on role strengthens the hepatoprotective effect of NAC on APAP-induced liver damage and resolute the inflammatory infiltration. Meanwhile, the combination of two reagents attenuates the decreased glutathione (GSH) and activation of the p38/JNK pathway. The combination of MLT and NAC can further ameliorate APAP-induced liver injury, which provides a novel strategy for drug-induced liver injury (DILI).

1. Introduction

Various inflammatory mediators could aggravate liver damage during the process of APAP overdose intoxication [1]. In the clinical context, different conditions can lead to the impairment of liver function and the occurrence of acute liver injury. Drug poisoning is a leading cause of acute liver failure, where APAP overdose nearly accounts for 50% of all liver injuries [2].

Widely used in analgesics and antipyretics, APAP is considered effective in therapeutic doses [3], and the dose of APAP varying from 1 to 4 g/day is considered clinically safe [4]. Mainly metabolized by UDP-glucuronosyltransferase (UGT) and sulfotransferase (SULT), it can be expelled through urine [4]. However, APAP overdose can cause severe liver damage to both patients and laboratory animals [5]. As for the underlying mechanism behind hepatotoxicity, it is caused by the saturation of sulfation and glucuronidation metabolic pathways. More importantly, the production of N-acetyl-p-benzoquinone imine (NAPQI) during hepatotoxicity can be induced by some hepatic cytochrome P-450 (CYP) isoenzymes, especially CYP2E1 [6]. NAPQI depletes the GSH in a critical process and is regarded as an electrophile that binds covalently to essential proteins, which subsequently creates an environment conducive to oxidative stress that leads to hepatocyte death [5]. In particular, APAP causes mitochondrial ROS by affecting the ATP/ADP ratios and c-jun N-terminal kinase (JNK) activation, which can further aggravate liver damage [7, 8]. Excessive APAP intake not only causes metabolic acidosis but also elevated transaminases. In addition, it activates damage-related molecular patterns (DAMPs), produces various proinflammatory cytokines and chemokines, and consequentially amplifies liver damage [9].

At present, the following mechanisms are mainly identified as protective against APAP-induced liver damage: the stimulation of glutathione synthesis, CYP2E1 inhibition, HSP induction, and the inhibition of oxidative stress [10, 11]. The antioxidant N-acetylcysteine (NAC), a sort of cysteine prodrug, is clinically most used to treat APAP

intoxication. Besides, it is also treated as what replenishes the intracellular stores of hepatic GSH [12]. The treatment should be administered intravenously in a timely manner and last 20 hours. Despite this, it can still lead to such adverse events as allergic reactions, nausea, vomiting, diarrhea or constipation, fever, headache, lethargy, and hypotension [13].

Melatonin (MLT) is responsible for various physiological processes and plenty of studies suggest the beneficial effects of melatonin on liver damage and diseases [14]. Shown as a free radical scavenger, MLT can produce antioxidant enzymes to become an antioxidant, including antilipid peroxidation and protein peroxidation [15]. Apart from that, MLT can also induce γ-glutamylcysteine synthetase (γ-GCS), the rate-limiting enzyme of GSH synthesis, thus increasing the concentration of cellular GSH in human vascular endothelial cells [16]. MLT treatment can significantly inhibit the APAP-induced activation of serine/threonine kinase receptor-interacting protein 1 (RIP1) and suppress JNK phosphorylation and mitochondrial Bax translocation, thus preventing AIF-dependent cell death [17].

As a leading cause of DILI, APAP overdose might result in acute liver failure and mortality. As an effective treatment for APAP-overdose patients, the administration of NAC is subject to some limitations in the protection against liver injury [6]. In this study, a new investigation was conducted based on a favorable combinator application of NAC with MLT in mitigating liver damage.

2. Methods

2.1. Animals and Liver Injury Model. Male wild-type C57BL/6 mice were purchased from Shanghai SLAC Laboratory, and mice liver injury models were constructed as previously reported [18]. APAP (obtained from Sigma-Aldrich) was dissolved in PBS at 55°C before the immediate heating to 37°C. Then, mice, after overnight fasting, received intraperitoneal (i.p.) PBS or APAP (500 mg/kg) injection. 500 mg/kg of NAC [9] (Sigma-Aldrich, i.p., 30 min before APAP injection) either separately or combined with 100 mg/kg of melatonin (MLT) [19] (Sigma-Aldrich, intragastrical, 30 min before APAP injection) was given to the required mice groups. These mice, after overnight fasting, only received i.g. PBS and were treated as a control group. All mice were sacrificed 24 hours or an indicated time after APAP injection by isoflurane inhalation (concentration of 5%) and cervical dislocation. No heartbeat was considered death in this study. The experiment was approved by the Laboratory Animal Ethical and Welfare Committee of Ningxia Medical University.

2.2. Liver Histology Analyses. Liver tissue was fixed in paraformaldehyde, and low to high concentration alcohol was used as a dehydrating agent to gradually remove water from tissue blocks. Then the tissue block was placed in the transparent agent xylene, which is soluble in alcohol and paraffin wax, to replace the alcohol in the tissue block with xylene, to dip wax embedding. Prepare a container (such as folding a small paper box), pour the melted paraffin into it, and quickly clip the paraffin-soaked tissue into it. After cooling, it solidifies into blocks. The embedded tissue blocks harden before they can be cut into very thin slices on a slicer. The embedded wax block is fixed on the slicer and cut into thin slices, usually 5–8 microns thick. HE staining is commonly used to increase the color difference of each part of tissue cell structure, which is convenient for observation.

2.3. Western Blot. Briefly, liver tissue was harvested and extracted by RIPA lysis buffer (Thermo Fisher). After protein BCA quantification (Thermo Fisher), the samples were separated by SDS-PAGE gel electrophoresis and immunoblotted to nitrocellulose membranes. Subsequently, the membranes obtained were blocked with 5% milk and incubated with 5% BSA dissolved antibodies overnight at 4°C. The antibodies used in this study are detailed as follows: β-actin, anti-Rabbit (all from Jackson, 1 : 10000), phosphor-p38 (CST,4511), p-38 (CST, 8690), phosphor-JNK1(CST, 9259), JNK1(CST, 3708), and RIP1(CST, 3708) (all from Cell Signaling Technology, 1 : 1000). Besides, the second antibodies were diluted in 5% BSA and incubated for 1 hour at room temperature.

2.4. Acute Toxicity Analyses and Inflammation Detection. Mice serum ALT, AST, and the activities of liver superoxide dismutase (SOD) and catalase (CAT) were detected using a biochemical kit (Nanjing Jiancheng Institute, China) in line with the applicable protocols. TNFα and IL-6 levels were tested using the ELISA kits provided by Neo Bioscience, China. In accordance with the commercially available protocol (ab118970, Abcam), malondialdehyde (MDA) was equivalently represented to indicate the lipid peroxide expression. The percentage of neutrophils was obtained through cytometrical flow. The flow antibodies CD11b and Ly6G were added as instructed and then detected by the machine. The populations were analyzed by using Cytoflex S Flow Cytometer (Beckman Coulter, USA), while the data was analyzed using a CytExpert software package.

2.5. Statistical Analysis. The data used in this study are all denoted as means ± SD through GraphPad Prism 9.0 (San Diego, USA). The one-way analysis of variance (ANOVA) and posthoc Tukey tests were conducted to analyze the difference between the two groups. When p values are less than 0.05, it would be treated as statically significant (*means $p < 0.05$, ** means $p < 0.01$, *** means $p < 0.001$, respectively).

3. Results

3.1. MLT Strengthens the Hepatoprotective Effect of NAC in Liver Damage. Given MLT has been demonstrated as capable to interrupt APAP's toxicity [14], NAC is accepted as a standard method applied to treat acetaminophen-induced liver injury (AILI). Firstly, it was placed conditionally on the

effect of combining MLT as the standard method with the mono treatment of NAC. In this study, APAP overdose could produce a satisfactory outcome of liver injury in wild-type (WT) mice, which exhibited a significantly elevated level of serum transaminase (ALT, AST, both $p < 0.05$) (Figure 1(a)). Meanwhile, hepatic necrosis was much severe in actively APAP-intoxicated mice than in untreated mice (NAC, MLT, both $p < 0.05$) (Figures 1(b)–1(f)). Additionally, compared with the mice with AILI that received the vehicle, either NAC or MTL could induce a favorable reduction in serum ALT (NAC, MLT, both $p < 0.05$) and AST levels (NAC, MLT, both $p < 0.05$) after AILI (Figure 1(a)). The combination of NAC and MLT resulted in a significant reduction in the levels of serum transaminase (AST, ALT, both $p < 0.05$) and alleviation of liver necrosis ($p < 0.05$), as indicated by both lower necrosis in comparison with NAC monotherapy (Figure 1(g)).

3.2. The Add-On Role of MLT Dampens Inflammation Resolution after APAP Overdose. Then, the characteristics of the MLT combined effect on APAP-overdose-induced intoxication were analyzed. The elevated hepatic levels of tumor necrosis factor-α (TNFα) and IL-6 (both $p < 0.001$) were observed in APAP-overdose mice as well (Figure 1(a)). Accordingly, the single APAP-overdosed mice have a higher level of neutrophil infiltration in the liver. Besides, through flow cytometric analysis, it was found that the volume of hepatic neutrophils was reduced in the combined group after APAP treatment ($p < 0.01$) (Figures 2(b)–2(f)). It appears that a single therapy of NAC or MLT exhibits the same tendency. Nevertheless, there was still no significant difference observed in our data compared with the APAP-induced liver injury group, respectively ($p > 0.05$) (Figure 2(g)).

3.3. Treatment of MLT and NAC Attenuates the Decreased GSH Caused by APAP. Given that lipid, the peroxidation in membrane lipids is a typical index for oxidative stress [20]. The next investigation was conducted into lipid peroxidation production. The GSH content characterizes oxidative stress [21]. According to our results, APAP could lead to a sharp decrease of hepatic GSH levels around 6 hours, while the GSH level partially reverses back to normal as time elapsed. It is noteworthy that the addition of MLT to NAC triggers a more effective release in GSH level at 24 hours ($p < 0.01$) (Figure 3(a)). Meanwhile, there are no significant differences in separated treatment groups at an early time points (6 or 12 hours). As indicated by the formation of MDA, APAP is capable of significantly upregulating MDA. As shown in Figure 3(b), APAP-challenged mice manifested a more considerable accumulation in MDA level as time elapsed, compared with the control group ($p < 0.001$), whereas the treatment of adding MLT could enhance the decreased effect of NAC on MDA significantly ($p < 0.01$). Notably, compared with the APAP-challenged group, the add-on of MLT to NAC is more effective in alleviating liver superoxide dismutase (SOD), and catalase (CAT) depletion (all $p < 0.01$) at 24 hours but not in the early time points (Figures 3(c) and 3(d)).

3.4. A Combination of the two Reagents Ameliorates APAP-Induced Activation p38/JNK Pathway. An analysis was conducted regarding the effects of MLT addition on NAC-treated liver injury. As shown in Figures 4(a) and 4(b), the level of hepatic phosphate p38 was significantly upregulated in APAP-challenged mice. As expected, the pretreatment with MLT to NAC could also suppress the induction of APAP-treated hepatic RIP1, and JNK phosphorylation is illustrated in Figure 4(a). It can be seen from this figure that the level of phosphorylated JNK was significantly increased in the liver of mice administered with APAP, while there were no significant changes observed in the level of p38 and JNK. Notably, the pretreatment with MLT inhibited the signaling pathway of APAP-evoked hepatic RIP1/JNK.

4. Discussion

Due to the absence of the previous experiments on the combination of these two drugs for treating APAP-challenged liver injury. So far, there has been a report that both NAC and MLT can produce a hepatocyte-protective effect on APAP-induced liver injury. As indicated by our data, ALT, AST, and liver necrosis levels were remarkably elevated in these mice. Then a dose of NAC or MLT separately was therapeutically administered, both partially as antioxidant drugs. Since Sener et al. noted that a combination of two drugs plays a beneficial role in hepatic ischemia and reperfusion [22]. Unanimously, it was presented as the damage attenuating role in each medication [6, 17] and manifested a promising liver function recovery when combined with these two reagents in APAP-induced liver injury, suggesting that MLT can enhance the protective effect of NAC. In this study, it found that the add-on of MLT was effective in reversing the APAP-induced liver damage.

Considering that APAP-induced hepatocyte necrosis releases Kupffer cells, monocytes, and neutrophils, the increased level of neutrophils is significant to the hepatic sterile inflammatory response in acute liver injury [23]. Such staining methods could help identify the extent of inflammatory inflammation, which is a limitation of our study. Nevertheless, further evaluation was conducted regarding their effect on hepatic inflammatory infiltration. Though separately applicated, either NAC or MLT has a mild inflammation resolution, it exhibited a promising recovery for neutrophil ($Ly6G^+CD11b^+$) infiltration when adding MLT on NAC. Meanwhile, the combined treatment could also alleviate the release of APAP-induced inflammatory cytokines such as TNFα and IL-6. Mechanically, it has been reported that MLT is capable to reverse the tacrolimus-induced increase of TNFα and IL-6 [24]. NAC can improve the attraction of TNFα and neutrophils in APAP-induced liver injury [9] and inhibit the production of IL-6 in hemodialysis patients [25]. The effect of MLT is mediated through receptor-dependent pathways [26] and regulated by other mechanisms [27]. On the other side, liver cytotoxicity is initiated by the production of NAPQI after APAP-challenge and subsequent generation of proinflammatory cytokines as well as chemokines by Kupffer cells, recruiting neutrophils and monocytes into the liver [9]. Although neutrophils are

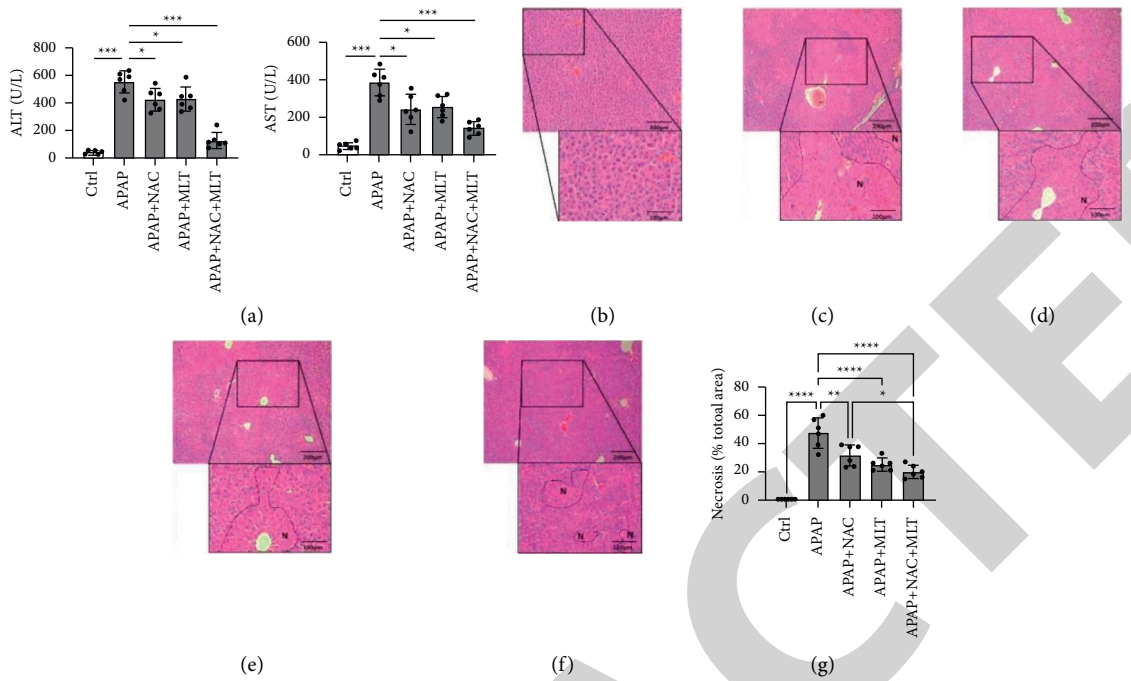

Figure 1: MLT displays a strengthened role in hepatic protective NAC therapy. (a) Serum level of ALT and AST for each group. H&E staining for wild-type mice (b), single APAP treated mice (c), APAP with NAC treated mice (d), APAP with MLT treated mice (e), and APAP with two drugs (f) and statistical quantification of necrosis in liver tissue for each group (g). The columns are shown as means ± SD ($n = 6$). N represents necrosis area. ($^{*}p < 0.05$, $^{**}p < 0.01$, $^{***}p < 0.001$).

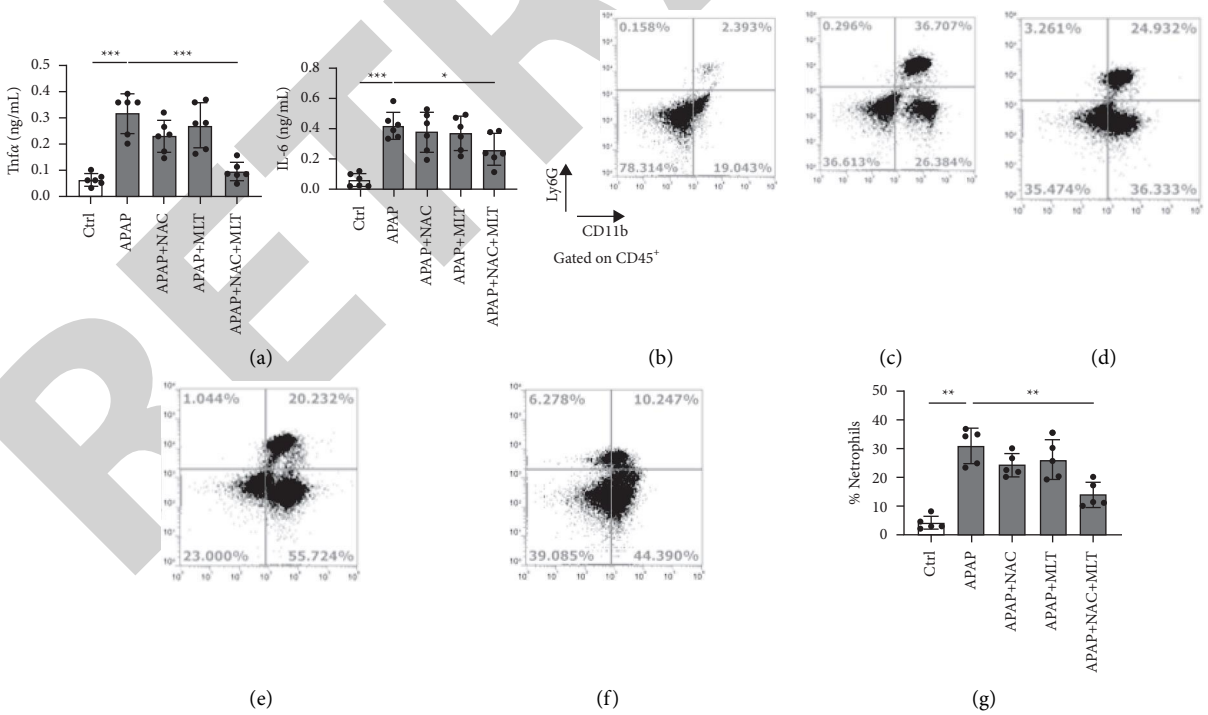

Figure 2: Enhanced inflammation resolution in mice treated with double drugs. (a) Serum levels of TNFα and IL-6 for each group. Representative FACS plots for control wild-type mice (b) ($n = 6$), single APAP treated mice (c), APAP with NAC treated mice (d), APAP with MLT treated mice (e), and APAP with two drugs (f) and statistical quantification of neutrophils in liver tissue for each group (g) ($n = 5$). The columns are shown as means ± SD. ($^{*}p < 0.05$, $^{**}p < 0.01$, $^{***}p < 0.001$).

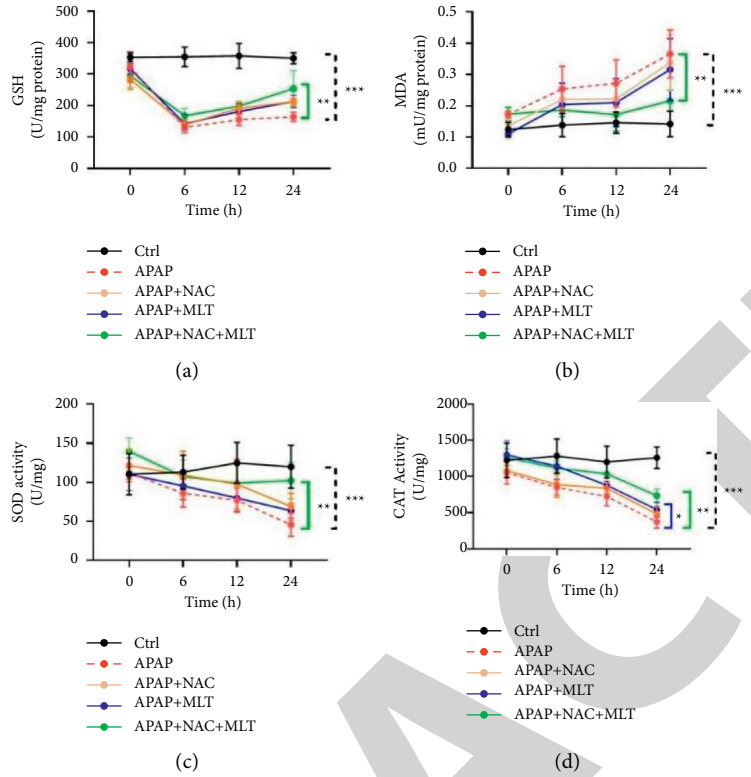

Figure 3: The effect of MLT, NAC, and combined treatments on glutathione (GSH) (a), malondialdehyde (MDA) (b), superoxide dismutase (SOD) and (c), catalase (CAT) activities levels (d) at an indicated time. The columns are shown as means ± SD ($n = 5$). ($^{*}p < 0.05$, $^{**}p < 0.01$, $^{***}p < 0.001$).

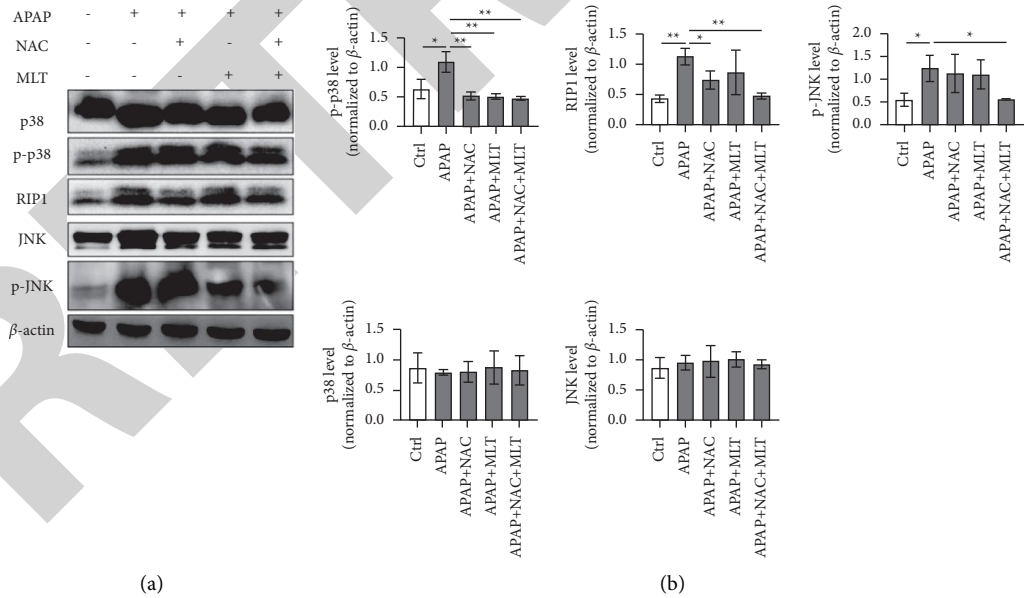

Figure 4: The effect of MLT, NAC, and combined drugs in RIP1/JNK associated apoptosis in APAP-induced liver damage. (a) Representative binds and (b) statistical grey-value analysis of protein level for each group. The columns are shown as means ± SD ($n = 3$). ($^{*}p < 0.05$, $^{**}p < 0.01$).

the first of the liver leukocytes to increase during AILI [28]. it is also thought that neutrophils only have an effect in the early stages and do not contribute to liver injury [29]. Our data support the involvement of neutrophils in the progression of acute liver injury during the early phase of AILI. But our main purpose is to find out the favorable impact of

combined drugs in APAP-induced liver injury but not the fundamental mechanism. Thus, the combined therapy method in other hepatic proinflammatory markers and the influx of proinflammatory monocytes remains unknown.

However, the protective effect mediated by melatonin or its metabolites remains inconclusive [30]. MLT and its metabolites all produce the same effect in suppressing ROS [31]. It has a direct antioxidant function or indirectly regulates the anti-oxidative and cytoprotective pathways, despite the rapidly metabolizing in peripheral tissues [32]. Besides, it is also involved in complex anti-oxidative activities by activating NRF2-dependent pathways [33, 34]. In this study, the single dose of melatonin in APAP-related hepatic toxicity failed to recover the hepatic GSH, which is consistent with the previous study [35]. Combined with NAC, however, it reinforces the inhibition in the consumption of GSH, by reportedly elevating γ-GCS to increase the intracellular GSH level [16]. The results obtained from this study provide a new therapeutic method for inflammation-related alleviation in liver injury. NAC has a positive effect on the hepatic GSH level exhausted by N-acetyl-p-benzoquinone and reactive oxygen species [1, 2, 36, 37]. MLT plays a limited role in inhibiting GSH depletion [17], which is associated with APAP-induced hepatotoxicity. MLT can induce γ-glutamylcysteine synthetase to affect GSH synthesis [16], thus significantly reducing the APAP-induced downregulation of hepatic GSH reductase and GSH peroxidase [17] and displaying an indirect antioxidant function in activating GSH peroxidase [38]. Moreover, this study exhibited a non-pronounced tendency to recovery in single MLT administration, which is confronted with little effect in APAP-related GSH depletion [17].

Concerning the mechanism of APAP-related liver injury, it has been well demonstrated that NAC can partially block the p38/JNK pathway [39]. There is a characteristic activation of JNK involved in APAP-related hepatotoxicity [40]. The RIP1-mediated activation of ASK1-interacting protein 1 (AIP1) is significant to ASK1-JNK/*p*38 apoptotic signaling pathway [41]. RIP1 is upstream of JNK and subsequent cell death [42, 43]. Meanwhile, RIP1 is associated with ROS-induced hepatotoxicity in APAP-related liver injury [44]. MLT is effective in inhibiting the APAP-induced activation of RIP1 and phosphorylation of JNK [17]. APAP could induce the activation of JNK and the phosphorylation of p38 in mouse models [45]. Currently, a conclusion consistent with the previous study is drawn. The overdose of APAP induces an elevation of p38/JNK pathway activation. Despite there being no significant difference observed between these groups for the single use of NAC or MLT, the suppressed APAP-induced phosphorylation of the p38 and JNK, and the combination of two drugs could reverse the activation of p38/JNK pathway, which provides a mechanistic basis for combined therapy.

However, there are also limits to this study. First, there are no clinical species in this study, which will verify the effect of melatonin. Second, the mechanism of this study is not clear, which needs further study to detect it.

5. Conclusion

In conclusion, it might produce a more favorable outcome when combined MLT with NAC in APAP-challenged liver injury, thus providing a novel therapeutic method for clinical practice.

Data Availability

The data and materials are available from the corresponding author upon reasonable request.

Ethical Approval

The experiment was granted approval from the Laboratory Animal Ethical and Welfare Committee of Ningxia Medical University.

Consent

The authors affirm that human research participants provided informed consent for publication.

Conflicts of Interest

The authors have no relevant financial or non-financial interests to disclose.

References

[1] H. Jaeschke, C. D. Williams, A. Ramachandran, and M. L. Bajt, "Acetaminophen hepatotoxicity and repair: the role of sterile inflammation and innate immunity," *Liver International*, vol. 32, no. 1, pp. 8–20, 2012.

[2] W. Bernal, W. M. Lee, J. Wendon, F. S. Larsen, and R. Williams, "Acute liver failure: a curable disease by 2024?" *Journal of Hepatology*, vol. 62, no. 1, pp. S112–S120, 2015.

[3] J. J. Zhang, X. Meng, Y. Li et al., "Effects of melatonin on liver injuries and diseases," *International Journal of Molecular Sciences*, vol. 18, no. 4, p. 673, 2017.

[4] E. M. Lancaster, J. R. Hiatt, and A. Zarrinpar, "Acetaminophen hepatotoxicity: an updated review," *Archives of Toxicology*, vol. 89, no. 2, pp. 193–199, 2015.

[5] J. A. Hinson, D. W. Roberts, and L. P. James, "Mechanisms of acetaminophen-induced liver necrosis," *Handbook of Experimental Pharmacology*, vol. 196, pp. 369–405, 2010.

[6] M. Alipour, C. Buonocore, A. Omri, M. Szabo, K. Pucaj, and Z. E. Suntres, "Therapeutic effect of liposomal-N-acetylcysteine against acetaminophen-induced hepatotoxicity," *Journal of Drug Targeting*, vol. 21, no. 5, pp. 466–473, 2013.

[7] M. R. McGill, M. R. Sharpe, C. D. Williams, M. Taha, S. C. Curry, and H. Jaeschke, "The mechanism underlying acetaminophen-induced hepatotoxicity in humans and mice involves mitochondrial damage and nuclear DNA fragmentation," *Journal of Clinical Investigation*, vol. 122, no. 4, pp. 1574–1583, 2012.

[8] M. R. McGill, C. D. Williams, Y. Xie, A. Ramachandran, and H. Jaeschke, "Acetaminophen-induced liver injury in rats and mice: comparison of protein adducts, mitochondrial dysfunction, and oxidative stress in the mechanism of toxicity,"

Toxicology and Applied Pharmacology, vol. 264, no. 3, pp. 387–394, 2012.

[9] S. Raevens, S. Van Campenhout, P. J. Debacker et al., "Combination of sivelestat and N-acetylcysteine alleviates the inflammatory response and exceeds standard treatment for acetaminophen-induced liver injury," *Journal of Leukocyte Biology*, vol. 107, no. 2, pp. 341–355, 2019.

[10] J. Y. Akakpo, A. Ramachandran, and H. Jaeschke, "Novel strategies for the treatment of acetaminophen hepatotoxicity," *Expert Opinion on Drug Metabolism and Toxicology*, vol. 16, no. 11, pp. 1039–1050, 2020.

[11] H. Jaeschke, J. Y. Akakpo, D. S. Umbaugh, and A. Ramachandran, "Novel therapeutic approaches against acetaminophen-induced liver injury and acute liver failure," *Toxicological Sciences*, vol. 174, no. 2, pp. 159–167, 2020.

[12] W. Klein-Schwartz and S. Doyon, "Intravenous acetylcysteine for the treatment of acetaminophen overdose," *Expert Opinion on Pharmacotherapy*, vol. 12, no. 1, pp. 119–130, 2011.

[13] M. C. Yarema, D. W. Johnson, R. J. Berlin et al., "Comparison of the 20 hour intravenous and 72 hour oral acetylcysteine protocols for the treatment of acute acetaminophen poisoning," *Annals of Emergency Medicine*, vol. 54, no. 4, pp. 606–614, 2009.

[14] S.-I. Kanno, A. Tomizawa, T. Hiura et al., "Melatonin protects on toxicity by acetaminophen but not on pharmacological effects in mice," *Biological and Pharmaceutical Bulletin*, vol. 29, no. 3, pp. 472–476, 2006.

[15] G. Sener, A. Ö Sehirli, and G. Ayanoglu-Dülger, "Protective effects of melatonin, vitamin E and N-acetylcysteine against acetaminophen toxicity in mice: a comparative study," *Journal of Pineal Research*, vol. 35, no. 1, pp. 61–68, 2003.

[16] Y. Urata, S. Honma, S. Goto et al., "Melatonin induces γ-glutamylcysteine synthetase mediated by activator protein-1 in human vascular endothelial cells," *Free Radical Biology and Medicine*, vol. 27, no. 7-8, pp. 838–847, 1999.

[17] Y. L. Liang, Z. H. Zhang, X. J. Liu et al., "Melatonin protects against apoptosis-inducing factor (AIF)-dependent cell death during acetaminophen-induced acute liver failure," *PLoS One*, vol. 7, no. 12, Article ID e51911, 2012.

[18] M. Li, X. Sun, J. Zhao et al., "CCL5 deficiency promotes liver repair by improving inflammation resolution and liver regeneration through M2 macrophage polarization," *Cellular and Molecular Immunology*, vol. 17, no. 7, pp. 753–764, 2020.

[19] R. Yang, C. Song, J. Chen et al., "Limonin ameliorates acetaminophen-induced hepatotoxicity by activating Nrf2 antioxidative pathway and inhibiting NF-κB inflammatory response via upregulating Sirt1," *Phytomedicine*, vol. 69, Article ID 153211, 2020.

[20] K. Uchida, "Future of toxicologylipid peroxidation in the future: from biomarker to etiology," *Chemical Research in Toxicology*, vol. 20, no. 1, pp. 3–5, 2007.

[21] N. Patsoukis and C. D. Georgiou, "Determination of the thiol redox state of organisms: new oxidative stress indicators," *Analytical and Bioanalytical Chemistry*, vol. 378, no. 7, pp. 1783–1792, 2004.

[22] G. Sener, O. Tosun, A. Ö şehirli et al., "Melatonin and N-acetylcysteine have beneficial effects during hepatic ischemia and reperfusion," *Life Sciences*, vol. 72, no. 24, pp. 2707–2718, 2003.

[23] O. Krenkel, J. C. Mossanen, and F. Tacke, "Immune mechanisms in acetaminophen-induced acute liver failure," *Hepatobiliary Surgery and Nutrition*, vol. 3, no. 6, pp. 331–343, 2014.

[24] A. B. Karabulut and C. Ara, "Melatonin ameliorates tacrolimus (FK-506)'s induced immunosupressive effect in rat liver," *Transplantation Proceedings*, vol. 41, no. 5, pp. 1875–1877, 2009.

[25] M. M. Nascimento, M. E. Suliman, M. Silva et al., "Effect of oral N-acetylcysteine treatment on plasma inflammatory and oxidative stress markers in peritoneal dialysis patients: a placebo-controlled study," *Peritoneal Dialysis International*, vol. 30, no. 3, pp. 336–342, 2010.

[26] R. M. Slominski, R. J. Reiter, N. Schlabritz-Loutsevitch, R. S. Ostrom, and A. T. Slominski, "Melatonin membrane receptors in peripheral tissues: distribution and functions," *Molecular and Cellular Endocrinology*, vol. 351, no. 2, pp. 152–166, 2012.

[27] A. T. Slominski, M. A. Zmijewski, I. Semak et al., "Melatonin, mitochondria, and the skin," *Cellular and Molecular Life Sciences*, vol. 74, no. 21, pp. 3913–3925, 2017.

[28] Z. X. Liu, S. Govindarajan, and N. Kaplowitz, "Innate immune system plays a critical role in determining the progression and severity of acetaminophen hepatotoxicity," *Gastroenterology*, vol. 127, no. 6, pp. 1760–1774, 2004.

[29] C. D. Williams, M. L. Bajt, M. R. Sharpe, M. R. McGill, A. Farhood, and H. Jaeschke, "Neutrophil activation during acetaminophen hepatotoxicity and repair in mice and humans," *Toxicology and Applied Pharmacology*, vol. 275, no. 2, pp. 122–133, 2014.

[30] A. T. Slominski, I. Semak, T. W. Fischer et al., "Metabolism of melatonin in the skin: why is it important?" *Experimental Dermatology*, vol. 26, no. 7, pp. 563–568, 2017.

[31] A. T. Slominski, T. K. Kim, K. Kleszczynski et al., "Characterization of serotonin and N-acetylserotonin systems in the human epidermis and skin cells," *Journal of Pineal Research*, vol. 68, no. 2, Article ID e12626, 2020.

[32] T. K. Kim, K. Kleszczynski, Z. Janjetovic et al., "Metabolism of melatonin and biological activity of intermediates of melatoninergic pathway in human skin cells," *The FASEB Journal*, vol. 27, no. 7, pp. 2742–2755, 2013.

[33] Z. Janjetovic, S. G. Jarrett, E. F. Lee, C. Duprey, R. J. Reiter, and A. T. Slominski, "Melatonin and its metabolites protect human melanocytes against UVB-induced damage: involvement of NRF2-mediated pathways," *Scientific Reports*, vol. 7, no. 1, p. 1274, 2017.

[34] C. Skobowiat, A. A. Brozyna, Z. Janjetovic et al., "Melatonin and its derivatives counteract the ultraviolet B radiation-induced damage in human and porcine skin ex vivo," *Journal of Pineal Research*, vol. 65, no. 2, Article ID e12501, 2018.

[35] T. Matsura, T. Nishida, A. Togawa et al., "Mechanisms of protection by melatonin against acetaminophen-induced liver injury in mice," *Journal of Pineal Research*, vol. 41, no. 3, pp. 211–219, 2006.

[36] C. Saito, C. Zwingmann, and H. Jaeschke, "Novel mechanisms of protection against acetaminophen hepatotoxicity in mice by glutathione and N-acetylcysteine," *Hepatology*, vol. 51, no. 1, pp. 246–254, 2010.

[37] D. P. Lopez, "Emergency: acetaminophen poisoning," *AJN, American Journal of Nursing*, vol. 109, no. 9, pp. 48–51, 2009.

[38] I. Crespo, B. S. Miguel, A. Laliena et al., "Melatonin prevents the decreased activity of antioxidant enzymes and activates nuclear erythroid 2-related factor 2 signaling in an animal model of fulminant hepatic failure of viral origin," *Journal of Pineal Research*, vol. 49, no. 2, pp. 193–200, 2010.

[39] M. Zafarullah, W. Q. Li, J. Sylvester, and M. Ahmad, "Molecular mechanisms of N-acetylcysteine actions," *Cellular and Molecular Life Sciences*, vol. 60, no. 1, pp. 6–20, 2003.

Hindawi
Emergency Medicine International
Volume 2023, Article ID 9813103, 1 page
https://doi.org/10.1155/2023/9813103

Retraction

Retracted: An Image Fusion Algorithm Based on Improved RGF and Visual Saliency Map

Emergency Medicine International

Received 19 December 2023; Accepted 19 December 2023; Published 20 December 2023

This article has been retracted by Hindawi following an investigation undertaken by the publisher [1]. This investigation has uncovered evidence of one or more of the following indicators of systematic manipulation of the publication process:

(1) Discrepancies in scope

(2) Discrepancies in the description of the research reported

(3) Discrepancies between the availability of data and the research described

(4) Inappropriate citations

(5) Incoherent, meaningless and/or irrelevant content included in the article

(6) Manipulated or compromised peer review

The presence of these indicators undermines our confidence in the integrity of the article's content and we cannot, therefore, vouch for its reliability. Please note that this notice is intended solely to alert readers that the content of this article is unreliable. We have not investigated whether authors were aware of or involved in the systematic manipulation of the publication process.

Wiley and Hindawi regrets that the usual quality checks did not identify these issues before publication and have since put additional measures in place to safeguard research integrity.

We wish to credit our own Research Integrity and Research Publishing teams and anonymous and named external researchers and research integrity experts for contributing to this investigation.

The corresponding author, as the representative of all authors, has been given the opportunity to register their agreement or disagreement to this retraction. We have kept a record of any response received.

References

[1] Y. Li, H. Yang, and Y. Gao, "An Image Fusion Algorithm Based on Improved RGF and Visual Saliency Map," *Emergency Medicine International*, vol. 2022, Article ID 1693531, 10 pages, 2022.

Hindawi
Emergency Medicine International
Volume 2022, Article ID 1693531, 10 pages
https://doi.org/10.1155/2022/1693531

Research Article

An Image Fusion Algorithm Based on Improved RGF and Visual Saliency Map

Yang Li, Haitao Yang, and Yuge Gao

Center for Space Security Studies, University of Aerospace Engineering, Beijing, China

Correspondence should be addressed to Haitao Yang; yanghtt@126.com

Received 30 May 2022; Accepted 30 June 2022; Published 25 August 2022

Academic Editor: Jacek Smereka

To solve the artifact problem in fused images and the lack of enough generalization under different scenarios of existing fusion algorithms, the paper proposes an image fusion algorithm based on improved RGF and visual saliency map to realize fusion for infrared and visible light images and a multimode medical image. Firstly, the paper uses RGF (rolling guidance filter) and Gaussian filter to decompose the image into the base layer, interlayer, and detail layer by a different scale. Secondly, the paper obtains a visual weight map by the calculation of the source image and uses the guided filter to better guide the base layer fusion. Then, it realizes the interlayer fusion through maximum local variance and realizes the detail layer fusion through the maximum absolute value of the pixel. Finally, it obtains the fused image through weight fusion. The experiment demonstrates that the proposed method shows better comprehensive performance and obtains better results in fusion for infrared and visible light images and medical images compared to the contrast method.

1. Introduction

As an image enhancement technology, image fusion basically aims to form a fused image that is more useful for human vision or subsequent image processing by superimposing and complementing all information of two or more images under the same scenario for different sensors or different positions, time, and illumination. The process shall follow three basic rules: firstly, the fused image must retain distinct features of the source image. Secondly, artificial information cannot be added in the fusion process. Thirdly, the valueless information (e.g., noise) shall be restrained as much as possible.

Among medical images, the multimode image can provide various types of information, of which importance on the clinical diagnosis increases continuously. Based on different imaging mechanisms, the multimode medical image provides different types of organizational information. For example, CT (computed tomography) provides information on the dense structure (e.g., skeleton and implantation material), whereas MR-T2 (T2-weighted magnetic resonance imaging) indicates high-resolution anatomical information (e.g., soft tissue). To obtain enough information for accurate diagnosis, doctors often need to make sequence analyses for captured medical images under different modes. In many cases, such a separated diagnosis mode is not convenient. An effective method of solving the problem is medical image fusion, which aims to generate a combined image and integrate complementary information in different forms of medical images.

With the rapid development of image technology in theory and application, how to improve information content in the fused image and how to improve the speed of fusion algorithm and generalization under different application scenarios are widely studied. Based on Laplacian Pyramid transform [1] and wavelet transforms [2], the early multiscale fusion method combines with different fusion rules or optimizes the decomposition method to improve the fusion effect or speed. However, the algorithm based on the above two methods has theoretical defects, i.e., the Pyramid decomposition-based method has no translation invariance but excessive redundant information, whereas the wavelet variation-based method has no translation invariance and few directions of decomposition. Therefore, the derived

algorithm from the above methods obtains an unclear target edge of the fused image and a bad overall effect. Although the NSCT (nonsubsampled contourlet)- [3] and NSST (nonsubsampled shearlet transform)-based [4] methods can overcome the above problems, realize good direction selection and translation invariance, generate less redundant information and more details in the fused image when decomposing the image, the methods cannot ensure spatial consistency in the fusion process and may result in an artifact in the fused image and noise because of the algorithm.

For the problems and defects of the above algorithm, the paper proposes the RGF-based improvement method for decomposing the source image on the basis of a conventional algorithm, and it designs a new fusion algorithm in combination with the maximum local variance, the maximum absolute value of the pixel, and a visual saliency map. Through the experimental verification of visual light and infrared image fusion and medical image fusion, the proposed algorithm indicates a better fusion effect, clearer edge in the fused image, higher illumination of the infrared target, more complete background information of visible light in the fused image, and better generalization under different scenarios compared to the classical algorithm.

2. Related Algorithm Research

2.1. Guided Filter and Rolling Guidance Filter (RGF). He et al [5] proposed the guided filter in 2010, which attracted wide attention because of its salient boundary effect, good gradient retention, and low linear complexity. Compared to other filters, the method can enhance detailed information and the overall feature of an image while retaining good image edge information.

The basic principle of the guided filter can be explained as follows: if the input image is p, the output image is q, and the guided image is I, then the output image q in the window ω_k with the center of k can be expressed as

$$q_i = a_k I_i + b_k, \quad \forall i \in \boldsymbol{\omega}_k, \tag{1}$$

where i & k are pixel coordinates, a_k & b_k are linear constants in the window, and ω_k is the square window with a size of $(2r+1)(2r+1)$. It can be seen that $\nabla q = a\nabla \mathbf{I}$ is true and ensures edge consistency between the output image q and the guided image I.

The constants a_k and b_k can be calculated by minimizing the square error between the input image p and the output image q:

$$E(a_k, b_k) = \sum_{i\in\omega_k} \left[\left(a_k I_k + b_k - p_i\right)^2 + \varepsilon a_k^2 \right], \tag{2}$$

where ε is the regularization parameter that can avoid too large a coefficient. Then, a_k and b_k can be calculated as follows:

$$\begin{aligned} a_k &= \frac{(1/|\omega|)\sum_{i\in\omega_k} I_i p_i - \mu_k \overline{p_k}}{\sigma_k^2 + \varepsilon}, \\ b_k &= \overline{p_k} - a_k \mu_k, \end{aligned} \tag{3}$$

where μ_k and $\overline{p_k}$ are the mean values of I and p in the window ω_k, σ_k^2 is the variance of I in the window ω_k, and $|\omega|$ is the pixel of window ω_k.

It is given that the guided image I has a linear correlation in the window ω_k, and the window includes all pixel points p_i, so that the value of the output image will vary with the transform of the window ω_k. Then, the final filter output q_i can be expressed as follows:

$$q_i = \frac{1}{|\omega|} \sum_{i\in\omega_k} \left(a_k I_k + b_k\right) = \overline{a_i} I_i + \overline{b_i}. \tag{4}$$

The final guided filter can be expressed as follows:

$$q = G_{r,\varepsilon}(I, p), \tag{5}$$

where G is the guided filter, and r, ε are the sizes of the filter window and structural erasing scale.

RGF [6] (rolling guidance filter) is an iteration method of combining the guided filter with other filters. It can obtain the outline of the object when filtering an image. Compared to other filters, RGF can avoid the loss of outline and boundary when erasing the texture structure or area details. Figure 1 shows the key idea of iteratively processing an image by RGF.

2.1.1. Small Structure Removal. The paper, firstly, erases the edge of the source image J to obtain J_1. Then, it considers the source image J as the guided image and uses the guided filter for J_1 to recover the edge and obtains J_2. Compared to J_1, J_2 has a clearer edge, and it loses some detail texture. The paper repeats the above steps and gradually increases the scale of erasing details to obtain the filtering results of a different scale.

The materials and methods section should contain sufficient details, so that all procedures can be repeated. It may be divided into headed subsections if several methods are described.

2.2. Visual Saliency Analysis. Visual saliency is an expression method of extracting salient points or areas in an image in a visual form by simulating human eyes, observing various features under different scenarios and generating related strong and weak stimulation. The first step of obtaining a visual saliency map is to get its high-pass image. The basic method is to use the difference between the mean filtering result and median filtering result of the source image to

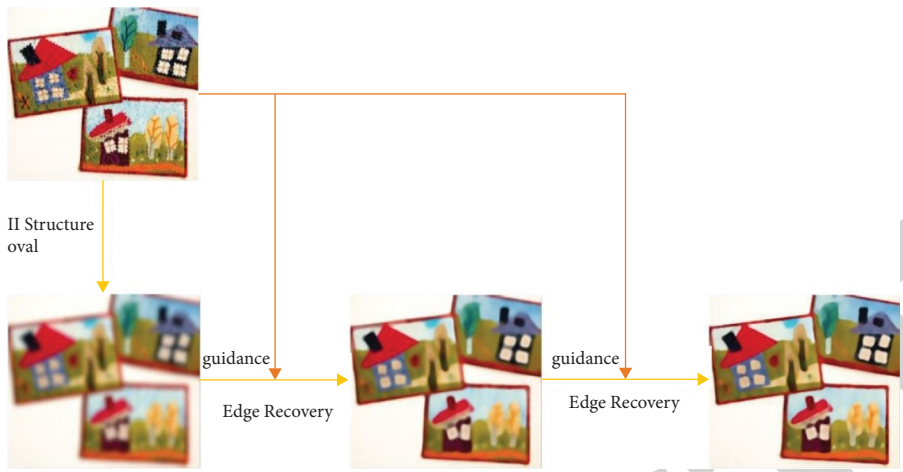

Figure 1: RGF diagram.

obtain the corresponding high-pass image, with the expression given as follows:

$$H_n(x, y) = \text{Average filter}(x, y, \mu_n) - \text{Median filter}(x, y, \rho_n), \quad n = 1, 2, \tag{6}$$

where (x, y) is the pixel coordinate of the source image in the corresponding position, and μ_n and ρ_n are the sizes of the mean filtering window and median filtering window.

The visual saliency map of two source images can be obtained by the smooth operation of the Gaussian filter based on the high-pass image, with the expression given as follows:

$$\mathbf{S}_n = \text{Gaussian filter}\left(H_n, r_g, \sigma_g\right), \tag{7}$$

where $(2r_g + 1)(2r_g + 1)$ is the window size of the Gaussian filter, σ_g is the standard deviation of the filter, and $\mathbf{S}_n$ is the obtained visual saliency map.

3. Fusion Algorithm Design

3.1. RGF-Based Image Decomposition Algorithm. As a filter with good dimensional perception and edge retention characteristic, RGF is widely used for extracting the edge outline and denoising the image. RGF consists of structural erasure and edge recovery. The first step is to eliminate a small structure with the filter, in which a Gaussian filter and median filter can be used. The proposed improved RGF structure consists of a guided filter and a mean filter. If the mean filter is used for structural erasure, it indicates high mean filtering efficiency, simple and fast computation, and the stable erasure of information in the spatial scale. As a result, the extracted features of different scales are separated more thoroughly. If the input image is I, the obtained output filtering image G can be expressed as follows:

$$G = \text{Average}\left(I, \sigma_s\right), \tag{8}$$

where σ_s is the scale parameter. Theoretically, the step can erase the structure with a smaller spatial scale than σ_s. Secondly, the paper uses the guided filter, recursive bilateral filter, or bilateral filter for edge recovery. Although the bilateral filter has a better edge retention effect, it requires calculating the spatial filtering kernel function and the grey filtering kernel function simultaneously, of which the frequency response has a correlation with the input image. Hence, the bilateral filter is not applicable here because it is nonlinear and takes a long execution time. The paper selects the guided filter for the second step of edge recovery. If the iterative recovery for edge is made for the image J^t, then the obtained iterative image J^{t+1} can be expressed as follows:

$$J^{t+1} = \text{Guided Filter}\left(J^t, I, \sigma_s, \sigma_r^2\right), \tag{9}$$

where I is the guided image. The paper selects the source image as a guided image to recover the edge structure to the largest extent. σ_r is the distance weight, and σ_s is the scale parameter.

The above formula can be expressed as follows:

$$u = \text{RGF}\left(I, \sigma_s, \sigma_r, T\right), \tag{10}$$

where the number of iterations is set to $T = 4$, and u is the output image.

The front four images show the results of iterative smoothness with RGF (mean value—guided filter), and the final image shows the fuzzy result of the Gaussian filter. It can be seen that the edge structure is erased by different scales during iterative smoothness with RGF (mean value—guided filter). The change in the image is shown in Figure 2. Compared to the first image, the wall detail, small bicycle in the far distance, and texture on the ground are erased in the second image. Compared to the second image, the outline of the small structure is vague, and the edge of some large structures is dissolved in the third image. The fourth image includes the edges of the large structure and target. The iterative results accommodate the demand hereof.

Figure 2: Iterative smoothness with RGF (mean value—guided filter).

Figure 3: Iterative decomposition with RGF (mean value—guided filter).

Figure 3 shows the multiscale decomposition results of the extracted image from different iterative results. The image is decomposed into four layers here. The final image shows the Gaussian blur result of the source image, which is considered the base layer. The base layer generally includes the overall contrast ratio and grey distribution in the image and erases the edge detail information in the source image. The paper considers the 5^{th} layer as the base layer, which can be obtained directly through Gaussian filter processing to include rough grey distribution and an overall contrast ratio of the image. Compared to the method of obtaining the base layer through continuous iteration, direct processing for the source image is simpler, faster, and better. The detail layer and interlayer are obtained from the front four images, where J_1J_2 correspond to the portions with small structure and J_3J_4 correspond to the portions with large structure. Different scale of information is decomposed to different images.

Image decomposition can be expressed as follows:

$$u^j = \text{RGF}\left(u^{j-1}, \sigma_s^{j-1}, \sigma_r, T\right), \quad (j = 1, \ldots, N-1), \tag{11}$$

$$d^j = u^{j-1} - u^j, \quad (j = 1, \ldots, N-1), \tag{12}$$

$$u^j = \text{Gaussian}\left(u^{j-1}, \sigma_s^{j-1}\right), \quad (j = N), \tag{13}$$

$$d^j = u^{j-1} - u^j, \quad (j = N), \tag{14}$$

where formulas (11) and (12) are the iterative expressions of the detail layer and interlayer, u^j is the image in the j^{th} iteration, d^j is the image in the j^{th} decomposition, and N is the number of decomposed layers. Formulas (13) and (14) are used for solving the base layer. With the above formulas, the paper decomposes the source image into a base layer, interlayer, and detail layer.

3.2. Design of Fusion Method. Figure 4 shows the overall design of the proposed fusion method. Firstly, the paper decomposes the image into the base layer, interlayer, and detail layer through MSD (multiscale decomposition) to include the different scale information of the image. Secondly, the paper uses the processed visual saliency map by the guided filter to guide the base layer fusion, uses the maximum local variance to guide interlayer fusion, and uses the maximum absolute value of the pixel to guide the detail layer fusion.

3.3. Interlayer and Detail Layer Fusion. The detail layer is separated from the source image and includes small structure and texture characteristics, of which the fusion effect directly influences the fusion result. The paper selects *L*1*L*2 as detail layers for fusion through the maximum absolute value of the pixel. The method is generally used for the fusion of high-frequency portions in the image. If the values of a pixel pair on the detail layer of the source image are d_1 and d_2, then the weight of the processed point through the maximum absolute value of pixel W is as follows:

$$W^j = \begin{cases} 1, & \left|d_1^j\right| > \left|d_2^j\right| \\ 0, & \text{otherwise} \end{cases} \quad (j = 1, 2, \ldots, N). \tag{15}$$

Then, the detail layer M^j can be expressed as follows:

$$M^j = W_d^j d_1^j + \left(1 - W_d^j\right) d_2^j \quad (j = 1, 2). \tag{16}$$

The information structure in the interlayer is larger than the detail layer and smaller than the base layer in scale, which includes the edge and outline of the large structure. For such information, the paper selects the fusion pixel through maximum local variance. The pixel region with a large local variance represents a larger information content, so that more salient characteristics in the source image can be retained in the fusion result. If the local region is $(2d + 1)(2d + 1)$ and the number of local pixel points is n, then the local variance can be expressed as follows:

$$V(x) = \sqrt{\frac{1}{n-1} \sum_{x=1}^{n} (i(x) - u)^2},$$
$$u = \frac{1}{n} \sum_{x=1}^{n} i(x)n. \tag{17}$$

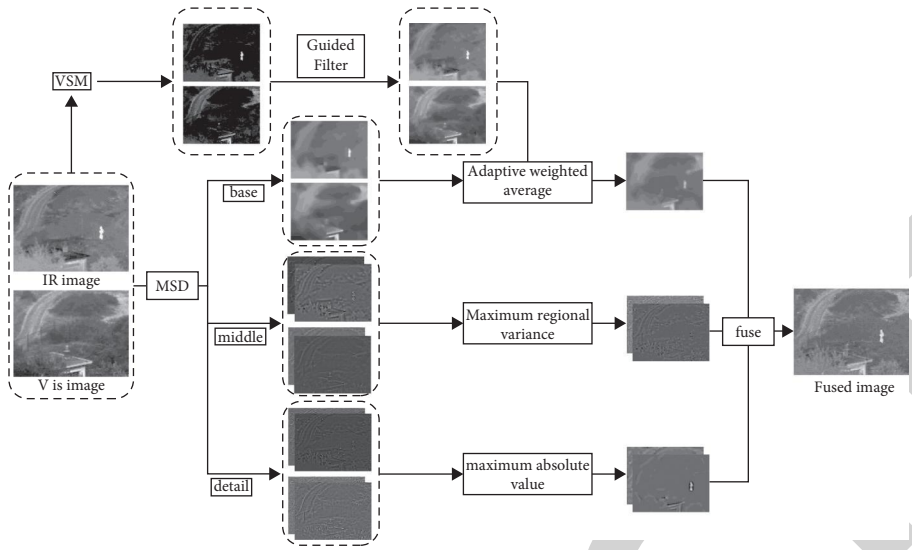

Figure 4: The proposed decomposition method.

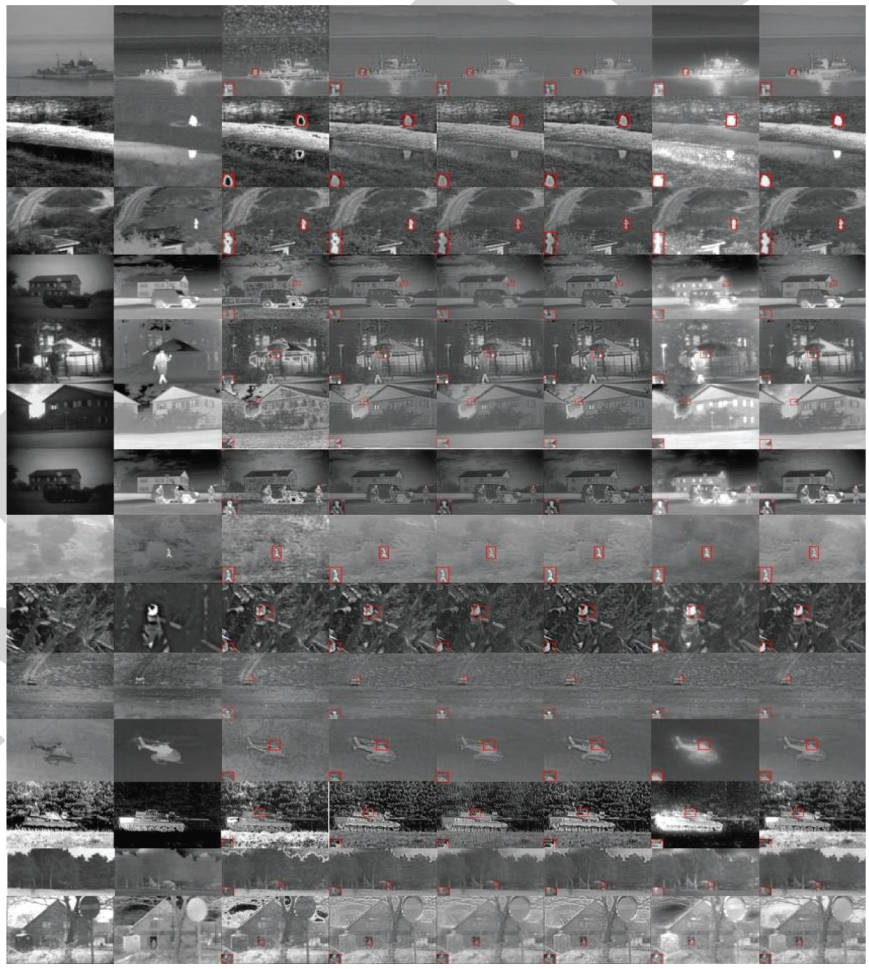

(1) IR (2) Visible (3) CBF (4) CVT (5) CVTSR (6) NSCT (7) RP (8) proposed

Figure 5: Comparison of the fusion results from different methods on the source images.

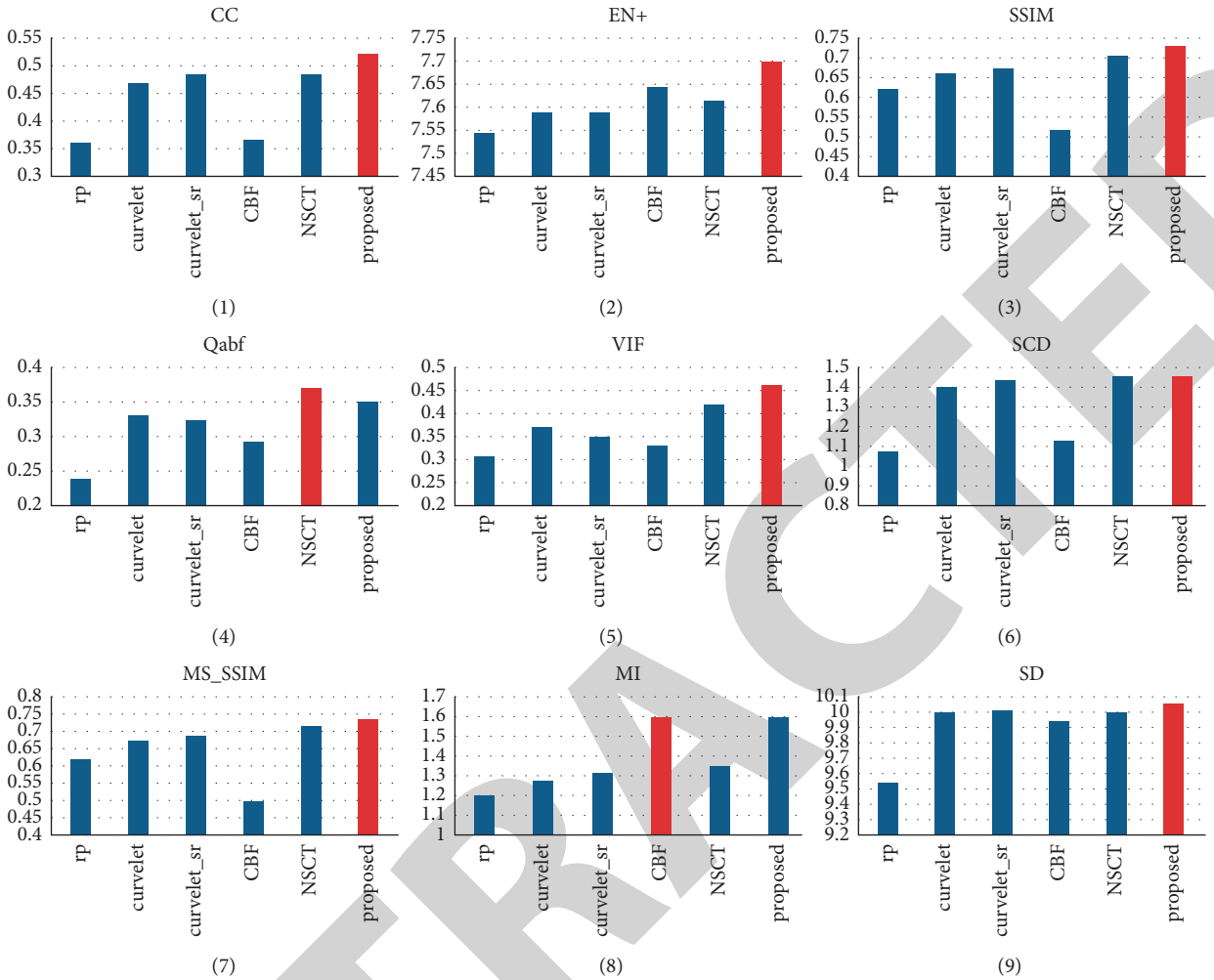

Figure 6: Comparison of the fusion results from different methods on the source images.

Table 1: Different fusion methods are compared quantitatively, and the best fusion results are highlighted in bold.

Indexes	Methods					
	rp	Curvelet	Curvelet_sr	CBF	NSCT	Proposed
CC	0.3576	0.4694	0.4824	0.3656	0.4830	**0.5245**
EN	7.5463	7.5871	7.5863	7.6432	7.6142	**7.6970**
SSIM	0.6172	0.6617	0.6690	0.5136	0.7049	**0.7310**
Qabf	0.2387	0.3333	0.3228	0.2922	**0.3727**	0.3493
VIF	0.3059	0.3684	0.3513	0.3293	0.4215	**0.4637**
SCD	1.0800	1.3965	1.4432	1.1196	1.4535	**1.4569**
MSSSIM	0.6147	0.6707	0.6906	0.4963	0.7190	**0.7388**
MI	1.2008	1.2772	1.3150	**1.5968**	1.3481	1.5894
SD	9.5468	9.9837	10.0149	9.9406	9.9828	**10.0604**

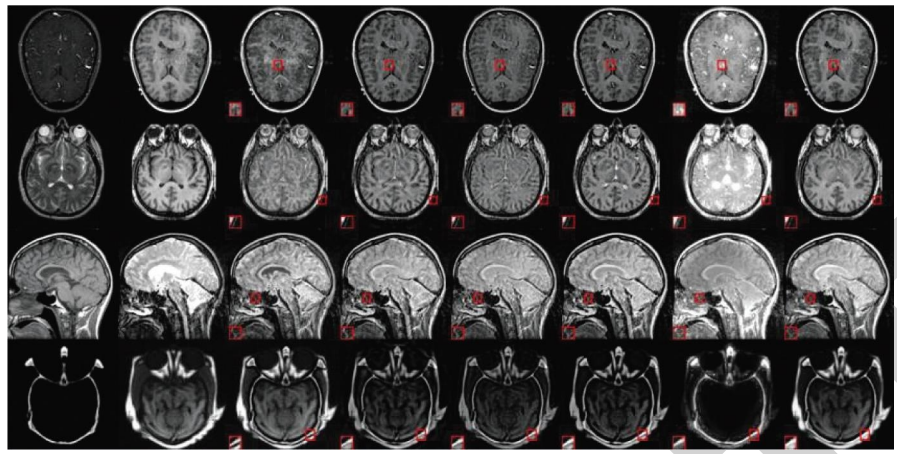

(1) IR (2) Visible (3) CBF (4) CVT (5) CVTSR (6) NSCT (7) RP (8) proposed

Figure 7: Comparison of the fusion results from different methods on the source images.

In the local variance map of the above two images, if the weight of the pixel point with large variance is 1 and the weight of the pixel point with small variance is 0, then the fused image M^j on the interlayer is expressed as follows:

$$W^j = \begin{cases} 1, & V_1^j(x) > V_2^j(x) \\ 0, & \text{otherwise} \end{cases} \quad (j = 3, 4), \tag{18}$$

$$M^j = W_d^j d_1^j + \left(1 - W_d^j\right) d_2^j \quad (j = 3, 4).$$

3.4. Base Layer Fusion. In the decomposition method, the obtained base layer includes grey distribution and a contrast ratio of the source image to regulate the overall visual perception of the fused image. The simple fusion rule is generally selected during the fusion. On the one hand, it can improve the fusion speed. On the other hand, the low-frequency information is not useful and cannot be processed by a complex method. However, these simple fusion rules with representative "averaging" fusion rule have low utilization for low-frequency information and neglect the difference of low-frequency information in different source images, resulting in a decrease in contrast ratio in the fused image and a bad fusion effect.

For the above problem, the paper proposes an adaptive fusion method for a visual saliency map under the guidance of a guided filter to realize the base layer fusion. The visual saliency analysis is widely used in the field of computer vision, which can reflect the salient characteristics of the image and recognize visual structure and object with salient perception in the image different from adjacent regions. The paper uses the method of Literature [7] to build VSM, which considers the comparison between a pixel point and an adjacent pixel point as the definition of pixel saliency. If I_p is the intensity value of a pixel point p in the image, then the visual saliency $V(p)$ of the pixel p is defined as follows:

$$V(p) = \left|I_p - I_1\right| + \left|I_p - I_2\right| + \cdots + \left|I_p - I_N\right|, \tag{19}$$

where N is the total number of pixel points in the image I. If two pixels have the same intensity values, then they have the same saliency. The larger the intensity value, the stronger the saliency. The formula can be updated as follows:

$$V(p) = \sum_{j=0}^{L-1} M_j \left|I_p - I_j\right|, \tag{20}$$

where j is the different pixel intensity, M is the number of pixels with intensity j, and L is the number of grey levels (total 256). The weight map from direct calculation indicates a bad fusion effect for the base layer. The paper uses the guided filter and selects the original image I as the guided image for filtering the weight map.

$$V' = \text{Guided Filter}\left(V, I, \sigma_s, \sigma_r^2\right). \tag{21}$$

The paper uses an adaptive "mean value" rule during fusion. The formula is as follows:

$$W_b = 0.5 + \frac{V_1' - V_2'}{2}, \tag{22}$$

where $V1$ and $V2$ are processed visual saliency maps by the guided filter, respectively. If $V_1 = V_2$, then $W_b = 0.5$. It is the weight of the mean value at the point. If $V_1 > V_2$, then the weight W_b will increase, and more information in the fusion result will be obtained from V_1. Otherwise, the weight will decrease and more information in the fusion result will be obtained from V_2. Then, the fused result from the weighting average can be expressed as follows:

$$B_F = W_b B_1 + \left(1 - W_b\right) B_2. \tag{23}$$

4. Experiment and Result Analysis

4.1. Experimental Environment and Design. In the experiment, the hardware configuration is a PC with Intel (R) Core (TM) i5-9600k 3.7 GHz CPU and NVIDIA GeForce RTX 1080ti GPU, and the software configuration is MATALB 2021b.

Table 2: Different fusion methods are compared quantitatively, and the best fusion results are highlighted in bold.

Methods	Indexes					
	rp	Curvelet	Curvelet_sr	CBF	NSCT	Proposed
CC	0.7504	0.7093	0.7401	0.7533	0.7250	**0.7807**
EN	6.9483	7.5573	7.5092	7.1027	7.5090	**7.6053**
SSIM	0.6789	0.6990	0.7107	0.7647	0.7778	**0.8214**
Qabf	0.3325	0.3995	0.4071	0.4887	0.4891	**0.5009**
VIF	0.5328	0.4246	0.4103	**0.6002**	0.5038	0.5912
SCD	0.6646	0.6468	0.6991	0.7658	0.7557	**0.8521**
MSSSIM	0.7305	0.7715	0.7865	0.8007	0.8378	**0.8429**
MI	3.0110	2.5652	2.6563	2.8093	2.8856	**3.2338**
SD	9.9432	10.1073	10.1456	10.3472	10.1509	**10.4893**

The paper selects 15 pairs of infrared and visible light images from the TNO dataset, which can verify the validity and advancement of the fusion algorithm because the image subjects include character, carrier, building, and hidden target. Besides, the paper selects CT and MRI image pairs to verify the generalization of the algorithm.

The experiment compares the proposed algorithm with five classical algorithms, i.e., RP (ratio pyramid) transform-based method, CVT (curvelet) variation-based method [8, 9], curvelet_sr transform-based method [10], CBF (cross bilateral filter)-based method [11], and NSCT transform-based method [12].

4.2. Analysis of Experimental Results for Infrared and Visible Light Image Fusion

4.2.1. Comparison of Subjective Results. Figure 5 shows a parallel comparison of fusion results for infrared and visible light images under different scenarios, where Figures 5 (1) and (2) show the infrared and visible light images, and Figures 5 (3) to (8) show algorithm comparison. To conveniently show algorithm results, the paper selects and magnifies some portions and the above images.

It can be concluded through intuitive observation that the fusion results of the CBF algorithm include much meaningless noise, bad edge fusion effect, and more serious distortion of fused images. For CVT and CVTSR algorithms, the infrared target is generally reflected. The fused image includes a small number of noises. The CVT algorithm results in a serious artifact, whereas the CVTSR algorithm results in a slight artifact and a relatively low contrast ratio. The NSCT algorithm indicates a good contrast ratio, more complete information of visible light, but low illumination of the infrared target, and a nonsalient target. The RP algorithm indicates relatively high illumination of fusion, fluorescent characteristic, salient infrared information, however, it results in the serious erasure of visible light information, and a serious loss of edge details. The proposed algorithm can realize better fusion for the information of infrared and visible light images, avoid artifacts at the edge boundary, indicate salient infrared characteristics, and retain the good details of visible light and good visual effect as a whole. Therefore, the method can realize a better fusion effect for infrared and visible light images compared to contrast algorithms.

4.2.2. Comparison of Objective Results. The paper evaluates the fusion results of the proposed algorithm through 9 indexes, i.e., CC (correlation coefficient) [13], EN (entropy) [14], SSIM (structural similarity) [15], Qab/*f* [16], VIF (visual information fidelity) [17], SCD (sum of correlation difference) [18], MS-SSIM (multilevel structural similarity) [7], MI (mutual information) [19], and SD (standard deviation) [20].

To avoid the contingency of a single image, the paper considers the mean values of evaluation indexes of 14 images from Figure 5 as contrast indexes, implements visualization for data in Figure 6, and marks optimal results in red. It can be seen from Table 1 and Figure 6 that the paper obtains optimal and suboptimal values from CC, SSIM, SCD, MS-SSIM, and MI. It indicates that the proposed algorithm has a good correlation with the source image and retains more useful information. The best values from EN, VIF, Qab/*f*, and SCD that the fusion results of the proposed algorithm indicate a better visual effect and larger information content.

To sum up, the analysis of objective data demonstrates the superiority of the proposed algorithm.

4.3. Analysis of Experimental Results for Medical Image Fusion.

To verify the generalization and application effect of the proposed algorithm in the medical image, the paper selects four groups of multimode brain lesion images with the size of 256×256 for the contrast experiment. Figures 7 (1) and (2) show the multimode images. Figures 7 (3) to (8) show result comparisons of different algorithms.

4.3.1. Comparison of Subjective Results. As shown in Figure 7, the CBF method indicates a good contrast ratio of fusion results but serious artifact and noise. CVT and CVTSR methods indicate the overall dark image and vague edge structure. The NSCT method indicates overall vague fusion result, which is not beneficial to the human eye recognition and subsequent computer processing. The RP method indicates overall excessive illumination of the fusion result and incomplete image information. Compared to the fusion effect hereof, the proposed algorithm indicates a good contrast ratio and detailed information, integrates different information of multimode images, and realizes the purpose of image fusion well.

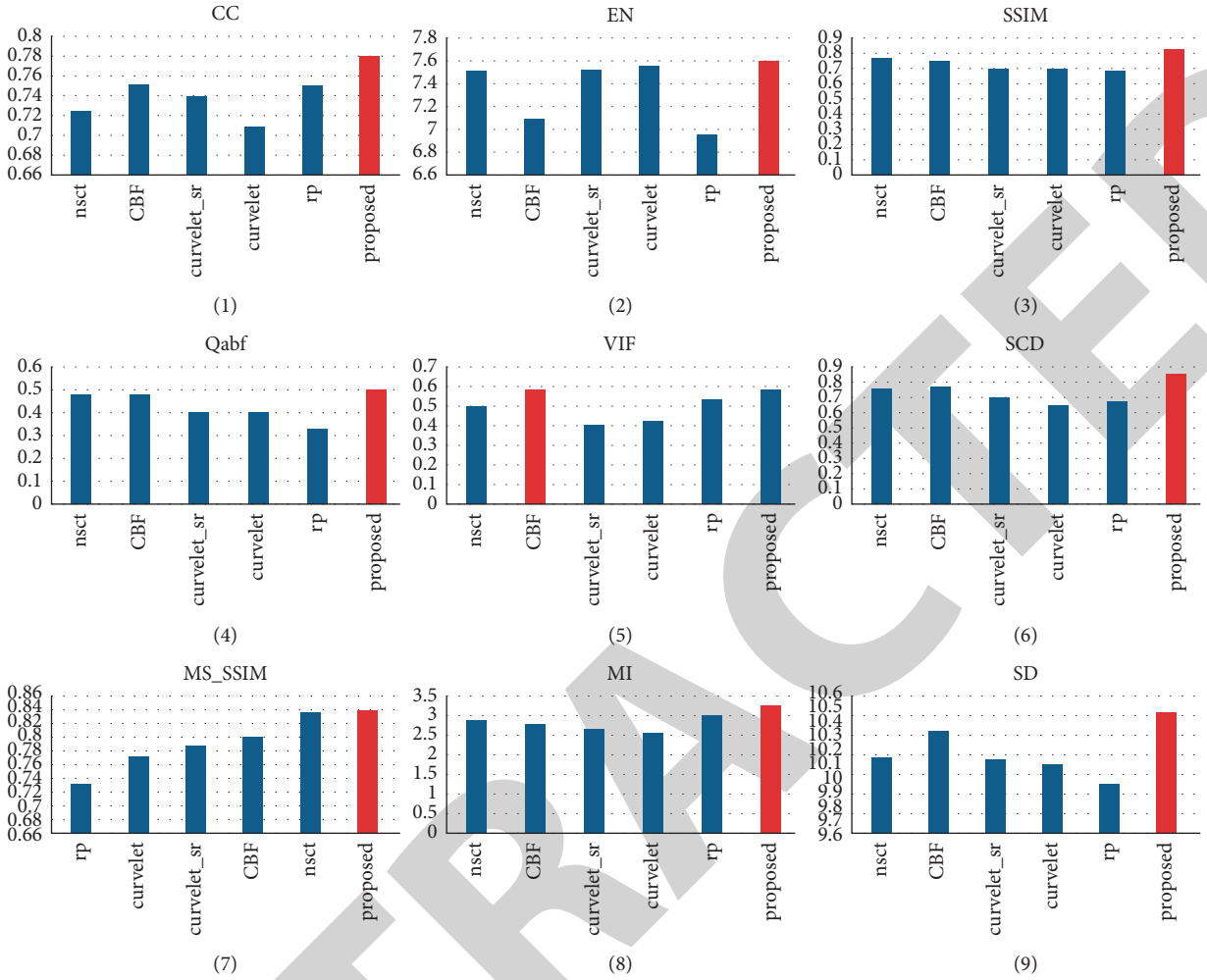

Figure 8: Comparison of the fusion results from different methods on the source images.

4.3.2. Comparison of Objective Results. Table 2 shows the mean values of results for four groups of multimode medical image fusion, where bold values are optimal, and visual processing is shown in Figure 8. It can be seen that the proposed algorithm obtains optimal or suboptimal values among all contrast indexes. According to all subjective and objective evaluations, the proposed algorithm can realize the optimal fusion effect in multimodel medical images, integrate information from the source image, and benefit subsequent human eye judgment or computer processing compared to contrast algorithms.

5. Conclusions

The paper proposes an image fusion algorithm based on improved RGF and visual saliency map. Firstly, the paper uses RGF to decompose the image into the base layer, interlayer, and detail layer at different scales. Secondly, the paper obtains a visual weight map through the calculation of the source image and uses the guided filter to better guide the base layer fusion. Then, it realizes the interlayer fusion through maximum local variance and realizes the detail layer fusion through the maximum absolute value of the pixel. Finally, it obtains the fused image through weight fusion. The experiment uses the infrared and visible light image pair and multimode medical image pair to compare and verify the proposed algorithm. The experimental results indicate that the proposed method is better than the contrast algorithm in subjective effect and objective evaluation. Besides, the fused image with better details, edge, and texture retention capacity and good overall contrast ratio can be obtained with the proposed algorithm.

Data Availability

The basis of data from TNO_Image_Fusion_Dataset is used this article, and the details can be found in https://figshare.com/articles/TN_Image_Fusion_Dataset/1008029.

Conflicts of Interest

The authors declare that they have no conflicts of interest.

References

[1] P. J. Burt and E. H. Adelson, "The laplacian pyramid as a compact image code," in *Readings in Computer Vision: Issues, Problem, Principles, and Paradigms*, M. A. Fischler and O. Firschein, Eds., Elsevier, Amsterdam, Netherlands, 1987.

Hindawi
Emergency Medicine International
Volume 2023, Article ID 9784847, 1 page
https://doi.org/10.1155/2023/9784847

Retraction

Retracted: An Auxiliary Scoring Model for Patients with Acute Pulmonary Embolism Complicated with Atrial Fibrillation Was Established Based on Random Forests

Emergency Medicine International

Received 28 November 2023; Accepted 28 November 2023; Published 29 November 2023

This article has been retracted by Hindawi, as publisher, following an investigation undertaken by the publisher [1]. This investigation has uncovered evidence of systematic manipulation of the publication and peer-review process. We cannot, therefore, vouch for the reliability or integrity of this article.

Please note that this notice is intended solely to alert readers that the peer-review process of this article has been compromised.

Wiley and Hindawi regret that the usual quality checks did not identify these issues before publication and have since put additional measures in place to safeguard research integrity.

We wish to credit our Research Integrity and Research Publishing teams and anonymous and named external researchers and research integrity experts for contributing to this investigation.

The corresponding author, as the representative of all authors, has been given the opportunity to register their agreement or disagreement to this retraction. We have kept a record of any response received.

References

[1] C. Zhang, Q. Guan, J. Qin, D. Huang, and J. Wu, "An Auxiliary Scoring Model for Patients with Acute Pulmonary Embolism Complicated with Atrial Fibrillation Was Established Based on Random Forests," *Emergency Medicine International*, vol. 2022, Article ID 2596839, 8 pages, 2022.

Hindawi
Emergency Medicine International
Volume 2022, Article ID 2596839, 8 pages
https://doi.org/10.1155/2022/2596839

Research Article

An Auxiliary Scoring Model for Patients with Acute Pulmonary Embolism Complicated with Atrial Fibrillation Was Established Based on Random Forests

Chuang Zhang,[1] Qiongchan Guan,[1] Jie Qin,[1] Daochao Huang,[1] and Jinhong Wu[2]

[1]*Department of Emergency, Taizhou Hospital of Zhejiang Province Affiliated to Wenzhou Medical University, Linhai 317000, Zhejiang, China*
[2]*Department of Obstetrics and Gynecology, Taizhou Hospital of Zhejiang Province Affiliated to Wenzhou Medical University, Linhai 317000, Zhejiang, China*

Correspondence should be addressed to Daochao Huang; huangdc6549@163.com and Jinhong Wu; wujinhong6070@163.com

Received 28 June 2022; Accepted 1 August 2022; Published 22 August 2022

Academic Editor: Hang Chen

The purpose of this study was to explore the establishment of an auxiliary scoring model for patients with acute pulmonary embolism (APE) complicated with atrial fibrillation (AF) based on random forest (RF) and its application effect. A retrospective analysis was performed on the general data, underlying diseases, laboratory indicators, and cardiac indicators of 100 patients with APE admitted to our hospital from 2018 to 2021. The occurrence of atrial fibrillation in patients with pulmonary embolism was taken as a categorical variable, and the general data, underlying diseases, laboratory indicators, and cardiac indicators were taken as input variables. Then, the risk auxiliary scoring model for patients with APE complicated with AF was established based on RF and logistic regression. Finally, the accuracy, sensitivity, specificity, recall rate, accuracy, F1 value, and the receiver operator characteristic (ROC) curve were used to evaluate the predictive value of the models. After statistical analysis, the optimal node value was 3 and the optimal number of decision trees was 500 in the RF model. The importance of predictors in descending order were Hcy, diabetes mellitus, FT3 level, UA level, left atrial diameter, hypertension, and smoking history. The prediction accuracy of the RF model was 0.934, sensitivity 0.966, specificity 0.876, recall rate 0.9660, accuracy 0.934, and F1 value 0.950. The logistic regression model prediction accuracy was 0.816, sensitivity 0.915, specificity 0.125, recall rate 0.902, accuracy 0.811, and F1 value 0.896. The RF model and logistic regression prediction model AUC values were 0.984 and 0.883, respectively. From this, we conclude that the RF model was better than the logistic regression model in predicting AF in APE patients. So, the RF model had the clinical application value.

1. Introduction

Acute pulmonary embolism (APE) is caused by a thromboembolic artery and its branches or venous system in the right heart [1]. APE can not only cause pulmonary circulation disorder but also cause increased right ventricular load and expansion of the right heart, resulting in atrial fibrillation (AF) [2]. Relevant studies have pointed out that AF-induced abnormal atrial electrical activity can affect patients' cardiac systolic and diastolic functions, lead to dysfunction of heart pumping, and cause irregular ventricular contraction and electrical response in patients, thus inducing heart failure [3]. Other studies have shown that AF was closely related to the prognosis of APE patients, and AF can promote the further formation and shedding of emboli, thus inducing cardiovascular diseases such as cerebral infarction and myocardial infarction and greatly increasing the risk of poor prognosis for patients [4]. Early warning and early intervention are the keys to reducing AF. However, there is a lack of prediction methods for APE concurrent AF. Age, height, obesity, hypertension, left ventricular ejection fraction (LVEF), and having a history of AF were influential factors for the occurrence of AF in a multivariate logistic regression analysis [5, 6]. However, the logistic regression

model is not fit and its accuracy is not high. In addition, the conclusions of each study differ greatly. Random forest (RF) is a classifier that uses multiple trees to train and predict samples. It is a classical machine learning algorithm proposed by Leo Breiman in 2001. In machine learning, RF is a classifier that contains multiple decision trees, and the class of its output is determined by the mode of the class of the output of individual trees. RF can be used to generate highly accurate classifiers, deal with a large number of input variables, and evaluate the importance of variables in determining categories. It can be used for classification and regression analysis with high accuracy and can deal with a large number of input variables and balance errors. This method has been successfully applied to the early prediction and prognosis assessment of various diseases [7]. Therefore, we speculated that RF may also help clinicians predict the risk of AF in patients with APE. This study retrospectively analyzed the general data, underlying diseases, laboratory indicators, and cardiac indicators of APE patients and established auxiliary scoring models for APE patients complicated with AF based on RF and logistic regression, respectively. The application effects of the two models were compared and analyzed. It was expected to provide new ideas for the early detection and treatment of AF in patients with APE.

2. Materials and Methods

2.1. Data Sources. A retrospective analysis was performed on the general data, underlying diseases, laboratory indicators, and cardiac indicators of patients with AP admitted to our hospital from 2018 to 2021. Conditions of selection included the following: (1) according to the criteria in Chinese expert consensus on diagnosis and treatment of acute pulmonary embolism (2015), APE was clearly diagnosed by pulmonary angiography [8]; (2) the time from onset to admission was less than 2 weeks; (3) patients who received normal treatment, such as symptomatic anti-infection and improvement of cardiac function; and (4) normal coagulation function and immune system. Conditions of elimination included the following: (1) combined with serious organ diseases such as congenital heart disease, hypohepatia, and kidney failure; (2) complicated with malignant tumors; (3) complicated with infectious pneumonia or other infectious diseases; (4) complicated with serious cardiovascular and cerebrovascular diseases such as myocardial infarction, cerebral infarction, and so on.; and (5) in-hospital deaths occurred. One hundred patients in total were enrolled, including 57 males and 43 females. The average age was (53.55 ± 3.35) years. The time from onset to admission was 3–12 days, with an average of (7.86 ± 1.47) days. This study was approved by the Ethics Committee of Taizhou Hospital of Zhejiang Province, affiliated with Wenzhou Medical University.

2.2. Data Collection. A uniformly designed case data sheet was used for collecting clinical data from patients. (1) The general data included age, sex, height, time from onset to admission, body mass index (BMI), obesity, pregnant women, risk degree of disease, AF history, APE, drinking history, and smoking history. (2) The underlying diseases included diabetes, hypertension, and hyperlipidemia. (3) The laboratory indicators included D-dimer, albumin, Hcy, UA, creatinine, serum-free triiodothyronine (FT3), and serum-free tetraiodothyronine (FT4). (4) The cardiac indicators included ventricular rate, left ventricular ejection fraction (LVEF), left atrial internal diameter, and right atrial internal meridian.

2.3. Relevant Variables and Definitions. (1) BMI = weight (kg)/height^2 (m): 18.5–23.9 kg/m^2 was defined as normal, 24.0–27.9 kg/m^2 was defined as overweight, and 28.0 kg/m^2 was defined as obese [9]. (2) Smoking history: the average smoking volume was ≥1 cigarette per day, and the duration was more than 1 year. (3) Drinking history: drinking at least once a month for more than 6 months. (4) Hypertension: systolic blood pressure ≥140 mmHg (1 mmHg = 0.133 kPa) and diastolic blood pressure ≥90 mmHg [10]. (5) Diabetes: fasting blood glucose ≥70 mmol/L and (or) 2 h postprandial blood glucose ≥11.1 mmol/L [11]. (6) Hyperlipidemia: low density lipoprotein concentration ≥3.37 mmol/L [12]. (7) Detection of D-dimer, albumin, homocysteine (Hcy), and uric acid (UA): before treatment, 5 mL of fasting elbow venous blood was collected from the patients and placed in two test tubes, one of which was centrifuged at 3000 r/min for 10 min with a low-speed centrifuge. The serum was separated and the plasma D-dimer level was determined by immunoturbidimetry. The other one was centrifuged at 4000 r/min for 10 min. The serum albumin level was determined by the colorimetric method, the Hcy level was determined by HPLC, and the UA level was determined by the uric acid oxidase method. The test kits were purchased from Shanghai Canspec Scientific Instruments Co., Ltd., and the test procedures were carried out in strict accordance with the kit instructions.

2.4. AF Evaluation Criteria and Grouping. AF diagnostic criteria [13]: (1) Symptoms: common symptoms include palpitations, fatigue, chest tightness, chest pain, and decreased exercise tolerance. Some patients may not have any clinical symptoms. (2) Signs: auscultation of the first heart sound is not strong or weak, the rhythm is extremely irregular, and the pulse rate is short when the ventricular rate is fast. (3) ECG manifestations: the P wave disappeared, replaced by an atrial fibrillation wave (f-wave) with inconsistent size, shape, and amplitude; the frequency of the *f*-wave was 350 times/min–600 times/min; absolutely irregular spacing of QRS groups is usually accompanied by irregular shapes and amplitudes. Patients complicated by AF were assigned to the AF group, and patients without AF were assigned to the non-AF group.

2.5. Statistical Methods. Statistical analysis was performed using R4.1.2 language software and SPSS 23.0 software. The measurement data conforming to normal distribution were represented by mean ± standard deviation and an

independent sample t-test was performed. The constituent ratios of the count data were expressed as percentages of frequency and were analyzed using the chi-square test or Fisher's exact probability method. The dataset was randomly divided into a training set and a validation set according to 0.67 : 0.33. The training set was used to establish the RF algorithm and multivariate logistic regression analysis, and the validation set was used to test the prediction effect of the model. $P < 0.05$ was considered a statistically significant difference .

(1) Establishment of a multivariate logistic regression model: a single factor analysis was used to screen variables, and the inclusion criterion for variables was $P < 0.05$. The maximum likelihood method was used to construct a prediction model of APE patients complicated with AF based on a multivariate logistic regression analysis. (2) Establishment of the RF model: use Random Forest package to realize the application of the RF algorithm and specify the random sampling method of Bootstrap, and the default was sampling with putting back. The RF model had two important parameters, which were the number of decision trees, ntree, and the number of preselected variables of split node mtry. The RF warning model was constructed by training set data, and the optimal mtry and ntree were selected to reduce the prediction error rate of the model. The importance function was used to calculate the importance of a model variable, with a larger value indicating that the variable was more important. (3) Model evaluation: application of accuracy, sensitivity, specificity, recall rate, accuracy rate, F1 value, and area under the curve AUC and other indicators were used to evaluate the performance of the risk warning model for APE patients complicated with AF, and a relative operating characteristic (ROC) curve was drawn to compare the size of AUC. The larger AUC (or the closer to 1) was, the better the model's predictive performance.

3. Results

3.1. Basic Information of the Patients and Univariate Analysis of Risk Factors for AF in Patients with APE

(1) Among the 100 patients in this study, 24 patients were complicated by AF, and 76 patients were not complicated by AF, with an incidence of 24%

(2) Univariate analysis showed that there were statistically significant differences in smoking history, diabetes, hypertension, Hcy, UA, FT3, and left atrial diameter between the AF group and the AF group ($P < 0.5$), as shown in Table 1

3.2. Multivariate Logistic Regression Analysis of APE Patients Complicated with AF. Statistically significant variables in the results of the univariate analysis were included as independent variables in the multivariate logistic regression, and the variable assignment is shown in Table 2. Multivariate logistic regression analysis was performed with AF (yes = 1, no = 0) as the dependent variable. The results showed that the smoking history, diabetes, hypertension, high Hcy, high UA, FT3, and low left atrial diameter were independent risk factors for APE patients with AF. The results of multivariate logistic regression analysis are shown in Table 3.

3.3. RF Model Predicts Model Analysis Results. The results of multivariate logistic regression analysis of APE patients complicated with AF were used to establish the RF model. The relationship between model error and the number of random trees was analyzed to define the number of random trees (ntree) and determine the optimal feature selection (mtry). When Mtry = 3 and ntree = 500, the error was based on stability and the optimal model could be established, as shown in Figure 1.

3.4. Order the Importance of RF Model Variables. This study attempted to use the average reduction of the Gini value as a measure of the importance of variables in the RF model to further clarify the important predictors of APE patients with AF. The results showed that the Hcy score was the highest, indicating that Hcy played a major role in the model. The relatively important predictors in this model were diabetes mellitus, FT3 level, UA level, left atrial diameter, hypertension, and smoking history in sequence. These predictors also played a certain role in the model classification. The analysis results are shown in Table 4 and Figure 2.

3.5. Comparison of Two Prediction Models. Validation set data were used to compare the prediction effect of APE patients complicated with AF based on RF and logistic regression. The accuracy, sensitivity, specificity, recall rate, accuracy, and F1 value of the RF prediction model were all higher than those of the logistic regression model, and the analysis results are shown in Table 5. The AUC of the RF prediction model was 0.984, and the ROC curve based on the RF prediction model is shown in Figure 3. The AUC of the logistic regression prediction model was 0.883. The ROC curve based on the logistic prediction model is shown in Figure 4. The AUC of the RF prediction model was larger than that of the logistic regression model.

4. Discussion

APE is a common clinical emergency with a complex etiology. Previous studies believed that the occurrence of APE was related to factors such as long-term bed rest and chronic lung disease [14]. APE was easy to cause AF, which posed a threat to patients' life safety, so the hidden danger of APE complicated with AF cannot be ignored [15]. Relevant investigation results showed that the incidence of AF in APE patients was as high as 15%–21%, which was significantly higher than that of healthy peers [16]. In this study, 24 out of 100 APE patients were complicated by AF, and the incidence of AF was 24%, which was similar to previous reports, suggesting that APE patients were still at high risk of

Table 1: Univariate analysis of risk factors for AF in patients with AP ($\overline{x} \pm s/n$ (%)).

Variable	AF group ($n = 24$)	Non-AF group ($n = 76$)	t/χ^2	P
General data				
Age (year)	51.31 ± 3.50	50.59 ± 3.20	0.940	0.350
Sex (male/female)	14 (58.33)/10 (41.67)	43 (56.58)/33 (43.42)		
Height (cm)	166.42 ± 3.06	167.42 ± 2.39	1.666	0.099
Time from onset to admission (*d*)	7.66 ± 1.79	7.96 ± 1.15	0.965	0.337
BMI (kg/m^2)	21.53 ± 1.12	21.47 ± 1.22	0.214	0.831
Obesity (yes/no)	5 (20.83)/19 (79.17)	17 (22.37)/59 (77.63)	0.025	0.874
Pregnant women (yes/no)	3 (12.50)/21 (87.50)	5 (6.58)/71 (93.42)	0.869	0.351
Risk degree of disease (low risk/moderate risk/high risk)	3 (12.50)/9 (37.50)/12 (50.00)	11 (14.47)/27 (35.53)/38 (50.00)	0.070	0.965
AF history (have/not have)	6 (25.00)/18 (75.00)	18 (23.68)/58 (76.32)	0.017	0.895
APE (first confirmed/not first confirmed)	20 (83.33)/4 (16.67)	69 (90.79)/7 (9.21)	1.036	0.309
Drinking history (have/not have)	7 (29.17)/17 (70.83)	26 (34.21)/50 (65.79)	0.210	0.647
Smoking history (have/not have)	8 (33.33)/16 (66.67)	7 (9.21)/69 (90.79)	8.325	0.004
Underlying diseases				
Diabetes (have/not have)	12 (50.00)/12 (50.00)	8 (10.53)/68 (89.47)	17.763	<0.001
Hypertension (have/not have)	12 (50.00)/12 (50.00)	15 (19.74)/61 (80.26)	8.476	0.004
Hyperlipidemia (have/not have)	6 (25.00)/18 (75.00)	17 (22.37)/59 (77.63)	0.071	0.789
Laboratory indicators				
D-Dimer (μg/L)	234.66 ± 30.36	235.18 ± 28.27	0.077	0.939
Albumin (g/L)	33.45 ± 4.86	33.27 ± 5.03	0.154	0.878
Hcy (μmol/L)	18.13 ± 3.34	15.85 ± 2.59	3.497	<0.001
UA (mmol/L)	446.26 ± 35.81	415.86 ± 44.87	3.025	0.003
Creatinine (μmol/L)	80.26 ± 7.75	82.16 ± 6.41	1.202	0.232
FT3 (mmol/L)	3.85 ± 0.90	4.26 ± 0.85	2.031	0.044
FT4 (mmol/L)	17.55 ± 3.41	17.46 ± 3.35	0.114	0.909
Cardiac indicators				
Ventricular rate (time/min)	83.26 ± 15.39	82.88 ± 16.42	0.100	0.920
LVEF (%)	45.58 ± 12.25	45.35 ± 8.64	0.102	0.919
Left atrial internal diameter (mm)	40.00 ± 4.38	37.51 ± 4.18	2.515	0.014
Right atrial internal meridian (mm)	47.39 ± 5.52	47.28 ± 5.41	0.086	0.931

Note. BMI, body mass index; AF, atrial fibrillation; APE, acute pulmonary embolism; Hcy, homocysteine; UA, uric acid; FT3, free triiodothyronine; FT4, free tetraiodothyronine; LVEF, left ventricular ejection fraction.

Table 2: Variable assignment.

Independent variable	Assignment
Smoking history	have = 1, not have = 0
Diabetes	have = 1, not have = 0
Hypertension	have = 1, not have = 0
Hcy	Continuous variable
UA	Continuous variable
FT3	Continuous variable
Left atrial diameter	Continuous variable

complicated AF and clinical vigilance should be raised. Early identification of influencing factors of APE patients complicated by AF and timely targeted intervention management for them had important guiding significance for reducing the probability of the patients complicated by AF. This would help to reduce the economic burden on patients, improve clinical treatment benefits, and reduce mortality [17]. A logistic regression model was used to analyze the influencing factors of APE patients with AF in the past. However, because of the lack of a fitting degree, accuracy of the logistic regression model, and the quite different conclusions of various studies, it was necessary to find a prediction model with higher accuracy to further identify the risk factors of AF.

RF is one of the most important machine learning algorithms at present. The model has been applied to establish the prediction of different diseases and achieved good results. In this study, auxiliary scoring models for APE patients with AF were established based on the RF model and multivariate logistic regression, respectively. The results showed that the RF model could effectively distinguish the individuals with AF and those without AF, and its prediction accuracy was higher than that of the logistic regression model. Moreover, the accuracy, sensitivity, specificity, recall rate, accuracy rate, and F1 value of the RF model were higher than those of the logistic regression model, and the AUC of the two models were 0.984 and 0.883, respectively. In addition, the factors predicted by the RF model were Hcy, diabetes mellitus, FT3 level, UA level, left atrial diameter, hypertension, and smoking history in descending order of importance. Using the effect size analysis of the multivariate logistic regression prediction model, it was concluded that smoking history, diabetes, hypertension, Hcy, UA, left atrial diameter, and FT3 were related to AF in APE patients. (1) Imtiaz and his research team conducted a follow-up investigation on 11047 patients. Finally, they statistically found that the detection rate of AF in smokers was 9.5%, while that in nonsmokers was 7.8% [18]. Their study also found that

Table 3: Multivariate logistic regression analysis of APE patients complicated with AF.

Variable	β	SE	Wald χ^2	P	OR	95% CI	
						Lower limit	Upper limit
Smoking history	2.785	1.078	6.676	0.010	16.196	1.959	133.908
Diabetes	1.758	0.773	5.172	0.023	5.800	1.275	26.383
Hypertension	1.882	0.772	5.941	0.015	6.567	1.446	29.832
Hcy	0.024	0.009	6.540	0.011	1.025	1.006	1.044
UA	0.159	0.079	4.091	0.043	1.172	1.005	1.367
FT3	0.377	0.150	6.303	0.012	1.457	1.086	1.956
Left atrial diameter	−0.932	0.435	4.594	0.032	0.394	0.168	0.923
Constant	−22.071	7.021	9.881	0.002	<0.001	—	—

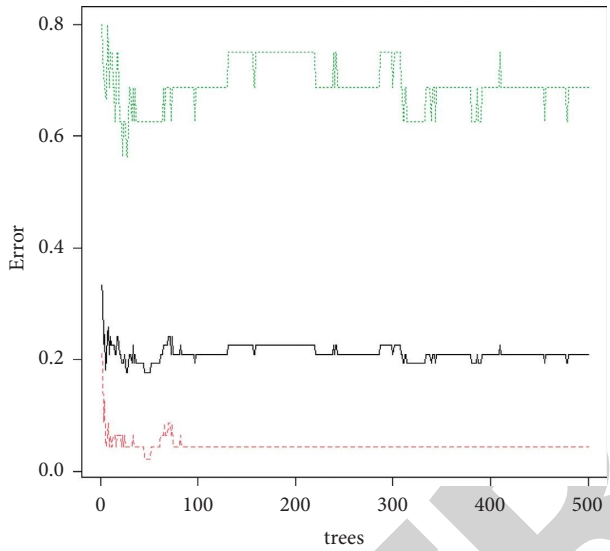

Figure 1: Prediction model of relationship between model error and number of random trees.

Table 4: Mean decrease Gini of RF model variables.

Variable	Mean decrease Gini
Hcy	6.290
Diabetes mellitus	4.115
FT3	3.859
UA	3.646
Left atrial internal meridian	3.600
High blood pressure	2.390
Smoking history	1.755

smoking was strongly associated with a 15 percent increased risk of AF over 10 years. Smoking increased susceptibility to atrial fibrillation through indirect and direct mechanisms. Smokers were more likely to develop abdominal obesity, atherosclerosis, hypertension, diabetes, chronic obstructive pulmonary disease, coronary heart disease, and heart failure [19]. These adverse events were risk factors for atrial fibrillation and could indirectly promote the occurrence of atrial fibrillation. As the main ingredient in tobacco, nicotine could stimulate the body to release hormones such as catecholamines, which activated the sympathetic nervous system and raise blood pressure and heart rate. It had been confirmed that nicotine directly promoted the occurrence of AF [20]. (2) Toxicity caused by long-term hyperglycemia would damage myocardial cells, resulting in abnormal cardiac structure [21]. In addition, insulin resistance and chronic inflammation in diabetic patients would affect cardiac function, which may increase the risk of AF in patients with APE. Therefore, we suggested that hypoglycemic drugs or insulin intervention should be given to patients with APE complicated with diabetes according to their actual situation to regulate their blood glucose level and prevent the occurrence of AF [22]. (3) Long-term hypertension could cause abnormal changes in left atrial hemodynamics, resulting in an increase in thickness and hardness of the left ventricular wall and damage to ventricular diastolic function, thus promoting increased ventricular pressure and ventricular remodeling, which could lead to increased risk of AF in patients with APE [23]. Therefore, for APE patients with hypertension, antihypertensive drug intervention should be given to actively control blood pressure levels and prevent the occurrence of AF. (4) Hcy was an intermediate product of the metabolism of methionine and cysteine [24]. Under normal circumstances, the Hcy would be metabolized by the body, so its serum concentration was low. However, the occurrence of APE would affect the metabolism of Hcy, leading to an increase in serum Hcy levels. Relevant research reports indicated that the increase in Hcy level would lead to the imbalance of the antioxidant and pro-oxidation system, promote the generation of reactive oxygen species, and trigger the oxidative stress response of the body. The resulting large amount of peroxide would lead to cellular calcium overload, resulting in ventricular remodeling [25]. In addition, an increased Hcy level could also promote the generation of various inflammatory factors, damage myocardial cells, and promote the occurrence and development of AF. Therefore, patients with elevated Hcy levels should be vigilant and their Hcy levels should be actively reduced. Folic acid combined with vitamin B6 or vitamin B12 would reduce the risk of AF. (5) UA was the metabolite of purine, which was mainly metabolized by the kidney and had an antioxidant effect [26]. It had been reported that increased UA indicated increased activity of xanthine oxidase, which could activate the protein kinase pathway, promote the generation of inflammatory cells, cause atrial remodeling, and promote S-nitrosylation of ion channel, eventually causing AF. (6) Thyroid hormone had a significant impact on the cardiovascular system [27]. Hyperthyroidism was associated with an increased risk of arrhythmia and hypothyroidism may lead to atherosclerosis.

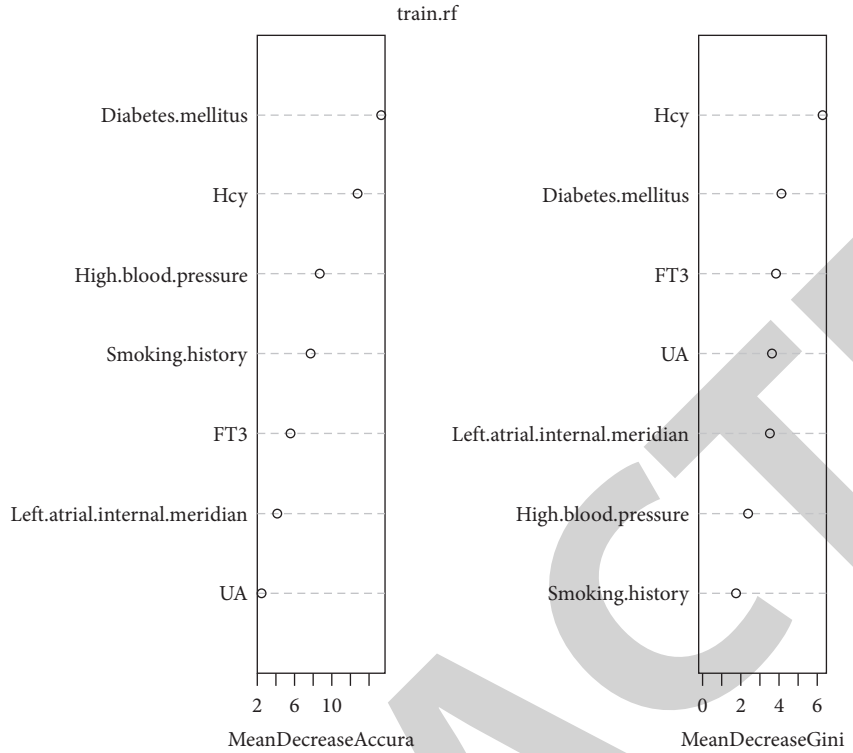

Figure 2: Order of importance of modeling variables.

Table 5: Comparison of prediction performance between the two models.

Model	Accuracy	Sensitivity	Specificity	Recall rate	Accuracy	F1 value
RF model	0.934	0.966	0.876	0.966	0.934	0.950
Logistic regression model	0.816	0.915	0.125	0.902	0.811	0.896

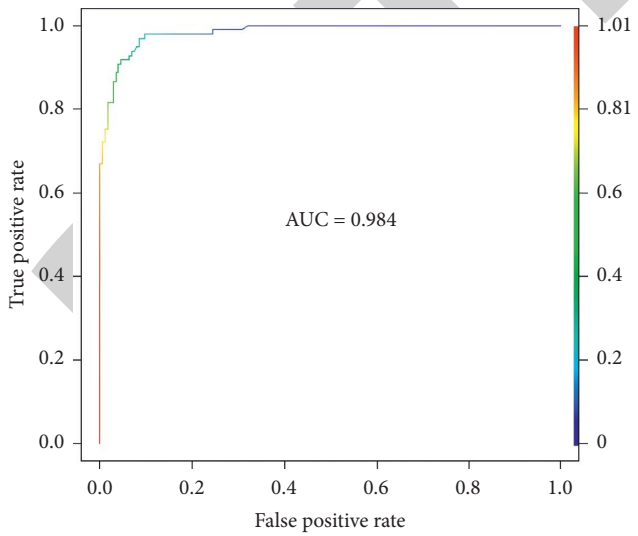

Figure 3: ROC curve based on the RF prediction model.

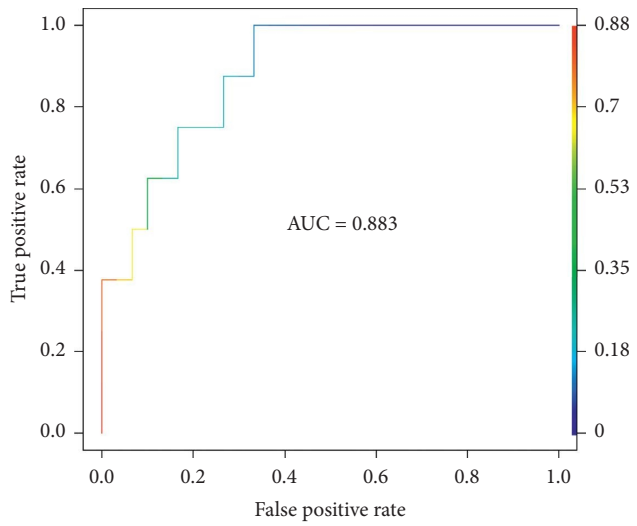

Figure 4: ROC curve based on the logistic prediction model.

At present, there were few reports on the relationship between FT3 and atrial fibrillation, which required further study. (7) Left atrial diameter was a major indicator of changes in cardiac structure, which could be used to predict the risk of cardiovascular disease. APE could cause increased ventricular load, decrease ventricular systolic function, and cause acute left atrial dilation, finally resulting in an increase in left atrial diameter [28]. The enlargement of left atrial diameter lead to increased atrial pressure, which lead to atrial remodeling and increases the risk of AF.

5. Strengths and Limitations

This study had certain advantages. On the one hand, RF could be used to train all available variables, and hundreds of variables could be directly used in model construction without manual selection of variables in advance. At the same time, relevant influencing factors of APE patients with concurrent AF could be screened out from the perspective of algorithm. On the other hand, the data needed to establish the prediction model could be directly obtained in the clinic, which was conducive to the clinical medical staff to quickly assess the risk of APE patients with AF, so as to realize the early and personalized intervention for high risk and critical patients. However, there were shortcomings in this study, that was, some potential factors that may be related to the occurrence of AF were not included in the analysis, which would affect the accuracy of the prediction model to a certain extent. In addition, this study was a single-center study and lacked the support of external data. Therefore, we had doubts about whether the RF model could also achieve good prediction results when used in a wider range. Considering this problem, future studies should extend the thinking to the external data of the multicenter to enhance the reliability of the results of this study.

6. Conclusions

In conclusion, the RF model was better than the logistic regression model in predicting AF in APE patients. However, considering that the logistic regression model could directly explain the results, we suggested that clinicians combine the two models in practical application to more systematically describe the factors affecting APE patients with AF, so as to provide new guidance for APE treatment and patients rehabilitation.

Data Availability

The data used to support the findings of this study are available from the corresponding author upon request.

Disclosure

Jinhong Wu and Daochao Huang are the co-authors.

Conflicts of Interest

The authors declare that they have no conflicts of interest.

Authors' Contributions

Jinhong Wu and Daochao Huang contributed equally to this work.

References

[1] C. Wang, Z. Zhai, Y. Yang et al., "China venous thromboembolism (VTE) study group, efficacy and safety of low dose recombinant tissue-type plasminogen activator for the treatment of acute pulmonary thromboembolism: a randomized, multicenter, controlled trial," *Chest*, vol. 137, no. 2, pp. 254–262, 2010.

[2] P. Osmancik, D. Herman, P. Neuzil et al., "Left atrial appendage closure versus direct oral anticoagulants in high-risk patients with atrial fibrillation," *Journal of the American College of Cardiology*, vol. 75, no. 25, pp. 3122–3135, 2020.

[3] N. A. Chatterjee, C. U. Chae, E. Kim et al., "Modifiable risk factors for incident heart failure in atrial fibrillation," *Journal of the American College of Cardiology: Heart Failure*, vol. 5, no. 8, pp. 552–560, 2017.

[4] R. L. Antikainen, R. Peters, N. S. Beckett, C. Rajkumar, and C. J. Bulpitt, "Atrial fibrillation and the risk of cardiovascular disease and mortality in the hypertension in the very elderly trial," *Journal of Hypertension*, vol. 38, no. 5, pp. 839–844, 2020.

[5] U. M. Mogensen, P. S. Jhund, W. T. Abraham et al., "Type of atrial fibrillation and outcomes in patients with heart failure and reduced ejection fraction," *Journal of the American College of Cardiology*, vol. 70, no. 20, pp. 2490–2500, 2017.

[6] S. Masson, A. Aleksova, C. Favero et al., "Predicting atrial fibrillation recurrence with circulating inflammatory markers in patients in sinus rhythm at high risk for atrial fibrillation: data from the GISSI atrial fibrillation trial," *Heart*, vol. 96, no. 23, pp. 1909–1914, 2010.

[7] L. Jiang, S. Sun, J. Chen, and Z. Sun, "Random forest algorithm-based ultrasonic image in the diagnosis of patients with dry eye syndrome and its relationship with tear osmotic pressure," *Computational and Mathematical Methods in Medicine*, vol. 2022, Article ID 9437468, 8 pages, 2022.

[8] A. Andersen, F. Waziri, J. G. Schultz et al., "Pulmonary vasodilation by sildenafil in acute intermediate-high risk pulmonary embolism: a randomized explorative trial," *BMC Pulmonary Medicine*, vol. 21, no. 1, p. 72, 2021.

[9] M. E. Lean, W. S. Leslie, A. C. Barnes et al., "Primary care-led weight management for remission of type 2 diabetes (DiRECT): an open-label, cluster-randomised trial," *The Lancet*, vol. 391, no. 10120, pp. 541–551, 2018.

[10] S. Barco, M. Russo, E. Vicaut et al., "Incomplete echocardiographic recovery at 6 months predicts long-term sequelae after intermediate-risk pulmonary embolism. A post-hoc analysis of the pulmonary embolism thrombolysis (PEITHO) trial," *Clinical Research in Cardiology*, vol. 108, no. 7, pp. 772–778, 2019.

[11] J. M. Lachin, I. Bebu, R. M. Bergenstal et al., "Association of glycemic variability in type 1 diabetes with progression of microvascular outcomes in the diabetes control and complications trial," *Diabetes Care*, vol. 40, no. 6, pp. 777–783, 2017.

[12] T. J. Wang, A. S. Y. Lien, J. L. Chen, C. H. Lin, Y. S. Yang, and S. H. Yang, "A randomized clinical efficacy trial of red yeast rice (*monascus pilosus*) against hyperlipidemia," *American Journal of Chinese Medicine*, vol. 47, no. 2, pp. 323–335, 2019.

[13] W. Qureshi, E. Z. Soliman, S. D. Solomon et al., "Risk factors for atrial fibrillation in patients with normal versus dilated left atrium (from the atherosclerosis risk in communities study)," *The American Journal of Cardiology*, vol. 114, no. 9, pp. 1368–1372, 2014.

[14] A. B. Kay, D. S. Morris, S. C. Woller et al., "Trauma patients at risk for venous thromboembolism who undergo routine duplex ultrasound screening experience fewer pulmonary emboli: a prospective randomized trial," *The Journal of Trauma And Acute Care Surgery*, vol. 90, no. 5, pp. 787–796, 2021.

Hindawi
Emergency Medicine International
Volume 2023, Article ID 9754041, 1 page
https://doi.org/10.1155/2023/9754041

Retraction

Retracted: 3D Automatic Segmentation of Brain Tumor Based on Deep Neural Network and Multimodal MRI Images

Emergency Medicine International

Received 8 August 2023; Accepted 8 August 2023; Published 9 August 2023

This article has been retracted by Hindawi following an investigation undertaken by the publisher [1]. This investigation has uncovered evidence of one or more of the following indicators of systematic manipulation of the publication process:

(1) Discrepancies in scope
(2) Discrepancies in the description of the research reported
(3) Discrepancies between the availability of data and the research described
(4) Inappropriate citations
(5) Incoherent, meaningless and/or irrelevant content included in the article
(6) Peer-review manipulation

The presence of these indicators undermines our confidence in the integrity of the article's content and we cannot, therefore, vouch for its reliability. Please note that this notice is intended solely to alert readers that the content of this article is unreliable. We have not investigated whether authors were aware of or involved in the systematic manipulation of the publication process.

In addition, our investigation has also shown that one or more of the following human-subject reporting requirements has not been met in this article: ethical approval by an Institutional Review Board (IRB) committee or equivalent, patient/participant consent to participate, and/or agreement to publish patient/participant details (where relevant).

Wiley and Hindawi regrets that the usual quality checks did not identify these issues before publication and have since put additional measures in place to safeguard research integrity.

We wish to credit our own Research Integrity and Research Publishing teams and anonymous and named external researchers and research integrity experts for contributing to this investigation.

The corresponding author, as the representative of all authors, has been given the opportunity to register their agreement or disagreement to this retraction. We have kept a record of any response received.

References

[1] Z. Qian, L. Xie, and Y. Xu, "3D Automatic Segmentation of Brain Tumor Based on Deep Neural Network and Multimodal MRI Images," *Emergency Medicine International*, vol. 2022, Article ID 5356069, 9 pages, 2022.

Hindawi
Emergency Medicine International
Volume 2022, Article ID 5356069, 9 pages
https://doi.org/10.1155/2022/5356069

Research Article

3D Automatic Segmentation of Brain Tumor Based on Deep Neural Network and Multimodal MRI Images

Zhuliang Qian, Lifeng Xie, and Yisheng Xu

Department of Imaging, Xiaoshan District Hospital of Traditional Chinese Medicine, Hangzhou 311201, Zhejiang, China

Correspondence should be addressed to Yisheng Xu; 18403033@masu.edu.cn

Received 9 May 2022; Revised 14 June 2022; Accepted 28 June 2022; Published 21 August 2022

Academic Editor: Hang Chen

Brain tumor segmentation is an important content in medical image processing, and it is also a very common research in medicine. Due to the development of modern technology, it is very valuable to use deep learning (DL) and multimodal MRI images to study brain tumor segmentation. In order to solve the problems of low efficiency and low accuracy of brain tumor segmentation, this paper proposes DL to conduct research on multimodal MRI image segmentation, aiming to make accurate diagnosis and treatment for doctors. In addition, this paper constructs an automatic diagnosis system for brain tumors, uses GLCM and discrete wavelet transform (DWT) to extract features from MRI images, and then uses a convolutional neural network (CNN) for final diagnosis; finally, through four. The comparison of the results between the two algorithms proves that the CNN algorithm has the better processing power and higher efficiency.

1. Introduction

In recent years, through quantitative analysis of a large number of medical images, the relationship between the features contained in these images and their respective diseases has been discovered, and some progress has been made in automated omics imaging methods. Automatic classification is of great significance to the diagnosis of diseases. With the successful application of imaging in clinical medicine, quantitative analysis of imaging will play an increasingly important role in imaging. When classifying the volume image, in order to facilitate subsequent processing and segmentation results, the tumor part needs to be separated from the image to affect the subsequent processing of the information. The reliance on manual fragmentation is time-consuming and painful, mainly depends on the operator, and may lead to the loss of some useful information. Therefore, it is very important to study the automatic segmentation method of tumor images.

When the receiver is equipped with a limited number of radio frequency (RF) chains in a beam space millimeter wave (mmWave) large-scale multiple-input and multiple-output system, the channel estimation will be very challenging. To solve this problem, He H uses a learning-based noise reduction-based approximate message passing (LDAMP) network. The neural network can learn the channel structure and estimate the channel from a large amount of training data. However, the efficiency of DL in the communication process is not very high [1]. Brain tumor segmentation is the process of separating the tumor from the normal brain tissue. Michael's research introduced a new segmentation algorithm called DeepJoint segmentation and multiclassifier to classify the severity of glioma tumors. Initially, the brain image is preprocessed, and then the region of interest is extracted. Then, use the suggested DeepJoint segmentation to complete the segmentation of the preprocessed image. After segmentation, information theory methods are used to extract features from core and edema tumors. Finally, classification is performed by a deep convolutional neural network (DCNN), which is trained by an optimization algorithm called Fractional Jaya Whale Optimizer (FJWO). However, there are some errors in the segmentation process of multimodal MRI images, resulting in inaccurate results [2]. Sérgio Pereira proposed an automatic segmentation method based on CNN and explored 3×3 small cores. Considering that there are fewer weights in the network,

using a small kernel can design a deeper architecture, in addition to having a positive effect on overfitting. However, the complexity of the segmentation method is too high, leading to errors in the results [3].

The innovations of this article are (1) Magnetic resonance imaging (MRI) is a commonly used auxiliary diagnostic tool for brain diseases. It has the advantages of noninvasive, harmless to the human body, and high soft tissue resolution. Magnetic resonance imaging, as a multiparameter imaging method, has a high sensitivity to the display of tissue morphology and pathological changes. (2) Brain tumor segmentation plays an important role in assisting doctors in diagnosis and formulating treatment plans. The goal is to segment abnormal brain tissues.

2. Brain Tumor Segmentation Method Based on DL and Multimodal MRI Images

2.1. Automatic Diagnosis Method of Brain Tumor

2.1.1. DWT. After performing a two-dimensional discrete wave transformation on each image, an approximate low-pass sub-region and three high-pass sub-regions representing detailed information can be used. The four sub-regions are marked as LL, LH, HH, and HL. HH, HL, and LH, respectively, correspond to the high-frequency part of the image and reflect the detailed information of the image. LL corresponds to the low-frequency part of the image. The two parts, respectively, contain most of the energy information in the image [4, 5]. The two-dimensional discrete wave transform can repeat the discrete wave transform in the low-frequency sub-region, which can obtain any decomposition from the formula to obtain the decomposition of multiple analyses. In the experiment, considering the accuracy of calculation and classification, we only perform a one-level decomposition of the initial image. Since the main image information is concentrated in the low-frequency range (by comparison, it can be seen that the low-frequency sub-region has a good visual effect and is almost too close to the original image), the gray coexistence table is calculated in the low-frequency subset. Since the high-frequency part also contains some image features, it cannot be rejected immediately. Therefore, the change of the transformation factor is calculated in the high-frequency and low-frequency sub-regions of the image as a statistical feature [6, 7].

2.1.2. GLCM. GLCM is obtained by counting the number of occurrences of pixel pairs in a certain direction and a distance of d in the image. The GLCM takes into account the number of pixels in the image, factors such as the grayscale relationship, spatial distance, and mutual direction [8, 9]. Furthermore, the texture information can be represented by a relative frequency matrix. This frequency is the number of times two pixels with a distance of d appear on the entire image. The GLCM can be expressed as a function of two pixels with a distance of d in a certain direction and the positional relationship between the gray values of related pixels [10, 11]. In order to reflect the probability of pixel pairs appearing on the entire image, according to the literature, this frequency relative matrix needs to be normalized, and the normalization process is carried out according to formulas (1) and (2) [12, 13]. Normalization is a dimensionless processing method that turns the absolute value of the physical system value into a relative value relationship.

$$p(i, j) = \frac{T(i, j)}{R}. \tag{1}$$

$$R = \begin{cases} 2a(b-d), \theta = 0^{\circ} \text{ or } \theta = 90^{\circ}, \\ 2(b-d)(a-d), \theta = 45^{\circ} \text{ or } \theta = 135^{\circ}. \end{cases} \tag{2}$$

Among them, D is the distance between two pixels with gray value i and gray value j, a is the number of rows in the original image, b is the number of columns in the original image, and R represents the occurrence of all pairs of pixels with a spacing of d in the θ direction The total number of times, θ is the four directions when calculating GLCM.

Figure 1 shows the specific implementation process of the feature extraction method in this chapter [14]. After the image undergoes two-dimensional DWT, the GLCM and variance are calculated in the low-frequency part; in order to obtain the rotation invariant characteristics of the high-frequency part, the three high-frequency parts are added together to find the variance in the experiment [15, 16]. Finally, the three are connected together as the texture feature of the image.

2.1.3. CNN. CNN is a special model of a deep neural network. The structure of this network is inspired by the neural mechanism of the optical system. It is a multilayer perceptron specially designed to recognize two-dimensional shapes [17]. The convolutional neural network is constructed by imitating the visual perception mechanism of biology and can grid features with a small amount of calculation. The main neural network generally consists of an input layer, an aggregation layer, a down-sampling layer (concentration layer), a fully connected mattress, and an outlet mattress.

The basic structure of CNN consists of two parts: among them, the feature extraction layer is used to extract local regional features, and the input of each neuron is related to its local receptor field. After deriving a local attribute, it is necessary to determine its relationship with other local attributes. The second is the feature mapping level. Each layer of the computer in the network consists of many feature maps, and each feature map is flat, and the weights of all neurons at this level are equal [18, 19]. The feature map structure uses the Sigmoid function with a small influence function kernel as the activation function of the convolution network, so that the feature map has displacement invariance.

The convolutional layer is the main component of CNN. The definition of subsequent operations is as follows:

$$C_{ij} = \sum_{s=1}^{p} \sum_{t=1}^{q} a_{i+p-s, j+q-t} \bullet b. \tag{3}$$

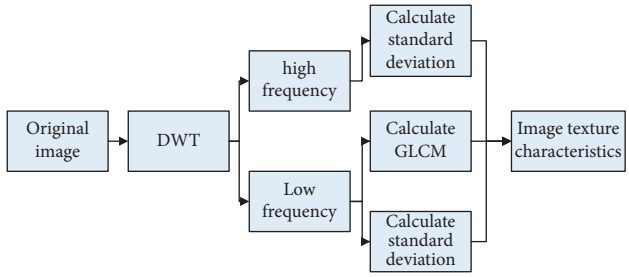

Figure 1: Feature extraction process based on GLCM.

Among them, the size of matrix A is P * Q, and the size of matrix B is expressed by p * q. Each element in their convolution C can be calculated by the above formula.

2.1.4. Classification of Sparrow Search Algorithms (ESSAs). In the standard sparrow search algorithm, when the values of the inertia factor w_n for inducing motion and the inertia factorw_h for foraging motion are large, it is helpful for the algorithm to avoid falling into the local minimum, thereby improving the global search ability; when the two factors have relatively high values it is helpful to improve the algorithm's ability to search for the local area where the sparrow is currently located; therefore, it can be known that a reasonable adjustment of the value of a factor is the key to improving the performance of the algorithm. In order to improve the convergence speed and accuracy of the algorithm, this paper proposes a sparrow search algorithm that dynamically adjusts the inertia weight. The inertial weight decreases linearly with the increase in the number of repetitions. It effectively prevents the decline of local search capabilities and has significant advantages in local and global search capabilities. The improvement strategy is

$$w_n = w_h = \frac{xsd(i,j) + w_{\min} - w_{\max}}{t_{\max}}\left(t_{\max} - t\right), \tag{4}$$

Among them, $xsd(i, j) \in (0,1)$ represents the similarity value of krill individuals i and j in the krill population, t represents the current iteration number, $t_{\max}$ represents the maximum iteration number, and $w_{\max}$ represents the induced inertia factor and foraging. The maximum value of the inertia factor and $w_{\min}$ represents its minimum value [20]. This improvement strategy allows the two factors of the algorithm to be adjusted according to the current krill population situation, which can effectively adjust the algorithm's global search and local survey capabilities. However, in practical applications, this linear reduction of information strategy exists locally in the initial stage of replication. The shortcomings of weak research ability and weak global ability; search in the later stage of the repetition. This will make the best points in the world easy to lose at the beginning of the repetition, and local optimization in the later price stage [21]. Aiming at the shortcomings of the linear decreasing update strategy, this paper continues to study the influence of the inertia weight on the algorithm based on it, in order to further improve its convergence speed and accuracy, and proposes an improved sparrow search optimization algorithm (IKHA). Here is a time-varying nonlinear decrement strategy, namely:

$$w_n = w_h = w_{\min} * \text{rand} + \left(w_{\max} - w_{\min}\right)\left(2 - e^{\log(2)*t/MI}\right). \tag{5}$$

In the formula, MI represents the current maximum number of iterations [22, 23]. This strategy makes the overall algorithm $w_{\max}$ and$w_{\min}$ gradually decrease, allowing the algorithm to better adjust the current search capability during the entire optimization process to avoid falling into the local optimal value, thereby further improving the algorithm's global search capability and convergence speed (the speed at which a convergent sequence approaches its limit).

The optimization process of the Improved Sparrow Search Optimization Algorithm (IKHA) can be described as follows:

$$X_i(t + \Delta t) = X_i(t) + \Delta t \frac{dX_i}{dt} + r1\left(X_{\text{best}}(t) - X_i(t)\right). \tag{6}$$

2.2. Principles of MRI Imaging. Magnetic imaging is based on the quantum mechanical properties of proton rotation, such as electrons and atomic nuclei, which also have angular momentum. The specific value of the angular torque should be determined according to the quantum torque of the magnetic core. Magnetic resonance imaging is an imaging technology that uses the signal generated by the resonance of atomic nuclei in a strong magnetic field to reconstruct the image. It is a nuclear physical phenomenon. In different magnetic fields, such as the brain, protons can be excited to generate radio frequency signals, and this signal can be recognized by the receiving circuit [24]. At present, only atomic nuclei whose rotation quantum number is equal to 1/2 can identify the NMR signal of the receiving circuit.

The most commonly used MRI scan is from a spin echo imaging sequence. The image input in this order is a function of two parameters of the instrument, one parameter is coordination time (TD), and the other is repetition time (TR). MRI can obtain images of the body's transverse, coronal, sagittal, and cross-sections in any direction, which is beneficial to the three-dimensional localization of lesions. An image blood vessel in the MR-wing image represents the nuclear magnetic coordination signal of the volume element hydrogen in the body. The image of the MR image of the body tissue can be expressed by the following equation:

$$S(TR, TE) = \sum\nolimits_i p_i\left(1 - e^{-\left(TR/t1_i\right)}\right)\left(e^{-TE/t2_i}\right). \tag{7}$$

Among them, $t1$ is the rotation relaxation time, also known as the relaxation length time, which reflects the time required for the switch core to transfer the absorbed energy to the surrounding power grid. It is also the time required for the 90 RF pulsed proton to recover to its original state before the magnetism is triggered. $t2$ is the torque rotation relaxation time, also known as the

transverse relaxation time, which reflects the decomposition and loss process of transverse magnetism [25]. The weakening of $T2$ is caused by the mutual magnetization between coordinating protons, which is different from $t1$ which causes the phase change. p is the density of the rotation type in the voxel.

The proton is positively charged and continues to rotate around its axis like the Earth, generating its own magnetic field. Generally speaking, the arrangement of the rotation axis of the small magnet is unstable and chaotic, but if a strong external magnetic field is applied, the rotation axis of the small magnet should be rearranged according to the direction of the magnetic force line. When protons are in a chaotic state, and now they are placed in a strong external magnetic field, the split state of the protons will change. It only points in two directions parallel or antiparallel to the external magnetic field. If it is stimulated by a pulse of a specific frequency, it will be used as a small magnet. The hydrogen core of the magnet absorbs a certain amount of energy and resonance, that is, magnetic coordination occurs.

2.3. Brain Tumor Segmentation Method

2.3.1. FCM Segmentation Method. Fuzzy clustering method (FCM) is an unsupervised classification method, which is widely used in brain tumor image segmentation. The FCM clustering method is based on the minimization of the objective function (the form of the goal pursued in terms of design variables), which becomes the c-mean function.

$$J(X;U,V) = \sum_{i=1}^{c}\sum_{a=1}^{N} (u_{ia})^m \left\| x_a - v_i \right\|_A^2. \tag{8}$$

$$D_{\text{iaA}}^2 = \left\| x_a - v_i \right\|_A^2 = (x_a - v_i)^t A (x_a - v_i). \tag{9}$$

For the data $X = [x_1, x_2, \ldots, x_n]$, $x_i \in R^s$, s is the number of features and $V = [v_1, v_2, \ldots, v_n]$ is the prototype of geometric clustering. u_{ia} stands for cluster center, and v_i is c prototype. The number of classes c must be given, and D_{iaA}^2 is the cluster center of each region. The stagnation point of the objective function can also be found by the following formula:

$$\bar{J}(X;U,V,\rho) = \sum_{i=1}^{c}\sum_{a=1}^{N} (u_{ia})^m D_{\text{iaA}}^2 + \sum_{a=1}^{N} \rho_a \left(\sum_{i=1}^{c} u_{ia} - 1 \right). \tag{10}$$

The minimization of $\bar{J}$ is based on the appropriate selection of U and V through the following formula:

$$u_{ia} = \frac{1}{\sum_{j=1}^{c} \left(D_{\text{iaA}} / D_{\text{jaA}} \right)^{2/(m-1)}}, \quad 1 \le i \le c, \quad 1 \le a \le n. \tag{11}$$

$$v_i = \frac{\sum_{a=1}^{n} u_{ia}^m x_a}{\sum_{a=1}^{n} u_{ia}^m}, 1 \le i \le c. \tag{12}$$

The algorithm can be summarized in the following steps:

(1) Give the number of clusters c, the weight index m, the norm induction matrix A, and the termination tolerance e.

(2) Initialize the segmentation matrix U.

(3) Use U and the formula v_i to calculate the cluster prototype.

$$v_i^{(l)} = \frac{\sum_{a=1}^{N} u_{ia}^{(l-1)} x_a}{\sum_{a=1}^{N} \left(u_{ia}^{(l-1)} \right)^m}, 1 \le i \le c. \tag{13}$$

(4) Calculate the distance as

$$D_{\text{iaA}}^2 = (x_a - v_i)^t A (x_a - v_i), \quad 1 \le i \le c; 1 \le a \le N. \tag{14}$$

(5) Update distance as

$$v_{i,a}^{(l)} = \frac{1}{\sum_{j=1}^{c} \left(D_{\text{iaA}} / D_{\text{jaA}} \right)^{2/(m-1)}}, \tag{15}$$

until

$$\left\| U^{(l)} - U^{(l-1)} \right\| < e. \tag{16}$$

2.3.2. Gaussian Kernel Fuzzy C-Means Clustering. The commonly used Gaussian Kernel Fuzzy C-Means Clustering Algorithm (KFCM) can be divided into KFCM-1 algorithm and KFCM-2 algorithm. Here, we mainly introduce the KFCM-1 algorithm. This method forms a mapping relationship through the kernel function, converts the points in the original space to the feature space for calculation and analysis, and finally obtains the optimal division of the original space. The main idea of the KFCM-1 algorithm is to use the kernel function to transform the data from a low-dimensional feature space into a high-dimensional feature space, so that the features that were not well displayed can be displayed and the difference between different categories is improved. This method is somewhat similar to the solution of a support vector machine (SVM). Support vector machines use kernel tricks to classify nonlinear data. When supervised learning is not possible and the numbers are not labeled, data clustering is used to classify the data. At this time, the learning is unsupervised and the support vector clustering algorithm is used. The specific mathematical description is that there are generally two steps for clustering in the feature space. First, transform the space to a high-dimensional space F through a nonlinear mapping o: $\lambda \longrightarrow F(x \in R^p \longrightarrow o(\lambda))$, $q > p$, and then cluster in the space F. Comparing the expression form of the low-dimensional cluster center, we can remember the cluster center in the high-dimensional space F as d_i as follows:

$$d_i = \sum_{j=1}^{n} \beta_{ij} o\left(x_j \right), \quad \forall i = 1, 2, \ldots, n. \tag{17}$$

The objective function of KFCM-1 is as follows:

$$J_m(U,d) = J_m(U,\beta_1,\beta_2,\ldots,\beta_d) = o(x_j)^T o(x_j) - 23\sum_{l=1}^{n}\beta_{il}(x_l)^T o(x_j) + \sum_{l=1}^{n}\sum_{k=1}^{n}\beta_{il}(x_j)^T o(x_j). \quad (18)$$

The calculations in (18) are all in the form of the inner product of the elements. The inner product is a vector operation, that is, the corresponding elements are multiplied and added, and the result is a scalar.

3. Construction Experiment of Brain Tumor Automatic Diagnosis Auxiliary System Based on Multimodal MRI Images

3.1. Computer-Aided System for Automatic Diagnosis of Brain Tumors. The workflow of the computer-aided system for the automatic diagnosis of brain tumors is shown in Figure 2. A preprocessing device-automatic smear device is used in the system to make cell smears used in the test, which is an auxiliary device of this system. The system adopts modular design ideas, each module is closely related to other modules, and connects up and down.

In traditional micro preparation, the doctor artificially melts the cell sample into a glass plate. Recent studies have shown that the coating made by this traditional manual method can only collect 20% of the cells, while more than 80% of the cell samples remain in the sample and are discarded together. In addition, more than 40% of the coating will become turbid due to the action of blood, mucus, and inflammatory tissue. These defects are the reason for the inaccurate results of most routine tests. The automation of cell smears not only improves the efficiency of the system, but also ensures the consistency of the system and the standardization of cell staining, thereby reducing the difficulty of identifying machines and improving the correct identification rate. The task of the pretreatment equipment is to automatically prepare cell staining. The working procedure of the instrument is as follows: using the principle of adsorption, diluting the cell sampling with a diluent, then uniformly stirring and filtering with an appropriate semipermeable membrane, staining with an appropriate staining method, forming a very thin cell coating on the window pane, use a fixative for fixation, and finally a drying process, coating extremely thin cells, the cell shape is well preserved and evenly distributed.

The computer-aided diagnosis instrument shall include microscopic visual inspection devices and automatic identification software. One is the foundation of the inspection system, and the other is the core and key of the inspection system. The two complement each other and are indispensable. The material system mainly includes an optical microscope, a precision workbench, an optical collection device, and a computer. The software system mainly includes image algorithm modules, cell segmentation (including core and coil segmentation) modules, export characteristics, and analysis and identification. Under the coordinated control of the computer, the unit controller drives the desktop to scan in the X and Y directions and focus correction in the Z direction. The CCD camera collects clear images of the cells magnified by the microscope and transmits them to the computer for processing and analysis.

3.2. Brain Tumor Segmentation Processing Steps. Magnetic resonance image preprocessing is a very active research area, which is dedicated to improving and correcting magnetic resonance images for future analysis. In the unsupervised method, the brain tissue data learning model without reference or nonauto-labeling will encounter common problems such as noise or gray inconsistency, which will cause the system to accumulate errors as the error categories increase. MRI brain tumor segmentation usually follows the following steps:

Denoising is a typical work of magnetic imaging preprocessing, its purpose is to reduce or ideally eliminate noise in the original magnetic imaging image. Although MRI noise is usually Gaussian, by definition, MRI noise generally obeys the Rician distribution. The main source of MRI image noise is the detection object, mainly thermal noise, and sometimes physiological noise.

Skull dissection is the process of removing the skull, hemorrhage, and nonbrain tissue from the MRI sequence. Brain Suite software can be used to improve data preprocessing, recalculate the autopsy masks of all patients, and delete unnecessary tissues in MRI images.

Abnormal intensity is another common artificial target during MRI data acquisition. Magnetic field anomalies are an inevitable result, including low-frequency signals destroying images and affecting grayscale. Grayscale uses black tones to represent objects, that is, black is used as the base color, and black with different saturations is used to display images.

In brain tumor injury plans, many magnetic imaging sequences are usually obtained through different analyses. Furthermore, introducing spatial inconsistency in multiple MRI studies.

3.3. Feature Extraction. There is a high degree of correlation between adjacent voxels in medical images, and the grayscale patterns between adjacent voxels are different, and the volumes are the same. This method uses patch prediction based on small image regions, which can make full use of these local correlation information, and can predict a set of limited image block vocabularies based on small image regions. This method has been widely used in the fields of image denoising, image reconstruction, and image pattern synthesis. This method converts the image segmentation

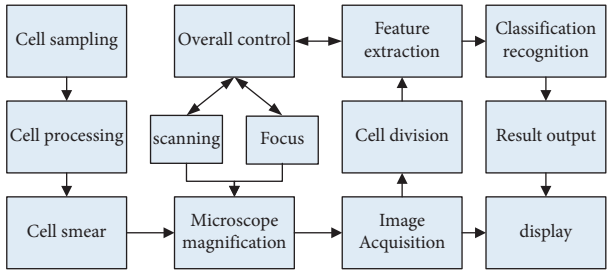

Figure 2: Work flow chart of the brain tumor automatic diagnosis system.

problem into the image unit classification problem by predicting the most likely label category of the central image unit and has achieved great success. All methods are similar to this focus on the study of the similarity between unnecessary local image information and its image features in near pixels. This article directly derives the target image and the small-area m and organizes them as features in the form of a one-dimensional vector $m \times \mathrm{m} \times m$.

Due to the imbalance between volume samples and nonvolume samples, a sampling method is used to reduce the positive and negative samples to 10 W data volume for training.

3.4. Results Evaluation. This experiment uses the training and testing data set provided by BRATS2015. In order to evaluate the performance of algorithm segmentation, the segmentation results are uploaded to the online evaluation system of the competition. Four indicators of Dice score, PPV, Sensitivity, and Kappa are used to evaluate the performance. The relevant definitions are as follows:

$$\mathrm{Dice}(U,V) = \frac{2\left(\left|U_1 \cap V_1\right|\right)}{\left|U_1\right| + \left|V_1\right|}. \tag{19}$$

$$\mathrm{ppv}(U,V) = \frac{\left(U_1 \cap V_1\right)}{\left|V_1\right|}. \tag{20}$$

$$\mathrm{sensi}(U,V) = \frac{\left(U_1 \cap V_1\right)}{\left|U_1\right|}. \tag{21}$$

$$\mathrm{Kappa}(U,V) = \frac{|U \oplus V|/\left|U_0 + V_1\right| - \left|U_0\right| \bullet \left|V_0 + \left|U_1\right| \bullet \left|V_1\right|\right| / \left(\left|U_0\right| + \left|V_0\right|\right) \bullet \left(\left|U_1\right| + \left|V_1\right|\right)}{\left|U_0\right| \bullet \left|V_0\right| + \left|U_1\right| \bullet \left|V_1\right| / \left(\left|U_0\right| + \left|V_0\right|\right) \bullet \left(\left|U_1\right| + \left|V_1\right|\right)}. \tag{22}$$

G represents the result of manual segmentation by experts, and S represents the result of segmentation by the algorithm in this chapter. U0 and U1 are manually divided into negative and positive samples. Similarly, $V0$ and $V1$, respectively, represent the negative and positive samples predicted by the algorithm.

4. Brain Tumor Segmentation Algorithm Based on Machine Learning and Multimodal MRI Images

4.1. Brain Tumor Segmentation Algorithm Based on Multimodal MRI Images. This article uses some segmented MR images in the public data set in the Whole Brain Atlas (WBA) database as training data. The first part shows the segmentation results on the No. 4 instance of the high-level whole brain Atlas WBA_TA; the second part is the segmentation results on the No. 20 instance of the low-level whole brain Atlas WBA_TB. Divide between $W1$ and $W2$, W1C, and WBA numbers.

This paper evaluates the segmentation efficiency of the algorithm based on the measurement of the Dice factor. The measured value of the Dice factor is in the range of [0,1], where 1 means a perfect match, and 0 means a complete disagreement. Use the training data set to simulate 20 WBA-TA and 20 WBA-TB instances, and record the measured value of the Dice factor. Table 1 and Figure 3, respectively, correspond to the results of 8 simulation examples.

Comparing the algorithm in this article with the current three technologies, Table 2 and Figure 4 list the average results of measuring the dice factors of these algorithms used to split the image into the data set. It can be seen that the algorithm in this paper achieves the best results when segmenting the volume and the volume of different images.

In addition, many existing segmentation algorithms require additional model training, so it takes a lot of time and depends on a specific training set. This algorithm realizes volume segmentation based on gray distribution matching and does not require manual calibration of large amounts of data for model training, which effectively reduces segmentation time. Experiments show that the average segmentation time of this algorithm for each image is about 0.5 s. For some automatic segmentation algorithms that do not require training, the segmentation time of these

Table 1: Dice coefficient metrics for image segmentation.

Numbering	1	2	3	4	5	6	7	8
WBA_TA-tumor	0.942	0.933	0.904	0.866	0.968	0.854	0.954	0.964
WBA_TA-edema	0.912	0.844	0.925	0.909	0.929	0.555	0.951	0.879
WBA_TB-tumor	0.954	0.800	0.815	0.933	0.905	0.912	0.872	0.821
WBA_TB-edema	0.954	0.850	0.890	0.920	0.900	0.917	0.895	0.644

Figure 3: Dice coefficient metrics for image segmentation.

Table 2: The mean value of the dice coefficient measurement of each segmentation algorithm.

Different algorithms	FCM	KFCM	CNN	Algorithm
WBA_TA-tumor	0.72	0.61	0.69	0.88
WBA_TA-edema	0.70	0.64	0.57	0.83
WBA_TB-tumor	0.65	0.48	0.72	0.87
WBA_TB-edema	0.43	0.33	0.39	0.81

algorithms is close to or slightly less than the algorithm in this article, but its segmentation accuracy is also obvious lower. In practical applications, the accuracy of subdivision is more important than the time of division. In short, the algorithm proposed in this paper significantly improves the accuracy of the segmentation while keeping the segmentation time low.

4.2. Results and Analysis of Brain Tumor Image Segmentation Based on MRI. This experiment uses a synthetic MRI data set with fewer artifacts and grayscale variables compared with real MRI images. This verification experiment does not include rough extraction.

The experiment uses an image patch with a size of $3 \times 3 \times 3$, and the dictionary atomic sequence $K = [2\ 4\ 8\ 16\ 32\ 64\ 128\ 256\ 512]$ is used to test and explore the optimal K

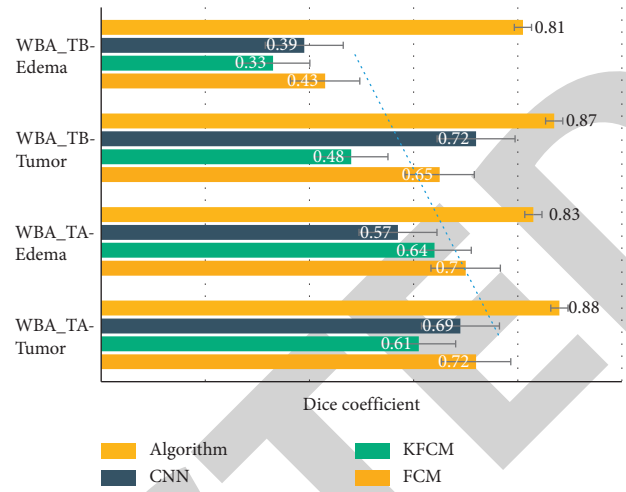

Figure 4: The mean value of the dice coefficient measurement of each segmentation algorithm.

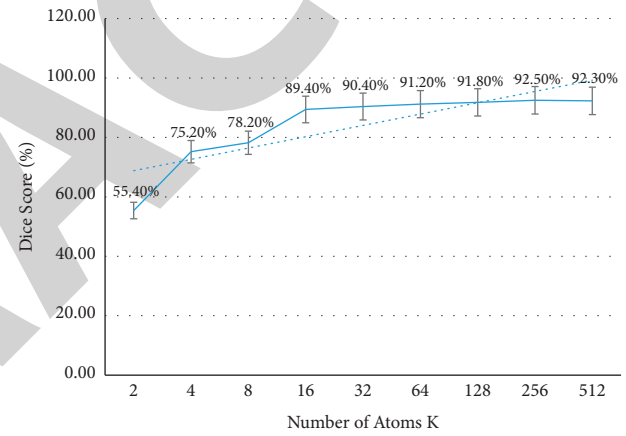

Figure 5: The number of dictionary atoms and the accuracy of segmentation.

Table 3: The average correct rate of 200 patients with segmentation in the training data set.

Validation	HGG	LGG
Dice-complete	0.86	0.80
Dice-core	0.76	0.64
Dice-enhancing	0.83	0.73
PPV-complete	0.95	0.83
PPV-core	0.72	0.57
PPV-enhancing	0.81	0.77
Sensitivity-complete	0.75	0.83
Sensitivity-core	0.79	0.76
Sensitivity-enhancing	0.84	0.66
Kappa	1.00	1.00

value. As shown in Figure 5, as the number of dictionary atoms increases, the average accuracy of segmentation increases very rapidly, and the accuracy does not stabilize until $K = 128$.

In order to compare the average segmentation performance of the segmentation method proposed in this article on the training data set and the test data set, the four

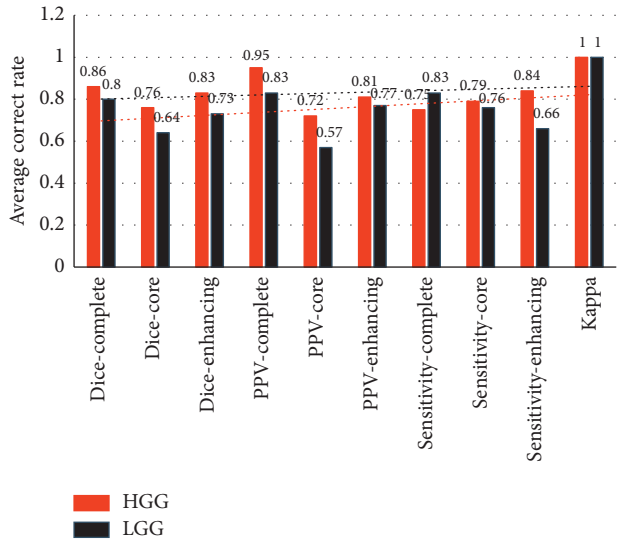

Figure 6: The average correct rate of 200 patients in the training data set with segmentation.

Table 4: The average correct rate with the segmentation of 100 patients in the tested data set.

Split task	Dice	PPV	Sensitivity	Kappa
Complete	0.84	0.83	0.80	1.00
Core	0.71	0.77	0.78	1.00
Enhancing	0.59	0.60	0.66	1.00

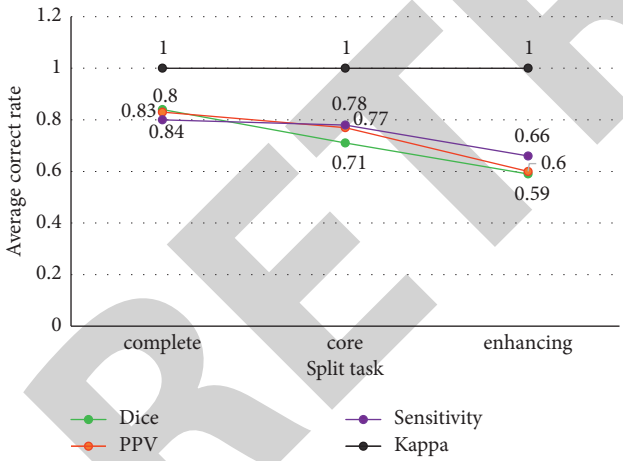

Figure 7: The average correct rate with the segmentation of 100 patients in the tested data set.

indicators of the two are counted and calculated. Among them, the segmentation method proposed in this article is in the training data set of BRATS 2019; the average segmentation performance of the above is shown in Table 3 and Figure 6.

In addition, the average segmentation performance of the segmentation method proposed in this paper on the BRATS 2019 test data set is shown in Table 4 and Figure 7.

According to the requirements of the BRATS competition, the experiment has three different segmentation tasks: complete tumor area R1 (label 1 + 2+3 + 4), tumor core area R2 (label 1 + 3+4), enhanced tumor area R3 (label 4). According to the comparison of the results of the algorithm segmentation in this paper, the segmentation method adopted in this paper has great potential.

5. Conclusions

The medical imaging scan of the MRI brain has a high degree of correlation between the target and neighboring voxels, as well as the grayscale calculation of different image modes between the same data volume. The prediction method using small-area image coding can make full use of this locally relevant information can be based on a limited set of image block vocabularies. This paper successfully applies these methods to image segmentation operations by providing the most likely label of the central pixel of the image block. This method focuses to a large extent on exploring the similarity information of the features of adjacent regions of the image.

This article mainly focuses on the uneven grayscale in the segmentation of MRI brain tumor images and the large differences in the size, location, and structure of brain tumors in different patients, such as the large differences in MRI images of different patients. Starting from the segmentation of the entire tumor structure, to the detailed description of the tumor substructure, the self-organizing active contour model and neural decoding network technology are introduced into the segmentation problem based on changeable images, and then the automatic tissue mapping based on the changeable MRI image and the deep deconvolution neural network hybrid active mapping model of brain tumors are proposed Segmentation strategy.

Tumor cell-assisted visual diagnosis system is an important application of computer automatic visual inspection in medical image processing. Based on the analysis of the clinical diagnosis of pathologists, and referring to the results and experience of previous studies, this article conducts an in-depth study on the principle of visual detection of microscopic cell smears, and proposes a set of implementation plans for a tumor cell-assisted diagnosis system. Based on the scheme, a preliminary software identification system is given. Focusing on cell image preprocessing, segmentation, cell classification, and identification, etc., this article has done a lot of research and achieved good preliminary research results. There is still room for improvement in the method in this paper. This paper deals with two-dimensional data. Subsequent work will extend the method to three-dimensional and further optimize the segmentation results.

Data Availability

No data were used to support this study.

Conflicts of Interest

The authors declare that there are no conflicts of interest with any financial organizations regarding the material reported in this manuscript.

Hindawi
Emergency Medicine International
Volume 2023, Article ID 9823909, 1 page
https://doi.org/10.1155/2023/9823909

Retraction

Retracted: Application of Image Processing Technology in Aerobics Injury Diagnosis

Emergency Medicine International

Received 8 August 2023; Accepted 8 August 2023; Published 9 August 2023

This article has been retracted by Hindawi following an investigation undertaken by the publisher [1]. This investigation has uncovered evidence of one or more of the following indicators of systematic manipulation of the publication process:

(1) Discrepancies in scope
(2) Discrepancies in the description of the research reported
(3) Discrepancies between the availability of data and the research described
(4) Inappropriate citations
(5) Incoherent, meaningless and/or irrelevant content included in the article
(6) Peer-review manipulation

The presence of these indicators undermines our confidence in the integrity of the article's content and we cannot, therefore, vouch for its reliability. Please note that this notice is intended solely to alert readers that the content of this article is unreliable. We have not investigated whether authors were aware of or involved in the systematic manipulation of the publication process.

In addition, our investigation has also shown that one or more of the following human-subject reporting requirements has not been met in this article: ethical approval by an Institutional Review Board (IRB) committee or equivalent, patient/participant consent to participate, and/or agreement to publish patient/participant details (where relevant).

Wiley and Hindawi regrets that the usual quality checks did not identify these issues before publication and have since put additional measures in place to safeguard research integrity.

We wish to credit our own Research Integrity and Research Publishing teams and anonymous and named external researchers and research integrity experts for contributing to this investigation.

The corresponding author, as the representative of all authors, has been given the opportunity to register their agreement or disagreement to this retraction. We have kept a record of any response received.

References

[1] D. Zhang and Y. Tian, "Application of Image Processing Technology in Aerobics Injury Diagnosis," *Emergency Medicine International*, vol. 2022, Article ID 2553048, 13 pages, 2022.

Hindawi
Emergency Medicine International
Volume 2022, Article ID 2553048, 13 pages
https://doi.org/10.1155/2022/2553048

Research Article

Application of Image Processing Technology in Aerobics Injury Diagnosis

Duo Zhang[1] and Yan Tian[2]

[1]*Physical Education Department, Civil Aviation Flight University of China, Guanghan 618307, Sichuan, China*
[2]*College of Physical Education, Chengdu University of TCM, Chengdu 611137, Sichuan, China*

Correspondence should be addressed to Yan Tian; tianyan@cdutcm.edu.cn

Received 17 May 2022; Revised 8 July 2022; Accepted 18 July 2022; Published 6 August 2022

Academic Editor: Hang Chen

Aerobics sports injury diagnosis is a rapid diagnosis of sports injuries caused by athletes in the process of aerobics training or competition. The purpose of this paper is to use image processing technology to study and analyze the diagnosis of aerobics sports injury, so that the diagnosis results can be obtained more quickly and effectively. This paper first introduces the image processing technology and then analyzes the sports injury in colleges and universities. Firstly, the algorithm formula of image processing technology is given, and then the algorithm is introduced into the dynamic analysis of aerobics injury diagnosis. The two are compared through example analysis. The experimental results show that joint strain, sprains, and muscle strain are the main types of sports injury of College Aerobics students, reaching 59, 50, and 31 times, respectively. When using image processing technology in the diagnosis of sports injury, the diagnosis results can be obtained quickly and effectively.

1. Introduction

With the rapid development of image processing technology in China, we can find that it has been applied in various fields of real life. At the same time, image processing technology is also widely used in the detection of sports injuries. Most sports injuries can be diagnosed by image processing technology. Image processing technologies are a kind of using computers to deal with image messages. It primarily deals with image digitization, image intensification and repair, image data codes, image division, and image definition. Image processing technology has successfully entered people's lives and affected people's lives. And the image processing technology is excellent in the diagnosis of sports injury, especially in the diagnosis of aerobics sports injury.

Today, with the diversified and multiproject development of image processing technology, how to apply image processing technology perfectly in aerobics sports injury diagnosis and use image processing technology to obtain the best sports injury judgment also has far-reaching significance for the development and expansion of image processing technology. Image processing technology is also widely used. In recent years, scholars have used image processing technology to solve the problem of sports injury diagnosis, but there is relatively little application and research in aerobics sports injury diagnosis. How to reduce the occurrence of sports injuries in high-level competitive aerobics athletes is an important problem that needs to be solved urgently in the development of Chinese competitive aerobics. Therefore, the application of image processing technology to solve the problem of aerobics injury diagnosis has both theoretical and practical significance.

With the progress of society, increasing scholars have done relevant research on the application of image processing technology in aerobics injury diagnosis. In recent years, Wang J has normalized the image based on image recognition technology. And he carried out feature recognition on gray-scale images, ignoring small fluctuations. Combined with the characteristics of inventory images, he removed the drying process and proposed an algorithm model based on feature recognition [1]. However, the data used in his research is not the latest, and the results of the

output are not very ideal. In the same year, Huang et al. studied the application of image processing technology in high-frequency vibration direction and amplitude measurement. According to the corresponding relationship between the vibration blurred images and the still images in the spectrum, they preprocessed the image [2]. However, their expressions on blurred images and still images were not clear enough. Before them, Oho E proposed an efficient and fast scanning method, such as TV scanning, combined with digital image processing technology to replace the traditional slow scanning mode as the standard acquisition model [3] of general scanning electron microscope (SEM). However, the combination of the two lacks theoretical support.

After studying the image processing technology of other scholars, Zhang D used the methods of literature, questionnaire, and mathematical statistics to investigate and analyze the common sports injuries of aerobics athletes. The results show that the common sports injury parts of aerobics athletes are waist, knee, shoulder, and ankle [4]. However, he did not make a systematic analysis of his research themes in the conclusion. Subsequently, Zhu et al. used big data analysis technology and computer vision technology based on convolutional neural network to establish the loss risk prediction model of aerobics athletes according to the relevant theories of sports biomechanics and computer image recognition [5]. However, the application effect of the prediction model created in real life is not very good. Later, Mmfa introduced the application of nuclear medicine technology in the diagnosis of bone and soft tissue injury, focusing on the important contribution of bone scintigraphy and hybrid research (SPECT/CT) [6]. However, his own arguments expressed in the article were relatively few, and most of them are a study of the research results of others. Unlike him, Jyoti et al. discussed a range of imaging options available in clinical settings for sports injuries and provided an in-depth understanding of the role of each imaging modality and image guidance procedure in enabling athletes to resume activities at an early stage [7]. Zhang observed and analyzed the effects of *Astragalus* and Salvia miltiorrhiza on skeletal muscle injury in aerobics athletes [8]. However, there is too much overlap in the methods he has used in his research.

The innovation of this paper lies in the following: (1) in the diagnosis of aerobics sports injury, it can use image processing technology to diagnose more quickly and effectively. It makes it easier for athletes to manage their physical condition. (2) Image processing technology algorithm is applied to the research of aerobics sports injury diagnosis. In other applications, image processing technology is often used as a method to check product quality problems. This paper is committed to deeply mining the internal characteristics and advantages of image processing technology and finds out the similarities between image processing technology and medical image diagnosis. It uses the characteristics of the algorithm to diagnose medical images to get a faster diagnosis result.

2. Application of Image Processing Technology in Aerobics Injury Diagnosis

2.1. Image Processing Technology

2.1.1. Overview of Digital Image Processing. Digital image processing refers to a technology that takes corresponding operations on digital images with the help of computers to achieve the expected purpose, so we can also use the concept of computer image processing to represent digital image processing. Image is the representation of a natural landscape. It can be presented in various ways objectively. It includes visible images, such as light images, photos, graphics, and pictures. It also includes abstract mathematical functions and physical images that cannot be seen by human eyes [9]. From the perspective of whether the computer can recognize and process it, images can be divided into two categories. The first category is analog images, and the other category is digital images. Digital images are the research object of digital image processing technology.

2.1.2. Content of Digital Image Processing. In real life, when processing digital images, if there is no other program to process the images directly, we will encounter many difficult places. For example, there is an interference signal in the image when the image is encoded and compressed. At this time, when we change the data of the original image into another way with obvious features, the image can be processed quickly and effectively. The most widely used image transformation methods are the following [10].

(1) Fourier Transform. Fourier transform is actually sending a signal from the time domain to the frequency domain, and the reciprocal of the time domain is its frequency. The speed of changing the gray level of an image is the frequency of the image. Figure 1 shows the spectrum display of a medical image.

(2) Wavelet Transform. Wavelet transform is similar to Fourier transform. The function of wavelet transform is to send image data from the spatial domain to the wavelet domain. The wavelet coefficients obtained in this way are not single-layer, but multilayer. Wavelet transform is also a great tool for multilevel image decomposition. As shown in Figure 2, after the image is changed by wavelet, the subsequent work of the image is completed by reading and changing the wavelet coefficient. For example, changing the wavelet coefficient can change one aspect of the characteristics of the original image [11].

(3) Main Contents of Image Processing Technology. As shown in Figure 3, classic digital image processing mainly includes image enhancement, image transformation, image restoration, image edge detection, image segmentation, image feature parameter extraction, and image morphological processing, and the output is the processed image [12].

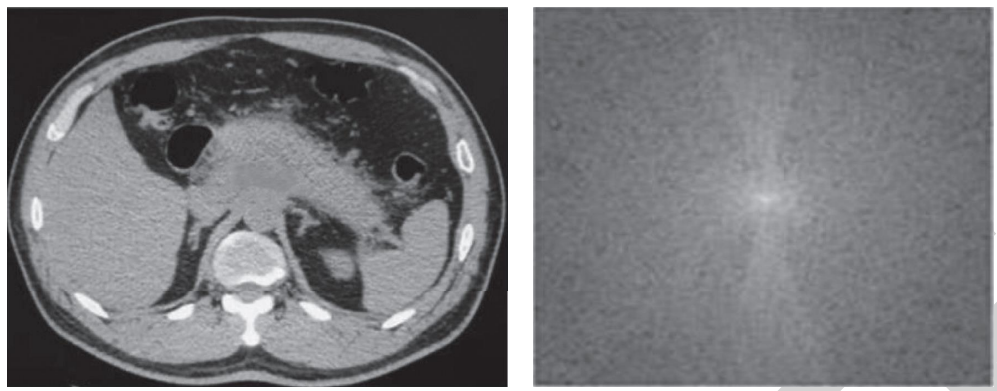

(a) (b)

Figure 1: Medical image and its frequency domain spectrum display. (a) Medical image. (b) Frequency domain spectrum.

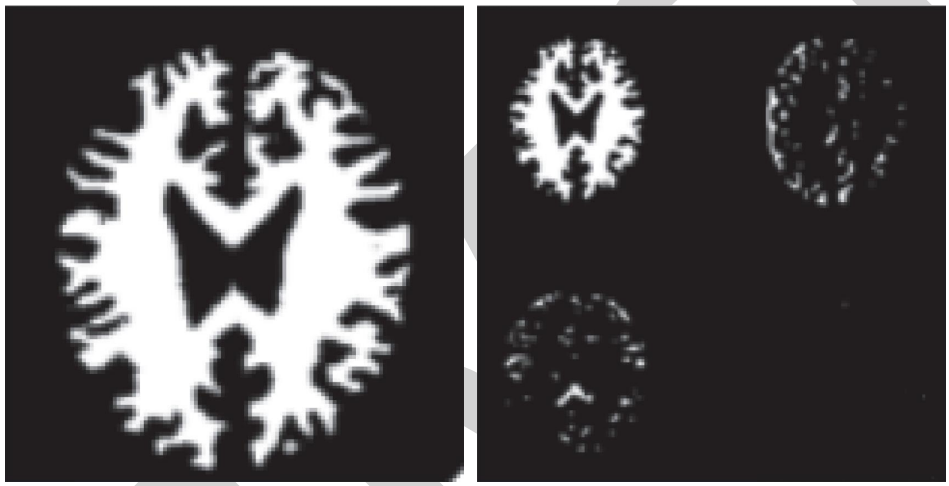

Figure 2: Binary wavelet decomposition of image.

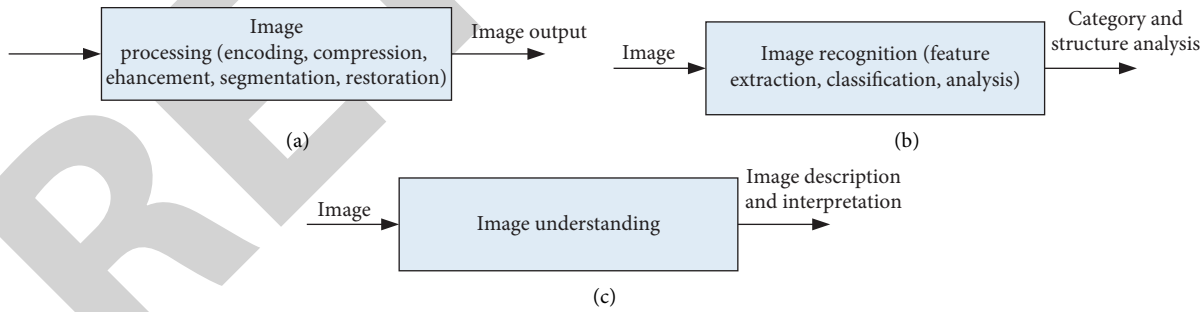

Figure 3: Main content of image processing technology. (a) Schematic diagram of image processing. (b) Schematic diagram of image recognition. (c) Schematic diagram of image understanding.

The main task of image analysis and recognition is to extract the features and measure the parameters of the target object obtained by image segmentation, to form the representation and description of non-images such as characters and values [13].

Image understanding is a kind of advanced digital image processing, which is a continuation and development of digital image processing and image analysis. It enables the computer to have the ability to understand the surrounding scenery like human beings, to replace human beings to solve practical application problems. After the operation of digital image understanding technology, the output is the description and interpretation of the image [14].

2.2. Image Preprocessing Algorithm. Image preprocessing is to transform the part image captured by the image acquisition device to achieve the purpose of image feature

extraction and recognition. Many algorithms are involved in the process of image filtering, binarization, morphology, and edge detection. Therefore, the main research content of this chapter is to select suitable digital image processing methods and algorithms according to the actual characteristics of aerobics injury diagnosis [15].

2.2.1. Filter Processing. The image captured by the camera may be disturbed by noise in the process of digitization, resulting in poor quality. Therefore, when further processing the digital image, it must be filtered first to eliminate or reduce the noise and restore the original image [16].

(1) Mean Filtering. It is a typical linear filtering algorithm. Its basic principle is to determine a template for the target image from the digital image. Its common template is square. Common 3×3 mean filtering 4-domain and 8-domain templates are shown as follows:

$$\frac{1}{5} \times \begin{bmatrix} 0 & 1 & 0 \\ 1 & 1 & 1 \\ 0 & 1 & 0 \end{bmatrix} \frac{1}{9} \begin{bmatrix} 1 & 1 & 1 \\ 1 & 1 & 1 \\ 1 & 1 & 1 \end{bmatrix}. \tag{1}$$

(2) Gaussian Filtering. Gaussian filtering (also known as weighted filtering, it is also a kind of linear smoothing filtering) is suitable for eliminating Gaussian noise and is widely used in the noise reduction process of image processing [17]. Its function is expressed as

$$j(c,u) = \frac{1}{2\pi\sigma} r^{\left(c^2+u^2\right)/\left(2r^2\right)}. \tag{2}$$

Among them, 2 $\pi\sigma$ 2 represents the weighted average of the pixel values of the entire image, and the value of each pixel is obtained by the weighted average of its own value and other pixel values in the field. The commonly used templates for Gaussian filtering are similar to the mean template. The commonly used templates include 3×3 templates, 5×5 templates, and 7×7 templates. The commonly used 3×3 Gaussian template is shown as follows [18]:

$$\frac{1}{16} \times \begin{bmatrix} 1 & 2 & 1 \\ 2 & 4 & 2 \\ 1 & 2 & 1 \end{bmatrix}. \tag{3}$$

2.2.2. Binarization Treatment. Image binarization processing is the basic technology of image preprocessing and a very active branch of image processing. Especially, it plays an important role in image information compression, edge extraction, and shape analysis. It has a wide range of applications and has become a basic segment in its processing process [19].

Binary image refers to the image with only two gray levels, which has small storage space and fast processing speed. It can conveniently carry out logical operation on the image [20]. After binarization, the image has only black and white, so the degree range is divided into target and background, and the binarization of the image is realized.

$$(h(c,u)) = \begin{cases} 255\,(\text{white}) & g(c,u) \geq y \\ 0\,(\text{black}) & g(c,u) < y \end{cases} \tag{4}$$

2.2.3. Global Threshold Method. In some simple images, the background region and the target region form two peaks in the histogram of the image, and a trough is formed between the two peaks [21]. Then, the gray value y represented by the trough between the two peaks is selected as the threshold to realize the segmentation of the two regions. This method is also known as the bimodal method, as shown in Figure 4.

If the image has 256 gray values, the gray value range is 0~255, and then select a gray value y to divide the gray histogram into two categories H_0 and H_1. M represents the total number of image table points in the image, and m_l represents the number of image table points with gray value L [22]. Assuming that the number of pixels in H_0 and H_1 areas accounts for e_0 and e_1 in the overall image, and the average gray values of the two areas are i_0 and i_1, we can get the following:

Probability:

$$E_0 = \sum_{l=0}^{y} q_l = \frac{\sum_{l=0}^{y} m_l}{M}, \tag{5}$$

$$e_1 = \sum_{l=k=1}^{n-1} q_l = 1 - e_0. \tag{6}$$

Average gray value:

$$i_0 = \sum_{l=0}^{k} l q_l, \tag{7}$$

$$i_1 = \sum_{l=y+1}^{n-1} l q_l. \tag{8}$$

Then, the total average gray value:

$$i = e_0 \times i_0 + e_1 \times i_1. \tag{9}$$

Interclass variance:

$$h(y) = e_0 \times \left(i_0 - i\right)^2 + e_1 \times \left(i_1 - i\right)^2 = e_0 e_1 \left(i_0 - i_1\right)^2. \tag{10}$$

The optimal threshold is

$$Y = \text{ARGMAX}\left(H(Y)\right). \tag{11}$$

2.2.4. Maximum Entropy Threshold. According to the concept of entropy, for the image with a gray-scale range of 0, 1, 2, . . ., N–1, the entropy of the histogram is defined as

$$J = -\sum_{L=0}^{N-1} Q_L \in Q_L. \tag{12}$$

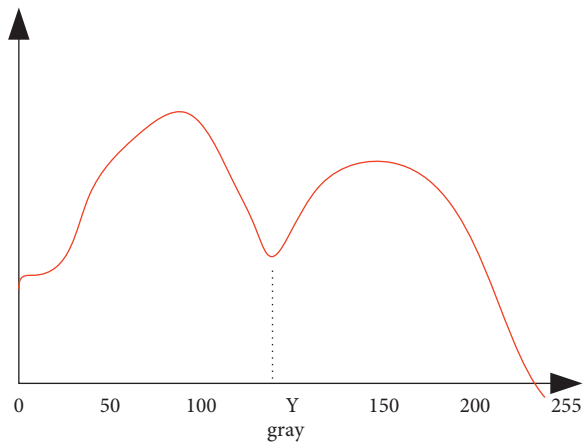

Figure 4: Schematic diagram of bimodal method.

Q_L is the probability of pixels with gray value L in the overall image. If the threshold y is set, the image is divided into target P and background n, and their probability distributions are as follows:

Zone P:

$$\frac{Q_L}{Q_Y} L = 0, 1, 2, \ldots Y \, Q_Y = \sum_{L=0}^{Y} Q_L. \tag{13}$$

Zone V:

$$\frac{Q_L}{1 - Q_Y} L = Y + 1, Y + 2, \ldots, N - 1. \tag{14}$$

If

$$J_Y = -\sum_{L=0}^{Y} Q_L \in Q_L, \tag{15}$$

then it can get the following formula:

$$J(Y) = -\sum_{L=0}^{N-1} Q_L \in Q_L, \tag{16}$$

$$J_P(Y) = -\sum_{L=0}^{Y} \frac{Q_L}{Q_L} \in \frac{Q_L}{Q_L} = \mathrm{IN} Q_Y + \frac{J_L}{Q_Y}. \tag{17}$$

Then, the total entropy of the image is

$$J_N(Y) = -\sum_{L=Y+1}^{N-1} \frac{Q_L}{1 - Q_Y} \in \frac{Q_L}{1 - Q_Y} = \mathrm{IN}(1 - Q_Y) + \frac{J - J_Y}{1 - Y_Y}. \tag{18}$$

2.2.5. Principle of Mathematical Morphology. There are two basic operations in mathematical morphology: expansion and decay. Based on these basic operations, we can also deduce and combine various practical algorithms of mathematical morphology, such as open operations and closed operations.

(1) Swell. Image s is expanded with a structural element n and can be written as

$$S \oplus N = \left\{ C \middle| (\widehat{N})_C \cap S \neq \varnothing \right\}. \tag{19}$$

It first makes an image of the structural element n about its origin and then shifts the image C to the image s. Then, the set of elements formed when the image after translation intersects at least one nonzero common element of the target point in the image s is the result of the expansion operation. As shown in Figure 5, the shapes of structural elements can be rectangular, square, circular, diamond, and other shapes. In this example, only one structural element in rectangular form is selected.

(2) Corrode. The image S is etched by a structural element N to write $S\Theta N$, which is defined as

$$S\Theta N = \left\{ C \middle| (N)_C \in S \right\}. \tag{20}$$

When the structural element N is completely still contained in the image S, the set of the origin of the structural element N is the result of corrosion operation, as shown in Figure 6.

2.3. Aerobics Sports Injury

2.3.1. Overview of Sports Injury. Some people say that the concept of sports injury is because external factors act on the human body, resulting in the normal operation of human organ function. It also causes discomfort in the human body, which is called injury. Similarly, we can know that the injury in sports is a sports injury. The injury caused by different sports has its remarkable characteristics, but one thing is common: the impact of sports injury on sports participants is extremely serious.

2.3.2. Analysis on the Current Situation of Sports Injury of Aerobics Majors in Colleges and Universities

(1) Through the survey, we can get Tables 1 and 2. Among the 160 students majoring in Aerobics selected by 8 colleges and universities in China, one male is an international athlete from Guangzhou Institute of Physical Education. There are 3 national athletes, 2 boys and 1 girl, from D University and a university, respectively. The proportion of students at the master level accounted for 2.49% of the respondents. The proportion of students at the national level and the national level is 8.13% and 20%, respectively. The proportion of students below national level II is the largest, 69.38%.

It can be seen that, with the continuous deepening of the training mode of sports talents combined with sports education in China, college students have also made good achievements in international Chinese competitions. However, it should also be noted that the number of students who have obtained the master level is small, accounting for only 2.49% of the selected research objects. From the perspective of

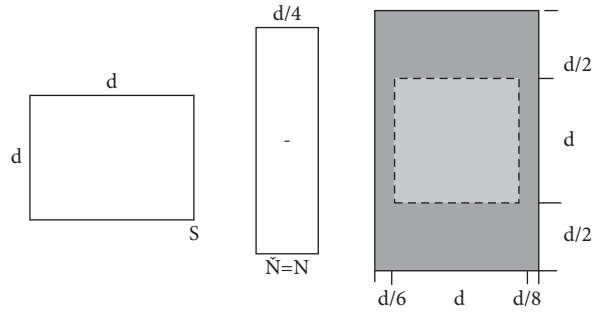

Figure 5: Schematic diagram of expansion.

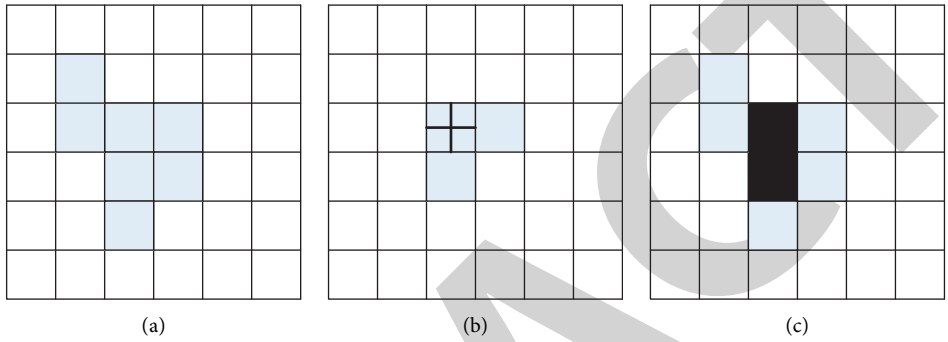

Figure 6: Corrosion schematic diagram. (a) Image s. (b) Image n. (c) Image $S \Theta N$.

Table 1: Sports grade of students majoring in aerobics.

	International master class	National elite level	The national level	National secondary	National level 2 or below	A combined
Male	1	2	9	33	33	65
Female	0	1	4	78	78	95
A combined	1	3	13	32	111	160
A combined %	0.63%	1.86%	8.13%	20%	69.38%	100%

Table 2: Regional distribution of sports grades of aerobics majors.

University name	International master class	National elite level	The national level	National secondary	National level 2 or below
A	0	2	3	9	6
B	0	0	2	4	14
C	0	0	0	6	14
D	1	1	5	8	5
E	0	0	0	1	19
F	0	0	3	4	13
G	0	0	0	0	20
H	0	0	0	0	20
A combined	1	3	13	32	111

gender, the number of girls majoring in aerobics is greater than that of boys, indicating that aerobics is more favored by girls.

(2) Incidence and duration of sports injury: in the investigation on the incidence of sports injury of aerobics majors (Tables 3 and 4), we can see that there are many phenomena of sports injury of aerobics students during training. Among the 160 aerobics majors surveyed, 132 students have experienced sports injuries. Among them, the number of injured girls is more than that of boys. The incidence of sports injuries among students is 83%, which is quite amazing. Some students have sports injury accidents more than once, with a total of 186 injuries. In each stage of aerobics practice, no one was injured in the preparatory activities, which is related to the

Table 3: Incidence of sports injury in aerobics majors.

	The number of survey	The number of injured	Incidence of injury (%)	The number of injured	Average number of injured
Male	64	51	78	97	1.48
Female	96	81	87	172	2.66
A combined	160	132	84	186	1.16

Table 4: Exercise period of sports injury of aerobics majors.

	Preparation activities	Difficulty movement training	Flexible training	Complete set of training	Strength training
Male	0	20	13	12	5
Female	0	42	10	15	15
A combined	0	62	23	27	20

low intensity of preparatory activities. Sports injuries mostly occur in the process of difficult training, and 62 people's sports injuries occur in this practice stage. This shows that, with the continuous development of aerobics, the requirements for difficult movements are higher and higher, and the requirements for students' physical reserves are also higher and higher. This leads to the emergence of a series of sports injuries in the process of practicing difficult movements and complete sets of movements.

In the investigation of the occurrence time of sports *injuries*, it is found that aerobics majors in different regions have phased characteristics in the occurrence time of sports injury and show regional differences. As shown in Figure 7, in terms of time, October and December are the high incidence stage of sports injuries. During this period, 86 students majoring in aerobics had sports injuries, accounting for 46% of the total number of injuries.

(3) Location and type of sports injury: through the *investigation* of the parts and types of sports injury of aerobics majors in colleges and universities, it is found that there are 8 easy parts of sports injury of aerobics majors in total. They are shoulder, elbow, wrist, waist, thigh, knee, calf, and ankle. Among the 186 cases of sports injury, the highest part of sports injury was the wrist, with 36 cases. The second is the knee joint with 32 people times, and the third is the ankle joint with 30 people times. Thighs, lower legs, waist, shoulders, and hips ranked fourth to eighth.

It is found from the survey results (as shown in Table 5) that joint strain, sprains, and muscle strain are several main types of sports injuries of college aerobics majors, reaching 59, 50, and 31 times, respectively. The prone parts of joint strain are the wrist, waist, and knee. This is related to the content and method of aerobics training. Sprains often occur in the ankle and knee.

3. Experiment and Application of Image Processing Technology in Aerobics Injury Diagnosis

3.1. Preprocessing of Aerobics Sports Injury Diagnosis Surface Image. The surface image of aerobics sports injury diagnosis is affected by image acquisition, image transmission, and on-site working environment, resulting in the reduction of the visual effect of the image, such as insufficient contrast, unclear image edge contours, noise in the image, image blur, and deformation, which will bring inconvenience to computer image processing and analysis. To enable the computer to analyze and process the image well, this paper first needs to preprocess the collected aerobics injury diagnosis surface image. Image enhancement is the basic content of digital image preprocessing, which lays a good foundation for subsequent image processing, especially image segmentation.

Image enhancement can enhance the contrast of the image and increase the difference between the target and the background. It removes the useless interference information in the image and enhances the target features in the image. The algorithms of image enhancement mainly include gray histogram enhancement, noise elimination, piecewise linear enhancement, Laplace operator, and various filtering methods. By using image enhancement technology, the quality of aerobics sports injury diagnosis images has been significantly improved. It improves the definition of aerobics injury diagnosis image and obtains good visual effect. It greatly reduces the influence of ambient noise on aerobics injury diagnosis image and reduces the difficulty of image segmentation in the next step.

3.1.1. Gray Histogram. From the gray histogram of the image, we can get the gray range of the image, the distribution of gray level, and the average brightness of the whole image, so we can get the important basis for further image processing. In addition, the histogram represents the gray distribution of the object image, and the shape of this gray distribution will not scale with the rotation of the object. It

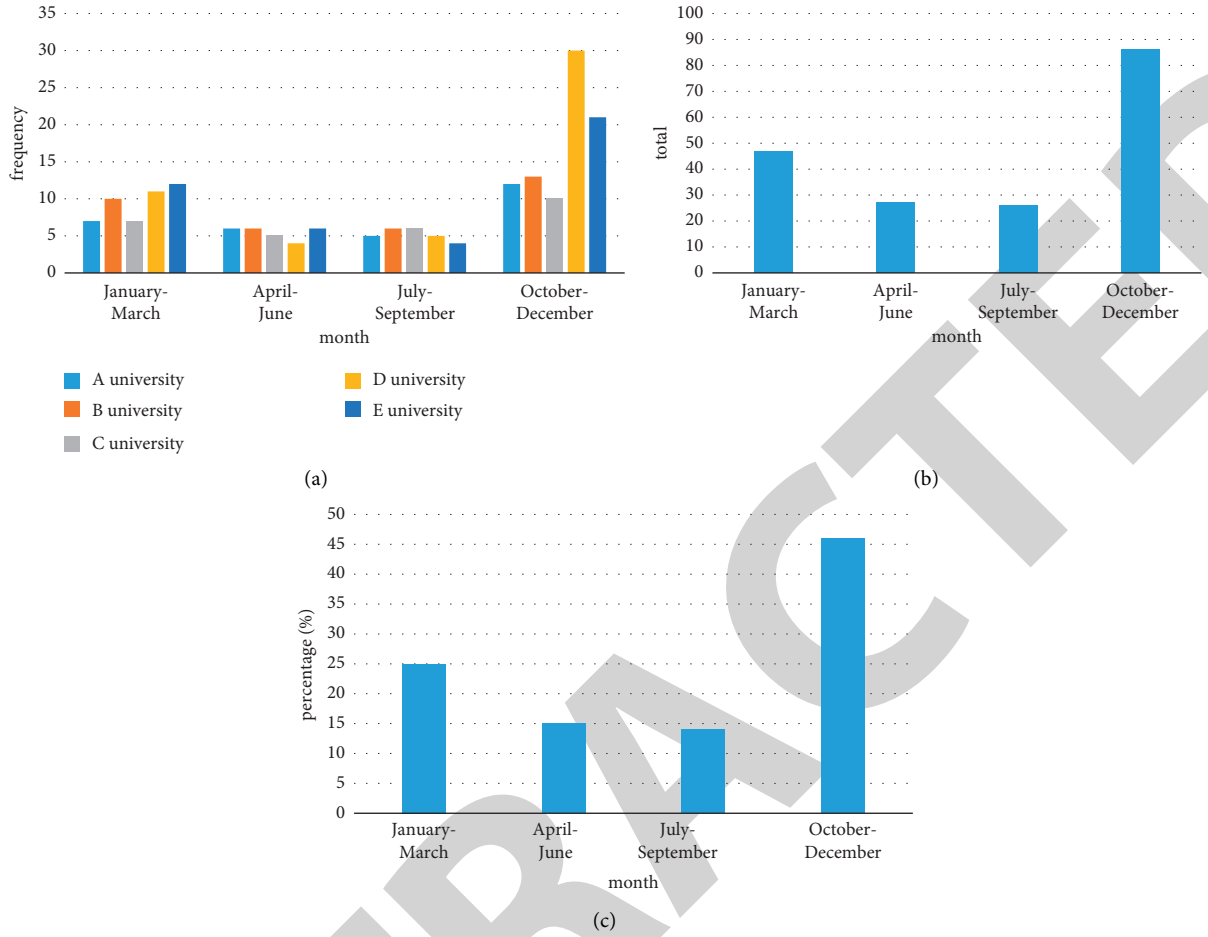

Figure 7: time statistics of sports injury. (a) Time of sports injury. (b) Total damage of each month. (c) Percentage of damage at each time.

Table 5: Parts and types of sports injury of aerobics majors.

	Joint sprains	Strain	Strain	A cramp	Contusion	Scratch	Fractures	A combined
The head								
The shoulder	6	3						9
The elbow					6	2	2	8
Wrist			34		2			36
The waist	5		10					15
Thighs, hips		28						28
The knee joint	9		15			8		32
Ankle	30							30
The calf				20		8		28
A combined	50	31	59	20	8	16	2	186

will not even change due to external light. Therefore, to a certain extent, using the histogram of the object can effectively identify the object.

The surface histogram and equalization histogram of the aerobics injury diagnosis diagram are shown in Figure 8. It has been operated by the gray histogram of the original surface image of aerobics injury diagnosis, and the histogram corresponding to the gray image is obtained. It then performs histogram equalization on the gray histogram. It improves the quality of the image. The clarity, brightness, and contrast of the image have been enhanced, which provides convenience for subsequent image processing.

3.1.2. Motion Injury Image Denoising. In the process of collecting and transmitting aerobics sports injury diagnosis images, it is affected by the industrial field environment, which will inevitably produce noise, resulting in some

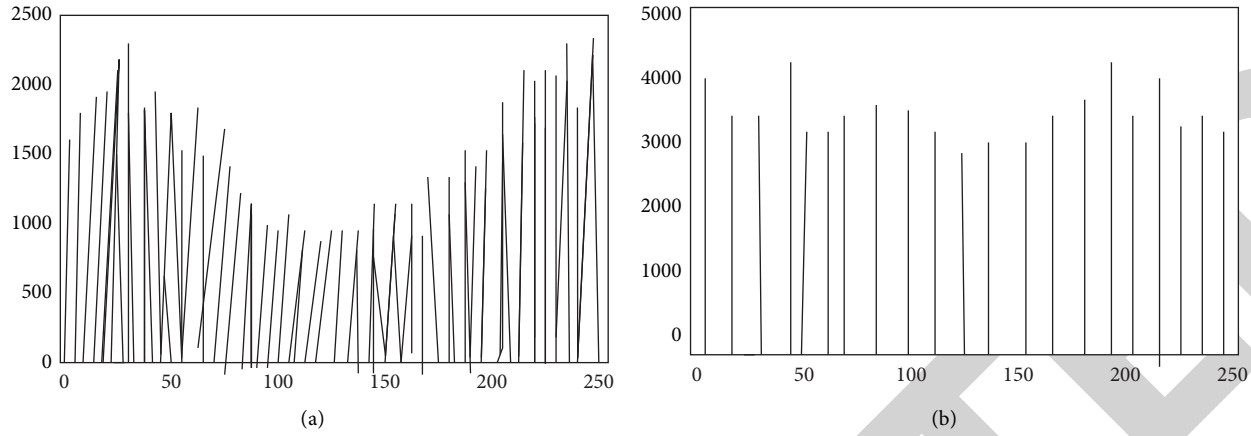

Figure 8: Gray histogram. (a) Histogram corresponding to the gray image. (b) Histogram homogenization effect.

unknown black and white spots on the image. This not only affects the visual effect of the image, but also increases some interference information, which also leads to the decline of image quality. It is not conducive to the operation and processing of subsequent computers. To eliminate the interference of image noise, we need to study a suitable low-pass filter. It filters out the interference of high-frequency noise signal through low-pass filters, to achieve the purpose of removing noise, so the selection of low-pass filters is particularly critical. For noise removal, various filtering techniques can be used to remove noise, such as mean filter, median filter, and improved median filter. These technologies are based on low-pass filtering technology to achieve the effect of noise reduction.

This paper uses a median filter. Median filtering technology can not only reduce noise, but also preserve the contour of the original image to the greatest extent. The specific implementation is to sort the gray value of the pixel and the gray value of the pixels in the surrounding window for a point in the image disturbed by noise and the area centered on the point. The intermediate value is obtained to replace the original pixel value of a certain point, to neutralize the abrupt points in the image and achieve the purpose of image noise removal. The flow chart of the median filtering algorithm can be shown in Figure 9.

3.2. Segmentation of Aerobics Injury Diagnosis Image. The most basic function of image segmentation is to segment the image into target and background. The ultimate purpose of segmentation is to segment the required parts according to the application requirements and remove the useless information areas such as background. The basic image segmentation techniques include edge segmentation and threshold segmentation. These basic technologies can realize the binarization of images. However, according to different objectives, it combines different application requirements. When appropriate, it needs to take special image segmentation. Combined with the particularity of sports injury medical images, this topic adopts a special image segmentation technology, that is, the image segmentation algorithm based on mathematical morphology to realize the segmentation of sports injury medical images.

Generally speaking, it is necessary to carry out binary threshold segmentation on the preprocessed sports injury image. Through the binary threshold segmentation operation of the image, the gauze image is separated from the background, and then, with the help of the reconstruction technology in mathematical morphology, the features in the sports injury image are finally segmented and extracted. Through image segmentation, it provides an important basis for feature extraction of sports injuries. At the same time, it is also convenient for the subsequent analysis of the computer image processing systems. The quality of image segmentation seriously affects the result of feature parameter extraction and ultimately affects the accuracy of recognition and judgment of computer image processing system.

After binarization, all regions of the image are black except warp and weft, and the feature region we need to extract; that is, the target is in the black region. Therefore, it is necessary to reverse the image and convert the target of the defect area into a white image. The essence of image inversion is to perform nonoperation on each pixel value after binarization. The black-and-white conversion of the original binary image is realized through the operation of taking and repairing to analyze and process the target defects in the future.

Edges can be defined as the region with discontinuous gray change in the image. Image edge is the basis of image segmentation and feature parameter extraction. The edge detection algorithm can detect the gray discontinuous part and then extract the edge of the target image, which is convenient for the subsequent target segmentation. The common image edges are shown in Figure 10, from which we can see the type of gray mutation. To segment the edge of the image, we need to study the appropriate edge detector algorithm. Classical edge detection algorithms include

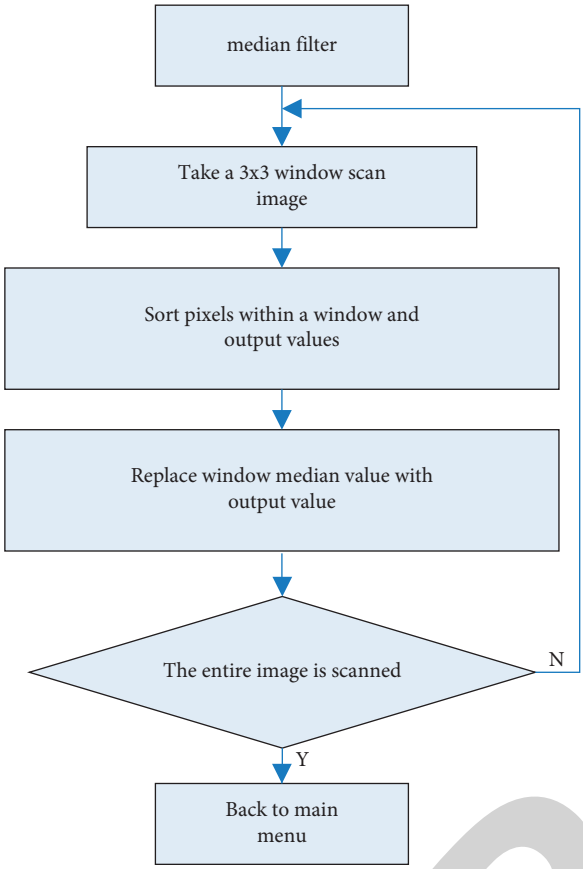

Figure 9: Flowchart of median filtering algorithm.

Prewitt operator, Roberts operator, Sobel operator, Laplacian operator, LOG operator, and wavelet transform.

3.3. Feature Extraction and Aerobics Injury Diagnosis Map. In the previous chapters, we used a series of image preprocessing, image segmentation, and other technologies for the surface image of sports injury, which belong to the field of image processing. When processing the image of a sports injury diagnosis, what we send to the computer image processing system is the original digital image to be processed. After the application of a series of image processing algorithms in a computer image processing system, the output is still image. At this time, the image is a binary image, the amount of information of the image is greatly compressed, and the quality of the image has been significantly improved. Image preprocessing and image segmentation technology are ready for the analysis and recognition of defect images. The process of image analysis mainly includes image feature extraction and measurement of feature parameters, image classification, and feature judgment results. During image analysis, what we send to the computer is the segmented image of the sports injury surface. After the analysis and judgment of the image, it outputs the data information and representation of the feature rather than the image information. Finally, the surface feature detection system gives the judgment result. It mainly goes through three processes to complete the recognition and classification of sports injury surface images.

3.3.1. Feature Extraction. To identify the types of sports injury images, feature extraction is needed first. In this paper, when extracting the features of sports injury images, the input is the binary image segmented by morphology. The output is the data of the motion injury image; that is, the motion defect image is described from another non-image field of view. It needs a process to make the computer have the ability to analyze and understand images like people. The first step is to measure the parameters of image features. The measured data also directly affect the result of image discrimination.

Feature extraction is the feature extraction and parameter measurement of the target object obtained by image segmentation to form a description of image data. This description is non-image, which can be character data or digital. The main extracted image features include edge features, gray features, texture features, and geometric features. The result of image feature extraction directly affects the accuracy of image analysis and recognition. If the method is not suitable, the image classification cannot be carried out. What kind of features are selected for the image and the parameter measurement of the selected features is the key to the accuracy of the detection results.

3.3.2. Image Recognition. Generally speaking, image recognition is to recognize and classify images. The research of image recognition technology in this subject is to develop a sports injury feature detection system, which replaces manual automatic detection and recognition of surface features. The specific implementation process of sports injury recognition system is as follows: the first step is to collect the original sports injury image and convert the image information of the analog signal into digital image. It is then transmitted to the computer surface feature detection system for image processing. The second step is to preprocess the surface feature image of a sports injury, which can enhance the contrast between the image feature target and the background. It reduces the influence of noise on the image and improves the quality of the image. In the third step, firstly, the threshold segmentation algorithm is used to binarize the image, and then the main features such as broken hole, missing longitude, and broken weft are extracted from the background with the help of the segmentation method of mathematical morphology. The fourth step is the extraction of image features and the measurement of parameters. The focus of this step is to select effective features that can reflect the commonness and individuality of defects. The last step is to complete the identification and classification of aerobics injury diagnosis by using a certain discrimination principle through the extracted data information.

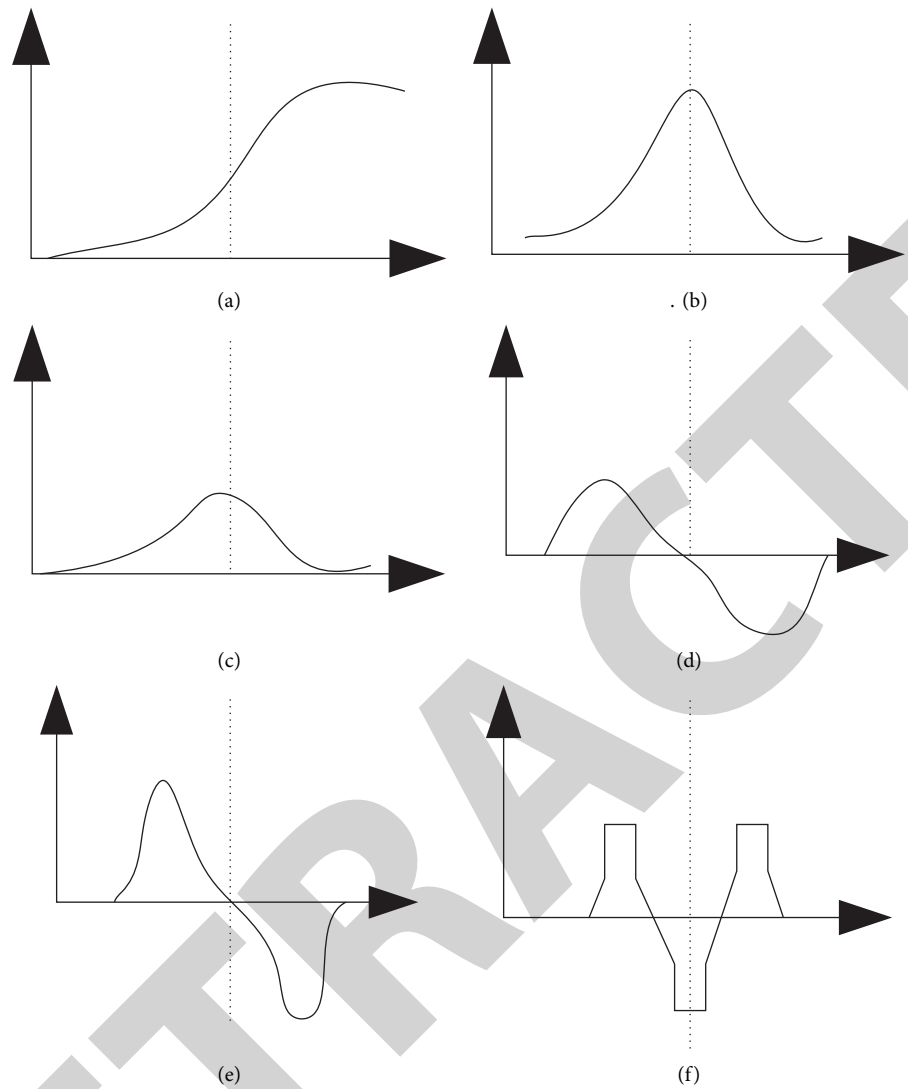

Figure 10: Edge of image. (a) Stepped edge. (b) pulsed edge. (c) Stepped edge first-order difference. (d) Pulsed edge first-order difference. (e) Stepped edge difference. (f) Pulsed edge second-order difference.

It is to automatically recognize the surface of the sports injury images and classify these surface features, which involves pattern recognition technology. Pattern recognition is a comprehensive application of a series of digital image processing algorithms. Through pattern recognition technology, the surface feature detection system can finally complete the recognition and classification of sports injury images. In fact, sports injury recognition is such a process: first, extract the geometric features of the image and measure the feature parameters, then classify and judge the sports injury image according to the designed classifier, and finally output the recognition results.

4. Discussion

This document is committed to the application research and design of image processing technology in the diagnosis of bodybuilding injury, and it is ideal for intricate analyzes and processing of bodybuilding injury diagnosis. It not only expands the scope of applying image processing technology, but also is a new venture to research the intricacies of diagnosing fitness injuries. Through the study of the process of image processing technology, this paper mines image processing technology as an important tool to study the complexity of the system. It holds great value in the study of the intricacy of injuries in exercise and health. In addition, based on the existing research of Chinese scholars, this paper draws on and summarizes it. The algorithm of image processing technology is listed one by one, making the algorithm suitable for the environment of sports injury medical images. For the research of image processing technology, this paper starts with the overview of the most basic image processing technology and analyzes the content and algorithm of the basic image processing technology. It was successfully combined and concluded with aerobic exercise injury diagnosis. In the empirical analysis stage, this paper uses the image preprocessing, segmentation and feature description algorithms listed in this paper to study the medical images of bodybuilding

sports injury diagnosis. Several factors were analyzed, and the outcome indicates that the findings are in fact in line with the real world.

Discussion of the incident: it shows that image-based processing technology is more effective than a single observation of medical images. Athletes with sports injuries can judge the injury more quickly. This can greatly reduce the time to study sports injuries. In the specific practical decision-making, image processing technology can still analyze the medical image of sports injury and obtain the diagnosis results reasonably and flexibly, to obtain the most effective and rapid diagnosis.

This paper makes a case study on the medical image of aerobics injury diagnosis. Firstly, this paper makes a qualitative analysis of the concept and algorithms of image processing technology. Then, it studies the injury of aerobics athletes and uses the algorithm to combine and analyze according to the sports injury medical image. Through the analysis of the data, this paper concludes that the injury diagnosis of aerobics athletes based on image processing technology is indeed faster and more effective than human naked eyes.

5. Conclusion

Through the case study, this paper draws an important conclusion: through the application of image processing technology in aerobics sports injury diagnosis, we can find that using image processing technology can diagnose sports injury medical images more quickly. However, this is not absolute. It does not rule out the fixed nature of medical images. Some small details may not be seen by experienced doctors, such as the diagnosis of various injury degrees of Aerobics Athletes in this case. This requires more detailed research and quantitative analysis to determine a more effective diagnostic report. To reduce the injury rate of aerobics, it can reasonably supplement nutrition, adjust work and rest time, reduce exercise fatigue, do stretching and relaxation exercises, strengthen medical supervision and rehabilitation training, etc. The items discussed in this article are based on the combination of image processing technology and bodybuilding injury medical images, and the selection of items is relatively limited. The general reality of medical imaging of sports injuries will face more detailed diagnostic problems. In reality, aerobics injuries should also be studied in combination with many factors. If the study is more careful, it will be more valuable and more difficult. However, we can still choose to believe that there will be increasingly such research reports in the near future. And the image processing technology will be increasingly developed. Even subtle problems in medical images can be diagnosed in a short time.

Data Availability

The data underlying the results presented in the study are available within the manuscript.

Conflicts of Interest

The authors declare that they have no conflicts of interest.

References

[1] J. Wang, "Application of wavelet transform image processing technology in financial stock analysis," *Journal of Intelligent and Fuzzy Systems*, vol. 40, no. 2, 2021.

[2] X. Huang, Z. Wei, and F. Wen, "Image processing technology in high frequency vibration direction and amplitude measurement," *Journal of Intelligent and Fuzzy Systems*, vol. 35, no. 2, pp. 1–8, 2021.

[3] E. Oho, K. Suzuki, and S. Yamazaki, "Applying fast scanning method coupled with digital image processing technology as standard acquisition mode for scanning electron microscopy," *Scanning*, vol. 2020, no. 6, 9 pages, Article ID 4979431, 2020.

[4] D. Zhang, N. Zhang, F. F. Ma et al., "One-step fabrication of functionalized poly(l-lactide) porous fibers by electrospinning and the adsorption/separation abilities," *Journal of Hazardous Materials*, vol. 360, no. 7, pp. 150–162, 2018.

[5] D. Zhu, H. Zhang, Y. Sun, and H. Qi, "Injury risk prediction of aerobics athletes based on big data and computer vision," *Scientific Programming*, vol. 2021, no. 1, 10 pages, Article ID 5526971, 2021.

[6] B. Mmfa, "Clinical applications of nuclear medicine in the diagnosis and evaluation of musculoskeletal sports injuries [J]," *Revista Española de Medicina Nuclear e Imagen Molecular*, vol. 39, no. 2, pp. 112–134, 2020.

[7] R. Jyoti, T. Jain, and M. Damiani, "The expanding role of imaging in the diagnosis and management of sports injuries," *Australian Journal of General Practice*, vol. 49, no. 1, pp. 12–15, 2020.

[8] M. Zhang, "Research on college students' sports aerobics teaching from the perspective of personality shaping[J]," *Agro Food Industry Hi-Tech*, vol. 28, no. 1, 2017.

[9] B. Subba Reddy and D. Shakthi Prasad, "Digital image processing techniques for estimating power released from the corona discharges," *IEEE Transactions on Dielectrics and Electrical Insulation*, vol. 24, no. 1, pp. 75–82, 2017.

[10] M. E. Kew, M. D. Miller, and B. C. Werner, "Chapter 5: techniques for ACL revision reconstruction," *Sports Medicine and Arthroscopy Review*, vol. 28, no. 2, pp. e11–e17, 2020.

[11] M. Nadim, H. Ahmadifar, M. Mashkinmojeh, and M. R. Yamaghani, "Application of image processing techniques for quality control of mushroom," *Caspian Journal of Health Research*, vol. 4, no. 3, pp. 72–75, 2019.

[12] C. Fang and S. Labi, "Image-processing technology to evaluate static segregation resistance of hardened self-consolidating concrete," *Transportation Research Record*, vol. 2020, no. 1, pp. 1–9, 2018.

[13] G. Yang, J. Wu, and Q. Hu, "Rapid detection of building cracks based on image processing technology with double square artificial marks," *Advances in Structural Engineering*, vol. 22, no. 5, 2019.

[14] Y. Bu, "Research on the application of image processing technology based on SIFT features extraction in the retrieval and classification of art works," *Revista de la Facultad de Ingenieria*, vol. 32, no. 6, pp. 162–170, 2017.

[15] L. Zhu, A. Wang, and F. Jin, "Using image processing technology and general fluid mechanics principles to model smoke diffusion in forest fires," *Fluid Dynamics and Materials Processing*, vol. 17, no. 5, 2021.

[16] D. Forsdyke, A. Smith, M. Jones, and A. Gledhill, "Infographic: psychosocial factors associated with outcomes of sports injury rehabilitation in competitive athletes," *British Journal of Sports Medicine*, vol. 51, no. 7, p. 561, 2017.

Hindawi
Emergency Medicine International
Volume 2023, Article ID 9840632, 1 page
https://doi.org/10.1155/2023/9840632

Retraction

Retracted: Meta-Analysis of Predictive Role of Early Neurological Deterioration after Intravenous Thrombolysis

Emergency Medicine International

Received 28 November 2023; Accepted 28 November 2023; Published 29 November 2023

This article has been retracted by Hindawi, as publisher, following an investigation undertaken by the publisher [1]. This investigation has uncovered evidence of systematic manipulation of the publication and peer-review process. We cannot, therefore, vouch for the reliability or integrity of this article.

Please note that this notice is intended solely to alert readers that the peer-review process of this article has been compromised.

Wiley and Hindawi regret that the usual quality checks did not identify these issues before publication and have since put additional measures in place to safeguard research integrity.

We wish to credit our Research Integrity and Research Publishing teams and anonymous and named external researchers and research integrity experts for contributing to this investigation.

The corresponding author, as the representative of all authors, has been given the opportunity to register their agreement or disagreement to this retraction. We have kept a record of any response received.

References

[1] H. Jiang, J. Zuo, D. Wang, Y. Huang, C. Gao, and Y. Wan, "Meta-Analysis of Predictive Role of Early Neurological Deterioration after Intravenous Thrombolysis," *Emergency Medicine International*, vol. 2022, Article ID 2894426, 11 pages, 2022.

Hindawi
Emergency Medicine International
Volume 2022, Article ID 2894426, 11 pages
https://doi.org/10.1155/2022/2894426

Research Article

Meta-Analysis of Predictive Role of Early Neurological Deterioration after Intravenous Thrombolysis

Haiwei Jiang, Jing Zuo, Dan Wang, Yi Huang, Chang Gao, and Yue Wan

Department of Neurology, Hubei No. 3 People's Hospital of Jianghan University, Wuhan 430033, Hubei Province, China

Correspondence should be addressed to Yue Wan; 20161750101@stu.gzucm.edu.cn

Received 8 April 2022; Revised 25 May 2022; Accepted 2 June 2022; Published 22 July 2022

Academic Editor: Hang Chen

With the popularization of intravenous thrombolysis, more and more people use intravenous thrombolysis to treat related diseases, but problems also arise. There are still a considerable number of patients with early disease after thrombolytic therapy not only not significantly improving, but also progressing, that is, early neurological deterioration (END). In view of this problem, the prediction of END after intravenous thrombolysis becomes very important. With the development of medical technology, research on the prediction of END after intravenous thrombolysis has gradually been carried out. Effective prediction is of great significance for the prevention and treatment of END after intravenous thrombolysis. This article aimed to carry out a meta-analysis of the predictive role of END after intravenous thrombolysis. Through an informed analysis of all studies of this type in this field, this article determines a method for predicting END after intravenous thrombolysis. The actual effect of its role is revealed in this paper, and its purpose is to promote the development of this field. This article addresses the same type of study on the predictive role of neurological deterioration after intravenous thrombolysis. The article performs test and meta-analysis of its role by conditionally searching for literature studies. It is explained using the relevant theoretical formulas. The analysis results show that the prediction of END after intravenous thrombolysis in this paper can effectively help make a preliminary judgment on the possible later neurological deterioration. Although there is an error between the predicted curve and the actual curve, the difference between the two is between 1% and 5%. It can basically effectively predict the occurrence of END. Therefore, the prediction of END after intravenous thrombolysis has a very large preventive effect on the END after intravenous thrombolysis.

1. Introduction

With the increasingly serious aging, cerebrovascular disease occupies an important position in the increasing incidence rate year by year, and people's life and health are facing a huge threat. Cerebrovascular disorder refers to various diseases of blood vessels in the brain including cerebral arteriosclerosis and thrombosis. Its common feature is to cause ischemia or hemorrhage in the brain tissue, resulting in disorder or death. The most common cerebrovascular disease is acute ischemic stroke. For patients with acute cerebral infarction within 4.5 hours after the onset, intravenous thrombolysis therapy with recombinant tissue plus plasminogen activator (rt-PA) is recommended. Intravenous thrombolysis is the injection of thrombolytic drugs into the body through a peripheral or central vein. However, there are some patients with neurological changes and persistent or staged progression after intravenous thrombolytic therapy. It eventually presents with poor prognosis, residual impairment, and even death. There are two types of venous thrombosis. One is thrombophlebitis. That is, inflammation is the first and thrombosis is the second. Another is venous thrombosis. That is, thrombosis is the initial phenomenon, and inflammation of the vein wall is secondary, with deep vein thrombosis of the lower extremities being the most common.

The short-term improvement of neurological function in patients after intravenous thrombolysis, followed by deterioration, progressive or staged deterioration, is called END after intravenous thrombolysis. The incidence of END may vary widely due to the different definitions of END in different studies; however, the occurrence of END is not

uncommon. There are still no unified diagnostic criteria for END. This is mainly due to inconsistent scoring scales and scoring criteria for the severity of END, as well as controversy over the time window of END. The definition of END should be simple and effective in helping medical staff identify patients with neurological deterioration for timely management and improved prognosis. At present, researchers have different opinions on the criteria for judging END. Regarding the neurological deterioration in the initial stage after venous thrombolysis, most academic studies use the NIHSS score of more than 4 points at the time of hospitalization or death within 24 hours after venous thrombolysis. In recent years, scholars have studied the problem of early prediction of neurological deterioration after intravenous thrombolysis. However, the overall grasp and research on the role of prediction of neurological deterioration after intravenous thrombolysis are relatively rare. Therefore, this paper will conduct a meta-analysis of the role of existing studies in the prediction of END after intravenous thrombolysis through literature research. It has very important theoretical and practical significance for the prognosis of patients with this disease.

The innovations of this paper are as follows: (1) This paper introduces the relevant theoretical knowledge of intravenous thrombolysis and the prediction of END after thrombolysis. In this paper, the principles and methods of END prediction after intravenous thrombolysis are used to analyze the role of meta-analysis in the prediction of END after intravenous thrombolysis. (2) This paper expounds the advantages of early prediction of neurological deterioration after intravenous thrombolysis. Through experiments, it is found that the prediction of END after intravenous thrombolysis in this paper has a very important and positive effect on the prognosis of patients.

2. Related Work

With the continuous development of social economy and medical industry, more and more people have conducted in-depth research on the prediction of END after intravenous thrombolysis. Tanaka et al. investigated differences in predictors of END due to hemorrhagic and ischemic injury [1]. Wu et al. evaluated the safety and efficacy of early low dose casein therapy for early end patients within the first 24 hours after IVT [2]. Although it has carried out drug evaluation for the early treatment of END patients, it has certain promotion significance. They extracted and analyzed from a large national stroke registry [3]. Zhang et al. have studied the incidence, composition, and outcomes of END after acute ischemic stroke by IVrt-PA and EVT and identified risk factors for END [4]. Although the study identified risk factors for END, there has been insufficient research on large artery occlusion as a significant predictor of END or poor prognosis in patients with mild ischemic stroke. Based on this, Kim proposed that intravenous thrombolysis of recombinant tissue plus plasminogen activator within 4.5 hours is an effective treatment for acute ischemic stroke. However, the risk-benefit ratio of this treatment in patients with mild stroke remains unclear [5]. Based on this, the Chi and Chan study compared safety and short-term treatment outcomes in patients who met criteria and those who did not [6]. Although they have studied safety and efficacy in different patients, there are insufficient studies on the risk of mild stroke symptoms and END in patients with acute large vessel occlusion (LVO). Therefore, Gwak et al. identified the best imaging variables for predicting END in this population. However, the improvement of symptoms after intravenous thrombolysis with recombinant tissue plasminogen activator (rt-PA) has not been studied [7]. On this basis, Bouchal et al. explained the 58-year-old case of recurrent ischemic stroke who received intravenous thrombolysis every 10 days and was significantly improved. They suggested that the carotid septum was the cause of this recurrent stroke [8]. Although the studies have promoted the development of research related to the prediction of END after intravenous thrombolysis, the meta-analysis research on the prediction of END after intravenous thrombolysis is still insufficient.

3. Methods for Predicting END after Intravenous Thrombolysis

3.1. Intravenous Thrombolytic Therapy. Intravenous thrombolysis refers to the injection of thrombolytic drugs into the body through a peripheral vein or a central vein through an intravenous infusion. These thrombolytic drugs act on the thrombus to produce a thrombolytic effect. Intravenous thrombolysis is often divided into peripheral thrombolysis and intubation thrombolysis, as follows.

Peripheral thrombolysis is a superficial intravenous infusion thrombolysis device, and there are commonly used thrombolysis agents such as urokinase and rt-PA. Through blood circulation, it circulates to the thrombus site and acts on the thrombus to produce a thrombolytic effect. Intubation thrombolysis is direct contact thrombolysis, requiring interventional therapy. In addition to the hole at the head end, the catheter with multiple side holes has many small side holes on the tube, and the catheter is inserted into the thrombus to be in direct contact with it. Thrombolytics are injected through the distal end of the catheter, which is typically pumped into a vein. It sprays thrombolytic drugs onto the thrombus through such side holes, resulting in direct thrombolysis [9]. The thrombolytic efficiency of direct contact thrombolysis is higher, and the effect of thrombolysis is better. It is more efficient and effective than peripheral intravenous thrombolysis [10].

As shown in Figure 1, the core part of the brain tissue undergoes ischemia-hypoxic necrosis due to various reasons. The surrounding brain tissue cannot maintain its original physiological function due to insufficient cerebral blood perfusion, but its activity has not been lost. This portion of marginal tissue is called the ischemic penumbra. The original concept of the ischemic penumbra is the termination of the electrical activity of cells within ischemic tissue, but the preservation of transmembrane ionic potential. The term was later used to describe the peri-infarct area of potentially reversible damage. If the area fails to restore blood flow within the time window or take other

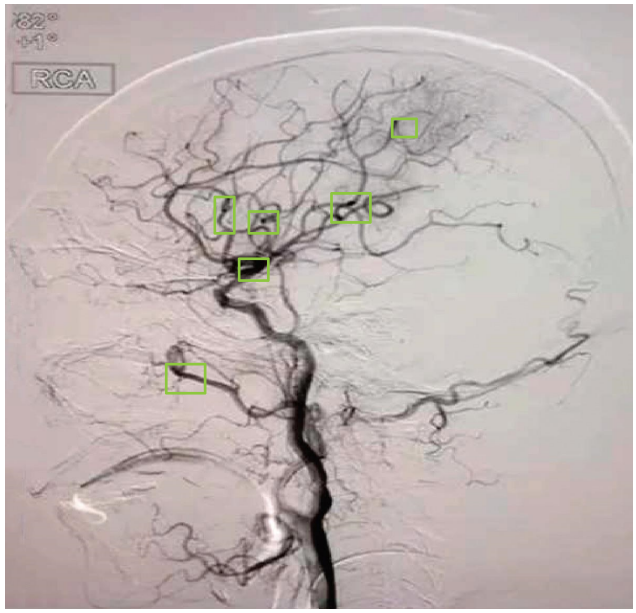

Figure 1: Cerebrovascular blockage.

measures to prevent the cell death process, it can develop into an infarction. The latter concept is closer to clinical practice [11]. The ischemic penumbra is the brain tissue surrounding necrotic tissue following cerebral ischemia. Its blood flow rate is lower than that required to maintain normal brain function, but higher than the blood flow rate that causes changes in brain morphology [12]. Within the time frame of reperfusion, it is possible to develop infarcted areas. Therefore, the main purpose of treating acute cerebral infarction is to preserve the brain tissue of the ischemic penumbra, restore its function as soon as possible, and avoid long-term ischemic death. Due to insufficient energy supply, cells in the ischemic penumbra cannot perform their original normal physiological functions and can only maintain their own shape without being destroyed. It is generally believed that the ischemic penumbra appears about 1 hour after cerebral ischemia and can be maintained for about 6–24 hours. A small percentage of patients persisted for days afterward. Therefore, the medical community proposed the concept of "time frame." The so-called time frame refers to the reopening of originally occluded cerebral arteries or the formation of new collateral blood circulation through effective treatment. Originally ischemic brain tissue restores blood irrigation during a period of restoring normal neurological function [13]. This effective treatment is called intravenous thrombolysis.

As shown in Figure 2, rt-PA is a thrombolytic drug. Its main component is glycoprotein, containing 526 amino acids. rt-PA can bind to fibrin through its lysine residue and activate the conversion of fibrin-bound plasminogen to plasmin. This effect was significantly enhanced compared to that of rt-PA to activate circulating plasminogen. rt-PA is also the main thrombolytic drug currently used. However, in the early stage of acute ischemic stroke, since various risk factors are not paid attention to, the risk factors are not effectively managed. So, there is a risk of recurrence. Even

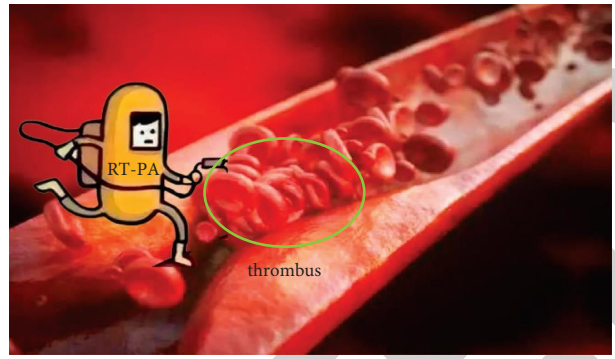

Figure 2: Schematic diagram of RT-PA drug intravenous thrombolysis.

after aggressive thrombolytic therapy in the early stage, 5%–40% of patients with acute cerebral infarction will experience aggravation of symptoms, resulting in poor prognosis and even death [14].

3.2. Application of Machine Learning Model in Prediction after Intravenous Thrombolysis. Machine learning is a specific form of artificial intelligence that uses algorithms to analyze and learn from data to make predictions and decisions about actual events. The classic algorithms of machine learning include logistic regression, decision tree, support vector machine, artificial neural network, and convolutional neural network [15]. Machine learning is a multidisciplinary interdisciplinary major, covering knowledge of probability theory, statistics, approximate theory, and complex algorithms. It uses computers as tools and aims to simulate the way humans learn in real time. It divides the existing content into knowledge structure to effectively improve learning efficiency [16]. At present, the research on the prediction of the prognosis of intravenous thrombolysis by machine learning models is still insufficient, and the existing research scale is small and lacks external validation evidence. Therefore, there is still a certain distance from clinical application. However, with the advent of the era of big data, machine learning technology will eventually become an important tool for assisting clinical decision-making and predicting clinical prognosis.

3.3. Application of Neural Network to Prediction of END after Intravenous Thrombolysis

3.3.1. Neuron Model. Neurons are the simplest basic components that make up a neural network. In biological neural networks, nerves are connected to neurons. When neurons are stimulated, chemicals are sent to change electrical potential. Each neuron has a threshold, and if the potential exceeds this threshold, the neuron is activated by MP [17]. A neural network is a simple network that abstracts this process. This is the simplest neural network structure, as shown in Figure 3.

In Figure 3, x_n is the input value, Y is the weight, and y is the output value.

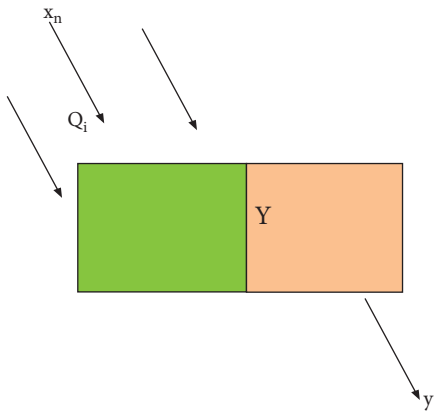

Figure 3: Schematic diagram of MP neural network structure.

The commonly used activation function is the sigmoid function—the sigmoid function is a common function in biology, which is also called the sigmoid growth curve; in information science, the sigmoid function is often used as the activation function of neural networks due to its properties such as single increase and inverse function single increase; it maps variables between 0 and 1—which is continuous and smooth, and its expression is as follows:

$$f(x) = \frac{1}{(1 + e^{-z})}. \tag{1}$$

BP neural network is nested from multiple such structures. The sigmoid function is shown in Figure 4.

3.3.2. Multilayer Neural Network Structure. A perceptron is a two-layer neural network that does not contain hidden layers, only an input layer and an output layer [18]. Figure 5 is a perceptron with two input variables. When the input sample is determined, the final model can be obtained by learning the weight $Q_i\,(i = 1, 2, \ldots, n)$ and the threshold Y. Threshold Y can be regarded as another fixed input of -1; that is, the process of learning Y becomes the same as the process of learning weights. The perceptron also has a simple learning process. If the sample (z, x) is given and the output value of the perceptron is $\hat{b}$, the perceptron will make the following adjustments in the next training:

$$\Delta Q_i + Q_i \longrightarrow Q_i, \tag{2}$$

$$\Delta Q_i = \partial(b - \hat{b})z_i, \tag{3}$$

where $\partial \in (0, 1)$ is the learning rate. If the prediction is correct, b and $\hat{b}$ are equal, that is, the weights will not be updated, and the model is stable. Otherwise, the weights are continuously updated [19]. The perceptron can easily implement the linear model, but it cannot be implemented for the nonlinear model, because the perceptron is only processed by one layer of activation function [20]. The perceptron structure is shown in Figure 5.

To solve nonlinear problems, a neural network with multiple layers of neurons is required. That is, a hidden layer needs to be added between the input layer and the output

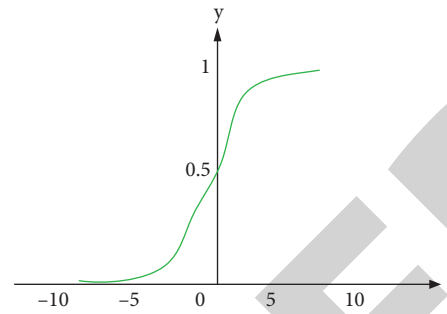

Figure 4: Sigmoid function image.

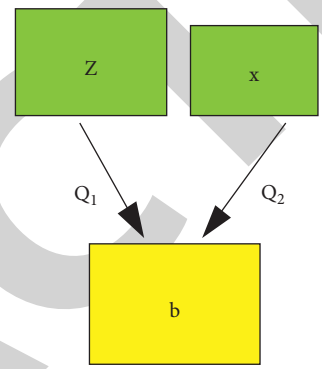

Figure 5: Perceptron block diagram.

layer [21]. A single hidden layer neural network has a hidden layer between the input and output; that is, the output of the input layer is the input of the hidden layer. The product of the output of the hidden layer and the corresponding weight is the input of the output layer, and the output of the output layer is the final output [22]. In this network structure, each neuron is connected to all the neurons in the next layer, and the neurons in the same layer are not connected to each other and cannot be connected to each other. The network structure formed by this connection method is called a fully connected structure, which is also usually called a feed-forward neural network [23], as shown in Figure 6.

The neural network structure shown in Figure 6 includes an output layer, an input layer, and a hidden layer. The input layer is not processed by the activation function and only plays the role of transmitting the input signal, so it is usually called a double-layer neural network [24]. In computational networks, the activation function of a node defines the output of that node with respect to a specific input or set of inputs. A standard computer chip circuit can be thought of as an activation function of a digital circuit that turns the output on or off depending on the input. In artificial neural networks, this function is also called the transfer function. The learning process of the neural network is the same as that of the perceptron, that is, updating its weights and thresholds to continuously reduce the error between the predicted result and the true value.

3.3.3. Error Backpropagation Neural Network. The error backpropagation algorithm is called the BP algorithm, and the structure formed using it in the training of the multilayer neural network is the BP neural network. The so-called BP

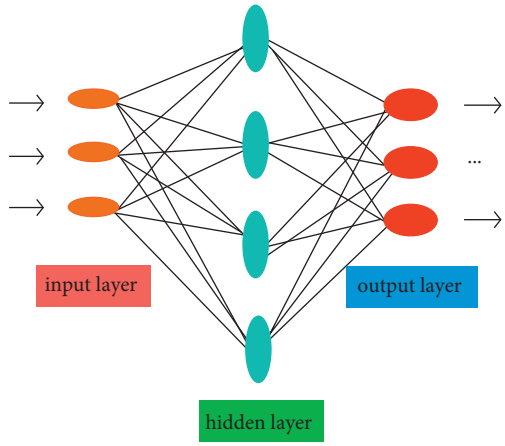

Figure 6: Structure diagram of feedforward neural network.

neural network is a structure in which the BP algorithm is applied to a multilayer feedforward neural network. The mathematical principle and training process of the BP neural network will be described in detail below.

Assuming that the training set is $J = \{(a, b_1), (a_2, b_2), \ldots, (a_n, b_n)\}$, $a_i \in R^d, b_i \in R^l$, the input samples are d-dimensional space and the outputsamples are l-dimensional space. A neural network structure including d input neurons and l output neurons is given, the corresponding neuron of the mth output layer is denoted by ∂_m, and the neuron threshold of the kth hidden layer is denoted by ∞_k.

It is assumed here that there is a training instance (a_n, b_n), and $\hat{u}^n = (\hat{u}_1^n, \hat{u}_2^n, \ldots, \hat{u}_l^n)$ is used to represent the output value of the neural network, so the output is shown in the following formula:

$$\hat{u}_m^n = \text{sigmoid}(\partial_m - \infty_m). \tag{4}$$

The mean square error w_n is used to represent the error of the neural network; that is, the error w_n is expressed as the following formula:

$$w_n = \frac{1}{2\sum_{m=1}^{l}(\hat{u}_m^n - u_m^n)^2}. \tag{5}$$

The learning process of the BP neural network is carried out round by round, and each round of learning will be accompanied by the update of the weights. The update method is similar to that of the perceptron, as shown in the following formulas:

$$v \longrightarrow v + \Delta v, \tag{6}$$

$$Q \longrightarrow Q + \Delta Q. \tag{7}$$

The learning process of the BP neural network is based on the gradient descent method, and the parameters are adjusted according to the negative gradient direction of the parameters in each round of training. Gradient descent is an iterative method that can be used to solve least squares problems (linear and nonlinear). For the error w_n, if the learning rate is $\partial \in (0, 1)$, it is shown in the following formula:

$$\Delta Q_{mn} = -\sigma \frac{\varepsilon_{w_n}}{\varepsilon_{Q_{mn}}}, \tag{8}$$

$\hat{u}_n^m$ is obtained by Q_{mn} through the input β_j of the output layer and then through the activation function. w_n is affected by the output. The partial derivative of w_n for Q_{mn} is equivalent to the derivative of the composite function, as shown in the following formulas:

$$\frac{\Psi_{w_n}}{\Psi_{Q_{mn}}} = \frac{\Psi_{w_n}}{\Psi_{\hat{y}_m^n}} * \frac{\Psi_{\hat{u}_n^m}}{\Psi \infty_m} * \frac{\Psi \infty_m}{\Psi_{Q_{mn}}}, \tag{9}$$

$$\frac{\Psi \partial_m}{\Psi Q_{nm}} = x_n. \tag{10}$$

The sigmoid function is derived as shown in the following formula:

$$f'(x) = f(x)[1 - f(x)]. \tag{11}$$

According to (4) and (5), the following formulas can be obtained:

$$b_m = \frac{\Psi w_n}{\Psi \hat{u}_m^n} * \frac{\Psi \hat{u}_m^n}{\Psi \partial_m}, \tag{12}$$

$$b_m = \hat{u}_m^n \left(1 - \hat{u}_m^n\right)\left(u_m^n - \hat{u}_m^n\right). \tag{13}$$

Among them, ∂_m is the input of the mth neuron; its expression is shown in the following formula:

$$\partial_m = \sum_{i=1}^{q} Q_{nm} x_n. \tag{14}$$

By arranging the above formula, the update formula of Q_{mn} can be obtained as follows:

$$\Delta Q_{nm} = \sigma b_m x_n. \tag{15}$$

The same can be obtained as follows:

$$\Delta \infty_m = -\sigma b_m, \tag{16}$$

$$\Delta v_{in} = \sigma w_n x_i, \tag{17}$$

$$\Delta \lambda_n = -\sigma w_n. \tag{18}$$

Among them, λ_n is the threshold of the hidden layer; w_n is expressed as follows:

$$w_n = \frac{\Psi w_n}{\Psi x_n} * \frac{\Psi x_n}{\Psi \mu_n} = x_n(1 - x_n)\sum_{m=1}^{l} Q_{nm} b_m. \tag{19}$$

μ_n is the input of the nth output neuron, as shown in the following formula:

$$\mu_n = \sum_{i=1}^{d} v \text{in} x_i. \tag{20}$$

The learning rate is a parameter used to control the update step size in each round of learning. Its value cannot be too large or too small, because being too large will make it easy to cross the optimal solution when learning the weight, resulting in the phenomenon of oscillation, as shown in Figure 7. On the other hand, being too small will make the convergence rate too slow and the training time too long. Therefore, the setting of the learning rate should be adapted to the trained model.

As shown in Figure 7, when learning the weights, because the weights are too large to stay at the optimal solution, they show repeated horizontal jumps on both sides of the optimal solution, resulting in oscillations.

3.4. Meta-method for Predicting Neurological Deterioration after Intravenous Thrombolysis

3.4.1. Literature Search Strategy. This article used a computerized system search for studies on the role of early prediction of neurological deterioration after intravenous thrombolysis until January 1, 2022. The language of the literature is limited to Chinese and English. References of the included articles were screened to supplement the search results.

3.4.2. Search Terms. This article searches using the following keywords in combination with their synonyms: "intravenous thrombolysis," "END," "predicted risk," "risk factors," etc.

3.4.3. Literature Screening. We read the titles and abstracts of the retrieved articles, read the full text of studies that may meet the selection criteria, and cross-checked the screening results of the articles. Inconsistencies were resolved through group discussions.

3.4.4. Inclusion Criteria. Inclusion criteria are shown in Table 1.

3.4.5. Exclusion Criteria. Exclusion criteria are shown in Table 2.

3.4.6. Final Events

① Hemorrhagic transformation (HT) occurs within 24 hours after intravenous thrombolysis, which includes symptomatic intracerebral hemorrhage and parenchymal hematoma.

② The prognosis of neurological function was poor 3 months after intravenous thrombolysis, which was defined as modified Rankin scale (mRS) ≥3 points. The mRS scoring scale is shown in Table 3.

③ Mortality occurred 3 months after intravenous thrombolysis.

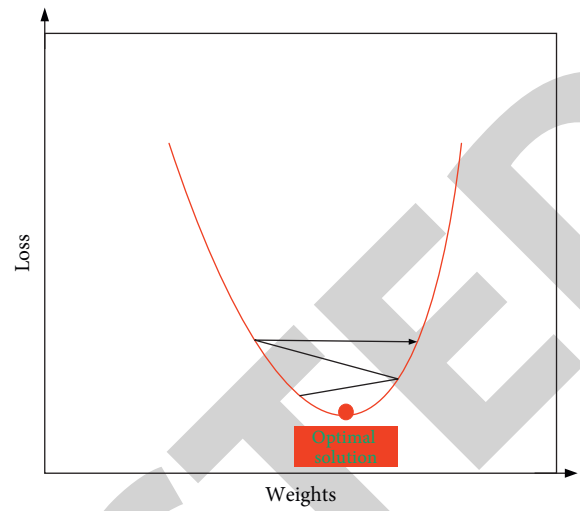

Figure 7: Diagram of the oscillation process.

4. Meta-experiment and Predictive Effect of END after Intravenous Thrombolysis

4.1. Literature Screening Results on Predictive Role of END after Intravenous Thrombolysis. The results of the screening revealed that a total of 340 studies were retrieved, 228 duplicates were removed, and 74 irrelevant studies were removed after reading the titles and abstracts of the articles. The remaining 48 articles have been read in full, and 5 abstracts, 5 reviews, and 17 irrelevant articles have been excluded. Finally, a total of 11 studies were included in this meta-analysis. The flowchart of literature search and screening is shown in Figure 8:

The algorithm shown in Figure 8 included 11 studies with a total of 3578 patients. All 11 studies used standardized intravenous thrombolysis in patients, and the basic characteristics of the included studies are shown in Figure 9.

As shown in Figure 9, a total of 3578 cases and patients were included in this study, of which the highest number in a single study was 653 and the lowest was 86. The sample blood collection time in the study was mainly about 24 hours. Through the analysis of different samples included in the study, it was found that blood collection of samples in different time periods after intravenous thrombolysis had an impact on the different results after intravenous thrombolysis. It led to the occurrence of END in different time periods through statistical analysis, as shown in Figure 10.

It can be seen from Figure 10 that the occurrence probability of END between 0 and 12 hours in the blood collection period is low, between 0 and 0.3. The occurrence of END in the blood collection period of 12–24 hours is relatively unstable, and it can reach about 0.5.

4.2. Meta-results on Predictive Effect of END after Intravenous Thrombolysis. In this paper, a literature search was conducted using keywords such as "intravenous thrombolysis," "END," "prediction of risk," and "risk factors." This paper conducts a meta-analysis of the searched papers. By analyzing the pathogenesis of END after intravenous

Table 1: Literature inclusion criteria.

Serial number	Standard
1	Study subjects were patients with AIS receiving intravenous thrombolysis
2	NLR was measured before or within 24 hours of intravenous thrombolysis
3	At least one of the following outcomes was reported: HT, poor neurological outcome (mRS ≥3), and death rate
4	The type of study design was cohort study or case-control study

Table 2: Literature exclusion criteria.

Serial number	Standard
1	Animal research
2	Studies with duplicate publications or overlapping data
3	Case reports, meeting abstracts, letters, and comments
4	Studies not available in full text

Table 3: mRS rating scale.

Project	Grading
0	Completely asymptomatic
1	Despite symptoms, there is no apparent functional impairment and is able to perform all daily duties and life activities
2	Mild disability, unable to perform all activities before the illness, but able to take care of own things without assistance
3	Moderately disabled, some assistance required, but no assistance needed to walk
4	Severely disabled, unable to walk independently, unable to meet own needs without the help of others
5	Severely disabled, bedridden, incontinent, requiring ongoing care and attention

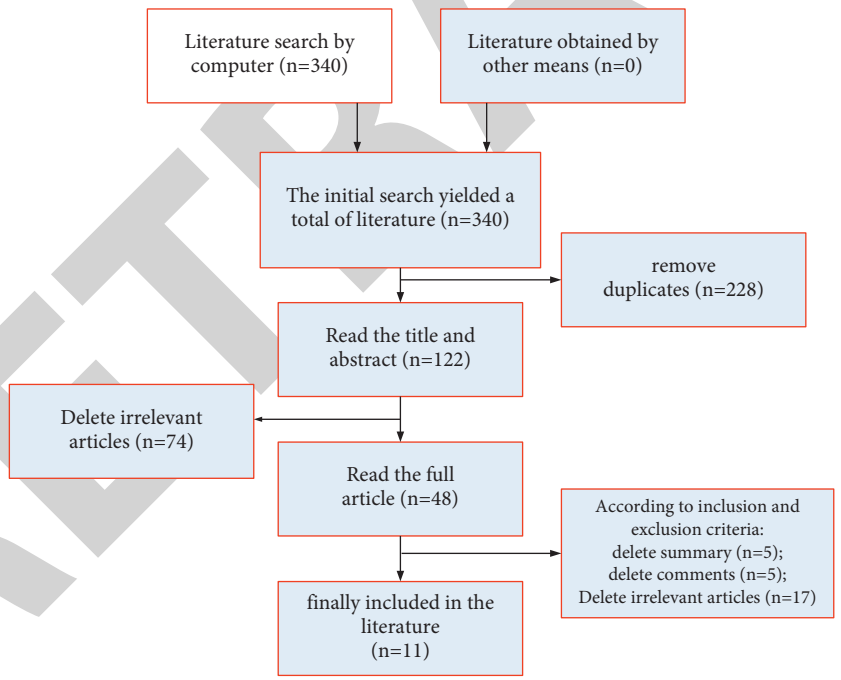

Figure 8: Flowchart of literature search and screening.

thrombolysis, this article identifies which factors have a positive effect on the prevention of END. In this paper, the pathogenesis of END was obtained by statistical analysis of the cases included in the study, as shown in Figure 11.

As shown in Figure 11, there are four main etiological mechanisms for END after venous thrombolysis: I is ischemic development of cerebral infarction, H is hemorrhagic trait transition, B is cerebral edema, and C is cardiovascular event. It can be seen from the analysis that cerebral edema and ischemic development of cerebral infarction are the main pathogenic mechanisms leading to END, accounting for as high as 34% and 33% of the study cases. On the contrary, the proportion of cardiovascular events is only 5%, which is not the main pathogenesis compared with the former two.

END in acute ischemic stroke patients is closely related to poor prognosis. END prolongs hospital stay in patients with cerebral infarction. It also leads to a significant increase

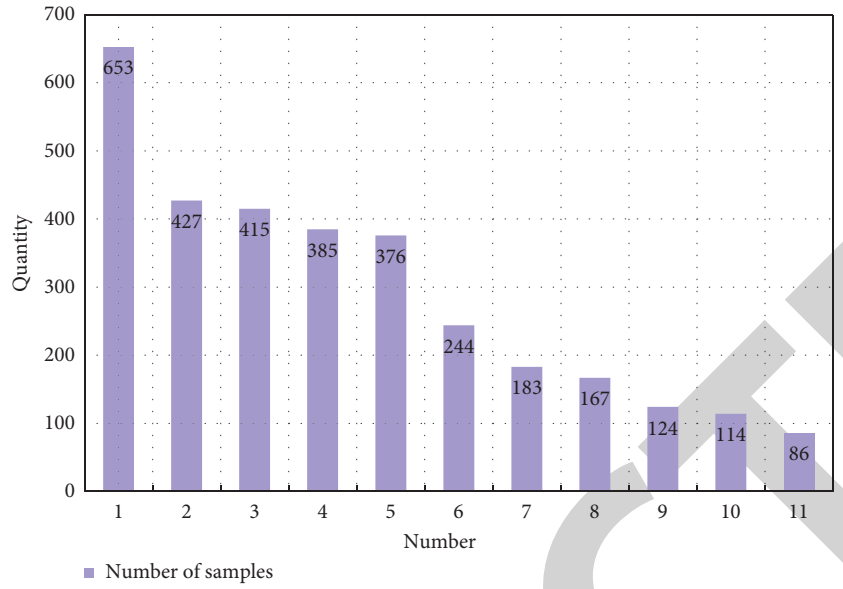

(a)

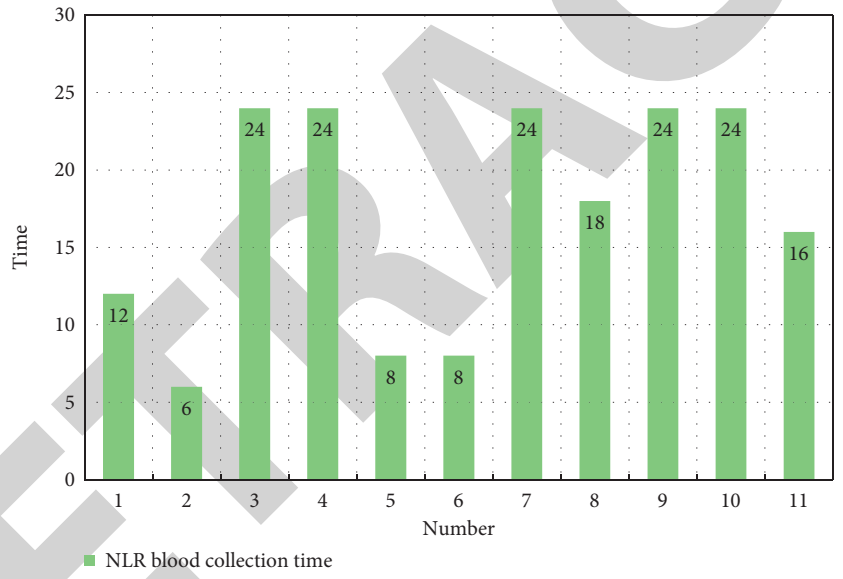

(b)

Figure 9: Basic characteristics of included studies. (a) The sample size of the included studies. (b) Study sample blood collection time.

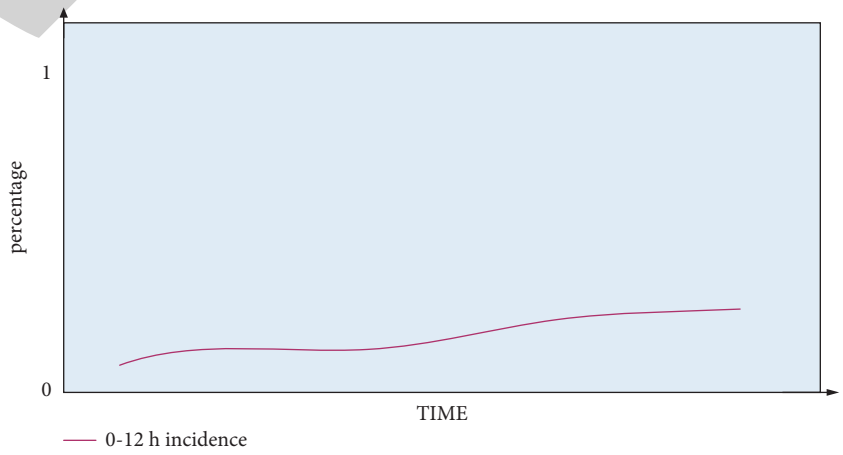

(a)

Figure 10: Continued.

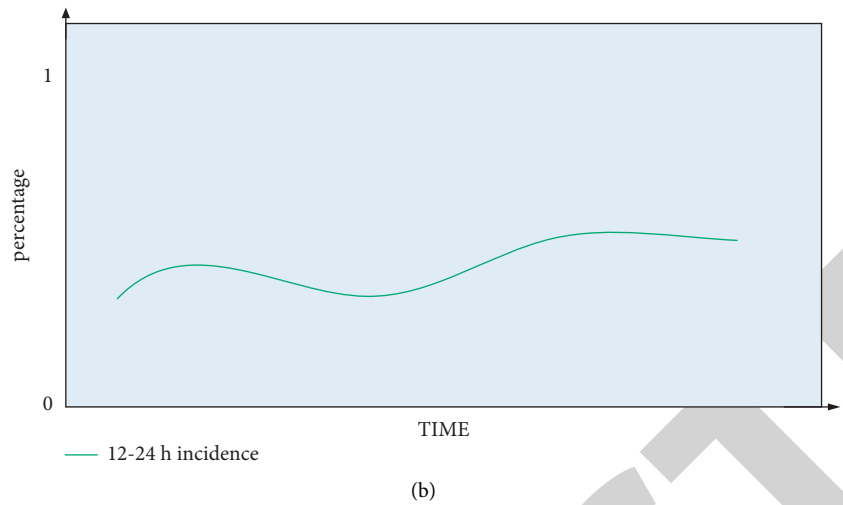

(b)

Figure 10: The occurrence of END in different blood collection time periods. (a) The occurrence of END in the blood collection period of 0–12 hours. (b) The occurrence of END in the blood collection period of 12–24 hours.

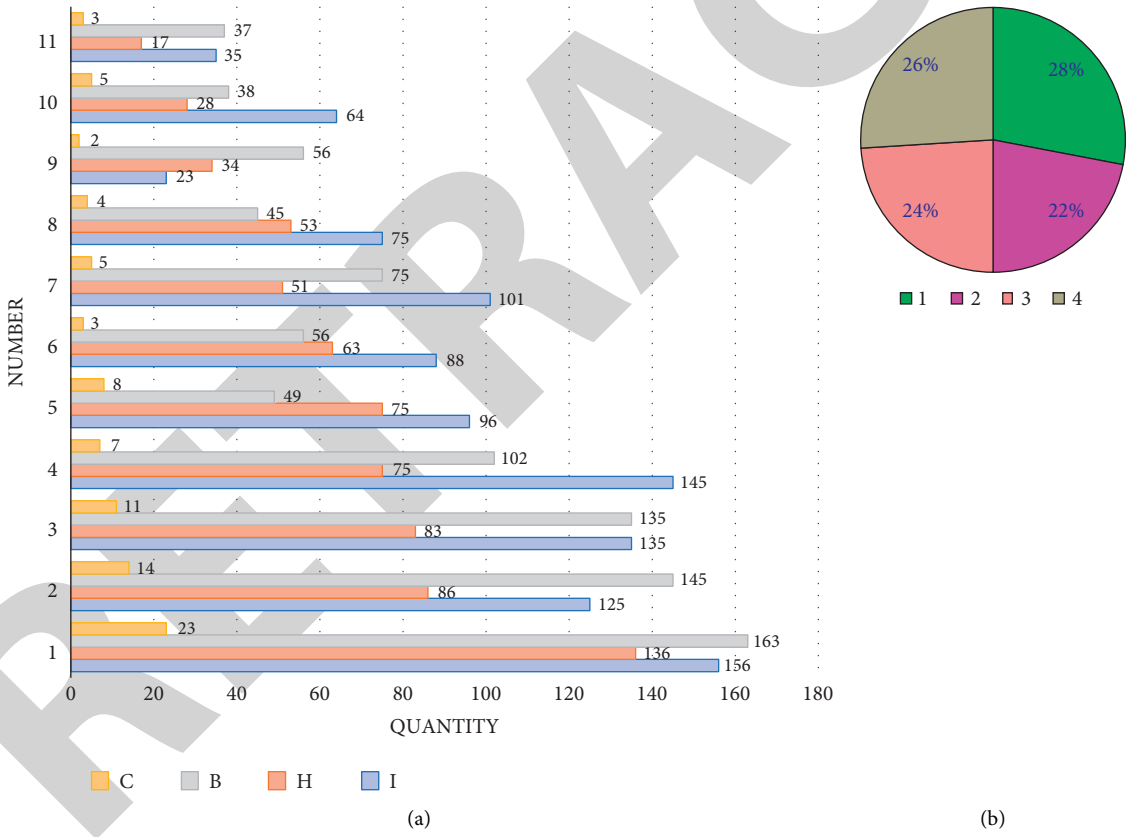

(a) (b)

Figure 11: Analysis of the pathogenesis of END in the cases included in the study. (a) Statistical map of the pathogenesis of END in the included cases. (b) Probability of the pathogenesis of END in the included cases.

in in-hospital mortality and disability in patients with cerebral infarction. This is the main cause of increased infarction and mortality. The predictive effect of intravenous thrombolysis on END is shown in Figure 12.

As shown in Figure 12, the predictable risk factors for neurological deterioration in the early stage of intravenous thrombolysis were hypertension and blood pressure variability (z), hyperglycemia (x), arterial stenosis (c), degree of neurological deficit at admission (v), inflammation (b), elevated body temperature (n), and other hematological indicators (m). These indicators are used to predict the END after intravenous thrombolysis, and the predicted curve obtained in this paper is compared with the actual incidence. The results were basically similar to the actual incidence

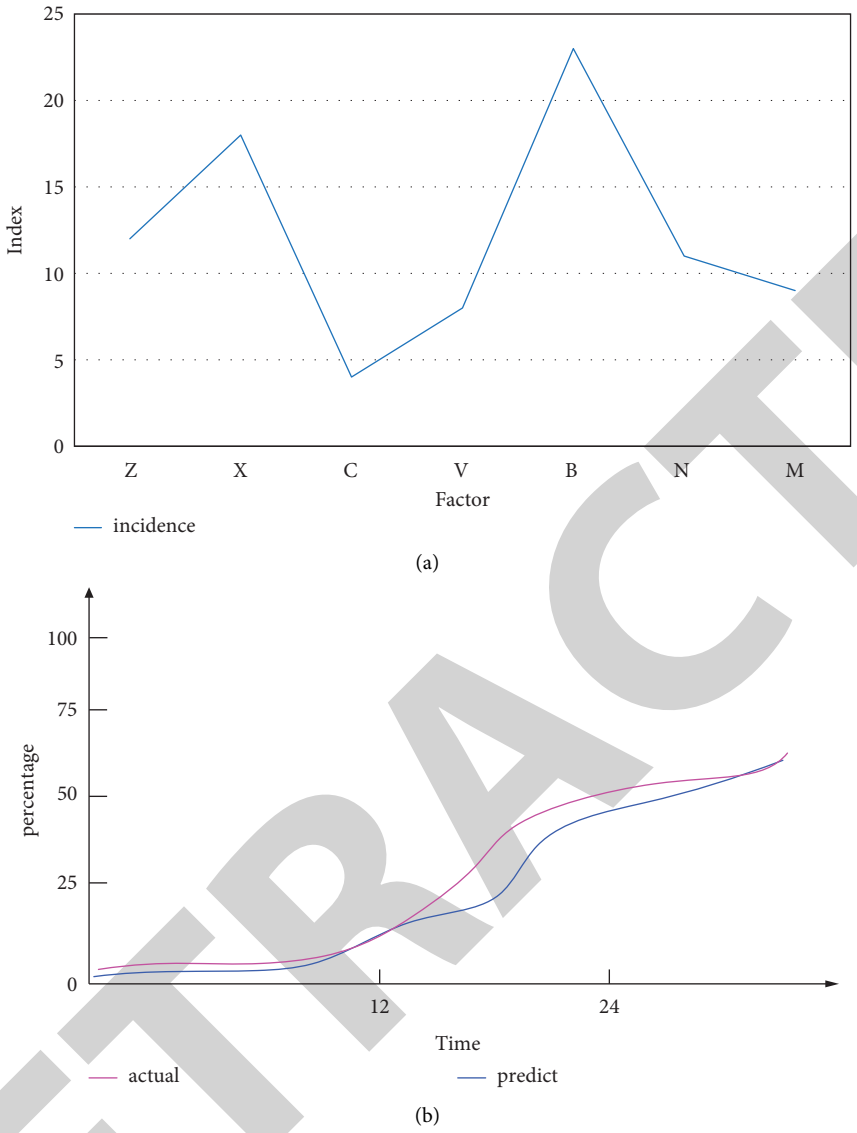

Figure 12: Analysis of the predictive effect of END after intravenous thrombolysis. (a) Distribution of predictable risk factors for END in intravenous thrombolysis. (b) Predictive effect and actual comparison of END after intravenous thrombolysis.

curve. Among them, inflammation (*b*) was an important predictable risk factor in the prediction of END after intravenous thrombolysis, accounting for 23%. The ratio of the predicted curve to the actual curve shows that the difference between the two is less than 5%. It shows that its accuracy is sufficient to effectively predict the deterioration of neurological function in the early stage of intravenous thrombolysis.

Through comprehensive experimental tests, it can be seen that the prediction of early neurological function deterioration after intravenous thrombolysis in this paper can effectively help make a preliminary judgment on the possible late neurological function deterioration. Although there is an error between the predicted curve and the actual curve, the difference between the two is between 1 and 5%, which can basically effectively predict the occurrence of END. This prediction of END after intravenous thrombolysis is very important for the prevention and treatment of END after intravenous thrombolysis. Of course, the analysis results of this experiment are different and not completely reliable, because there are many unstable factors.

5. Conclusion

With the continuous improvement of material life, people's demand for life and health is also increasing. The development of healthcare is inseparable from the development of science and technology. The application of various technical advantages in the medical field has enabled some diseases to be effectively prevented and treated. In this paper, a general introduction to intravenous thrombolytic therapy and early prediction of neurological deterioration is made, so that people can understand the related principles and functions of the two. This paper then uses the relevant principle formulas to analyze their functional roles. Finally, it is found that the combination of the two can be of great significance.

Hindawi
Emergency Medicine International
Volume 2023, Article ID 9845275, 1 page
https://doi.org/10.1155/2023/9845275

Retraction

Retracted: Electron Microscope Observation of Acupuncture and Nerve Repair in the Treatment of Peripheral Facial Paralysis

Emergency Medicine International

Received 8 August 2023; Accepted 8 August 2023; Published 9 August 2023

This article has been retracted by Hindawi following an investigation undertaken by the publisher [1]. This investigation has uncovered evidence of one or more of the following indicators of systematic manipulation of the publication process:

(1) Discrepancies in scope
(2) Discrepancies in the description of the research reported
(3) Discrepancies between the availability of data and the research described
(4) Inappropriate citations
(5) Incoherent, meaningless and/or irrelevant content included in the article
(6) Peer-review manipulation

The presence of these indicators undermines our confidence in the integrity of the article's content and we cannot, therefore, vouch for its reliability. Please note that this notice is intended solely to alert readers that the content of this article is unreliable. We have not investigated whether authors were aware of or involved in the systematic manipulation of the publication process.

In addition, our investigation has also shown that one or more of the following human-subject reporting requirements has not been met in this article: ethical approval by an Institutional Review Board (IRB) committee or equivalent, patient/participant consent to participate, and/or agreement to publish patient/participant details (where relevant).

Wiley and Hindawi regrets that the usual quality checks did not identify these issues before publication and have since put additional measures in place to safeguard research integrity.

We wish to credit our own Research Integrity and Research Publishing teams and anonymous and named external researchers and research integrity experts for contributing to this investigation.

The corresponding author, as the representative of all authors, has been given the opportunity to register their agreement or disagreement to this retraction. We have kept a record of any response received.

References

[1] Z. Shan, "Electron Microscope Observation of Acupuncture and Nerve Repair in the Treatment of Peripheral Facial Paralysis," *Emergency Medicine International*, vol. 2022, Article ID 5432223, 10 pages, 2022.

Hindawi
Emergency Medicine International
Volume 2022, Article ID 5432223, 10 pages
https://doi.org/10.1155/2022/5432223

Research Article

Electron Microscope Observation of Acupuncture and Nerve Repair in the Treatment of Peripheral Facial Paralysis

Zhenggen Shan

Sichuan Vocational College of Health and Rehabilitation, Zigong, Sichuan, China

Correspondence should be addressed to Zhenggen Shan; 18409224@masu.edu.cn

Received 29 April 2022; Revised 31 May 2022; Accepted 22 June 2022; Published 13 July 2022

Academic Editor: Hang Chen

The repair of peripheral facial paralysis is a long-term problem in neurosurgery, and nerve repair is often needed. Due to the high differentiation of nerve tissue and the slow regeneration of peripheral nerve fibers, the repair effect after peripheral nerve injury is not ideal. In recent years, studies have found that the inflammatory response after peripheral nerve injury also has an important impact on the repair of peripheral nerve defects. This study depends on the utilization of traditional needle therapy in the treatment of fringe facial loss of motion, and the clinical adequacy of needle therapy in addition to nerve fix in the intense period of fringe facial loss of motion was seen with an electron magnifying lens. Endeavor to give significant exploration results to the clinical treatment of fringe facial loss of motion gives a straightforward, simple, protected, and successful new treatment innovation for the clinical treatment of the infection and enriches the treatment plan for peripheral facial paralysis. Transmission electron microscopy observations showed that 21 days after the artificial nerve was repaired, the nerve injury showed different degrees of recovery, and the myelin sheath was forming and gradually wrapping the new axons, which was similar to the catheter group (NC) and hydrogel group (HC). In contrast, the myelin layer of the fibroblast group (FHC) is more obvious, and the repair effect is better. In the maintenance of fringe nerve surrenders, irritation is an unavoidable interaction, and moderate needle therapy is useful to advance the maintenance of fringe nerve abandons. Talking about the law of nerve fix reaction in fringe nerve imperfection fix is helpful to the examination of fringe nerve deformity fix. Tests have shown that utilizing needle therapy and moxibustion joined with nerve fixes has accomplished great outcomes in the treatment of fringe facial loss of motion, and the patient's recuperation rate has expanded by over 30%.

1. Introduction

Fringe facial nerve paralysis (PFP) is additionally called Bell's paralysis, idiopathic facial nerve paralysis, and facial neuritis. It is the reason for fringe facial nerve paralysis, its goal is not clear, and there could be no different side effects and qualities. Modern medicine speculates that the disease may be caused by perifacial paralysis caused by nonspecific inflammation of the facial nerve in the trunk organ. It was first described by Charles Bell in 1821. To commemorate Bell, the descendant doctor William The Gowers was named after Bell. Peripheral facial nerve palsy usually comes on suddenly. Before it starts, the patient may have wind, cold, or fatigue, and there may be pain or fever from the back of the ear to the skin behind the ear bones and cheeks. The affected side may be paralyzed, the nasolabial fold may flatten, and the corners of the mouth may tilt. It is completely different from the healthy side. The wrinkles on the forehead disappear, the eyes are swollen, and the face is dull and numb. Peripheral facial paralysis is called facial neuritis, which is caused by the acute inflammation and edema of the stylomastoid foramen of unknown origin, but 10% to 25% of the patients cannot fully recover due to mistreatment or serious illness and even suffer from severe disease—leaving serious sequelae, causing great harm to the patient's body and mind. Therefore, how to cure facial paralysis at the best time is imminent.

In modern medicine, the cause of peripheral facial nerve palsy is not yet fully understood. Hormone therapy is the main treatment method, but the effect is not very

satisfactory. Sun summarized the academic thoughts and clinical experience of Professor Sun Shentian's acupuncture treatment of peripheral facial nerve palsy. According to the different stages of facial paralysis, Professor Sun's treatment plan has its own focus. In the acute phase, Professor Sun emphasized the importance of standardized western medicine treatment and made recommendations for early acupuncture treatment. Treatment is mainly focused on dispelling wind and cold, promoting blood circulation, and dredging collaterals. In the rehabilitation phase, Professor Sun emphasized the "needle removal method" and repeated transcranial acupuncture according to the functional direction of the cerebral cortex. In the sequelae stage, Professor Sun emphasized the value of regulating thoughts. During the treatment, Professor Sun paid great attention to flexible acupuncture point selection, repeated transcranial acupuncture, "needle removal" method, acupoint pressing, and giant needle method, as well as the combined use of electric acupuncture and directional injection. However, the treatment method is too slow to suppress the condition in time [1]. Lv et al. investigated the impact of back rub on quality articulation in rodents with sciatic nerve injury (SNI). They explained the maintenance component of back rub to advance the recuperation of fringe nerve injury. In the joke activity bunch, the right sciatic nerve was uncovered without a brace. The SNI model was laid out on the right leg with sciatic forceps and afterward arbitrarily isolated into SNI gathering and back rub bunch. Seven days in the wake of demonstrating, the back rub group utilized the "Back rub Massage Manipulation Simulator" for treatment consistently. The simulator was used to stimulate the silver gate (BL37) every day. The stimulation force was 4N and the stimulation frequency was every minute. Use each method and each acupuncture point for 1 minute, for a total of 9 minutes. However, this method has sequelae to the patient and needs to be treated according to the situation [2]. Lovaglio AC accepts that fringe nerve and brachial plexus injury typically prompts extreme harm to the impacted appendage. The rate of neuropathic torment is exceptionally high, particularly on account of cervical root separation, as high as 95% of cases. Neuropathic torment is brought about by harm to the somatosensory framework, and its ongoing advancement process relies upon the harm that influences the encompassing and focal sensory system. The treatment of these agonies is extremely convoluted and should be finished by a multidisciplinary group. From the first-line pharmacological treatment (Such as tricyclic antidepressants and calcium channel ligands) start with physical and word-related treatment, transcutaneous electrical feeling, and mental help. For patients who experience issues getting introductory treatment, a few neurosurgery choices are accessible, including nerve decompression or reproduction and removal/molding systems. Yet, this will defer the ideal time of patient treatment, and the condition might change [3].

This article depends on the utilization of needle therapy and treatment of fringe facial loss of motion and the utilization of an electron magnifying instrument to screen the clinical impacts of needle therapy and nerve fix in the intense period of fringe facial loss of motion [4]. Aiming at the research on limbic facial nerve palsy, and comparing many treatment methods, find out the advantages and disadvantages of different treatment methods, accumulate experience, and make more contributions to traditional Chinese medicine. It gives significant exploration results to the treatment of intense fringe facial loss of motion and gives a solid premise to bed rest. After the beginning of fringe facial nerve paralysis, the facial nerve is compacted in the intense stage, and the facial nerve tube is ischemia and hypoxia, bringing about degeneration, edema, and even demyelination. The more pressure on the facial nerve, the more degeneration, and it is difficult to recover. The degree of facial nerve injury determines the severity and prognosis of facial paralysis [5, 6]. Early consultation and timely intervention are protective factors in restoring facial nerve palsy. Therefore, treatment in the acute phase is very important. The research on the repair of peripheral facial paralysis is a convenient reference for future medical development.

2. Treatment of Peripheral Facial Paralysis

Modern medicine believes that the treatment of peripheral facial paralysis through the functional recovery of the facial nerve is the most scientific and simple method; since ancient research, TCM has formed a sound TCM theoretical system in the treatment of "slanting eyes and mouth." The etiology and pathogenesis of this disease have been perfected under the continuous research and exploration of senior Chinese medicine practitioners.

2.1. Diagnostic Criteria of Chinese Medicine. Allude to the New Century (Second Edition) course book "Needle therapy and Moxibustion Therapy" (altered by Wang Qicai, China Press of Traditional Chinese Medicine, 2007) [7, 8]:

(1) The onset is sudden, usually in winter and summer, and often has a history of cold and cold or pain in the bone behind the ear when some patients first onset;

(2) Muscles on the side of the disease are numb and stiff, forehead lines become shallow or disappear, eye fissures become wider, eyes open and tear, nasolabial fold becomes shallow, mouth corners droop and crook to the healthy side;

(3) The sick side cannot do actions such as frowning, closing eyes, bulging cheeks, and showing teeth [9, 10].

Inadequate qi and blood classification: more normal in patients with recuperation period or a long course of sickness, appendages languor and shortcoming, pale composition, wooziness, short breath, lethargic discourse, palpitations, perspiring, pale tongue, dainty white fur, slim and frail heartbeat [11, 12].

2.2. Western Medicine Diagnostic Criteria. In line with the "Neurology" of Western medicine, the diagnostic criteria for idiopathic facial nerve palsy and facial neuritis:

(1) The onset is rapid, and the symptoms of facial nerve palsy often rise to the peak in a short period of time; it is more common on one side;

(2) The facial expression muscles of the disease are paralyzed, the forehead lines disappear, the forehead frowning cannot be performed, and the eye fissures become enlarged;

(3) When the eyes are closed, the white sclera of the diseased eye is exposed;

(4) The nasolabial folds become shallow, the mouth corners droop during static observation, and the mouth corners are skewed toward the healthy side when performing tooth-exposing movements;

(5) The sick side often leaks air when doing puffing movements, and food residues are easy to keep on the sick side's gums;

(6) In some cases, abnormal taste in the front 2/3 of the tongue, or hyperacusis can be seen;

(7) The electromyography is abnormal [13, 14].

2.3. Adverse Events and Treatment Methods.

(1) Needle dizziness: the patient has symptoms such as nausea and vomiting, pale complexion, cold limbs, dizziness, and palpitation, etc., and the needle should be taken immediately, and the patient should be assisted to lie supine with the head low and the feet high, and keep warm [15, 16]. Give patients appropriate warm water orally. Generally recoverable, if the situation is serious, emergency treatment should be taken immediately.

(2) Hematoma: local small bruises after needle removal are mostly caused by a small amount of subcutaneous hemorrhage, which usually resolves spontaneously and does not require special treatment. If the bruising area is large and accompanied by local pain and swelling, apply cold compresses to stop the bleeding first, and then slowly rub or apply heat to the local area to dissipate and absorb blood stasis.

(3) Scald: the flash tank operation causes small blisters to appear locally. As long as they are not rubbed, they can not be treated, and they can be absorbed naturally. If the blisters are large, the local skin should be strictly disinfected first, and then the blisters should be pierced with a thick needle to release the liquid, and the blisters should be disinfected again and then wrapped with gauze.

2.4. Principles of Peripheral Nerve Injury Repair. The main function of nerve fibers is to conduct nerve impulses. The conduction speed of various nerve fibers is different, roughly between 3 and 120 meters per second. Those that transmit nerve impulses from receptors to the central nervous system are called afferent fibers; those that transmit impulses from the central nervous system to effector organs are called efferent fibers. Nerve fibers are the protrusions of neurons, and the neuron cell body is the nutrient center of neurons [17, 18]. Due to injury or other reasons, nerve fibers may be cut out of the cell body, which may cause damage and death. This process is called nerve fiber ulcer. At this point, the peripheral shaft and myelin sheath and some proximal shafts first expand, then collapse, and collapse into fragments and droplets called plaques. Protective inflammation is an important part of innate immunity after peripheral nerve injury, and it is a necessary step to promote wound healing and functional reconstruction. After 3 days of nerve injury, fibroblasts migrate from a calm state to a migrating state and gradually migrate to the center of the wound. At the same time, they multiply rapidly and synthesize a large amount of collagen and fibronectin. On the 14th day after the injury, fibroblasts transform into a contractile phenotype to induce various cytokines, namely myofibroblasts, and the extracellular matrix is regulated by integrins on the surface of fibroblasts, leading to wound contraction [19, 20]. After wound healing, the number of myofibroblasts decreases due to programmed death. On the one hand, fibroblasts multiply, synthesize, and secrete a large amount of extracellular matrix to fill tissue defects. On the other hand, the extracellular matrix acts as a framework and binding role. It regulates the migration, differentiation, and proliferation of fibroblasts and also acts as a "reservoir" for regulating fibroblasts through local accumulation and release of growth factors. During the regeneration of peripheral nerves, fibroblasts multiply and migrate to fill the defect. Then, they migrate Schwann cells from the proximal end to the distal end through signal transduction pathways and finally make the axons lower than the Schwann cells. The guide extended to the end [21].

As shown in Figure 1, regeneration of nerve fibers usually occurs 2–3 weeks after injury. The Nissl body corresponding to the damaged nerve fiber gradually returned to its normal shape, the nucleus returned to the center, the proximal end of the damaged nerve axis was connected and oriented to the cell body, and many steps grew on the edge. Some of these young shoots passed through the tissue gap in the injury, grew long distances along with Schwann cells, and finally reached the original tissues and organs [22, 23]. Some young shoots penetrate the connective tissue of the nerve and form neuroma, while the rest of the young shoots degenerate or disappear. The axial shoots growing along Schwann cells continue to thicken, myelin sheath gradually forms, and the function of nerve fibers gradually recovers. At that time, the regeneration process of nerve fibers is also completed in advance.

3. Peripheral Nerve Injury Repair Correlation Experiment

3.1. Determination of Pla/Go Conductivity. The electrical conductivity was analyzed by measuring the volume resistivity of the fiber membrane, and the volume resistivity of the PLA/GO electrospun fiber membrane was tested with a four-point probe measuring instrument. At room temperature, test each group of samples five times and calculate the average value. The calculation formula (1) of the volume resistivity (R) of PLA/GO is as follows:

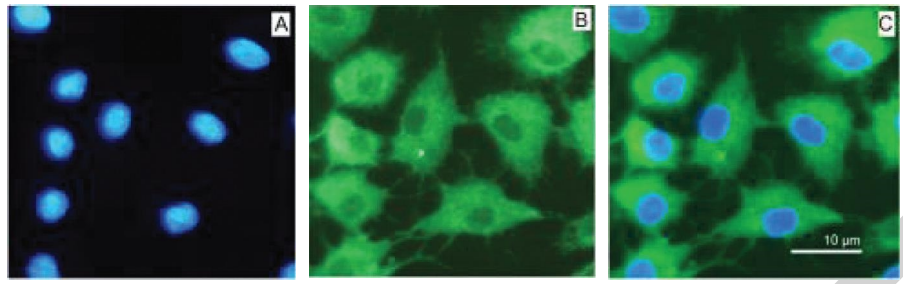

Figure 1: Primary culture and identification of fibroblasts.

$$R = 0.628 \times \frac{V}{I} \times \text{Thick.Correct} \times \text{Temp.Correct} \times \text{Edge.Correct}. \quad (1)$$

In the formula, V/I is the surface resistance of the PLA/GO electrospun fiber membrane, Thick.Correct is the thickness correction coefficient, Temp.Correct is the temperature correction coefficient, and Edge.Correct is the side length correction coefficient.

Take out the fiber membrane soaked in ethanol, weigh the mass of the remaining pycnometer and ethanol as M3, measure each sample 5 times in parallel, and take the average value. The porosity is shown in the following formula (2):

$$\text{porosity}(\%) = \frac{M_2 - M_3 - M_0}{M_1 - M_3 \times 100\%}. \quad (2)$$

According to the experimental load and the size of the fiber membrane, the corresponding stress value is calculated, and the stress-strain curve can be obtained from the load-deformation curve. Each valid sample was tested in parallel 5 times, and the average value was taken [24, 25]. The tensile strength (MPa) is calculated according to formula (2):

$$\delta = \frac{F}{b \times d}. \quad (3)$$

The elongation at break (%) is calculated as shown in formula (3):

$$\varepsilon = \frac{L - L_0}{L_0}. \quad (4)$$

Because the pH environment exceeds a certain range of pH, the degradation of the fiber membrane in the solution is affected. In order to ensure that the pH value of the solution environment is around 7.4, new PBS solution needs to be added regularly, twice a week. Calculate as follows to obtain the weight loss rate of the fiber membrane:

$$W(\%) = \frac{(W_0 - W_1)}{W_0} \times 100\%, \quad (5)$$

where W is the weight loss rate; the initial mass of W_0 fiber membrane [26]; the mass of W_1 after different degradation times. According to formula (4), calculate the cumulative release percentage of NGF and draw the release curve.

$$Q(\%) = \frac{V_0 \times C_t + V \times \sum_{n-1}^{t-1} C}{M}. \quad (6)$$

3.2. Electron Microscope Observation Method. Electron microscopy is an instrument that replaces light beams and optical lenses with electron beams and electron lenses based on the principles of electron optics to image the fine structures of matter under very high magnification. In recent years, the research and manufacture of electron microscopes have made great progress: on the one hand, the resolution of electron microscopes has been continuously improved, the point resolution of transmission electron microscopes has reached 0.2–0.3 nm, and the lattice resolution has reached about 0.1 nm, people have been able to directly observe atomic images; on the other hand, in addition to transmission electron microscopes, a variety of electron microscopes have been developed, such as scanning electron microscopes, analytical electron microscopes, etc. Silicon is anisotropic during wet etching. As shown in Figure 2, the schematic diagrams of the etching of silicon with (100) crystal orientation and (110) crystal orientation in KOH solution are shown, respectively.

When the size of (100) crystal phase silicon is small, it will automatically stop on the (111) crystal plane after KOH etching, forming a pyramid shape. The relationship between the etching depth and the shorter side length of the uncovered silicon is shown in the formula [27]:

$$h = \frac{L}{2} * TG(63.2°), \quad (7)$$

where h is the depth of etching and L is the shorter side length of the exposed surface. When the silicon is etched through, the relationship between the etched size formed on the other side of the silicon and the size not covered by silicon nitride is as shown in the formula:

$$w = W - 2H * ctg(63.7°). \quad (8)$$

The observation of the Coulomb blockade effect generally needs to meet two conditions.

$$R_T > R_K - c, \quad (9)$$

$$\frac{e^2}{C \gg kT}. \quad (10)$$

Here, C is the tunneling junction capacitance and T is the measured temperature. The smaller the junction capacitance C, the higher the measurement temperature T, k is Boltzmann's constant, and T is the temperature of the nanometer point [28, 29]. When the size of nanomaterials decreases, the

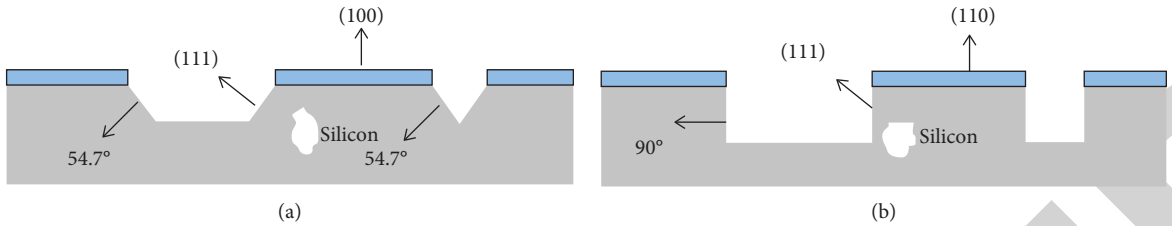

Figure 2: Etching of silicon with different crystal phases in KOH.

self-capacitance of nanomaterials also decreases, which means that it is easier to observe the Coulomb blockade.

$$\frac{77k \ll e^2}{C \ll 300k}. \tag{11}$$

For the spherical nanodots of InAs, the capacitance of the nanodots is as follows:

$$C = \pi\varepsilon_r\varepsilon_0 r - 200k + \frac{cd}{\sum_R t - 3}. \tag{12}$$

The calculation shows that when the 10 nm nanodots of InAs nanodots exhibit Coulomb blockage at liquid nitrogen temperature, the Coulomb blockage phenomenon will disappear at room temperature.

4. Effect of Acupuncture on Peripheral Facial Paralysis

4.1. H-B Facial Nerve Classification before and after Treatment. Before treatment, the two groups were analyzed by Ridit, $t = 0.587$, $P = 0.560 > 0.05$, indicating that the difference between the two groups before treatment was not significant; after treatment, the two groups were analyzed by Ridit, $t = -0.583$, $P = 0.012 < 0.05$, indicating that after treatment, there is a statistical difference between the two groups; in the comparison of the treatment group before and after treatment, through Ridit analysis, it can be obtained: $t = 2.122$, $P = 0.044 < 0.05$, indicating that the effect of the treatment group before and after treatment is obvious, and the difference can be considered as statistical significance. In the comparison between before and after treatment in the control group, Ridit analysis showed: $t = 2.618$, $P = 0.019 < 0.05$, indicating that the HB facial nerve grading of the treatment group was significantly different before and after treatment. It can be seen from the results of statistical data analysis that during the course of treatment, the HB classification changes of the treatment group and the control group before and after treatment were more obvious, and the treatment effect of the treatment group (acupuncture + acupuncture) was obvious, as shown in Table 1.

After all the treatment courses are completed, through the comparison of various evaluation indicators and after statistical technical analysis, it is determined that the evaluation indicators are statistically significant, and it is concluded that the scoring results after treatment have significant changes compared with those before treatment, as shown in Figure 3.

After the completion of all treatment courses, through the comparison of various evaluation indexes and the statistical technical analysis, it is determined that the evaluation indexes are statistically significant. Furthermore, it is reasoned that the scoring results after treatment have massive changes contrasted and those before treatment. To be specific ($P < 0.05$), looking at the treatment bunch (needle therapy + needle therapy) and the benchmark group (needle therapy), the treatment gathering's recuperation rate is more huge than the benchmark group; the treatment bunch (needle therapy + needle therapy) and the benchmark group (needle therapy) all out compared with the powerful rate, the successful pace of the treatment bunch is more critical than that of the benchmark group. Through the examination of trial information, it tends to be seen that needle therapy joined with needle therapy treatment is more successful in the treatment of patients with "fringe facial loss of motion" in the recuperation time frame, as shown in Figure 4.

The fix rate and successful pace of the treatment bunch were 60.00% and 83.33% separately; the fix rate and compelling pace of the benchmark group were 46.67% and 73.33%, individually; the fix rate and powerful pace of the treatment bunch were more huge than those of the benchmark group. The position total test information examination shows that $2w = 19.733$, $P = 0.006 < 0.01$; there is a tremendous distinction; this indicates that this experiment has research significance.

As shown in Table 2, the treatment process of the two groups of cases progressed smoothly. Another 5 people had a certain psychological rejection of acupuncture during the treatment process, which had a certain impact on the treatment effect, but did not have much impact on the overall treatment effect, including 3 cases in the treatment group and 2 cases in the control group.

The comparison of the curative effects of the three groups is shown in Figure 5. Through moxibustion on acupoints and local points, the vascular permeability of the local skin is increased and the pores are expanded, thereby promoting the absorption of drugs and giving full play to the curative effect of drugs. Combining the functions of acupoints, it can harmonize internal and external effects, improve the body's immune function, promote the elimination of local inflammatory factors, accelerate the absorption of inflammatory exudate, and promote swelling, pain elimination, and skin lesion recovery. This also reflects the role of traditional Chinese medicine in "strengthening the body and eliminating evils," which can relieve pain, promote qi and blood circulation, clear heat, relieve fire, expel wind, relieve

Table 1: Two groups before treatment in patients with H—B level of facial nerve.

Group	Number of cases	Before treatment		After treatment	
		I	II	I	II
Therapy group	30	0	1	15	9
Control group	30	0	1	11	6

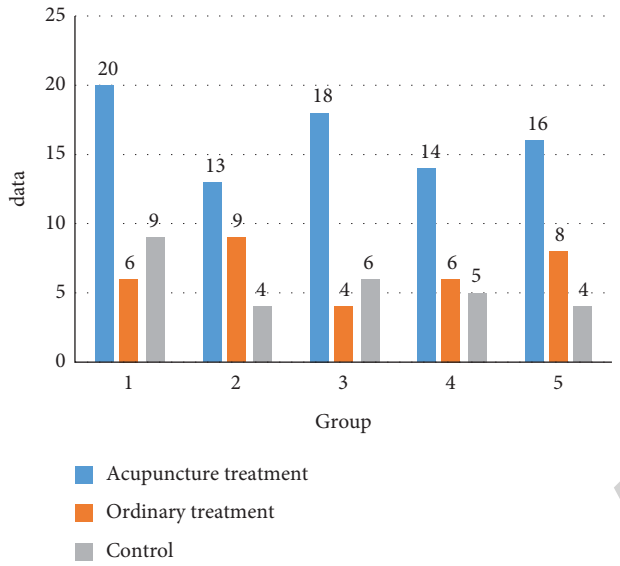

Figure 3: Comparison of different treatment methods for patients with facial paralysis.

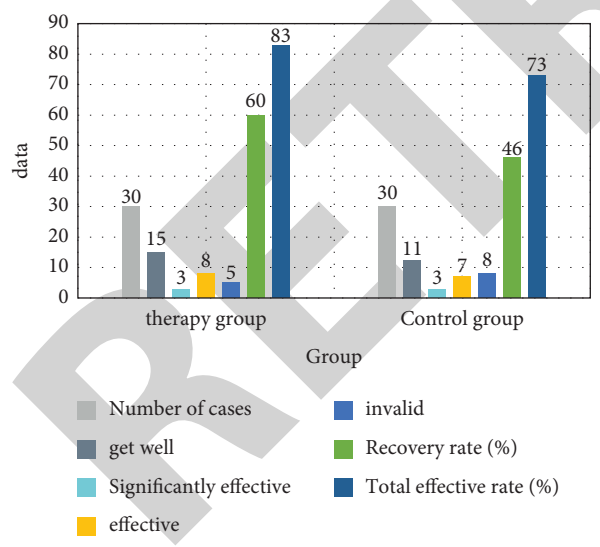

Figure 4: Comparison of two groups after treatment efficiency.

Table 2: Two groups of treatment comparisons (n).

Group	Number of cases	Level 1	Level 2	Level 3	Level 4
Therapy group	20	17	3	0	0
Control group	20	18	2	0	0

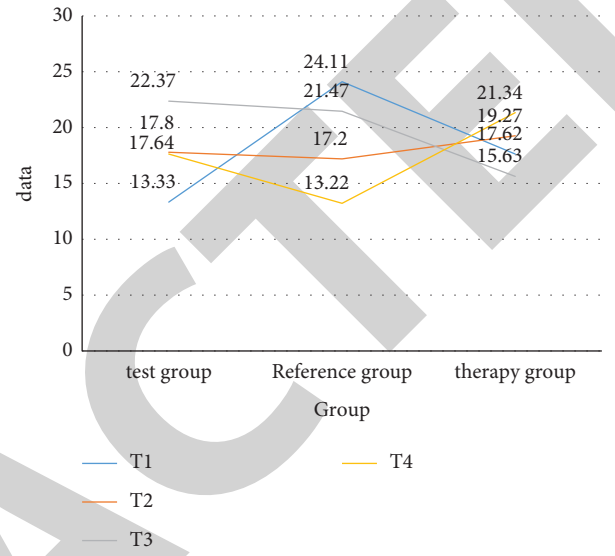

Figure 5: FDIP evaluation of the two groups at the four time nodes of T1, T2, T3, and T4.

itching, and reduce swelling. The medicinal thread moxibustion therapy is simple in operation, rigorous in theoretical content, and effective. In a sense, it has the function of auxiliary treatment.

4.2. Microscopic Observation of Nerve Recovery Analysis. It is understandable that fibroblasts and Schwann cells are contained in the fibroblast group, but they are also contained in the catheter group and hydrogel group, indicating that the regeneration activity of peripheral nerve injury has been carried out at 14 days. Other cells that do not develop color correspond to the figure. It is guessed that they are red blood cells or inflammatory cells, indicating that the inflammatory response is still going on at this time. There are more fibroblasts and Schwann cells in the fibroblast group than in the catheter group and the hydrogel group, indicating that the fibroblast group has more active cell repair after peripheral nerve injury, and the repair may be faster, as shown in Figure 6.

The normal nerve longitudinal section was used for immunofluorescence staining of the fibroblast marker Fibronectin (green fluorescence) and nuclear DAPI (blue fluorescence). The picture shows that after a normal nerve longitudinal section, clear-textured nerve fibers can be seen. These nerve fibers are composed of neuron axons and outer glial cells (Schwann cells), so only weak fluorescence can be seen. Green fluorescence (Fibronectin, a marker for fibroblasts) can also see obvious nuclei in nerve fibers [30, 31]. Compared with the fluorescence intensity of normal nerve

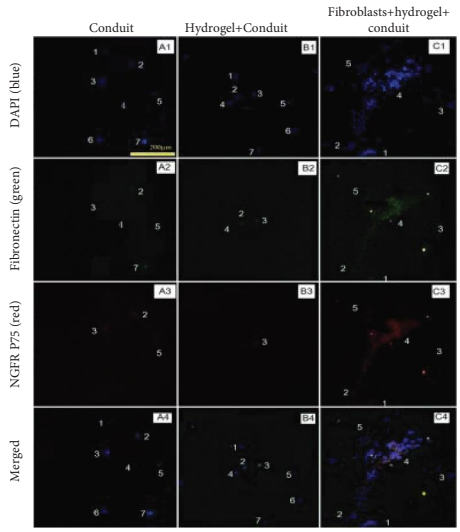

Figure 6: Immunofluorescence staining of Schwann cells and fibroblasts on the 14th day of nerve repair.

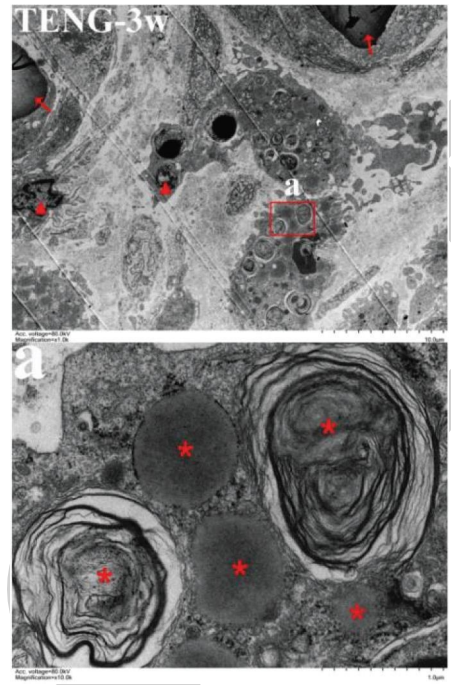

Figure 7: Electron microscope ultrastructure of the regenerated nerve tissue proximal to the catheter 3 w after operation in the TENG group.

longitudinal section Schwann cells, the fluorescence intensity of Schwann cells in the hydrogel group is weaker, and the fluorescence intensity of normal nerve Schwann cells is stronger. This shows that the Schwann cells in the hydrogel group are less than those in the normal nerves, and the proximal and tube wall fibroblasts in the hydrogel group are slightly more than those in the normal nerves. There was little difference in the number of fibroblasts in the distal and normal nerves in the group.

The nervous system is the most important tissue system in the human body. It regulates the sensation and movement of various parts of the body. Therefore, once the nerves are damaged, the normal functions of various organs will also be affected. As shown in Figure 7, with the help of light microscopy or electron microscopy technology, we can visually observe from the morphology that Schwann cells guide axon regeneration from dedifferentiation, proliferation, migration, and then differentiation and sparing axons after nerve injury. Hence, behind these interesting biological phenomena, which molecules are involved? In order to understand this complex gene network in depth, we still use the above three different types of rat sciatic nerve defect/repair models, namely the Sca group, the TENG group, and the Auto group. At the same time, a sham operation (Sham) group is set up to eliminate surgical factors. Interference, at different time points after surgery (1 d, 4 d, 1 w, 2 w, 3 w, 4 w, 8 w, 12 w), the bridging segment tissues of each group of animals were obtained. In the Sham group, the sciatic nerve at the same position was taken, and the tissue RNA was extracted to perform gene Chip detection. Search for myelin-related genes (including related genes involved in Schwann cell dedifferentiation, proliferation, migration, differentiation, myelination, myelin thickness, etc.) through the IPA (Ingenuity Pathway Analysis) database, and then extract these genes with the chip data Intersection, a total of 383 myelin-related genes were obtained (it may increase after the IPA database is updated); Hierarchical cluster analysis (Hierarchical clustering analysis) was performed on the myelin-related genes at all time points in the Sca, TENG, and Auto groups using bioinformatics analysis tools. Clustering, HCL, or Principal Component Analysis (PCA) analyzes the clustering situation of each group of samples at each time point or the positional relationship in three-dimensional space and conducts gene network analysis on the biological process of remyelination through the IPA database, through the Venn diagram to show the similarities and differences of the molecules involved in each biological process of the Sca, TENG, and Auto groups, and perform immunohistochemistry and PCR verification.

As shown in Table 3, observe the tissue sections of the four groups of regenerated nerves at various time points through a microscope, compare and analyze the regeneration of each group of nerves and the differences between groups, and observe the formation of regenerated nerves and the growth of myelinated nerve fibers. Nikon picture analyzer: each cut arbitrarily chooses 5 fields of view, counts the number of myelinated nerve strands per unit region, and measures the thickness of the myelin sheath of the myelinated nerve. The recuperation of facial nerve work was decided by the inertness of the activity capability of the orbicularis oris muscle, the conduction speed of the recovering nerve, and the sufficiency of the compound neuromuscular activity potential in trial creatures. Use SPSS22.0 statistical analysis software to analyze neuromuscular action potential latency, amplitude, regenerative nerve conduction velocity, number of myelinated nerve fibers, and myelin thickness, etc., use one-way analysis of variance, and then use LSD-*t* test for pairwise analysis. For comparison, the

Table 3: Comparison of the latency, amplitude, and conduction velocity of nerve regeneration in each group at 8 weeks after the operation.

Group	Incubation period (ms)	Amplitude (mV)	Conduction speed (m/s)
Group A (chitosan plus PRP)	1.90 ± 0.21	3.05 ± 0.15	22.19 ± 1.19
Group B (chitosan plus saline)	2.37 ± 0.12	1.94 ± 0.06	17.85 ± 0.28
Group C (silicone tube plus saline)	2.50 ± 0.17	1.88 ± 0.03	17.45 ± 0.39
Group D (silicone tube plus PRP)	1.90 ± 0.31	2.99 ± 0.15	22.17 ± 1.22
F value	46.447	157.254	44.020
P value	0.000	0.000	0.000

measurement data is expressed as ($\pm s$), and the test level is $\alpha = 0.05$, $P < 0.05$, the difference is considered to be statistically significant.

As shown in Table 4, the examination between the two gatherings before treatment was not measurably huge ($P > 0.05$), and the correlation between the treatment bunch when treatment $Z = -5.092$, $P = 0.000 < 0.01$; there was a massive distinction. When treatment in the benchmark group, $Z = -5.090$, $P = 0.000 < 0.01$, there is a tremendous contrast. The examination between the two gatherings after treatment was measurably huge ($P < 0.05$). Note: the two gatherings are practically identical after treatment. After treatment, the fringe facial nerve paralysis scale scores of the treatment bunch and the benchmark group are worked on contrasted with before treatment, and there is a distinction in the scores of the fringe facial nerve paralysis scale between the two gatherings.

The neural network abstracts the human brain neuron network from the perspective of information processing, establishes a certain simple model, and forms different networks according to different connection methods. As shown in Figure 8, on the 3rd, 7th, and 14th days of nerve repair, white blood cells, red blood cells, and cells of nonblood cell lines can be observed in each group. These cells have different morphologies. It may be fibroblasts or Schwann cells. For the group of fibroblasts, since fibroblasts are added to artificial nerves, it is expected that cells of nonblood cell lines can be observed. In the nerve conduit group and the hydrogel group, since no cells were added, cells of nonblood cell lines were observed. Theoretically, these cells may be derived from the distal or proximal end of the recipient sciatic nerve or may be caused by the differentiation of hematopoietic stem cells, which seems to mean that on the third day of artificial nerve repair, nerve defect repair activities have started. At the same time, the appearance of white blood cells indicates that the inflammatory response has started on the third day of artificial nerve repair. The distribution of capillaries in the sciatic nerve is underdeveloped, and material exchange mainly depends on tissue fluid [32]. The appearance of red blood cells indicates that blood is directly involved in the repair of peripheral nerve defects. From the 14th day to the 21st day of artificial nerve repair, the proportion of nonblood-line cells gradually increased, indicating that the repair process of peripheral nerve defects is proceeding more quickly, and a large number of nonblood-line cells are secreted to promote the regeneration of peripheral nerves. The gradual decrease of white blood cells indicates that the intensity of the inflammatory response is gradually weakening. There are

Table 4: Comparison of Nerve Palsy Scale scores before and after treatment.

Group	Number of cases	Before treatment	After treatment
Therapy group	34	30.29 ± 13.35	87.43 ± 18.03
Control group	34	30.88 ± 13.69	76.62 ± 22.80
Z		−0.321	−2.172
P		0.748	0.030

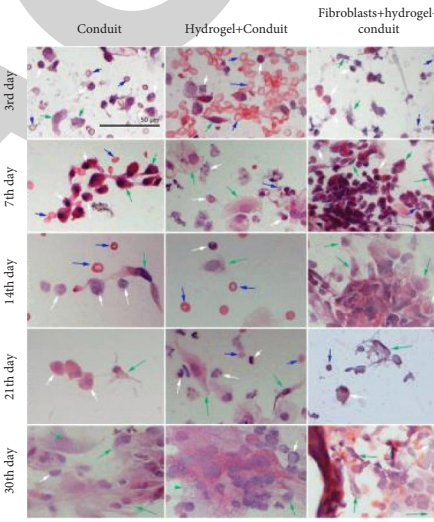

Figure 8: Observation diagram of coating preparation containing artificial nerve components obtained after implantation.

fewer white blood cells in the fibroblast group, indicating that the inflammatory response is weaker. From the 21st to the 30th day of nerve repair, nonblood cells increased in the three groups, indicating that nerve regeneration was more vigorous. There was a limited quantity of white platelets in the fibroblast bunch, the nerve channel bunch, and the hydrogel bunch, demonstrating that the provocative response in the fibroblast bunch, the nerve conduit bunch and the hydrogel bunch was going to end.

5. Conclusions

The treatment method in this study has a certain improvement in the treatment effect of "peripheral facial paralysis" in the recovery period and has a good performance in clinical application. In this study, traditional acupuncture treatment was used as the basic treatment. By comparing the

clinical efficacy of nerve repair combined with acupuncture in the treatment of "peripheral facial paralysis" during the recovery period, the results of this project can be summarized as follows: The treatment effect of "facial paralysis" during the recovery period has been improved to a certain extent, and it has a better performance in clinical application. By comparing the results of 4 evaluation indicators displayed by several groups of patients in different treatment time periods, it can be concluded that in the treatment of "peripheral facial paralysis" during the recovery period, ordinary acupuncture is used as the basic treatment, supplemented by acupuncture and moxibustion treatment. The effect is more significant. In this trial design, the treatment group used acupuncture on the basis of the control group to treat "peripheral facial paralysis" during the recovery period. The experiment showed that $t = 2.618$, $P = 0.019 < 0.05$, indicating that there was a significant difference in the HB facial nerve grading in the treatment group before and after treatment. The method is relatively novel and has a certain degree of innovation. The results show that acupuncture therapy can not only promote local qi and blood circulation in the treatment of "peripheral facial paralysis" but also solve the problem of muscle disability left by "peripheral facial paralysis" and confirm that acupuncture can treat muscle paralysis caused by motor nerve injury. This article also uses a variety of evaluation indicators to evaluate efficacy. These indicators are the main indicators for evaluating the effect of "peripheral facial paralysis" during the recovery period. The evaluation is relatively comprehensive, and the conclusions obtained are true and reliable. Because I have certain limitations in my energy, ability, time, funding, etc., this study did not conduct a large sample survey and analysis. Therefore, the accuracy, stability, avoidance of errors, and improvement of the persuasiveness of the research results are relatively lacking. The number and types of research subjects are limited to some extent. Due to limited conditions, it is impossible to carry out laboratory collection of more information (such as blood, body immune function, etc.). The inference of sexuality has not been studied with a more scientific method. I will perfect it in my work and study in the future, hoping to contribute my own strength to acupuncture and moxibustion medicine.

Data Availability

No data were used to support this study.

Conflicts of Interest

The author declares that there are no conflicts of interest in this paper.

References

[1] P. Y. Zhu, M. M. Sun, T. Y. Yu, Y. Li, and S. T. Sun, "Professor SUN Shen-tian's clinical experience of acupuncture and moxibustion for peripheral facial paralysis," *Zhongguo zhen jiu = Chinese acupuncture & moxibustion*, vol. 41, no. 2, pp. 189–191, 2021.

[2] T. Lv, Y. Mo, T. Yu et al., "An investigation into the rehabilitative mechanism of tuina in the treatment of sciatic nerve injury," *Evidence-based Complementary and Alternative Medicine*, vol. 2020, no. 1, Article ID 5859298, 11 pages, 2020.

[3] A. C. Lovaglio, M. Socolovsky, G. Di Masi, and G. Bonilla, "Treatment of neuropathic pain after peripheral nerve and brachial plexus traumatic injury," *Neurology India*, vol. 67, no. 7, p. S32, 2019.

[4] J. Cao, A. Yuan, Y. Zhang, J. Yang, and Xg. Song, "Effect of warm needling therapy and acupuncture in the treatment of peripheral facial paralysis: a systematic review and meta-analysis," *World Journal of Acupuncture-Moxibustion*, vol. 28, no. 4, pp. 278–286, 2018.

[5] Qin, "Clinical study on acupuncture and moxibustion in the treatment of peripheral facial paralysis at acute stage," *Modern Distance Education of Chinese Medicine*, vol. 016, no. 021, pp. 139-140, 2018.

[6] Jing-Hua, Wang, Yao-Hui et al., "Effect of acupuncture at "reflection points" of the affected side on the peripheral facial paralysis in acute phase," *Zhongguo zhen jiu = Chinese acupuncture & moxibustion*, vol. 39, no. 6, pp. 588–592, 2019.

[7] T. Li, J. Ren, and X. Peng, "Therapeutic observation on superficial needling with different frequencies for intractable facial paralysis," *Journal of Acupuncture and Tuina Science*, vol. 17, no. 6, pp. 432–437, 2019.

[8] S. M. Rozen, "Discussion: incomplete facial paralysis: the use of the ipsilateral residual facial nerve as a donor nerve for facial reanimation," *Plastic and Reconstructive Surgery*, vol. 142, no. 1, pp. 215-216, 2018.

[9] Y. Zheng, P. Wang, and J. Zhao, "Professor Jiping ZHAO's experiences in the differentiation and treatment of peripheral facial paralysis with acupuncture," *World Journal of Acupuncture-Moxibustion*, vol. 29, no. 1, pp. 76–79, 2019.

[10] Y. Han, R. Liu, T. R. Wang et al., "Bibliometric analysis of refractory facial paralysis based on CNKI database," *Zhongguo zhen jiu = Chinese acupuncture & moxibustion*, vol. 41, no. 2, pp. 229–232, 2021.

[11] W. H. Wang, R. W. Jiang, and N. C. Liu, "Electroacupuncture is effective for peripheral facial paralysis: a meta-analysis," *Evidence-based Complementary and Alternative Medicine*, vol. 2020, Article ID 5419407, 11 pages, 2020.

[12] M. Wang, X. Zhang, F. Wang, and H. Ying, "Therapeutic observation of acupoint Application with ban Ba gao for peripheral facial paralysis in acute stage," *Shanghai Journal of Acupuncture*, vol. 038, no. 008, pp. 861–864, 2019.

[13] P. Liu and M. He, "Physiotherapy assisted treatment of 154 cases of peripheral facial paralysis%154 cases of peripheral facial paralysis by physical assisted therapy," *Agricultural Reclamation Medicine*, vol. 041, no. 001, pp. 46–48, 2019.

[14] W. Yan, S. Ge, W. Chunbo, and L. Wenhui, "Bilateral peripheral facial paralysis combined with HIV meningitis during acute HIV-1 infection: a case report," *Chinese Medical Sciences Journal*, vol. 34, no. 1, pp. 55–59, 2019.

[15] G. Colini Baldeschi, A. Dario, G. De Carolis et al., "Peripheral nerve stimulation in the treatment of chronic pain syndromes from nerve injury: a multicenter observational study," *Neuromodulation: Technology at the Neural Interface*, vol. 20, no. 4, pp. 369–374, 2017.

[16] T. Mindos, X. P. Dun, K. North et al., "Merlin controls the repair capacity of Schwann cells after injury by regulating Hippo/YAP activity," *Journal of Cell Biology*, vol. 216, no. 2, pp. 495–510, 2017.

[17] C. Atam, Z. Orhan, G. Toplu, M. Serin, Z. O. Karaduman, and A. Ozturk, "Comparison of peripheral nerve repair using

Hindawi
Emergency Medicine International
Volume 2023, Article ID 9843571, 1 page
https://doi.org/10.1155/2023/9843571

Retraction

Retracted: Clinical Treatment and Nursing Intervention Study of Clipping Treatment of Cerebral Aneurysm under the Health Model of Data Analysis

Emergency Medicine International

Received 8 August 2023; Accepted 8 August 2023; Published 9 August 2023

This article has been retracted by Hindawi following an investigation undertaken by the publisher [1]. This investigation has uncovered evidence of one or more of the following indicators of systematic manipulation of the publication process:

(1) Discrepancies in scope
(2) Discrepancies in the description of the research reported
(3) Discrepancies between the availability of data and the research described
(4) Inappropriate citations
(5) Incoherent, meaningless and/or irrelevant content included in the article
(6) Peer-review manipulation

The presence of these indicators undermines our confidence in the integrity of the article's content and we cannot, therefore, vouch for its reliability. Please note that this notice is intended solely to alert readers that the content of this article is unreliable. We have not investigated whether authors were aware of or involved in the systematic manipulation of the publication process.

In addition, our investigation has also shown that one or more of the following human-subject reporting requirements has not been met in this article: ethical approval by an Institutional Review Board (IRB) committee or equivalent, patient/participant consent to participate, and/or agreement to publish patient/participant details (where relevant).

Wiley and Hindawi regrets that the usual quality checks did not identify these issues before publication and have since put additional measures in place to safeguard research integrity.

We wish to credit our own Research Integrity and Research Publishing teams and anonymous and named external researchers and research integrity experts for contributing to this investigation.

The corresponding author, as the representative of all authors, has been given the opportunity to register their agreement or disagreement to this retraction. We have kept a record of any response received.

References

[1] Y. Huang and L. Huang, "Clinical Treatment and Nursing Intervention Study of Clipping Treatment of Cerebral Aneurysm under the Health Model of Data Analysis," *Emergency Medicine International*, vol. 2022, Article ID 8178963, 12 pages, 2022.

Hindawi
Emergency Medicine International
Volume 2022, Article ID 8178963, 12 pages
https://doi.org/10.1155/2022/8178963

Research Article

Clinical Treatment and Nursing Intervention Study of Clipping Treatment of Cerebral Aneurysm under the Health Model of Data Analysis

Yuyou Huang and Liping Huang

Emergency Intensive Care Unit, Longhua People's Hospital, Shenzhen 518000, Guangdong, China

Correspondence should be addressed to Liping Huang; 1420150221@st.usst.edu.cn

Received 29 March 2022; Accepted 30 May 2022; Published 30 June 2022

Academic Editor: Hang Chen

Middle cerebral artery aneurysm is a common type of intracranial aneurysm in neurosurgery, accounting for about 20% of intracranial aneurysms, and is the third most common site of intracranial aneurysms. The surgical success rate and postoperative recovery ability of today's treatment plans are not satisfactory. Therefore, this paper designs a health model based on data analysis to clinically apply clipping surgery for cerebral aneurysm. This paper studies data analytics health models in the context of big data analytics. The model combines the characteristics of cerebral aneurysms for targeted analysis, and then through the understanding of the clipping treatment of cerebral aneurysms, this paper combines the deep learning in the neural network to train the treatment plan under the data analysis health model. Finally, this paper designs a therapeutic plan for clipping treatment of cerebral aneurysm based on a data analysis health model. To verify its data analysis ability, this paper designs experiments on unbalanced data sets and experiments to improve the execution efficiency of the algorithm. After analyzing the results obtained from the experiment, this paper will apply them to the clinic. The final experiment showed that the surgical success rate of the clipping treatment for cerebral aneurysm based on the data analysis health model was increased by 21.84% compared with the traditional clipping treatment for cerebral aneurysm.

1. Introduction

With the advent of the era of big data, medical informatization has had a huge impact on the domestic medical industry and promoted the advancement and reform of the entire industry. Medical information is based on various basic medical data such as clinical and monitoring data collected directly from hospitals, research data from medical research institutions, and personal health data collected directly by individuals.

Brain aneurysms can be divided into three types: aortic aneurysm, branch aneurysm, and distal aneurysm according to the location of growth, usually at the origin of the anterior cranial artery. The neck of the tumor is generally wide and closely associated with perforated blood vessels. The risk of postoperative brain aneurysms is much higher than elsewhere. Branch aneurysms have the highest incidence, about 80–85%, usually in the initial branch of the middle cerebral artery, mainly in cerebral aneurysms or giant aneurysms. Distal aneurysms are mainly caused by infectious factors, which are rare in clinical diagnosis and treatment. If data analysis can be applied to a healthy model to improve the clipping treatment of cerebral aneurysms and optimize its postoperative care, it can improve the surgical success rate and postoperative recovery of patients with cerebral aneurysms.

The innovation of this paper is that this paper combines the health data analysis model of big data and then analyzes the surgical plan for the clipping treatment of the cerebral aneurysm. Then, through the application of deep learning of neural network in data analysis health model, a treatment plan for clipping treatment of cerebral aneurysm based on

big data analysis health model is finally designed. This paper designs experiments on unbalanced data sets and experiments to improve the execution efficiency of the algorithm, and tests and improves the performance of the data analysis model.

2. Related Work

Mobile devices are increasingly becoming an integral part of people's daily lives, facilitating a variety of useful tasks. Tawalbeh LA describes a cloudlet-based mobile cloud computing infrastructure for healthcare big data applications. He reviews the techniques, tools, and applications of big data analytics and concludes the design of networked healthcare systems using big data and mobile cloud computing technologies [1]. He applied big data to the medical system. If he can design a data analysis health model, it will be more useful for this article. To explore the risk factors and intervention strategies of cerebral arteriovenous malformation complicated with aneurysm hemorrhage, Li X collected and analyzed the clinical and imaging data of 42 cases of cerebral arteriovenous malformation complicated with aneurysm [2]. According to the results of intraoperative angiography and the characteristics of vascular structure, the treatment plan is formulated. Brain aneurysm rupture is closely related to aneurysm size. Because aneurysms often have complex shapes, using only the size of the aneurysm dome and neck may be inaccurate, and important geometric information may be overlooked. Dong B proposed a level-set-based surface capture algorithm to first capture aneurysms from the vessel tree [3]. Since aneurysms are described by level-set functions, the volume, curvature, and other geometric quantities of the aneurysm surface can be easily calculated for medical research. The purpose of Byndiu AV is to study the characteristics of early clinical neurological manifestations after intraoperative rupture of an aneurysm (AA) [4]. He then conducted a retrospective study of the surgical outcomes of 69 patients with hemorrhagic acute cerebrovascular disease due to ruptured cerebral aneurysms, including intraoperative ruptures. The increasing popularity and development of data mining technology have brought a serious threat to the security of sensitive personal information. Xu L takes a broader perspective on privacy issues related to data mining and studies various methods that help protect sensitive information [5]. He identified four different types of users involved in data mining applications, namely data providers, data collectors, data miners, and decision-makers. Machine learning prediction methods are highly effective in applications ranging from medicine to assigning city fire and sanitation inspectors. Thus, Athey S's research is mainly focused on making predictions and making decisions and requires an understanding of the underlying assumptions to optimize data-driven decision-making [6]. Advances in information technology have witnessed tremendous advancements in healthcare technology in various fields today. However, these new technologies have also made healthcare data not only larger but more difficult to process. To provide a more convenient healthcare service and environment, Zhang Y proposed a cyber-physical system for patient-centric healthcare applications and services based on cloud and big data analysis technology, called Health-CPS [7]. To sum up, most of the cited literature is about big data and cerebral aneurysms. If the data analysis of big data can be applied to the health model, and then analyzed for clipping treatment of cerebral aneurysms, it will be more in line with the theme of the article. Therefore, it is necessary to further study the application of data analysis of big data in health models.

3. Design Method of Health Model Based on Big Data

3.1. Big Data Analysis Model

3.1.1. Big Data. In recent years, with the rapid development of the Internet society, a large amount of information has been digitized, and big data [8] has emerged as the times require. Modern people are all surrounded by this massive amount of data. The most notable feature of big data is its huge amount of data. Common computer storage units of measurement have developed from GB to TB, PB, EB, ZB, YB, etc. Taking the world's largest search engine Google as an example, its daily data processing volume has exceeded 24 PB, which is already equivalent to 2 to the 50th power of bytes, and a 4 MB ordinary MP3 song can be played for 48,000 years. The fields involved are shown in Figure 1.

3.1.2. Characteristics of Big Data. Big data involves a huge amount of data with a wide variety of types. It is necessary to use software to complete the processing of relevant data sets within a certain period and analyze the basis for decision-making references to reflect the value of big data. Big data has the following characteristics:

(1) The amount of data is huge and complex [9], and the amount of data is huge. In general, traditional databases do not have the function of collecting and saving, and there are various types of data, which come from various aspects, and the sources are extremely complex, presenting various structures and various media forms, which far exceed the previous database capabilities. To realize the role of big data technology in promoting economic development, management and analysis need a database with powerful functions, which can lead to the potential value of data [10].

(2) The processing speed is fast [11]. Big data has higher and higher requirements for computer technology, and data will change in various ways, so it is particularly important to process data on time. In addition to data collection, data analysis and mining are required [12]. Therefore, to meet real-time reference requirements, data must be analyzed and processed rapidly and continuously.

(3) It uses data analysis to obtain valuable information [13]. The core of big data is not the storage and simple processing of huge amounts of data, but the

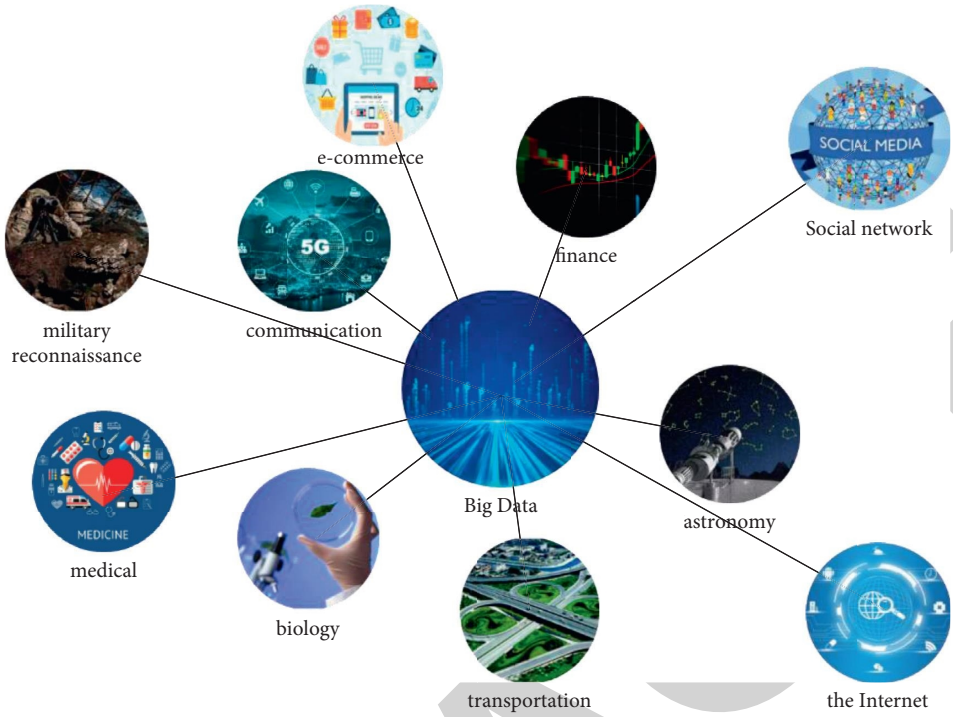

Figure 1: Fields covered by big data.

specific analysis of these data, and then draw some important information from it. For example, after analyzing the shopping lists of a large number of customers, a supermarket found that beer often appeared on the same shopping list as diapers. The supermarket concluded that customers who buy beer usually also buy diapers, so they put beer and diapers together on the product placement, which not only makes it easier for customers to get the product but also increases the sales of these two products. In the above case, the supermarket has obtained valuable information for its operation through the analysis of the data. The same is true for big data technology, but the amount of data is larger, and the processing and analysis methods are more complicated.

3.1.3. The Basic Value of Big Data. Today, big data has become a key element in transforming production relations and improving social productivity. When it comes to the value of big data, we cannot avoid considering the huge economic benefits contained in it from the perspective of social attributes. The concept of "data is an asset" is particularly important in the era of big data. The industrial chain derived from the element of "data" covers data itself, technology, and thinking.

From the perspective of big data itself, the possession of massive data by an enterprise is equivalent to obtaining a "rich mine" of future competition, which is tantamount to controlling a large number of production materials and winning the ownership of data [14]. Big data owners can not only use big data resources but also make secondary use of data, improve user experience, and improve their operations and services [15]. It is also possible to transfer the use value of massive data to third-party technology companies through data authorization, so as to obtain its value and improve economic benefits. It is foreseeable that a large number of such "data middlemen" will emerge shortly, such as banks, search engines, e-commerce platforms, social industries, government departments, and so on. Mastering big data itself occupies the core position of the big data industry chain. Taking the gold mine as an analogy, whether it is its miner or its seller, the owner who benefits the most is ultimately its owner.

From the perspective of big data skills, in the early days of the big data era, only those who take the lead in mastering advanced data processing methods can capture the greatest commercial value. What has to be mentioned here is a big data technology and big data talents. Big data technology is to "make data sound" through technical means, that is, to develop the potential value and innovative uses of data from the vast ocean of data. Undoubtedly, the monopoly of related technologies in data mining, data analysis, and data presentation in the future will be enough to make consulting service companies, technology suppliers, and information analysis companies become industry leaders. At the same time, big data talents will also gain a pivotal position. Today, conclusions based on technical and data facts are far more convincing than those guided by traditional experience, and data scientists will replace industry experts as the dominant force in future strategic decisions.

From the perspective of big data thinking, the value of big data lies in the emancipation of the mind, that is, to get rid of the influence of inherent patterns and vested interests, and to "dissect sparrows" from the height of top-level design.

From a methodological point of view, it is to jump out of the shackles of thinking in the era of small data and use quantitative thinking, overall thinking, relevant thinking, and fault-tolerant thinking in the era of big data to guide people to understand and transform the world from a new perspective.

3.1.4. Application of Big Data. The arrival of the era of big data has affected all aspects of social development in all countries in the world, from business and economics to healthcare, technology, education, and more. As long as it is closely related to people's lives, big data is everywhere [16]. Therefore, whether it is the rise and development of the big data industry or as a technical means, big data has been widely used in various fields. Therefore, the application of big data mentioned here is not only the application of big data technology in other fields but also the positive impact of the integration of the big data industry in other industries.

Big data is a strategic resource that is vigorously developed in China, mainly because big data can be extended to various fields as a technology. After the Internet of Things and cloud computing [17], the development and application of big data technology have received attention from all walks of life. The biggest achievement of big data applications is their integration. It is not only the integration and development of related industries but also integration with industrial clusters. Only in the process of integration and application can big data play its role. The subdivision of its application can be summarized into three aspects, the application of data storage; the application of data analysis; and the application of data fusion. It is the application of these three aspects that allows big data to penetrate all aspects of other industries, and even more subtle links.

3.1.5. Research on Health Big Data. Health big data [18, 19] refers to all data closely related to human health and public health, including birth, infant health management, vaccination, admission inspection, employment inspection, medical treatment, hospitalization, exercise, sleep, death, and other life cycles. It can be roughly divided into structured data such as inspection data and semi-structured and unstructured data such as medical record data and medical images. Test data mainly refer to data generated by routine blood tests, cell tests, and pathological tests of various organs. Medical record data refers to data related to personal medical diagnosis information records and health status, etc., which are usually managed electronically. Medical image data refer to images such as internal tissue structures obtained from the human body. Through this part of the data, a more detailed understanding of the health status of the human body can be obtained.

The rapid development of information technology and social changes have gradually transformed traditional medical and health records from paper files to digital storage and gradually entered the era of big data in the medical industry. The development process of China's healthcare informatization is shown in Figure 2.

Health big data has the characteristics of redundancy, polymorphism, privacy, timeliness, and incompleteness, so the analysis and processing of health big data is a new challenge. Common methods for data analysis of health big data include feature analysis, classification, regression analysis, clustering, and visualization. Combining machine learning technology to reason and judge different types of test data, medical record data, medical images, and other data is a new means to strengthen medical services, predict disease conditions and reduce medical costs.

3.1.6. Traditional Algorithm of Health Big Data. Classification is to use the known attribute data of the data set [20] to infer an unknown discrete attribute data. The key to making accurate predictions is to establish an effective model between known attribute information and unknown discrete attributes, that is, a classification model. Therefore, the classification problem includes two processes of learning and classification, as shown in Figure 3.

Traditional health data classification methods [21] are mainly based on supervised learning. In machine learning, common classification algorithms include SVM [22], decision tree [23], and so on. The classification of health data is actually to map the patient's inspection information to specific categories, so as to achieve the right medicine and accurate treatment.

When traditional supervised learning algorithms classify different types of healthy big data, preprocessing and feature selection are performed first, and then the classifier is trained. The conventional classification process of health big data is shown in Figure 4.

3.2. Clipping Therapy for Cerebral Aneurysms. Patients with cerebral aneurysms [24, 25] are often accompanied by intracranial hematomas. In the case of an intracranial hematoma, coma, or worsening of state after a brief hemorrhage, mainly due to cerebral vasospasm, not hematoma compression or brain herniation. Therefore, in patients with middle cerebral aneurysms and large intracranial hematomas, early aneurysm debridement and intracranial hematoma removal are recommended to prevent secondary rupture of the aneurysm.

Due to the special anatomical location and complex structure of MCA, most aneurysms have wide or irregular heads, and intracranial hematomas are easily formed after rupture, so they are not suitable for endovascular interventional therapy.

The release of ISAT in 2002 indicated that endovascular therapy is safer and more effective than surgical clipping. More and more clinicians use endovascular therapy to treat intracranial aneurysms, but ISAT results are clinical results 12 months after treatment. Although the study was for ruptured intracranial aneurysms, its publication also has major implications for how unruptured aneurysms are treated. Although in recent years ISAT showed that the difference between the two treatments decreased with the extension of follow-up time, the latest ISAT showed no significant difference between the two treatments. And only

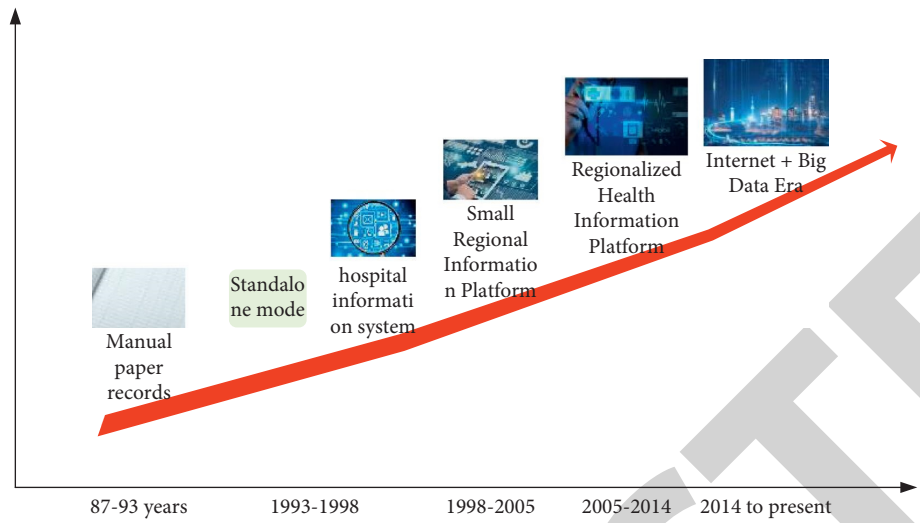

Figure 2: The development process map of China's health and medical informatization.

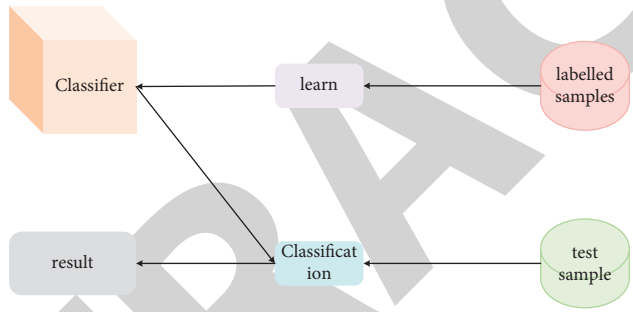

Figure 3: Classification problem.

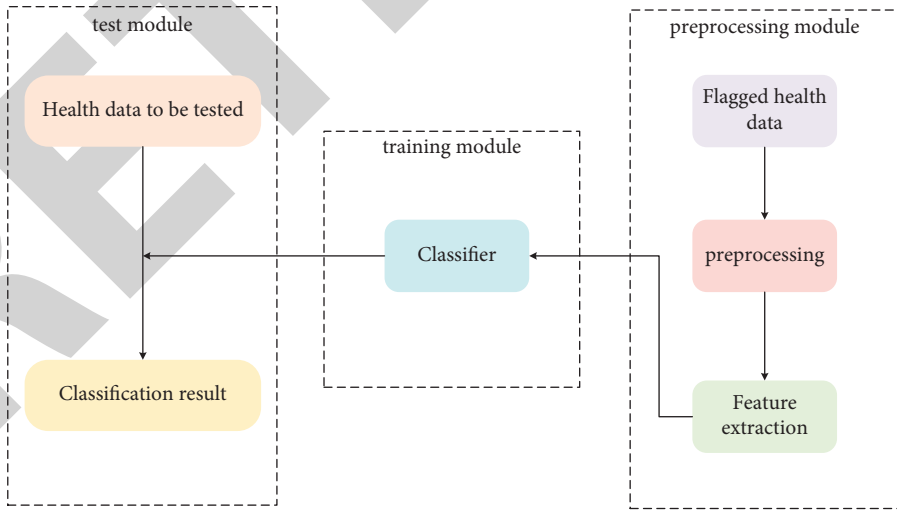

Figure 4: Flow chart of health big data classification.

303 of the 2143 patients in ISAT were MCAA, and middle cerebral aneurysms were underrepresented, but the endovascular treatment of intracranial aneurysms has become an important treatment method for aneurysms. There is no consensus on which of the two approaches provides long-term security. Although the location of the middle cerebral aneurysm makes it more likely that craniotomy clipping is a straightforward, feasible approach, there is both early vasospasm and additional damage from the craniotomy (for example, traction injury of brain tissue and perioperative hematoma). These difficulties and complications can be avoided with interventional therapy. However, there is no

high-level, high-quality evidence that its therapeutic efficacy and safety are superior to craniotomy clipping.

The specific operation process of craniotomy clipping treatment is as follows:

The main surgical instruments include microscopes and microscopic instruments, various types of aneurysm clips, and bipolar coagulation.

With the patient supine, the head is rotated 30 degrees in the opposite direction so that the zygomatic protrusion reaches the highest point of the surgical site. Due to the shallow position of the middle cerebral artery, during the craniotomy, the periosteum of the skull, lateral head muscle, and skull is squeezed from the subperiosteal to the front and lower parts, which shortens the time of the craniotomy. This prevents damage to the craniotomy, including the anterior branches of the facial nerve and the supraorbital nerve. In the internal carotid cistern, the bone hole on the junction of the coronary artery and the upper head line was pulled out, the flap was opened with a grinding knife, the sericoid bulge was removed, and the meninges were suspended, and the dura was cut into an arc. The sericin fissure was isolated under a microscope while opening to release cerebrospinal fluid to reduce intracranial pressure, and the middle cerebral artery was explored retrogradely along the internal carotid artery. Rupturing or hemorrhage may occur during dissection, and temporary clips are recommended to temporarily block the proximal parent artery, usually within 15 minutes. Choosing the appropriate aneurysm clip based on the size and orientation of the aneurysm neck. In the case of a large aneurysm, blood flow may be temporarily cut off. When the aneurysm sac remains, multiple clips can be used for clipping. Since the aneurysm is so large that complete clamping of one or more aneurysms is expected to be difficult, the aneurysm can be cauterized around the head of the aneurysm by bipolar low-frequency conduction, thus allowing the tumor to be clipped before resection. The temporary occlusion clip was released, and intraoperative fluoroscopy revealed that the parent artery was not occluded and no aneurysm was found. Bleeding was completely stopped before surgery, and the decision to replace the bone flap was based on intracranial pressure. Dehydration and decreased intracranial pressure, prophylaxis of vasospasm, hemostasis, anti-infectives, and other symptomatic and supportive treatments are routinely performed after surgery.

3.3. Principles and Models of Neural Networks. Assuming that there is a training sample set, $(a^{(i)}, b^{(i)})$, taking the supervised learning neural network as an example, a high-order complex nonlinear hypothesis model $g_{W,y}(a, b)$ is constructed by using the neural network algorithm, and the parameters W and y are the parameters of the function. As shown in Figure 5, the general complex neural network model is described first from the simplest single neuron consisting of only one "neuron".

In Figure 5, a_k, $(k = 1, 2, 3 \ldots)$ is the input vector and wk, $(k = 1, 2, 3 \ldots)$ is the weight of each input component. The function of the weight can be regarded as the connection strength of each component, and the input component can

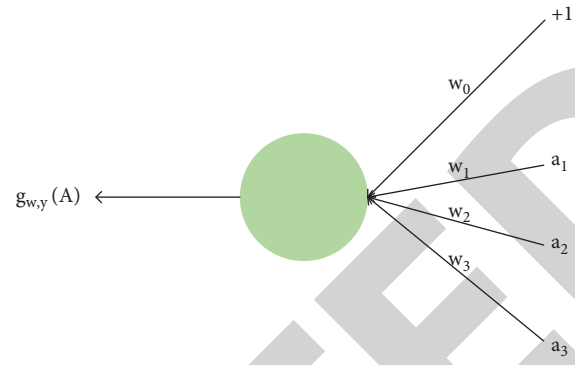

Figure 5: Sketch of the neuron model.

be enlarged or reduced by changing the size of the weight. d is the excitation function, also known as the activation function, the transfer function. The y value is an offset value, also called a threshold.

When using data sets a_1, a_2, a_3 as the input of the neuron model to train the network parameters, it is necessary to add a bias + 1 to it, and then use it as the input data of the neuron. Its output is expressed as

$$g_{w,y}(a) = g\left(W^T a\right) = d\left(\sum_{i=1}^{3} W_i a_i + y\right). \tag{1}$$

Among them, the function $d(\cdot)$ is an activation function, and there are many choices, and specific choices are made according to different data objects. In general, the sigmoid function is used as the activation function $d(\cdot)$ in the neural network

$$d(c) = \frac{1}{1 + \exp(-c)}. \tag{2}$$

In addition to the sigmoid function, the hyperbolic tangent function tanh, ReLu (Rectified Linear Units), etc., can be selected, and different activation functions can be selected according to the specific application background.

$$\begin{aligned} d(c) &= \tan g(c) = \frac{q^c - q^{-c}}{q^c + q^{-c}}, \\ d(c) &= \max(0, c). \end{aligned} \tag{3}$$

As shown in Figure 6, layer1 is the input layer of the network, layer3 is the output layer of the network, and the middle layer layer2 is the hidden layer. Respectively, adding a bias unit in addition to the output layer:

In the specific calculation, it is necessary to transpose the original feature matrix, so that the features of the same data object are all in the same row of the training matrix and then use matrix multiplication to calculate, namely

$$\begin{aligned} c^{(2)} &= \theta^{(l)} A^T, \\ x^{(2)} &= h\left(c^{(2)}\right). \end{aligned} \tag{4}$$

Since the $g_{\theta(a)}$ calculated by the forward propagation algorithm cannot obtain the best feature representation, it is

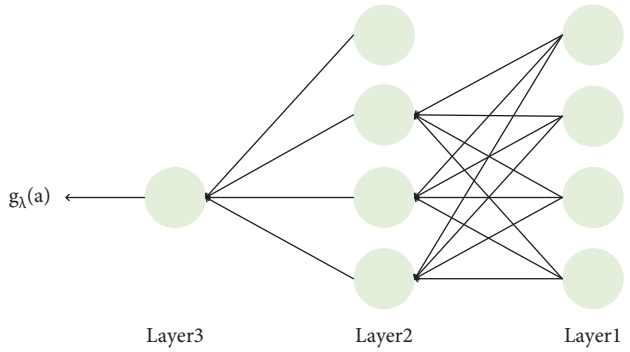

Figure 6: Three-layer neural network model diagram.

also necessary to adjust the weights of the network to obtain the best network model.

Here, it is necessary to optimize the network model by calculating the partial derivative $(\partial/\partial\theta_{ij}^{(l)})J(\theta)$ of the cost function $J(\theta)$ through the back-propagation algorithm, starting from the last layer of the network, and adjusting the weights of the network in reverse.

If the neural network model is a four-layer network training model, with $(A(1), B(1))$ as the training set of the network, the forward propagation algorithm is briefly described as:

$$\begin{aligned} x^{(1)} &= a, \\ c^{(2)} &= \theta^{(1)} x^{(l)}, \\ x^{(2)} &= h\left(c^{(2)}\right)\left(\text{add}x_0^{(2)}\right), \\ c^{(3)} &= \theta^{(2)} x^{(2)}, \\ x^{(3)} &= h\left(c^{(3)}\right)\left(\text{add}x_0^{(3)}\right), \\ c^{(4)} &= \theta^{(3)} x^{(3)}, \\ x^{(4)} &= h_\theta(a) = h\left(c^{(4)}\right). \end{aligned} \tag{5}$$

When the forward propagation is calculated, the back-propagation can be started based on the idea of the error (the deviation between the output value $x^{(4)}$ and the actual value $b(n)$ of the training set). The specific steps are as follows:

Taking the variable δ to represent the error, then

$$\delta^{(4)} = x^{(4)} - b. \tag{6}$$

Using formula (9) to calculate the error of the previous layer

$$\delta^{(3)} = \left(\theta^{(3)}\right)^T \delta^{(4)} * h'\left(c^{(3)}\right), \tag{7}$$

where $h\prime(c^{(3)})$ is the derivative of the S-function.

$$h\prime\left(c^{(3)}\right) = x^{(3)} * \left(1 - x^{(3)}\right). \tag{8}$$

Then continue to calculate the error of the next layer

$$\delta^{(2)} = \left(\theta^{(2)}\right)^T \delta^{(3)} * h\prime\left(c^{(2)}\right). \tag{9}$$

Because the input layer of the network uses raw data as input, its error is 0. Finally, calculate the partial derivative $(\partial/\partial\theta_{ij}^{(l)})J(\theta)$ of the cost function

$$\frac{\partial}{\partial\theta_{ij}^{(l)}} J(\theta) = x_j^l \delta_j^{l+1}. \tag{10}$$

The meanings of the superscript and subscript in the above formula: l represents the currently calculated network layer, and j represents the subscript value of the activation unit of the current calculation layer. This is also the next layer of additional characters for the jth input variable. i is represented as an additional character for neural network errors.

When $\Delta_{ij}^{(l)}$ is calculated, the error representation of the cost function can be expressed as:

$$\begin{aligned} D_{ij}^{(l)} &= \frac{1}{m}\Delta_{ij}^{(l)} + \lambda\theta_{ij}^{(l)} \text{ if } j \neq 0, \\ D_{ij}^{(l)} &= \frac{1}{m}\Delta_{ij}^{(l)} \text{ if } j = 0. \end{aligned} \tag{11}$$

4. Data Analysis Model Performance Test Experiment

4.1. Experiments with Unbalanced Data Sets. In three groups of class-imbalanced purely numeric data sets, the traditional SMOTE algorithm and the improved SMOTE algorithm based on the centroid were used to balance the data sets and use random forests to predict the classification. By comparing the two results, the effect of the improved SMOTE algorithm can be verified. The information of these three sets of data sets is described in detail in Table 1:

As can be seen from Table 1, since the imbalance rates of these three data sets are all low, it is difficult to use the random forest to classify and predict the sample data set if there are few samples from the minority class. Therefore, both the traditional SMOTE algorithm and the modified gravity-based SMOTE algorithm are used to improve the imbalance of the data set. The data set will then be classified and predicted according to the random forest. Then, the experimental results are compared and analyzed using classification accuracy, ROC curve (AUC field), and F1-measure evaluation metrics.

From Tables 2–4, it can be seen that.

(1) Due to the low imbalance rate of these three data sets, that is, due to the low proportion of the minority class in the entire data sample. Therefore, when using the random forest algorithm to directly classify these three data sets, although the classification effects of different data sets will change, it can be seen that the overall classification performance is not high.

(2) Using the traditional SMOTE algorithm to synthesize a small number of samples, after improving the imbalance rate of the data set, use the random forest algorithm to classify and predict the data set. The classification performance on the three data sets has improved by an average of 10%. The results show

Table 1: Detailed description of the three data sets.

Data set	Number of attributes	Number of samples	Minority class samples	Majority class samples	Nonequilibrium rate (%)
Glass	10	214	29	185	13.6
Adult	14	48842	12732	36110	26.1
Haberman	3	306	81	225	26.5

Table 2: Comparison of classification accuracy results.

Data set	Glass	Adult	Haberman
Original data set	0.6542	0.6669	0.6937
Traditional SMOTE processing	0.7319	0.7523	0.7875
Improved SMOTE handling	0.7748	0.7842	0.8273

Table 3: AUC area result comparison table.

Data set	Glass	Adult	Haberman
Original data set	0.6812	0.7043	0.7137
Traditional SMOTE processing	0.7511	0.7685	0.7963
Improved SMOTE handling	0.7885	0.7933	0.8273

Table 4: F1-Measure result comparison table.

Data set	Glass	Adult	Haberman
Original data set	0.7041	0.6829	0.7337
Traditional SMOTE processing	0.7897	0.8185	0.8212
Improved SMOTE handling	0.8159	0.8433	0.8533

Table 5: AUC area of different algorithms on different data sets.

Algorithm	Original data set	Outlier detection	Improve outlier detection
Tri-training	0.7692	0.8533	0.8704
K-means	0.7014	0.7473	0.7562
SVM	0.7852	0.8221	0.8312

that when the random forest algorithm is used to classify the data set, the imbalance of the data will have a certain impact on the classification results.

(3) Balancing the data set using the improved SMOTE algorithm and then using the random forest algorithm to classify and predict the data set. By using the traditional SMOTE algorithm, the classification performance of the three sets of data is further improved, with an average increase of 3–5%. This result shows that the quality of the new samples synthesized by the improved SMOTE algorithm is very good.

The original data set is balanced and transformed using the traditional SMOTE algorithm and the improved SMOTE algorithm. The experimental comparison results are shown in Figure 7.

Obviously, the average classification accuracy of the improved SMOTE algorithm is 4% higher than that of the traditional SMOTE algorithm, and the classification accuracy of the original data set without SMOTE algorithm is much lower. If the original data set is improved with the improved SMOTE algorithm, the AUC area will reach a maximum of 0.88, which is 0.04 higher than the traditional SMOTE algorithm, but the AUC area is only 0.72, using random forest to classify the original data set, but the classification performance is poor. This shows that using the traditional SMOTE algorithm to improve the imbalanced data set can improve the random forest classification performance. At the same time, the new samples synthesized by the improved SMOTE algorithm are of higher quality than the traditional SMOTE algorithm, and the classification effect of random forest is better.

4.2. Experiments to Improve the Efficiency of Algorithm Execution. To further demonstrate the impact of the improved algorithm in detecting global outliers, this paper uses a classification model to test the data sets processed by two different algorithms on the cerebral aneurysm test data set and analyzes and compares them through experiments. As in the supervised algorithm experiment, the labeled data in the data set are divided into two parts, one part is training data and the other part is test data, and the training data account for 70%. The difference is that the training data in the semi-supervised algorithm are also divided into two categories, one part is labeled data and the other part is unlabeled data. This division enables three different types of

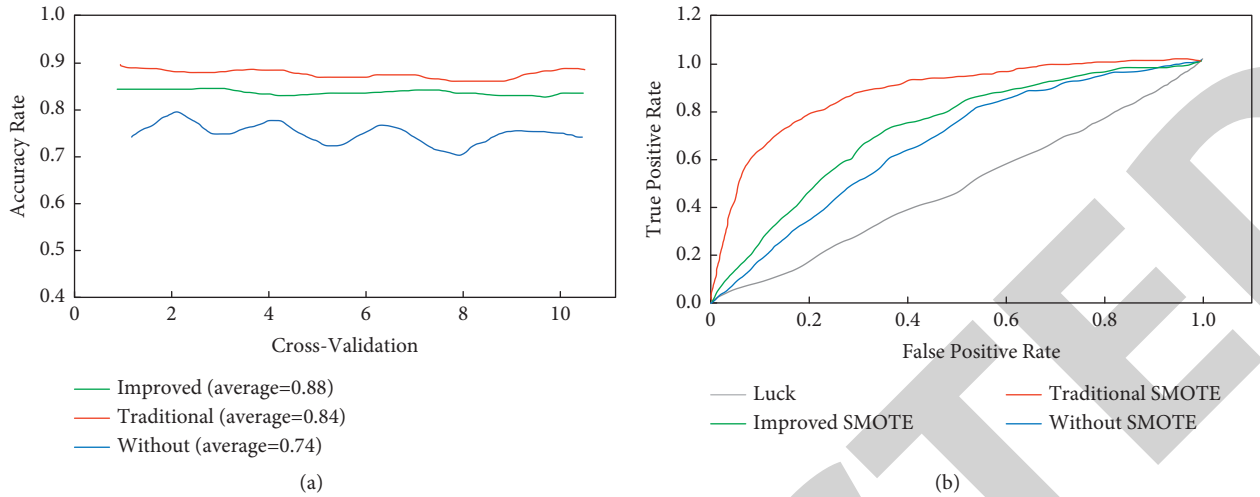

Figure 7: Comparison of experimental results. (a). Comparison of classification accuracy results when cv = 10. (b). Comparison of ROC curve results.

algorithms (supervised, unsupervised, and semi-supervised) to be trained and tested on the same data set, thereby improving the performance of the algorithms based on the performance analysis of different algorithms. The trained model is verified using the test set, and the experimental results obtained are shown in Table 5:

The outlier alignment before and after improvement, and the AUC change are shown in Figure 8.

It can be seen from Figure 8 that the increase in the data set size also brings more outliers, and the improved algorithm can identify outliers more comprehensively than the original algorithm. The analysis shows that the improved algorithm further improves the performance of subsequent data analysis. Overall, the improved algorithm is better than the original algorithm in terms of execution time and detection of outliers. Among them, the reduction of the algorithm execution time becomes more and more obvious with the increase of the data set, and the performance of the classification model has also been improved to varying degrees.

5. Results of Cerebral Aneurysm Clipping Treatment

5.1. Tumor Observation and Analysis. The current gold standard for the diagnosis of intracranial aneurysm is whole-brain angiography. In this study, the image data selected for constructing the 3D model of the intracranial aneurysm were head CTA image data. To verify whether DSA and CTA measurement results were statistically different, the imaging data (data acquisition is performed under the same field of view, and the long and short diameters of the aneurysm body and the width of the aneurysm neck are measured, respectively, of 50 patients with intracranial aneurysms confirmed by head CT angiography and whole cerebral angiography were collected. SPSS 17.0 statistical software was used for data analysis and processing, and $P < 0.05$ was considered statistically significant. The experimental results are shown in Figure 9.

The measured values of the longest diameter, shortest diameter, and aneurysm neck width on 3D-CTA and 3D-DSA obeyed normal distribution. There was no significant difference in the mean value of aneurysm (long diameter, short diameter, and width) measured between the two groups ($P < 0.05$).

5.2. Control Experiments. The data collected through the experiment optimize the clipping treatment of cerebral aneurysm based on the data analysis healthy model designed in this paper. To explore the clinical treatment effect and postoperative nursing effect of this treatment plan, a set of controlled experiments were designed in this paper. The experiment was divided into two groups, one group used the clipping treatment plan for cerebral aneurysm based on the data analysis healthy model designed in this paper and the other group adopted the traditional clipping treatment plan for cerebral aneurysm. The success rate of surgery and the degree of postoperative recovery are shown in Figure 10.

As can be seen from Figure 10, the surgical success rate of the clipping treatment for cerebral aneurysm based on the data analysis healthy model reached 92.93%. The traditional clipping treatment for cerebral aneurysm has a surgical success rate of only 71.09%. In contrast, the clipping treatment plan for cerebral aneurysm based on the data analysis health model designed in this paper has a 21.84% higher surgical success rate than the traditional clipping treatment plan for cerebral aneurysms. In contrast, the degree of postoperative recovery of the clipping therapy for cerebral aneurysm based on the data analysis healthy model recovered from 72.31% to 93.62% in the 5-month recovery period. The degree of postoperative recovery of the conventional clipping regimen for cerebral aneurysms only recovered from 65.41% to 73.41% in the 5-month recovery period. In summary, the surgical success rate and

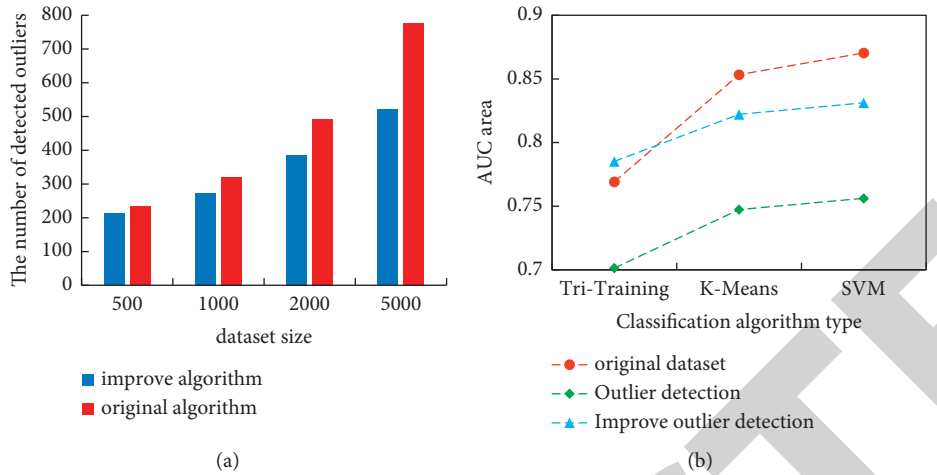

Figure 8: Experimental results. (a). Comparison of detection of outliers by the algorithm before and after improvement. (b). Comparison of AUC changes of different algorithms.

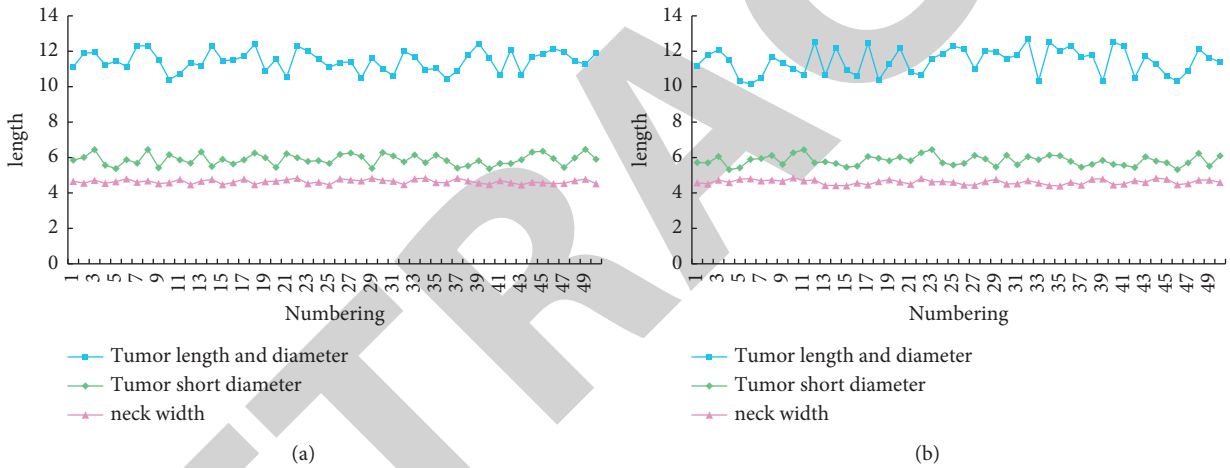

Figure 9: Results of tumor observation experiment. (a). DSA measurement results. (b). 3D-DSA measurement results.

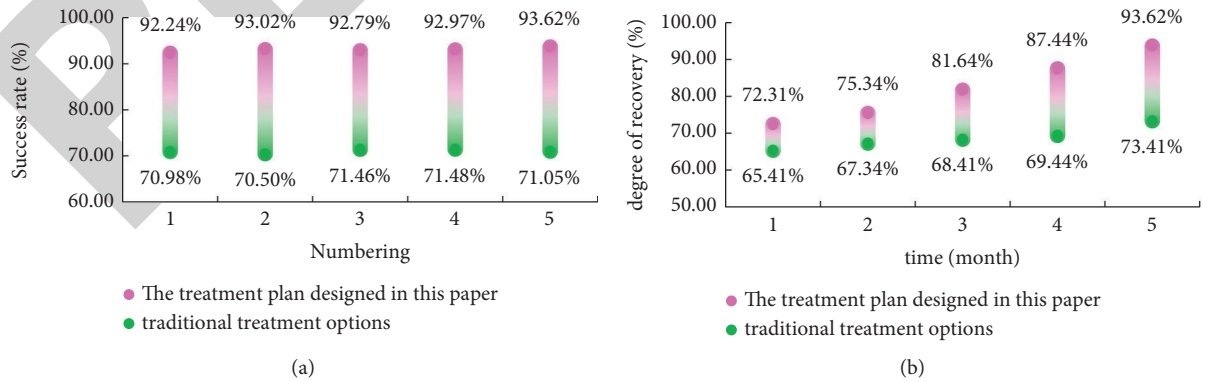

Figure 10: Comparison of results with traditional treatment regimens. (a). Surgical treatment success rate. (b). Degree of recovery after surgery.

postoperative recovery ability of the clipping treatment plan for cerebral aneurysm based on the data analysis health model designed in this paper have been greatly improved.

6. Conclusions

This paper mainly studies the treatment plan and clinical care of clipping surgery for cerebral aneurysm based on a data analysis health model. Therefore, this paper formulates a health model based on the data analysis in big data and the content of cerebral aneurysm and then conducts data analysis and training on the health model through deep learning in the neural network. Then, the clipping treatment of cerebral aneurysm was analyzed, and finally, the treatment plan of clipping treatment of cerebral aneurysm based on the data analysis health model was designed. To verify the performance of the data analysis health model, this paper designs experiments on unbalanced data sets and experiments to improve the efficiency of algorithm execution. The data obtained through the experiment are analyzed, and then the data analysis health model is optimized, and finally, the clinical experiment is concluded. Compared with the traditional clipping treatment of cerebral aneurysm, the surgical success rate and postoperative recovery of the clipping treatment plan for cerebral aneurysm based on the data analysis health model designed in this paper are significantly improved.

Data Availability

No data were used to support this study.

Conflicts of Interest

The authors declare that there are no conflicts of interest regarding the publication of this article.

References

[1] L. A. Tawalbeh, R. Mehmood, E. Benkhelifa, and H. Song, "Mobile cloud computing model and big data analysis for healthcare applications," *IEEE Access*, vol. 4, no. 99, pp. 6171–6180, 2017.

[2] X. Li, W. Zhao, J. Yang, C. Chen, H. Fan, and A. Li, "Risk factors and interventional therapy of hemorrhage in brain arteriovenous malformation associated with aneurysm," *Chinese Journal of Interventional Imaging and Therapy*, vol. 15, no. 4, pp. 204–208, 2018.

[3] B. Dong, A. Chien, M. Yu, Y. Jian, F. Viñuela, and S. Osher, "Level set based brain aneurysm capturing in 3D," *Inverse Problems and Imaging*, vol. 4, no. 2, pp. 241–255, 2017.

[4] A. V. Byndiu, M. Y. Orlov, M. Y. Orlov, and V. V. Cheburachin, "Influence of intraoperative rupture of brain aneurysm on results of surgical treatment in the early postoperative period," *Endovascular Neuroradiology*, vol. 23, no. 1, pp. 24–32, 2018.

[5] L. Xu, C. Jiang, J. Wang, J. Yuan, and Y. Ren, "Information security in big data: privacy and data mining," *IEEE Access*, vol. 2, no. 2, pp. 1149–1176, 2017.

[6] S. Athey, "Beyond prediction: using big data for policy problems," *Science*, vol. 355, no. 6324, pp. 483–485, 2017.

[7] Y. Zhang, M. Qiu, C.-W. Tsai, M. M. Hassan, and A. Alamri, "Health-CPS: healthcare cyber-physical system assisted by cloud and big data," *IEEE Systems Journal*, vol. 11, no. 1, pp. 88–95, 2017.

[8] J. C. Caicedo, S. Cooper, F. Heigwer et al., "Data-analysis strategies for image-based cell profiling," *Nature Methods*, vol. 14, no. 9, pp. 849–863, 2017.

[9] W. Xu, H. Zhou, N. Cheng et al., "Internet of vehicles in big data era," *IEEE/CAA Journal of Automatica Sinica*, vol. 5, no. 1, pp. 19–35, 2018.

[10] P. Singh and S. Aggarwal, "A cognitive research tendency in data management of sensor network," *International Journal of Wireless and Ad Hoc Communication*, vol. 3, no. 1, pp. 26–36, 2021.

[11] M. Rathore, A. Paul, A. Ahmad, B.-W. Chen, B. Huang, and W. Ji, "Real-time big data analytical architecture for remote sensing application," *IEEE Journal of Selected Topics in Applied Earth Observations and Remote Sensing*, vol. 8, no. 10, pp. 4610–4621, 2017.

[12] M. Ismail, N. El-Rashidy, and N. Moustafa, "Mobile cloud database security: problems and solutions," *Fusion: Practice and Applications*, vol. 7, no. 1, pp. 15–29, 2022.

[13] J. W. Xue, X. K. Xu, and F. Zhang, "Big data dynamic compressive sensing system architecture and optimization algorithm for internet of things," *Discrete and Continuous Dynamical Systems - Series S*, vol. 8, no. 6, pp. 1401–1414, 2017.

[14] K. Sharma, A. Shankar, and P. Singh, "Information security assessment in big data environment using fuzzy logic," *Journal of Cybersecurity and Information Management*, vol. 5, no. 1, pp. 29–42, 2021.

[15] M. Nasir and A. N. Al-Masri, "Multi-source heterogeneous ecological big data adaptive fusion method based on symmetric encryption, fusion," *Practice and Applications*, vol. 5, no. 1, pp. 08–20, 2021.

[16] Z. Lv, R. Lou, J. Li, A. K. Singh, and H. Song, "Big data analytics for 6G-enabled massive internet of things," *IEEE Internet of Things Journal*, vol. 8, no. 99, p. 1, 2021.

[17] Y. Wang, L. Kung, and T. A. Byrd, "Big data analytics: understanding its capabilities and potential benefits for healthcare organizations," *Technological Forecasting and Social Change*, vol. 126, pp. 3–13, 2018.

[18] H. Xing, A. Qian, R. C. Qiu, W. Huang, L. Piao, and H. Liu, "A big data architecture design for smart grids based on random matrix theory," *IEEE Transactions on Smart Grid*, vol. 8, no. 2, pp. 674–686, 2017.

[19] L. Kuang, F. Hao, L. T. Yang, M. Lin, C. Luo, and G. Min, "A tensor-based approach for big data representation and dimensionality reduction," *IEEE Transactions on Emerging Topics in Computing*, vol. 2, no. 3, pp. 280–291, 2017.

[20] C. S. Calude and G. Longo, "The deluge of spurious correlations in big data," *Foundations of Science*, vol. 22, no. 3, pp. 595–612, 2017.

[21] M. Janssen, H. van der Voort, and A. Wahyudi, "Factors influencing big data decision-making quality," *Journal of Business Research*, vol. 70, pp. 338–345, 2017.

Hindawi
Emergency Medicine International
Volume 2023, Article ID 9783534, 1 page
https://doi.org/10.1155/2023/9783534

Retraction

Retracted: Clinical Observation of Computer Vision Technology Combined with Music Therapy in the Treatment of Alzheimer's Disease

Emergency Medicine International

Received 28 November 2023; Accepted 28 November 2023; Published 29 November 2023

This article has been retracted by Hindawi, as publisher, following an investigation undertaken by the publisher [1]. This investigation has uncovered evidence of systematic manipulation of the publication and peer-review process. We cannot, therefore, vouch for the reliability or integrity of this article.

Please note that this notice is intended solely to alert readers that the peer-review process of this article has been compromised.

Wiley and Hindawi regret that the usual quality checks did not identify these issues before publication and have since put additional measures in place to safeguard research integrity.

We wish to credit our Research Integrity and Research Publishing teams and anonymous and named external researchers and research integrity experts for contributing to this investigation.

The corresponding author, as the representative of all authors, has been given the opportunity to register their agreement or disagreement to this retraction. We have kept a record of any response received.

References

[1] A. Zhang, Y. Yang, and M. Xu, "Clinical Observation of Computer Vision Technology Combined with Music Therapy in the Treatment of Alzheimer's Disease," *Emergency Medicine International*, vol. 2022, Article ID 2567340, 12 pages, 2022.

Hindawi
Emergency Medicine International
Volume 2022, Article ID 2567340, 12 pages
https://doi.org/10.1155/2022/2567340

Research Article

Clinical Observation of Computer Vision Technology Combined with Music Therapy in the Treatment of Alzheimer's Disease

Anshuang Zhang,[1] Yunpeng Yang,[2] and Ming Xu [1]

[1]*Department of Creative Arts Psychotherapy, Jeonju University, Jeonju 55068, Republic of Korea*
[2]*Information Office, Shandong Modern College, Jinan 250000, Shandong, China*

Correspondence should be addressed to Ming Xu; 2009040226@st.btbu.edu.cn

Received 6 May 2022; Revised 25 May 2022; Accepted 2 June 2022; Published 29 June 2022

Academic Editor: Hang Chen

With the world's population aging, Alzheimer's disease has attracted more and more attention as a common elderly disease. The clinical manifestations of cognitive function decline in Alzheimer's disease are mainly memory decline, which will seriously damage the patient's sense of self-worth. The purpose is to use the method of song recall to conduct individual music therapy intervention for Alzheimer's disease patients, to help Alzheimer's disease patients activate autobiographical memory, trigger positive emotions, improve behavioral symptoms, and delay the development of the disease. This paper proposes to combine computer vision technology with music therapy to obtain relevant data before and after intervention through the literature method, measurement method, case study method and experimental method. It helps AD patients to improve and slow down the forgetting and confusion of autobiographical memory, thereby enhancing the mood and cognition of AD patients. It observes the changes of AD patients before and after intervention by song recall and provides new ideas and practical basis for the application of music therapy in the field of Alzheimer's disease research. The experimental results showed that the subjects' autobiographical memory test (AMT) after 16 sessions of music therapy, from 12 points before the test to 14 points after the test. The scores were significantly positively correlated, and the improvement of autobiographical memory could improve the patient's orientation and memory.

1. Introduction

With the rapid development of China's social undertakings and economic construction, as well as the improvement of life expectancy and the change of fertility concept, China's aging problem has become increasingly prominent. Dementia, including Alzheimer's disease (AD), has become the fourth leading cause of death in the elderly. The cognitive decline of AD is mainly manifested as memory deterioration, and autobiographical memory decline is one of the core symptoms of AD patients. Due to the decline of autobiographical memory in AD patients, it can lead to confusion in patients' memory for objective facts and their own experiences. This leads to a decrease in self-identity and self-cognition impairment as well as emotional problems such as anxiety and depression, which reduce self-well-being.

The research on improving cognition and memory in patients with Alzheimer's disease through music therapy is relatively mature, while the research on music therapy in China in the field of Alzheimer's disease is relatively rare. It is possible to improve the memory ability of patients with Alzheimer's disease by learning to sing new songs, hoping to provide a reference for the treatment and research on the improvement of memory ability of patients with Alzheimer's disease in China. Music therapy is a convenient, effective, and least side effect method among nondrug treatments. Using music therapy as a nondrug intervention helps dementia patients activate memory, trigger positive emotions, and improve behavioral symptoms. It is of great significance

to the current life of dementia patients and can help patients delay the disease process, improve their quality of life, and increase their happiness in life.

The innovations of this paper are as follows: (1) this paper discusses the clinical status of memory in patients with Alzheimer's disease and the influence of music therapy on it, in order to make up for the lack of individual music therapy in the memory research of elderly Alzheimer's disease. It has important theoretical value for perfecting the music therapy system. (2) This article will use the intervention method of individual music therapy to investigate the status of his autobiographical memory after the intervention. It uses experimental scale data to understand the correlation between autobiographical memory and cognitive function and emotion in AD patients. (3) This paper further explores the improvement of autobiographical memory in elderly patients with Alzheimer's disease through individual music therapy and enriches the form of rehabilitation therapy for this population. It provides a reference intervention method and hopes to provide a more mature paradigm through research to provide reference for clinical practice in other regions.

2. Related Work

Music therapy is recommended for the treatment of Alzheimer's disease (AD), but only a few tools are available to measure musical skills in AD patients. Berruchon et al. developed an assessment tool, the MOT (Music Therapy Orientation Test), designed to assess patients' musical cognitive abilities and guide music therapy planning. They present guidelines and scoring terminology for all items as well as normal ranges for elderly patients. He performed MOT on 50 healthy elderly subjects (mean 74.3 ± 8.7 years) and 50 AD patients (mean 82.8 ± 8.0 years) [1]. Alzheimer's disease (AD) is increasingly common in the world's aging population, including a persistent decline in mental function and the onset of dementia. Music therapy has been shown to provide health benefits when used as an adjunct therapy. To determine whether music therapy can improve clinical outcomes in AD, Wang et al. analyzed its effects on cognitive function and behavior in patients with mild AD, combined with conventional medical therapy [2]. There is currently no cure for Alzheimer's disease, and patients can only rely on quality care to prolong their lives. Furthermore, the onset of pneumonia has been found to accelerate the progression of dementia and even lead to death. This has resulted in increased caregiver burdens and unbearable emotional stress for caregivers. The purpose of Lyu and Yuan's research is to build a smart dog music therapy and pneumonia detection system. He combines robotic dogs, cloud technology, multiagent systems, adaptive network-based fuzzy inference systems (ANFIS), web applications, and sensor technologies to provide care for Alzheimer's patients and help alleviate the difficulties faced by caregivers. After using the system, he interviewed nursing staff to determine its usefulness in nursing and whether it improved their overall nursing experience [3]. A previous systematic review of nonpharmacological interventions for clinical symptoms in patients with dementia demonstrated efficacy. It includes cognitive stimulation therapy (CST) for cognitive impairment, exercise therapy for activities of daily living, and music therapy and behavior management techniques for behavioral and psychological symptoms in people with dementia. It is also important for informal and formal caregivers to learn behaviour management techniques. Therefore, Kazui tried to promote the use of behavior management techniques in Japan. It is even more important for him to incorporate nonpharmacological interventions into the daily life of people with dementia and to prevent the development of BPSD [4]. Today, Alzheimer's disease (AD) is widely recognized as a real societal problem. The prevention and treatment of AD is a new challenge faced by the pharmaceutical industry, institutions, physicians, patients and their families. It is urgent to discover a new, safe way to cure this neurodegenerative disease and should not be delayed. Due to the multiple origins of this pathology, Piemontese and Hiremathad are currently strongly pursuing multitarget strategies, and they discuss novel structures aimed at improving the activity of classical AD targets [5]. Behavioral and psychological symptoms of target dementia (BPSD) are nearly universal in dementia, which occurs in more than 40 million people worldwide. BPSD presents considerable treatment challenges for prescribers and healthcare professionals. The aim of Kales et al. is to prioritize existing and emerging BPSD treatments in Alzheimer's disease (AD) as a whole, specifically targeting agitation and psychosis. The participant expert panel consisted of 11 international members with clinical and research expertise in BPSD management. Consensus results showed a clear preference for an escalating approach to managing BPSD in AD, starting with the identification of the underlying cause [6]. Music therapy has shown effectiveness in treating general behavioral and cognitive symptoms in people with various types of dementia to evaluate the effect of music therapy on memory in patients with Alzheimer's disease (AD). As of June 2017, Moreira et al. conducted a systematic search of PubMed (Medline), Cochrane Library, PsycINFO, and Lilacs databases. It included all randomized controlled trials using music interventions to assess memory in AD patients, identified 42 studies, and selected 24 studies. These studies showed the benefit of using music to treat memory impairment in AD patients [7]. Alzheimer's disease (AD) patients often experience behavioral and psychological symptoms of dementia (BPSD), which may include anxiety, depression, and agitation, resulting in reduced quality of life. Nagy et al.'s program assessed the perceived impact of this outreach on students. In addition to having a profound impact on residents, this outreach provides an excellent educational channel for students to build and practice skills in working with AD patient populations [8]. While building and practising skills for working with AD patient populations, the experimental effect is still not very clear.

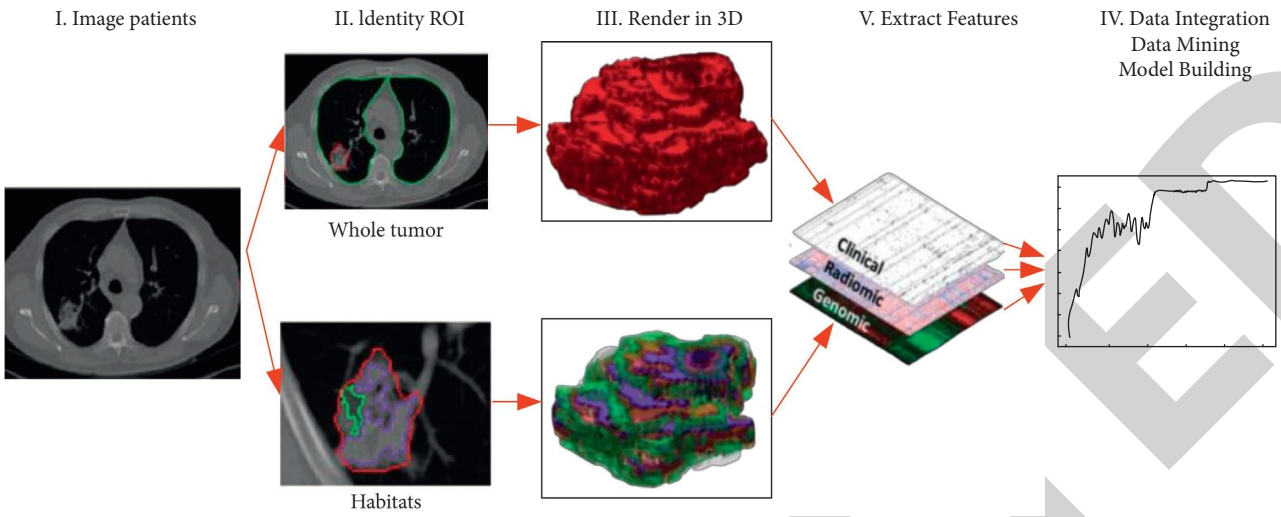

Figure 1: The application framework of radiomics methods in medical imaging.

Figure 2: The basic framework of the auxiliary diagnosis method of Alzheimer's disease based on radiomics.

3. Computer Vision-Aided Diagnosis Method for Alzheimer's Disease

3.1. Auxiliary Diagnostic Methods of Imaging Group. The term radiomics refers to a technology that extracts and analyzes high-throughput, high-dimensional quantitative features from medical images, and performs data mining and analysis on them [9]. The core key of radiomics is to extract a large number of high-order features from medical images. These radiomics signatures are not only effective in diagnosing diseases but also revealing deep-seated information hidden in images, which may help doctors to formulate accurate individualized medical plans and improve the accuracy of diagnosis, prognosis, and prediction. The application framework of the radiomics method in medical imaging is shown in Figure 1.

As shown in Figure 1, the method framework of radiomics can be roughly divided into four parts: (1) data collection and segmentation of regions of interest; (2) feature extraction; (3) feature analysis; (4) establishment of application models (such as classification diagnosis, or cancer cell metastasis prediction, etc.). The main part of the method flow framework used in this study will follow the traditional radiomics framework, which consists of image preprocessing, region of interest segmentation, feature extraction, and feature selection and application. Figure 2 shows the basic framework of a radiomic-based auxiliary diagnosis method for Alzheimer's disease.

As shown in Figure 2, in order to adapt to the characteristics of AD and MCI brain images, we mainly made improvements in three parts: image preprocessing, ROI segmentation, and feature selection.

3.2. Pathological Overview and Research Significance of Alzheimer's Disease. AD is a degenerative disease of the central nervous system with different clinical features depending on the age of onset and living environment. According to the report, the average survival time of AD patients is 8 years, and some can live for 20 years, and the course depends on the age of diagnosis and the health status of the patient. A schematic diagram of the normal brain and AD brain and the comparison between the two is shown in Figure 3.

As shown in Figure 3, as the brain structure of AD patients changes, their cognitive function gradually declines. Its main manifestations are memory loss from "near to far," confusion of time and space positioning, decreased language ability, and emotional problems such as depression and anxiety gradually appear, and other functions gradually deteriorate [10–12]. Until the final stage, there will be no self-recognition, and the schematic diagram of senile plaques and neurofibrillary tangles is shown in Figure 4.

As shown in Figure 4, from the mild to moderate stages of Alzheimer's disease, due to the formation of more plaques and tangles in the brain, patients' memory and thinking abilities are impaired, interfering with their normal work and life. At this stage, as AD progresses, the patient's personality and behavior will change, gradually losing sight of friends and family, and memory will deteriorate. Senile plaques and neurofibrillary tangles at various stages in AD patients are shown in Figure 5.

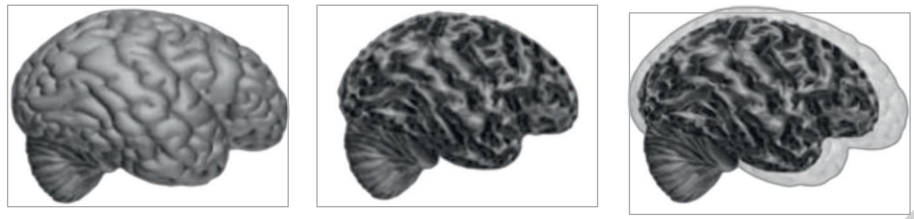

(a) (b) (c)

Figure 3: Schematic diagram of normal brain and AD brain and their comparison. (a) Normal brain. (b) Brains of AD patients. (c) Comparison of two.

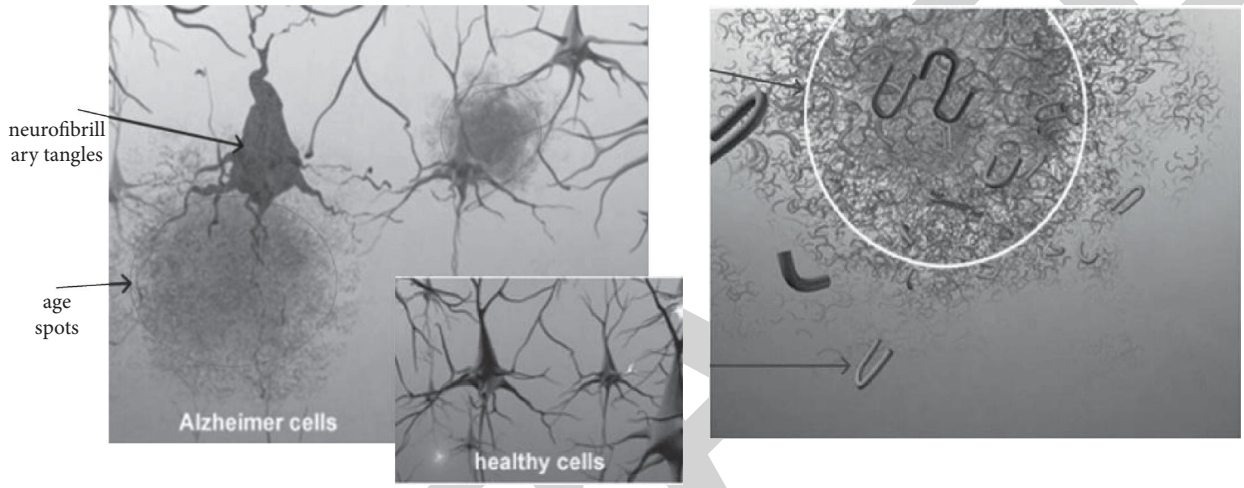

(a) (b)

Figure 4: Schematic diagram of senile plaques and neurofibrillary tangles. (a) Schematic diagram of senile plaque. (b) Schematic diagram of neurofibrillary tangles.

Figure 5: Senile plaques and neurofibrillary tangles in various stages of AD patients.

As shown in Figure 5, clinically Alzheimer's disease has an insidious onset, and the main symptoms are progressive memory impairment, cognitive dysfunction, personality changes, behavioral disturbances, speech impairments, and impairments in daily living activities. It is important to note that the symptoms are slowly progressive and irreversible [13].

3.3. Region of Interest Segmentation. Cognitive degenerative diseases do not have as clearly defined ROI as tumors. Therefore, for this topic, locating and segmenting ROIs related to AD and MCI is a key issue. The process framework of this research is shown in Figure 6.

As shown in Figure 6, the process framework of this study consists of five parts: image preprocessing, region of interest localization, feature extraction, feature selection, and support vector machine-based classification prediction [14–16]. In this topic, we intend to use two methods for ROI segmentation: voxel-based morphometry (VBM)-based methods and deep learning-based ROI segmentation.

3.3.1. Voxel Morphology Method. The VBM method is a classic comparative method of brain structure analysis, which locates relevant local brain regions by quantitatively calculating the density differences of brain tissue

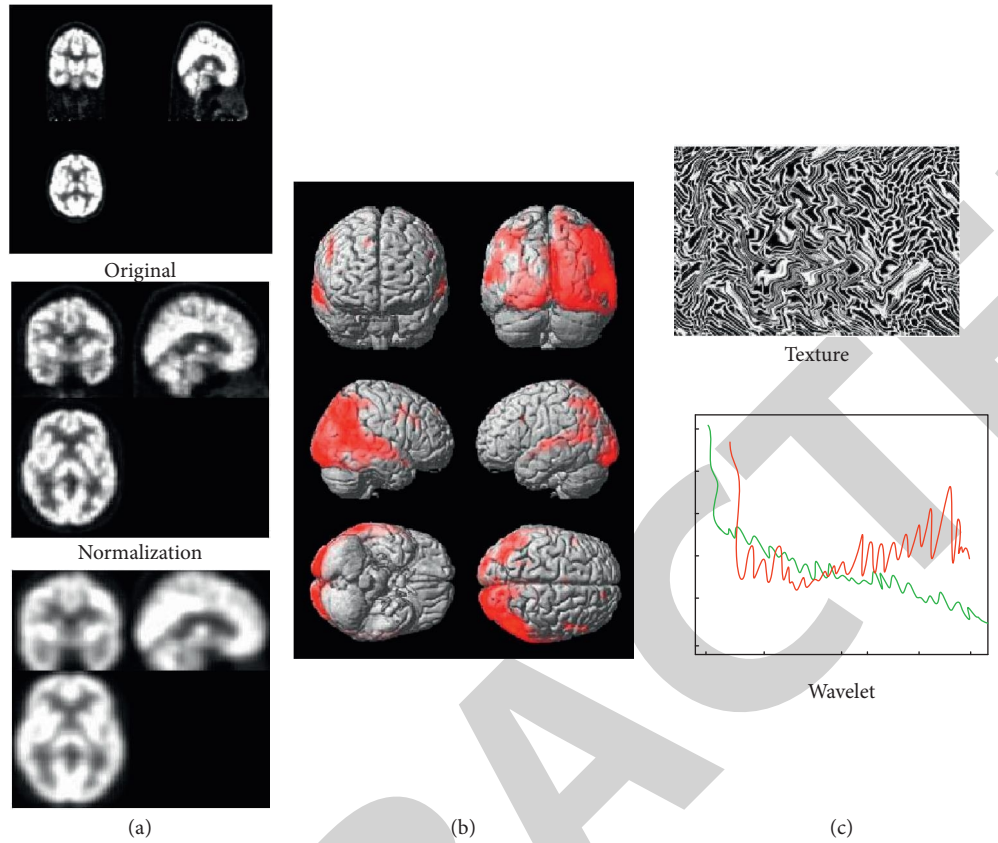

Figure 6: Research process. (a) Preprocessing. (b) Region of interest. (c) Feature extraction.

components between different groups of samples (such as AD and HC) [17, 18]. This method is data-driven and enables morphological analysis of the entire brain based on sample groups and discovers very subtle structural differences between groups, locating brain regions of interest associated with disease.

The commonly used models for this method include analysis of variance, paired t-test, and two-sample t-test. In this study, two-sample t-test was used as the model for VBM analysis. Let P denote the gray level of a voxel in brain imaging, which are independent of each other and obey a normal distribution with variance δ^2:

$$P_{qj} \sim N\left(\mu_q, \delta^2\right), \quad \begin{cases} q = 1, \ j = 1, 2, \ldots, n_1, \\ q = 2, \ j = 1, 2, \ldots, n_2. \end{cases} \tag{1}$$

The formula is equivalent to

$$\begin{cases} P_{qj} = \mu_q + e_{qj}, \\ e_{qj} \sim N\left(0, \delta^2\right), \end{cases} \quad \begin{cases} q = 1, \ j = 1, 2, \ldots, n_1, \\ q = 2, \ j = 1, 2, \ldots, n_2. \end{cases} \tag{2}$$

Among them, q is used to distinguish the sample group to which the sample belongs, j represents each sample in the sample group, and $x_{1qj}$and x_{2qj} are the number of samples in the two sample groups. If variables x_{1qj} and x_{2qj} are introduced, formula (2) can be expressed as

$$\begin{aligned} P_{qj} &= x_{1qj}\mu_1 + x_{2qj}\mu_2 + e_{qj}, \\ x_{1qj} &= \begin{cases} 1, & q = 1, \\ 0, & q = 2, \end{cases} \\ x_{2qj} &= \begin{cases} 0, & q = 1, \\ 1, & q = 2. \end{cases} \end{aligned} \tag{3}$$

The formula can be rewritten in matrix form:

$$Y = X\beta + e, \tag{4}$$

where $X{=}X = \begin{bmatrix} 1 & \ldots & 1 & 0 & \ldots & 0 \\ 0 & \ldots & 1 & 1 & \ldots & 1 \end{bmatrix}^T, \beta = [\mu_1, \mu_2]^T.$

Using the least squares method to estimate the parameters, we can get

$$\widehat{\beta} = \left(X^T X\right)^{-1} X^T Y = \left(\overline{\mu_1}, \overline{\mu_2}\right)^T, \tag{5}$$

$$\delta^2 = \frac{e^T e}{n_1 + n_2 - 2}. \tag{6}$$

In the model base, the null hypothesis H_0: $\mu_1 = \mu_2$ is proposed, specifically, there is no difference between the voxel gray mean values between the two sample groups. This null hypothesis can be tested by the following statistics:

$$S_1^2 = \frac{1}{n_1}\sum_{j=1}^{n_1}\left(P_{1j} - \overline{\mu_1}\right)^2, \tag{7}$$

$$S_2^2 = \frac{1}{n_2}\sum_{j=1}^{n_2}\left(P_{2j} - \overline{\mu_2}\right)^2. \tag{8}$$

If the calculated statistic of a voxel at a certain spatial position can reject the null hypothesis, it can be considered that the voxel at this spatial position is different between the two sample groups [19, 20]. By performing the analysis on all voxels of the whole brain, the positions of brain voxels that are significantly different between groups can finally be obtained, that is, the final determined ROI positions.

3.3.2. Feature Extraction. Previous radiomics studies have uncovered vast feature sets, including texture, shape, wavelet, intensity, and more. These features have good predictive, classification, and diagnostic capabilities for various types of cancers and tumors [21]. These features are mainly divided into global gray level features, texture features, shape features, and wavelet features (defined as texture, shape, and other features extracted from the image after wavelet filtering) [22–24]. The features included in this topic are introduced, mainly including global features, shape features, wavelet features (features extracted after wavelet filtering), and texture features based on four texture matrices including:

(1) Global Feature. Let P define a histogram with an isotropic voxel-sized volume $V(x, y, z)$. The $p(i)$ of the ith gray level of the normalized histogram is defined as

$$P(i) = \frac{P(i)}{\sum_{i=1}^{N_g} P(i)}. \tag{9}$$

(2) Gray-Level Co-Occurrence Matrix (GLCM). N_g represents the number of gray levels in P. By simultaneously summing the co-occurrence frequencies of all voxels with their 26 connected voxels in 3D space, all voxels (including edge voxels) are considered to be a central voxel [25]. Only GLCMs of size $N_g{}^*N_g$ are calculated for each volume V. Then, $p(i, j)$ for normalized GLCM is defined as follows:

$$p(i, j) = \frac{P(i, j)}{\sum_{i=1}^{N_g}\sum_{j=1}^{N_g} P(i, j)}. \tag{10}$$

Also, define the following parameters:

$$\mu_i = \sum_{i=1}^{N_g}\sum_{j=1}^{N_g} P(i, j), \mu_j = \sum_{j=1}^{N_g}\sum_{i=1}^{N_g} P(i, j), \tag{11}$$

$$\sigma_i = \sum_{i=1}^{N_g}(i - \mu_i)^2\sum_{i=1}^{N_g} P(i, j), \sigma_j = \sum_{j=1}^{N_g}\left(j - \mu_j\right)^2\sum_{i=1}^{N_g} P(i, j). \tag{12}$$

(3) Gray-Level Run-Length Matrix (GLRLM). N_g represents the number of gray levels in P, and L_r represents the longest run length of any gray level in the volume [26]. By accumulating all possible longest run lengths simultaneously in 13 directions in 3D space, a GLRLM of size $N_g{}^*L_r$ can be calculated for each volume V. The $p(i, j)$ of the normalized GLRLM is defined as follows:

$$p(i, j) = \frac{P(i, j)}{\sum_{j=1}^{N_g}\sum_{i=1}^{N_g} P(i, j)}. \tag{13}$$

Also, define the following parameters:

$$\mu_i = \sum_{i=1}^{N_g} i\sum_{j=1}^{N_g} P(i, j), \mu_j = \sum_{j=1}^{N_g} j\sum_{i=1}^{N_g} P(i, j), \tag{14}$$

$$p(i, j) = \frac{P(i, j)}{\sum_{i=1}^{N_g}\sum_{j=1}^{L_z} P(i, j)}. \tag{15}$$

The transformation function $T(X)$ in "Transformation" represents the spatial mapping relationship from the point on the reference image to the point on the image to be registered, as shown in Figure 7.

As shown in Figure 7, the degree to which the reference image matches the image to be registered is provided and a quantitative criterion is formed. This criterion can be optimized by the "optimizer" by finding the space defined by the passed parameters [27, 28].

$$\mu_i = \sum_{i=1}^{N_g} i\sum_{j=1}^{N_g} P(i, j), \mu_j = \sum_{j=1}^{L_z} j\sum_{i=1}^{N_g} P(i, j). \tag{16}$$

3.3.3. Neighborhood Gray-Tone Difference Matrix (NGTDM). In order to take into account the discretization length difference, when calculating the mean value of the surrounding voxel gray value, the voxel weight of $\sqrt{3}$ voxel distance around the central voxel is $\sqrt{3}$. The voxel weight of $\sqrt{2}$ voxel distance around the center voxel is $v2$, and the voxel weight of 1 voxel distance around the center voxel is 1. The definition of NGTDM is as follows:

$$P(i) = \begin{cases} \sum_{\text{allvoxelsÎ}\{N_i\}} \left|i - \overline{A_i}\right|, \text{if } N_i > 0, 0, \text{if } N_i = 0, \end{cases} \tag{17}$$

$$\overline{A_i} = \overline{A_i}(j, k, l) = \frac{\sum_{m=-1}^{m=1}\sum_{n=-1}^{n=1}\sum_{o=-1}^{o=1} w_{m,n,o}\cdot V(j+m, k+n, l+o)}{\sum_{m=-1}^{m=1}\sum_{n=-1}^{n=1}\sum_{o=-1}^{o=1} w_{m,n,o}}, \tag{18}$$

$$\text{where } w_{m,n,o} = \begin{cases} \frac{1}{\sqrt{2}}, & \text{if } |j-m| + |k-n| + |l-o| = 2, \\ \frac{1}{\sqrt{3}}, & \text{if } |j-m| + |k-n| + |l-o| = 3, \\ 0, & \text{if } V(j+m, k+n, l+o) \text{is undefiend.} \end{cases} \tag{19}$$

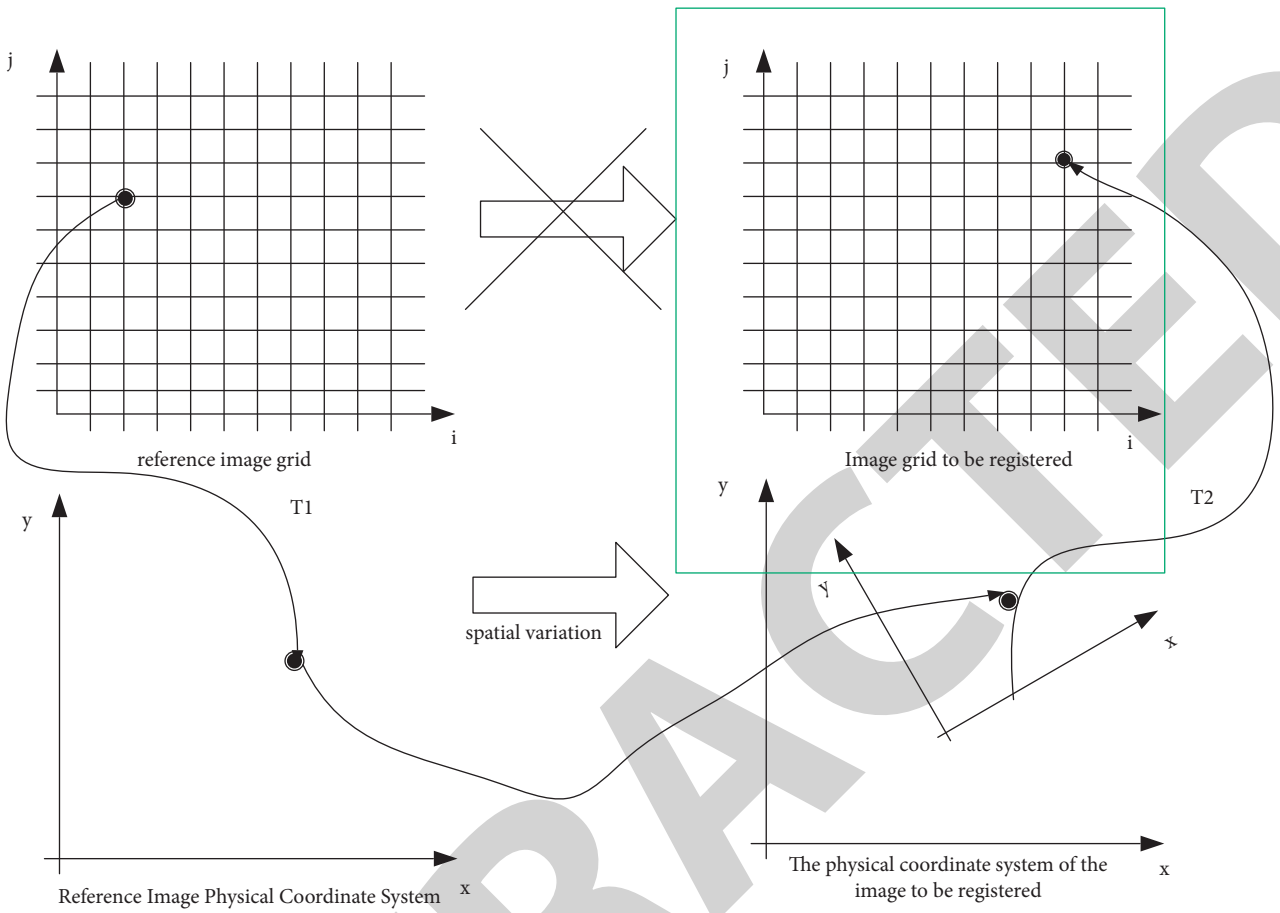

Figure 7: Spatial mapping relationship between points on the reference image and points on the image to be registered.

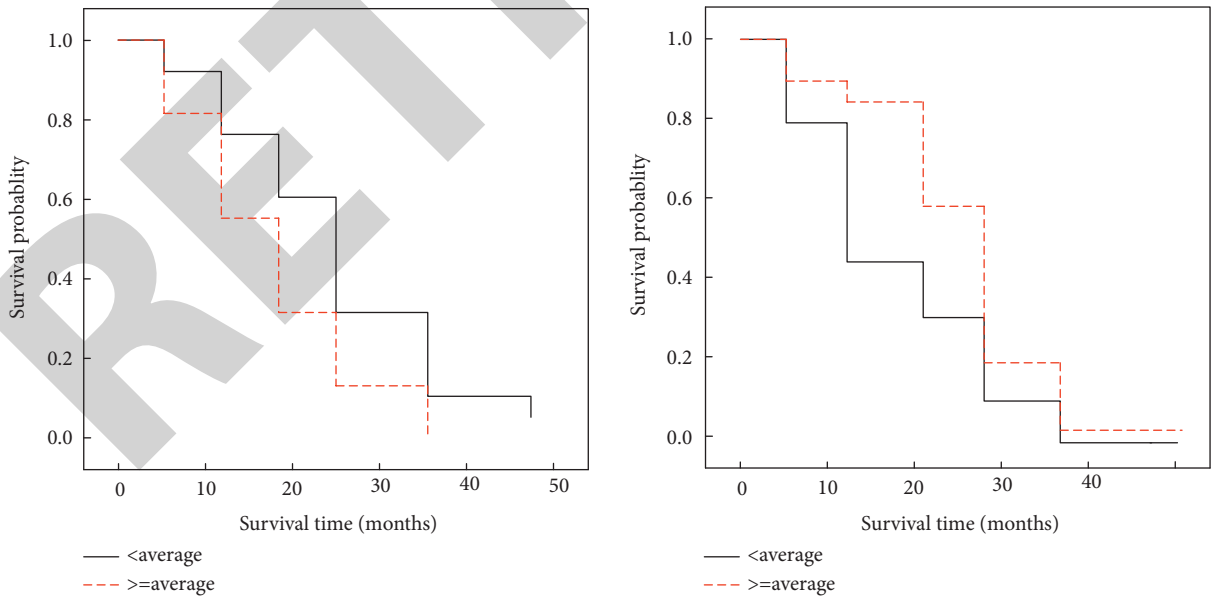

Figure 8: Two radiomics characteristic curves.

Also, define the following parameters:

$$n_i = \frac{N_i}{N}. \tag{20}$$

If a certain feature in the imaging at a certain time point is regarded as an initial feature, then the feature imaged at the kth time point is equivalent to the combination of the

Table 1: Basic information of the subjects.

	A	B	C
Gender	Female	Female	Male
Age	Eighty-one	Seventy-nine	Eighty-two
Degree of illness	Light	Light	Moderate
Basic family information	Two sons	One son and one daughter	1 son
Family economic situation	Preferably	Preferably	Preferably
Educational level	Undergraduate college	Primary school	Undergraduate college
Work before retirement	Math teacher	Self-employed person	Math teacher
Primary caregiver	Nursing workers	Nursing workers	Lover

feature at the $k-1$ time point and the initial test feature. The two radiomics characteristic curves are shown in Figure 8.

Figure 8 statistical test results show that their "high" and "low" values are closely related to the transformation process. Correspondingly, this means that MCI patients with "low" Left_2/3R_Contrast values and "high" Right_1/2R_Variance values are more likely to convert to AD at any point in time. The combination of k calculations of this kind of feature is formed, then the alpha coefficient of this kind of feature is

$$r_{xx'} = \frac{k\left(\overline{r_{ij}}\right)}{1+(k-1)\overline{r_{ij}}} = \left(\frac{k}{k-1}\right)\left(1-\frac{\sum_{i=1}^{k} S_i^2}{S_T^2}\right). \quad (21)$$

Among them, $\overline{r_{ij}}$ is the average value of the correlation coefficient between the same features in the k time point scans. $\sum_{i=1}^{k} S_i^2$ is the variance of the feature, and $r_{xx'}$ is the Cronbach's Alpha coefficient.

4. Clinical Observation of Music Therapy Intervention in Alzheimer's Disease

4.1. Experiment Objects. The subjects of this study were elderly people diagnosed with Alzheimer's disease in the memory impairment area of a nursing home in Wuhan, with an average age of about 80 years old. Through the recommendation of supervisors and nursing staff in the nursing home, interviews and assessments were conducted on 9 elderly people in the nursing area.

4.1.1. Inclusion Criteria. (1) According to the National Neurological Language Disorders and Stroke Institute AD and Related Disorders Association (NINCDS-ADRDA) criteria, the elderly who have been clinically diagnosed with mild or moderate AD. (2) Recommended by the senior care center supervisor and nursing staff, suitable for music therapy. (3) With the consent of the family members and the patient themselves, they can understand the test content, participate in music therapy voluntarily, and are willing to complete the pre- and post-test questionnaires.

4.1.2. Exclusion Criteria. (1) Patients with Lewy body disease, dementia, cerebrovascular disease, traumatic brain injury, and other diseases. (2) Serious agitation and violent tendencies. (3) Those with severe hearing impairment and unable to carry out speech dialogue. (4) The ability of daily living is normal, and the ability to talk independently.

According to the inclusion criteria and exclusion criteria, after understanding with supervisors and nursing staff, 3 people finally met the criteria. The basic situation is shown in Table 1.

As shown in Table 1, through interviews with 3 subjects and their families, they were all willing to participate in this experiment and signed the informed consent. All subjects received routine medication and nursing home care and daily activities. Through understanding with the family members of the three subjects, the hospital supervisor and their nursing staff, the research method is the following steps: measurement method, case study method, experimental method, and observation method.

(1) Measurement Method. The autobiographical memory test (AMT) and geriatric depression scale (GDS-15) were used to investigate the current situation and influencing factors of patients with Alzheimer's disease, and pre- and post-tests were conducted to collect the data.

(2) Case Study Method. The experimental design in the case study method is adopted, and the treatment plan is designed according to the individual according to the subject's hobby and familiarity with the song.

(3) Experimental Method. Combined with Autobiographical Memory Scale (AMT), and Simple Geriatric Depression Scale (GDS-15), individual music therapy programs for Alzheimer's disease patients were designed in advance. It uses the experimental method to intervene in the experimental subjects.

(4) Observation Method. During the intervention, the therapist and assistant therapist observed the subjects' response to music in real time, discussed after each treatment, and adjusted the treatment plan in time according to each observation.

(5) Statistical Analysis Method. SPSS 22.0 was used for data analysis and processing, and paired t-test was used to compare the difference of scores of different scales before and after treatment. Pearson correlation was used to analyze whether the scales were correlated.

4.2. Experiment Procedures

4.2.1. Experiment Time. The study period was from November 2021 to January 2022. During the whole process, each participant received 2 times a week, each time was 45 minutes, for a total of 16 times of music therapy.

4.2.2. Experimental Steps

(1) Confirm the patients with Alzheimer's disease in the nursing home, communicate with supervisors and nursing staff to select suitable candidates, communicate with suitable candidates and their families, and determine the subjects to be tested.

(2) Sign an informed consent form with the subjects, and use the GDS-15 Simple Geriatric Depression Scale and AMT Autobiographical Memory Test to conduct pretests on the subjects and retain the results as pretest data.

(3) Interview the subjects, according to the three important life stages (childhood, early adulthood, and old age) in autobiographical memory. The subjects were asked to learn about the favorite song styles and the song names or melodies that they could recall during the three periods. If the subject cannot recall, ask the supervisor of the area and the subject's nursing staff (the hospital will organize a singing activity once a week) or communicate with the subject's family. Learn about songs that are important to the subject. If it is still uncertain, it will be formulated according to the age of the song's release relative to the age of the subjects.

(4) According to the collected information, the key points are marked from the paper playlist made by the author. If the songs are not included in the paper playlist, they will be supplemented in time.

(5) Perform music therapy activities, each with a duration of 45 minutes, twice a week, for a total of 16 times. After the 14th session of music therapy, the 16th session of activity should be informed in advance to separate.

(6) After the last music therapy intervention, GDS-15 Simple Geriatric Depression Scale and AMT Autobiographical Memory Test were used for post-test again, and the results were retained as post-test data.

(7) SPSS22.0 was used for statistical analysis of pre- and post-test data.

(8) A return visit will be conducted one month later, and the supervisor and nursing staff will be asked whether there is a persistent change after the experimental intervention.

4.3. Design of Music Therapy Activity Plan. After understanding with the supervisors and nursing staff of the hospital, and after comprehensive evaluation and investigation in various aspects such as the actual situation of the subjects, a music therapy activity of 45 minutes is set each time, and a structured music therapy method is used to intervene. The schedule of music therapy activities is shown in Table 2.

Table 2: Schedule of music therapy activities.

Step	Activity name	Time (min)
Activity 1	Hello song	2
Activity 2	Song singing	10
Activity 3	Song memories	30

Table 3: Comparison before and after AMT treatment.

	Pretest	Post-test	t	P value
Forward	5 ± 2	5.33 ± 1.53	−1.000	0.423
Neutral	4.33 ± 2.08	4.33 ± 2.08	—	—
Negative direction	2.33 ± 1.16	5 ± 2.65	−3.024	0.094
Total score	11.67 ± 5.13	14.67 ± 16.11	−5.196	0.035*

It can be seen from Table 2 that due to the presence of memory confusion in the symptoms of AD, false memories are formed. Therefore, after each intervention, the recollection of the subject should be confirmed with family members, supervisors, and nurses in time to determine whether the subject's recollection in this intervention is correct and recorded. In the following activities, observe whether the subjects can recall the correct memory.

5. Clinical Observation Results

5.1. Comparison of Scores in the AMT Autobiographical Memory Test before and after Treatment. The differences in AMT scores before and after treatment were compared by using paired t-test, as shown in Table 3.

It can be seen from Table 3 that the total score of autobiographical memory test was significantly different before and after treatment ($P = 0.035 < 0.05$), and the total score of autobiographical memory test after treatment was significantly higher than that before treatment. Positive and negative lexical retrieval autobiographical memory scores improved after treatment, but did not reach a significant difference. Neutral lexical retrieval autobiographical memory scores were unchanged. The author used paired t-test to compare the difference of GDS-15 scores before and after treatment as shown in Table 4.

It can be seen from Table 4 that the statistical analysis and comparison of the pre- and post-test data of the GDS-15 showed that each $P > 0.05$, and the comparison of the pre- and post-test data did not reach a significant difference. Therefore, it cannot be proved by data analysis that after the intervention of song recall, the situation has been significantly improved.

5.2. Intervention Results

5.2.1. Song Recall Improves Autobiographical Memory in Alzheimer's Disease. The author classified the pre- and post-test data of the three subjects according to the retrieval of

Table 4: Comparison of scores between groups before and after GDS-15 treatment.

	Pretest	Post-test	t	P value
Directional force	4.67 ± 3.79	5 ± 3	−0.378	0.742
Memory	2.67 ± 0.58	3 ± 0	−1.000	0.423
Attention and computational power	3.33 ± 1.16	3 ± 2	0.500	0.667
Recall ability	0.33 ± 0.58	0 ± 0	1.000	0.423
Language ability	8.33 ± 1.16	8.33 ± 0.56	0.000	1.000
GDS-15 total score	19.33 ± 5.51	19.33 ± 4.73	0.000	1.000

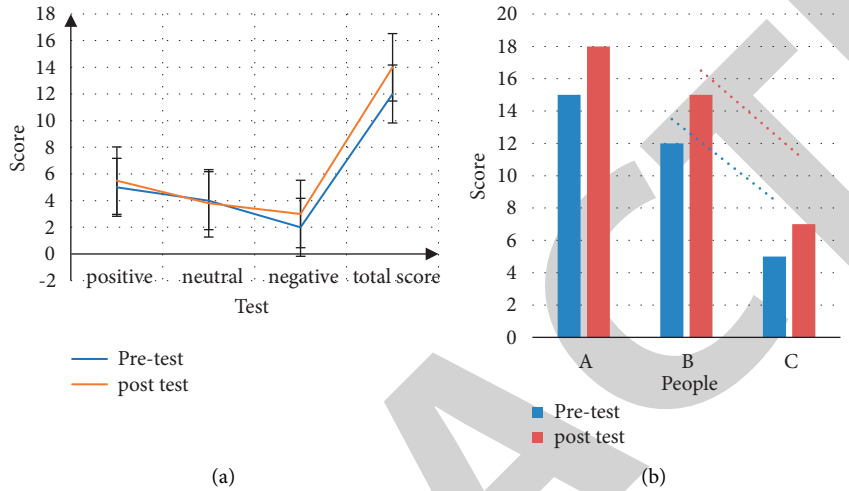

Figure 9: Autobiographical memory test and autobiographical memory total score. (a) Comparison of autobiographical memory test scores before and after the test. (b) Total autobiographical memory scores of 3 subjects.

three different emotional words in the autobiographical memory test. It calculated the average scores of the three emotions and the final total score before and after the test, and the total score of the autobiographical memory test, and made a statistical chart to compare the longitudinal and lateral comparisons before and after treatment as shown in Figure 9.

As shown in Figure 9, the scores of the subjects' corresponding emotions before and after treatment can be compared longitudinally, and the score differences between different emotions before and after treatment can be compared horizontally. Before the experimental intervention, the three subjects had lower autobiographical memory scores on negative emotional word retrieval. The difference in the autobiographical memory scores between neutral words and positive words was smaller, but both were higher than those of negative emotional words. After 16 times of music therapy, although the increase is not large, it can be seen from the figure that the positive word retrieval score is still the highest. Negative emotional word retrieval scores increased most significantly, surpassing neutral word retrieval memory scores. However, the differences in the pre- and post-test comparisons of neutral words changed little. Therefore, it can be concluded that after the experimental intervention, the improvement of autobiographical memory with emotional color is more obvious, and the retrieval of autobiographical memory recalling negative emotions has the most obvious change.

Due to the influence of symptoms, the episodic memory in the autobiographical memory of AD patients will develop semantically with the progress of the disease process, which will lead to confusion and forgetting of important past experiences, living places, and even their own identities. According to the degree of AD, the damage degree of autobiographical memory also has obvious differences. The difference between subjects A and B in the pretest is small, and the score of subject C is lower. After the experiment, the post-test scores of the three members are all higher than the pretest, and the improvement of subject A is more obvious.

5.2.2. Song Recall Improves Other Cognitive Conditions in Alzheimer's Disease. According to the clinical symptoms of AD, with the development of the disease course, the cognitive function of patients gradually declines. The decline in cognitive function is mainly manifested as orientation problems, difficulty concentrating, and decreased thinking ability and calculation ability. Even highly educated patients are unable to complete addition and subtraction within 100, and their language skills are unable to write or speak a paragraph because they cannot find familiar words. The author used the GDS-15 scale to measure the orientation, memory, attention, and calculation ability, recall ability, and language ability of the patients before and after treatment, and calculated the average scores of the

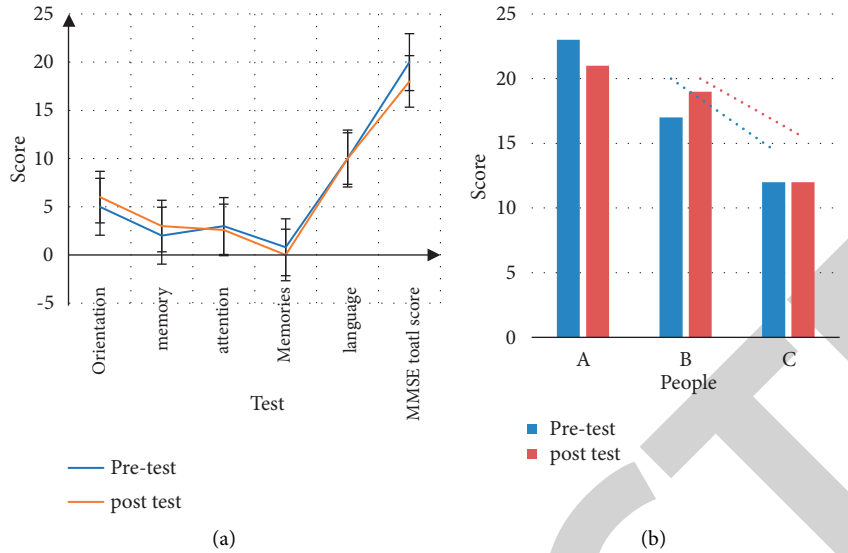

Figure 10: GDS-15 total score and GDS-15 scale total score. (a) GDS-15 total score and comparison of each subitem before and after the test. (b) GDS-15 total score of 3 subjects.

three groups of patients before and after treatment, and made a statistical chart. It compares the pre- and post-test changes in each cognitive domain of the subjects vertically through visual illustrations, and compares the degree of change in different cognitive domains horizontally. In order to have a clearer understanding of the changes of intervention before and after treatment for each subject, as well as patients in different periods of symptoms, this paper uses the changes in cognitive status after experimental intervention. It made a statistical graph of the total GDS-15 scores of the three subjects for comparison. The GDS-15 total score and the GDS-15 scale total score are shown in Figure 10.

As shown in Figure 10, in this intervention, the scores of the GDS-15 scale fluctuated less before and after the test, and the patients' orientation and memory scores after the intervention were better than those before the treatment, showing an upward trend. Therefore, it can be deduced that AD patients recall past experiences, characters, and other related events after the intervention of song recall. It also has a positive impact on the orientation and memory of reality, which has also been demonstrated in the correlation analysis of this conclusion. It can be clearly seen that according to the different stages of AD, the degree of cognition is in a downward trend, and the A subject is in the mild stage. Therefore, the pre- and post-test scores are higher, while the C subject is in the middle stage, and the pre- and post-test scores are the lowest.

6. Conclusion

The research object of this paper is Alzheimer's disease patients. The main clinical symptom of Alzheimer's disease is memory loss. It involves the decline of autobiographical memory leading to a semantic development of episodic memory. The forgetting of various life events in their own life will make AD patients gradually forget the familiar people and things around them. Due to the loss of episodic memory, the patient's language skills decline, making it difficult to find words when speaking. As a result, they will become reluctant to communicate, and the lack of social skills will lead to further deterioration of the patient's symptoms, thus creating a vicious circle. For most elderly people, they like to sing and listen to music, so the use of music therapy is more acceptable to AD patients. By using the intervention of song recall, it allows the therapist to have the opportunity to interact with the patient. Through this experiment, the intervention method of song recall has a good effect on the improvement of autobiographical memory in AD patients. It can improve the cognitive symptoms of AD patients to a certain extent, relieve the negative emotions of patients, and improve the positive emotions to some extent. Due to the influence of the experimental environment and conditions, only 3 AD patients in a nursing home were selected for intervention in this experiment, and the sample size of the study was small. Therefore, the obtained data results and analysis have limitations. In the future experimental process, a large sample method can be adopted to make the experimental data more convincing.

Data Availability

The data that support the findings of this study are available from the corresponding author upon reasonable request.

Conflicts of Interest

The authors declare no potential conflicts of interest with respect to the research, authorship, and/or publication of this article.

Hindawi
Emergency Medicine International
Volume 2023, Article ID 9789785, 1 page
https://doi.org/10.1155/2023/9789785

Retraction

Retracted: Effects of Amiodarone and Esmolol for Heart Rate and Cardiovascular Changes

Emergency Medicine International

Received 8 August 2023; Accepted 8 August 2023; Published 9 August 2023

This article has been retracted by Hindawi following an investigation undertaken by the publisher [1]. This investigation has uncovered evidence of one or more of the following indicators of systematic manipulation of the publication process:

(1) Discrepancies in scope
(2) Discrepancies in the description of the research reported
(3) Discrepancies between the availability of data and the research described
(4) Inappropriate citations
(5) Incoherent, meaningless and/or irrelevant content included in the article
(6) Peer-review manipulation

The presence of these indicators undermines our confidence in the integrity of the article's content and we cannot, therefore, vouch for its reliability. Please note that this notice is intended solely to alert readers that the content of this article is unreliable. We have not investigated whether authors were aware of or involved in the systematic manipulation of the publication process.

In addition, our investigation has also shown that one or more of the following human-subject reporting requirements has not been met in this article: ethical approval by an Institutional Review Board (IRB) committee or equivalent, patient/participant consent to participate, and/or agreement to publish patient/participant details (where relevant).

Wiley and Hindawi regrets that the usual quality checks did not identify these issues before publication and have since put additional measures in place to safeguard research integrity.

We wish to credit our own Research Integrity and Research Publishing teams and anonymous and named external researchers and research integrity experts for contributing to this investigation.

The corresponding author, as the representative of all authors, has been given the opportunity to register their agreement or disagreement to this retraction. We have kept a record of any response received.

References

[1] H. Wang, F. Lei, L. Bai, and A. Zhang, "Effects of Amiodarone and Esmolol for Heart Rate and Cardiovascular Changes," *Emergency Medicine International*, vol. 2022, Article ID 9197369, 7 pages, 2022.

Hindawi
Emergency Medicine International
Volume 2022, Article ID 9197369, 7 pages
https://doi.org/10.1155/2022/9197369

Research Article

Effects of Amiodarone and Esmolol for Heart Rate and Cardiovascular Changes

Hao Wang,[1] Fengping Lei,[2] Lei Bai,[3] and Anping Zhang [4]

[1]*Department of Cardiology, The First People's Hospital of Li County, Longnan 742500, Gansu, China*
[2]*Department of Pharmacy, Pharmacy, Xi'an Aerospace General Hospital, Xi'an 710199, Shaanxi, China*
[3]*Nursing Department, Children's Hospital of Xi'an Jiaotong University, Xi'an 710002, Shaanxi, China*
[4]*Department of Vascular Surgery, Lanzhou University Second Hospital, Lanzhou 730030, Gansu, China*

Correspondence should be addressed to Anping Zhang; 201105081@email.poe.edu.pl

Received 25 March 2022; Accepted 26 May 2022; Published 27 June 2022

Academic Editor: Hang Chen

Objective. To probe into the effects of amiodarone and esmolol for heart rate disorders and myocardial infarction. *Methods.* 76 cases of cardiopathy in our hospital from July 2019 to October 2021 were analyzed for myocardial infarction. The control group applied amiodarone treatment. Blood pressure, treatment effect, adverse reactions, myocardial marker levels, electrocardiogram, and heart function indicators were compared. *Results.* There were no statistical differences in two groups of diastolic pressure ($P > 0.05$). The analysis of the systolic pressure in the study group was greater than the control group ($P < 0.05$); The effective rate was higher than that of the control group ($P < 0.05$); the incidence of adverse reactions in the study group and control group was 28.95% and 31.58%, respectively, and there was no statistically significant difference between groups ($P > 0.05$). The standards of markers were significantly reduced compared with the control group ($P < 0.05$). After treatment, the heart rate of the two groups was significantly reduced, and the QT intervals were significantly shortened. But compared with the control group, reduction was larger in the research group ($P < 0.05$). Compared with the control group, the resolution rate was higher ($P < 0.05$). After treatment, the two groups of quality of life were significantly increased, and compared with the control group, the increase in the quality of life of the study group was greater ($P < 0.05$). *Conclusion.* Application of amiodarone and esmolol joint treatment can improve the quality of life, improve the level of heart function and myocardial marker, and can reduce Q-T intervals and prognosis. Therefore, amiodarone and esmolol treatment is worth promoting.

1. Introduction

Myocardial infarction is a clinically multiexpressive cardiovascular disease. This disease often induces a variety of complications such as arrhythmias, usually in the early stage of myocardial infarction. [1]. In patients with myocardial infarction combined with arrhythmia, the contraction frequency in the room is significantly increased, the corresponding amount of myocardial oxygen is increased, and the symptoms of myocardial necrosis are significantly aggravated. This is the main cause of sudden death and cardiogenic shock in patients [2]. There is a significant decrease in myocardial infarction combined with arrhythmia patients, and it has seriously threatened the safety of patients [3]. Clinical use of amiodarone is effective up to 80%, but because amiodarone has a classic drug loss, there are short absorption, half-life, and individual differences [4]. More and more studies have confirmed that esmolol can also be used in the clinical treatment of patients with myocardial infarction and can be rapidly alleviated by the compression symptoms of the ventricular period, and the early sudden death rate is significantly reduced, which is conducive to the improvement of patient prognosis [5].

The study selected 76 cases of myocardial infarction from July 2019 to October 2021 from our hospital, and the two drugs—amiodarone and esmolol—were used and therapeutic effects and electrocardiogram variations were analysed and reported as follows.

2. Data and Methods

2.1. General Information. 76 cases of of myocardial infarction were chosen from our hospital from July 2019 to October 2021.

2.1.1. Inclusion Criteria. (1) Compliance with arrhythmias and cardiomyopathy; (2) 48 hours of morbidity; (3) treatment compliance height; (4) did not accept other beta-adrenergic receptors to block drugs before the study by the patient.

2.1.2. Exclusion Criteria. (1) Cardiological shock, room transmission block, loss of compensatory heart failure, and (4) malignant tumor. The study group ($N = 38$) included 26 males and 12 females, with an average BMI of $22.57 \pm 3.25\,kg/m^2$, average disease of 3.12 ± 1.07, and average age of 46.34 ± 2.35 years. The control group ($N = 38$) included 25 males, 13 females, with an average BMI of $22.54 \pm 3.24\,kg/m^2$, average disease of 3.13 ± 1.05, and an average age of 46.34 ± 2.33 years. This study has been approved by the ethical department. The general data difference between the two groups is statistically significant ($P > 0.05$).

2.2. Method

2.2.1. Control Group. 5% glucose solution and 20 ml + 3 mg/kg amiodarone injection (national medicine quasi-word H20044923, production enterprise: Shandong Fang Ming Pharmaceutical Group Co., Ltd.) were used, and each intravenous injection time is 10 min. 7 days were required for treatment, and 6 months of prognosis for patients was required.

2.2.2. Study Group. Apply amiodarone treatment based on the treatment of the control group, and the treatment method is the same. Intravenous injection volume is $0.5\,mg/(kg{\cdot}min^{-1})$ Ezolol (National Medicine Standard H19991059, Production Enterprise: Qilu Pharmaceutical Co., Ltd.), for about 1 min, and the next vein drop control is controlled at $0.05\,mg/(kg{\cdot}min^{-1})$. After 4 minutes, continue to maintain the dose, and if the effect is not ideal, it can be gradually incremented by $0.05\,mg/(kg{\cdot}min^{-1})$, but the optimal dose should be controlled at $0.3\,mg/(kg{\cdot}min^{-1})$. Internally, a total of 7D continuous treatment is received, and the patient was followed up for 6 months prognosis.

3. Observation Indicator

3.1. Blood Pressure [6]. Blood pressure coupling was used for to patient's blood pressure measurement. Attention should be paid to the patient before the measurement, and patients need to sit still for 5 minutes. The right arm blood pressure was measured by a corrected standard desktop hydraulometer, and the 5th sound of Coriolis is the diastolic pressure. The first sound of Coriolis is the systolic pressure, and the blood pressure is measured. Measurement time interval for each time is 1-2 min, and each blood pressure average is taken as the final value of blood pressure.

3.2. Treatment Effect [7]. Nominal symptoms disappear, and electrocardiogram was normal. On further aggravation, the heart rate change is small. Efficiency = (productive + effective) number/total number × 100%.

3.3. Adverse Reactions. The incidence of adverse reactions is inversely relative to the prognosis of patients.

3.4. Myocardial Marker Level [8]. 5 ml of venous blood was drawn and centrifuged at 3000 rpm to obtain serum for N-terminal B-type sodium peptide (NT-probnp), creatine kinase uNP (CK-MB), and myocardial index testing such as hypermorriamalone protein T (HS-TNT). The operation is strictly carried out in accordance with the manufacturer's instructions.

3.5. ECG Indicator [9].

3.6. Sinus Turpoli Rate. The patients were followed up for 6 months, the sinus rhythm infusion volume was counted, and the transparency rate was calculated to judge the prognosis of patients.

3.7. Heart Function Indicators. These include left ventricular ejection fraction (LVEF), left ventricular diastolic volume (LVEDV), and left ventricular shrinkage vector (LVESV) 3 indicators.

3.8. Quality Rating [10]. Apply SF-36 meter to assess the patient's social, psychological, emotional, and cognitive functions, forming a total of 100 points. The score is proportional to the quality of life.

3.9. Statistical Method. Utilized statistical SPSS22.0 software for data analysis, such as data compliance with normal distribution. Counting data are compared with the comparison ratio and the intergroup differential analysis selection card test. Measurement data (metric ± standard difference) indicate that $P < 0.05$ is statistically significant.

Table 1: Two sets of blood pressure contrast (N, %).

Group	Count	Shuxo pressure (mmHg)	Sealing pressure (mmHg)
Control group	38	70.47 ± 8.65	103.33 ± 10.51
Research group	38	70.53 ± 10.93	116.83 ± 11.34
T	—	1.685	17.524
P	—	>0.05	<0.05

Table 2: Comparison of two groups of treatment results.

Group	Count	Descendant	Efficient	Invalid	Efficient
Control group	38	20 (52.63)	10 (26.32)	8 (21.05)	78.95%
Research group	38	27 (71.05)	9 (23.68)	2 (5.26)	94.74%
X^2	—	—	—	—	6.325
P	—	—	—	—	<0.05

Table 3: Analysis of two groups of preparation.

Group	Count	Liver function injury	Nausea	Sinus arrhythmia	Phlebitis	Hypotension	Incidence
Control group	38	3 (7.89)	2 (5.6)	2 (5.26)	2 (5.26)	2 (5.26)	28.95%
Research group	38	2 (5.26)	3 (7.89)	2 (5.26)	2 (5.26)	3 (7.89)	31.58%
X^2	—	—	—	—	—	—	6.325
P	—	—	—	—	—	—	<0.05

4. Results

Two groups of blood pressure comparison between the two sets of diastolic pressure show significant differences ($P > 0.05$) (Table 1).

Two groups of treatment effect contrast control group, the effective rate of the study group was 78.95%, 94.74%, and the research team was efficient than the control group ($P < 0.05$) (Table 2).

The incidence of adverse reactions in two groups was 28.95% and 31.58%, and there was no statistically significant difference in comparison between groups ($P > 0.05$) (Table 3).

After comparison of myocardial markers in two groups, the levels of myocardial markers in the two groups were significantly reduced, but compared with the control group, the research group decreased larger and has statistical significance ($P < 0.05$) (Figure 1).

Two sets of electrocardiogram indicators were compared and showed that the heart rate of two groups was significantly reduced, and the QT intervals were significantly shortened. But compared with the control group, the research group decreased larger and has statistical significance ($P < 0.05$) (Figure 2).

Sinus rhythm removal rate of two groups: compared to the control group, the resolution rate of the group was higher ($P < 0.05$) (Figure 3).

Heart function indicators of two sets were compared to the control group; the LVEDV and LVESV indicators were lower; and the LVEF indicator was higher ($P < 0.05$) (Figure 4).

After the comparison of two groups of quality of life, the two groups of life rating increased significantly, compared with the control group, and the quality of life rating increased larger ($P < 0.05$) (Figure 5).

5. Discussion

The data show that the incidence population tends to be young, in which unhealthy lifestyle is the main induced factor [11]. At present, the use of amiodarone treatment can be improved on the symptoms of paroxysmal tachycardia, and it is also suitable for myocardial infarction treatment [12]. Amiodarone is an antiarrhythmic first-line drug, which can block the L-type Ca^{2+}, Na^{+}, and K^{+} channel, sinus, and junction zone, and the in-room conduction speed is significantly slowed [13]. Another study confirmed that amiodarone will be self-regulatory inhibition of sinus nodules and room interruption; the potential time history is prolonged, which is conducive to the mitigation of ventricular fibrillation and atrial fibrillation; and the clinical treatment is higher [14].

Esmolol is a selective β1-receptor blocker. At present, it is increasingly widely used in clinical treatment of cardiopathy with myocardial infarction, and it is of great significance to the improvement of heart function indicators [15]. The QTCD reflects the unevenness of myocardial positivity, but amiodarone is not only used for the transfer but also for sinus regulation. The drug can be extended to the time course of each of the cardiomyoma action potentials and can be excited to return. The process is eliminated, and the speed is significantly slowed [16]. The drug also plays an important role in vascular expansion and improving blood flow. After treatment, the patient's heart rate is significantly reduced [17]. Nevertheless, since the auxiliary of the amiodate is relatively long, the index is large, and it is necessary to reduce the amount of amiodarone in order to reduce the degree of liver function. Esmolol will compete in the binding site of catechine phenol, the function of β1-receptor is inhibited, the movement and resting heart rate is slow, and myocardial consumption is significantly reduced

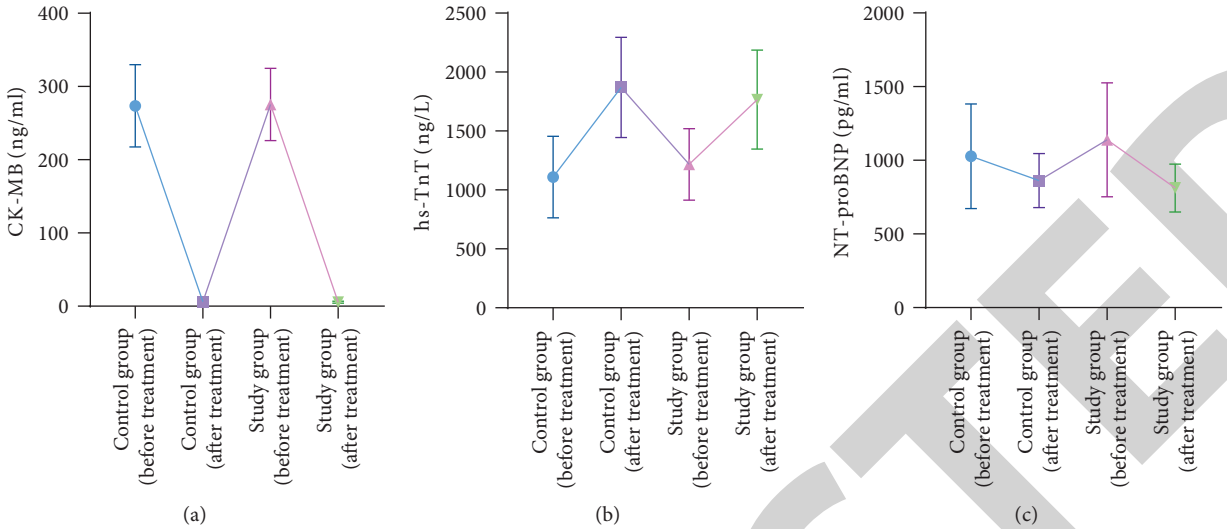

Figure 1: Experimental result.

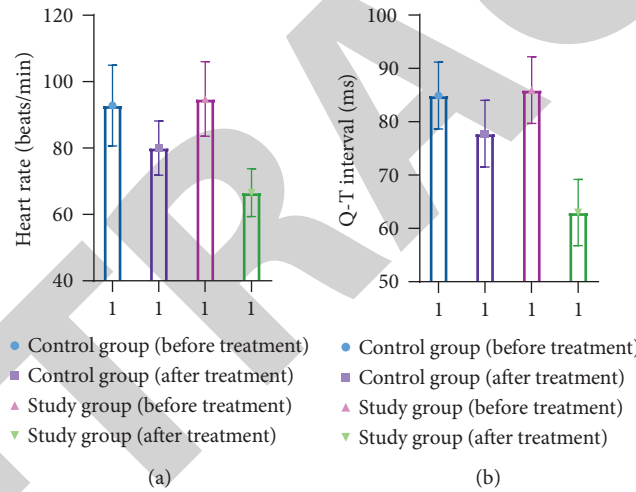

Figure 2: Experimental result.

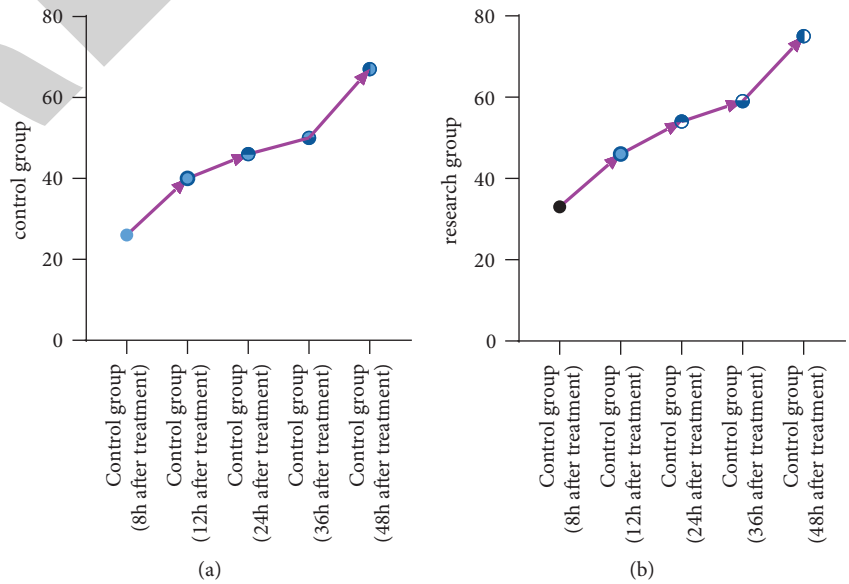

Figure 3: Experimental result.

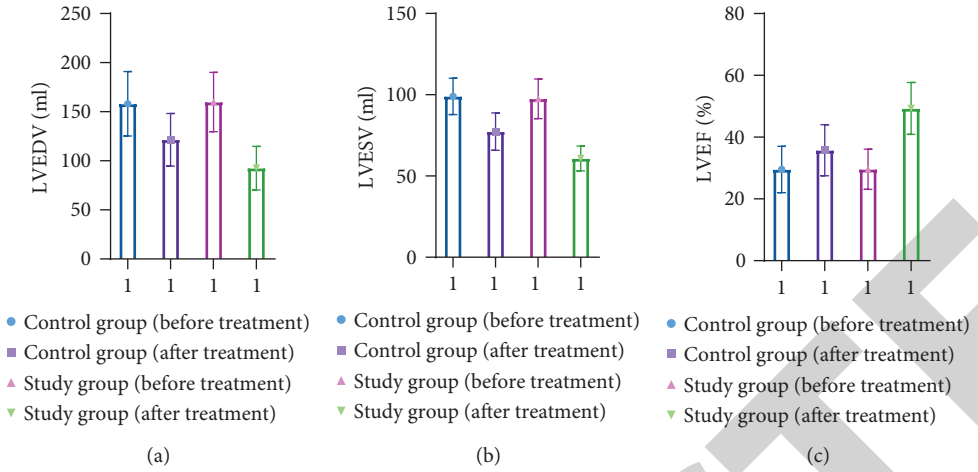

Figure 4: Experimental result.

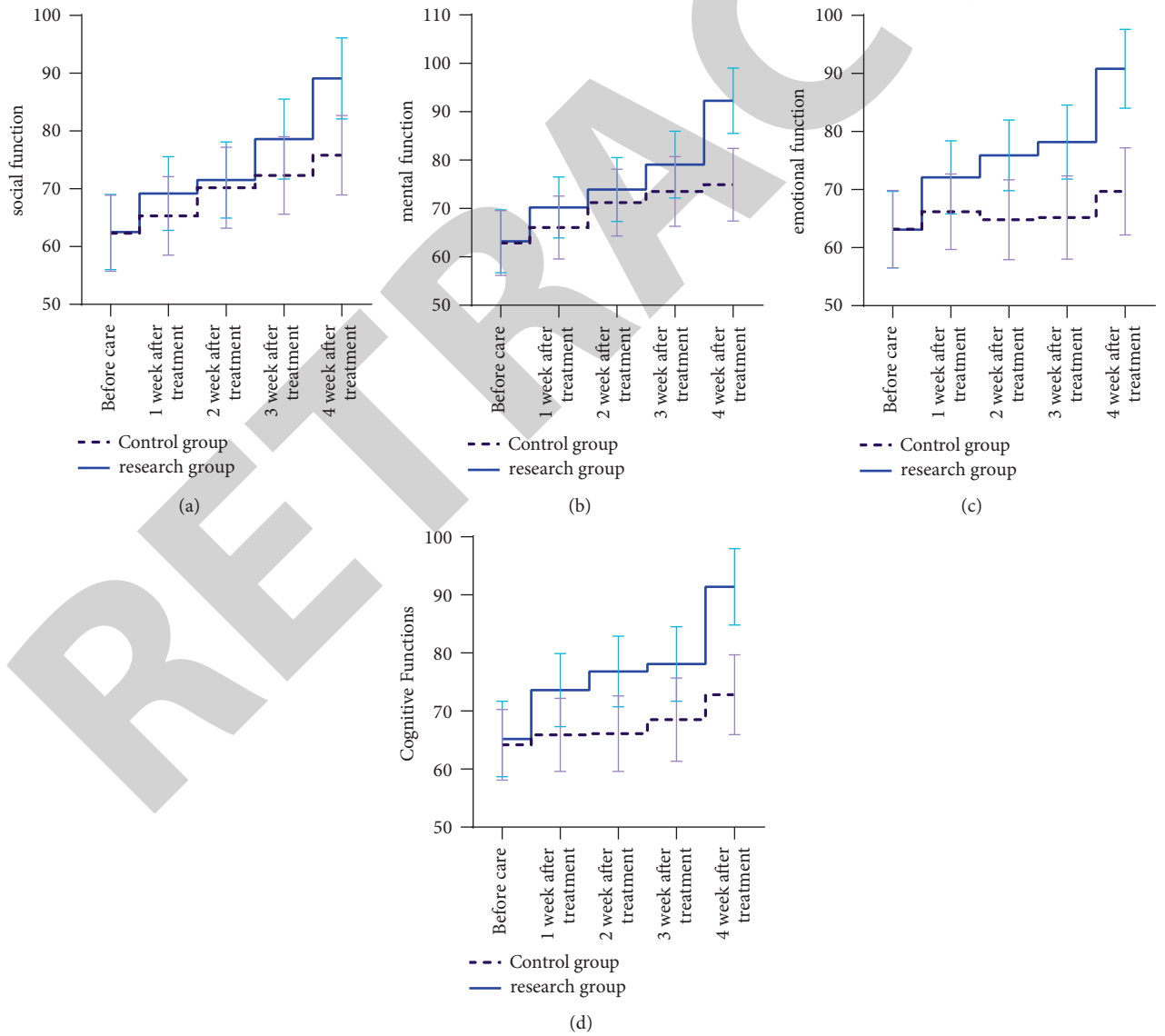

Figure 5: Experimental result.

[18]. Esmolol is shorter, and it is possible to control atrial fibrillation, which is conducive to ventricular rate control [19]. The study analyzed the influence of the two drugs—esmolol and amiodarone—on patients. The results showed that, after treatment, the two sets of heart rate were significantly reduced, and QT intervals were significantly shortened, but compared with the control group, the research group reduced the magnitude ($P < 0.05$). The results confirmed that amiodarone is safe and effective. Expanding the blood vessels around the coronary artery increased coronary blood flow, and the myocardial oxygen consumption is significantly reduced. In addition, the results showed that the effectiveness of the control group and the study group was 78.95% and 94.74%, and the efficiency of the study group was higher than the control group, but the two groups of adverse reactions were not significantly different. The results confirmed that combined drugs can improve the treatment efficiency, but does not increase adverse reactions, which facilitates the improvement of patient prognosis. And, amiodarone and esmolol have higher safety.

Studies use esmolol treatment, while improving myocardial oxygen consumption, and it can reduce blood pressure. After treatment, the patient's systolic pressure is significantly improved, which is conducive to the clinical symptoms of patients, which can be used as arrhythmia combined with myocardial infarction preferred treatment [20, 21]. Esmolol can reduce the peripheral resistance of coronary artery, which can effectively control the blood volume, while weakening myocardial contraction ability and reducing myocardial infarction, and can improve patient social, psychological, emotional, and cognitive functions. The results showed that, after treatment, the two sets of quality of life were significantly increased, compared with the control group, and the increase in the quality of life of the study group was greater ($P < 0.05$). The results confirmed that amiodarone treatment is conducive to the patient's return to society and can alleviate the negative emotions of patients, and patients can face disease with good attitudes, which is conducive to follow-up treatment and intervention. On the basis of amiodone treatment, the treatment of Esmolol is synergistic, and it is possible to compensate the drug for amiodarone, and it will enhance the drug efficacy [14, 22]. The study showed that, after treatment, the two sets of myocardial markers and cardiac function levels were significantly improved, but the research team improved the improvement. The study was consistent with the study of Liu [23]. However, as arrhythmia is a faster progression, the results will be affected by many factors such as research objects, so subsequent research needs to increase sample quantity and multicenter research and analyze two drugs to prognosis on patients' value and mechanism.

In summary, the use of amiodarone and esmolol in patients with myocardial infarction can improve the quality of life, improve the level of heart function and myocardial marker, and can reduce Q-T intervals and prognosis. Therefore, amiodarone and esmolol treatment is worth promoting [24, 25].

Data Availability

The raw data supporting the conclusions of this article will be made available by the authors, without undue reservation.

Conflicts of Interest

The authors declare that they have no conflicts of interest regarding this work.

References

[1] Y. Lu, Y. Duan, Li Zhi et al., "Efficacy of esmolol combined with amiodarone in patients with acute cardiac arrhythmia combined with rapid myocardial infarction and its effect on ECG," *Journal of Clinical Internal Medicine*, vol. 37, no. 11, pp. 31–34, 2020.

[2] N. Scaturo, E. Shomo, and M. Frank, "Current and investigational therapies for the treatment of refractory ventricular fibrillation," *American Journal of Health-System Pharmacy*, vol. 79, no. 12, pp. 935–943, 2022.

[3] "Drugs for atrial fibrillation," *Medical Letter Drugs Therapeutics*, vol. 61, no. 1580, pp. 137–144, 2019.

[4] K. Milojevic, A. Beltramini, M. Nagash, A. Muret, O. Richard, and Y. Lambert, "Esmolol compared with amiodarone in the treatment of recent-onset atrial fibrillation (RAF): an emergency medicine external validity study," *Journal of Emergency Medicine*, vol. 56, no. 3, pp. 308–318, 2019.

[5] E. Pontali, S. Volpi, A. Signori et al., "Efficacy of early anti-inflammatory treatment with high doses of intravenous anakinra with or without glucocorticoids in patients with severe COVID-19 pneumonia," *Journal of Allergy and Clinical Immunology*, vol. 147, no. 4, pp. 1217–1225, 2021.

[6] National Institute of Diabetes and Digestive and Kidney Diseses, *Livertox: Clinical and Research Information on Drug-Induced Liver Injury*, National Institute of Diabetes and Digestive and Kidney Diseses, Bethesda, Maryland, USA, 2012.

[7] F. Ye, W. Jiang, Y. Wang, W. Lin, H. Chen, and B. Pan, "Aggravation of atrial arrhythmia by amiodarone during the perinatal period: a case report," *Medicine*, vol. 98, no. 7, 2019.

[8] Z. Bao and X. Li, "The efficacy and safety analysis of puerarin injection and compound Danshen injection combined with amiodate in the treatment of acute myocardial infarction," *Chinese and Western medicine combined cardiovascular and cerebrovascular disease magazine*, vol. 18, no. 6, pp. 924–928, 2020.

[9] A. Chowdhury, B. Fernandes, T. M. Melhuish, and L. D. White, "Antiarrhythmics in cardiac arrest: a systematic review and meta-analysis," *Heart Lung & Circulation*, vol. 27, no. 3, pp. 280–290, 2018.

[10] H. Wang, Y. Zhang, F. Xin et al., "Calcium-induced autonomic denervation in patients with post-operative atrial fibrillation," *Journal of the American College of Cardiology*, vol. 77, no. 1, pp. 57–67, 2021.

[11] C. Mackin, E. S. Dewitt, K. J. Black et al., "Intravenous amiodarone and sotalol impair contractility and cardiac output, but procainamide does not: a langendorff study," *Journal of Cardiovascular Pharmacology and Therapeutics*, vol. 24, no. 3, pp. 288–297, 2019.

[12] M. Kohlhauer, S. Dawkins, A. S. Costa et al., "Metabolomic profiling in acute ST-segment–elevation myocardial infarction identifies succinate as an early marker of human ischemia–reperfusion injury," *Journal of the American Heart Association*, vol. 7, no. 8, Article ID e007546, 2018.

Hindawi
Emergency Medicine International
Volume 2023, Article ID 9821382, 1 page
https://doi.org/10.1155/2023/9821382

Retraction

Retracted: Effect of Bodybuilding and Fitness Exercise on Physical Fitness Based on Deep Learning

Emergency Medicine International

Received 8 August 2023; Accepted 8 August 2023; Published 9 August 2023

This article has been retracted by Hindawi following an investigation undertaken by the publisher [1]. This investigation has uncovered evidence of one or more of the following indicators of systematic manipulation of the publication process:

(1) Discrepancies in scope
(2) Discrepancies in the description of the research reported
(3) Discrepancies between the availability of data and the research described
(4) Inappropriate citations
(5) Incoherent, meaningless and/or irrelevant content included in the article
(6) Peer-review manipulation

The presence of these indicators undermines our confidence in the integrity of the article's content and we cannot, therefore, vouch for its reliability. Please note that this notice is intended solely to alert readers that the content of this article is unreliable. We have not investigated whether authors were aware of or involved in the systematic manipulation of the publication process.

In addition, our investigation has also shown that one or more of the following human-subject reporting requirements has not been met in this article: ethical approval by an Institutional Review Board (IRB) committee or equivalent, patient/participant consent to participate, and/or agreement to publish patient/participant details (where relevant).

Wiley and Hindawi regrets that the usual quality checks did not identify these issues before publication and have since put additional measures in place to safeguard research integrity.

We wish to credit our own Research Integrity and Research Publishing teams and anonymous and named external researchers and research integrity experts for contributing to this investigation.

The corresponding author, as the representative of all authors, has been given the opportunity to register their agreement or disagreement to this retraction. We have kept a record of any response received.

References

[1] M. Sun and L. Wang, "Effect of Bodybuilding and Fitness Exercise on Physical Fitness Based on Deep Learning," *Emergency Medicine International*, vol. 2022, Article ID 3891109, 2 pages, 2022.

Hindawi
Emergency Medicine International
Volume 2022, Article ID 3891109, 12 pages
https://doi.org/10.1155/2022/3891109

Research Article

Effect of Bodybuilding and Fitness Exercise on Physical Fitness Based on Deep Learning

Manman Sun[1] and Lijun Wang[2]

[1]*College of Sports and Leisure, Xi'an Physical Education University, Xi'an, 710000, Shaanxi, China*
[2]*College of Physical Education, Shaanxi Normal University, Xi'an, Shaanxi 710000, China*

Correspondence should be addressed to Lijun Wang; wlj0713@snnu.edu.cn

Received 31 March 2022; Revised 9 May 2022; Accepted 1 June 2022; Published 21 June 2022

Academic Editor: Hang Chen

With the rapid development of society and economy, people's living standards are improving day by day, and increasingly attention is paid to physical health, which has set off a fitness upsurge. The purpose of this paper was to analyze the impact of bodybuilding exercise on physical fitness based on deep learning. It provides a reference for fitness enthusiasts to choose scientific and targeted exercise methods, and provides a theoretical basis for the promotion of bodybuilding and fitness. This paper first gives a general introduction to deep learning and adds image segmentation technology to design experiments for bodybuilding and fitness. The experiment was divided into groups A and B, and control group C. In this paper, recurrent neural network and gated recurrent neural network are introduced to compare and analyze the data, and the stability of data processing with different activation functions is compared. The data results show that under the scientific and reasonable arrangement of exercise conditions, bodybuilding and fitness exercises have a corresponding positive effect on the body shape and posture of the subjects. It is more practical to choose a combination of aerobic and anaerobic exercise. In this paper, based on the deep learning algorithm, compared with the recurrent neural network, the gated recurrent neural network is more suitable for processing sequence problems. In the experimental analysis part, this paper compares and analyzes the experimental results of the data under different activation functions, sigmoid function, and tanh function. It is found that the tanh activation function and the gated recurrent neural network are more stable for data processing. The highest AUC value of the traditional recurrent neural network differs by 0.78 from the highest AUC value of the gated recurrent neural network. The data analysis results are in line with the actual situation.

1. Introduction

The national physical quality is not only one of the material foundations for considering the progress of a country and society but also an important manifestation of national strength and social development. However, with the development of society, the way of life and entertainment is diversified. On the one hand, it increases people's income and spare time activities, and enriches people's spare time life and spiritual world. However, on the other hand, economic pressures such as buying a house and unhealthy lifestyles such as staying up late all endanger people's health. Therefore, to meet people's pursuit of physical health, fitness and bodybuilding exercises are increasingly favored by people. Since the effectiveness of bodybuilding and fitness for fat loss has been affirmed by many professionals, many people who have requirements for their own body and posture love bodybuilding and fitness a lot. Fitness bloggers have also sprung up, causing a fitness craze, which has also led to some people's lack of awareness of themselves. It blindly followed the trend and did not take scientific and reasonable fitness methods to exercise. It not only fails to achieve the desired results but also may lead to sports injuries. Therefore, it is necessary to study the impact of bodybuilding and fitness on the body. Deep learning is a network model algorithm emerging in the era of big data. It has demonstrated the superiority of deep learning

models for data analysis in many fields such as computer and face recognition.

With the popularity of the Internet, various fitness bloggers' fitness methods have appeared in people's field of vision. However, many enthusiasts do not know enough about bodybuilding and fitness itself. They do not have a scientific and reasonable understanding of how to choose and formulate their own exercise goals and exercise methods, and the arrangement of exercise and exercise is also lacking in pertinence. This also leads to the failure to achieve the expected results after exercising and even sports injuries in severe cases. As a branch of machine learning, deep learning has achieved many achievements in data mining, multimedia learning, recommendation and personalization technology, and other related fields. As an algorithmic method for learning the inherent laws and representation levels of sample data, deep learning is more accurate in studying the impact of bodybuilding and fitness on physical fitness. It has certain theoretical significance for the expansion of the research field of deep learning algorithms. The research on the effect of bodybuilding and fitness on physical fitness in actual exercise can provide a theoretical reference for fitness enthusiasts to choose appropriate exercise plans, which has certain practical significance.

The innovation of this paper is (1) how to choose a more targeted exercise method according to one's own situation when making a bodybuilding and fitness exercise plan. (2) This paper introduces the deep learning algorithm into the research on the impact of bodybuilding and fitness exercise on physical fitness. It can find some hidden laws and characteristics in the research object, which is more valuable for the reference of choosing a scientific fitness method. And this paper compares and analyzes the effect of two different neural network models on data analysis. It breaks the traditional mode of the questionnaire analysis method, and the analysis of data is simpler and more intelligent.

2. Related Work

Fitness exercise refers to the use of various exercise methods combined with different forms of exercise in accordance with the principles of human life science. It is a sport that ultimately enhances people's physique, quality of life, and longevity. In foreign countries, many researchers have also conducted research on bodybuilding and fitness exercises and gave interpretations. Dobrescu *T* conducted a sociological study in which bodybuilding can even be used as a professional sport, aiming to promote physical function, psychological development, and esthetic awareness of practitioners [1]. Kashuba V found in the study of the effect of fitness exercise on adult women: in the case of using reasonable water fitness methods, exercise can improve the physical function of women. Therefore, fitness exercise can be regarded as an effective tool for adult women's health improvement and weight management [2].

Deep learning is a general term for a class of pattern analysis methods, and it is also one of the machine learning methods. Deep learning has played an effective role in computer, audio, robotics, information retrieval, and other fields. Yu used a convolutional network algorithm for research to identify Moyamoya disease and predict bleeding events. Combining with research data, he believed that the data obtained through deep learning algorithm analysis is more accurate, sensitive, and specific [3]. Gong *M* studied the detection of changes in synthetic aperture radar images through deep learning. He proposed the feasibility and superiority of deep learning algorithms in different research fields [4]. So, W used the linear activation function of the output layer and the global mean variance of the target features to analyze and process various reverberation times through a deep neural network framework [5]. C Sánchez-Sánchez and Izzo studied the application of deep learning to spacecraft navigation and control systems. In the article, he proposed that the analysis results based on deep learning can allow the design of an on-board real-time optimal control system [6]. Jiang et al. compared deep neural network with other traditional methods and believed that deep neural network is more suitable for video semantic modeling [7]. Various research results have shown the superiority of deep learning algorithms. In different research fields, the types of neural networks are used, such as deep convolutional neural networks [5], and the models are also different.

3. Brief Description of Deep Learning Model Algorithm

3.1. Deep Neural Networks. Deep learning builds a deep neural network by simulating the neuron activity of the human brain [8]. The basic structure of each neuron is shown in Figure 1.

The output of the previous neuron is the input of the neuron in this layer. Each neuron is similar to a function, receiving n parameters and outputting the result through the calculation of the neuron. However, the last layer of neurons is different from the previous layer, and the output of this layer is generally activated or not activated. The formula is as follows:

$$h(m) = \begin{cases} 1, & \text{if } h(m) > t, \\ 0, & \text{if } h(m) \le t. \end{cases} \tag{1}$$

Among them, $m = X1, X2, \ldots. Xn$, h (m) represents the activation function of the neuron. There are also many types of neuron activation functions, among which the more common is the sigmoid function and the tanh function. The sigmoid function is an activation function commonly used in early multilayer perception [9]. However, when dealing with a relatively large-scale neural network, the tanh function is generally used. The sigmoid function is more commonly used in binary classification problems, but because the gradient of the sigmoid function is very small, when the input is extremely large or extremely small, it will affect the gradient, resulting in a large error in the data. Compared with the sigmoid function, the tanh function has less influence on the gradient [10].

The sigmoid function formula is as follows:

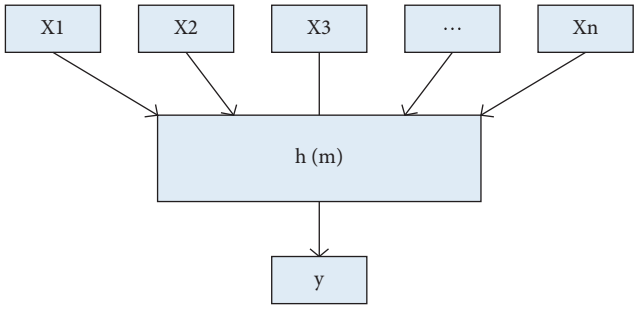

Figure 1: Basic structure of neurons.

$$h(u) = \frac{1}{1 + e{-}u}. \tag{2}$$

The tanh function formula is as follows:

$$T(x) = 2h \times 2x - 1. \tag{3}$$

The sigmoid function image and the tanh function image are shown in Figure 2.

Neither of the two functions completely solves the gradient problem. On this basis, the ReLU function and the Elu function appear in the researcher's field of vision. These two functions can effectively solve the gradient problem as stage functions.

The formula of the ReLU function is as follows:

$$F(x) = Max(0, x). \tag{4}$$

The Elu function formula is as follows:

$$F(x) = \begin{cases} (e^x - 1)m, & \text{if } x < 0, \\ x, & \text{if } x \geq 0. \end{cases} \tag{5}$$

The ReLU function image and the Elu function image are shown in Figure 3.

The effect of different activation functions is shown in Table 1.

When a large number of neurons are used as hidden layers, plus the last layer of output neurons, a simple neural network is formed. Figure 4 is a simple neural network structure.

The figure represents the input layer, hidden layer, and output layer from left to right, and each circle represents a node. The input layer inputs the initial value, and the output layer outputs the result. In the deep neural network algorithm, it is necessary to initialize the weights first, then input the data, and then compare the output layer with the marked value to calculate the error. The output error formula is as follows:

$$E = \frac{1}{2}(T - O)^2 + I^2, \tag{6}$$

where T represents the tag value O represents the output and I represents the regularization term.

The traditional neural network model calculation formula is as follows:

$$f = h(w \times x + a), \tag{7}$$

where f represents the output node at a certain moment, x is the input node at this moment, w is the weight, and h is the activation function of the neuron. Activation function is a general term. It can be seen from the formula that the output information f of the traditional neural network model at different times does not affect each other. However, the influence of fitness exercise on physical quality includes time series. At different time nodes, the degree of influence of bodybuilding and fitness exercise on physical fitness is also inconsistent. Moreover, the impact of fitness exercise on the body is multidimensional. Therefore, traditional neural network models are not suitable for data analysis of the impact of fitness exercise on the body.

The limitations of the traditional neural network model are broken by another neural network model, which is the recurrent neural network model. The peculiarity of recurrent neural networks is their recurrent nature, which makes them more efficient in processing sequence data than traditional neural network models. In sequence data, the training data before and after are not independent, and the sequence of the sequence can also reflect the characteristics of the data, and the recurrent neural network model can handle the ordered data well. Figure 5 is a data diagram of the recurrent neural network model.

As can be seen from Figure 5, when the recurrent neural network performs data analysis, the hidden layer and the layer can also be transmitted to each other. In the traditional neural network model, each node is connected but independent of each other, although the layers are connected to each other. However, the nodes at the same layer cannot transmit data, and the recurrent neural network model solves this problem well. Data can also be transmitted between nodes in each layer. That is to say, in the recurrent neural network model, the output of the hidden layer is not only related to the output of the input layer. It is also related to the output of the hidden layer at the previous moment [11]. The correlation formula between the value of the hidden layer corresponding to the current node and the value of the hidden layer at the previous moment is as follows:

$$f_{t-1} = h(w_t + u f_{t-1}). \tag{8}$$

Among them, h is the activation function, and w is the weight of the input process.

The input function of the hidden layer of the recurrent neural network at a certain time t is as follows:

$$m_t^{\ h} = \sum_{i=1}^{i} W_{ih} \times u_t^i, + \sum_{(h-1)=1}^{h} w_{(h-1)h} \times n_{t-1}^{h-1}. \tag{9}$$

The output function at this time t is as follows:

$$n_t^h = f_h\left(m_t^h\right). \tag{10}$$

Among them, u_t^i is the input at time t, n_{t-1}^{h-1} is the output at time t − 1, and w_{ih} is the weight between the input layer and the hidden layer. $w_{(h-1)h}$ is the weight between the

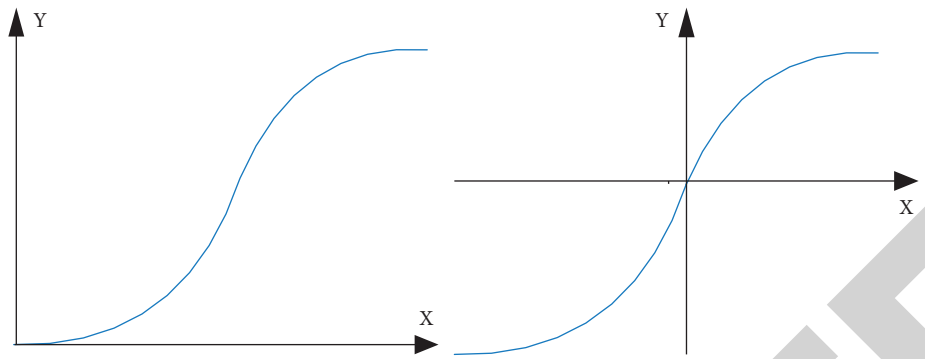

Figure 2: Sigmoid function image (left) and tanh function image (right).

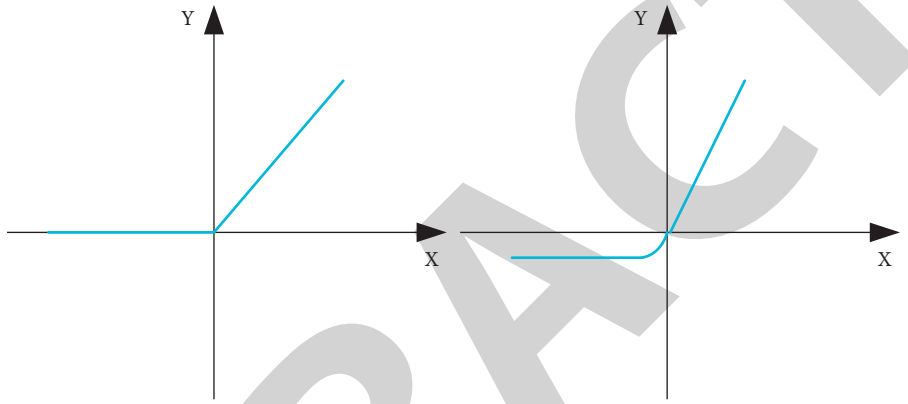

Figure 3: ReLU function image (left) and Elu function image (right).

Table 1: Comparison of activation function effects.

Function type	MAPE	MAE	RMSE
Sigmoid	0.0076	2.16	3.03
Tanh	0.0064	1.93	2.56
ReLU	0.0040	1.14	1.2
Elu	0.0062	1.91	2.51

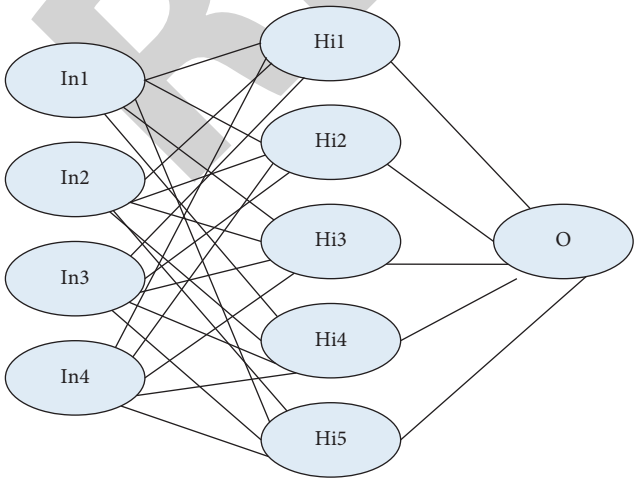

Figure 4: Simple neural network architecture.

hidden layer at the previous moment and the current hidden layer, and f_h is the activation function of the hidden layer.

The input function of the output layer of the recurrent neural network at a certain time t is as follows:

$$m_t^x = \sum_{h-1}^{h} w_{xh} \times n_t^h. \tag{11}$$

The output function at this time t is as follows:

$$g_t^x = f_x(m_t^x). \tag{12}$$

Among them, w_{xh} is the weight between the hidden layer and the output layer, and f_x is the excitation function of the output layer.

Similarly, in the cyclic neural network, the error also needs to be calculated. The error formula of the output layer of the cyclic neural network at a certain time t is as follows:

$$e_t^x = g_t^x - \phi_t^x. \tag{13}$$

At this moment t, the hidden layer error formula is as follows:

$$e_t^h = f_{(h-1)}\left(m_t^h\right)\left(\sum_{x=1}^{x} e_t^x \times w_{xh} = \sum_{(h-1)=1}^{h} e_{t+1}^{h-1} \times w_{(h-1)h}\right). \tag{14}$$

After the error value is calculated, the partial derivative of each parameter is obtained to obtain the rate of change.

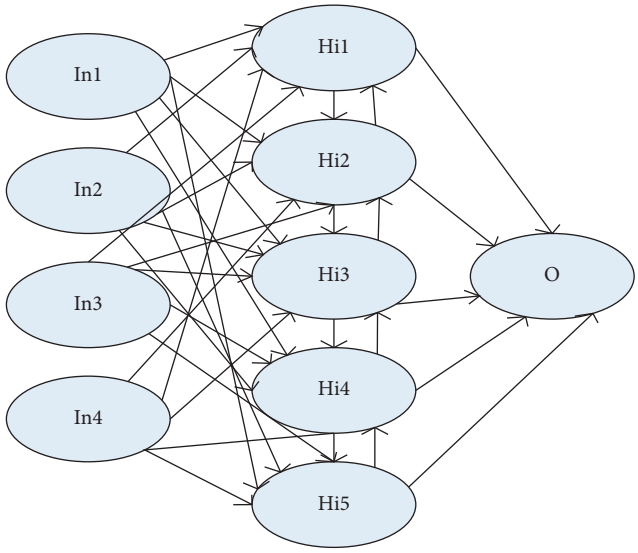

Figure 5: Recurrent neural network model diagram.

The hidden gradient function formula at this time t is as follows:

$$e_t^k = \frac{\partial E}{\partial m_t^a}, \tag{15}$$

where E is the error function and ϕ_t^x is the label of u_t^i as shown in formula. At the same time, to better solve the gradient problem and make the error function approximation minimum, it is necessary to use the gradient descent method to process the data [12, 13]. It obtains the minimized loss function and model parameter values to approximately minimize the error function. It needs to be solved iteratively step by step. The gradient descent method formula is as follows:

$$\Delta w_t = -\lambda e_t, \tag{16}$$

$$\Delta w_t = w_{t+1} - w_t, \tag{17}$$

where λ is the learning rate and e_t is the gradient at time t. This is the general formula of the gradient descent method, but when there are too many calculation samples, the training speed will be slowed down [14], so to make up for this deficiency, the Adagrad algorithm appeared. In this algorithm, a minimum value is added. To ensure that the denominator will not be 0, the calculation formula of the algorithm is as follows:

$$\Delta w_t = -\frac{\lambda}{\sqrt{\sum_{t=1}^{t-1} e_t^2 + \delta}} e_t. \tag{18}$$

The formula for the partial derivative function for each gradient weight is as follows:

$$\Delta E(W_{ik}) = \sum_{t=1}^{t} e_t^k \times n_t^i. \tag{19}$$

Combining with the gradient descent method to find the update function of the weightthe formula is as follows:

$$w_{(ik+1)} = w_{ik} - m \times \Delta E(w_{ik}). \tag{20}$$

Since the cyclic neural network needs to expand the entire network structure and show the characteristics of full connection in the whole neural network [15], more detailed algorithms are needed to solve the gradient problem.

3.2. Bodybuilding and Fitness. Fitness and bodybuilding can not only promote the normal development of the human body but also have a positive effect on the body, physical function, and mental health [16]. During adolescence, scientific and appropriate exercise can help promote physical development and greatly improve the physique of adolescents. For ordinary adults, a reasonable arrangement of exercise in leisure time can eliminate part of the impact of life stress on the body and can also delay aging. Bodybuilding and fitness also have related items in sports competitions, which require higher physical fitness of individuals. And they need to devote themselves to sports, but most of them are just public fitness models, using spare time for exercise. Bodybuilding and fitness exercise mainly consists of three parts: stretching exercise, aerobic exercise, and muscle load exercise. When carrying out bodybuilding and fitness exercises, they should scientifically and reasonably arrange the exercises of these three parts according to their own conditions. The selection of the exercise sequence can generally be done with reference to Figure 6.

It can be seen from the figure that a complete fitness exercise should first activate the stretching exercise of the body. After the body adapts to the exercise state, the addition of aerobic exercise can increase the heart rate as part of the warm-up activity. When the body is fully prepared for exercise, it performs muscle-loading exercises to achieve the purpose of shaping the body and finally performs stretching to stretch the muscles to relax the tight muscles.

There are many kinds of bodybuilding and fitness methods for the public, such as aerobics, running, swimming, or exercising with weights such as dumbbells. These sports can generally be divided into aerobic and anaerobic. The more common fitness method is the combination of anaerobic and aerobic. Aerobic exercise is the way to provide the energy required for exercise by aerobic metabolism. Common aerobic exercise mainly includes jogging, rope skipping, swimming, Tai Chi, yoga, aerobics, and others, as shown in Figure 7.

The exercise method carried out in the state of anaerobic function metabolism is anaerobic exercise. Most of the anaerobic exercises are high-intensity and instantaneous sports, such as sprinting, push-ups, weightlifting, muscle strength training, and other long-term muscle contraction exercises as shown in Figure 8.

The bodybuilding and fitness activities of the public are mainly to meet the pursuit of modern people's health. According to a report released by the World Health Organization, the global obesity rate is on the rise. Therefore, in addition to adjusting the diet, proper exercise is also essential. China has also formulated corresponding physical

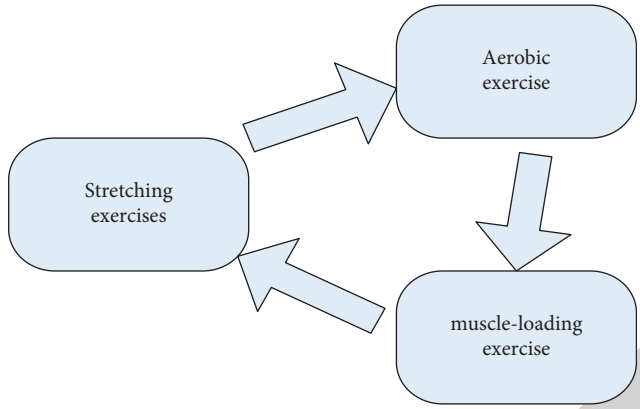

Figure 6: Bodybuilding and fitness exercise flow chart.

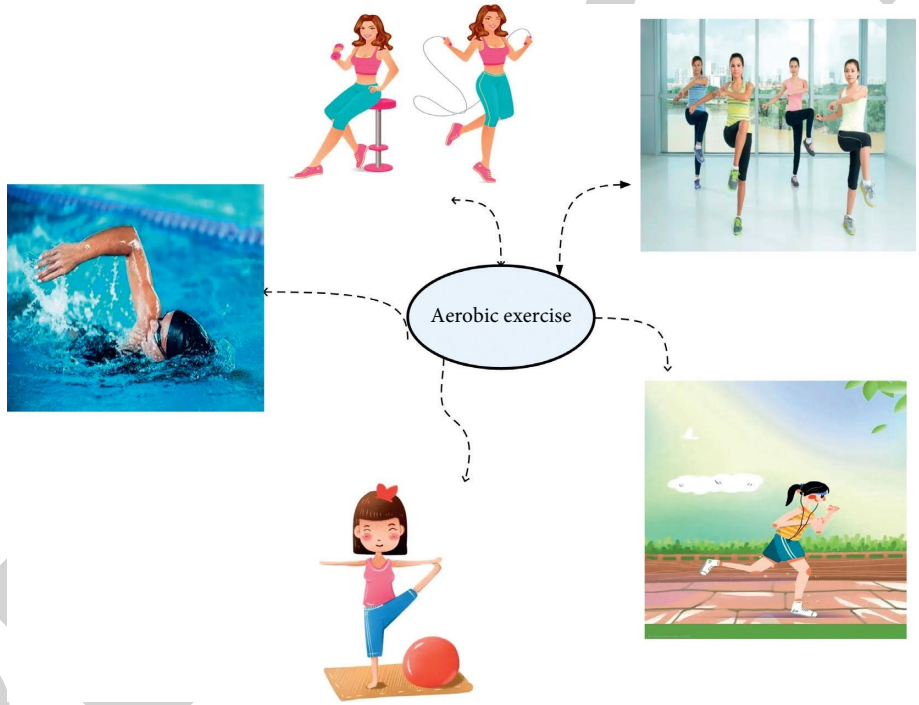

Figure 7: Some common forms of aerobic exercise.

health standards. The normal standards of body mass index, body fat percentage, and vital capacity are shown in Table 2.

3.3. Application of Image Segmentation Technology in Human Movement. The application of image segmentation technology in human motion is mainly realized by detecting, identifying, tracking, understanding, and describing the human body in a set of image sequences containing people. Since the human body moves during the motion, this paper chooses the method based on video frame difference to construct the background image.

Assuming that the number of frames is represented by v, M is the sum of the number of frames, and the pixel position is (a, b). Then, the video frame difference that can reflect the brightness change between adjacent frames is calculated as follows:

$$L_v(a,b) = \begin{cases} c, c \geq D, \\ 0, c < D, \end{cases} \quad (21)$$
$$c = \left| V_v + Q(a,b) - V_v(a,b) \right|.$$

Among them D represents the threshold for controlling noise removal. The midpoint of the longest segment is selected to fill the corresponding position in the video background among the detected static partsand the reconstructed background obtained is as follows:

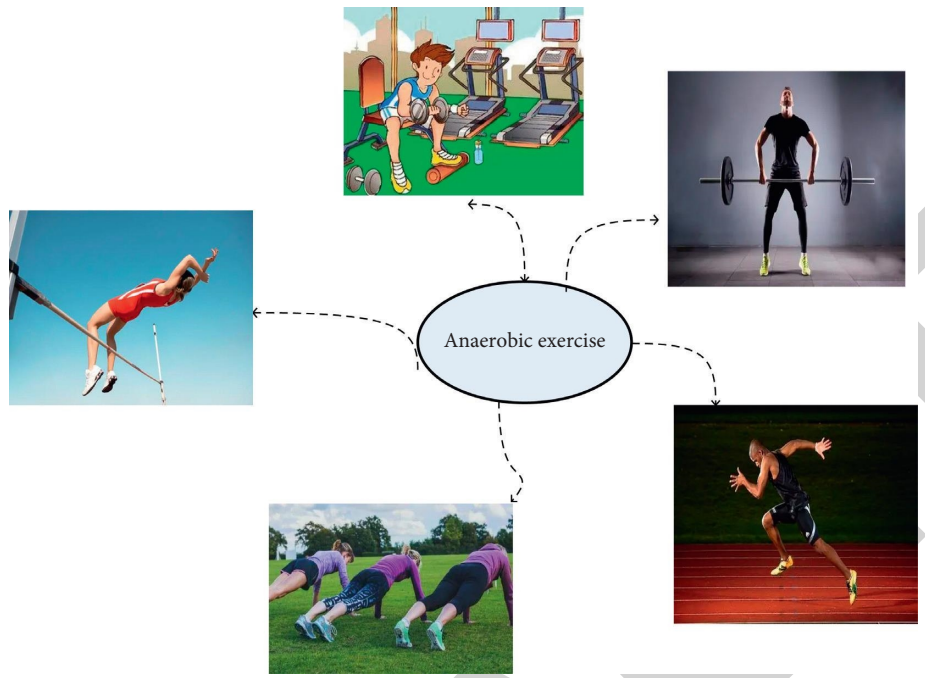

Figure 8: Some common anaerobic exercise methods.

Table 2: Brief list of physical health standards.

Index	Male	Female
BMI	18.5~23.9	18.5~23.9
Body fat percentage (%)	15~18	20~25
Lung capacity (ml)	3500~4000	2500~3500

$$J(a,b) = V(a,b,H(a,b)),$$
$$H(a,b) = \frac{H_q(a,b) + H_z(a,b)}{2}, \tag{22}$$

where $H_q(a,b)$ and $H_z(a,b)$ represent the start and end points of the longest stationary sectionrespectively.

Then, we use the background difference method to extract the moving human body. The calculation method is the color value of the pixel point of the current frame minus the color value of the pixel point in the background town, which takes a positive number. After the color difference value is obtained, the value is weighted according to different colors, so as to eliminate the interference of the environment, which can be expressed as follows:

$$g(a,b) = \omega_1 F_{ab}(\mathrm{Red}) + \omega_2 F_{ab}(Green) + \omega_3 F_{ab}(Blue). \tag{23}$$

Among them, ω represents the weight value, and F_{ab} represents the color difference value of different colors.

We set the global threshold ΔD on the image, and the binary image is obtained as follows:

$$J(a,b) = \begin{cases} \text{background}, 0; g(a,b) \le \Delta D, \\ \text{foreground}, 0; g(a,b) > \Delta D. \end{cases} \tag{24}$$

Double thresholds are used to perform binary processing on the image. First, the low threshold is obtained from the average value of the difference image and the absolute difference of the average value, and the high threshold is obtained by multiplying the ratio of the high and low thresholds by the low threshold. Perform mathematical morphological expansion operation on the low-threshold processed binarized image to obtain the result, and then jointly process the high-threshold processed binary image to obtain a complete moving human body.

This paper will use image segmentation technology to capture the motion of the participants in the experimental part and conduct action guidance.

3.4. Impact of Bodybuilding and Fitness Exercises on Physical Fitness Based on Deep Learning. The influence of bodybuilding and fitness exercise on physical quality is multifaceted, and the data of body fat rate, body mass index, and lung capacity in physical function are visualized, and the influence of exercise on the body shows the characteristics of stages. Combined with the deep learning algorithm, a layer of connection GRU between the input layer and the output layer is established between the time points before and after the data; in order to shorten the distance between the relevant characteristics, it includes long-distance data, and another layer is added to allocate the attention coefficient. It is used to reinforce the role of data-focused. The basic structure is shown in Figure 9.

At the same time, to reduce the influence of weights and better solve the error problem, different positional states in the neural network structure of the gated recurrent unit have different effects on the current hidden layer nodes. It can be used to alleviate the problem of vanishing or exploding

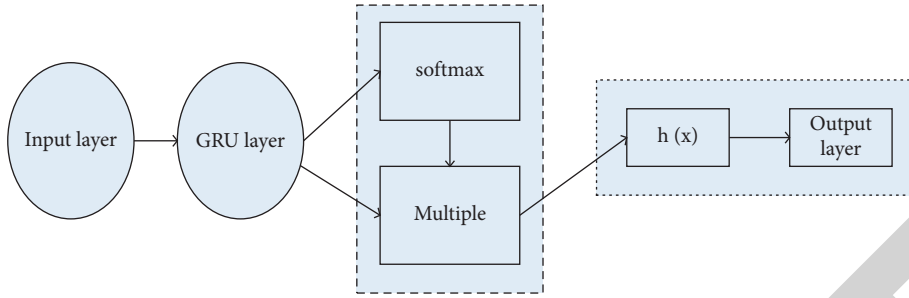

Figure 9: GRU basic structure.

gradients [17, 18]. It occupies less computer memory resources and is more efficient, which is an advantage compared to recurrent unit networks. The gated recurrent unit neural network structure is shown in Figure 10.

It can be seen from the structure diagram that the gated recurrent unit neural network includes several major structures such as update gate, reset gate, and memory unit [19]. When analyzing the impact on physical fitness, the data are reset and updated according to the time, node, and data type. The function formula is as follows:

$$m_t = \mathrm{Tanh}\left(a_{x_t} + w_r b O_{t-1}\right), \tag{25}$$

$$h_t = w_u O_{t-1} + (1 - w_u) m_t. \tag{26}$$

Among them, h_t is the hidden layer state, w_u is the update gate weight, O_{t-1} is the input of the hidden layer in the past, m_t is the memory unit, a is the input variable, and b is the hidden layer parameter.

Considering that the sample data will be unbalanced, that is to say, the proportion of positive and negative samples will change with the test time. This paper introduces AUC to analyze the data [20]. The AUC value is the area under the ROC curve (receiver operating characteristic curve), which represents the ratio of negative and positive cases in the divided instance. The larger the AUC value, the better the effect of fitness and bodybuilding on quality.

4. Experiments and Analysis of the Impact of Fitness and Bodybuilding on Physical Fitness Based on Deep Learning

4.1. Bodybuilding and Fitness Exercise Combination Design. According to the classification of bodybuilding and fitness, this article compares different combinations of bodybuilding and fitness. It analyzes the impact of different exercise methods on the body. The experiment provides aerobic and aerobic and anaerobic exercise methods. It first controls the duration of each exercise to be 1 hour, and a group of aerobic exercises is one hour. The second group of aerobic exercise and anaerobic exercise is half an hour, and the rest interval between the two groups is the same. It can rest for five minutes to half an hour during exercise to adjust breathing. The specific time arrangement is shown in Figure 11.

Because the exercise program is highly targeted, the arrangement of the exercise program is essential to the experimental results. According to the principles of human life science, the set exercise plan is arranged as shown in Table 3.

This study recruited 20 volunteers between the ages of 22 and 40 who were passionate about bodybuilding and fitness. There are 10 males and 10 females. All subjects have no contraindications that affect sports under the evaluation of professionals, and they can all perform bodybuilding and fitness exercises. To improve the reliability of the data, a control group was added to this experiment, with 5 males and females, and all volunteers aged 22 to 40. The control group did not participate in fitness exercises. The exercise plan is selected according to the body fat rate of the group members and the physical ability of the body. Therefore, this experiment was divided into three groups: A, B, and C. Group A implemented exercise program 1, and group B implemented exercise program 2. This experiment was divided into groups according to the health level of the test indicators, body mass index, body fat rate, and lung capacity before the test. Among them, group A is member with high body fat rate, and group B is member with slightly lower body fat rate and normal range. The various test indicators before participating in the test members are shown in Table 4.

The duration of this experiment was 12 weeks, and subjects were tested for experimental indicators every four weeks. During this experiment, the exercising personnel who participated in the experiment did not participate in other physical exercises except for the exercise during the experiment. The diet is based on a normal diet, not overeating. It also guarantees protein intake during the experiment, guided by professionals during the process. The dietary requirements of the control group were the same as those of the experimental group.

4.2. Influence of Bodybuilding and Fitness on Physical Fitness. After three months of exercise, the subject index values are shown in Table 5.

Since the amount of data is not very large, sigmoid and tanh activation functions are selected for comparative analysis. According to the data in the table and the test values in the fourth and eighth weeks, the data results are shown in Figure 12.

As can be seen from the figure, the AUC value increases steadily with the increase of the number of iterations. The highest value of the sigmoid function is higher than the

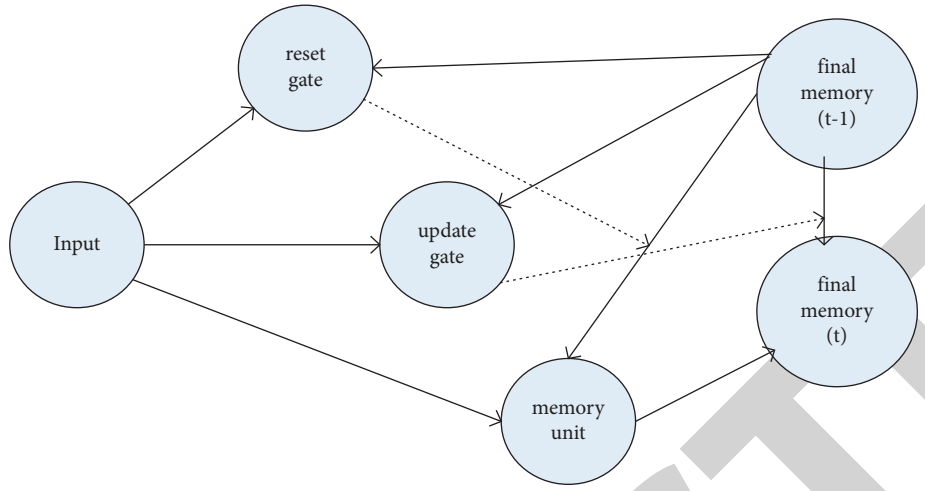

Figure 10: Gated recurrent unit neural network.

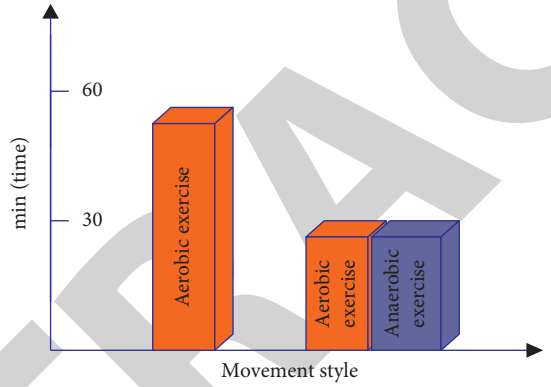

Figure 11: Movement time design.

Table 3: Exercise program arrangement.

Frequency (week)	Adapt to the object	Main function
1~5	Intermediate and advanced	Development force
4~6	Beginner and intermediate	Build muscle and build strength
5~7	Fat beginner	Reduce fat and increase muscle endurance

highest value of the tanh function. Compared with the sigmoid functionthe tanh function is more robust in the same neural network model.

Under the same activation function tanh, the comparison of data analysis based on recurrent neural network (RNN) and gated recurrent unit neural network (GRU) models is shown in Figure 13.

It can be seen from the figure that, under the same stable activation function, the AUC value of the gated recurrent unit neural network rises faster and more smoothly, thus proving the effectiveness of the gated recurrent unit neural network based on traditional recurrent neural network optimization.

4.3. Control Experiments. To better reflect the validity of the data on the impact of bodybuilding and fitness on physical fitness, the data of the control group were also briefly analyzed. In this paper, the relevant data of the control group C are collected. The values of body mass index, body fat percentage, and vital capacity are also used every four weeks. Under different activation functions, the AUC value changes of GRU and the AUC value changes of different neural network models under the tanh activation function are shown in Figure 14.

According to the graph, it can also be concluded that the tanh function and the gated recurrent neural network model are more stable.

5. Discussion

This paper mainly studies the data analysis model based on deep learning, and it applies it to the analysis of the impact of bodybuilding and fitness on physical fitness. This paper not

Table 4: Numerical table of test indicators for subjects before the experiment.

Group	Number	BMI	Body fat percentage	Lung capacity
A	1	24.3	19.1	3500
	2	24.7	20.3	3500
	3	25.1	20.4	3600
	4	26.3	21.2	3600
	5	24.9	20.3	3500
	6	26.1	25.2	3200
	7	24.6	25.0	2600
	8	25.3	25.6	3000
	9	27.2	25.8	3100
	10	25.6	25.3	3200
B	1	18.2	15	3600
	2	19.1	15.9	3800
	3	22.3	16.7	3600
	4	23.1	18.0	3700
	5	18.4	15.1	3900
	6	21.7	20.1	2800
	7	23.9	23.5	3000
	8	23.6	23.7	3100
	9	23.6	24.3	3200
	10	23.9	24.6	3100

Table 5: Numerical table of test indicators after subject experiment.

Group	Number	BMI	Body fat percentage	Lung capacity
A	1	23.9	17.6	3600
	2	24.1	19.7	3600
	3	24.2	19.8	3700
	4	25.0	20.7	3600
	5	23.9	18.3	3900
	6	24.6	23.7	3200
	7	23.7	23.5	2800
	8	24.9	24.8	3000
	9	26.1	25.0	3200
	10	24.2	23.1	3300
B	1	18.5	15.2	3600
	2	19.3	15.7	3900
	3	21.9	16.1	3600
	4	22.9	17.9	3800
	5	18.7	15.3	3900
	6	21.0	20.1	2900
	7	22.6	22.8	3200
	8	23.1	23.1	3100
	9	22.9	23.8	3200
	10	23.1	23.6	3200

only expands the research field of deep learning algorithms but also increases the data channels for influencing factor analysis. When analyzing data using deep learning algorithms, this article first introduces the application of deep neural networks in different fields. And based on the deep neural network, this paper introduces the optimized deep neural network. In this paper, the algorithm is simply optimized according to the advantages and disadvantages of different neural networks. This paper specifically compares and analyzes the traditional recurrent unit neural network and the gated recurrent unit neural network model under deep learning. This paper derives the utility of using gated recurrent unit neural networks for the analysis of such data. To make the experimental analysis more accurate and the error smaller, this paper compares and analyzes different activation functions in the data analysis model. And in the construction of the neural network model, this paper uses the gradient descent method to optimize the model, to ensure that the error value of the data is approximately the smallest.

Due to the limitations of the experiment, in this data analysis, this paper only uses the gradient descent method and does not compare other optimization algorithms. Under different optimization algorithms, the effect of the model is

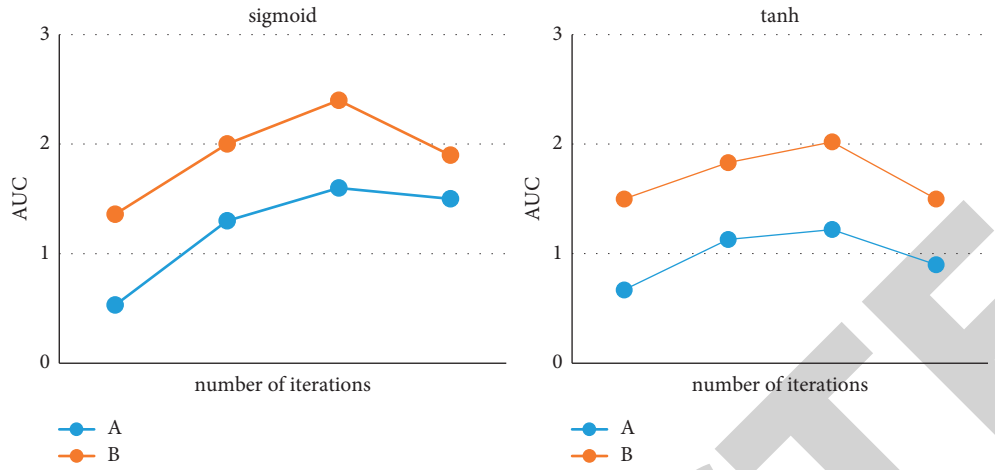

Figure 12: AUC change graph of GRU under different activation functions.

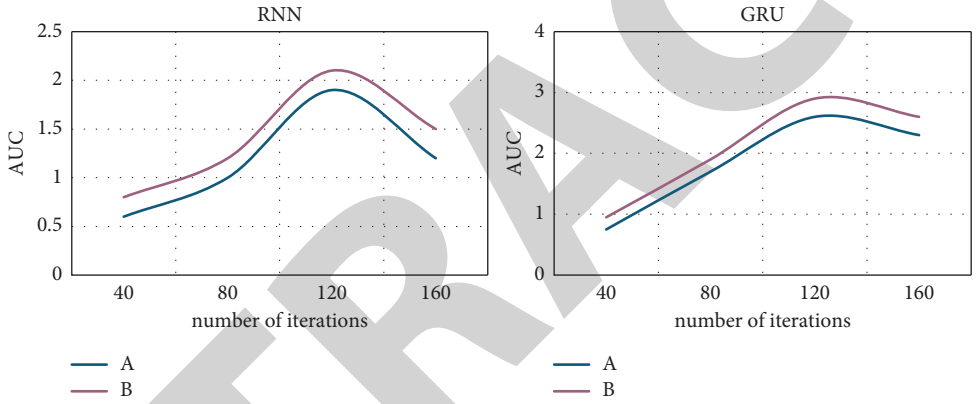

Figure 13: AUC changes in different neural network models.

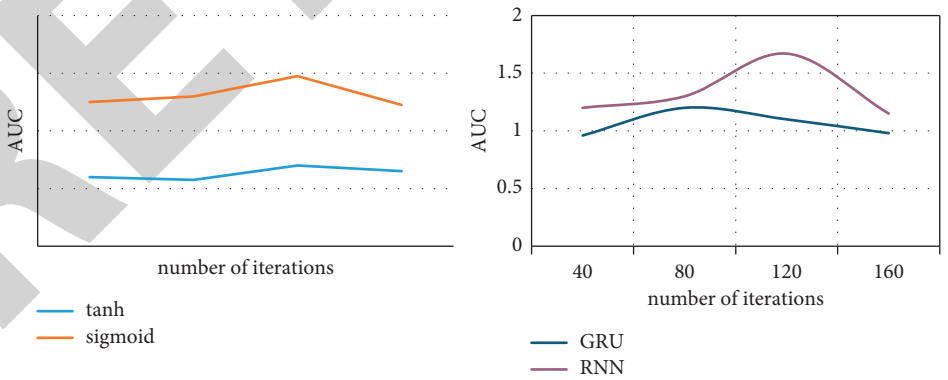

Figure 14: Changes in the AUC value of the model in group C.

also different. Therefore, in the future experimental analysis, we can try to use different optimization algorithms to update and train the model to make the data analysis more effective. During the experiment, although the subjects have been restrained according to the relevant requirements, it is difficult to control the suddenness of the physical condition, and there may be errors in the relevant data. Since both body mass index and body fat percentage require body weight data, in terms of city experimental data, body weight is not used as a test indicator alone. Considering that some subjects love fitness, but they do not perform high-intensity exercise. And due to the differences in the physical quality of the

Hindawi
Emergency Medicine International
Volume 2023, Article ID 9801869, 1 page
https://doi.org/10.1155/2023/9801869

Retraction

Retracted: Application of Low-Intensity Laser in the Treatment of Skeletal Muscle Injury in Runners

Emergency Medicine International

Received 8 August 2023; Accepted 8 August 2023; Published 9 August 2023

This article has been retracted by Hindawi following an investigation undertaken by the publisher [1]. This investigation has uncovered evidence of one or more of the following indicators of systematic manipulation of the publication process:

(1) Discrepancies in scope
(2) Discrepancies in the description of the research reported
(3) Discrepancies between the availability of data and the research described
(4) Inappropriate citations
(5) Incoherent, meaningless and/or irrelevant content included in the article
(6) Peer-review manipulation

The presence of these indicators undermines our confidence in the integrity of the article's content and we cannot, therefore, vouch for its reliability. Please note that this notice is intended solely to alert readers that the content of this article is unreliable. We have not investigated whether authors were aware of or involved in the systematic manipulation of the publication process.

Wiley and Hindawi regrets that the usual quality checks did not identify these issues before publication and have since put additional measures in place to safeguard research integrity.

We wish to credit our own Research Integrity and Research Publishing teams and anonymous and named external researchers and research integrity experts for contributing to this investigation.

The corresponding author, as the representative of all authors, has been given the opportunity to register their agreement or disagreement to this retraction. We have kept a record of any response received.

References

[1] Y. Chen and Q. Li, "Application of Low-Intensity Laser in the Treatment of Skeletal Muscle Injury in Runners," *Emergency Medicine International*, vol. 2022, Article ID 1211602, 9 pages, 2022.

Hindawi
Emergency Medicine International
Volume 2022, Article ID 1211602, 9 pages
https://doi.org/10.1155/2022/1211602

Research Article

Application of Low-Intensity Laser in the Treatment of Skeletal Muscle Injury in Runners

Youdong Chen[1] **and Qiang Li**[2]

[1]*School of Clinical Medicine, Hunan University of Chinese Medicine, Changsha 410000, Hunan, China*
[2]*Hunan University of Chinese Medicine, Hunan Province Second People Hospital, Changsha 410000, Hunan, China*

Correspondence should be addressed to Youdong Chen; 20203482@stu.hnucm.edu.cn

Received 7 April 2022; Revised 13 May 2022; Accepted 23 May 2022; Published 17 June 2022

Academic Editor: Hang Chen

With the continuous improvement of people's economic level, running, as the most common sports, is not limited by sports venues and sports levels and deeply loved by people. However, during running, soft tissue resonates with the impact force, increasing the load on joints and tendons and potentially leading to sports injuries. The purpose of this article is to study the application of low-intensity laser in the treatment of muscle strain. This article analyzes running, muscle adjustment, and lower limb stiffness. On the basis of theory, 20 healthy male college students were selected as research objects in the experimental part. The subjects were allowed to run at three speeds: slow, medium, and fast. The kinematics, dynamics, and surface EMG signals of the subjects during running were collected to analyze the effect of low-intensity laser therapy on exercise muscle strain. The experimental results showed that a low-intensity laser can effectively alleviate muscle inflammation, reduce the number of cell damage, bring the mean and integral optical density of protein to the normal level significantly, and reduce the strain degree of exercise muscle. In this article, a statistical method was used to obtain the gait cycle time (P & LT; 0.01) and support cycle time (slow $P < 0.01$).

1. Introduction

With the continuous development of China's society and economy and the continuous improvement of people's requirements for quality of life, a healthy and high quality of life has become a lifestyle that people increasingly pursue. At the same time, the three high issues caused by obesity and poor living habits are seriously affecting people's health. Therefore, fitness has changed from the earlier emerging things to the normal state of people's daily life. Physical fitness can not only beautify the appearance of the body but also improve the regulation of the nervous system and promote the growth of bones and muscles. Among many fitness methods, running is widely accepted by the general public because of its simple technical requirements and not being restricted by too many venues, clothing, and equipment and has become an important fitness method. Running can enhance the body's metabolism and basal metabolic rate and has a good effect on weight loss, fat loss, exercise, and enhancement of body immunity, antiviral ability, and resistance. Running for a long time is a very effective aerobic exercise, which can have a good effect on the cardiovascular endothelial system and can effectively reduce the incidence of coronary atherosclerotic heart disease, acute stroke, cerebral infarction, and other serious cardiovascular and cerebrovascular diseases. Regular running can also reduce blood lipids and can significantly reduce the concentration of triglycerides, cholesterol, uric acid, and blood sugar, so it has a good effect on the prevention and healthcare of the above diseases. Long-term running will play a certain role in promoting and regulating gastrointestinal digestion and absorption and effectively improve sleep and the sleep quality of the human body.

In normal human movement, factors such as running speed, distance, and frequency are usually determined or selected by the athlete at will. Everyone has their own

suitable frequency, and the impact of this suitable frequency on human soft tissue is different. In this article, the effects of running frequency on stiffness and muscle tuning of the lower limbs are analyzed using microscope-based medical imaging diagnostic technology, simultaneous acquisition of dynamics and kinematics, and surface electromyography data. It provides a theoretical basis for people to choose a reasonable running frequency when running.

The purpose of Park et al. is to enable anyone to semiautomatically segment anatomical structures in MRI, CT, and other medical images on a personal computer. When performing semiautomatic segmentation in Adobe Photoshop, appropriate algorithms can be used, the degree of automation can be adjusted, a convenient user interface can be used, and software errors rarely occur [1]. Bailey's team aimed to compare the relationship between stride length (SL), stride frequency (SF), and speed when running on a treadmill and on the ground. Strategies for changing SL across speeds are different on treadmills and on the ground [2]. Faber and his team, due to their junior grades having little predictive value for future success, sought other solutions to assess the potential of young players. The purpose of this systematic review is to outline the tools that measure the personal determinants of young athletes in racket sports and to evaluate the effectiveness of these tools on talent development. The lack of longitudinal research makes it impossible to validate the instrument's ability to predict future performance [3].

In this article, 20 ordinary healthy male college students were selected as the research object, and the subjects were subjected to slow, medium, and fast. This kind of speed is used to run, and the kinematics, dynamics, and surface EMG signals of the subjects during running are collected simultaneously. In each speed mode, the subjects were divided into a low-cadence group and a high-cadence group; the stiffness of the lower limbs in the buffer phase and the active kick-extension phase were calculated based on the vertical reaction force peaks in the support phase and the vertical displacement of the center of gravity. Muscle vibration frequencies were analyzed prior to landing to analyze muscle tuning to analyze the effect of low-intensity laser therapy on exercise muscle strain [4].

2. Proposed Method

2.1. Lower Limb Stiffness. Stiffness is a physical term that refers to the ability of an object to resist deformation when it is loaded. The greater the stiffness of an object, the smaller its deformation [5]. For the human body, its stiffness value determines the strength of the supporting tissue and the body's ability to resist external forces. Generally speaking, the individual stiffness value is determined by muscles, tendons, ligaments, and bones. You can use a spring to simply show the relationship between the external force acting on the system and causing displacement. It will be found that under external force, the change in the displacement of the spring has a linear relationship with the applied external force, which is called the spring-mass model [6, 7]. For the human body, its overall skeletal muscle system also has elastic characteristics, which will change in length with external forces. In engineering applications, the stiffness of the structure is very important, so the elastic modulus is an important indicator when selecting materials. A high modulus of elasticity is necessary when there is an unpredictably large deflection. When the structure needs to have good flexibility, the elastic modulus is not required to be too high [8].

The elastic characteristics of the human skeletal muscle system are similar to springs. The self-regulation mechanism of human muscle stiffness helps the body better adapt to the external environment and can effectively maintain the stability of body posture [9, 10]. However, unlike the simple spring-mass model in the sense of general physics, a spring-mass model that can effectively restore the state of human movement should be able to integrate various soft tissue components, including human bones, muscles, tendons, and cartilage, and can contain biological tissue viscosity, muscle reflex time, central nervous system control, and many other factors. Obviously, the simple spring-mass model cannot take all the above factors into account. Therefore, this simple spring-mass model commonly used in the field of biomechanics to evaluate the stiffness of lower limbs is called quasistiffness.

In the field of biomechanics, the stiffness of lower limbs that people study can usually be divided into three types: vertical stiffness, leg stiffness, and joint stiffness. They have different ranges of action. In actual scientific research, vertical stiffness is mostly used to study vertical movements such as straight knee bouncing and jumping. The calculation method is to divide the peak vertical reaction force from the ground by the body divided by the vertical displacement distance of the center of gravity of the body; use vibration period and body mass to calculate by formula $K = m(2\pi/p)^2$ (p is the period of vertical vibration) or calculate the natural frequency of vibration according to the landing time and the vacant time between continuous movements, and then use the formula $K = m\omega^2$ to calculate the lower limb stiffness (m is the body mass and ω is the natural frequency of vibration). Leg stiffness is mainly used to describe walking or running. The calculation of leg stiffness is often performed using McMahon's formula $K = F/\Delta L$. F is the maximum vertical reaction force from the ground received by the lower limbs and ΔL is the maximum vertical displacement distance of the center of gravity of the body during the movement; joint stiffness is biased to describe the rotation characteristics of the joints during the lower limb movements. The change in joint torque is usually divided by Change ($K = \Delta M/\Delta\theta$, where$\Delta M$ is the change in joint torque and $\Delta\theta$ is the change in joint angle).

When the human body is performing a deep jump, the sensory system can sense the stretch load and falling height of the limbs, thereby acting on the neuromuscular system of the human body and judging the ground conditions during landing by the visual system, thereby activating the functional muscle groups in advance and making the human body better adapted to sports surfaces. That is, in the movement, when the human body makes reasonable judgments on the ground conditions through feedback from

the visual system and commands from the central nervous system, the muscles are adjusted to a suitable stiffness before landing, and when the muscles are eccentrically contracted, they are obtained by stretch reflection. After better activity, the muscle will be preactivated, and this phenomenon will be reflected in myoelectric activity. This regulating ability has been discovered by scientists and is considered to be an important mechanism for regulating the stiffness of the lower limbs to prevent sports injuries.

In addition, the regulation of human lower limb stiffness is also related to age. When performing the action of descending stairs, the lower limb joint angle of the elderly is smaller and the muscle stiffness is greater; when performing the vertical jump in place, the elderly have worse muscle strength and lower limb stiffness adjustment ability than those of the young adults. It is believed that the ability of self-regulation during muscle contraction will decrease with aging [11].

There is also a correlation between the stiffness of the lower limbs and the hardness of the moving surface. The stiffness of the lower limbs of the human body when running in soft shoes is greater than the stiffness of the lower limbs when wearing hard shoes. During exercise, the lower limbs can perform a series of self-regulation according to the ground conditions so that the human body can better adapt to the ground hardness and achieve an optimal lower limb-ground overall stiffness value, which also shows that the human body will use the sensory motor function system to exercise. The hardness of the surface is appropriately adjusted so that the body can maintain the accuracy and balance of movements on the ground with different hardness. The stiffness of the lower extremity when jumping on the softest sports surface is twice that of the hardest sports surface, and the stiffness of the ankle joint and the extent of knee straightening also increase. It can be seen that the adjustment of lower limb stiffness in human movement is closely related to the adjustment of limb position and joint angular stiffness. It is often necessary to adjust the joint angular stiffness and limb position to adapt to the condition of the sports surface so that the body maintains the same posture on different sports surfaces [12].

2.2. Muscle Tuning. During exercise, the soft tissue structure of the human body (muscles, tendons, fascia, surrounding tissues, and skin) has a certain natural frequency and has the characteristic of changing its own frequency with changes in exercise state (systolic, diastolic, and forced conditions) [13]. In the study of impact force, we can consider the soft tissue structure, including muscles, tendons, fascia, and skin, as a vibration system, and the impact force as a set of input signals from the outside has the characteristics of causing soft tissue to vibrate. When the frequency of the impact force from the outside is close to the natural frequency of the soft tissue, the muscle will have a resonance phenomenon, which will increase the amplitude, but this phenomenon will disappear after the soft tissue vibrates twice. This is a muscle tuning activity performed by the human body in order to avoid soft tissue resonance leading to sports injuries; it can reduce the frequency of muscle vibrations and avoid sports injuries [14].

It can be seen that before the human body performs a series of running and jumping movements, the neuromuscular system will preactivate according to the landing conditions (such as ground hardness and speed of movement) and will reduce the frequency of soft tissue vibration through its own muscle tuning mechanism to avoid sports injuries. This process is called muscle tuning [15, 16]. The purpose of muscle tuning is to prevent the occurrence of resonance phenomenon caused by the external input frequency being close to its own natural frequency during exercise so as to prevent sports injuries and helps the repair of muscles and tendons; stretching exercises can stretch muscles and tendons, help prevent muscle tension, and relieve muscle soreness that often occurs after intense exercise [17]. During the muscle tuning process, the human body adjusts joint stiffness and joint position, thereby activating the soft tissues involved in movement and avoiding resonance. In general, during the entire exercise of the human body, the preactivation phenomenon will occur before the muscles touch the ground. At the same time, the joint stiffness and joint position of the human body will change accordingly during exercise. This series of adjustments is the performance of muscle tuning. The purpose is to reduce resonance, adapt to the state of exercise, and avoid sports injuries [18].

Muscles adjust vibration in the workplace; that is, when muscles encounter the potential danger of resonance, they adjust themselves to avoid resonance. During the movement of the human body, the active state of the lower limb muscles will change with the change of the impact force. When the frequency of the impact force from the outside in the exercise is close to the natural frequency of the quadriceps, the preactivation of the muscle will be significantly enhanced. In addition, when the human body moves without predicting the condition of the sports surface, the adjustment of the muscles when they touch the ground will change greatly. In this state, when the input frequency is close to the natural frequency, the resonance effect of the muscle will be more obvious. During the pretouchdown phase of human movement, muscle activity is mainly preparing for the next movement. The degree of muscle activation at this time is the impact force (including vibration frequency and amplitude) received by the previous muscle.

Moreover, muscle tuning is a holistic concept. It is a series of adjustments made by the muscles to avoid resonance, including changes in the geometric position of the lower limbs, changes in the stiffness of the lower limbs; adjustment of the vibration frequency of the soft tissues, changes in the load of the joints of the lower limbs, stability during the support phase, and action advancement during the off-ground phase.

2.3. Running. Running is a kind of periodic motion in which one-leg support alternates with vacancy, step-and-swing coordination, and coordinated and coherent movements. It is one of the main ways for the human body to complete

displacement, and it is also a natural movement of human body movement. The human body experiences two single-leg supports and two emptyings in a running cycle. The support period is from the time when the foot hits the ground to the time when the foot is off the ground, including the front support stage and the rear kick stage, and the vacant period is from the time when one foot is off the ground to the time when the other foot is touched, including the back swing stage and the front swing stage. Running uphill (downhill) can stimulate the calf muscles, allowing rapid muscle strength growth. Fast running is an anaerobic exercise; anaerobic exercise can hone people's endurance and physical quality, can bring people many different benefits, and can also help calf muscles become more full and powerful [19].

Because the foot is the only part of the body that the runner contacts the ground and directly provides power during running, the landing of the foot plays a special role in running technology, especially in the process of contacting the ground. According to the foot strike pattern, the runner's running mode is mainly divided into three types: the hindfoot landing mode, the midfoot landing mode, and the forefoot landing mode. The hind foot landing mode is the initial heel contact with the ground. The study found that more than 85% of middle- and long-distance runners use the rear foot landing mode. The rest of the runners used the midfoot landing mode and the forefoot landing mode. The midfoot landing mode is when the heel and ball of the foot initially contact the ground at the same time, and the forefoot landing mode is when the metatarsal ball initially contacts the ground. Many factors may affect the landing mode, including the type of running shoes that the runner wears, running speed, and running surface. For example, when running on steep slopes, runners tend to use the forefoot landing mode, and when running downhill, they tend to use the hindfoot landing mode. The landing mode of running will affect the transmission of impact force and the change of the lower limb movement biomechanics during running, resulting in different movement patterns of the lower limbs and the conduction of the power chain of the runner, which may cause different locations and rates of sports injuries. Therefore, the landing mode of running is one of the important factors that researchers must consider in the research of running biomechanics, and it is also one of the focuses of current running-related research.

When initially touching the ground, the ankle joints of runners using the forefoot landing mode were slightly flexed, and the ankle joints of the runners using the hindfoot landing mode were slightly dorsiflexion. After initial contact with the ground, the ankle joint of runners using the hindfoot landing mode has a rapid plantar flexion. In contrast, runners who used the forefoot landing mode experienced dorsiflexion in the ankle joint after initial contact with the ground. In addition, runners who use the forefoot landing mode will have greater knee and hip flexion angles. The kinematic change of the ankle joint in different landing modes is one of the important reasons leading to the kinematic change of the knee and hip joints. Compared with runners who use the forefoot landing mode, runners who use the forefoot landing mode have a smaller range of ankle dorsiflexion during the support phase and a larger range of knee and hip joints on the sagittal plane. In terms of the motion of the lumbar vertebrae, compared with runners using the forefoot landing mode, runners using the hindfoot landing mode have a larger range of lumbar spine motion.

At the same running speed, runners who landed on the forefoot showed shorter stride length, higher stride frequency, and shorter ground contact time. This may be because the knee joint flexes more when the runner touches the ground at this time, which shortens the runner's step length. Moreover, runners have more flexed ankles when they touch the ground, which may correspond to increased stride frequency. The increased cadence means that each step has a shorter time to touch the ground.

Muscle activity is caused by nerve impulses. Surface electromyography (EMG), as an effective way to observe muscle activity, can be used to evaluate muscle recruitment, activation, and coordination among muscles. This information about muscle activity obtained by the EMG test can be used to determine the specific internal mechanisms of human biomechanical adjustment. However, the current research on the neuromuscular regulation of the human body when running in different landing modes is relatively limited, mainly focusing on the muscles on the front and back of the calf.

In the time when the ankle plantar flexor muscle (gastrocnemius) is activated before the initial contact with the ground, runners using the forefoot landing mode activate 11% earlier than runners using the hindfoot landing mode. Runners in back foot landing mode are 10% longer. This may have a causal relationship with the structure of the human body. The preactivation of the ankle plantar flexor muscles before contacting the ground can increase the Achilles tendon tension, which in turn helps absorb the impact when contacting the ground. This can not only prepare for contact with the ground but also increase the ability of the tissue structure around the ankle joint to store elastic energy at the beginning of the support phase. Before the foot initially touches the ground, the gastrocnemius muscles are activated, causing muscle contractions. Therefore, for runners using the forefoot landing mode, the impact force upon landing will be immediately counteracted by the gastrocnemius muscle activated earlier and longer, which will help stabilize the ankle joint and stabilize the Achilles tendon load ratio. A medical imaging picture of the plantar flexor muscle is shown in Figure 1.

Compared with runners who used the hindfoot landing mode, runners who used the forefoot landing mode had lower tibialis anterior muscle activity and higher muscle activity on the medial head of the gastrocnemius muscle. For the hindfoot landing mode, there is more muscle activity in the tibialis anterior muscle, while for the forefoot landing mode, there is more muscle activity in the gastrocnemius and soleus muscle.

Many human movements are characterized by the continuous repetition of some basic form of movement (such as walking, running, single-foot jumping, cycling, swimming, and rowing). For periodic exercise, the average

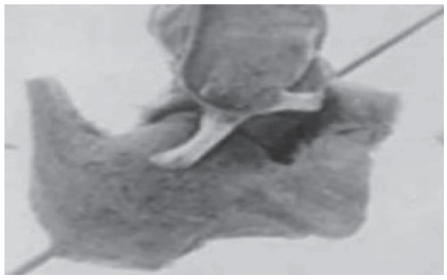

Figure 1: Plantar flexor muscle picture.

speed of the exercise is equal to the product of the average moving distance (such as the step size during running) and the average frequency or rhythm (such as the step frequency during running) of each exercise cycle. In normal human movement, these factors such as speed, distance, and frequency are usually arbitrarily determined or selected by the athlete, rarely fixed or determined in advance, and humans have an amazing ability to change speed, distance, and frequency to adapt to the environment demand. We call the frequency arbitrarily determined or selected by the athlete as the self-selected frequency or suitable frequency.

3. Experiments

3.1. Data Collection. This experiment selected 20 male students from a sports university. In order to reflect the difference between different running frequencies, the 20 subjects were randomly divided into two groups of low-frequency step and high-frequency step, with 10 boys in each group. The low-frequency step and high-frequency step are divided into three different speeds: low speed, medium speed and high speed.

3.2. Criteria for Recruiting Subjects. The criteria for recruiting subjects are as follows: (1) aged between 18 and 30; (2) male; (3) having a running exercise habit, running at least 10 km per week; (4) not receiving special system training. All subjects completed the informed consent form before the experiment to ensure that the subjects were healthy without motor system, neurological diseases, and other major medical histories. In the current state, there was no sports injury and the exercise ability was good. No strenuous exercise was performed within 24 hours before the test, and there was no muscle fatigue.

3.3. Experimental Instruments. The experimental instruments used in this study are as follows: infrared high-speed motion capture test system, three-dimensional force plate system, surface electromyography test system, laser speed measurement system, portable ultrasound system, height gauge, weight scale, morphometric ruler, and sports shoes need to be prepared, socks, tights, swimming cap, alcohol cotton ball, double-sided tape, elastic bandage, scissors, and other experimental consumables.

3.4. Experimental Methods. The application of a three-dimensional force plate system is studied to collect the ground reaction forces and related indicators in three directions during running, the acquisition frequency is 1000 Hz, and the surface electromyography test system is used to collect the subject's lower limb electromyographic parameters during running, and the acquisition frequency is 2000 Hz. The infrared high-speed motion capture system was used to collect the three-dimensional kinematic parameters of the reflective markers during running, and the instrument acquisition frequency was set to 200 Hz. The acquisition frequency of the experimental instrument is set to achieve frame synchronization between kinematics, dynamics, and surface EMG data. Before the experiment, inform and explain the subject's experimental content and experimental process in detail so that they fully understand and actively cooperate with the test.

The subject naturally stood on the force platform, with both arms raised sideways, feet separated, toes forward, and the positions of each point in the quiet state were marked. The subject then started at a position 13 m straight from the force plate and ran across the 26 m runway at speeds of 2.5 ± 0.2 m/s, 3.25 ± 0.2 m/s, and 4 ± 0.2 m/s, using portable speed measurement. The system monitors the running speed. The subject was not informed of the specific position of the force plate before the test. The subject was required to adjust without steps and step on the force plate with his left foot completely, no reflective landmarks fell off during the acquisition process, and no abnormal EMG signals were used as valid data. Data were recorded corresponding to each test file during the test. Each subject collected valid data 6 times at each speed, and the average value was obtained by excluding the maximum and minimum values.

The data were expressed as mean standard deviation and processed by statistical software. Paired tests were performed on the data of muscle stiffness, tendon stiffness, stiffness of muscle tendon complex, and vertical stiffness of lower limbs in each group. The significance level was $P < 0.05$.

4. Discussion

4.1. Analysis of Kinematic and Dynamic Parameters at Different Frequencies

4.1.1. Analysis of Kinematic Parameters at Different Frequencies. In this study, the stage where the vertical ground reaction force is greater than 10 N is regarded as the subject stepping on the force plate. According to the dynamic data, find the number of frames at the beginning and end of the left foot support phase, the magnitude of the vertical ground reaction force (the first peak, the second peak), and the number of frames at the time of occurrence; the critical frames of the buffer phase and the kick phase are calculated the support period and relative support period. The vertical ground reaction force value needs to be divided by the subject's weight for normalization to reduce the effect of weight on the force value. Kinematic indicators at different running frequencies are shown in Table 1 and Figure 2.

Table 1: Kinematic indicators at different running frequencies.

		Low-frequency step	High-frequency step
Slow	Stride (m)	1.9	1.8
	Gait cycle (s)	0.7	0.7
	Support period (s)	0.3	0.2
	Relative support period (%)	40	37
Medium speed	Stride (m)	2.4	2.2
	Gait cycle (s)	0.7	0.7
	Support period (s)	0.2	0.2
	Relative support period (%)	33	34
High speed	Stride (m)	2.9	2.7
	Gait cycle (s)	0.7	0.6
	Support period (s)	0.3	0.2
	Relative support period (%)	30	31

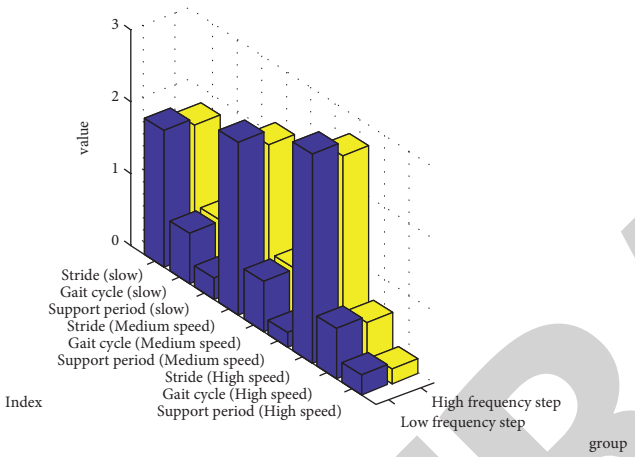

Figure 2: Kinematic indicators at different running frequencies.

From Table 1 and Figure 2, it can be seen that when the subjects are running at three speeds, there is no significant difference in step length between the low-cadence group and the high-cadence group, but both show an increase in running frequency and a decrease in step length. The small change trend is observed as follows: at three speeds, the gait period of the high-cadence group is significantly smaller than that of the low-cadence group ($p < 0.01$); at three speeds, the support period of the high-cadence group is shorter than that of the low-frequency group. And it is extremely significant at slow speeds ($p < 0.01$); when the subjects are jogging, the high stride group and the low stride group show a significant difference in the relative support period ($p < 0.05$), and the high stride frequency in the relative support period of the group was significantly shortened, but during the middle and fast running, the low-cadence group and the high-cadence group showed an increase in running frequency and a relative support period. In terms of the relative support period, at the three speeds, the values of slow steps are 40 and 30. It is suggested that the running frequency has an effect on step length, support period, and gait cycle.

4.1.2. Analysis of Dynamic Parameters at Different Frequencies. This study mainly analyzes the effect of different running frequencies on vertical ground reaction forces. After the dynamic data are collected and processed, the number of frames at the characteristic moments of the dynamic data (landing, off the ground, and the time when the maximum ground reaction force occurs) is synchronously converted into the number of frames at the characteristic moments of the kinematics data. Characteristic moments (landing, off the ground, and the moment when the maximum ground reaction force occurs), the lower limb joint angle, the maximum angle of the lower limb joint at the support stage, the minimum angle, and the range of motion (the difference between the maximum angle and the minimum angle) are also analyzed. The analysis of kinetic parameters at different frequencies is shown in Figure 3.

As shown in Figure 3, the first peak of the high-cadence group is larger than that of the low-cadence group when running at slow and medium speeds, and the opposite is true for fast running. The second peak of the high-cadence group is larger than that of the low-cadence group during slow and fast running, but the opposite is true at medium speed, but there is no significant difference.

4.2. Analysis of Lower Limb Stiffness and Muscle Vibration Frequency at Different Frequencies

4.2.1. Analysis of Lower Limb Stiffness at Different Frequencies. During running, the person's center of gravity is not always directly above the foot, so when calculating the stiffness, factors such as the speed of the runner, support time, leg length, and angle of the supporting leg and the ground must be considered. This study uses the following formula to calculate the stiffness of the lower limbs during the support phase, the buffer phase, and the active pedal extension phase:

$$k_{\text{leg}} = \frac{F_{\max}}{L - \sqrt{L^2 - \left(Vt_c/2\right)^2 + \Delta y}}. \quad (1)$$

Among them, $F_{\max}$ represents the maximum vertical ground reaction force, L represents the leg length, V represents the speed, t_c represents the ground time, and Δy represents the vertical displacement of the center of gravity.

The lower limb stiffness analysis at different frequencies is shown in Figure 4.

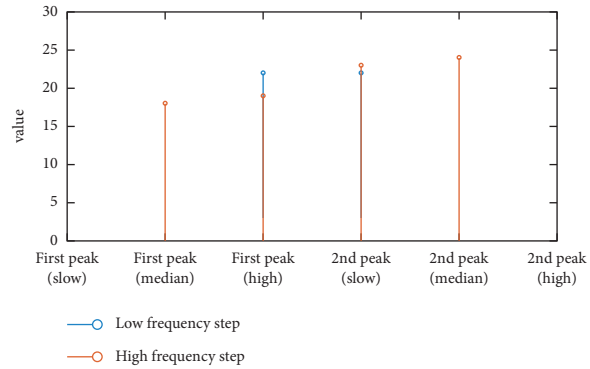

Figure 3: Analysis of kinetic parameters at different frequencies.

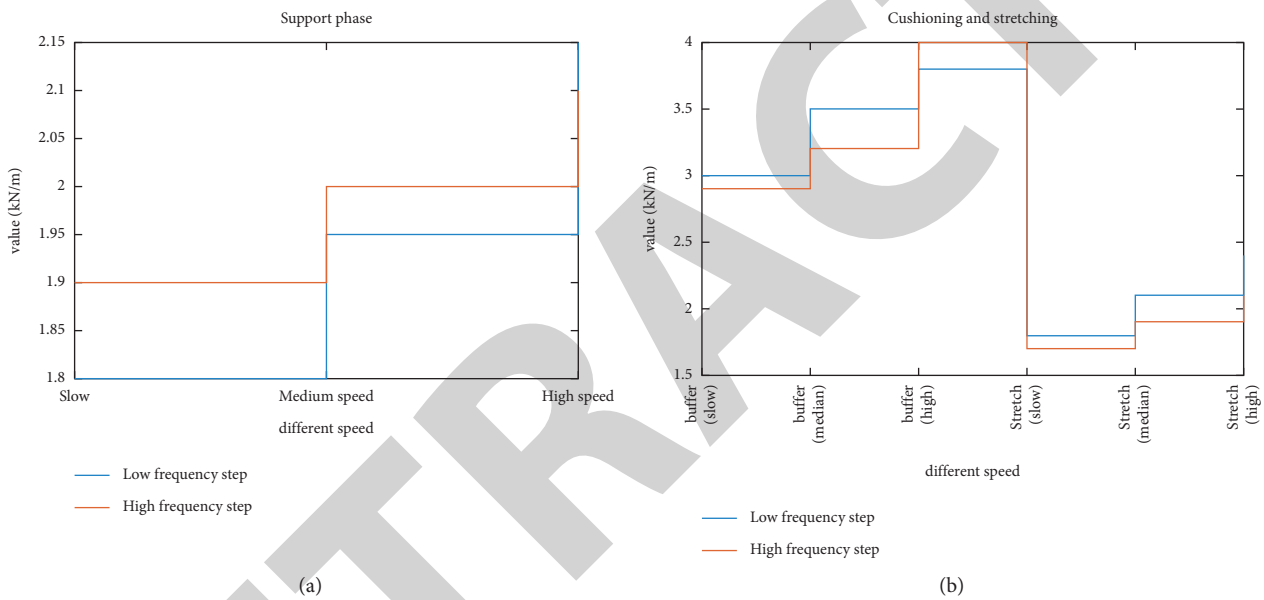

Figure 4: Analysis of lower limb stiffness at different frequencies. (a) Support phase; (b) cushioning and stretching.

It can be seen from Figure 4 that during the whole support period, the subjects' stiffness in the lower limbs of the high-cadence group was greater than that of the low-cadence group when running at slow and medium speeds, and the opposite was true during fast running, but there was no significant difference. In the buffer phase, the subjects' lower limb stiffness was lower in the high-cadence group than in the low-cadence group when running at slow and medium speeds, and the opposite during fast running. In the active kick-extension phase, the stiffness of the lower limbs of the high-cadence group was lower than that of the low-cadence group at three speeds.

4.2.2. Analysis of Muscle Vibration Frequency at Different Frequencies. A surface EMG signal is a combined wave composed of many sine waves with different frequencies and amplitudes in a certain time sequence. It is an electrical signal that is continuous in time and amplitude. The analysis of EMG signals includes time domain analysis and frequency domain analysis. This study mainly adopts time domain analysis methods, iEMG, and RMS. iEMG refers to the total discharge of motor units participating in activities in muscles within a certain period of time. The size of the iEMG value reflects the number of sports units participating in the work, the discharge size of each exercise unit, and, to a certain extent, muscle strength. RMS responds to the average level of muscle discharge over time. First, the original data are processed by zeroing, filtering (10–400 Hz), inversion, and low-pass filtering (0–20 Hz), and then iEMG and RMS are calculated. The lower limb stiffness analysis at different frequencies is shown in Figure 5.

From Figure 5, the activity of the rectus femoris, tibialis anterior muscle, medial head of gastrocnemius, lateral head of gastrocnemius, and biceps femoris, rectus, medial head of gastrocnemius, and lateral head of gastrocnemius at slow and fast can be seen; the higher the running frequency, the smaller the RMS trend. Moreover, the RMS of the medial head of the gastrocnemius muscle was significantly different between the low-cadence group and the high-cadence group at medium speed ($p < 0.05$).

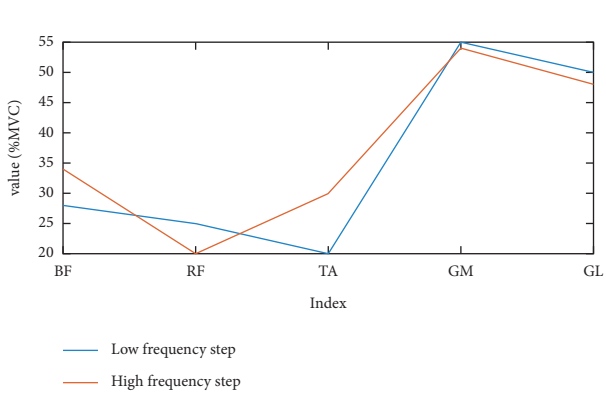

(a)

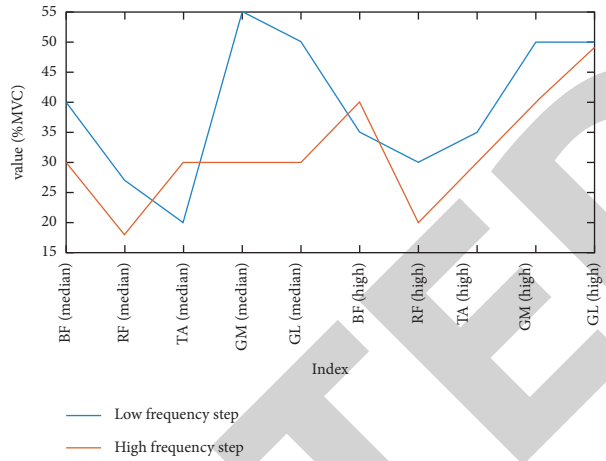

(b)

Figure 5: Analysis of lower limb stiffness at different frequencies. (a) Slow and (b) median speed and high speed.

5. Conclusions

The purpose of this article is to investigate the use of low-intensity lasers in the treatment of muscle strains, analyzing running, muscle conditioning, and lower extremity stiffness.

(1) This article analyzes the effects of different running frequencies on various spatiotemporal parameters. The results show that at three speeds, the higher the running frequency, the smaller the step size and gait cycle and the support period. The support period and relative support period of the high-cadence group at the slow speed are significantly lower than those of the low-cadence group. As the speed increases, the support period of the high-cadence group is still smaller than that of the low-cadence group, but there is no significant difference.

(2) This article finds that there is no difference in the impact force on the lower limbs at different running frequencies, and the kinematic indexes, such as the displacement of the center of gravity in the vertical direction, have a tendency to change, so it is theoretically inferred that the stiffness of the lower limbs at different running frequencies should be changed. The results calculated in this study are that during the buffer phase, the subjects' lower limb stiffness was lower in the high-cadence group than in the low-cadence group when running at slow and medium speeds, and the opposite was true during fast running. In the active kick-extension phase, the stiffness of the lower limbs of the high-cadence group was lower than that of the low-cadence group at three speeds.

(3) This article analyzes the effect of running frequency on muscle tuning and stiffness of lower limbs. It is recommended that people should try to choose a relatively high-cadence at the same speed when running, and runners who are used to lower cadence should appropriately choose professional sports equipment to reduce the risk of sports injuries.

Data Availability

The data that support the findings of this study are available from the corresponding author upon reasonable request.

Disclosure

The authors received no financial support for the research, authorship, or publication of this article.

Conflicts of Interest

The authors declare that they have no conflicts of interest.

References

[1] J. S. Park, H. Lee, B. W. Choi et al., "An MG53-IRS1-interaction disruptor ameliorates insulin resistance," *Experimental & Molecular Medicine*, vol. 50, no. 6, pp. 1–12, 2018.

[2] J. Bailey, T. Mata, and J. A. Mercer, "Is the relationship between stride length, frequency, and velocity influenced by running on a treadmill or overground?" *International Journal of Exercise Science*, vol. 10, no. 7, pp. 1067–1075, 2017.

[3] I. R. Faber, P. M. J. Bustin, F. G. J. Oosterveld, M. T. Elferink-Gemser, and M. W. Nijhuis-Van der Sanden, "Assessing personal talent determinants in young racquet sport players: a systematic review," *Journal of Sports Sciences*, vol. 34, no. 5, pp. 395–410, 2016.

[4] H. Zhu, H. Wei, B. Li, X. Yuan, and N. Kehtarnavaz, "Real-time moving object detection in high-resolution video sensing," *Sensors*, vol. 20, no. 12, p. 3591, 2020.

[5] M. A. Alsmirat, Y. Jararweh, M. Al-Ayyoub, M. A. Shehab, and B. B. Gupta, "Accelerating compute intensive medical imaging segmentation algorithms using hybrid cpu-gpu implementations," *Multimedia Tools and Applications*, vol. 76, no. 3, pp. 3537–3555, 2016.

[6] A. J. Greenup, B. Bressler, and G. Rosenfeld, "Medical mmaging in small bowel crohn's disease-computer

Hindawi
Emergency Medicine International
Volume 2023, Article ID 9754073, 1 page
https://doi.org/10.1155/2023/9754073

Retraction

Retracted: Study on the Changes of Liver and Kidney Function-Related Indicators and Clinical Significance in Patients with OSAHS

Emergency Medicine International

Received 19 December 2023; Accepted 19 December 2023; Published 20 December 2023

This article has been retracted by Hindawi following an investigation undertaken by the publisher [1]. This investigation has uncovered evidence of one or more of the following indicators of systematic manipulation of the publication process:

(1) Discrepancies in scope
(2) Discrepancies in the description of the research reported
(3) Discrepancies between the availability of data and the research described
(4) Inappropriate citations
(5) Incoherent, meaningless and/or irrelevant content included in the article
(6) Manipulated or compromised peer review

The presence of these indicators undermines our confidence in the integrity of the article's content and we cannot, therefore, vouch for its reliability. Please note that this notice is intended solely to alert readers that the content of this article is unreliable. We have not investigated whether authors were aware of or involved in the systematic manipulation of the publication process.

In addition, our investigation has also shown that one or more of the following human-subject reporting requirements has not been met in this article: ethical approval by an Institutional Review Board (IRB) committee or equivalent, patient/participant consent to participate, and/or agreement to publish patient/participant details (where relevant).

Wiley and Hindawi regrets that the usual quality checks did not identify these issues before publication and have since put additional measures in place to safeguard research integrity.

We wish to credit our own Research Integrity and Research Publishing teams and anonymous and named external researchers and research integrity experts for contributing to this investigation.

The corresponding author, as the representative of all authors, has been given the opportunity to register their agreement or disagreement to this retraction. We have kept a record of any response received.

References

[1] R. Liu and X. Kong, "Study on the Changes of Liver and Kidney Function-Related Indicators and Clinical Significance in Patients with OSAHS," *Emergency Medicine International*, vol. 2022, Article ID 9536617, 7 pages, 2022.

Hindawi
Emergency Medicine International
Volume 2022, Article ID 9536617, 7 pages
https://doi.org/10.1155/2022/9536617

Research Article

Study on the Changes of Liver and Kidney Function-Related Indicators and Clinical Significance in Patients with OSAHS

Rongyue Liu[1] **and Xiangdong Kong**[2]

[1]*Department of Otolaryngology, The First People's Hospital of Fuyang Hangzhou, Hangzhou 311400, Zhejiang, China*
[2]*Department of Nephrology, The First People's Hospital of Fuyang Hangzhou, Hangzhou 311400, Zhejiang, China*

Correspondence should be addressed to Rongyue Liu; liurongyue@st.btbu.edu.cn

Received 17 March 2022; Accepted 25 May 2022; Published 16 June 2022

Academic Editor: Roberto Cirocchi

Purpose. To study the changes of liver and kidney function-related indexes in patients with obstructive sleep apnea hypopnea syndrome (OSAHS) and analyze their clinical significance. *Method*. Ninety OSAHS patients treated in our hospital from April 2019 to April 2021 were selected. According to the apnea-hypopnea Index (AHI), they were divided into mild OSAHS group ($5 \le \text{AHI} < 15$ times/h, 35 people), moderate OSAHS group ($15 \le \text{AHI} < 30$ times/h, 35 people), and severe OSAHS group ($\text{AHI} \ge 30$ times/h, 20 people). In addition, 50 healthy people who underwent physical examination in our hospital at the same time were selected as the control group, and the liver and kidney function and polysomnography (PSG)-related indexes of the above subjects were detected, and the comparison between the groups was carried out. *Result*. The serum BUN and SCR levels of the severe group were significantly higher than those of the moderate group, the moderate group had significantly higher levels than the mild group, and the mild group had significantly higher levels than the control group ($P < 0.05$). The blood AST level of the severe group was significantly lower than that of the moderate group, the moderate group had a significantly lower level than the mild group, and the mild group had a significantly lower level than the control group ($P < 0.05$). The blood ALT level of the severe group was significantly higher than that of the moderate group, the moderate group had significantly a higher level than the mild group, and the mild group had a significantly higher level than the control group ($P < 0.05$). The proportions of abnormal liver and kidney function in the control group, mild group, moderate group, and severe group were significantly different ($P < 0.05$). The AHI of the severe group was significantly higher than that of the moderate group, the moderate group had a higher value than the mild group, and the mild group had a higher value than the control group ($P < 0.05$). The ASpO_2 and MSpO_2 of the severe group were significantly lower than those of the moderate group, the moderate group had significantly lower values than the mild group, and the mild group had significantly lower values than the control group ($P < 0.05$). Spearman correlation analysis showed that the liver and kidney function indexes of OSAHS patients were significantly correlated with PSG indexes ($P < 0.05$). *Conclusion*. Patients with OSAHS will have obvious liver and kidney dysfunction, and the monitoring of liver and kidney function in such patients should be strengthened. If abnormality occurs, early intervention is recommended.

1. Preface

Obstructive sleep apnea hypoventilation syndrome (OSAHS) is a sleep breathing disorder of unknown etiology [1], in which the main clinical manifestations include nocturnal snoring with apnea and daytime sleepiness. Clinical practice indicates that OSAHS is a potentially fatal sleep breathing disorder because of its tendency to cause recurrent episodes of nocturnal hypoxia and hypercapnia, which may lead to complications such as hypertension, coronary heart disease, diabetes mellitus, and cerebrovascular disease, and may even induce sudden death at night [2, 3]. Data from some large community-based population studies show that the prevalence of OSAS in recent years is about 4%–7.5% in men and 2% in women, and domestic epidemiological investigation suggests that the prevalence of OSAHS in adults is between 3% and 5% [4, 5].

In recent years, as research on OSAHS has intensified, more and more studies have pointed out that such patients may have concomitant hepatic and renal impairment [6]. Data show that about 51.7% of patients with OSAHS have concomitant polyuric symptoms, more than 30% of patients with OSAHS have concomitant chronic kidney disease, and some patients with OSAHS have decreased glomerular filtration rate [7]. A large number of studies have also concluded that although the site of OSAHS is the upper airway, the damage caused by the disorder is not limited to the upper airway itself. Systemic hypertension, atherosclerosis, coronary artery disease, arrhythmias, pulmonary hypertension, asthma, and Alzheimer's disease may be closely related to OSAHS [8]. Although the causal relationship between the above diseases and OSAHS is still being explored, an increasing number of scholars tend to define OSAHS as a multisystemic and multiorganic disease.

This study intends to investigate the changes of liver and kidney function-related indicators in patients with OSAHS by setting up a control group and attempts to investigate the necessity of liver and kidney function monitoring in patients with OSAHS, in order to provide clinical reference for improving the prognosis of patients with OSAHS.

2. Information and Method

2.1. General Information. Ninety patients with OSAHS treated in our hospital from April 2019 to April 2021 were selected. They were divided into mild OSAHS group ($5 \leq$ AHI < 15 times/h, 35 patients), moderate OSAHS group ($15 \leq$ AHI < 30 times/h, 35 patients), and severe OSAHS group (AHI ≥ 30 times/h, 20 patients) according to apnea-hypopnea index (AHI). 50 healthy individuals who underwent physical examination in our hospital at the same time were selected as the control group.

2.1.1. Inclusion Criteria. (1) Patients with OSAHS met clinical diagnostic criteria [9] and presented with appropriate clinical symptoms. (2) Patients were conscious and able to cooperate with the study. (3) Case data were complete and available. (4) Patients have good compliance with the study. (5) Patients have signed informed consent. (6) AHI score ≥ 5. (7) The study was approved by the ethics association to be conducted.

2.1.2. Exclusion Criteria. (1) Patients have combined psychiatric disorders. (2) Patients have combined malignant neoplasm. (3) Patients have combined liver and kidney dysfunction. (4) Patients have combined autoimmune diseases. (5) Patients have combined pulmonary diseases. (6) Patients have complicated blood system diseases, hyperthyroidism, hypothyroidism, etc. (7) Patients have been taking drugs with impaired liver and kidney function within the last 1 month.

2.2. Intervention Method. (1) Sleep monitoring: all patients in the study group completed PSG monitoring, and no sleeping pills or alcohol, tea, coffee, etc. could be taken within 24 h before the test. The subjects were mainly monitored for sleep structure, breathing, snoring, and body position, and their sleep conditions were judged according to the American Academy of Sleep Medicine sleep and its related events (AASM) criteria [10], and their AHI, $ASpO_2$, and $MSpO_2$ indicators were recorded. (2) Fasting elbow venous blood samples were collected from all subjects, and liver and kidney functions were tested by automatic biochemical analyzers, including AST and ALT for liver functions and BUN and SCr for kidney functions.

2.3. Observation Indicators and Evaluation Criteria. The patients in the study group were distinguished into mild OSAHS group ($5 \leq$ AHI < 15 times/h, 35 cases), moderate OSAHS group ($15 \leq$ AHI < 30 times/h, 35 cases), and severe OSAHS group (AHI ≥ 30 times/h, 20 cases), according to the AHI index [11]. The differences in liver and kidney function and PSG-related indicators between the above three groups and control individuals were compared between groups, and the correlation between liver and kidney function indicators of patients with OSAHS and their PSG indicators was also analyzed.

2.4. Statistical Method. Spss22.0 statistical software was selected to analyze the data collected in the study, in which the measured data were expressed as (standard deviation of mean value ± for standard deviation) normal distribution and chi square test, t-test was used for the differences between data groups that conform to normal distribution or chi square distribution, and Mann Whitney u test was used for statistics of data with inconsistent variance. The difference between groups was tested using the chi-square test, and the difference was considered statistically significant at $P < 0.05$. The GraphPad Prism 8.3 was used in this study [12].

3. Result

3.1. Comparison of Baseline Information between Groups of Patients. Age, gender, BMI, blood pressure, blood test-related indicators, and respiratory sleep monitoring-related indicators were included in the study and carried out to compare the difference between groups, and the result showed that the difference between groups in age, gender, BMI, blood pressure, blood glucose, total cholesterol, and triglycerides in several groups were not statistically significant ($P < 0.05$), suggesting that the groups were better comparable (see Table 1).

3.2. Comparison of Renal Function Indicators between Groups of Patients. The results showed that the serum BUN and SCr levels of patients in the severe group were significantly higher than those in the moderate group, the moderate group had significantly higher levels than the mild group, and the mild group had significantly higher levels than the

Table 1: Comparison of baseline information of patients in different groups ($\overline{x} \pm s$)/(n (%)).

General clinical information		Mild group ($n = 35$)	Moderate group ($n = 35$)	Severe group ($n = 20$)	Control group ($n = 50$)	F	P value
Gender	Male	20	19	8	25	1.211	0.723
	Female	15	16	12	25		
Average age (years)		49.89 ± 3.22	50.19 ± 2.98	50.11 ± 2.38	49.78 ± 3.89	0.123	0.946
Average BMI (kg/m^2)		23.29 ± 2.39	23.41 ± 2.09	23.89 ± 2.11	23.78 ± 2.01	0.571	0.635
Systolic blood pressure (mmHg)		124.38 ± 10.19	123.98 ± 9.98	123.78 ± 10.31	124.08 ± 10.78	0.016	0.997
Diastolic blood pressure (mmHg)		78.98 ± 5.44	79.01 ± 4.98	79.13 ± 5.01	79.33 ± 4.87	0.043	0.988
Blood glucose (mmol/L)		4.98 ± 0.98	5.01 ± 0.89	5.04 ± 0.87	4.99 ± 1.01	0.020	0.996
Total cholesterol (mmol/L)		4.49 ± 0.43	4.53 ± 0.39	4.51 ± 0.33	4.59 ± 0.29	0.6	0.616
Triglycerides (mmol/L)		2.29 ± 0.32	2.30 ± 0.29	2.34 ± 0.31	2.33 ± 0.28	0.201	0.896
High-density lipoprotein (mmol/L)		1.12 ± 0.12	1.14 ± 0.09	1.15 ± 0.12	1.18 ± 0.14	1.813	0.148
Low-density lipoprotein (mmol/L)		2.87 ± 0.54	2.78 ± 0.49	2.91 ± 0.31	2.84 ± 0.21	0.523	0.667

Table 2: Comparison of renal function indicators among patients in each group ($\overline{x} \pm s$).

Group	Number of cases	BUN (mmol/L)	SCr (μmol/L)
Mild group	35	5.11 ± 0.45^{①②③}	83.22 ± 4.22^{①②③}
Moderate group	35	5.39 ± 0.39^{①②}	88.98 ± 3.98^{①②}
Severe group	20	5.78 ± 0.29^{①}	93.29 ± 4.01^{①}
Control group	50	4.68 ± 0.33	76.11 ± 3.98
F	—	50.003	116.111
P value	—	<0.001	<0.001

Compared with the control group, $^{①}P < 0.05$; compared with the severe group, $^{②}P < 0.05$; compared with the moderate group, $^{③}P < 0.05$.

control group, and the differences between the groups were statistically significant ($P < 0.05$) (see Table 2 and Figure 1).

The serum BUN and SCr levels of patients in the severe group were significantly higher than those in the moderate group, the moderate group had significantly higher levels than the mild group, and the mild group had significantly higher levels than the control group, and the differences of the above indicators were statistically significant when comparing between groups ($P < 0.05$). # represents a statistically significant difference between groups comparing the same index.

3.3. Comparison of Liver Function Indicators between Groups of Patients. The AST and ALT level of blood samples from patients in the mild group, moderate group, severe group, and control group were tested and compared between the groups. The ALT level of blood samples of patients in the severe group was significantly higher than that in the moderate group, the moderate group had a significantly higher level than the mild group, and the mild group had a significantly higher level than the control group. The difference of the above indicators were statistically significant when comparing between groups ($P < 0.05$) (see Table 3 and Figure 2).

The AST level of blood samples of patients in the severe group were significantly lower than those in the moderate group, the moderate group had significantly a lower level than the mild group, and the mild group had a significantly lower level than the control group. The difference of above indicators were statistically significant when comparing between groups ($P < 0.05$). The ALT level of blood samples of patients in the severe group was significantly higher than that in the moderate group, the moderate group had a significantly higher level than the mild group, and the mild group had a significantly higher level than the control group. The difference of above indicators were statistically significant when comparing between groups ($P < 0.05$). # represents a statistically significant difference between groups comparing the same index.

3.4. Comparison of the Rate of Abnormal Liver and Kidney Function in Each Group of Patients. The percentage of liver and kidney function abnormalities in each group was compared between groups, and the results showed that there were large differences in the ratio of liver and kidney function abnormalities in the control, mild, moderate, and severe groups. The comparison between groups showed that

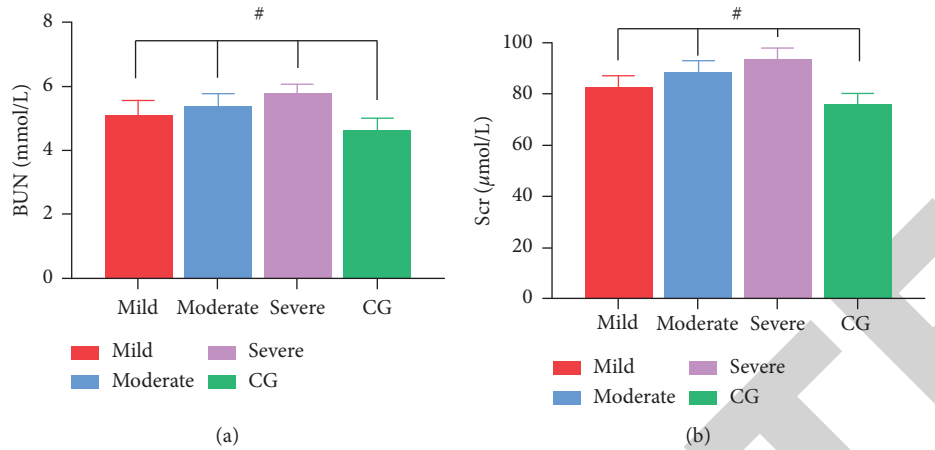

Figure 1: Comparison of renal function indicators among groups.

Table 3: Comparison of liver function indicators among patients in each group ($\bar{x} \pm s$).

Group	Number of cases	AST (U/L)	ALT (U/L)
Mild group	35	21.27 ± 3.22^{①②③}	33.18 ± 3.20^{①②③}
Moderate group	35	25.03 ± 2.39^{①②}	40.11 ± 4.10^{①②}
Severe group	20	27.19 ± 3.01^{①}	46.18 ± 3.98^{①}
Control group	50	29.89 ± 4.33	22.91 ± 3.20
F	—	367.330	271.976
P value	—	<0.001	<0.001

Compared with the control group, $^{①}P < 0.05$; compared with the severe group, $^{②}P < 0.05$; compared with the moderate group, $^{③}P < 0.05$.

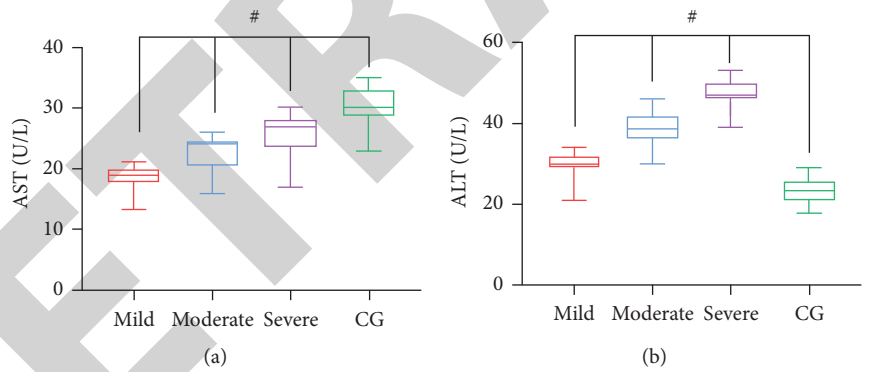

Figure 2: Comparison of liver function indicators of patients in each group.

Table 4: Comparison of abnormal liver and kidney function rates among groups (n (%)).

Observed indicators		Mild group ($n = 35$)	Moderate group ($n = 35$)	Severe group ($n = 20$)	Control group ($n = 50$)
Liver function	AST	0 (0.00)	4 (11.43)^{①②}	5 (20.00)^{①②}	0 (0.00)
	ALT	3 (8.57)	8 (22.86)^{①}	10 (50.00)^{①②}	1 (2.00)
Renal function	BUN	4 (11.43)	7 (20.00)^{①}	8 (40.00)^{①}	1 (2.00)
	SCr	2 (5.71)	6 (17.14)^{①}	9 (45.00)^{①②}	1 (2.00)

Compared with the control group, $^{①}P < 0.05$; compared with the mild group, $^{②}P < 0.05$.

the percentage of liver and kidney function abnormalities in the moderate and severe groups was significantly higher than that in the mild and control groups, and the difference in some indicators were statistically significant ($P < 0.05$) (see Table 4).

3.5. Comparison of PSG-Related Indicators between Groups of Patients. The PSG test was performed on each group of patients separately, and the indices of AHI, $ASpO_2$, and $MSpO_2$ of the subjects were tested and compared between the groups. The $ASpO_2$ and $MSpO_2$ of patients in the severe

Table 5: Comparison of PSG-related indicators among patients in each group ($\overline{x} \pm s$).

Group	Number of cases	AHI (times/h)	$ASpO_2$ (%)	$MSpO_2$ (%)
Mild group	35	13.22 ± 1.98^{①②③}	96.18 ± 3.49^{①②③}	83.18 ± 5.01^{①②③}
Moderate group	35	23.89 ± 3.21^{①②}	93.29 ± 4.01^{①②}	76.18 ± 4.22^{①②}
Severe group	20	60.19 ± 5.41^{①}	90.19 ± 2.30^{①}	64.29 ± 4.30^{①}
Control group	50	3.98 ± 0.43	99.28 ± 3.90	89.18 ± 3.49
F	—	240.465	36.619	189.593
P value	—	<0.001	<0.001	<0.001

Compared with the control group, $^{①}P < 0.05$; compared with the severe group, $^{②}P < 0.05$; compared with the moderate group, $^{③}P < 0.05$.

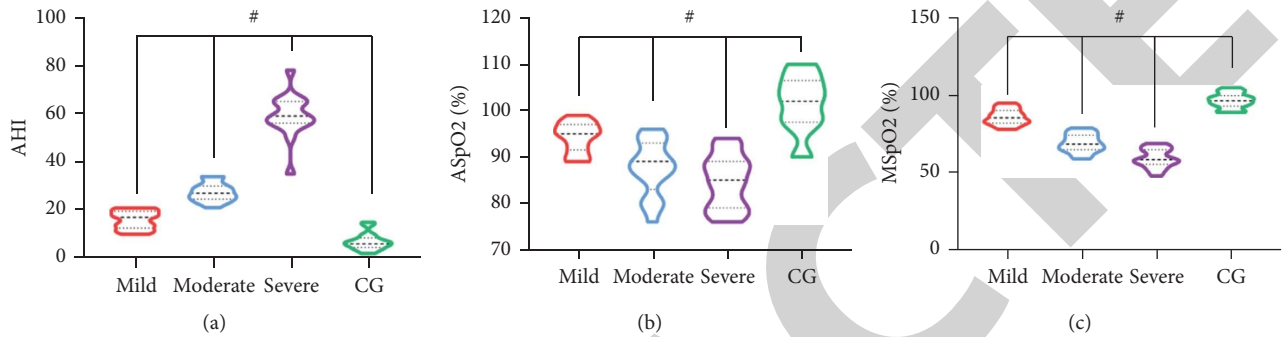

Figure 3: Comparison of PSG-related indicators among groups of patients.

Table 6: Correlation analysis of liver and kidney function indicators with PSG indicators in patients with OSAHS.

Indicators	AST	ALT	BUN	SCr	AHI	$ASpO_2$	$MSpO_2$
AST	—	—	—	—	−0.726	0.556	0.519
ALT	—	—	—	—	0.712	−0.772	−0.549
BUN	—	—	—	—	0.459	−0.771	−0.627
SCr	—	—	—	—	0.819	−0.728	−0.711
AHI	−0.726	0.712	0.459	0.819	—	—	—
$ASpO_2$	0.556	−0.772	−0.771	−0.728	—	—	—
$MSpO_2$	0.519	−0.549	−0.627	−0.711	—		—

group were significantly lower than those in the moderate group, the moderate group had significantly lower values than the mild group, and the mild group had significantly lower values than the control group. The difference between the groups were statistically significant ($P < 0.05$) (see Table 5 and Figure 3).

Comparison showed that the AHI of patients in the severe group was significantly higher than that in the moderate group, the moderate group had a higher value than the mild group, and the mild group had a higher value than the control group. The difference between the groups was statistically significant ($P < 0.05$). The $ASpO_2$ and $MSpO_2$ of patients in the severe group were significantly lower than those in the moderate group, the moderate group had significantly lower values than the mild group, and the mild group had significantly lower values than the control group. The difference between the groups were statistically significant ($P < 0.05$). # represents a statistically significant difference between groups comparing the same index.

3.6. Correlation Analysis of Liver and Kidney Function Indicators with PSG Indicators in Patients with OSAHS. Spearman analysis was performed on the correlation between liver function indicators (AST and ALT), kidney function indicators (BUN and SCr) and PSG indicators (AHI, $ASpO_2$, and $MSpO_2$) in patients with OSAHS. The results showed that AST showed significant correlation with AHI, $ASpO_2$, and $MSpO_2$ ($r = -0.726, 0.556, 0.519$, $P < 0.05$), ALT showed significant correlation with AHI, $ASpO_2$, and $MSpO_2$ ($r = 0.712$, -0.772, -0.549, $P < 0.05$), and BUN showed significant correlations with AHI, $ASpO_2$, and $MSpO_2$ ($r = 0.459, -0.771, -0.627$, $P < 0.05$), and SCr showed significant correlations with AHI, $ASpO_2$, and $MSpO_2$ ($r = 0.819$, -0.728, -0.711, $P < 0.05$) (see Table 6).

4. Discussion

Since the 1970s, there has been increasing concern about OSAHS worldwide [13]. Overseas epidemiological surveys for snoring and OSAHS began 20 years ago in the form of questionnaires and telephone calls, and some of these patients were even monitored for sleep breathing throughout the night. It was concluded that the prevalence of OSAHS in individuals under 65 years was about 0.3%–1%, with men prevalence significantly higher than that of women [14]. Less epidemiological investigation has been conducted for OSAS in China, but the prevalence of the disorder has shown a significant increase in recent

years with the rise in life and work stress among the population [15].

Medical practitioners believe that patients with OSAHS are superior to the collapse of the upper airway during sleep, prone to apnea and hypoventilation, followed by a series of changes such as endothelial damage, sleep structural fragmentation, endocrine hormone abnormalities, and inflammatory reactions, which can cause safety threats to the circulatory, neurological, metabolic, endocrine, respiratory, urinary, hematological, and other systemic systems of patients, especially cardiovascular, hepatic, and renal function damage are the most [16, 17]. Studies have confirmed the independent correlation between OSAS and cardiovascular diseases, and patients with OSAHS are significantly more likely to develop hypertension, stroke, pulmonary hypertension, chronic kidney disease, and other disorders [18, 19].

In this study, we investigated the changes in liver and kidney function in patients with OSAHS by setting up a control group, and the results showed that compared with the control group, patients with OSAHS showed a significant decrease in AST, a significant increase in ALT, and a significant increase in BUN and SCr. Both indicators of kidney function and the changes were also closely related to the condition of OSAHS.

In a study of 230 patients with OSAHS [20], the level of reactive oxygen species, hypoxia-inducible factor-1α, nitric oxide, urea nitrogen, creatinine, and uric acid in the serum of patients with moderate to severe OSAHS were significantly different from those of patients with mild OSAHS and normal controls, which is believed to be due to the presence of chronic hypoxia in patients with OSAHS. Chronic hypoxia, which in turn induces renal impairment, can be considered as a potential risk factor for chronic renal insufficiency in OSAHS. In a study conducted on 50 patients with OSAHS and 40 healthy controls [21], it was found that the level of ALT, TC, AST, BUN, and SCr were abnormally elevated in patients with mild to moderate and severe OSAHS compared to normal controls, while the elevation of AST and SCr was particularly severe in patients with severe OSAHS. In this study, we analyzed that AST and ALT can reflect the integrity of hepatocyte membrane or mitochondria, and their serum concentrations can reflect the damage status of hepatocytes more sensitively; thus, they are often used in clinical screening for impaired liver function [22]. BUN and SCr are both common indicators of renal function examination in clinical practice, among which SCr can also reflect glomerular filtration rate [23]. Due to impaired airway function and long-term hypoxia, several studies have confirmed that OSAHS is an independent risk factor for diseases such as cardiac arrhythmia, congestive heart failure, insulin resistance, and hyperlipidemia, and also a risk factor for the development of chronic kidney injury.

Continued exacerbation of OSAHS without better control will induce and aggravate the decline of liver and kidney function and eventually lead to the development of liver and kidney impairment [24]. Patients with OSAHS can develop significant liver and kidney dysfunction, and monitoring of liver and kidney function in such patients should be strengthened, and early implementation of interventional therapy is recommended in case of abnormalities. The limitations of this study are as follows: (1) There were more men than women in the study, and gender bias may have had an impact on the results. (2) Changes in the abovementioned indicators in patients with OSAHS after the intervention were not studied. (3) Detailed mechanisms of liver and kidney function impairment in OSAHS patients were not analyzed. Revisions and improvements are planned for later stages. In this paper, the authors analyzed that, in addition to the above mechanisms, there may be another reason for OSAHS-induced liver and kidney injury, namely, OSAHS causes the body to be in a state of inflammatory imbalance. Many studies have pointed out that the levels of superoxide dismutase, interleukin-2, and tumor necrosis factor are significantly elevated in patients with severe OSAHS, analyzing that OSAHS leads to a disturbance in the immune imbalance of the organism [25], and the present study suggests that this may also be related to the development of OSAHS, and further in-depth study of the mechanism is needed.

Data Availability

The raw data supporting the conclusions of this article will be made available by the authors, without undue reservation.

Conflicts of Interest

The authors declared that they have no conflicts of interest regarding this work.

Acknowledgments

This study was supported by the Zhejiang Medical and Health Science and Technology Plan Project No. 2020KY802.

References

[1] M. Otto-Yáñez, R. Torres-Castro, J. Nieto-Pino, and M. Mayos, "Obstructive sleep apnea-hypopnea and stroke," *Medicina (B Aires)*, vol. 78, no. 6, pp. 427–435, 2018.

[2] A. C. Stöwhas, M. Lichtblau, and K. E. Bloch, "Obstruktives schlafapnoe-syndrom obstructive sleep apnea syndrome," *Praxis (Bern 1994)*, vol. 108, no. 2, pp. 111–117, 2019.

[3] C. Perez, "Obstructive sleep apnea syndrome in children," *General Dentistry*, vol. 66, no. 6, pp. 46–50, 2018.

[4] Z. H. Wu, X. P. Yang, X. Niu, X. Y. Xiao, and X. Chen, "The relationship between obstructive sleep apnea hypopnea syndrome and gastroesophageal reflux disease: a meta-analysis," *Sleep and Breathing*, vol. 23, no. 2, pp. 389–397, 2019.

[5] C. Y. Ko, Q. Q. Liu, H. Z. Su et al., "Gut microbiota in obstructive sleep apnea-hypopnea syndrome: disease-related dysbiosis and metabolic comorbidities," *Clinical Science*, vol. 133, no. 7, pp. 905–917, 2019.

[6] C. F. Lee, C. H. Lee, W. Y. Hsueh, M. T. Lin, and K. T. Kang, "Prevalence of obstructive sleep apnea in children with down syndrome: a meta-analysis," *Journal of Clinical Sleep Medicine*, vol. 14, no. 5, pp. 867–875, 2018.

[7] S. García Castillo, M. d P. S. Hoyos Vázquez, R. Coloma Navarro et al., "Obstructive sleep apnoea syndrome," *Anales de Pediatría*, vol. 88, no. 5, pp. 266–272, 2018.

Hindawi
Emergency Medicine International
Volume 2023, Article ID 9809046, 1 page
https://doi.org/10.1155/2023/9809046

Retraction

Retracted: Key Technology of the Medical Image Wise Mining Method Based on the Meanshift Algorithm

Emergency Medicine International

Received 28 November 2023; Accepted 28 November 2023; Published 29 November 2023

This article has been retracted by Hindawi, as publisher, following an investigation undertaken by the publisher [1]. This investigation has uncovered evidence of systematic manipulation of the publication and peer-review process. We cannot, therefore, vouch for the reliability or integrity of this article.

Please note that this notice is intended solely to alert readers that the peer-review process of this article has been compromised.

Wiley and Hindawi regret that the usual quality checks did not identify these issues before publication and have since put additional measures in place to safeguard research integrity.

We wish to credit our Research Integrity and Research Publishing teams and anonymous and named external researchers and research integrity experts for contributing to this investigation.

The corresponding author, as the representative of all authors, has been given the opportunity to register their agreement or disagreement to this retraction. We have kept a record of any response received.

References

[1] J. Cui, Y. Wang, and K. Wang, "Key Technology of the Medical Image Wise Mining Method Based on the Meanshift Algorithm," *Emergency Medicine International*, vol. 2022, Article ID 6711043, 8 pages, 2022.

Hindawi
Emergency Medicine International
Volume 2022, Article ID 6711043, 8 pages
https://doi.org/10.1155/2022/6711043

Research Article

Key Technology of the Medical Image Wise Mining Method Based on the Meanshift Algorithm

Jinli Cui,[1] Yadong Wang,[2] and Ke Wang [3]

[1]*Department of Radiology, Affiliated Hospital of Changchun University of Traditional Chinese Medicine, Changchun 130000, Jilin, China*
[2]*Department of Computer Science and Technology, Changchun University of Technology, Changchun 130000, Jilin, China*
[3]*Department of Radiology, Xi'an Kidney Diseases Hospital of Traditional Chinese Medicine, Xi'an 710300, Shaanxi, China*

Correspondence should be addressed to Ke Wang; wangke1128520@njau.edu.cn

Received 2 April 2022; Revised 4 May 2022; Accepted 19 May 2022; Published 15 June 2022

Academic Editor: Hang Chen

Mean-shift originally refers to the mean vector of the offset. The algorithm idea is to assume that the data sets of different clusters conform to different probability density distributions, and the area with high sample density corresponds to the center of the cluster. With the wide application of hospital information system, especially the popularity of the meanshift algorithm in the outpatient system, it has greatly improved the efficiency of medical staff. Medical imaging refers to the technology and process of obtaining internal tissue images of the human body or a certain part of the human body in a noninvasive manner for medical treatment or medical research. It contains the following two relatively independent research directions: medical imaging system and medical image processing. In this paper, we expect to improve the mining ability of medical image information with the help of the meanshift algorithm based on the key technology of the medical image intelligent mining algorithm. This paper proposes a method to enhance image feature extraction and data mining and how to apply relevant analysis rules for mining. Applying this integrated algorithm to extract simplified rules is more beneficial to people's understanding than the raw data and helps doctors quickly understand the patient's condition.

1. Introduction

Today's society is an era of information and networking. The amount of information is growing rapidly. It also brings a lot of problems: the first is excessive information and difficult to digest; the second is true and false information. The fast-growing massive amounts of data are stored in large and large databases, without powerful tools, and understanding them has gone far beyond human capabilities, resulting in data being collected in large databases becoming "data graves" rare to visit again. Data archives and a lot of important information are hidden behind the surge of data. Decision makers' decisions are often not based on useful information in the database, but on intuition, because decision makers lack the tools to extract valuable knowledge from massive data [1–3]. There are many types of data available in the medical field [4], including complete code information, clinical information about the patient's medical history, testing, and treatment [5], drug management information [6], hospital management information, and [7], data mining theory is applied in medicine [8–10]. According to the amount of data, it is divided into memory level: the amount of data does not exceed the maximum memory of the cluster; BI level: the amount of data that is too large for memory; the amount of data that has completely failed or is too expensive for databases and BI products. The meanshift algorithm, also known as the mean shift method, has at its core the mean shift vector, which estimates the gradient of the probability density function. The meanshift algorithm needs to first calculate the offset mean of the current point, move the point to this offset mean, and then use this as a new starting point and continue to move until the final

conditions are met. The function does not require the aid of a priori knowledge and is classified as a nonparametric estimation method. The meanshift algorithm provides an effective means of analyzing medical data and extracting valuable and meaningful information. The study of genetic patterns of human disease and health is extremely important in promoting human health and maintaining a healthy quality of life [11, 12].

Electronic devices have been widely used in the medical field [13, 14]. However, most hospitals currently deal with databases as low-end operations in medical databases, lacking data integration and analysis, not to mention medical decision-making and automatic acquisition of knowledge. A large amount of data are described as "rich data, but information is poor." How to use data mining technology to find valuable knowledge and rules from these massive data is a problem that needs to be solved at present [15, 16], and mining the hidden rules in the data to use them to provide scientific decisions for the diagnosis and treatment of diseases, summarizing various treatments. The efficacy of the program, better for hospital decision-making management, medical, scientific research, and teaching services, has become a very important research topic. Rough sets are widely used, including a variety of logical, mathematical, and philosophical aspects of rough sets [17, 18]. Rough sets are also associated with many other methods and are also associated with a very broad hybrid system. Rough sets are now associated with data mining and knowledge discovery and decision systems. Rough sets have been used in reasoning and computational fields [19, 20].

This paper combines the meanshift algorithm with medical image intelligent mining technology, by mining association rules and useful information from a large number of images, and investigates the feature extraction and loading method of medical image data [21, 22], the classification method of medical image data, and the coarse set mining data aspect of brain tumor MRI images, which helps doctors identify the relationship between the high incidence of disease population, the severity of disease, and various hidden information, aids the decision-making diagnosis process, and improves the accuracy rate, with important theoretical significance and broad application prospects.

2. Proposed Method

2.1. Data Mining. Data mining is a cross-cutting discipline. Data mining is the process of getting valuable information of scrappy data. Data mining refers to the use of data mining technology on a very large amount of irregular data to obtain hidden information that is beneficial to value. The complexity of the data can thus be seen. Data mining can derive a new value from the complexity of information. Through data mining, new data rules can be found from the data and the data can be analyzed from different perspectives to obtain new values. Figure 1 shows a schematic diagram of the data mining model:

Data mining is a hot problem in the field of artificial intelligence and database research, which can save time and improve efficiency by quickly capturing the needed information from a large amount of complicated information according to the condition constraints. Data mining is a decision support process that can also make inductive reasoning and uncover potential information to help decision makers make the right decisions. Data mining technology has experienced four steps of data collection, data access, data warehouse, and data mining, which can meet the needs of query and storage and provide a basis for auxiliary decision-making.

Data mining not only can query and traverse past data but also can predict future trends and behaviors and automatically detect patterns that have not been discovered before so that people can make good decisions. The object of data mining can be any type of data source: it can be a relational database, which contains structured data; it can also be data warehouse, text, and multimedia data, which contains semistructured data or even heterogeneous data source. The discovered knowledge can be used for knowledge management, decision support, process control, and many other applications. The functions of data mining are mainly divided into the following categories: Association analysis: the correlation analysis refers to finding the similarity of values in the database, that is, the hidden association rules between the discovered data, which is the description of the data correlation in the database. Clustering: the process of grouping data in a database into multiple classes of similar data is called clustering, and its purpose is to establish a macroscopic concept of objective reality. Each class generated by clustering is a collection of data, the data in the same class are similar to each other, and the data in different classes are different. Figure 2 shows a diagram of the data mining process.

In recent years, data mining technology has been widely used in the medical field. Promising results have been obtained in disease diagnosis, treatment, and scientific research. In the pathological study, a large amount of data of pathological sections were analyzed by data mining and the key indicators were summarized to establish a normal and pathological virtual cell model. Virtual cell is an emerging discipline that analyzes, integrates, and applies the structure and function of cells through mathematical calculation and analysis to simulate and reproduce the phenomena of cells and life. This can be used to understand the physiological mechanisms of the occurrence, activity, and regulation of virtual cells. It can also understand and reveal the pathogenesis of diseases, find effective pathogenic molecules and marker molecules, conduct early warning diagnosis of diseases, and propose prevention and intervention measures. Data mining can make better use of these data, help physicians improve the efficiency and accuracy of diagnosis, reduce the work intensity of physicians, discover new medical laws, explore human mysteries,, minimize medical risks, and improve the success rate of cure.

2.2. Meanshift Algorithm. The core of the meanshift algorithm is the mean shift vector, which is classified as a nonparametric probability density estimation, which

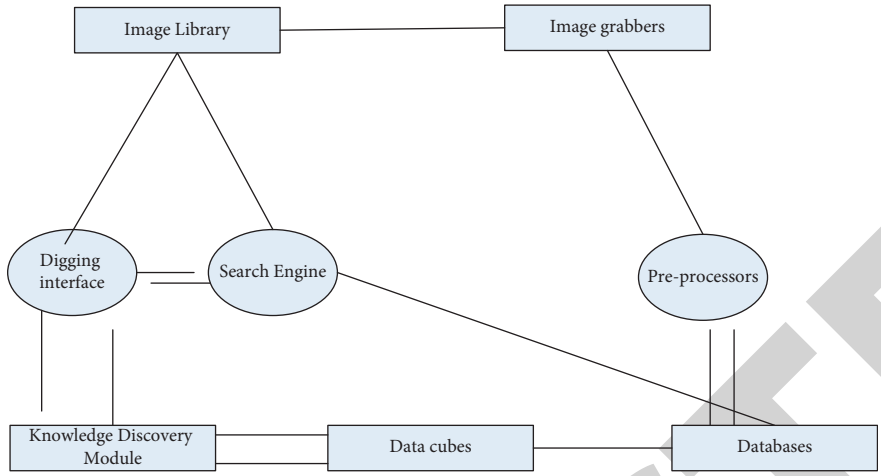

Figure 1: Data mining model.

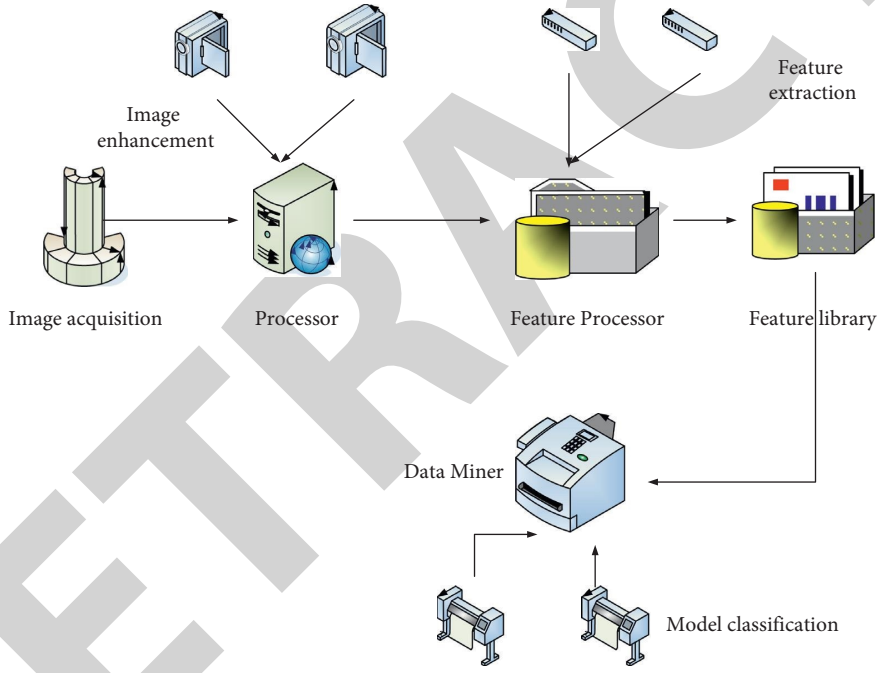

Figure 2: Data mining process.

includes histogram estimation and kernel density estimation methods, among others.

$$\widehat{g}(a) = \frac{1}{m}\sum_{z=1}^{m}\beta\left(h\left(Q_z\right) - a\right). \tag{1}$$

The estimation algorithm is a histogram estimation algorithm, and $g(a)$ represents the probability density function and $h(a)$ represents the index.

$$\widehat{g}(v) = \frac{1}{ti}\sum_{z=1}^{t} W\left(\frac{v - V_z}{i}\right), \tag{2}$$

W represents the kernel function and V represents the sample set.

$$\sup_{a\in t}|W(a)| < \infty, \tag{3}$$

$$\int_{-\infty}^{+\infty}|W(a)|\mathrm{d}a < \infty, \tag{4}$$

$$\lim_{a\longrightarrow\infty} a^m|W(a)| = 0, \tag{5}$$

$$\int_{-\infty}^{+\infty}|W(a)|\mathrm{d}a = 1. \tag{6}$$

As the nonreference functions are generally continuous single-peaked, they need to satisfy the aforementioned function expression conditions in the practical

application process. Table 1 shows a comparison of the number of iterations.

2.3. Medical Images. Medical imaging refers to the technology and processing of the human body or a part of the human body to obtain images of internal tissues in a noninvasive manner for medical treatment or medical research. The former is the process of image generation; the latter is to recover images that are not clear enough, or to highlight certain features in the image, or to classify patterns in the image, etc. In addition to X-ray, there are also techniques such as MRI. Medical imaging has been developed so far. While techniques such as MRI focus on measurement and recording, but have no data display capabilities, the derived data can be considered an alternative form of sonography due to their locational characteristics. MRI applies a radio frequency pulse of a certain frequency to the human body in the static magnetic field, so that the hydrogen protons in the human body are excited and the magnetic resonance phenomenon occurs.

Medical images have many unique features compared to general images such as natural landscapes and art paintings. Among them, multimodality is one of them, which causes the multimodality of medical images because the imaging principles of modern medical imaging equipment are different. However, according to their application range, medical images are mainly divided into two types: anatomical images and functional images. Anatomical images have higher resolution and can more clearly reflect the structural information of a tissue or organ. Functional images can reflect information about the body's metabolism but at a lower resolution. Specific to clinical applications, according to different imaging parameters and imaging conditions, each modality can also produce different performance images, such as T1 and T2 imaging modes in MRI. If you can combine this information, you can get more medical information for the doctor to diagnose, and image registration technology is the main tool to combine different modal image information. Compared with ordinary images, medical images have intrinsic nonuniformity and blur characteristics. Medical images have gradation in the gray scale. There is a large change in CT values of the same tissue. For example, the density of the femur, sinus bones, and teeth in the bones is very different. The CT values are not uniform for the same object, such as the density of the outer surface of the femur and the internal bone marrow. In addition, the noise signal caused by technical reasons tends to blur the high-frequency signal at the edge of the object and the ambiguous effect of the image due to the conscious or unconscious activity of the human body. In a voxel on a boundary, the relationship between the edge, the corner, and the region of the object in the image of both the boundary and the object is often difficult to accurately describe. Some of the diseased tissue cannot be clearly defined due to its infiltration into the surrounding tissue.

Table 1: Comparison of the number of iterations.

Number of frames		18	19	20	21	22
Number of iterations meanshift algorithm		3	3	4	4	5
	Improved algorithm	1	1	2	2	3
	Average	2	2	3	3	4

2.4. Image Enhancement. Image enhancement is to purposefully emphasize the overall or local characteristics of the image, make the original unclear image clear, expand the difference between the characteristics of different objects in the image, and improve the visual effect of the image. Traditional contrast enhancement algorithms are divided into direct and indirect methods. The direct method mainly achieves the purpose of enhancement by correcting the histogram, and the overhead calculation first borders the contrast and then enhances the contrast based on this. Image enhancements include a wide range of content; for example, it can enhance comparison, improve noise, reduce shadow, refine, and filter margins. Traditional contrast enhancement techniques are mostly based on global and neighborhood, and the results of these methods tend to fall under under-enhancement or overenhancement. In the global histogram equalization, since a small number of adjacent gradations are combined into one gradation during the equalization process, the contrast is lowered. Through histogram equalization, the image brightness can be better distributed on the histogram, which can be used to enhance the local contrast without affecting the overall contrast. In order to overcome this defect, the equalization function can be obtained in a small area. In the equalization process, the combination of adjacent pixels is reduced and the image contrast is less reduced than the global equalization. It is called adaptive neighborhood histogram equalization. There are many factors that cause low image quality: uneven lighting will make the grayscale image too concentrated, transmission lines are generated when the noise pollution and image quality inevitably reduced; the lighter the noise, the more difficult it is to see the details of the image; and then, the image will be blurred. Therefore, before the image analysis and processing, the image must be improved, that is, the image must be enhanced. Table 2 shows the evaluation of the image enhancement effect.

Using image gray histogram processing technology, there are many ways to enhance the image in the spatial domain, such as enhanced contrast and dynamic range compression. The grayscale histogram is to arrange all the pixels in the digital image according to the size of the grayscale value. It represents the number of pixels with a certain gray scale in the image and reflects the frequency of a certain grayscale in the image. This kind of processing method is more flexible and convenient, and the processing effect is also good, but for some images with dense gray distribution or weak contrast. Although it has a certain enhancement effect, it is not obvious to identify. The gradation transformation processing of an image is realized by changing the probability distribution of each pixel of the original image at each gray level. Table 3 shows the image enhancement metrics for the different regions.

Table 2: Evaluation of image enhancement effects.

Indicators	Based on uniformity	Mathematical morphology	Histogram equalization
DSM	12	20	1
TBCs	27	7	2
TBCe	29	6	1

Table 3: Image enhancement metrics for different regions.

Name	Average value	Variance	Smoothness	Peak state
Background category	175	2.158	0.639	0.254
Function bundle category 1	141	13.15	0.852	0.059
Function bundle 2	91.2	7.69	0.789	0.156

The histogram function expressions can be obtained by counting the images.

$$p(sk) = \frac{nk}{n}, \quad k = 0, 1, \ldots, L-1. \tag{7}$$

This expression is expressed in the first k, the number of pixels at the gray level is nk, total number of pixels is n, ratio is $p(sk)$, and the right sk should be given, which is an estimate of the probability of occurrence. Through this function, you can clearly understand the dynamic range of the image and you can understand the main concentration range of the grayscale image.

The purpose of enhancing an image is to sharpen the original image to emphasize certain features of the image, making it easier to improve the visual effect on the picture or perform other processing. The histogram equalization enhancement method is a grayscale enhancement algorithm performed in the spatial domain.

2.5. Feature Extraction. A single measurement is defined in eigen extraction treatment. Feature extraction is a major action in picture processing, which examines pixels. The input image, which is a prerequisite for feature extraction action, has usually been processed before the final result is produced. Figure 3 shows the block diagram of an image enhancement algorithm.

The first step in SIFT feature extraction is to design the space, the second step is to target the image focus, and the third step is to perform orientation assignment. The fourth step is to describe the key points. In order to ensure the stability of the image when describing the key points, the angle is adjusted in the area near the key points beforehand and then the histogram of the sampled area is calculated. Finally, a vector technique is applied to the image.

2.6. Rough Set. Rough set theory is a powerful data analysis tool that does not require prior knowledge in the application. Rough set theory has some unique viewpoints, which makes it irreplaceable in many fields and makes it particularly suitable for data analysis. It does not need any prior knowledge beyond the set of data the problem needs to deal with and is highly complementary to theories dealing with other uncertainty problems. Different attribute knowledge

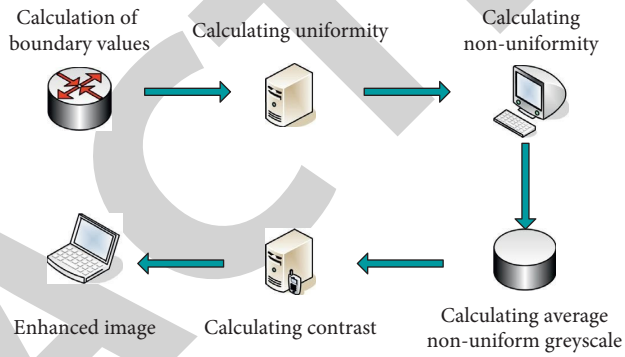

Figure 3: Image enhancement algorithm.

descriptions can be used to generate different categories. It divides the knowledge of the research domain by the indistinguishable relationship and forms the knowledge expression system to use above and below approximation sets to approximate the description object through knowledge reduction so as to obtain the simplest knowledge. A main goal of rough set theory is to obtain the conceptualization of the target through background knowledge. Its more prominent feature is its objectivity. It does not need to prescribe certain features or quantitative descriptions of attributes, such as the membership of fuzzy sets, degree, and the probability distribution of statistics, but directly from the description set of a given problem, it finds the inherent law in the problem through the indiscernible relationship and the approximate domain. Table 4 shows examples of rough set decision-making.

Rough theory differs from theory as it does not require a priori information, so rough theory is a more objective description of the uncertainty of the problem. Rough theory extends the old set theory by embedding the knowledge used for classification into the set as a collective component. Rough theories are thus divided into three types: (1) object a must belong to set X; (2) object a must not belong to set X; and (3) object a may or may not belong to set X.

3. Experiments

Tumors that grow in the brain are collectively referred to as brain tumors, including primary tumors caused by changes in the brain's own parenchyma and secondary tumors that

Table 4: Rough set decision-making.

Decision table	Conditional properties			Decision attributes
A	1	2	3	4
B	1	0	1	1
C	2	1	0	1
D	1	1	0	2

occur from other parts of the body and metastasize to the brain. It can occur at any age, and the cause is still unknown. The correct diagnosis of brain tumor grade has a great influence on the treatment and prognosis. Generally, low-grade brain tumor (LGG) has a survival time of 5 to 10 years, while high-grade brain tumor (HGG) has a survival time of about 1 year. The grading examination and diagnosis of brain tumors currently rely heavily on the analysis of medical images such as CT, angiography, and MRI. Among them, MRI examination is generally considered to be more sensitive than CT in the medical field and has three-dimensional imaging characteristics, which can reflect the brain more effectively and the essence of the tumor. At present, MRI diagnosis of brain tumors is mainly based on tumor location, tumor morphology, tumor occupying, tumor edge clarity, edema around the tumor, bleeding, calcification, and many other factors. In this experiment, MRI images of 120 pathologically confirmed brain tumors in a hospital were collected. The images were collected from the Maconi 1.5 T superconducting nuclear magnetic resonance system and organized in an image database, as shown in Figure 4 (image comes from the network) and collected according to the WHO classification. The classification of image data is shown in Table 5.

4. Discussion

The acquired MRI image has a large original size and needs to be compressed. The image format directly collected from the medical instrument is 512×512, which is compressed into 128×128 format, so as to improve the analysis efficiency. In Clementine, you can directly input the MRI image using the image database as the data source and perform cluster analysis based on the different settings of the edges, occupancy, bleeding, edema, and other factors of the MRI image. The data flowchart is shown in Figure 5; through the user input node, input source data after preprocessing, and K-mean cluster analysis.

The user input node is used to input the original data, and the features of the image are input into the data stream from the user input node in the form of a table. The middle type node, the derive node, and the SPSS transform node are feature inputs for processing the MRI image. Similarly, the characteristics of the MRI image are entered in a discrete type indicating discrete data and a flag type indicating Boolean data. Finally, the data are analyzed by the K-mean node.

Figure 6 shows the analysis results, according to the edge, hemorrhage, calcification, edema, and occupancy of a total of five MRI signs into a total of 9 categories, cluster1 to cluster9. In order to facilitate the subsequent data mining rough set, it is also required to carry out its treatment before discrete excavation, the attribute value range into a plurality of breakpoints through a number of discrete sections, and then different symbols representing each attribute value of the interval. After that, a rough set analysis data stream is established and the data are input into the input stream for rule mining. The rules explained in the excavation are shown in Table 6.

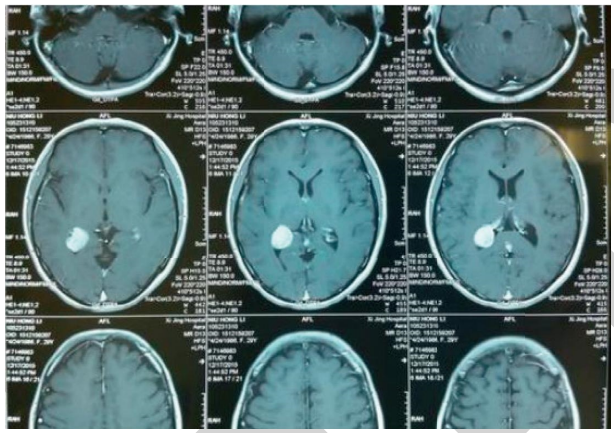

Figure 4: Brain MRI image data.

Table 5: Image grading statistics.

WHO level		Percent
Class I	LGG	14%
Class II		42%
Class III	HGG	33%
Class IV		11%

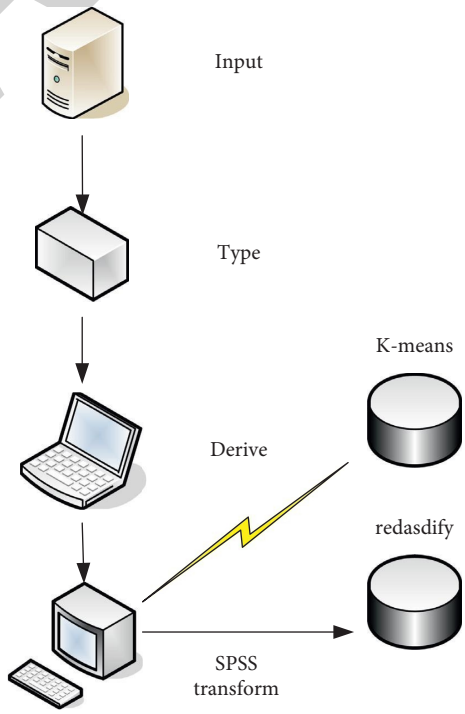

Figure 5: K-mean clustering analysis process of MRI images.

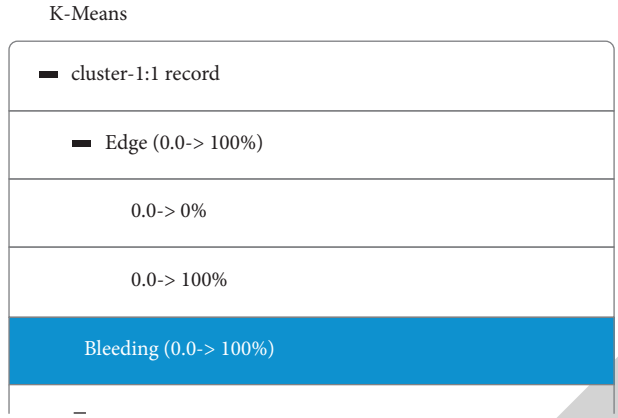

Figure 6: Cluster analysis of MRI images.

Table 6: The input stream for rule mining.

Rule	Composition	Conf (%)
Edge = very clear ⟶ WHO level = HGG	2	100
Edge = relatively clear ∧ placeholder = heavy placeholder ⟶ WHO level = HGG	3	100
Edge = relatively clear edema = severe edema ⟶ WHO level = HGG	3	100
Occupancy = mild occupation ∧ edema = mild edema ⟶ WHO level = LGG	3	100
Edge = fuzzy ∧ placeholder = mild place ∧ edema = severe edema ⟶ WHO level = LGG	4	100

Table rules and inference rules presubstantially are the same as the remaining samples of the resulting test sample were evaluated rule, and the diagnostic rules using the WHO level above an 80% accuracy rate.

5. Conclusions

With the continuous development in health care, health care is gaining more and more attention. In this system, a wide variety of patient information can be stored. If this information could be reused, it would greatly facilitate the development of medical care. But this data simply record the surface information and do not analyze the deeper content of the information to its fullest extent.

In this paper, we focus on the meanshift algorithm, which provides an in-depth understanding of the vectors that are at the heart of the algorithm and provides an optimal optimisation algorithm for data analysis. Combining the meanshift algorithm with medical data will be of great use in disease diagnosis and treatment, medical research and teaching, and hospital management, greatly contributing to the advancement of healthcare.

Data Availability

This article does not cover data research. No data were used to support this study.

Conflicts of Interest

The authors declare that they have no conflicts of interest.

References

[1] Z. He, B. Fan, T. C. E. Cheng, S.-Y. Wang, and C.-H. Tan, "A mean-shift algorithm for large-scale planar maximal covering location problems," *European Journal of Operational Research*, vol. 250, no. 1, pp. 65–76, 2016.

[2] O. Hyrien and A. Baran, "Fast nonparametric density-based clustering of large datasets using a stochastic approximation mean-shift algorithm," *Journal of Computational & Graphical Statistics*, vol. 25, no. 3, pp. 899–916, 2016.

[3] H. Abulkasim, A. Farouk, S. Hamad, A. Mashatan, and S. Ghose, "Secure dynamic multiparty quantum private comparison," *Scientific Reports*, vol. 9, no. 1, pp. 17818–17916, 2019.

[4] W. Y. Zhu, "Video target tracking algorithm with combining robust estimation and Meanshift," *Journal of Shenyang University of Technology*, vol. 39, no. 2, pp. 177–182, 2017.

[5] G. Beck, T. Duong, M. Lebbah, H. Azzag, and C. Cérin, "A distributed approximate nearest neighbors algorithm for efficient large scale mean shift clustering," *Journal of Parallel and Distributed Computing*, vol. 134, no. Dec, pp. 128–139, 2019.

[6] O. I. Khalaf, G. M. Abdulsahib, and B. M. Sabbar, "Optimization of wireless sensor network coverage using the bee algorithm," *Journal of Information Science and Engineering*, vol. 36, no. 2, pp. 377–386, 2020.

[7] T.-Y. Kim, S.-H. Kim, and H. Ko, "Design and implementation of BCI-based intelligent upper limb rehabilitation robot system," *ACM Transactions on Internet Technology*, vol. 21, no. 3, 2021.

[8] W. Jianhong, Q. Welliang, and W. Xiaogang, "Convergence and stability analysis of mean-shift algorithm on large data sets," *Statistics and Its Interface*, vol. 9, no. 2, pp. 159–170, 2016.

Hindawi
Emergency Medicine International
Volume 2023, Article ID 9869764, 1 page
https://doi.org/10.1155/2023/9869764

Retraction

Retracted: Influence of Aerobic Exercise Load Intensity on Children's Mental Health

Emergency Medicine International

Received 8 August 2023; Accepted 8 August 2023; Published 9 August 2023

This article has been retracted by Hindawi following an investigation undertaken by the publisher [1]. This investigation has uncovered evidence of one or more of the following indicators of systematic manipulation of the publication process:

(1) Discrepancies in scope
(2) Discrepancies in the description of the research reported
(3) Discrepancies between the availability of data and the research described
(4) Inappropriate citations
(5) Incoherent, meaningless and/or irrelevant content included in the article
(6) Peer-review manipulation

The presence of these indicators undermines our confidence in the integrity of the article's content and we cannot, therefore, vouch for its reliability. Please note that this notice is intended solely to alert readers that the content of this article is unreliable. We have not investigated whether authors were aware of or involved in the systematic manipulation of the publication process.

Wiley and Hindawi regrets that the usual quality checks did not identify these issues before publication and have since put additional measures in place to safeguard research integrity.

We wish to credit our own Research Integrity and Research Publishing teams and anonymous and named external researchers and research integrity experts for contributing to this investigation.

The corresponding author, as the representative of all authors, has been given the opportunity to register their agreement or disagreement to this retraction. We have kept a record of any response received.

References

[1] S. Zhao, "Influence of Aerobic Exercise Load Intensity on Children's Mental Health," *Emergency Medicine International*, vol. 2022, Article ID 7827980, 11 pages, 2022.

Hindawi
Emergency Medicine International
Volume 2022, Article ID 7827980, 11 pages
https://doi.org/10.1155/2022/7827980

Research Article

Influence of Aerobic Exercise Load Intensity on Children's Mental Health

Sihong Zhao

School of Preschool Education, Xi'an University, Xi'an 710065, Shaanxi, China

Correspondence should be addressed to Sihong Zhao; zhaosihong@xawl.edu.cn

Received 1 April 2022; Revised 13 May 2022; Accepted 26 May 2022; Published 11 June 2022

Academic Editor: Hang Chen

As people have become more aware in recent years, aerobic physical exercise plays an important role in alleviating people's mental health problems. However, traditionally, it is believed that young children do not have mental health problems. To help people change this fixed idea, and to study how to correctly adjust the load intensity of aerobic physical exercise under the condition of limited physical fitness of young children, and accurately help children's mental health development, this paper studies the influence of aerobic physical exercise load intensity on children's mental health. In this paper, the detection and tracking technology of video moving objects is used to analyze the data of the research object. This technique includes several commonly used and improved video analysis algorithms. The use of moving target and tracking technology and algorithms can completely extract moving targets, eliminate the phenomenon of void and nothingness, and improve data acquisition and analysis capabilities. The results show that taking part in aerobic exercise with appropriate intensity is beneficial to regulating children's emotional state, reducing their psychological burden, enhancing their negative energy resistance, and arousing their positive participation. Compared with before aerobic exercise, the learning efficiency was improved by 6.36%.

1. Introduction

Children's mental health of the mental is the focus of increasing social concern. Children's mental health of mental is an important prerequisite for preschool education. Preschool education is the foundation of the national quality education system, which can lay a good foundation for children's future life and provide them with good development conditions. Therefore, it is more important and urgent to actively explore the relationship between aerobic exercise load intensity and children's health, and the influence of physical exercise activities on children's mental health and positive results.

Aerobic exercise is a key part of physical exercise and plays a heavy role in enhancing students' physical fitness. Many teams have studied this. Gregory team studied the effects of dual-task gait training and aerobic exercise intervention on cognition. It investigated the activity and cardiovascular health of elderly people living in a community without dementia. The conclusion is that aerobic exercise improves the performance of many cognitive results [1]. Several studies by Innocenti have shown that aerobic exercise can improve the cognitive ability of MCI patients [2]. Chan studied that exercise training can improve insulin sensitivity and RBP4 [3]. The purpose of Callegari's research was to investigate the muscle response of creatine kinase (CK) and lactate dehydrogenase (LDH) after different levels of resistance and aerobic exercise programs. Immediately after the end of the protocol, it was observed that LDH in some groups increased significantly compared with other groups [4]. The AJA team tested whether Mk III GLCS was the second largest aerobic exercise. The feasible auxiliary means of VO_2 max prediction produced by this method is to compare the obtained VO_2 max prediction with pa [5]. Leeuwis had evidence that aerobic exercise is beneficial to cognition and provided insight into the potential mechanisms of aerobic exercise in improving hemodynamic status [6]. The research by Moghadasi indicated that high-intensity aerobic exercise training greatly affected serum A-FABP [7]. The results of these

studies show that aerobic exercise plays an essential role in the human body.

In the process of children's development, it is important to pay attention to their physical and mental health. Considering children's health, it should not only consider the healthy development of young children. Children's mental health is related to their healthy development in the future. Caring for children's mental health means paying attention to children's healthy development. Many teams have studied this. Freeman's research held that psychological health problems are intimately related to the environment [8]. Silove considered the contemporary problems in the field of refugee mental health. He discussed developing ecological research model focusing on the dynamic relationship among past traumatic experiences, continuous daily stressors, and background destruction of the core social psychological system [9]. Butterworth's research has shown that adolescents and young people have high psychological stress, but the utilization rate of treatment is very low [10]. Emma studied and compared parents' and children's reports on children's mental health to determine the relationship between parent-child differences and parents' psychological and attitude factors, and how parent-child differences are related to the use of professional services [11]. Leese measured different types of service provision and considered that the influence on the views of service users was essential for planning mental health services [12]. Based on the PREPARE/ENRICH program, Muhammad found the influence of communication and conflict resolution skills training on the mental health of Iranian couples [13]. Tsanava believed that early intervention for children and adolescents with mental health problems is essential to ensure that these problems will not continue into adulthood [14]. The results have shown that it is essential to solve children's mental health problems, which will have an important impact on their future.

The points of innovation in this document are as follows:

(1) In the field of aerobic psychology, experienced experts and researchers have done a great deal of research and different degrees of research on the effects of exercise on health. In addition, there is no uniform standard for training intensity, duration, and frequency.

(2) According to children's age, under the condition that the same exercise cycle, the same number of exercises per week, and intensity are close to three emotional factors, the topics are grouped into three types of functions. It is an exercise plan to analyze each mental health level. It adjusts the relationship between different physical activities and mental health plans according to different mental health levels and provides some clues for the influence of different physical activity plans on mental health.

(3) This work is the first time to use the human motion search and tracking system, which uses a video imaging algorithm to study the influence of aerobic exercise weight on children's mental health. It improves the efficiency of data analysis, ensures the accuracy of the data, and provides a new basis for future research.

2. Methods

The research focus of this paper is to detect and track aerobic exercise videos, which needs to gather and parse a large amount of data. To facilitate data analysis, this paper uses a new video processing algorithm to help obtain and process data on the relationship between young children and physical exercise load intensity. It simplifies the extracted image to reduce the interference elements of key algorithms in the later stage, including the subsequent processes and algorithms [15].

2.1. Gray-Scale Processing. Color images are divided into three categories: black and white, gray, and color. The natural video images taken by digital cameras are all color images. To speed up the program, it is important to convert the downloaded image into a gray image. Gray scale can represent the total area and distribution area of the whole image as well as the color and brightness characteristics [16].

The relationship usually adopts the formula:

$$grey(x, y) = 0.11r(x, y) + 0.59(x, y) + 0.3b(x, y). \quad (1)$$

2.2. Image Enhancement Algorithms. Image enhancement technology can increase users' interest in images, such as edges, borders, and contrast, and increase the contrast between different parts of images [17]. It can provide a good foundation for extracting image information and applying other analysis techniques. Improving image information, lighting and shadow, and sharpening image edges are the main concerns of image enhancement. Gray-scale conversion technology is an important way to enhance the effect of image recognition, which makes the details of the image easy to find.

$$S = T(r). \quad (2)$$

Among them, r and s represent the image pixel values before and after processing. It is a transformation method that maps the original domain r_o, r_k to the latest domain S_o, S_k.

Different interpretations of t may lead to different conversion results. Typical gray-scale modification includes linear inversion transformation, logarithmic transformation, contrast rendering, and histogram alignment.

(1) Contrast stretching:

$$s = T(r) = \frac{1}{1 + (m/r)E}. \quad (3)$$

Among them, E is a given parameter of control degree and M is the maximum value of the gray scale. Histogram averaging changes the input gray level according to the formula (x, x) [18] to obtain the gray output level s.

$$s = E(a) = \int_0^1 P_a(u)\mathrm{d}u. \tag{4}$$

In the above formula, $pa(u)$ represents the probability density function of the gray level in a given image and w is the variable of sum. Next, it can be assumed that the probability weight function of the bright gray scale is uniform, that is:

$$p_a(a) = \begin{cases} 1, & 0 \le a \le 1 \\ 0, & \text{others} \end{cases}. \tag{5}$$

After histogram adjustment, the gray scale is more balanced, and the final image has higher contrast and wider intensity.

(2) Two-dimensional median filtering: in a digital image, because it is a 2-dimensional data image, the intermediate processing is also 2-dimensional. It selects a 2-dimensional recording model with specific settings. The process of presenting the 2D filter is as follows:

$$h(x, y) = \mathrm{Med} f(x - u, y - v), \quad (u, v) \in D. \tag{6}$$

Among them, $f(x, y)$ is the original image, $h(x, y)$ is the median filtered image, and D is the two-dimensional template.

(3) Mean filtering: assuming that the size of video $f(x, y)$ with noise is $M * N$. The formula of processed image $\widetilde{f}(i, j)$ is as follows, where W is the domain of point (x,y).

$$\widetilde{f}(i, j) = \frac{1}{M * N} \sum_{i,jeW} f(i, j). \tag{7}$$

(4) Gaussian filtering: Gaussian smoothing filter is the most widely used algorithm in image processing [19].

$$f'(i, j) * g(i, j), \tag{8}$$

$$g(i, j) = \frac{1}{\sqrt{2\pi}\alpha} \exp\left(-\frac{i^2 + j^2}{2\alpha^2}\right). \tag{9}$$

Among them, α is the characteristic parameter of Gaussian low-pass filtering. To blur the edge of the image, so as not to affect the normal performance of the next algorithm, this effect can be achieved by adjusting the filter.

(5) Three-frame difference algorithm: the algorithm of frame difference method is simple and clear, and background update is not considered. The shortcomings are also very obvious. Difference images always have a lot of noise. To solve this problem, a three-frame difference method is proposed, and its formula is

$$mx(x, y) = \left|f_{t-1}(x, y) - f_1(x, y)\right| * \left|f_x(x, y) - f_{t+1}(x, y)\right|, \tag{10}$$

$$M_x(x, y) = \begin{cases} 255, m_x\left(x, y\right) > T. \\ 0 \end{cases} \tag{11}$$

Among them, the first frame of the three-frame difference image is $f_{t-1}(x, y)$, the second frame is $f_t(x, y)$, the third frame is $f_{t+1}(x, y)$, and $m_t(x, y)$ is the three-frame conversion part.

(6) Background subtraction method: background subtraction is the process of removing each image frame with a fixed background pattern. This is also a common algorithm for moving target detection. The expression formula is as follows:

$$R(x, y) = F(x, y) - G(x, y). \tag{12}$$

Among them, $R(x, y)$ is the moving target to be detected and $F(x, y)$ is the video sequence image. $G(x, y)$ is the background model image.

(7) Optical flow constraint method: when the recording time is t, the gray value of the moving object of the image in space (x, y) is E (x, y, and t). When it reaches the $(x + \Delta x, y + \Delta y)$ point and its gray matter is recorded as $E(x + \Delta x, y + \Delta y, t + \Delta t)$, according to the constant light hypothesis, there are

$$\frac{\mathrm{d}E}{\mathrm{d}t} = 0. \tag{13}$$

According to the chain rule,

$$\frac{\partial E}{\partial x}\frac{\mathrm{d}x}{\mathrm{d}t} + \frac{\partial E}{\partial y}\frac{\mathrm{d}y}{\mathrm{d}t} + \frac{\partial E}{\partial t} = 0. \tag{14}$$

Marking it as $\mu = \mathrm{d}x/\mathrm{d}t, v = \mathrm{d}y/\mathrm{d}t$. It is the time of the moment projection component (x, y) in the μ, v image plane in the X direction and Y direction, that is, the bright flux. This provides us with the linear equation of visual flow:

$$E_x u + E_y v + E_t = 0. \tag{15}$$

This is a well-known optical flow constraint equation, and the value of $E_x = \partial E/\partial x, E_y = \partial E/\partial y, E_t = \partial E/\partial t$ can be obtained from the image. The Laplacian operator of U and v is defined as follows:

$$\begin{aligned} \nabla^2 u &= \left(\frac{\partial u}{\partial x}\right)^2 + \left(\frac{\partial u}{\partial y}\right)^2, \\ \nabla^2 v &= \left(\frac{\partial v}{\partial x}\right)^2 + \left(\frac{\partial v}{\partial y}\right)^2. \end{aligned} \tag{16}$$

According to the optical flow constraint equation, the error reflection of bright flux deviation from normal light is

$$\Gamma_b = E_x u + E_y y + E_t. \tag{17}$$

The error of deviation from the smoothness requirement is

$$\Gamma_e = \left(\frac{\partial u}{\partial x}\right)^2 + \left(\frac{\partial u}{\partial y}\right)^2 + \left(\frac{\partial v}{\partial x}\right)^2 + \left(\frac{\partial v}{\partial y}\right)^2. \tag{18}$$

Minimizing error:

$$\Gamma^2 = \int\int \alpha^2 \Gamma_c^2 + \Gamma_b^2, \mathrm{d}x\mathrm{d}x y. \tag{19}$$

Solving the equation:

$$u^{n+1} = \begin{matrix} -n \\ u \end{matrix} - \frac{\left[\begin{matrix} -n & -n \\ E_x & + E_y \\ u & v \end{matrix} + E t \right]}{\left(\begin{matrix} 2 & 2 \\ \partial^2 + E & + E \\ x & y \end{matrix} \right)}, \tag{20}$$

$$v^{n+1} = \begin{matrix} -n \\ v \end{matrix} - \frac{E_x \left[\begin{matrix} E_x \begin{matrix} -n \\ u \end{matrix} + E_y \begin{matrix} -n \\ v \end{matrix} \end{matrix} + E t \right]}{\left(\begin{matrix} 2 & 2 \\ \alpha^2 + E & + E \\ X & y \end{matrix} \right)}. \tag{21}$$

With the development of computer, Internet, and other technologies, the data processing technology of physical exercise video is also increasingly widely used in various fields. By making good use of the video processing technology and its algorithm, the data of aerobic physical exercise can be accurately obtained, the influence of the load intensity of physical exercise on the mental health of young children can be observed, and a quick response can be made. This provides a firm foundation for improving the mental health of young children.

3. Intelligent Surveillance and Video System

3.1. Intelligent Surveillance and Video Composition. By finding targets and monitoring systems [20], it collects and processes information on the effects of aerobic physical activity and load intensity, which play an important role in early childhood development and people's mental health. It analyzes and evaluates this, providing accurate data for research. Therefore, this paper uses the search sports video streaming media site and tracking system to enable the results. The main users of this program include system administrators, temporary users, and sponsors. Users use Ethernet to access the Internet and then use firewalls to connect to routers and gateways for data mining, as shown in Figure 1.

3.2. System Modules. (1) Physical exercise video management module: the physical exercise video control module is an important part of the search engine module. The video control module is mainly managed and maintained by video managers. Its functions mainly include video control functions and video management functions. Among them, the main function of sports video management is to maintain sports videos, including adding videos, deleting, and converting videos. [21]. The video administrator inputs the corresponding user name and password to enter the settings, then accesses the physical exercise video control module, and completes the video recovery process by prompting the video method, as show in Figure 2.

(2) Target tracking management module: the most important part of the target search and tracking system is the target tracking module. The main function of the unit is to monitor the transfer position in real time, and then retrieve the corresponding data and analyze it with the help of monitoring. The function of this part is to support children's mental health, and its primary responsibility is the video analyst. The main tasks of this project are the development of a space models and the monitoring of space events. The specific operation procedure is as follows: First, design a fixed shooting position, and then design the correct monitoring position, as shown in Figure 3.

Intelligent monitoring and video systems are mainly used in the fields of vehicle monitoring, electric energy measurement, on-site monitoring, and so on [22]. The purpose of this book is to explore the intensity of teenagers' aerobic exercise by using search and stadium tracking system, video monitoring, tracking, and stadium tracking activities. The use of intelligent monitoring and video systems to detect the impact of aerobic physical activity on child program implementation has an important and positive role in the development of children's mental health. In addition, the use of this system can also simplify the complicated data collection process and improve the research efficiency.

3.3. Simulation of Actual Space Scene. Figure 4 shows the actual space scene. It selects the direction OX perpendicular to the ground plane as the reference direction. HF represents the footprint to be measured. L is the predicted plane image of the zero line on the infinite surface. When the pedestrian stands with his feet locked, the top line of the pedestal can be approximately a part of the line perpendicular to the ground. That is, the field of vision of the head and feet, so HF is equivalent to the reference direction OZ. H0F0 represents the reference point selected in the real scene. C refers to the movement of the camera, and its vertical distance from the ground plane is represented by dc. It draws a plane parallel to the ground plane by moving the camera, and the extension line of the line segment HF intersects with the plane A at point P, so the distance from point P to the ground plane [14] is equal to dc.

4. Specific Methods of Aerobic Exercise

Research object: to study the influence of aerobic exercise on children's mental health, this paper selects 80 children aged 61–70 months in kindergarten and divides them into two teams. One team is the experimental team and the other team is the control team. There are 20 children in each group. The reason the kindergarten is chosen is that the children in large classes are suitable in age and easy to control process. All children who participated in the study obtained the consent and support of parents and the school in advance. In addition, before the start of the test, the test group and the control group were randomly divided into groups to conduct a preliminary mental health test at the time of group selection. The two groups of children were almost identical, which allowed the test to ignore the differences and randomly determine the experimental group and the control group of young children.

Since all children who participate in the training are young, organized training is unique to children's basic sports, but the simple content is related to aerobic exercise. It

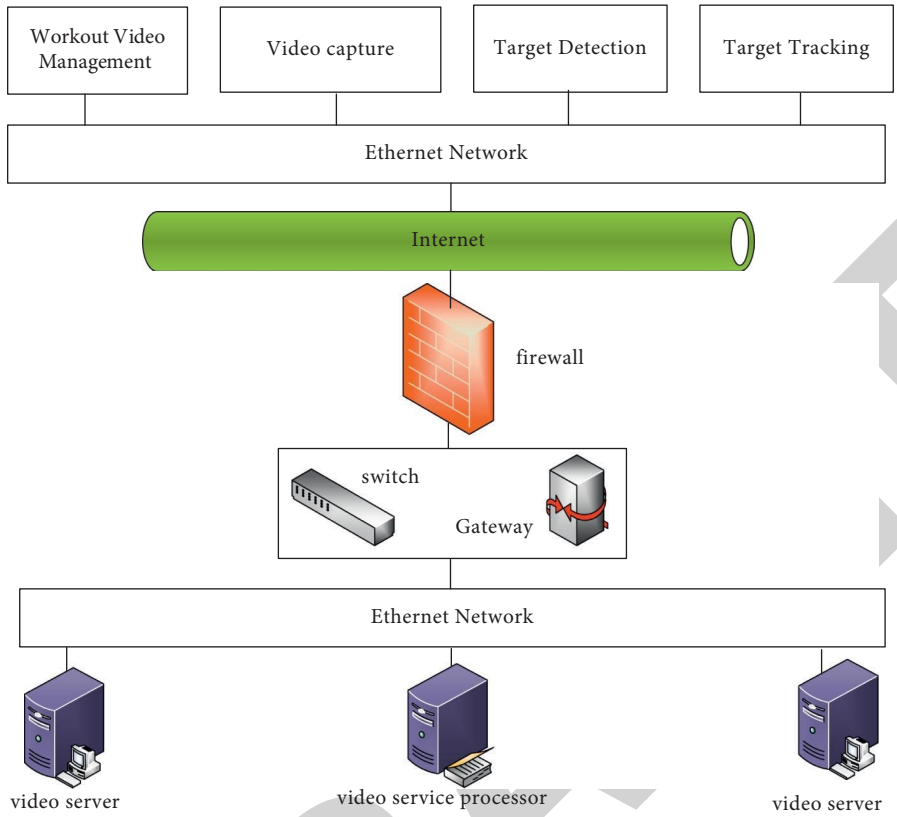

Figure 1: System information collection diagram.

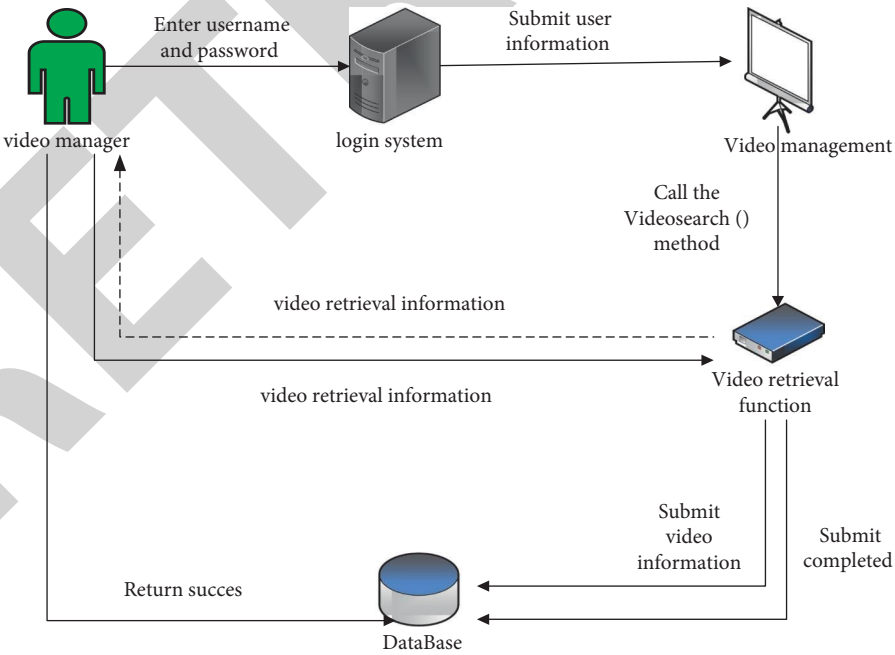

Figure 2: Physical exercise video management module diagram.

allows children in the experimental group to take part in aerobic exercise and uses unconventional aerobic exercise methods to have extra influence on the test group. Basic gymnastics for children is a simple and easy-to-operate aerobic exercise program. It compiles 3 sets of infant aerobics, supplemented by small games. Children in the control

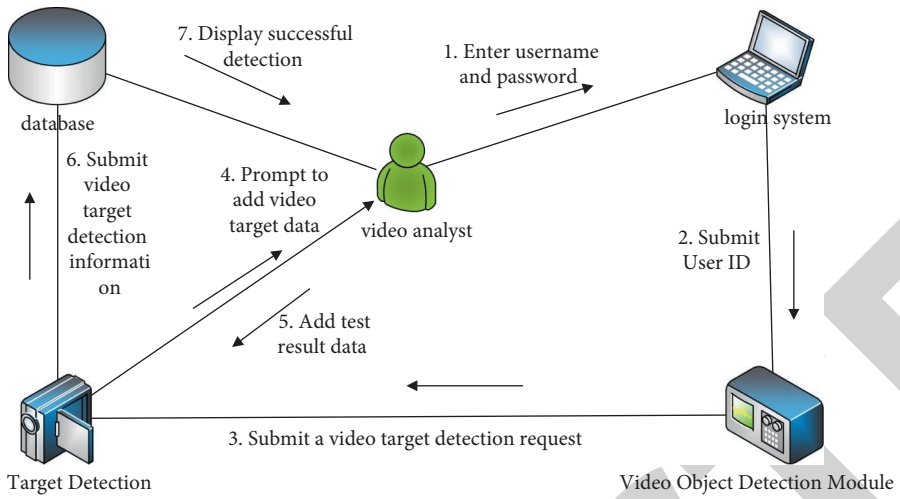

Figure 3: Target tracking management chart.

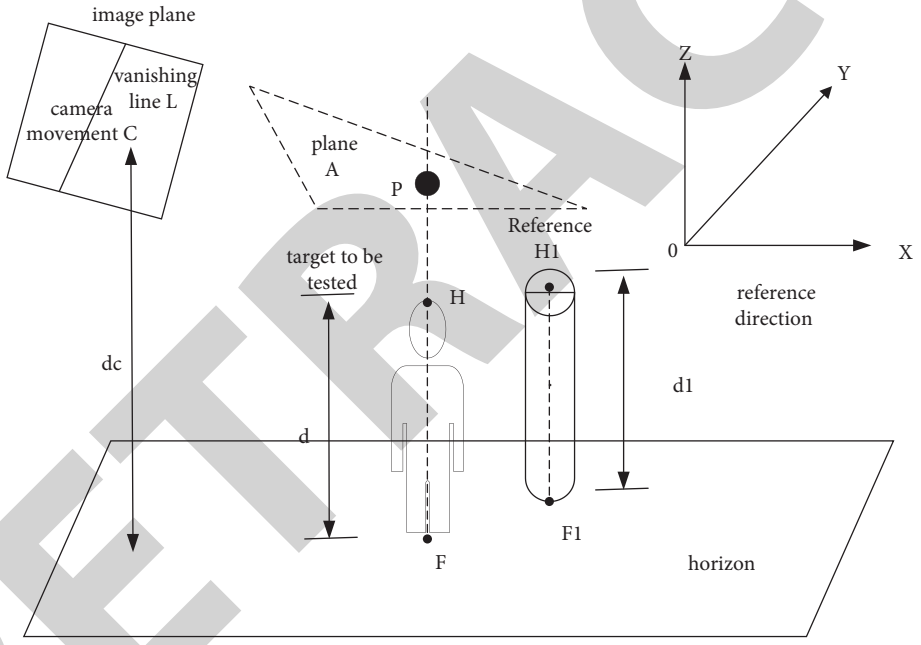

Figure 4: Simulation diagram of actual space.

group were intervened by the high, medium, and low intensity of basic gymnastics. Each group of children participated in the same load intensity exercise for 2 months, 8 times a month, and 2 times a week, and the time of each exercise was 30 minutes. Time arrangement: one time is arranged in the physical education class, one time is arranged after class, and the control group is the same as usual. To show the intensity of aerobic exercise, it needs to apply the heart rate index. High-intensity exercise requires the heart rate to reach more than 140 beats/min, 110 ~ 130 beats/min is suitable for the goal of medium-intensity exercise, and less than 100 beats/min is the goal of low-intensity exercise.

It tests the mental health of children. After the experiment, the children's mental health status was checked again by preventive mental health test and the results of both were carried out. At the same time, sports emotion measurement is used to measure cognitive emotion and sports satisfaction after different degrees of exercise, and make statistical analysis, as shown in Figure 5.

Control factors of the experiment: during the period, children's gymnastics basic training was used to intervene, and all training items were carried out on the plastic playground. To ensure proper physical exercise improvement and normal operation, teachers must implement the protection system. To ensure the effectiveness of exercise, the duration of each exercise is 30 minutes.

Experimental control factors: in the whole process of this study, only the trainers know the course, but the children do not know that they are the subjects. This is to prevent the

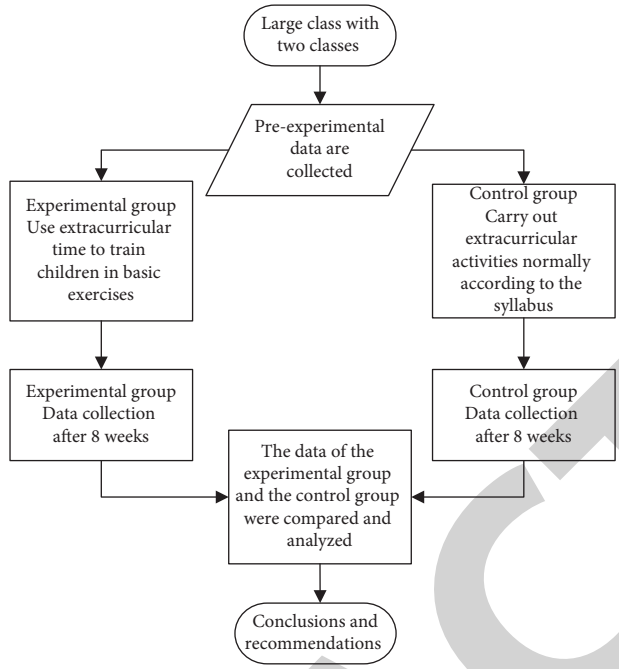

Figure 5: Flow chart.

Hawthorne effect of the controller from affecting the result. The Hawthorne effect refers to the artifact of the method in field behavioral experiments, as subjects realize they are being trained. This knowledge allows them to respond to the social context of the data collection process, rather than to the experimental methods the researchers are trying to investigate. It is similar to the "guinea pig effect" in laboratory studies. During the experiment, in the physical activity classes of the two classes, the experimental group carried out a well-designed basic exercise plan for children, while the control group received the contents of preschool textbooks for routine activities. Other conditions being completely equal, two groups of children were tested.

Posttreatment: after the experiment, two groups of children were tested, excluding various factors (taking part in additional training such as dancing and roller skating). Mathematical statistics: SPSS 20.0 is used for statistical calculation based on experimental data, and its related data are essential for statistical analysis. Gender analysis is used to evaluate the influence of basic sports on children's mental health in many fields.

5. Outcomes of Aerobic Exercise Experiment

5.1. Comparison of Mental Health Status of Children in Experimental Group and Control Group before Exercise. (1) Before the experiment, the health level of the students in the experimental class, the control class, and the research class in aspects of insight, intelligence, emotional experience, sense of responsibility, thinking, language, anxiety level, self-esteem, self-confidence, and memory was checked. Physical exercise experiments are based on differences, as shown in Figure 6.

From Figure 6, the average success rate of children's mental health in the experimental group is 70.04%, and that of girls is 69.51%. The average pass rate of boys in the control group and the mental health of children in the experimental group reached 70.62%, and the average of the two groups was 70.61%. There is no significant age difference, and they are at the same level.

In addition, it can be seen from Figure 6 that there is no significant difference in the mental health level between the experimental group and the control group before the experiment, which can be related and studied. The data thus obtained is more reliable.

5.2. Comparison of Mental Health Status between Experimental Group and Control Group before the Experiment. As can be seen from Figure 7, before the experiment, we analyzed the test results of several indexes of children's mental health in the experimental group and the control group and found that there was no significant difference in each index. The experimental group is almost the same as the control group. The experiment can begin formally.

5.3. Comparison of Mental Health Status of Postnatal Children. The students were tested and investigated in aspects of mental health level, insight, intelligence, emotional experience, sense of responsibility, thinking, language, anxiety level, self-esteem and self-confidence, memory, etc.

To make the data clearer, the numerical values are averaged and expressed by P^*100. When $P^*100 < 5$, the difference is significant; $P^*100 < 1$, the difference is highly significant. When $P^*100 > 5$, there was no significant difference.

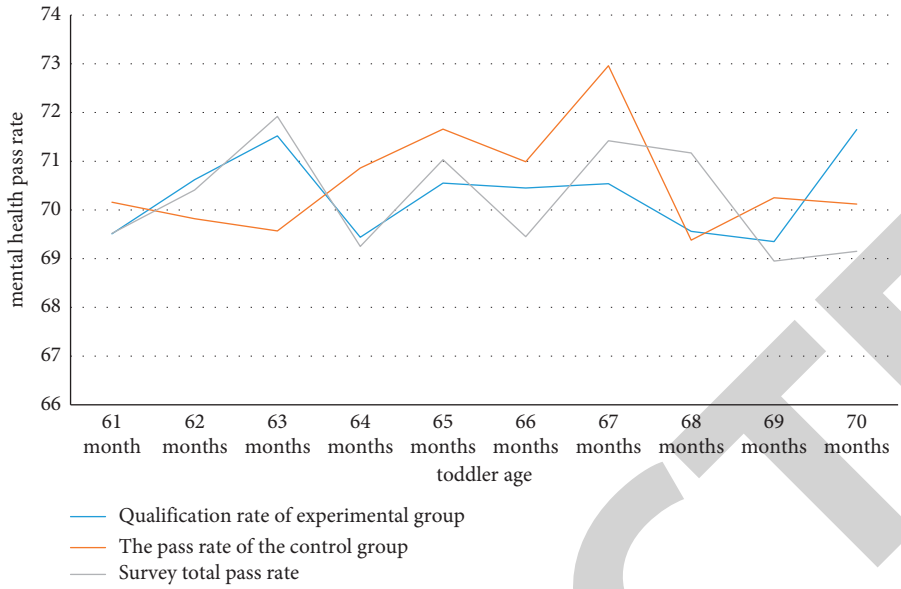

Figure 6: Qualified of children's mental health.

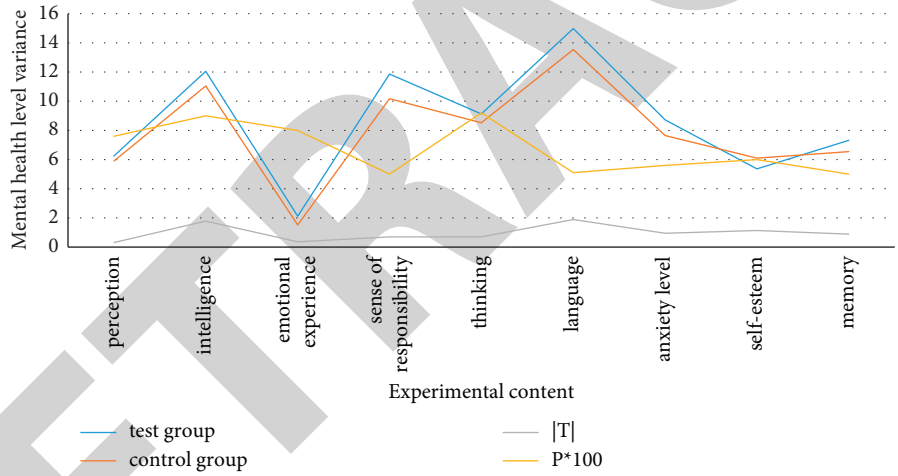

Figure 7: Comparison of mental health status between experimental group and control group before the experiment.

From the data in Figure 8, it can be seen that there are differences in the scores of insight, intelligence, emotional experience, sense of responsibility, thinking, language, anxiety level, self-esteem, and self-confidence and memory during the whole experiment ($P^*100 - 5$). Comparing the mental health level of the experimental group and the control group, the growth rate of different positions is different. Comparing the increase of scores before and after, it is concluded that there are significant differences in intelligence and thinking. The scores of self-esteem and anxiety levels are not as obvious as those of other parts, and there are obvious changes in language and emotional experience. During the whole experiment, the sense of responsibility and memory scores will increase rapidly.

5.4. Comparison of Mental Health Indexes of Children in Experimental Group and Control Group before and after Treatment. After the experiment, it is necessary to compare and analyze the data obtained from the control group and the experimental group, as shown in Figure 9.

As can be seen from Figure 9, after children's basic gymnastics training, there are significant differences in the mental health categories of children in the experimental group, such as insight, intelligence, emotional experience, sense of responsibility, thinking, language, anxiety level, self-esteem and self-confidence, and memory. ($P^*100 < 5$). Among them, the scores of thinking and language in the experimental group are quite different. The scores of intelligence, emotional

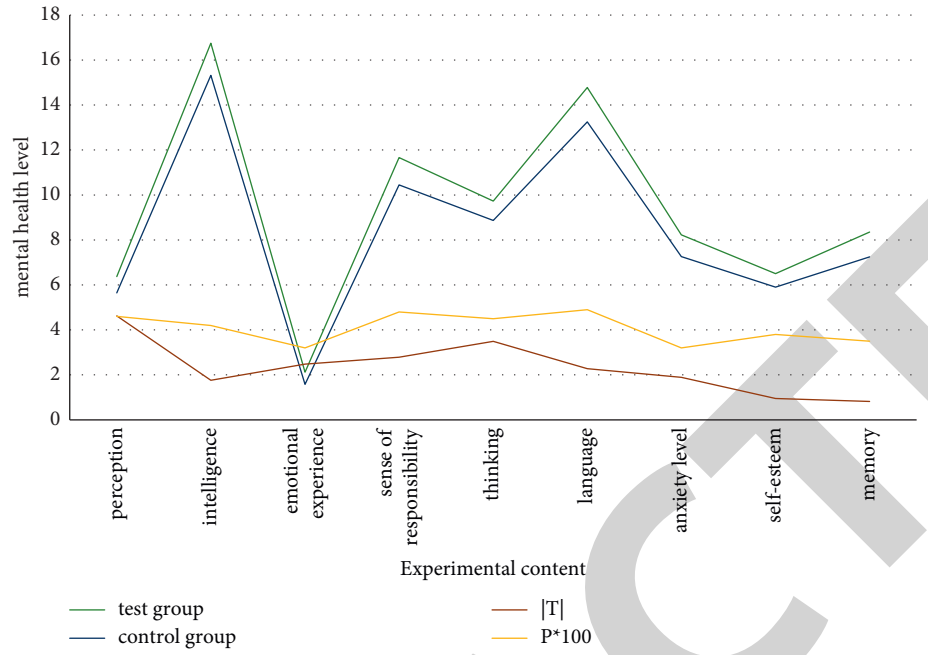

Figure 8: Statistical table of children's mental health in experimental group and control group experiment.

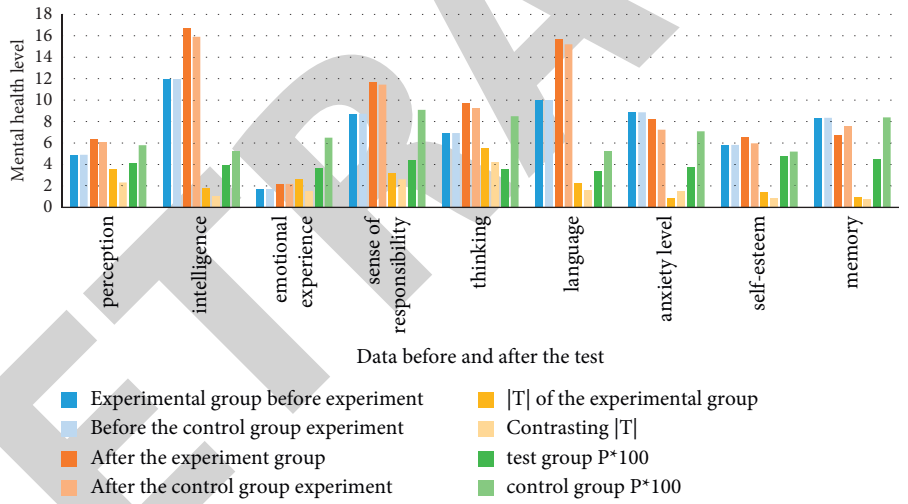

Figure 9: Comparative analysis of children's mental health level between experimental group and control group before and after the experiment.

experience, and anxiety level vary greatly. By comparing the scores of the mental health test report of the experimental group before and after the test, the average scores of several modules have been significantly improved, which shows that children's basic gymnastics has a significant impact on the improvement. In addition, from Figure 9, it can be found that there is no significant difference in the scores of several aspects of children's mental health in the control group ($P^*100 - 5$), but the overall trend score increases. The mental health level of children in the control class has no basic exercise. Each specific part changes at a different speed under the intervention.

6. Discussion and Conclusions

6.1. Discussion. Through this study, the following results are obtained:

(1) Participating in aerobic exercise of appropriate intensity is helpful to regulate children's emotional state and enhance their mental health. It is necessary

to renew ideas, reduce children's learning burden and homework, guide them to actively participate in physical exercise, and cultivate their interest and behavior in physical exercise, to lay a solid foundation for life sports.

(2) Children from 65 to 70 months participating in high- and medium-intensity aerobic exercise can achieve greater psychological effects of exercise and more pleasure in exercise. From 61 to 65 months, children participating in moderate and low-intensity aerobic exercise can achieve greater psychological effects of exercise and more pleasure in exercise. 61–65 months of young children participating in high-intensity exercise did not benefit their mental health.

(3) There were no gender differences in children participating in different intensities of aerobic exercise. The development of children's aerobic exercise programs should take into account physical, psychological, age and gender and other factors.

6.2. Conclusion. To study the influence of aerobic exercise and its load intensity on children's mental health, this paper adopts the classical pedestrian detection algorithm. It detects pedestrians in every frame of the video in this paper. There are more than 140 frames in the video, and the detection accuracy is 89%. It successfully detects the human body in the moving window. Detecting the human body in the moving area saves a lot of calculation time compared to detecting the whole picture. However, the accuracy rate has declined to some extent, which is related to the size of the training samples. It fills the moving window to make it regular, so that it can be used for detection. It zooms in and out during detection and makes multiscale detection more accurate. Finally, aiming at the multiwindow fusion problem caused by multiscale detection, the local MeanShift method is adopted to fuse, which ensures the fusion effect and effectively avoids the problem of fusing multiple human bodies into one window.

To further study the influence of children's basic gymnastics on children's mental health, this study conducted in-depth research on children's cognition, emotion, and social interaction. Through this study, it is found that children's scores in all aspects of mental health will gradually increase with the increase of age, and the change speed of each specific aspect is different. Aerobic exercise can effectively improve children's mental health. Compared with the control group, there is a highly significant difference in the movement of children who take part in aerobic exercise. This shows that aerobic physical exercise can promote the healthy development of children's mental health. Children's aerobic exercise can be included in kindergarten teaching materials as one of the educational means of all-round development, so that it can develop along the scientific direction.

Data Availability

All the data used are included in the article.

Conflicts of Interest

The authors declare that they have no conflicts of interest.

Acknowledgments

This work was supported by Preschool Education Research Project of Shaanxi Province 2020 Program: Research on the Promotion Strategy of Kindergarten Teachers' Physical Education Curriculum Execution in Shaanxi Province (Project No.: ZdKT2002).

References

[1] M. A. Gregory, N. C. Boa Sorte Silva, D. P. Gill et al., "Combined dual-task gait training andAerobic exercise to improve cognition, mobility, andVascular health inCommunity-dwelling older adults atRisk for future cognitive Decline1," *Journal of Alzheimer's Disease*, vol. 57, no. 3, pp. 747–763, 2017.

[2] D. M. Ca Mmisuli, A. Innocenti, and F. Franzoni, "Aerobic exercise effects upon cognition in Mild Cognitive Impairment: a systematic review of randomized controlled trials," *Archives Italiennes de Biologie*, vol. 155, no. 1/2, pp. 55–62, 2017.

[3] K. E. Chan, "Short-term detraining does not change insulin sensitivity and RBP4 in rodents previously submitted to aerobic exercise," *Hormone And Metabolic Research*, vol. 49, no. 01, pp. 58–63, 2017.

[4] G. A. Callegari, J. S. Novaes, and G. R. Neto, "Creatine kinase and lactate dehydrogenase responses after different resistance and aerobic exercise protocols," *Journal of Human Kinetics*, vol. 58, no. 1, pp. 65–72, 2017.

[5] J. Attias, A. C. Philip, J. Waldie, T. Russomano, N. E. Simon, and A. G. David, "The Gravity-Loading countermeasure Skinsuit (GLCS) and its effect upon aerobic exercise performance," *Acta Astronautica*, vol. 132, no. 4, pp. 111–116, 2017.

[6] A. E. Leeuwis, A. M. Hooghiemstra, and R. Amier, "Design of the ExCersion-VCI study: the effect of aerobic exercise on cerebral perfusion in patients with vascular cognitive impairment," *Alzhmers & Dementia Translational Research & Clinical Interventions*, vol. 3, no. 2, pp. 157–165, 2017.

[7] M. Moghadasi, "Effects of 8 weeks high intensity aerobic exercise on serum adipocyte fatty acid binding protein levels," *Annals of Biological Research*, vol. 4, no. 12, pp. 150–154, 2017.

[8] D. Freeman, S. Reeve, A. Robinson et al., "Virtual reality in the assessment, understanding, and treatment of mental health disorders," *Psychological Medicine*, vol. 47, no. 14, pp. 2393–2400, 2017.

[9] D. Silove, P. Ventevogel, and S. Rees, "The contemporary refugee crisis: an overview of mental health challenges," *World Psychiatry*, vol. 16, no. 2, pp. 130–139, 2017.

[10] P. Butterworth, S. New, and C. Schilling, "Dynamics of mental health and healthcare use among children and young adults," *Australian Economic Review*, vol. 54, no. 1, pp. 130–142, 2021.

[11] B. Emma, D. H. Klemanski, and H. Mathilde, "Factors associated with parent-child discrepancies in reports of mental health disorders in young children," *Child Psychiatry & Human Development*, vol. 49, no. 6, pp. 1003–1010, 2019.

[12] M. Leese, S. Johnson, M. Slade et al., "User perspective on needs and satisfaction with mental health services. PRiSM Psychosis Study. 8," *British Journal of Psychiatry*, vol. 173, no. 5, pp. 409–415, 2018.

Hindawi
Emergency Medicine International
Volume 2023, Article ID 9803639, 1 page
https://doi.org/10.1155/2023/9803639

Retraction

Retracted: The Influence of Sports Dance on the Physical and Mental Development of Contemporary College Students Based on Health Detection

Emergency Medicine International

Received 8 August 2023; Accepted 8 August 2023; Published 9 August 2023

This article has been retracted by Hindawi following an investigation undertaken by the publisher [1]. This investigation has uncovered evidence of one or more of the following indicators of systematic manipulation of the publication process:

(1) Discrepancies in scope
(2) Discrepancies in the description of the research reported
(3) Discrepancies between the availability of data and the research described
(4) Inappropriate citations
(5) Incoherent, meaningless and/or irrelevant content included in the article
(6) Peer-review manipulation

The presence of these indicators undermines our confidence in the integrity of the article's content and we cannot, therefore, vouch for its reliability. Please note that this notice is intended solely to alert readers that the content of this article is unreliable. We have not investigated whether authors were aware of or involved in the systematic manipulation of the publication process.

In addition, our investigation has also shown that one or more of the following human-subject reporting requirements has not been met in this article: ethical approval by an Institutional Review Board (IRB) committee or equivalent, patient/participant consent to participate, and/or agreement to publish patient/participant details (where relevant).

Wiley and Hindawi regrets that the usual quality checks did not identify these issues before publication and have since put additional measures in place to safeguard research integrity.

We wish to credit our own Research Integrity and Research Publishing teams and anonymous and named external researchers and research integrity experts for contributing to this investigation.

The corresponding author, as the representative of all authors, has been given the opportunity to register their agreement or disagreement to this retraction. We have kept a record of any response received.

References

[1] H. Huang, "The Influence of Sports Dance on the Physical and Mental Development of Contemporary College Students Based on Health Detection," *Emergency Medicine International*, vol. 2022, Article ID 3715150, 11 pages, 2022.

Hindawi
Emergency Medicine International
Volume 2022, Article ID 3715150, 11 pages
https://doi.org/10.1155/2022/3715150

Research Article

The Influence of Sports Dance on the Physical and Mental Development of Contemporary College Students Based on Health Detection

Huali Huang

Department of Public Sports, Jingchu University of Technology, Jingmen 448000, Hubei, China

Correspondence should be addressed to Huali Huang; hhl@jcut.edu.cn

Received 14 April 2022; Revised 16 May 2022; Accepted 25 May 2022; Published 11 June 2022

Academic Editor: Hang Chen

The healthy growth of college students is related to the future development of the country and the prosperity of the nation. Under fierce social competition, college students are faced with academic pressure and employment pressure, resulting in the failure to improve their physical and mental health and their low self-acceptance level. Faced with such a situation, it is an important subject to solve the problem of the physical and mental health development of contemporary college students. As a sport that integrates sports and art, sports dance is worthy of in-depth discussion on the physical and mental development of college students. To analyze the impact of sports dance on the physical and mental development of contemporary college students, this paper uses an intelligent health monitoring system to monitor the health status of college students before and after physical dance exercise. It analyzes the influence of sports dance on the physical and mental development of college students from the aspects of cardiorespiratory endurance, muscular endurance, flexibility, and happiness. Finally, the results are obtained by conducting experiments with 10 college students. The experimental results show that the psychological well-being of college students who take physical dance exercise increases by 7.8%. Cardiorespiratory endurance and flexibility are both improved accordingly. Physical dance exercise promotes the physical and mental development of contemporary college students.

1. Introduction

With the progress of human beings and the continuous development of social economy, college education pays increasingly attention to the overall improvement of students' personal quality. In the education of colleges and universities, the physical and mental health and artistic development of students have become essential. The healthy development of students' physical and mental health has become an integral part of the quality education system. With the progress of human beings and the continuous development of social economy, higher education pays increasingly attention to the overall improvement of students' personal quality. In higher education, the physical and mental health and artistic development of students become essential. Students' mental health has become an integral part of the quality education system. College students face enormous pressure in academic, economic, interpersonal, and other aspects, and are prone to psychological barriers and emotional overload due to excessive pressure. Practicing sports dance in colleges and universities can effectively relieve students' stress, regulate their emotions, and reduce the occurrence of extreme mental states. Physical dance exercise can improve the quality of students, but also affect the physical health of college students. Physical dance teaching is closely related to the development of students' mental health. It can promote the improvement of college students' mental health and also plays an important role in the overall development of students' quality.

To promote the development of sports dance, a large number of researchers are devoted to the study of physical health. To study the effect of sports dance on the body shape of young men, C Lu chose young men as the subject of sports dance training. Through training, it is found that the

physical fitness of sports men is significantly improved [1]. SJ Zhang studied peripheral blood T cells of retired employees through dance experiments. It was found that the immune function of the elderly who exercised physical dance improved better [2]. HU Mi studied the effect of body dance on the balance ability of girls aged 6 to 7 years and trained the test group for 4 months. The results show that sports dance can significantly improve the static balance ability of girls aged 6 to 7 years [3]. Z Zhang studied the effect of physical dance on the body shape of overweight and obese elderly women through experimental methods, mathematical calculations, and comparisons. After 10 weeks of regular exercise and dancing, it was found that the subcutaneous fat in women was reduced, and the fat accumulation in the waist and abdomen was significantly improved [4]. R Wang studied the effects of participating in competitive dance training on the development of coordination and sensitivity in college students. The results show that sports dance can effectively improve the coordination and sensitivity of ordinary college students [5]. XF Zong has examined changes in college students' physical health through sports and dance programs. The results showed that the teaching and tutoring of a sports dance classes promoted the improvement of students' body shape, physique, physical function, and body balance [6]. MH Gao analyzed the comprehensive level requirements of sports dance coaches in the process of cultivating athletes from three aspects: professional skills, training level, and comprehensive management. It can enhance the ability of coaches to cultivate athletes, to cultivate excellent athletes [7]. These studies show that physical activity plays an important role in people's health. Although these studies have achieved rich results, with the emergence of new technologies and new situations, many college students have new psychological problems, and it is necessary to pay more attention to the psychological research of college students.

Physical dance exercise can not only help people have a healthy body but also promote the development of people's mental health. H. Sun believed that sports dance has become mainstream in sports. It examined the influence of sports dance practice on students' temperaments from aspects of participants' temperament and body shape, personal expression, and self-confidence in sports [8]. Q Lit found that good posture and gait rhythm can be created for adolescents through physical dance practice [9]. JiYoung conducted a three-month study of college students. The study found that exercise changed physical fitness, weight, and psychological values. Sports dance has a positive effect on women's physical health [10]. XB Dong had given extensive physical dance training to more than 200 physical education students. It is found that sports dance can improve the quality, self-esteem, self-confidence, and interpersonal skills of college students [11]. JH Zhu trained the students in gymnastics. It is found that physical dance teaching improves students' "aesthetic quality," reduces negative emotions, and promotes students' physical and mental health [12]. Using bibliography and comprehensive analysis methods, J. Yao discussed the role of sports dance in cultivating students' healthy beauty, athletic beauty, and shaping physical beauty. It promotes the cultivation of college students' aesthetic ability, creates beauty, and influences the work of aesthetic education [13]. T Cheng conducted a survey of children aged 9–12. Combining questionnaires and mathematical statistics with the Eysenck Children's Personality Questionnaire and a questionnaire tool, it was found that children who had learned sports dance were in better physical condition than children who had not learned sports dance. And their character is more optimistic and upward [14]. The above studies show that sports dance promotes the development of human mental health.

Dance Sports is a perfect combination of art and sports, an activity that includes dance, movement, and music. It has a variety of values such as sports, competition, aesthetics, and fitness and can achieve the purposes of entertainment, competition, and exercise. In this paper, the intelligent health tracking system is used to collect various physical fitness indicators of students in the process of sports dance training and send them to the database wirelessly. After the training, the physical, and mental indicators of the students were collected and compared with those before the experiment to observe the impact of physical and dance exercise on the physical and mental development of college students.

The innovations of this paper are as follows:

(1) This paper analyzes the importance of sports dance. It uses an intelligent health detection system to collect student physiological data to analyze the impact of sports dance on students.

(2) According to the age and gender of college students, this paper is tested under the same conditions. Each student's level of mental ability is analyzed and some indications of the impact of different physical activity programmes on mental health are provided.

(3) This paper uses the intelligent health detection system to study the impact of sports dance on the physical and mental health of students. It improves the effectiveness of data analysis, ensures the accuracy of data, and lays a new foundation for future research.

2. Intelligent Health Detection System

2.1. Collection of Sports Dance Information. This paper consists of four main parts: the main controller state search module, the remote control module, the smartphone software monitoring module, and the remote monitoring server module. The whole system is shown in Figure 1. The main controller mainly includes three sensing sensors: an oxygen sensing sensor for oxygen collection, diastolic pressure sensors, and a systolic pressure sensor for blood pressure measurement. The remote control unit cooperates with some external auxiliary tools to first record the physical data and parameter data obtained from the sensor. The physical data and parametric data collected by the physical sensors are then transmitted. The unit is monitored via WiFi transmission to smartphone software. The wireless WIFI module used to transmit data to the smartphone monitoring module adopts the serial port-Ethernet-wireless network

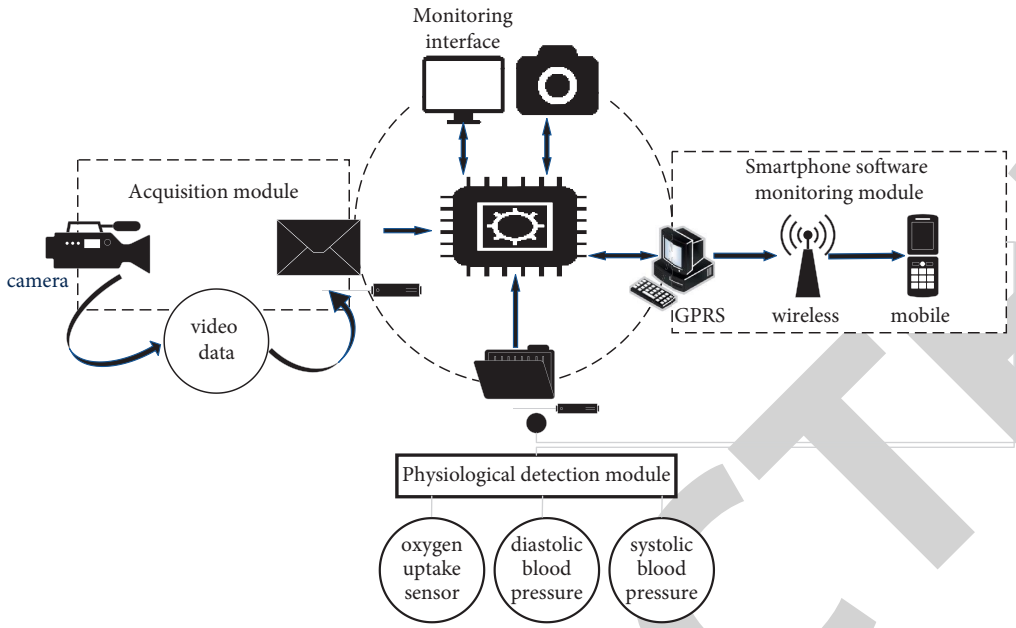

Figure 1: Framework diagram of intelligent health detection and collection.

function. Smartphone software monitoring involves partly managing user information and partly collecting normal student data [15]. The remote monitoring server platform is the same as the computer side. A Tomcat server specially designed for the Internet is installed on the computer. It is used to identify users using remote browsers and to record the physical activity of college students.

2.2. Android System. The Android system is divided into upper and lower layers. The upper layer has the application system layer and the application layer, and the lower layer has the kernel layer and the runtime system layer. The Android system architecture is shown in Figure 2. The basic Android server for the Linux kernel layer is called Linux Kernel Layer. It is based on Linux2.6, supports basic functions in Android, and is a movable layer that distinguishes software and hardware. Android kernel libraries are Android components provided by some core libraries. Developers can use it through the application process. Android time zone is configured by Android using Java language. To operate an Android application successfully, it needs to run in the Dalvik virtual machine. The Dalvik virtual machine must be run to run Android applications. The Dalvik virtual machine is a registry-based Linux kernel that provides basic functionality. The Android application framework can provide developers with any API framework they want to use. These technologies enable developers to better develop new applications, such as use of application resources, access to location information, and alarm settings. An Android application is a visual record of Android programming. It includes many source files of Java objects and finally starts the apk package for fetching [16, 17]. Android itself provides many basic applications such as Home, Contacts, Phone, and Browser. At the same time,

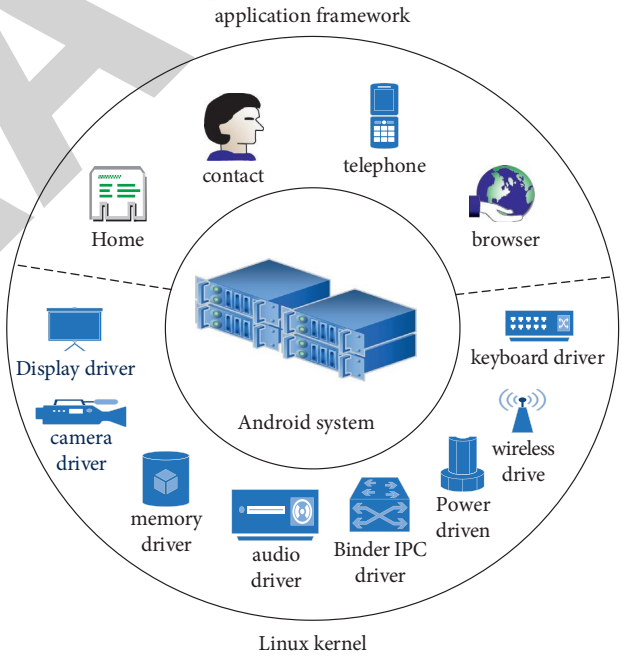

Figure 2: Android system architecture diagram.

developers can also use LayerLayerAPI to implement their own programs.

2.3. WiFi Wireless Transmission Technology. WiFi is a trade name in the industry. WiFi allows terminals to connect to the Internet anytime and anywhere, which is very convenient for human use. Like wireless technology, WiFi is a technology that can connect wireless devices such as computers, smartphones, and iPads. When using a wireless network, it should be noted that both the Infant network and

the ad hoc network belong to the wireless network. The location of the wireless AP network can create a wireless network, making it the central part of the network [18]. Any of these sites (computers, PDAs, and other Internet-enabled user devices) that are connected to a wireless network can be referred to as a site. As the center of the entire network, the wireless AP needs to communicate with other applications. Many STA devices are built in to create these wireless networks, while basic AP-based wireless networks are created by APs [19]. The basic network topology is shown in Figure 3. An ad hoc wireless network is a loose network. The AP is not in the network and only consists of two or more STAs, each of which can communicate with the outside world directly. The effect that the system wants to achieve in this paper is that the smartphone or PC can use WiFi connection to receive the physiological parameter information of college students and combine the data obtained from the home wireless network.

2.4. Gateway Workflow. The collection and transmission process of real sports dance training data needs to open the gateway and connect to the Internet. It uses the device to collect dance training data before and after the experiment. Different devices can have different transmission methods, for example, ECG first receives ECG data and then sends data through Bluetooth. The oximeter turns on Bluetooth before uploading data. After the data transmission is completed, the device will wait at the gateway port until it starts to search for data transmission. When the gateway is in standby mode (the delay may be in voting mode), the target Bluetooth device initiates a data request [20]. The device transmits the movement dance data received from the portal. After detecting the end of the data transfer, the Bluetooth is finally turned off. After the gateway analyzes and filters the received data, it processes the data packet of the data path and sends it to the data communication server through the data transmission model. If the gateway device is not connected to the network, the collected data is sorted and stored in a local file, and the data is resent after connecting to the network [21]. The workflow of the gateway is shown in Figure 4.

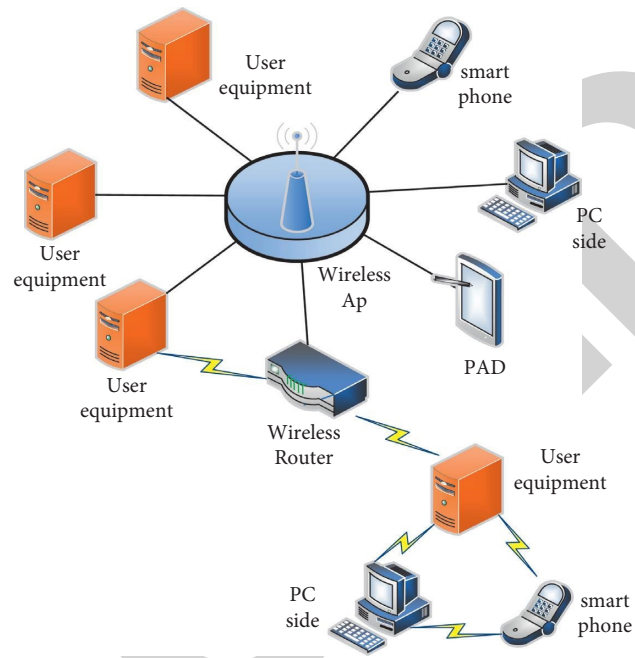

Figure 3: Analysis of WiFi wireless transmission technology.

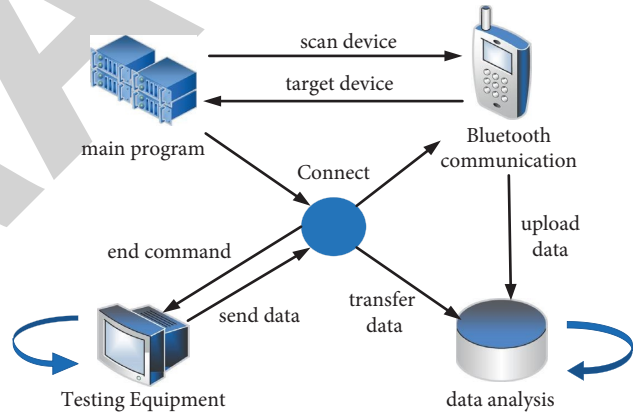

Figure 4: Gateway workflow.

3. Recommendation Algorithm

The focus of this study is to detect videos of college students' physical dance exercises. It uses the intelligent detection system to collect various physical indicators of college students during physical dance exercise and collects exercise videos. In a sequence of video images, the extracted images are simplified and sampled.

3.1. Active Contour Tracking Method. The moving edge function can provide target information about the moving position and moving shape of the object. The active contour algorithm is a common algorithm based on tracking edge information [22]. The contour model is an efficient segmentation and monitoring tool that requires parameters to render contours.

$$v(s) = [x(s), y(s)]. \tag{1}$$

The energy of the contour line is defined as

$$E_a[v(s)] = E_b[v(s)] + E_c[v(s)] + E_d[v(s)]. \tag{2}$$

In the formula, E_b represents the internal energy of the active contour, E_c represents the energy of the image force, and E_a represents the energy generated by the external restraint force. Then, the edge detection can get the contour edge of the image. Edge detection can be done by convolution with the help of gradient operators. It can be represented as a vector in position:

$$\nabla f(x, y) = \left[G_x G_y\right]^T = \left[\frac{\partial f}{\partial x} \frac{\partial f}{\partial y}\right]^T. \tag{3}$$

The direction of the vector is

$$\operatorname{mag}(\nabla f) = \left[G_x^2 + G_y^2\right]^{1/2}. \tag{4}$$

3.2. Optimal Bayesian Estimation. The mathematical model of the dynamic time-varying system can be described by formula (5) and formula (6). The state update equation of the system is described by

$$x_a = f_a(x_{a-1}, v_{a-1}). \tag{5}$$

Among them, f_a is a nonlinear function of the system state x_{a-1}, and v_{a-1} is a stationary noise sequence.

The measurement formula of the system is

$$z_a = h_a(x_a, n_a). \tag{6}$$

Among them, h_a is a nonlinear function of the system state x_a and n_k is a stationary noise sequence.

The basic idea of the Bayesian optimal filtering algorithm is that if the probability function of the initial condition is known, all measurement information can be used to construct the probability function behind the condition. Therefore, any filtering can lead to the theoretical optimal estimate [23]. In mathematical language, it can be described as follows:

$$p(x_a|z_{1:\,a-1}) = \int p(x_a|x_{a-1})p(x_{a-1}|z_{1:\,a-1})\mathrm{d}x_{a-1}, \tag{7}$$

The state update formula is

$$p(x_a|z_{1:\,a}) = \frac{p(z_a|x_a)p(x_a|z_{1:\,a-1})}{p(z_a|z_{1:\,a-1})}. \tag{8}$$

That is,

$$p(z_a|z_{1:\,a-1}) = \int p(z_a|x_a)p(x_a|z_{1:\,a-1})\mathrm{d}x_a. \tag{9}$$

It can be seen from formula (7) that the predictable probability weights can be obtained from the state transition function of formula (5). The probability function can be derived from the measurement model of formula (6). In formula (8), the measured value can be used to change the prepredicted probability to obtain the current state step.

3.3. Sequential Importance Sampling. The Bayesian sampling method mentioned above is a simple and commonly used Monte Carlo method. However, it is difficult to calculate over time. The main reason is that every time a desired observation is calculated, a new observation will appear. And the base density needs to be recalculated for each case. To address this issue, the next important sampling idea is proposed. That is, the specific gravity is calculated in the form of regression without changing the sampling time to the previous set of peaks [24].

The purpose of the sampling process is to find the frequency value of a specific sample. The main function must be written as follows:

$$q(x_{0:\,a}|z_{1:\,a}) = q(x_0)\prod_{b=1}^{a} q(x_b|x_{0:\,b-1}, z_{1:\,b}). \tag{10}$$

It can be concluded that

$$p\left(x_{0,a}\right) = p(x_0)\prod_{b=1}^{a} p(x_b|x_{b-1}). \tag{11}$$

That is,

$$p(z_{1:\,a}|x_{0:\,a}) = \prod_{b=1}^{a} p(z_b|z_{b-1}). \tag{12}$$

It is brought in to get the weight recursion formula:

$$w_a = \frac{p(z_{1:\,a}|x_{0:\,a})p(x_{0:\,a})}{q(x_a|x_{0:\,a-1}, z_{1:\,a})q(x_{0:\,a-1}|z_{1:\,a})}. \tag{13}$$

Reconsidering the described Bayesian estimation problem, using the sequential resampling idea, a complete recursive SIS can be obtained. From the point of view of practical application, most literature adopt the idea of sequential resampling. At this point it can be rewritten as follows:

$$w_a = w_{a-1}p(z_a|x_a). \tag{14}$$

Since the main function does not consider the latest data, the model produced by the main function is very different from the model created by the actual background distribution. Especially when the probability function has a probability type, the state setting density or model observations and precision are high. As shown in Figure 5, the sample becomes unusable due to its low density, making this sampling method inefficient.

3.4. Particle Scarcity and Resampling. The sampling process is an important part of particle filtering. While it increases particle hunger, it also reduces particle diversity. Therefore, the selection of evaluation should be based on certain criteria [25]. Currently, the most commonly used measurement is based on the number of active particles, defined as

$$N_f = \frac{1}{\sum_{i=1}^{N}\left(w_t^{(i)}\right)^2}. \tag{15}$$

The central idea of the particle filter algorithm is to use a random sampling system to represent the desired probability density function rather than based on general states. Figure 6 illustrates the implementation process of the particle filter algorithm.

The specific implementation steps of the particle filter algorithm are as follows:

$$w_a^{(i)} = w_{a-1}^{(i)}\frac{p\left(z_a|x_a^{(i)}px_a^{(i)}|x_{a-1}^{(i)}\right)}{q\left(x_a^{(i)}|x_{0:\,a-1}^{(i)}, z_{1-a}\right)}. \tag{16}$$

If a one-step transition posterior state distribution is used, the formula can be simplified to

$$w_a^{(i)} = w_{a-1}^{(i)}p\left(z_a|x_a^{(i)}\right). \tag{17}$$

The normalized weights are

$$\widehat{w}_a^{(i)} = \frac{w_a^{(i)}}{\sum_{b=1}^{N} w_a^{(b)}}. \tag{18}$$

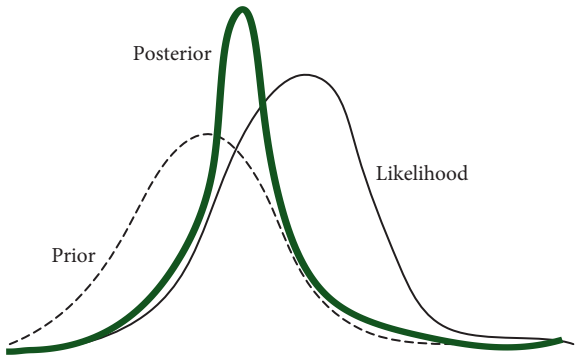

Figure 5: Comparison between importance function samples and real ones.

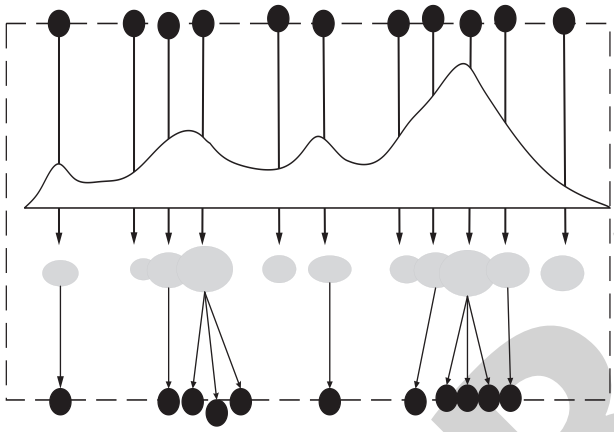

Figure 6: Implementation process of particle filter algorithm.

The output of the algorithm is the particle set, which is used to approximate the posterior probability and the expectation of the function:

$$\hat{p}\left(x_{0:\,a}|z_{1:\,a}\right) = \frac{1}{N}\sum_{i=1}^{N}\delta_{x_{0:\,a}^{(i)}}\left(\mathrm{d}x_{0:\,k}\right). \tag{19}$$

That is,

$$E\left(g_a\left(x_{0:\,a}\right)\right) = \frac{1}{N}\sum_{i=1}^{N} g_a\left(x_{0:\,a}^{i}\right). \tag{20}$$

4. Sports Dance Training Experiment

4.1. Experimental Design. Because the research design of this paper is carried out under natural conditions, it does not affect the students' class, and the students do not know the specific experiment, so it has good reliability and validity. It is often used in sports research. The subject and content of sports research often limits the practical application of this rigorous experimental design in many ways. This experimental model is a plan of equal groups before and after the test.

Combined with the research purpose of this paper, this experiment will randomly select from two universities. Students from different majors were randomly selected for the experiment and divided into an experimental group and a control group. Then, the two groups of students were measured with the mental health scale before receiving the experimental training, and the data were recorded. The experimental group was given physical dance exercise for up to 15 weeks, while the control group continued to live a normal life. After the experiment, the experimental group and the control group were remeasured. Finally, the two groups of outcome indicators were statistically analyzed.

4.2. Experimental Data. Students of different majors were selected as research subjects. Study and train in a 15-week sports dance class. The control group did not receive physical dance training, but only regularly studied and practiced, while the experimental group received physical dance training. To avoid the interference of age factors, this paper mainly selects sophomore students as the research objects. The age distribution is 20 years old, and 10 people are randomly selected. Among them, 1–5 are the control group, and 6–10 are the experimental group. The specific data are shown in Table 1.

4.3. Experimental Process. Before the experiment, it checks the results of physical fitness tests, including cardiopulmonary function, muscle strength and endurance, flexibility, body composition, and other physical fitness test results. The subjects were divided into an experimental group ($n = 5$) and a control group ($n = 5$). The experimental group conducted a 15-week sports dance intervention experiment. The control group followed the normal study and daily routine and did not do physical exercise outside the school physical education class. Cardiopulmonary function, muscle strength and endurance, flexibility, and body composition metrics were measured before and after surgery.

5. Experimental Results of Physical Dance Training

5.1. Cardiopulmonary Endurance Index. This paper selects three cardiorespiratory endurance indicators: maximal oxygen uptake, diastolic blood pressure, and systolic blood pressure to reflect the students' cardiovascular function. Among them, the unit of maximal oxygen uptake is mL/(kg·min). Table 2 is the measurement data results of the two groups of college students in terms of cardiorespiratory endurance before and after the experiment.

As can be seen from Table 2, there was a significant difference in the maximum oxygen uptake between the control group and the experimental group after the experiment. The maximal oxygen uptake of the control group changed from 30 ± 5 to 29 ± 6, and there was no significant change. In contrast, the VO2 max in the control group increased from 29 ± 4 to 33 ± 5. The systolic blood pressure and diastolic blood pressure in the experiment were significantly different from those before the experiment. The diastolic blood pressure in the control group decreased from 75.32 ± 12.45 to 74.36 ± 11.36. The diastolic blood pressure in the experimental group decreased from 72.23 ± 10.69 to

Table 1: Student data collection form.

Serial number	Gender	Height (cm)	Age	Weight (kg)	Profession
1	Male	178	20	71	Preschool education
2	Female	166	20	50	Nursing
3	Female	160	21	42	Film and television
4	Female	159	21	43	Psychology
5	Male	174	19	62	Mathematic major
6	Male	183	20	75	Management
7	Female	159	20	45	Preschool education
8	Male	179	21	71	Economics
9	Male	184	22	80	Law degree
10	Female	167	20	51	Nursing

Table 2: The test of cardiorespiratory endurance index of subjects in the control group and the experimental group before and after the experiment.

Test indicators	Control group ($n = 100$)		Experimental ($n = 100$)	
	Before experiment	Experimental	Before experiment	Experimental
Maximal oxygen uptake	30 ± 5	29 ± 6	29 ± 4	33 ± 5
Diastolic blood pressure	75.32 ± 12.45	74.36 ± 11.36	72.23 ± 10.69	66.02 ± 11.22
Systolic blood pressure	124.56 ± 12.56	122.18 ± 14.64	117.95 ± 14.23	112.85 ± 11.23

66.02 ± 11.22. The systolic blood pressure in the control group decreased from 124.56 ± 12.56 to 122.18 ± 14.64. The systolic blood pressure in the experimental group decreased from 117.95 ± 14.23 to 112.85 ± 11.23. It shows that regular participation in physical dance has a certain effect on increasing the maximum oxygen uptake and lowering blood pressure.

5.2. Muscle Strength/Muscular Endurance Index. In this study, three indicators, maximal inspiratory/expiratory pressure, maximal transdiaphragmatic pressure, and maximal maintenance ventilation, were selected to evaluate muscle strength/endurance. Table 3 shows the data changes between the experimental group and the control group before and after the experiment.

As can be seen from Table 3, there was no significant difference in the maximum inspiratory/expiratory pressure between the control group and the experimental group after the experiment. The maximum inspiratory/expiratory pressure of the control group changed from 90.9 ± 8.5 to 91.8 ± 6.6. The maximum inspiratory/expiratory pressure of the control group was 92.1 ± 7.9 and changed to 92.3 ± 4.4. The maximum transdiaphragmatic pressure and maximum maintenance ventilation in the test were significantly different from those before the test. The maximum transdiaphragmatic pressure in the control group increased from 150 ± 39 to 155 ± 40. The maximum transdiaphragmatic pressure in the experimental group increased from 147 ± 40 to 160 ± 30. The maximum maintenance ventilation in the control group increased from 90 ± 10 to 91 ± 8, and the maximum maintenance ventilation in the experimental group increased from 89 ± 6 to 96 ± 6. It shows that regular participation in physical dance has a certain effect on increasing the maximum transdiaphragmatic pressure and the maximum maintenance ventilation.

5.3. Flexibility Index. In this paper, 10 students were trained in physical dance for 15 weeks, including 5 in the control group and 5 in the experimental group. The effect of physical dance on flexibility was judged by observing weekly seat forward flexion. The results are shown in Figure 7.

It can be clearly seen that there is no significant difference in the index of sitting body forward flexion in the control group in the experiment. There were significant differences in the changes of sitting body forward flexion in the experimental group. It keeps increasing with the time of physical dance exercise.

5.4. Comprehensive Comparison of Mental Health Levels. Before the experimental intervention, each group was tested and analyzed to observe the changes in the psychological health of the experimenters, including the measurement of interpersonal relationships and self-esteem. 1 is before the experiment in the control group, 2 is after the experiment in the control group, 3 is before the experiment in the experimental group, and 4 is after the experiment in the experimental group. The results are shown in Figure 8.

After the experiment, the emotional indicators of the control group did not fluctuate much. However, the negative emotional indicators such as depression score and compulsion score of the subjects in the experimental group were significantly different from those before the experiment, and all of them were reduced to a certain extent. The interpersonal relationship score was significantly improved, which was 1.5 points higher than that before sports dance training.

5.5. Comparison of Subjective Well-Being Effects. Before the experiment, the subjective well-being of each group was analyzed to observe the changes in the mental health of the experimenters, including the measurement of emotion, satisfaction, and overall subjective well-being. 1 is before the

Table 3: Muscle endurance index matching test of subjects in the control group and experimental group before and after the experiment.

Test indicators	Control group ($n = 100$)		Experimental ($n = 100$)	
	Before experiment	Experimental	Before experiment	Experimental
Max inspiratory/expiratory	90.9 ± 8.5	91.8 ± 6.6	92.1 ± 7.9	92.3 ± 4.4
Max transdiaphragmatic	150 ± 39	155 ± 40	147 ± 40	160 ± 30
Max maintain ventilation	90 ± 10	91 ± 8	89 ± 6	96 ± 6

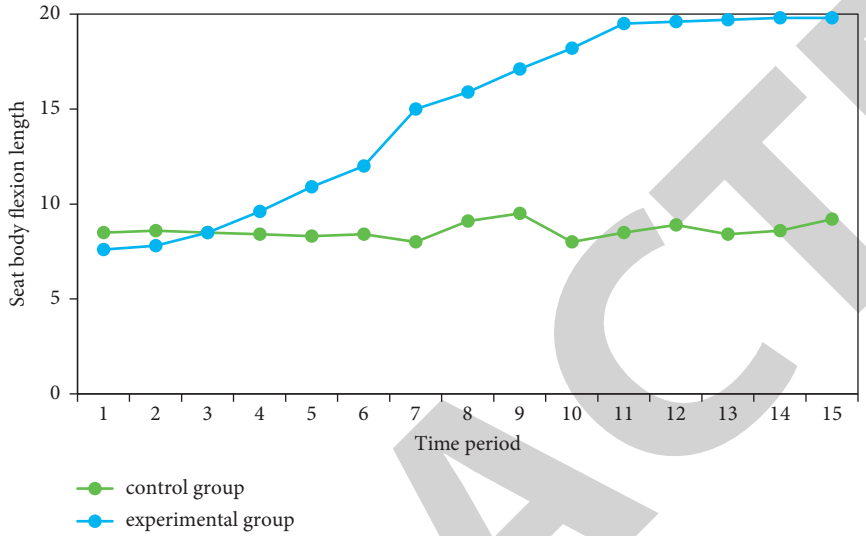

Figure 7: Flexibility index measurements.

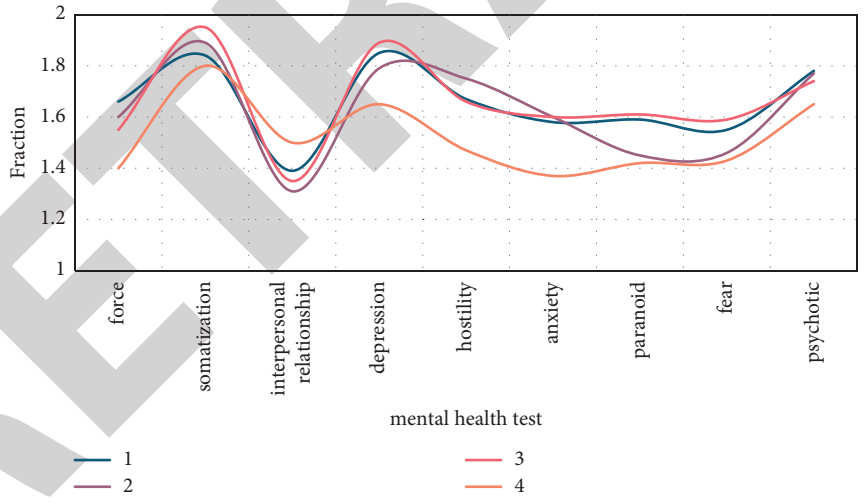

Figure 8: Comprehensive comparison of mental health levels.

experiment in the control group, 2 is after the experiment in the control group, 3 is before the experiment in the experimental group, and 4 is after the experiment in the experimental group. The result is shown in Figure 9.

As can be seen from Figure 9, there is not much difference between the control group before and after the experiment. The overall emotional scores of the subjects in the experimental group were significantly different from those before the experiment. After the experiment, the scores of the subjects in the experimental group were significantly different from those before the experiment. Happiness satisfaction increased by 7.8%.

5.6. Comparison of the Effect of Self-Acceptance on the Results. Before the experiment, a self-acceptance analysis was carried out for each group to observe the changes of the subjects' mental health, including measurement acceptance and evaluation acceptance. 1 is before the experiment in the control group, 2 is after the experiment in the control group, 3 is before the experiment in the experimental group, and 4 is after the experiment in the experimental group. The results are shown in Figure 10.

As can be seen from Figure 10, there is not much difference between the control group before and after the

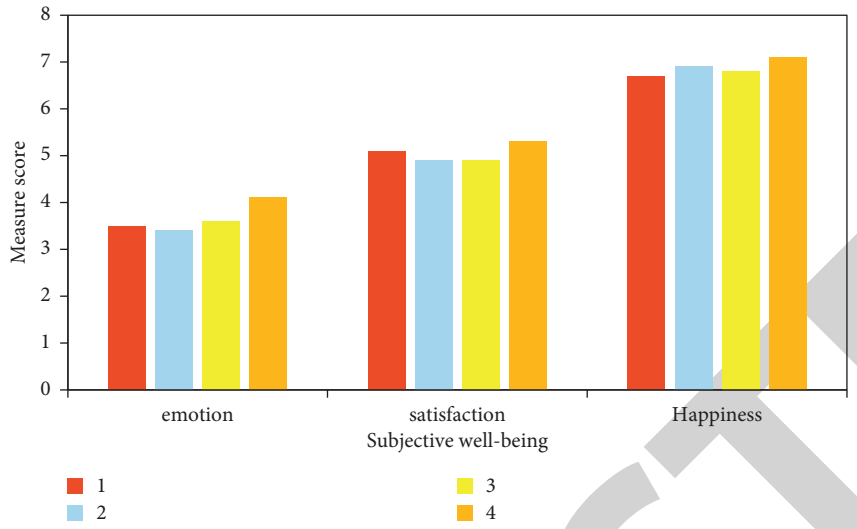

Figure 9: Comparison of subjective well-being effects.

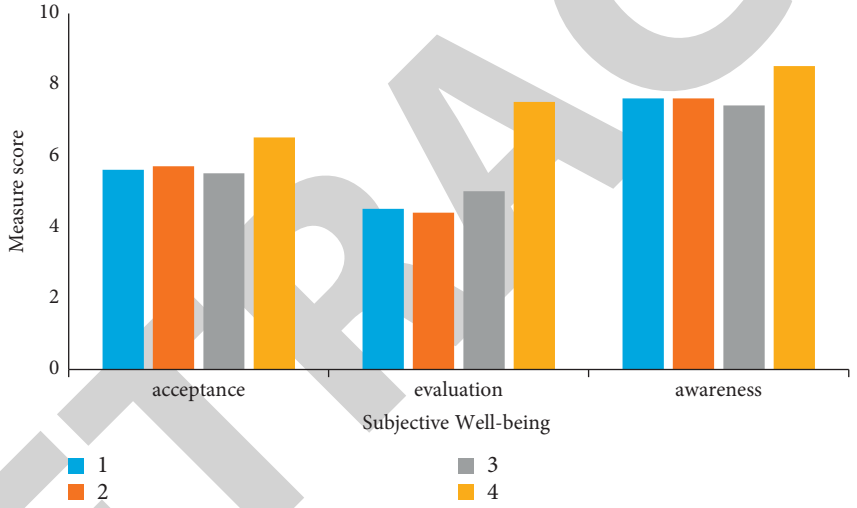

Figure 10: Comparison of self-acceptance impact results.

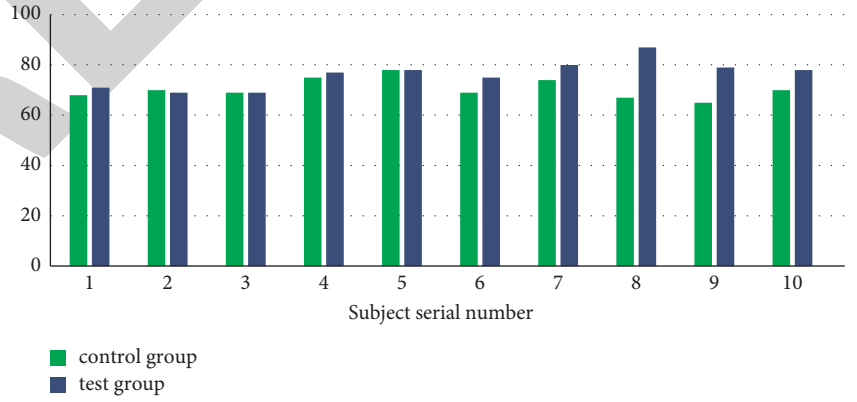

Figure 11: Comparison of self-assessment impact results.

experiment. The overall emotional scores of the subjects in the experimental group were significantly different from those before the experiment. After the experiment, the self-acceptance influence total score of the experimental group was higher than that before the experiment.

5.7. Comparison of Self-Evaluation Effects. Before the experiment, self-evaluation was scored for each group, and it was observed whether the subjects' self-score changed before and after the experiment. Among them, 1–5 are the control group, 6–10 are the experimental group, and the self-evaluation is scored out of 100 points. The results are shown in Figure 11.

As can be seen from Figure 11, there is not much difference between the control group before and after the experiment. The self-evaluation scores of the subjects in the experimental group were significantly different from those before the experiment. After the experiment, the self-evaluation total score of the experimental group was higher than that before the experiment.

6. Discussion

The positive effects of dance practice on the physical and mental health of modern students after sports dance intervention are consistent with previous studies. This study found that the effect of sports dance on the physical health of modern college students is particularly obvious in improving physical fitness and muscle strength. However, interventions in dance movements have not yet had a significant impact on students' cardiorespiratory capacity, muscular endurance, and body composition. Dance movement has a major impact on the mental health of modern students. Among them, the main ones were stress, depression, sleep and nutrition, relationships, paranoia, mental health determinants, and overall performance. There were also significant improvements in the happiness index and life satisfaction factors, as well as self-acceptance and self-confidence factors in the test group.

7. Conclusion

Through the health examination of modern college students, this paper finds that sports dance has a positive impact on students' physical and mental health and has a greater impact on students' mental health. It has a more obvious effect on physical health by improving the cardiovascular function of college students, improving muscle strength, and improving students' flexibility indicators, especially improving body shape and muscle strength. In terms of mental health, it can help relieve students' stress and anxiety in the learning process and improve their brain quality. It promotes positive attitudes and health in students, enables them to better accept themselves, and develops the ability to improve self-correction and facilitate interpersonal face-to-face communication. At the same time, it can also improve students' self-improvement abilities and improve their self-esteem. Therefore, regular participation in the practice of sports dance is a good choice to promote the physical and mental development of students. It plays an important and critical role in the process of physical and mental development and has an important position and importance in the process of school education quality reform.

Data Availability

The data underlying the results presented in the study are available within the manuscript.

Conflicts of Interest

The authors declare that there are no conflicts of interest.

References

[1] C. Lu, Y. S. Khan, M. Jouda et al., "COVID-19 pandemic fears and obsessive-compulsive symptoms in adolescents with pre-existing mental disorders: an exploratory cross-sectional study," *Clinical Child Psychology and Psychiatry*, vol. 27, no. 1, pp. 89–103, 2022.

[2] S. J. Zhang, T. Osadtsiv, V. Sosina, and O. Lykyanenko, "Control in the physical preparation of athletes aged 8-9 years in sport dancing," *Journal of Kinesiology and Exercise Sciences*, vol. 27, no. 80, pp. 21–25, 2017.

[3] M. Hu, V. Mitrousias, G. Halatsis et al., "Epidemiology of injuries in pole sports: emerging challenges in a new trend," *British Journal of Sports Medicine*, vol. 51, no. 4, 2017.

[4] E. López-Cañada, J. Devís-Devís, A. Valencia-Peris et al., "Physical activity and sport in trans persons before and after gender disclosure: prevalence, frequency, and type of activities," *Journal of Physical Activity and Health*, vol. 17, no. 6, pp. 650–656, 2020.

[5] R. Wang and Y. Liu, "Impact of sport dancing on the dynamics characteristic of foot movement of college students," *Leather and Footwear Journal*, vol. 18, no. 2, pp. 109–116, 2018.

[6] X. F. Zong, I. Grygus, N. Nesterchuk, S. Rabcheniuk, R. Hrytseniuk, and W. Zukow, "Correction of posture disorders with sport and ballroom dancing," *Medicni perspektivi (Medical perspectives)*, vol. 25, no. 1, pp. 174–184, 2020.

[7] M. H. Gao, K. K. Dhillon, E. E. Centeio, and S. Dillon, "Drumming and dancing: creative movement for convention refugee youth in a physical activity space," *Sport, Education and Society*, vol. 25, no. 3, pp. 318–331, 2019.

[8] H. Sun and A. C. E. Purser, "Dancing like a girl: physical competence and emotional vulnerability in professional contemporary dance," *Women in Sport & Physical Activity Journal*, vol. 25, no. 2, pp. 105–110, 2017.

[9] Q. Lit and D. Byczkowska-Owczarek, "Performing on the boundary of art and sport: the case of competitive ballroom dancers," *Czech Sociological Review*, vol. 55, no. 3, pp. 369–392, 2019.

[10] K. JiYoung, Y. JungEun, A. Hong, and S. Lee, "Finding the position of school dance: a review in accordance with policy and public law through the stakeholder analysis," *Korean Journal of Sport Pedagogy*, vol. 24, no. 2, p. 79, 2017.

[11] T. S. Jung and T. S. Jung, "Relations among tendency of perfectionism, self-management and competition anxiety of the high school students majoring in dancing," *The Korean Journal of Physical Education*, vol. 56, no. 5, pp. 607–619, 2017.

[12] M. Luiggi and J. Griffet, "Sport injury prevalence and risk by level of play and sports played among a representative population of French adolescents. a school-based study," *Revue d'epidemiologie et de sante publique*, vol. 67, no. 6, pp. 383–391, 2019.

[13] J. Yao and W. J. Lee, "A study on the dionysian elements in break dancing," *The Journal of the Korean Society for the*

Hindawi
Emergency Medicine International
Volume 2023, Article ID 9896378, 1 page
https://doi.org/10.1155/2023/9896378

Retraction

Retracted: Font Design in Visual Communication Design of Genetic Algorithm

Emergency Medicine International

Received 8 August 2023; Accepted 8 August 2023; Published 9 August 2023

This article has been retracted by Hindawi following an investigation undertaken by the publisher [1]. This investigation has uncovered evidence of one or more of the following indicators of systematic manipulation of the publication process:

(1) Discrepancies in scope
(2) Discrepancies in the description of the research reported
(3) Discrepancies between the availability of data and the research described
(4) Inappropriate citations
(5) Incoherent, meaningless and/or irrelevant content included in the article
(6) Peer-review manipulation

The presence of these indicators undermines our confidence in the integrity of the article's content and we cannot, therefore, vouch for its reliability. Please note that this notice is intended solely to alert readers that the content of this article is unreliable. We have not investigated whether authors were aware of or involved in the systematic manipulation of the publication process.

Wiley and Hindawi regrets that the usual quality checks did not identify these issues before publication and have since put additional measures in place to safeguard research integrity.

We wish to credit our own Research Integrity and Research Publishing teams and anonymous and named external researchers and research integrity experts for contributing to this investigation.

The corresponding author, as the representative of all authors, has been given the opportunity to register their agreement or disagreement to this retraction. We have kept a record of any response received.

References

[1] Y. Wang and W. Chung, "Font Design in Visual Communication Design of Genetic Algorithm," *Emergency Medicine International*, vol. 2022, Article ID 6897115, 10 pages, 2022.

Hindawi
Emergency Medicine International
Volume 2022, Article ID 6897115, 10 pages
https://doi.org/10.1155/2022/6897115

Research Article

Font Design in Visual Communication Design of Genetic Algorithm

Yue Wang [1,2] and Won-jun Chung [1]

[1]*Department of Visual Design, School of Architecture and Design, Dongmyong University, Busan 48520, Republic of Korea*
[2]*Department of Advertising, College of Media, Linyi University, Linyi 276000, Shandong, China*

Correspondence should be addressed to Yue Wang; wangyue@lyu.edu.cn

Received 8 April 2022; Revised 12 May 2022; Accepted 25 May 2022; Published 7 June 2022

Academic Editor: Hang Chen

The text has played an essential role in the advancement of human civilization. It is used now as a valuable cultural heritage that has been experienced for a thousand years. The passing text must have its irreplaceable advantages and charm. People are extremely sensitive to visual symbols, and it is also the first step in which people can know things. Most of the books in today's market focus on pictures and colors, which ignores the design of the text. This makes the text boring taste, causing the reader's visual fatigue, which is not conducive to readers absorbing information through books. Therefore, this paper studies the font design in the design of the visual algorithm based on the genetic algorithm, and the font design is analyzed by the particle swarming algorithm, the decision MIMO-SCMA system of the genetic algorithm. It aims to address the dryness of today's texts by constructing texts that are instantly recognizable and visually appealing to readers. Through innovative visual concepts, readers can enjoy the process of acquiring knowledge. In this paper, to investigate the effectiveness of the genetic algorithm in font design, the number of experimental research subjects was set to 300, and 280 valid questionnaires were collected to investigate the satisfaction of users with the newly designed fonts. Experiments showed that the visual communication design based on a genetic algorithm has increased by 6.52% for the design satisfaction and the number of fonts that use the system is also increasing.

1. Introduction

The text is a set of visual symbols, transformed from writing into a specific text, which is the value given to the text. The text is an important part of the information transfer, as an image color is an important visual element. In the context of visual communication, the visual meaning of "font" is personal. Whether it is e-mail, books, brochures, websites, and magazines, these designs have no difference in text. However, so far, the design and structure of "font" have been ignored. The genetic algorithm introduced in font design in visual communication design can make the font design provide valuable information to deep visual communication memory. In the development and design of the font, it integrates new features, making the creative design of the fonts widely spread, which has great significance for the development of the text.

With the development of intelligent terminals, the Internet of Things, the application of genetic algorithms is increasingly popular, and many teams are excavating and researching. Wenskovitch et al. explored the concept of using artificial intelligence factors in programming languages. He modeled the learning behavior of the adapter group and related rational factors in the financial system. The relationship between code encoding and genetic algorithm integration properties is described in detail [1]. Chun proposed a new method for improving power generation system maintenance. The proposed method uses the genetic algorithm to achieve the optimal solution to the annual Lole value of the energy system during analysis [2]. Zhou et al. used the genetic algorithm to diagnose cardiovascular disease and to increase its initial density, which provides the optimum density for neural networks, increasing the efficiency of neural networks by about 10% [3]. Devornique

et al. recommended optimizing the linear and longitudinal alignment of the *U* model. Digital samples are provided to compare the proposed technology with available methods, whose results prove the high efficiency of the proposed algorithm [4]. For multicenter optimization issues, Mercado-Borrayo et al. proposed a genetic algorithm to effectively solve these problems [5]. Xie et al. are testing a new hybrid calculation model in predicting future natural gas demand. They proposed a model binding on a genetic algorithm (GA) and other methods to construct a natural oil pipeline distribution model [6]. Wang proposed a new method based on static reactive energy recovery and traditional power system stability. This method is based on the connection between the genetic algorithm (GA) and the rough set process. What he proposed is designed to reduce the calculation time and reduce the storage capacity required for optimization and improve the performance stability of the power system [7]. From the above study, the current font design problems can be seen: first, the font is too monotonous compared to the picture, which cannot attract the reader's attention; second, the design of the font is about the transmission of culture, a single font form, which is not conducive to the transmission of colorful culture. Based on the above problems, this paper will focus on the analysis of font design to facilitate the inheritance and development of culture.

Visual communication is a communication service using a visual language, that is, a visual aid, which delivers information through optical media. Dawid and Kopel, to create a more beautiful graffiti, combined cloud computing and the Internet of Things, providing more visual communication elements. This provided resources for creators, which is a continuous creation enthusiasm [8]. Volkanovski et al. completed training through a visual exchange, providing the first algorithm for visual and social understanding of how to cooperate to support text processing to support visual exchange [9]. Zeinab et al. introduced signal flexibility to explain signal differences in different receivers and environments. Media reports are signals that accumulate from stock trading to games. Signal and visual kisses are used to affect funding decisions [10]. Alavidoost et al. determined many different stages of auditory interaction based on different time functions that affect the reaction of the audiovisual process (only affecting the auditory and audiovisual processes). It provided a unique way to explore acoustic interactions and measure the demand in short-term acoustic applications [11]. For multicenter optimization issues, Gong et al. and others proposed a genetic algorithm to effectively solve these problems [12]. Panapakidis and Dagoumas were testing a new hybrid calculation model in predicting future natural gas demand. They used their proposed model to construct a natural oil pipeline distribution model [13]. Fetouht Zakyms proposed a new method based on static reactive energy recovery and traditional power system stability. This method is based on the connection between the genetic algorithm (GA) and the rough set process. The proposed method is intended to reduce the calculation time and reduce the storage capacity required for optimization and improve the performance stability of the power system [14]. These studies have shown that genetic algorithms have been widely used in people's lives.

The font is the charm after the evolution of history and culture, which is the basis of cultural development and inheritance. It promotes not only the development of culture but also the enjoyment of readers' visual aesthetics. Based on the development of the state design, this paper analyzes the readers by using the genetic algorithm and transmits text through visual communication systems. In this study, under the support of the genetic algorithm, the fonts were designed in this article for reader and text development. In this paper, we will combine genetic algorithms to design fonts and change the problems in the evolution of fonts nowadays, to attract users to increase their usage of fonts and increase their satisfaction.

The font is the charm of historical and cultural evolution and is the basis of cultural development and transmission. It not only promotes the development of culture but also is a visual and aesthetic enjoyment for readers. However, due to the general neglect of the majority of people nowadays, there is a serious impact on the development of fonts. Based on the development of font design nowadays, this paper influences the development of the text by using genetic algorithms, visual communication design to analyze the psychology of readers, and design fonts that are more acceptable to readers.

This article has an innovative point as follows:

(1) In this paper, the genetic algorithm was introduced in the font design, analyzes the reader's psychology through a genetic algorithm, and designed the font that satisfies readers

(2) This paper proposed an information platform for professionalism, openness, and practical construction for visual communication design

(3) This article will also analyze the export methods and standard laws of words and then guide the application in modern design

2. Construction Based on the Visual Communication System

2.1. Relationship Chain in Visual Communication. Like the process of information visualization, visual conveyors ultimately help companies create value. Although there are many design categories and specific links, it is easy to customize business links. This article carefully develops internal visual conveying procedures by content and type, that is, from the outside: visual creativity, visual synthesis, process, control, and link. With the "external impact" as the main category, it encloses all external factors that affect the performance of the visual conveying process from different angles, which master the communication status of the internal and external communication links [15].

2.2. Value Link. In this article, based on economic-related theoretical boundary conditions, the value chain is only narrowly defined as a value chain produced by a series of value-added processes such as research, design, production,

and marketing. Visual conveying is a circulation communication in the value chain. It is an intermediate link in the value chain, interacts with other links, and is affected by a wide range of business and social foundations.

As shown in Figure 1, the "value chain link" during visual conveying is a process management process and integrated creativity that promotes visual communication. Absorbing and assimilating the background of the era, and based on the understanding of the work itself, the field of visual communication affects the performance of artistic creation. During the further process of visual conveying processes, the production process must be checked and calibrated again and again to make it not deviated from the visual communication space. At the same time, it is necessary to repeatedly test when operating multiple optical communication links to determine if the final visual work can achieve the intended purpose.

2.3. Process Control. In each visual communication link, the idea and behavior work together to complete a complex task. To achieve the final result of the communication, the process control connection is essential. Based on the information from the value chain and understanding of the entire project, the visual communication is controlled by various methods, which control the process of visual communication, such as planning and management of work conditions. In some cases, it ensures that the work can produce the expected results within the set time range.

Based on Figure 2, it can be seen that due to the factors involved in different visual communication tasks and the complexity of teamwork during operation, the process control links are more closely related. Compared with comprehensive ideas and visual ideas, it seems more intuitive and rationality.

2.4. Creative Synthesis. Creative logic refers to the rules that must be followed in the creative process to make meaningful tasks easier and more efficient. Most importantly, it is worth thinking about the creation of creative relationship logic before and after the creation. That is, creative logic not only represents the laws and relationships between the various steps and elements in the creative process but also represents how creativity must be best adapted to its creative goals and creation [16].

As shown in Figure 3, the focus of integrated creative connections in visual communication is not visual performance, but the design and arrangement of general information such as form, process, results, influence, and conveyance progress.

2.5. Creative Perfection. Visual creativity is the most important and simpler connection to present the final result of visual conveying. However, with the continuous change and upgrade of the market demand in the commercial world, the visual impact on the public is gradually subsidized under the initial visual fatigue. In the face of the status quo, visual ideas often need to expand and innovate with the overall creative and era background to achieve a strong visual impact, and it changes the visual level of the past, maximizing the impact of information transfer [17].

From Figure 4, it can be an intuitive understanding, and during design and operation, the links between the creative and value chains are integrated. It transfers the final design from the design language to the final product, thereby forming the full process of information communication space to meet its requirements and visual communication.

3. Genetic Algorithm

3.1. Genetic Algorithm. The genetic algorithm (GA) was first proposed by John Holland in the 1970s in the USA. The algorithm was designed and proposed according to the law of evolution of organisms in nature. It is a computational model of a biological evolutionary process that simulates the mechanism of natural selection and genetics of Darwinian biological evolution and is a method to search for the optimal solution by simulating the natural evolutionary process [18]. The flow chart of the genetic algorithm is shown in Figure 5.

3.2. Chaos Optimization Genetic Algorithm. The principle of this algorithm is to adjust the weight and threshold in the BP neural network through a chaotic genetic algorithm (CGA) and utilize the improved output function of the BP neural network [19]. The execution process of the algorithm is as follows.

3.2.1. Initial Population Chaotic Generation. For the original generator algorithm, the randomly generated initial populations will deviate from the optimal solution in algorithm training and optimization. To overcome these weaknesses, logistic mapping is used to add mixed variables to the initial population and to find the best variable optimization solution at the global level of the optimization scale using the universality of mixed motion, thus improving efficiency and accuracy. The logistics mapping is as follows:

$$\rho_i^{u+1} = u\rho_i^{(u)}\left(1 - \rho_i^{(u)}\right). \tag{1}$$

3.2.2. Moderate Functions. In the actual prediction of visual communication design, the predictive results often have a certain gap with the actual identification results, and the reciprocal of the error is used as a standard fitting measurement standard. The adaptation function is as follows:

$$f = \frac{1}{G}. \tag{2}$$

3.2.3. Select Operation. The main basis of this work is the adaptive function. The higher the appropriate value of the individual population, the greater the possibility of being selected. Depending on the appropriateness of the policy, the probability that all individuals are selected is

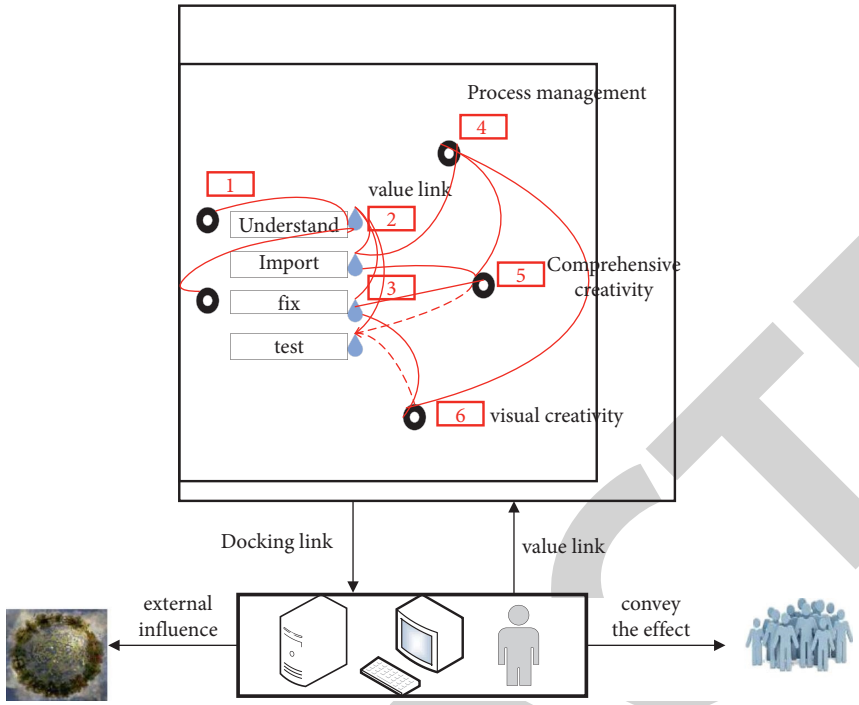

Figure 1: Operating logic map of the link.

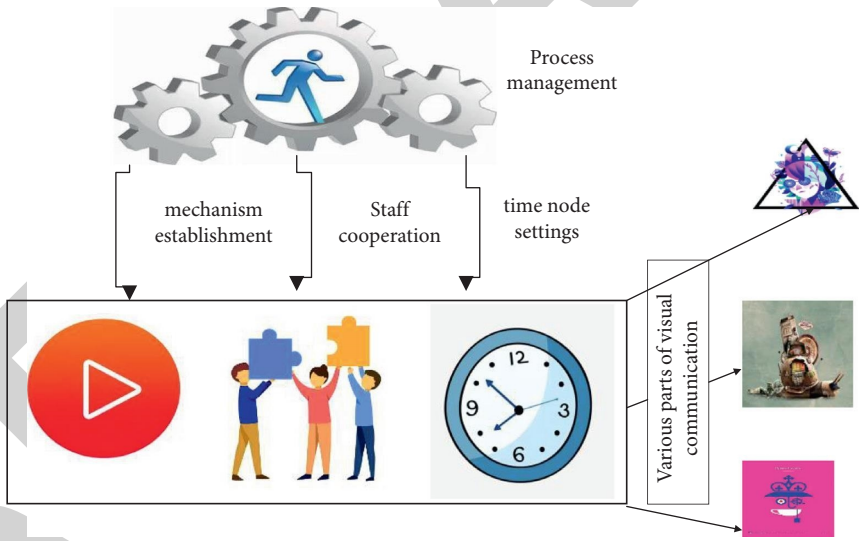

Figure 2: Logical structure diagram of the process control link.

$$f_i = \frac{l}{F_i},$$
$$p_i = \frac{f_i}{\omega_{i=1}^{N} f_i}. \tag{3}$$

3.2.4. Cross Operation. For genetic algorithms, following the theory of populations, cross the population and the best individuals generated by the system, that is, the real cross-specific. No. l chromosome α_l and No. k α_k in the i bits are as follows:

$$\begin{cases} \alpha_{lj} = \alpha_{lj}(1-b) + \alpha_{ij}b, \\ \alpha_{kj} = \alpha_{ij}(1-b) + \alpha_{lj}b. \end{cases} \tag{4}$$

3.2.5. Variation Operation. Species variation is a type of genetic variation, which produces a new population and then produces new individuals. Variation function in the genetic algorithm can divide a population to further expand the search. The function of selecting the individual genes is as follows:

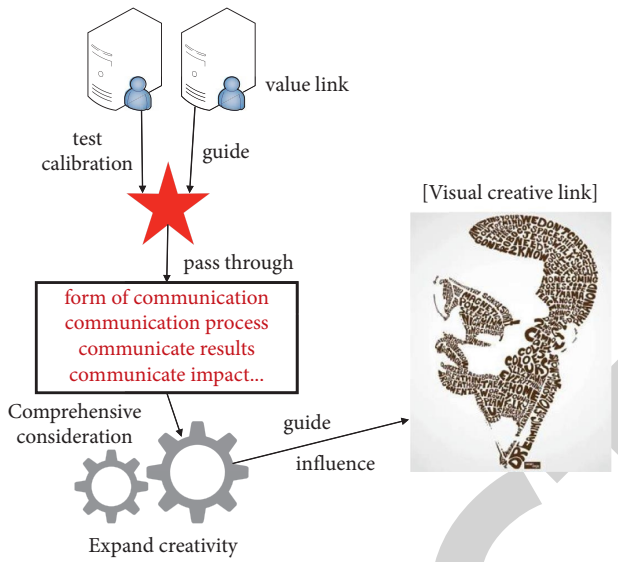

Figure 3: Logical structure diagram of creative integrated links.

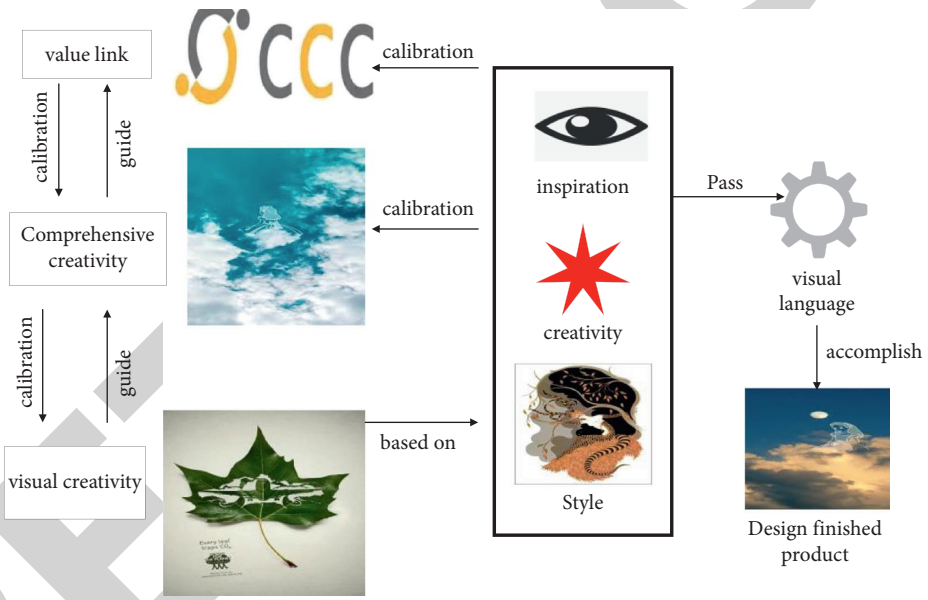

Figure 4: Visual creative link logic structure.

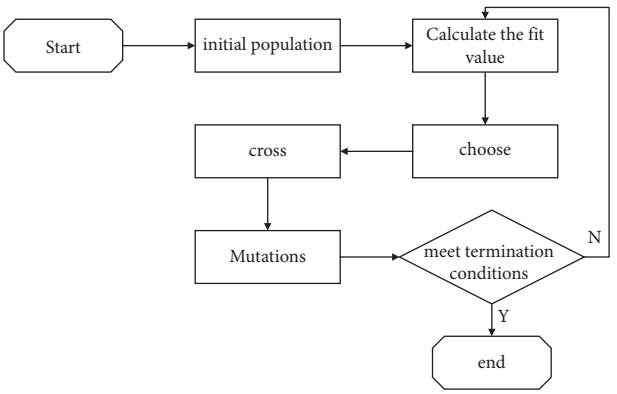

Figure 5: Genetic algorithm flow chart.

$$f(m) = r\left(1 - \frac{m}{M_{\max}}\right)^2,$$

$$\alpha_{ij} = \begin{cases} \alpha_{ij} + \left(\alpha_{ij} - \alpha_{\max}\right) f(m), & r > 0.5, \\ \alpha_{ij} + \left(\alpha_{\min} - \alpha_{ij}\right) f(m), & r \le 0.5, \end{cases} \tag{5}$$

where $\alpha_{\max}$ and $\alpha_{\min}$ represent the upper and lower limit values of α_{ij}, respectively, r is a random number whose value interval is [0,1], g represents the current number of iterations, and $M_{\max}$ represents the upper limit value of the number of evolutions.

3.2.6. Determining the Random Disturbance.

$$\alpha = 1 - \left(\frac{l-1}{l}\right)^m,$$

$$\Omega_k' = (1-\alpha)\Omega^{\Phi} + \alpha\Omega_k. \tag{6}$$

Here, the resulting vector is expressed by the current optimal solution on [0, 1], that is, the optimal chaotic vector. Ω_k represents the chaotic vector obtained by k iteration, Ω_k indicates the corresponding chaotic vector after scrambling, and k represents the number of iterations, where its value is [0, 1]. During the continuous iteration, the maximum value is analyzed, and m is an integer and is determined by the target function.

3.3. MIMO-SCMA System Based on Genetic Algorithm. For the MIMO-SCMA downlink system, after the final receiving antenna receives the signal, the MIMO signal is first detected, and then the next detection result is detected. MIMO detection is used to detect multidimensional signals, so it is very complicated in a single antenna system. In addition, multiple transmit antennas simultaneously increase the channel interference problem of the same channel source transmitted signal to find the difficulty of finding MIMO signals [20].

Suppose that the signal transmitted by the antenna at the base station is shown in Equation (7), and the signal received by the antenna at the user end is shown in Equation (8).

$$x = \left[\left(x^1\right)^T, \left(x^2\right)^T, \ldots, \left(x^{D_B}\right)^T\right] \in C^{N_B K \times 1}, \tag{7}$$

$$y = \left[\left(y^1\right)^T, \left(y^2\right)^T, \ldots, \left(y^{N_M}\right)^T\right] \in C^{N_M^{K \times 1}}. \tag{8}$$

The detection principles of the two types of algorithms are as follows.

3.3.1. ZF Detection. To detect the outgoing signal x from the received signal y, it is necessary to construct a matrix W satisfying WH = 1, where H denotes the channel parameters of the MIMO channel. In ZF detection, the construction matrix is

$$W = \left(H^h H\right)^{-1} H^h. \tag{9}$$

Therefore, the statistics of this detection method are shown in Equation (10), where n denotes the noise of the MIMO channel.

$$\hat{y} = Wy = x + \left(H^h H\right)^{-1} H^h n. \tag{10}$$

3.3.2. MMSE Detection Algorithm. MMSE detection can effectively eliminate the signal interference from other antennas, but it also increases the negative impact on the visual process. Low-Resolution Secondary Error (MMSE) effectively suppresses interference from other antennas while minimizing the effect of interference on detection. The principle is to create a table to minimize the squared error between the resolution and the transmitted signal. The matrix structure of the algorithm is as follows.

The judgment output is estimated as

$$\hat{y} = G_{\mathrm{MMSE}} y = \left(H^h H + \partial^2 I_T\right) H^h y. \tag{11}$$

Then, the mean square error arising from its verdict is

$$\varpi_{\mathrm{MMSE}} = E\left\{(\hat{y} - x)(\hat{y} - x)^h\right\} = \partial^2\left(H^h H + \partial^2 I_T\right)^{-1}. \tag{12}$$

3.4. Real-Time Communication of Image Features Based on Particle Swarm Optimization. Based on the received multiframe image capability, a real-time communication method based on particle font features is used to complete the visual communication of multiframe images [21]. To complete the real-time transmission of multiframe image data, this paper uses the population particle algorithm to compute multiframe image data for real-time target vision communication; the process is as follows.

To understand the distinguishability within each range of the multiframe images, the variance formula of the log-likelihood ratio function corresponding to the premise of the variance equation is

$$\mathfrak{R}_{ik}(P{:}\ e) = K\left[p(l)^2\right] - (H[P(l)])^2. \tag{13}$$

Within the equation, the log-likelihood ratio function is $p(l)$, and the foreground range scale and background range scale of the multiframe image are $K[p(l)^2]$ and $(H[P(l)])^2$, respectively, using a vector to describe the weights N; then,

$$N = [y_1, y_2, y_3]. \tag{14}$$

The multiframe image attributes y_1, y_2, y_3, and M' are the best resolutions of M, which is the best resolution of the individual elements of the larger image extracted using particles. The particle swarm optimization algorithm controls M' by assuming that the particles A,$\{t_1, t_2, \ldots, t_a\}$ and M have the same size points; then, each particle has a solution M. The orientation of each particle in the population determines the relative proportion of the particle eigenvalues. Assuming that the dimension of M is G, the particle size is u',

each particle in the cluster is l $(1 \le l' \le u')$, and the orientation of each particle at the s'th iteration is

$$\alpha_l(c') = \left(\alpha_{l1}, \alpha_{l2}, \ldots, \alpha_{lg}, \ldots, \alpha_{lG}\right). \tag{15}$$

Each particle currently collects the best fitness corresponding to the orientation of the local optimal solution:

$$W_{lr}(c') = \left(w_{l1}, w_{l2}, \ldots, w_{lg}, \ldots, w_{IG}\right). \tag{16}$$

The solution that best reflects the locally optimal solution of the particle fit is the current optimal solution of the particle population Ez. The population adjusts the current velocity and direction of each particle after several iterations, and the expression for the repetition is

$$\begin{aligned} W_{lr}(c'+1) = W_{lr}(c') + x_1 l_1 \left(E_{lr} - \alpha_{lr}(c')\right) \\ + x_2 t_2 \left(E_{lr} - \alpha_{lr}(c')\right), \end{aligned} \tag{17}$$

$$A_{lr}(c'+1) = A_{lr}(c') + W_{lr}(c'+1). \tag{18}$$

In Equations (17) and (18), the learning factor is also a unique random number in the range [0, 1], and the collection rate of each particle in step $c' - 1$ is the collection rate of each particle in step $W_{lr}(c'+1)$. The optimal solution N' sought in this paper is the Ez obtained at the end of the iterative probing of all particles within the population, when each particle orientation does not have any change, and the Ez obtained after the repetitive checking of all particles in the population change to complete the visual communication of the image target features.

4. Experiment of Introducing Genetic Algorithm into Font Design

To verify the effectiveness of the genetic algorithm in font design, this paper compares the evaluation results of different algorithm users. The number of experimental research subjects was set at 300, and 280 valid questionnaires were collected using the questionnaire method. The subjects investigated in this paper are all people who have more daily contact with words, such as students, teachers, and editors, based on their occupation, age, and the time of day they are exposed to the text as the basic information for the study. And Table 1 shows the specific information of the research subjects.

4.1. Experimental Process. Combined with the purpose of this paper's research, the experiment issued questionnaires to people of different occupations, and a total of 300 questionnaires were issued. 80 copies were distributed to students, 72 copies to teachers, 60 copies to editors, 48 copies to designers, and 40 copies to other people. The questionnaires were collected after completion, and a total of 280 valid questionnaires were collected. The relevant questionnaires were completed and collected, and the questionnaire data were used to analyze the font design studied in this paper and draw the corresponding conclusions.

4.2. Experiment Content. The experiments are mainly concerned with the impact of the design of fonts on readers' vision for the genetic algorithm, using different algorithms for the design of fonts, respectively, and transmitting different fonts to the range accessible to readers. Based on readers' feedback on fonts designed by different algorithms and different fonts designed by the same algorithm, readers' recognition and exposure to fonts are derived to compare the advantages of genetic algorithms in font design.

4.3. Experimental Data. In this paper, 300 readers of different occupations were selected and five different algorithms other than the genetic algorithm were used to study the amount of readers' attention to fonts and their satisfaction within 1 minute.

5. Results of Using Genetic Algorithm-Based Font Design

5.1. Amount of User's Attention at the Same Time. To test the effect of visual communication design based on a genetic algorithm on users' attention, an artificial intelligence algorithm and graph theory algorithm were used to compare with a genetic algorithm to test the amount of attention of test users at the same time. The test results are shown in Figure 6.

The results show that, according to Figure 6, the time was set to 0.9 s, 0.8 s, 0.75 s, 0.6 s, 0.45 s, and 0.3, respectively, to test the amount of user attention at the same time with different algorithms. As can be seen from the figure, the survey was conducted on 280 people who had returned the questionnaire, and at different times, the genetic algorithm always had a higher amount of user attention than the other algorithms. For example, at 0.3 seconds, the font designed by the genetic algorithm has 180 users' attention, which is much higher than other algorithms. It can also be concluded that genetic algorithm has a great advantage in the design of fonts.

5.2. Amount of Attention of Users in Different Age Groups Based on Genetic Algorithm. To test the effect of fonts designed based on a genetic algorithm on the amount of attention of readers in different age groups, people aged 18–25, 26–30, 35–40, and 45–50 years old were selected from 300 people. The test results are shown in Figure 7.

The results show that the font designed based on the genetic algorithm has the highest attention level among those aged 18–25 years old, followed by those aged 26–30 years old, and gradually increases with increasing time; the attention level of all different age groups basically reached the highest at 60 s. It can be concluded that the font designed by the genetic algorithm is more popular among young people.

5.3. The Attention of Users to Design Font Type under Different Algorithms. For the attention of users caused by different algorithms on font type design, five different algorithms

Table 1: Specific information on the study population.

Profession	Number of people	Average age/year	Time to touch text/hour
Student	80	21.16	10
Teacher	72	35.3	8
Editor	60	28.69	14
Designer	48	35.16	12
Others	40	32.6	6

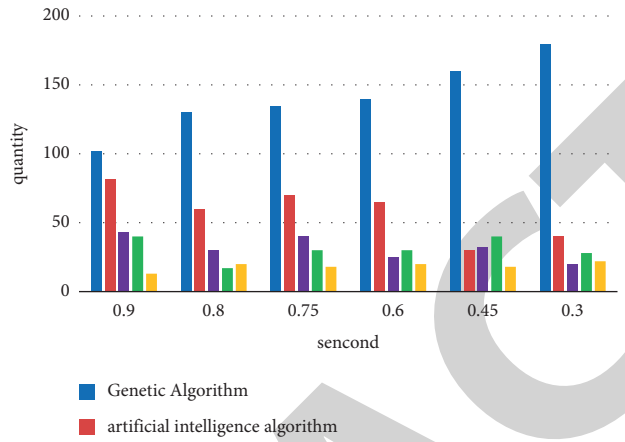

Figure 6: Amount of attention of users at the same time.

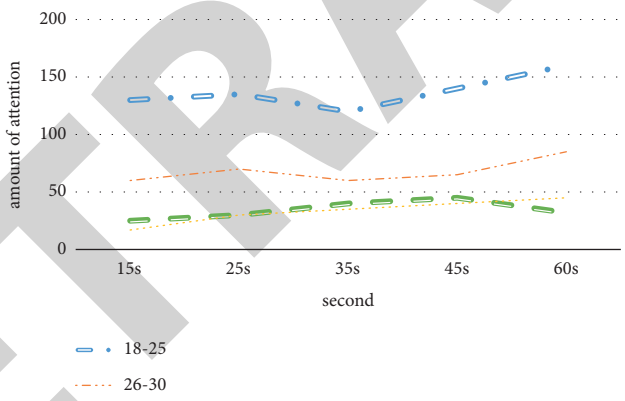

Figure 7: The amount of attention of users in different age groups.

were used to test seven different types of designed fonts, and the test results are shown in Figure 8.

The results show that the amount of user attention to font type design according to different algorithms is tested in this paper for bold advertising fonts, English, etc., respectively. According to Figure 8, no matter which algorithm designs the font type, the attention of genetic algorithm designing fonts is higher than other algorithms, among which users pay the highest attention to advertising fonts. Based on the graphical analysis, the font type designed by the genetic algorithm better caters to the needs of the reader.

The results show that the overall user satisfaction score of different algorithms is 10. As shown in Figure 9, the average user satisfaction of genetic algorithm-based font design is 8.16, the satisfaction of artificial intelligence algorithm is 7.66, and the other algorithms had a satisfaction rate of 6.732, 7, and 6.754. The comparison shows that the fonts designed by the visual communication system based on the genetic algorithm are more satisfactory. Compared with the fonts designed by other algorithms, users' satisfaction with the fonts designed by the genetic algorithm increased by 6.52%.

6. Discussion

In this paper, the visual communication system is improved based on the genetic algorithm, and the problems that need attention in the system and the main construction methods are introduced. After the system was constructed, experimental tests of the genetic algorithm-based system were conducted to evaluate the practicality and effectiveness of the system, which further pointed out the direction for the optimization of the system. At the same time, the particle swarm algorithm in image transmission was used to beautify

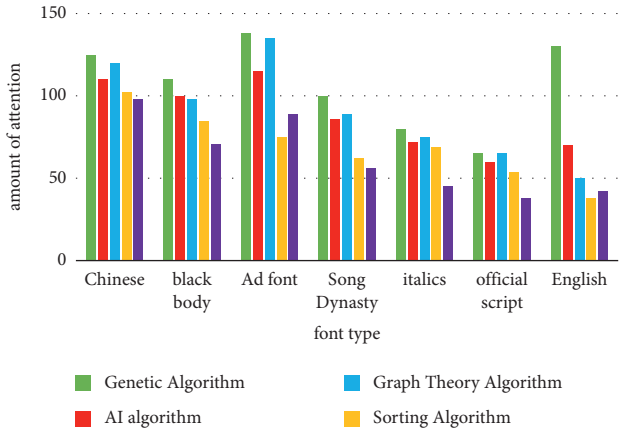

Figure 8: User attention to design font types.

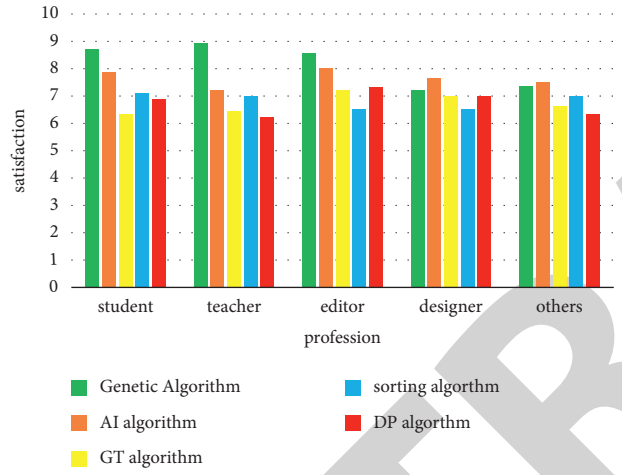

Figure 9: User satisfaction test chart.

the fonts in images, so that users can get visual enjoyment when reading the paper version of the reading materials and have fun in learning, which also lays the foundation for further development of the fonts.

7. Conclusions

This paper analyzed and composed the creative logic of visual communication based on a genetic algorithm, marked an outlook on its future development in the context of the current big data era, and drew the following research conclusions.

First, visual communication is an integrated design process that evolves with the business era and expands and updates as the business community changes. During this long process of development, certain patterns existed and changed over time between the internal links and multiple links of the visual communication process.

Secondly, the logical rules between links in the process of visual communication are a combination of sensibility and rationality and are based on the understanding and analysis of the goal of the work. The artistic inspiration and logical rigor of the visual communication process work at high speed in a seemingly chaotic but regular manner.

Thirdly, by comparing the internal links and internal logical relationships within visual communication, the whole process of visual communication can be made more clear. At the same time, research and exploration based on the concept of visual communication can complete the creative process more efficiently and accurately, thus making the final visual communication result more valuable.

Fourth, the field of visual communication can find the combination of its own logic and analysis with genetic algorithms, and then, it used big data thinking and related technology to optimize the internal aspects of visual communication and ultimately makes the value of visual communication on the existing basis to form a qualitative leap.

Data Availability

Data sharing is not applicable to this article as no datasets were generated or analyzed during the current study.

Conflicts of Interest

The authors declare that they have no conflicts of interest.

References

[1] J. Wenskovitch, I. Crandell, and N. Ramakrishnan, "Towards a systematic combination of dimension reduction and clustering in visual analytics," *IEEE Transactions on Visualization and Computer Graphics*, IEEE, no. 99, , p. 1, New York, NY, USA, 2017.

[2] C. H. Chun, "An analysis of change in Korean newspaper advertisement designs in the time of enlightenment(1876-1910)," *Archives of Design Research*, vol. 31, no. 1, pp. 211–223, 2018.

[3] S. Zhou, H. Ma, B. Gao et al., "Characterization of a novel disease-causing mutation in exon 1 of SH2D1A gene through amplicon sequencing: a case report on HLH," *BMC Medical Genetics*, vol. 18, no. 1, p. 15, 2017.

[4] G. Devornique, J. Fontchastagner, D. Netter, and N. Takorabet, "Three dimensional pole shape optimization of claw pole machines based on a hybrid model," *International Journal of Applied Electromagnetics and Mechanics*, vol. 57, no. 7, pp. 73–81, 2018.

[5] B. M. Mercado-Borrayo, R. Contreras, and A. Sánchez, "Optimisation of the removal conditions for heavy metals from water: a comparison between steel furnace slag and CeO2 nanoparticles," *Arabian Journal of Chemistry*, vol. 13, no. 1, pp. 1712–1719, 2018.

[6] Z. Xie, H. Fujioka, A. Hidaka, and H. Kano, "Modeling and manipulating dynamic font-based hairy brush characters using control-theoretic *B*-spline approach," *IFAC-PapersOnLine*, vol. 53, no. 2, pp. 4731–4736, 2020.

[7] F. Wang, "Comparative study on the effects of economic development on advertising between south Korea and China," *Korea Science & Art Forum*, vol. 32, pp. 169–182, 2018.

[8] H. Dawid and M. Kopel, "On economic applications of the genetic algorithm: a model of the cobweb type," *Journal of Evolutionary Economics*, vol. 8, no. 3, pp. 297–315, 2019.

[9] A. Volkanovski, B. Mavko, T. Boševski, A. Causevski, and M. Cepin, "Genetic algorithm optimisation of the maintenance scheduling of generating units in a power system," *Reliability Engineering & System Safety*, vol. 93, no. 6, pp. 779–789, 2008.

Hindawi
Emergency Medicine International
Volume 2023, Article ID 9862919, 1 page
https://doi.org/10.1155/2023/9862919

Retraction

Retracted: The Effect of Comprehensive Rehabilitation Nursing on the Rehabilitation of Sports-Induced Ankle Joint Injuries

Emergency Medicine International

Received 8 August 2023; Accepted 8 August 2023; Published 9 August 2023

This article has been retracted by Hindawi following an investigation undertaken by the publisher [1]. This investigation has uncovered evidence of one or more of the following indicators of systematic manipulation of the publication process:

(1) Discrepancies in scope
(2) Discrepancies in the description of the research reported
(3) Discrepancies between the availability of data and the research described
(4) Inappropriate citations
(5) Incoherent, meaningless and/or irrelevant content included in the article
(6) Peer-review manipulation

The presence of these indicators undermines our confidence in the integrity of the article's content and we cannot, therefore, vouch for its reliability. Please note that this notice is intended solely to alert readers that the content of this article is unreliable. We have not investigated whether authors were aware of or involved in the systematic manipulation of the publication process.

Wiley and Hindawi regrets that the usual quality checks did not identify these issues before publication and have since put additional measures in place to safeguard research integrity.

We wish to credit our own Research Integrity and Research Publishing teams and anonymous and named external researchers and research integrity experts for contributing to this investigation.

The corresponding author, as the representative of all authors, has been given the opportunity to register their agreement or disagreement to this retraction. We have kept a record of any response received.

References

[1] Y. Qiao, B. Zhang, and L. Zhang, "The Effect of Comprehensive Rehabilitation Nursing on the Rehabilitation of Sports-Induced Ankle Joint Injuries," *Emergency Medicine International*, vol. 2022, Article ID 4004965, 12 pages, 2022.

Hindawi
Emergency Medicine International
Volume 2022, Article ID 4004965, 12 pages
https://doi.org/10.1155/2022/4004965

Research Article

The Effect of Comprehensive Rehabilitation Nursing on the Rehabilitation of Sports-Induced Ankle Joint Injuries

Yu Qiao,[1] Bin Zhang,[2] and Lei Zhang[3]

[1]*Angeles University Foundation, Angeles City, Pampanga, Philippines*
[2]*Anhui Normal University, Wuhu 241000, Anhui, China*
[3]*Anhui Wannan Medical College, Wuhu 241000, Anhui, China*

Correspondence should be addressed to Lei Zhang; zhanglei@wnmc.edu.cn

Received 30 March 2022; Revised 25 April 2022; Accepted 5 May 2022; Published 24 May 2022

Academic Editor: Hang Chen

The purpose of participating in sports is to enhance physical fitness and promote physical and mental health. The occurrence of sports injuries will cause physical and mental injuries to athletes, especially the ankle joint injuries that often occur. Therefore, it is particularly important to understand the causes, symptoms, treatment, and prevention of athletes' ankle injuries. This article aims at studying the significance of comprehensive rehabilitation nursing for the rehabilitation of sports-induced ankle joint injuries and introduces the concepts of comprehensive rehabilitation nursing and ankle joint injuries. This article proposes how to use comprehensive rehabilitation nursing to recover ankle injuries caused by sports based on smart medical care. In the experiment of this article, it can be seen from Table 5 that the recovery speed of 5 athletes with ankle joint injuries before rehabilitation training was 8% (lowest) and 14% (highest). The recovery rate after rehabilitation care is up to 25%. It can be seen that comprehensive rehabilitation care is of great help to athletes with ankle injuries. As can be seen from Table 4, the number of ankle injuries in acute secondary injuries is 25, accounting for 33%, which is the highest; the number of contusions is 15, accounting for 21%, which is the lowest ratio, so it can be seen that the ankle joint injury in sports is the most serious. Therefore, the application of comprehensive rehabilitation care needs to be popularized, which is of great significance to ankle joint injuries. The ankle joint is one of the most easily sprained joints in the human body, not only because of the flexibility of the ankle joint, but also because of the anatomical characteristics of the ankle joint. The main cause of ankle injuries is inappropriate behavior in sports.

1. Introduction

Ankle joint injuries mainly include fractures of the ankle joint and damage to the surrounding ligaments. This is a relatively common sports injury. If an ankle joint injury occurs without timely and effective treatment or without thorough treatment, it will be easier to cause repeated attacks in the future, and it is not easy to recover. With the development of the national economy, the advancement of modern science, and technology and the improvement of people's living standards, the importance of rehabilitation medicine is increasingly recognized by people. Even in some foreign countries with advanced science, rehabilitation medicine is a relatively new discipline, and rehabilitation nursing must gradually form an independent system from nursing and become a new field of nursing [1].

The ankle joint injuries of students majoring in physical education are increasing year by year during the learning process. More and more educators are beginning to pay attention to ankle injuries and rehabilitation training after injuries. Improving students' awareness of their own protection is the main purpose. Due to the structure of the human body and the physiological characteristics of the ankle joint, students will suffer more injuries during the learning process. Making a reasonable and effective rehabilitation plan based on injury symptoms is a method of rehabilitation, and how to deal with ankle joint injuries is a problem that needs to be solved urgently.

Over the years, with the development of social economy and the change of cultural structure, the country has paid more and more attention to sports. Kai found that ankle ligament injuries often occur in sports, and the most common injuries include hands and feet. In general, conservative treatment is the first choice of treatment. The increasing severity of athletes' long-term injuries and the associated expensive treatment costs indicate that ankle joint injuries should not be underestimated. The scholar argued that ankle joint injuries should not be ignored, but there is a lack of data and authenticity [2]. Besting A found that due to supplier independence, new Internet service-oriented points of care and surgical equipment are the basis for improved operations. In order to improve efficiency, people should actively develop new methods. In this work, scholars discuss how to deal with these challenges and develop a descriptive model to determine key strategies. But the experiment did not mention what the new method is, and the concept is too vague [3]. Lacey and Donne found that ankle joint injuries not only lead to the destruction of static and dynamic balance, but also result in wasting a lot of exercise time, affecting athletes' daily activities, and may put athletes at greater risk of injury. Therefore, in order to identify athletes at risk of ankle injury, accurate and reliable balance assessment tools are needed. The balance test they proposed has strong reliability. The disadvantage of this experiment is that there is no experiment on the balance of the method, so the reliability cannot be confirmed [4]. Acosta-Olivo et al. found that overweight can also cause some injuries during sports. The purpose of his research is to assess whether there is a link between acute ankle injury and body mass index. But through experiments, they finally found that obesity is not a factor that affects ankle joint injury, and age is the key determinant of ankle joint injury. The disadvantage of this experiment is that it directly draws a conclusion. There is no object reference and process for the experiment, which makes the experiment very incomplete [5]. Lo et al. found that the mobile medical information system has a great impact on the traditional hospital information system, and the dynamic resource allocation table is very important for optimizing the performance of the mobile system. He designed an intelligent dynamic resource allocation model, using algorithms and cumulative allocation to optimize the resource allocation weights of the five main attributes in the cooperative communication system. Finally, it is found that the designed model can improve the efficiency of the medical system. This method does not propose what the specific model is and how the model is designed [6]. Ghoneim et al. found that with the invention of new communication technologies, artificial intelligence provides new functions and facilities for the smart medical framework. These functions and facilities are designed to provide customers with seamless, easy-to-use, accurate, and real-time healthcare services. Since health is a sensitive issue, it should be treated with the utmost safety and caution. The experiment did not compare artificial intelligence with traditional methods and did not compare the advantages of artificial intelligence [7]. Rana and Mishra found that the smart health medical system can not only improve the quality of medical services, but also improve the security of the system. The original system will have the problem of data insecurity and privacy insecurity in the smart health system. In order to overcome security and privacy risks, they designed effective access control for medical services. However, the program has not been proven, and no effective experiments are provided to solve [8]. Tian et al. found that with the development of information technology, smart medical care makes medical treatment more efficient, more convenient, and more personalized. In order to introduce the concept of smart medicine, Tian et al. first introduced the current situation of smart medicine in several important areas. Finally, they look to the future and evaluate the future prospects of smart medicine. Although they saw the advantages of artificial intelligence, they did not see the shortcomings of artificial intelligence and did not consider the pros and cons between the two [9]. Through the experimental analysis of scholars, we can see that as the field of sports expands, more and more people love sports. However, due to many factors, more and more people are causing ankle injuries. So scholars have conducted experiments on ankle joint injuries.

The innovations of this article are as follows: (1) introduced the relevant theoretical knowledge of smart medical treatment and ankle joint injury, and used data mining to analyze how comprehensive rehabilitation care plays a role in the rehabilitation of ankle joint injury, and (2) analyzed the data fusion, and conducted experiments and analysis on the injury factors and preventive measures of the ankle joint. Through experiments, it has been found that the proportion of ankle joint injuries has increased in recent years. There are many factors affecting the ankle joint. How to prevent ankle joints and use comprehensive rehabilitation care to recover ankle joint injuries is of great significance.

2. Data Mining Method and Multisource Data Fusion Algorithm Based on Smart Medical Care

Smart healthcare is a new term in medical care. By building a regional medical information platform for health records and using the most advanced Internet of Things technology, the interaction between patients and medical personnel, medical institutions, and medical equipment can be realized gradually, and information is gradually achieved [10, 11]. Ankle injuries are the most common sports injuries. It is mainly caused by the changes in the force acting position, direction, size, and other factors, as well as the different movement status of the lower limbs [12]. The degree of injury and the shape of the ankle joint are different, so the mechanism of the ankle joint injury is extremely complex and diverse.

The human body model uses high-resolution CT scanning to digitize the anatomical structure of the human body and is divided into fine finite element meshes to accurately simulate the geometric structure of the human body. The model reflects the anatomical characteristics of each organ. It can simulate damage at the tissue level by inputting the data of the physical material properties of organs and tissues reported in the latest research [13]. Simulated ankle injury is shown in Figure 1.

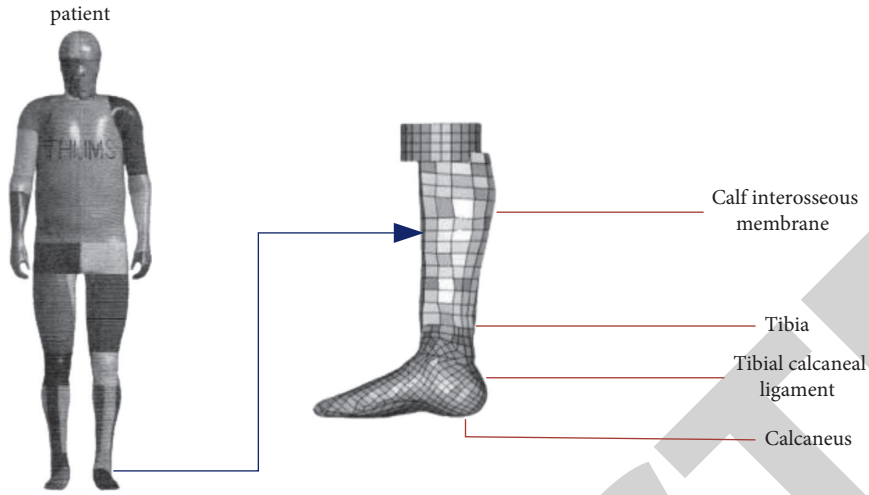

Figure 1: Simulated ankle injury.

As shown in Figure 1, the reasons for ankle joint injury during exercise are not being prepared for exercise before exercise, the muscles and ligaments of the ankle not being open, and the elasticity and stretchability of the joint ligaments being poor and not able to adapt to the needs of strenuous exercise [14].

2.1. Multisource Data Fusion Based on Smart Medical Care. The configuration of multisensor systems in medical care provides necessary conditions for the application of multisource data fusion. Multisource data fusion technology can realize applications such as behavior monitoring based on motion information and medical diagnosis based on physiological information by using the information collected by multisource sensors in smart medical care [15, 16]. Data-level fusion, also called pixel-level fusion, is a low-level fusion. After collecting the data, the sensor only performs simple processing or starts data fusion without processing. On the basis of the fusion, the characteristic information is extracted to obtain the final result. Data-level fusion generally requires the data collected by the sensor to be the same physical quantity. This level of fusion retains as much information as possible during the calculation process, and the fusion accuracy is the highest, but it is also accompanied by a large amount of calculation and a slow calculation speed [17].

The level of multisource data fusion is different, and the algorithms used are also quite different. Methods such as weighted average Kalman filtering are generally applied to low-level fusion. In high-level fusion, methods such as evidence theory, neural networks, and Bayesian inference are often used. Different levels of integration have their own advantages and disadvantages, and should be applied according to specific requirements. Choose an appropriate method to process the data at a specific level to achieve the best results [18]. The structure of multisource data fusion is shown in Figure 2.

As shown in Figure 2, according to the actual situation and application requirements of the obtained data, a certain degree of preprocessing is carried out on the data. Including inconsistency elimination, filling in missing data, and data

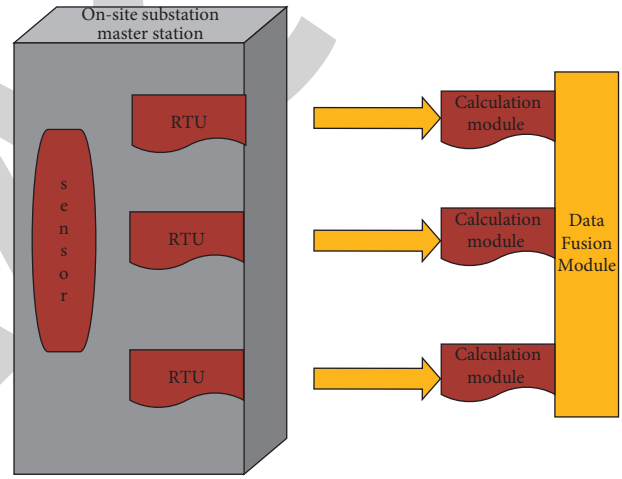

Figure 2: The structure of multisource data fusion.

standardization operations, the preprocessed data have higher quality [19]. Although the DS evidence theory can effectively deal with uncertain information, in the case of highly conflicting evidence, the classical DS evidence combination rules often produce unreasonable fusion results due to the normalization process. For this reason, many scholars have proposed many differences. Based on the modified method, the evidence distance is introduced, and the feature extraction of the evidence source is carried out, and the corresponding improvement scheme is put forward. The theoretical analysis and numerical experimental results show that the improved method can not only fully reflect the corresponding improvement ideas, but also can better realize the evidence combination, converge the real target faster, and get a reasonable fusion result.

Fusion computing is the use of one or more multisource data fusion algorithms to complete the fusion processing of feature data. Feature extraction and fusion calculation are the core of the entire fusion process. According to the data obtained by the fusion calculation, through certain decision rules, the final decision result is obtained for output. infusion computing is shown in Figure 3.

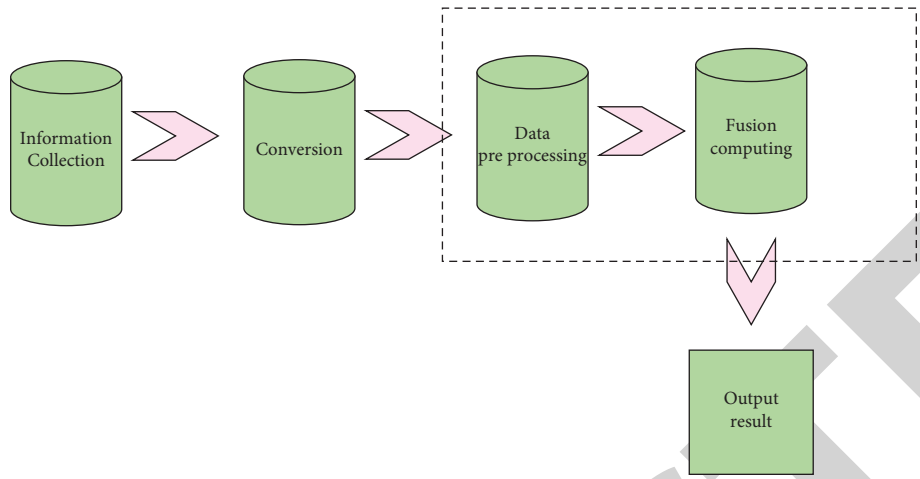

Figure 3: Fusion computing.

As shown in Figure 3, for data-level fusion with a lower fusion level, in order to retain more detailed information of the original data, there is often no data preprocessing link. In data processing, first go through fusion calculation and then extract features on the basis of the fusion result to obtain the final result [20].

2.1.1. Evidence Theory. Based on the historical data provided by the smart medical database and the rule method provided by the knowledge base, the system determines to adopt the membership function to obtain the initial credibility of the evidence theory. Membership function, also known as the membership function or fuzzy meta-function, is a function that will be used in fuzzy sets and is a generalization of indicator functions in general sets. An indicator function can tell whether an element in a collection belongs to a particular subcollection. The basic reliability distribution of the data to be tested in different physical states is given as

$$A_i = \frac{1}{e^{(u/\sigma^2)}}, \quad u = 1, 2, 3, \tag{1}$$

where $e^{(u/\sigma^2)}$ and A_i correspond to the historical data about body temperature provided by the database in the u-th physical sign state.

Through the combination of the evidence theory, the evidence is merged, and the reliability matrix H is obtained as

$$H = (H_A, H_B, H_C). \tag{2}$$

Evidence theory is widely used to solve uncertain reasoning problems, and it is an important data processing method for multisource data fusion. For an evidence theory problem model, all possible results are included in the identification framework Θ. The evidence theory uses sets to represent propositions, and Θ represents the set containing all the results of a problem. That is, $\Theta = \{\theta_1, \theta_2, \ldots, \theta_n\}$, where θ_n is called an element in the recognition frame, and different elements are mutually exclusive [21].

The reliability function is the main mathematical tool to describe the subjective uncertain phenomenon. The main difference between the reliability function and the probability function is that it does not satisfy the additivity. More importantly, there is Dempster's rule in the theory of reliability function, which can be used to combine two independent reliability functions into a comprehensive reliability function. The basic reliability function is used to express the degree of people's trust in the evidence. Suppose the recognition framework is Θ, and the basic reliability function is

$$\begin{cases} m(\varphi) = 0, \\ \sum\limits_{A \subseteq 2^{\Theta}} m(A) = 1, \end{cases} \tag{3}$$

where $m(\varphi) = 0$ means that the empty set does not have any reliability. For any subset A, as long as it satisfies $m(\varphi) > 0$, A is called a focal element.

How to merge the evidence is the key of the evidence theory algorithm, and this method is also called the D-S synthesis rule. Assuming that m_1 and m_2 are the basic reliability functions in the recognition framework Θ, the D-S synthesis rule is

$$m(A) = \frac{1}{1-k} \sum_{a \cap b} m_1(A_i) m_2(B_J), \tag{4}$$

where $m_2(B_J)$ is the conflict coefficient, and its size is between 0 and 1, indicating the degree of conflict between evidence. The larger the K, the higher the degree of conflict between the evidence.

Evidence theory can effectively distinguish "unknown" and "uncertain" information. And compared with the Bayesian theory in the probability theory, the evidence theory does not need to obtain conditions such as prior probability and conditional probability density, and has obvious advantages in dealing with uncertainty problems [22].

2.1.2. Improved Evidence Theory. Because the prior data required in the theory of evidence are more intuitive and easier to obtain than those in the theory of probabilistic

reasoning, with its own advantages, the evidence theory has played a huge role in solving related problems of uncertain reasoning and has become a basic algorithm in the field of data fusion [23]. However, its theory also has some problems, such as strict requirements on combination conditions, and each piece of evidence must be independent of each other.

Some scholars start by modifying the initial evidence reliability model, averaging the basic reliability values of different evidences, and then synthesize them with the D-S synthesis formula. The method of obtaining new evidence is

$$m(A) = \frac{1}{n}\left(m_1(A_i) + m_2(A_i) + \cdots + m_n(A_i)\right). \quad (5)$$

In order to describe and evaluate the relationship between evidences in multiple dimensions, some research scholars calculate the degree of similarity between evidences by designing functions and put forward the concept of evidence distance. Generally speaking, the greater the degree of similarity between $m_n(A_i)$ evidence, the smaller the distance of evidence. On the contrary, the smaller the degree of similarity between two pieces of evidence, the greater the distance between the evidence.

Assuming that m_1 and m_2 are the basic reliability functions of the evidence, the evidence distance between the evidences can be expressed as

$$d_{ij} = \sqrt{\frac{1}{2}\left(\|m_i\|^2 + \|m_j\|^2 - 2\langle m_i, m_j\rangle\right)}. \quad (6)$$

It is difficult to obtain the basic reliability function, and there is no unified solution in actual application. When the amount of evidence increases, the calculation of evidence theory may explode exponentially. The most prominent one is the failure of fusion when the evidence theory synthesizes conflicting evidence. The improved evidence algorithm effectively solves this problem [24].

2.2. Support Vector Machine Algorithm. Support vector machine, also known as "support vector network," is a discriminative machine learning classification algorithm. It uses decision boundaries (hyperplanes in this case) to separate data points into two classes at a time. Support vector machine (SVM) classification is based on the principle of structural risk minimization. Seek an optimal hyperplane, which maximizes the blank area on both sides of the hyperplane while ensuring the classification accuracy of the training samples [25]. For the linear case, support vector machine is shown in Figure 4.

As shown in Figure 4, straight line D is a dividing line with w as the normal vector, which can divide the two types of data as accurately as possible. $D2$ is the support vector point in the two types of samples and is a straight line parallel to the classification line. When D is in the middle, the straight line satisfies the principle of maximizing the interval between the two types of sample points and becomes the optimal dividing line, which is transformed into the problem of finding the normal vector w. Extending to a high-dimensional space, the optimal classification line

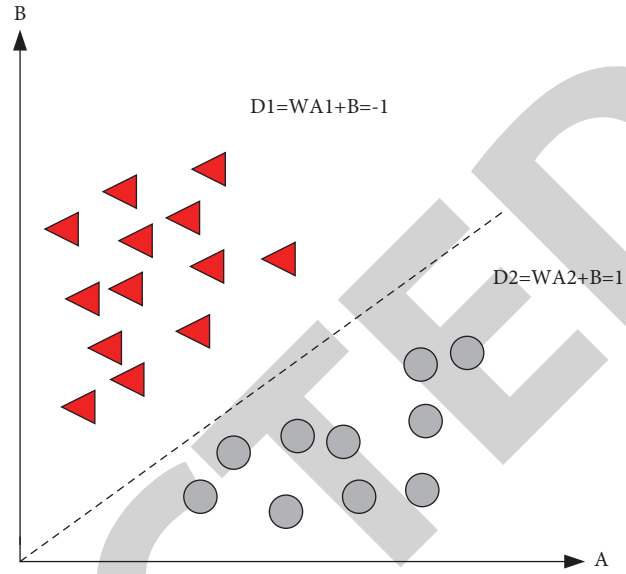

Figure 4: Support vector machine.

becomes the optimal hyperplane, that is, finding the normal vector of the optimal classification hyperplane, and classifying multiclass samples by finding the distance [26].

Taking the two-classification problem as an example, given the training sample set (a_i, b_i) of two types of data. In order to enable the hyperplane to correctly classify the two types of samples and to make the classification interval as large as possible, the hyperplane must satisfy

$$w \cdot a_i + b \geq 1. \quad (7)$$

Then, the classification interval can be expressed as

$$\min \Phi(w) = \frac{1}{2}\|w\|^2 = \frac{1}{2}\left(w^t \cdot w\right). \quad (8)$$

When there is a linear inseparable pattern, the optimal segmentation hyperplane is required to meet the principle of minimum average classification error probability for all training samples. At this time, only the constraint condition of equation (8) is relaxed; that is, a slack variable $\xi_i \geq 0$ is introduced, and then equation (8) becomes

$$b_i\left(w \cdot a_i + b\right) \geq 1 - \xi_i, \quad i = 1, 2, \ldots, n. \quad (9)$$

This is to introduce a cost function into the objective function; that is, add a penalty component with an adjustable factor C to the function. So the objective function is

$$\min \Phi(w) = \frac{1}{2}\|w\|^2 + c\sum_{i=1}^{n}\xi_i = \frac{1}{2}\left(w^t \cdot w\right) + c\sum_{i=1}^{n}\xi_i, \quad (10)$$

where c is the penalty factor, which controls the degree of punishment for the wrong sample. The larger the c, the heavier the penalty for the error. In order to solve this constrained optimal problem, the Lagrange function is introduced. For the following equation,

$$L(w, x, y) = \frac{1}{2}\|w\|^2 + c\sum_{i=1}^{n}\xi_i - \sum_{i=1}^{n}x_i\left(y_i\left(w \cdot x_i + y\right) - 1\right). \quad (11)$$

The Lagrangian function is only the function of conservative force in the mechanical system, and it is a function that describes the dynamic state of the whole physical system. Defined in analytical mechanics, the Lagrangian function of a dynamical system is a function that describes the dynamical state of the entire physical system. In the formula, $x_i \geq 0$ is called the Lagrange (Lagrange) factor. The solution of the constrained optimization problem is determined by the saddle point of the Lagrange function. The solution of the optimization problem satisfies the partial derivative of w and y to be 0 at the saddle point. By seeking the partial derivative, the above problem is transformed into a simple dual problem, which is

$$\min \frac{1}{2} \sum_{j=1}^{n} \sum_{j=1}^{n} \alpha_i \alpha_j y_i y_j - \sum_{i=1}^{n} \alpha_i. \tag{12}$$

For nonlinear classification problems, the sample can be projected to a high-dimensional space through an unknown mapping. The kernel function is the support vector machine that maps the input space to the high-dimensional feature space through a nonlinear transformation. The dimensionality of the feature space can be very high. If the solution of the support vector machine only uses the inner product operation, and there is a function in the low-dimensional input space, it is exactly equal to the inner product in the high-dimensional space. This mapping can be solved by using a kernel function. All functions that satisfy Mercer's theorem can be used as kernel functions, so that support vector machines can solve nonlinear problems in linear mode [27]. By constructing the optimization problem, only the inner product between samples appears in the solution process and in the final model. Therefore, when modeling nonlinear models, first defining the kernel function can solve the problem of unknown high-dimensional space mapping [28].

The kernel function method performs nonlinear classification, and the computational complexity of the algorithm itself does not increase. At this time, the dual problem can be expressed as

$$\sum_{i=1}^{n} \alpha_i b_i = 0, \tag{13}$$

where α_i is the Lagrangian factor and b_i is the number of support vectors.

It can be seen from equation (13) that for two classification problems, the algorithm seeks two hyperplanes, and each hyperplane corresponds to a class of samples. In the classification test, the distance between the data and the hyperplane is calculated, and the sample is classified into the category represented by the closer plane. In other words, Gemini Support Vector Machine contains one-to-two planning problems, each object function corresponds to one type of sample, and the constraint conditions are determined by the characteristics of another type of sample [29].

2.3. Taxonomy Based on Data Mining. Data mining refers to the process of searching for information hidden in a large amount of data through algorithms [30–32]. Data mining is usually related to computer science and achieves the above goals through a number of methods such as statistics, online analytical processing, intelligence retrieval, machine learning, expert systems, and pattern recognition. Classification plays an extremely important role in the field of data mining, analyzing data to extract data class models. This described model is called a classifier, which is specifically used to predict the class of data classification and give a unique class identification number. Classification technology can distinguish categories from samples of unknown categories, so as to provide a powerful reference for decision-making. Therefore, classification technology is widely used in systems with diagnostic and rating functions.

Suppose S is a set of data samples, the capacity is set to a, m different types of C, a_i is the number of samples of C_i, P_i is the probability of any sample belonging to C_i, and then, the entropy required for the classification of a given sample is

$$\text{Entropy}(a_1, a_2, \ldots, a_m) = -\sum_{i=1}^{m} p_i \log_2(p_i). \tag{14}$$

Suppose the value set of noncategory attribute A is $(a_{ij}, \ldots, a_{mj})$, divide A into v subsets $(a_1, \ldots, a_N)$, where a_j is the sample on A and a_{ij} is the number of samples of C_i in a_j, and the entropy is

$$\text{Entropy}(\text{A}) = -\sum_{i=1}^{m} \frac{a_{1j} + \cdots + a_{mj}}{a} \text{Entropy}\left(a_{ij}, \ldots, a_{mj}\right). \tag{15}$$

The information gain ratio is defined as

$$\text{Gainratio}(A, B) = \frac{\text{Gain}(A, B)}{\text{Split information}(A, B)}, \tag{16}$$

where $\text{Gainratio}(A, B)$ is the information gain, defined as

$$\text{Gainratio}(A, B) = \text{Entropy}(a_1, a_2, \ldots, a_m) - \text{Entropy}(A). \tag{17}$$

$\text{Split information}(A, B)$ is the split information, which indicates the uniformity of the attribute split data, which is

$$\text{Split information}(A, B) = -\sum_{I=1}^{C} \frac{|A_1|}{|A|} \log_2 \frac{|A_i|}{|A|}. \tag{18}$$

It is used to evaluate whether a classification model prediction is accurate, and the most recognized index by the industry is to consider the recall rate and the correct rate. The ratio of the number of correctly classified positives to the actual total number of positives is called the recall rate, which is

$$\text{Recall} = \frac{\text{TP}}{P}. \tag{19}$$

Recall is used to evaluate the reliability of the constructed classification model for the prediction of positive cases. In fact, in data research conducted in most engineering application environments, the attention paid to the positive target is far greater than the negative, so the recall rate is generally used as the most important indicator to measure

the performance of the classifier. In addition, it is more intuitive that the concept of correct rate Accuracy is

$$\text{Accuracy} = \frac{(\text{TP} + \text{TN})}{C}, \tag{20}$$

where TP stands for true positive and TN stands for true negative.

In order to fully illustrate the advantages of the improved algorithm compared to other classification algorithms, the recall rate is used to conduct experimental comparisons under different scale datasets to verify the improved effect. Improved algorithm under different dataset sizes is Figure 5:

The recall rate is for the original sample, which indicates how many positive examples in the sample are predicted correctly. As shown in Figure 5, it can be seen that the improved classification algorithm has a higher recall rate regardless of whether it is under the small-scale dataset or under the condition of big data. When the dataset size is below 1300, the advantage is not big, but when the dataset size reaches 1400, it has obvious advantages, and the gap is very obvious under the data level after 1700. Combining with the foregoing, the improved algorithm is very suitable for the medical intelligent diagnosis and classification business in the era of big data.

3. Investigation, Experiment, and Analysis of Factors and Measures for Athletes with Ankle Joint Injuries

3.1. Investigation and Analysis of Factors and Types of Ankle Injuries. Ankle injury is the most common sports injury in sports. Athletes' own technology, quality, self-defense awareness, etc. will cause varying degrees of injury and will inevitably cause mild or severe sports injuries. This not only damages the health and athletic ability of the enthusiasts, but also has a negative impact on daily life, study, and physical exercise. This will bring various psychological barriers to the athletes and affect their enthusiasm for participating in sports training.

In this article, the injury site is divided into the lateral malleolus, medial malleolus, ankle heel, and foot on the side of the dominant foot and the nondominant foot side according to the original location of the pain. Types of injuries on the side of the dominant foot are shown in Tables 1 and 2.

From the comparison of Tables 1 and 2, it can be seen that athletes' feet injured mainly include the outer ankle, the inner ankle, the heel, and the ankle heel. The number of ligament strains on the dominant foot of athletes is the largest, with 105, and the number of ligament strains on the nondominant foot is 87. This shows that the athlete's dominant foot is more likely to be injured than the nondominant foot.

This article investigates the proportion of athletes' ankle injuries in 2019 and 2020, as shown in Figure 6.

The percentage of athletes with ankle injuries in 2019 started at about 10%. Although it declined later, it has been on an upward trend, rising to about 25%; the percentage in

Figure 5: Improved algorithm under different data set sizes.

Table 1: Types of injuries on the side of the dominant foot.

Dominant foot	Ligament strain	Inflammation of the tendon	Fracture
Lateral malleolus	105	43	4
Medial malleolus	32	20	3
Ankle heel	15	5	2
Heel	10	2	0

2020 has risen from about 13% at the beginning to the best 33% of the total, which is faster than the increase in 2019. As shown in Figure 6, from 2019 to 2020, the proportion of athletes' ankle injuries is increasing. Ankle injuries are mostly caused by indirect external forces. The components of the ankle joint are photographed as physical damage, so that the ankle joint cannot be extended, rotated, and rotated normally. If it is not treated in time or treatment is not thorough, it will affect the ability of the ankle joint in the future.

This article divides the injuries of 100 sports personnel into 2 levels, as shown in Table 3.

As shown in Table 3, sports injuries can be simply divided into two levels. The first levelincludes acute injury and chronic injury. Among them, the number of acutely injured is 75, accounting for 75%; the number of chronically injured is 25, accounting for 25%. It can be seen that acute injury is much higher than chronic injury.

Among them, the secondary injury of acute injury includes the following points, as shown in Table 4.

Among them, the number of ankle injuries is the largest, with 25 people, accounting for 33%, the highest proportion. It can be seen from Table 4 that acute secondary injuries include ankle injuries, bruises, sprains, and strains. Among them, the proportion of ankle joint injuries is the highest. Because sports is a physical antagonistic sport, it has the characteristics of small playing field, fast offensive and defensive conversion, fierce competition, and strong physical antagonism. The athletes have poor self-protection consciousness. They can't pay attention to the control of their

Table 2: Types of nondominant foot side injuries.

Nondominant foot	Ligament strain	Inflammation of the tendon	Fracture
Lateral malleolus	87	35	2
Medial malleolus	25	15	0
Ankle heel	10	4	0
Heel	5	1	0

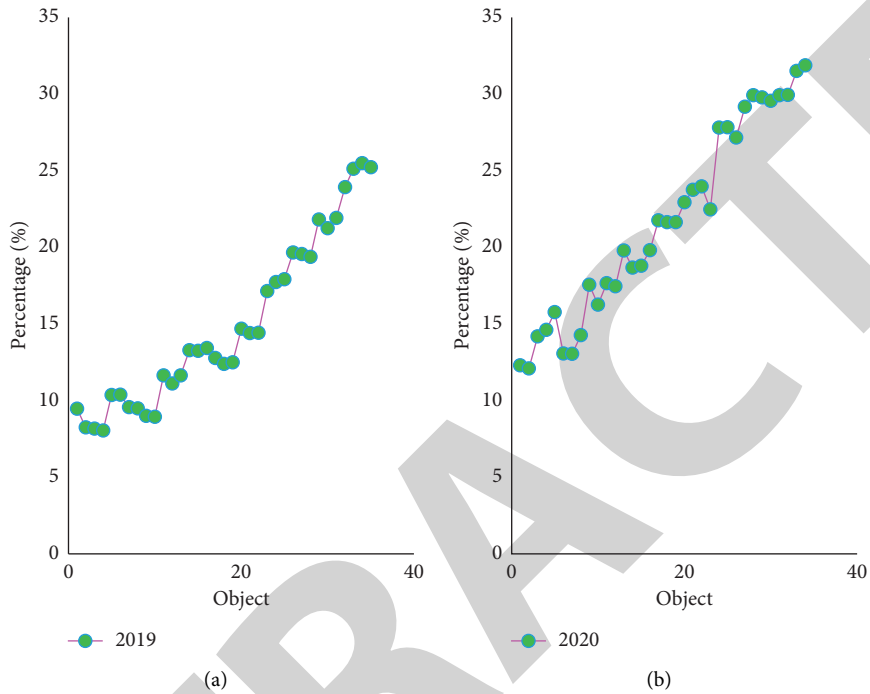

Figure 6: Proportion of athletes with ankle injuries in 2019 and 2020. (a) Proportion of athletes with ankle injuries in 2019. (b) Proportion of athletes with ankle injuries in 2020.

Table 3: Acute injury primary injury questionnaire.

First degree injury	Number of people	Percentage (%)
Acute injury	75	75
Chronic injury	25	25
Total	100	100

Table 4: Acute injury secondary injury questionnaire.

Secondary damage	Number of people	Percentage (%)
Ankle injury	25	33
Sprain	18	24
Strain	17	22
Bruise	15	21
Total	75	100

own movements during exercise, and often do quick and acute movements, which are more prone to ankle sprains, bruises, and contusions.

In order to verify the reliability of the data, this article conducted a survey of the types of injuries in the sports majors of 6 universities, as shown in Figure 7.

As shown in Figure 7, the injury sites of sports majors in 6 colleges and universities mainly include ankle joint injury, knee joint injury, thigh injury, calf injury, upper limb, and head injury. Among them, the proportion of ankle joint injuries is the highest, and the proportion range is 54%–70%. It can be seen that ankle joint injuries should be paid attention to.

In order to make the results of the experiment clearer, this article investigates the injury factors of sports players, as shown in Table 5.

As shown in Table 5, the main factors for athletes' injuries include incorrect technique, poor awareness of protection, overburdened ankle joints, other reasons, and poor physical fitness. Among them, the score of technically incorrect is 67 points, accounting for 32.5%, ranking first. The score for poor protection awareness is 35 points.

This article investigates the main injury factors of athletes from 2016 to 2020, as shown in Figure 8.

As shown in Figure 8, the main causes of injuries for athletes from 2016 to 2020 include incorrect technique, poor protection awareness, overburdened ankle joints, other reasons, and poor physical fitness. Among them, the proportion of incorrect technology is the highest, rising from 8% in 2016 to 14% in 2020; the percentage of poor protection awareness has risen from 7% in 2016 to 13% in 2020. Among them, the percentage of incorrect technology is the highest, reaching 14% in 2020. Therefore, it is necessary to strengthen the study of professional technology.

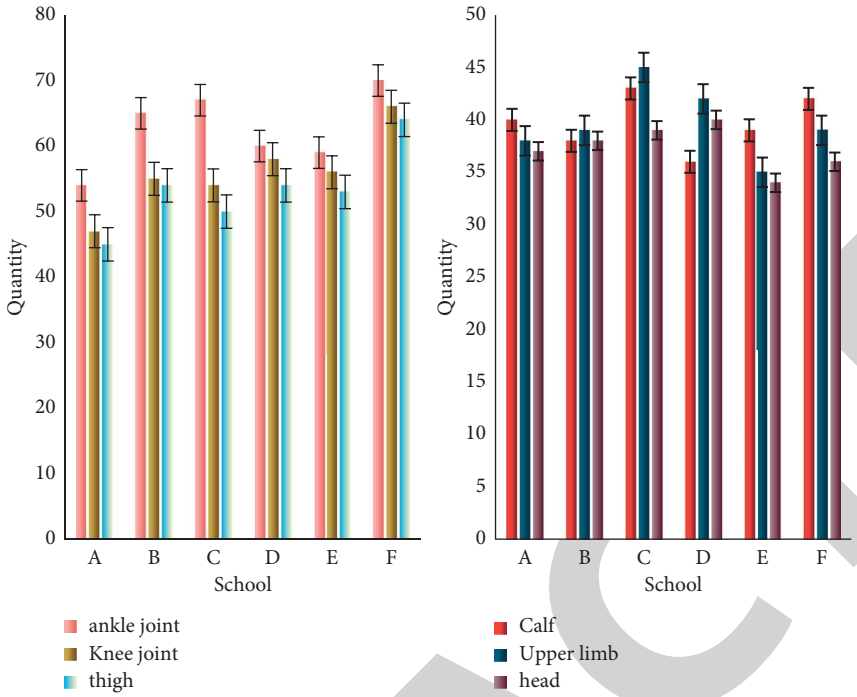

Figure 7: 6 injury types of sports professional athletes in colleges and universities.

Table 5: Injury factors of sports players.

Sort	Injury factor	Score	Percentage (%)
1	Incorrect technique	67	32.5
2	Poor protection awareness	54	26.2
3	Overburdened ankle	35	20
4	Other reasons	30	11.3
5	Poor physical fitness	20	10

In summary, the main causes of ankle joint injuries are as follows:

(1) Incorrect technology

The criterion of whether the technology is reasonable is to meet the requirements of the laws of human motion mechanics and biology. Technology is the performance of a general law with commonality, but it is necessary to consider the commonalities and the characteristics of each athlete at the same time. The unity of individuality and commonality is the best technique. Special technology is the basis for special sports. Therefore, the correct technical actions must be ensured.

(2) Poor protection awareness

Because sports is a combination of speed, endurance, strength, and skill, injuries are often accompanied by sports, and some injuries can be avoided by effective methods. The injury of the ankle joint happened suddenly and without warning, and only through the education of protective awareness and simulation measures to avoid the injury.

(3) Overburden on the ankle joint

In sports, every movement is based on the ankle joint, which is the key point of the entire sports. In sports, the rapid turning, sudden stop, and sudden rise all cause strong pressure on the ankle joint. Relevant studies have shown that the supporting stage of running is twice the load of the joints when walking. The joints bearing such a large force must undergo special training to strengthen the ankle joint's ability to bear the force.

(4) Other reasons

The remaining items include three factors: venue and equipment problems, clothing and shoes problems, and insufficient preparation activities. On the surface, these three factors are not related to ankle joint injury, but it is found through investigation that they are one of the main factors of sports ankle joint injury.

3.2. Experiment and Analysis of Comprehensive Rehabilitation Nursing for Ankle Joint Injury Rehabilitation. Nowadays, due to various reasons such as the aging of the city and the complexity of urban traffic, ankle joint fractures account for an increasing proportion of the whole body fractures, and they have become one of the most common fractures in trauma orthopedics clinics. Ankle fractures caused by sports can account for about 7% of ankle fractures, which have an important impact on the life of patients and the development of society. Since sports ankle fractures are intra-articular fractures, this has higher requirements for surgery. Anatomical reduction must be given to avoid serious complications such as traumatic arthritis as much as possible.

This requires targeted guidance of patients to carry out early rehabilitation exercises in order to restore the patients' normal physiological functions as much as possible. This

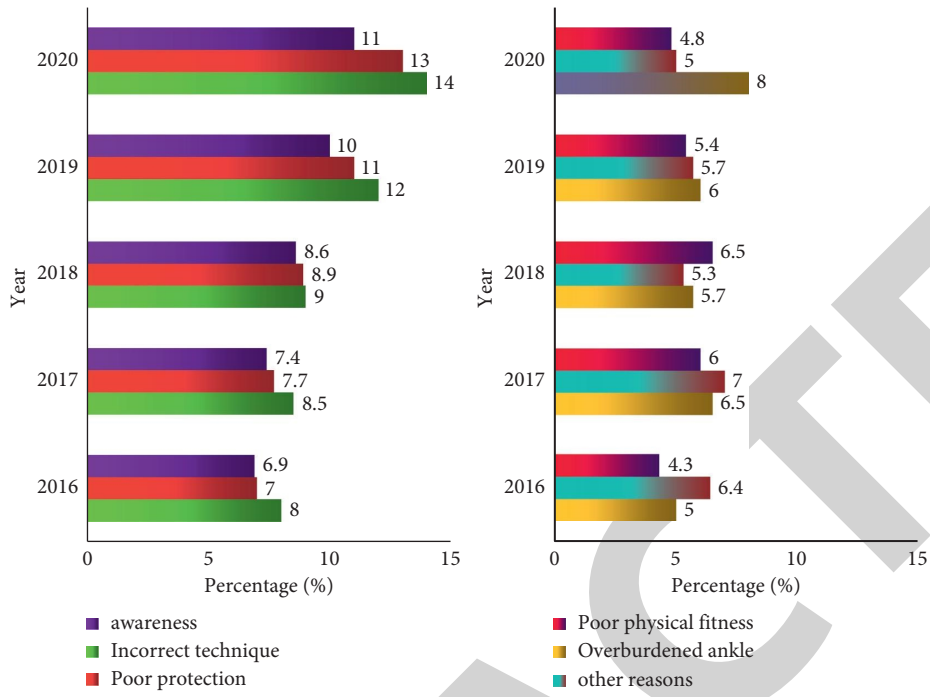

Figure 8: Major injury factors for athletes from 2016 to 2020.

article compares the recovery speed of ankle joint injuries before and after rehabilitation care, as shown in Table 6.

As shown in Table 6, the recovery speed of patients who underwent comprehensive rehabilitation care was significantly higher than that before recovery care. It can be seen that comprehensive rehabilitation care is of great importance to the degree of recovery of patients, and rehabilitation care is also necessary.

Table 6: Recovery speed of ankle joint injury before and after rehabilitation care.

Object	After care (%)	Before care (%)
1	20	14
2	25	12
3	19	8
4	17	9
5	27	10

3.2.1. Establish the Concept and Awareness of Early Rehabilitation. Rehabilitation of bone and joint injuries must be emphasized as early as possible, and interventional rehabilitation work should be carried out as soon as the patient's general condition permits. It creates favorable conditions for later functional recovery, actively prevents and reduces the occurrence of related complications, and must not separate treatment and rehabilitation. Those who think that after the treatment is over, the actions of the doctors who perform rehabilitation are even more inappropriate, which will be extremely unfavorable to the patient's functional recovery. Therefore, early functional exercise must be carried out.

3.2.2. "Combination of Dynamic and Static". Combination of fixation and exercise: After the fracture is reliably fixed by the operation, guided functional rehabilitation exercise is performed when the patient's pain is relieved, so as to restore the patient's normal physiological function as soon as possible. It is in the principle of fracture treatment of "combination of movement and static, equal emphasis on muscles and bones" in Chinese medicine. "Static" refers to the reliable fixation of fractures, including internal fixation and external fixation, while "movement" refers to functional exercise activities carried out under reliable fixation. "Dynamic" and "static" are inextricably related to each other. Functional exercise after fracture needs to be carried out under reliable fixation and does not affect fracture healing. The purpose of fracture fixation is to restore the patient's physiological function as much as possible. This kind of rehabilitation exercise method has great advantages and feasibility. It is a trustworthy, safe, and effective rehabilitation method.

4. Discussion

This article analyzes how to analyze the impact of comprehensive rehabilitation nursing on the rehabilitation of sports-induced ankle injuries based on the smart medical system. It expounds the concepts related to smart medical care and ankle joint injuries, and studies algorithms based on data mining and related theories of comprehensive rehabilitation care. It also explored how to prevent ankle joint injuries caused by exercise, and through experiments to discuss the importance of comprehensive rehabilitation care for the recovery of ankle joint injuries caused by exercise.

This article also makes reasonable use of data mining methods based on smart medical care. As the scope of

application of data mining methods has become larger and larger, the importance has also increased. According to this calculation, it is very important to discover the importance of comprehensive rehabilitation nursing for the recovery of ankle joint injuries caused by exercise based on data mining.

Through the experiments of many sports athletes, this article shows that with the development of the sports field in recent years, people are more and more likely to be injured in sports. Among them, ankle joint injury is a relatively common injury. There are many factors for ankle injury, such as insufficient professional skills, and weaker body, which requires athletes to improve their professional capabilities.

5. Conclusions

This article mainly discusses the effect of comprehensive rehabilitation nursing on the rehabilitation of sports-induced ankle joint injuries. This article adds an introduction to smart medical care. Based on smart medical care, it proposes a multisource data fusion and a classification method based on data mining and expounds the concepts of smart medical care and comprehensive rehabilitation care. The two algorithms are also specifically introduced in the method section. In the experimental part, a number of sports athletes in a number of universities were investigated, and it was found that the current ankle joint injury is one of the more frequent sports injuries. Through the comparison before and after rehabilitation care, it is found that comprehensive rehabilitation care plays a better role in the recovery speed of patients. The injury of the ankle joint will not only have a serious impact on the athlete's athletic ability, but also cause certain harm to the athlete's healthy development. If effective countermeasures are not taken to prevent sports injuries, it will have a serious adverse effect on the promotion and development of sports. Therefore, it is very important to analyze the causes of sports ankle joint injuries and propose comprehensive rehabilitation nursing measures.

Data Availability

No data were used to support this study.

Conflicts of Interest

The authors declare that there are no conflicts of interest with any financial organizations regarding the material reported in this article.

References

[1] T.-Y. Kim, S.-H. Kim, and H. Ko, "Design and implementation of BCI-based intelligent upper limb rehabilitation robot system," *ACM Transactions on Internet Technology*, vol. 21, no. 3, pp. 1–17, 2021.

[2] K. Fehske and C. Lukas, "Ligamentous ankle injury: an underestimated trauma?" *Sportverletzung—Sportschaden: Organ der Gesellschaft fur Orthopadisch-Traumatologische Sportmedizin*, vol. 34, no. 3, pp. 147–152, 2020.

[3] A. Besting, S. Bürger, M. Kasparick, B. Strathen, and F. Portheine, "Software design and implementation concepts for an interoperable medical communication framework," *Biomedical Engineering/Biomedizinische Technik*, vol. 63, no. 1, pp. 49–56, 2018.

[4] M. Lacey and B. Donne, "Does fatigue impact static and dynamic balance variables in athletes with previously ankle injury?" *International Journal of Exercise Science*, vol. 12, no. 3, pp. 1121–1137, 2019.

[5] C. Acosta-Olivo, Y. Tamez-Mata, J. Elizondo-Rodriguez, R. Rodriguez-Torres, A. Diaz-Valadez, and V. Pena-Martinez, "Investigation of the association between the acute ankle injury caused by fall from own height and body mass index," *Journal of Foot and Ankle Surgery*, vol. 58, no. 2, pp. 288–290, 2019.

[6] C. K. Lo, H. C. Chen, P. Y. Lee, M.-C. Ku, L. Ogiela, and C.-H. Chuang, "Smart dynamic resource allocation model for patient-driven mobile medical information system using C4.5 algorithm," *Journal of Electronic Science and Technology*, vol. 17, no. 3, pp. 231–241, 2019.

[7] A. Ghoneim, G. Muhammad, S. U. Amin, and B. Gupta, "Medical image forgery detection for smart healthcare," *IEEE Communications Magazine*, vol. 56, no. 4, pp. 33–37, 2018.

[8] S. Rana and D. Mishra, "Efficient and secure attribute based access control architecture for smart healthcare," *Journal of Medical Systems*, vol. 44, no. 5, pp. 97–11, 2020.

[9] S. Tian, W. Yang, J. M. L. Grange, P. Wang, W. Huang, and Z. Ye, "Smart healthcare: making medical care more intelligent," *Global Health Journal*, vol. 3, no. 3, pp. 62–65, 2019.

[10] J. Choi, C. Choi, S. H. Kim, and H. Ko, "Medical information protection frameworks for smart healthcare based on IoT," in *Proceedings of the 9th International Conference on Web Intelligence, Mining and Semantics (WIMS 2019)*, Seoul, South Korea, June 2019.

[11] V. Joseph Michael Jerard, M. Thilagaraj, K. Pandiaraj, M. Easwaran, P. Govindan, and V. Elamaran, "Reconfigurable architectures with high-frequency noise suppression for wearable ECG devices," *Journal of Healthcare Engineering*, vol. 2021, Article ID 1552641, 12 pages, 2021.

[12] D. S. Abdul Minaam and M. Abd-Elfattah, "Smart drugs: improving healthcare using smart pill box for medicine reminder and monitoring system," *Future Computing and Informatics Journal*, vol. 3, no. 2, pp. 443–456, 2018.

[13] S. P. irbhulal, W. Wu, G. Li, and A. K. Sangaiah, "Medical information security for wearable body sensor networks in smart healthcare," *IEEE Consumer Electronics Magazine*, vol. 8, no. 5, pp. 37–41, 2019.

[14] M. Jebraeily, Z. Z. Fazlollahi, and B. Rahimi, "The most common smartphone applications used by medical students and barriers of using them," *Acta Informatica Medica*, vol. 25, no. 4, pp. 232–235, 2017.

[15] S. Din and A. Paul, "RETRACTED: erratum to "smart health monitoring and management system: toward autonomous wearable sensing for Internet of Things using big data analytics," *Future Generation Computer Systems*, vol. 108, pp. 1350–1359, 2020.

[16] A. M. Fathollahi-Fard, M. Hajiaghaei-Keshteli, and S. Mirjalili, "A set of efficient heuristics for a home healthcare problem," *Neural Computing & Applications*, vol. 32, no. 10, pp. 6185–6205, 2020.

[17] Y. Yanagawa, K. Jitsuiki, H. Nagasawa et al., "A smartphone video transmission system for verification of transfusion," *Air Medical Journal*, vol. 38, no. 2, pp. 125–128, 2019.

Hindawi
Emergency Medicine International
Volume 2023, Article ID 9803581, 1 page
https://doi.org/10.1155/2023/9803581

Retraction

Retracted: A Multimodel Fusion Method for Cardiovascular Disease Detection Using ECG

Emergency Medicine International

Received 28 November 2023; Accepted 28 November 2023; Published 29 November 2023

This article has been retracted by Hindawi, as publisher, following an investigation undertaken by the publisher [1]. This investigation has uncovered evidence of systematic manipulation of the publication and peer-review process. We cannot, therefore, vouch for the reliability or integrity of this article.

Please note that this notice is intended solely to alert readers that the peer-review process of this article has been compromised.

Wiley and Hindawi regret that the usual quality checks did not identify these issues before publication and have since put additional measures in place to safeguard research integrity.

We wish to credit our Research Integrity and Research Publishing teams and anonymous and named external researchers and research integrity experts for contributing to this investigation.

The corresponding author, as the representative of all authors, has been given the opportunity to register their agreement or disagreement to this retraction. We have kept a record of any response received.

References

[1] G. Song, J. Zhang, D. Mao, G. Chen, and C. Pang, "A Multimodel Fusion Method for Cardiovascular Disease Detection Using ECG," *Emergency Medicine International*, vol. 2022, Article ID 3561147, 10 pages, 2022.

Hindawi
Emergency Medicine International
Volume 2022, Article ID 3561147, 10 pages
https://doi.org/10.1155/2022/3561147

Research Article

A Multimodel Fusion Method for Cardiovascular Disease Detection Using ECG

Guanghui Song,[1] **Jiajian Zhang**,[1] **Dandan Mao**,[2] **Genlang Chen**,[1] **and Chaoyi Pang**[1]

[1]*School of Computer and Data Engineering, Ningbo Tech University, Ningbo 315100, Zhejiang, China*
[2]*Department of Electrocardiogram, Ningbo Hospital of Traditional Chinese Medicine, Ningbo 315100, Zhejiang, China*

Correspondence should be addressed to Guanghui Song; songnbt@nbt.edu.cn

Received 17 March 2022; Revised 13 April 2022; Accepted 25 April 2022; Published 16 May 2022

Academic Editor: Hang Chen

Objective. Electrocardiogram (ECG) is an important diagnostic tool that has been the subject of much research in recent years. Owing to a lack of well-labeled ECG record databases, most of this work has focused on heartbeat arrhythmia detection based on ECG signal quality. *Approach*. A record quality filter was designed to judge ECG signal quality, and a random forest method, a multilayer perceptron, and a residual neural network (RESNET)-based convolutional neural network were implemented to provide baselines for ECG record classification according to three different principles. A new multimodel method was constructed by fusing the random forest and RESNET approaches. *Main Results*. Owing to its ability to combine discriminative human-crafted features with RESNET deep features, the proposed new method showed over 88% classification accuracy and yielded the best results in comparison with alternative methods. *Significance*. A new multimodel fusion method was presented for abnormal cardiovascular detection based on ECG data. The experimental results show that separable convolution and multiscale convolution are vital for ECG record classification and are effective for use with one-dimensional ECG sequences.

1. Introduction

The electrocardiogram (ECG), which reflects the heart's electrical activities, is widely used in clinics and hospitals worldwide to diagnose cardiac disorders. According to Bacquera et al. [1], the ECG signal itself is effective for predicting many cardiovascular-related diseases. However, because of the complexity and variability of ECG signals, it takes years to train a professional cardiologist to interpret them. Furthermore, the growing number of people with cardiac diseases makes the situation worse.

Therefore, an automatic and accurate system is needed to help doctors with ECG-based diagnoses. An ECG signal consists of five main waves, namely, *P*, *Q*, *R*, *S*, and *T*. Automatic classification systems can use the information hidden in ECG signals to assess heart-related diseases (e.g., atrial fibrillation), as different disorders result in different signal morphologies in both time and frequency domains. Thus, after the important features have been detected and a huge amount of data collected, it should be possible to automatically distinguish many heart-related diseases. As there are many types of heart-related disease, the first stage of ECG-based automatic diagnosis is to distinguish abnormal ECG signals from normal records. Then, cardiologists can concentrate on the signals that may reflect disease. More importantly, when used as an auxiliary diagnostic tool, such an automatic diagnosis algorithm could greatly reduce misdiagnosis rates. Thus, in this article, a binary ECG signal classification framework is presented and shown to achieve state-of-the-art results.

In recent years, most ECG classification research has fallen into two categories: ECG heartbeat classification and lead classification. The heartbeat is the basic component of an ECG record. Luz et al. [2] surveyed the latest techniques for the detection of abnormalities based on ECG heartbeat classification. The algorithms involved in ECG lead classification are similar to those used for heartbeat discrimination.

1.1. Signal Preprocessing. Normally, three steps are performed to identify the label of an ECG record: (i) signal preprocessing, (ii) feature extraction and analysis, and (iii) signal classification. Preprocessing of signals normally consists of making a judgment regarding the noise level of an ECG signal and denoising the signal. Clifford et al. [3] proposed six signal quality indices to evaluate the quality of 12-lead ECG signals in the PhysioNet/Computing in Cardiology Challenge 2011 [4] and achieved good results for classifying the signals as acceptable or unacceptable. Empirical mode decomposition (EMD) and discrete wavelet transform (DWT) were used by [5] to denoise ECG signals.

1.2. Feature Extraction. Features extracted from signals are vital for the final classification task because the obtained feature vector is used as the representation of a record. Features in either the time domain or in the frequency domain were used. A combination of ECG signal morphological and dynamic features was used by Ye et al. [6] to classify heartbeats from the MIT-BIH arrhythmia database. Sarkaleh et al. [7] used DWT to extract features and formed a feature vector, which was used by a multilayer perceptron (MLP) to classify heartbeats. DWT is the most popular method used to extract features from the frequency domain [8–10]. EMD has also been used as an effective tool to extract features [11]. Given the complexity of ECG features and the powerful capabilities of deep learning, neural networks have been employed as feature extractors. Kiranyaz et al. [12] realized a real-time ECG classification system based on a one-dimensional (1-D) convolutional neural network (CNN) in which feature extraction and classification were both performed by the CNN model. Kachuee et al. [13] implemented a 13-weighted-layer network to extract features from ECG signals and learn representations of the signals. They trained the network for arrhythmia detection and successfully used their model to diagnose myocardial infarction.

1.3. Classification Algorithms. After feature extraction, the formed feature vectors are fed into classifiers to obtain the final result. Over the past 20 years, a huge amount of work has been done on using machine learning and deep learning methods to classify ECG signals. The support vector machine (SVM) with kernel function is a popular method for classifying ECG signals [6, 14–16]. The random forest method is also widely used because of its simplicity and high classification accuracy [17–19]. As this method uses few parameters, it can achieve relatively good results without any tuning process. Based on its excellent performance in image classification tasks, deep learning is also used to classify ECG signals [8–11]. Furthermore, Moavenian et al. [16] performed a comparison between an SVM and an artificial neural network for classifying ECG signals. Their results showed that the SVM was more time-efficient, whereas the MLP had stronger generalization capability.

1.4. Record Classification. In addition to heartbeat classification, ECG signals can be classified based on the whole lead. The PhysioNet/Computing in Cardiology Challenge 2017 [20] aimed to classify ECG records into four classes based on a single ECG lead. Teijeiro et al. [21] used clinically meaningful features to train two classifiers, XGBoost and a long short-term memory network, to evaluate records globally and as a sequence. The outputs of the two classifiers were then combined to give the prediction result. Zabihi et al. [19] suggested a random forest model using features from time and frequency domains and phase space reconstruction; this model achieved high F1 scores. Hong et al. [22] extracted expert features and deep features (features extracted by a deep neural network) for classification. A cascaded binary classifier was implemented by Datta et al. [23] and proved to be very useful for record classification tasks. Normal and abnormal records differ from each other greatly, as shown in Figure 1. It is obvious from the figure that the abnormal ECG record has a much shorter R-R interval than the normal one.

Huang et al. [24] classified ECG signals from the Physikalisch-Technische Bundesanstalt database as normal or abnormal using three classifiers: stepwise discriminant analysis, SVM, and LASSO logistic regression. Zhang et al. [25] built the Chinese Cardiovascular Disease Database (CCDD), containing more than 100,000 12-lead ECG signals with well-labeled clinical diagnosis results, enabling classification of large-scale ECG records. Jin et al. [26] compared four traditional CNNs with a lead CNN (LCNN) in which they designed specifically for multilead ECG signals. The LCNN achieved the best results, with an 83.66% classification accuracy for distinguishing abnormal and normal ECG records. They then integrated two LCNNs and four rule-based classifiers; this combination yielded an accuracy of 86.22%. A Bayesian fusion method was used to combine two LCNN outputs; then, a Bayesian averaging method was applied to combine the results of the LCNN model and the rule-based classifiers and generate the final prediction [27]. Chen et al. [28] proposed a multibranch convolutional and residual network (MBCRNet), which had an average accuracy of 87.04%. Three feature fusion methods will be discussed in this paper.

On the basis of previous work, we find that different methods produce different advantages in ECG classification tasks. Most of the work has focused on heartbeat classification; there have been fewer studies of classification based on whole ECG records. Therefore, in this work, we focused on distinguishing abnormal ECG signals based on whole 12-lead records. We proposed and compared three classification frameworks based on traditional machine learning, a 1-D residual neural network (RESNET), and a 2-D RESNET. CCDD was chosen as our experimental dataset. We achieved state-of-the-art performance in the normal/abnormal classification task based on CCDD ECG records.

The main contributions of our proposed method are as follows:

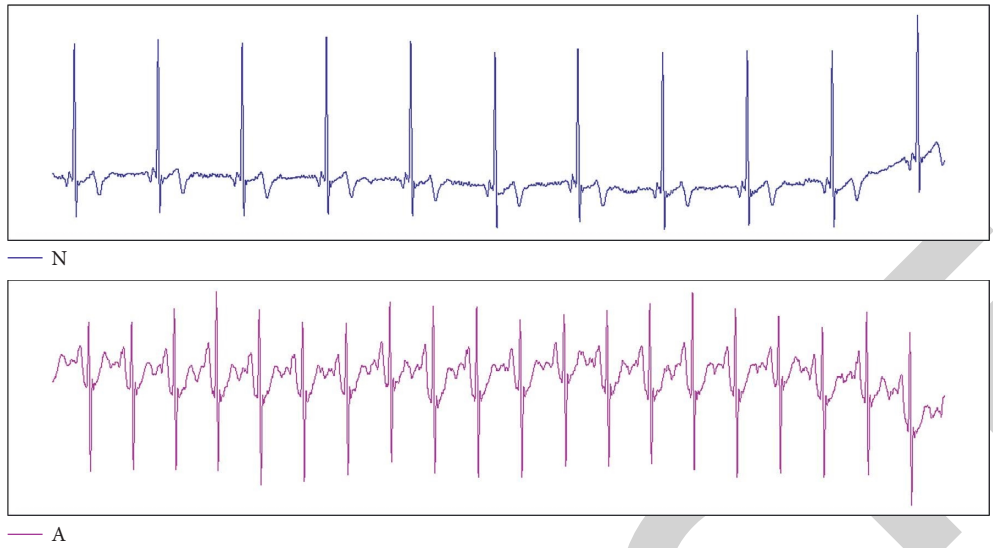

Figure 1: Normal (*N*) and abnormal (*A*) records from CCDD.

(i) We used both a signal quality filter and a record quality filter (RQF) to examine heavily polluted ECG records.

(ii) We proposed a feature fusion method combining both local and global features of ECG signals to form a record feature vector.

(iii) We analyzed the influence of multiscale convolution and separable convolution on multilead ECG records.

(iv) We implemented three classification baselines and applied model fusion to obtain RF-MLP (random forest fused with MLP) and RF-RESNET (random forest fused with RESNET) models. Better classification results were achieved with the RF-RESNET model. To the best of our knowledge, this is the highest accuracy achieved for record classification work on the CCDD database.

This paper is organized as follows. Section 1 summarizes related work on traditional and recently developed techniques applied to ECG diagnosis. In Section 2, we introduce the method and framework of our work. Detailed experiments and a discussion are presented in Section 3. Finally, we draw conclusions about our work in Section 4.

2. Method

2.1. Dataset and Preprocessing. We obtained approximately 140,000 records from CCDD, labeled as normal or abnormal with respect to least one type of disease. As in [26], we further relabeled the data as normal (0) or abnormal (1) for binary classification based on the original labels. In detail, records with labels of "0 × 0101" or "0 × 020101" were relabeled as normal (0); the others are relabeled as abnormal (1). A Butterworth filter (Bfilter) was used to remove noise such as baseline wander. Raw ECG signals from 12 channels are fed into the Bfilter, and the denoised ECG signal is output. The default parameters of the Bfilter were set to order = 4, type = "lowpass."

Records of less than 8 s in length and those mixed with too much noise were excluded using our proposed RQF algorithm, which will be described later. The original sampling rate was 500 Hz; for computational efficiency, we downsampled the signal to 200 Hz.

2.2. Record Quality Filtering. After applying various denoising methods, there were still some records that needed to be removed, as shown in Figure 2. These seriously damaged records were not suitable for use in classification work, as such noisy data do not retain the original pattern of real data and could cause the model to learn irrelevant features for the corresponding data type. Thus, based on the work of Orphanidou et al. [29], we developed our RQF, a fast feature-based ECG signal quality filter (Figure 3).

As shown in Figure 3, the first step was to detect *R* peaks and locate all the heartbeats in a record. Then, four rules were defined to set a threshold for unusable records. Here, HR is the heart rate, and max(|*RR*|) and min(|*RR*|) represent the maximum and minimum *R-R* intervals throughout the records, respectively. A feasible record should satisfy the following four conditions: HR less than 180 and more than 20; max(|*RR*|) not exceeding 3 s; the ratio of max(|*RR*|) to min(|*RR*|) less than 4; and, finally, number of *R* peaks more than 5 if a record is longer than 8 s.

Notably, our RQF does not need information about the QRS complex, *P* wave, or *T* wave; it only needs to identify all the *R* peaks in each record. The detection of an *R* peak yields the highest accuracy, as suggested by many studies.

Thus, our method also reduces the quality identification error originating from the wave delineation process. Through this filter, 1603 noisy records were removed from the dataset. Finally, we obtained 81,000 normal and 58,000 abnormal records for use as training and testing data, respectively.

2.3. Feature Fusion. Representative features are vital for distinguishing one type of record from others. An ECG record can be represented as signal = $\{L^1, L^2, ..., L^j\}$, where j

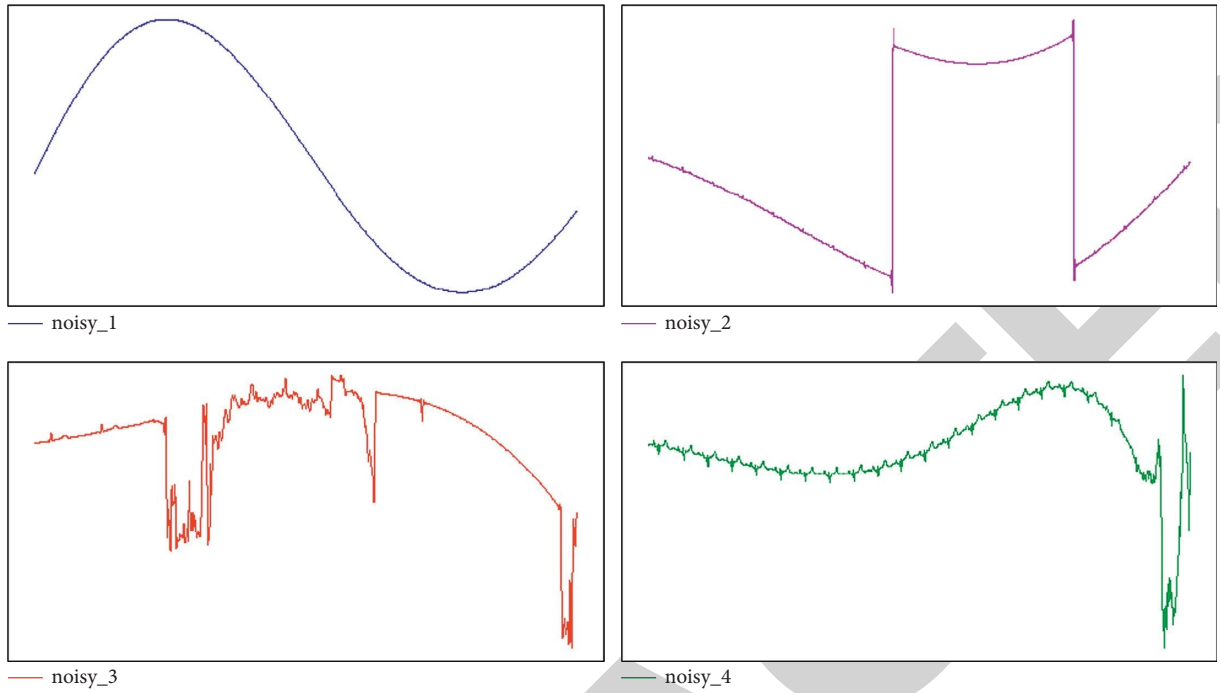

Figure 2: Noisy records.

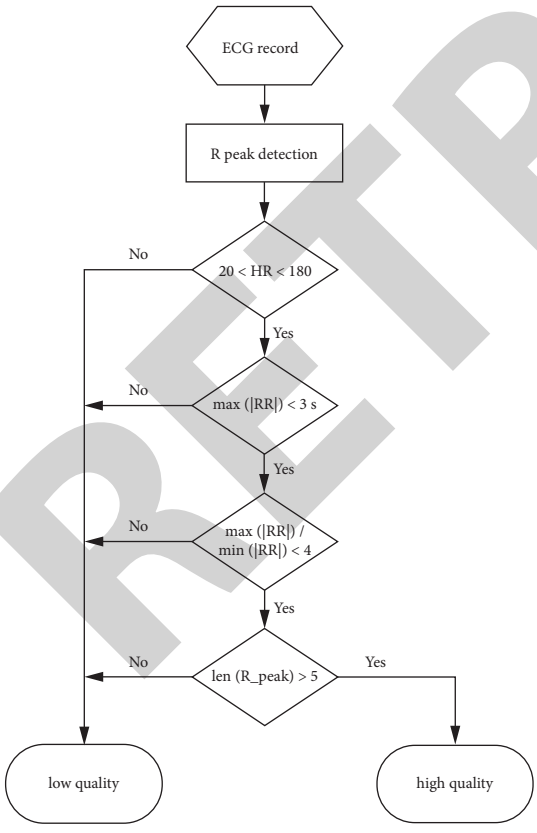

Figure 3: Record quality filter.

represents the number of leads. In this work, j is equal to 12, and L^i is the ith-lead, $L^i = \{a_1, a_2, \ldots, a_n\}$, where a_n represents the voltage value at time step n. The heartbeat is the basic component of ECG records, and the relationship between heartbeats in the same or different leads contains dynamic information on heart activities. As the shape forms of a time interval at different leads reflect heart activities from different angles, abnormal patterns may present differently in different leads.

We, therefore, present a novel feature fusion method combining local and global features from 12 leads to form discriminative feature representations of ECG records.

(i) Local features are the features obtained from each heartbeat. For each heartbeat, features from the time and frequency domains and the wave morphology are calculated and combined to form a local vector, which represents the heartbeat.

(ii) Global features consist of features computed from the whole ECG lead, namely, the R-R interval and DWT coefficients.

We implemented a modified QRS detection algorithm based on Pan et al. [30] to identify the R peak of each beat. We calculated the maximum amplitude, minimum amplitude, mean amplitude, and variation in amplitude for the obtained beats to describe the beat morphology. Based on [31], kurtosis signal quality indices were chosen to represent differences between the normal distribution and heartbeat data. We used skewness signal quality indices to measure the symmetry of a beat. A fast Fourier transform was performed on each beat to compute the wave energy (amplitude) and the frequency offset (phase). Fourth-order DWT coefficients were also used as features in the frequency domain. Based on our prior work [32], ten local features were chosen and are run on each of the 12 leads separately.

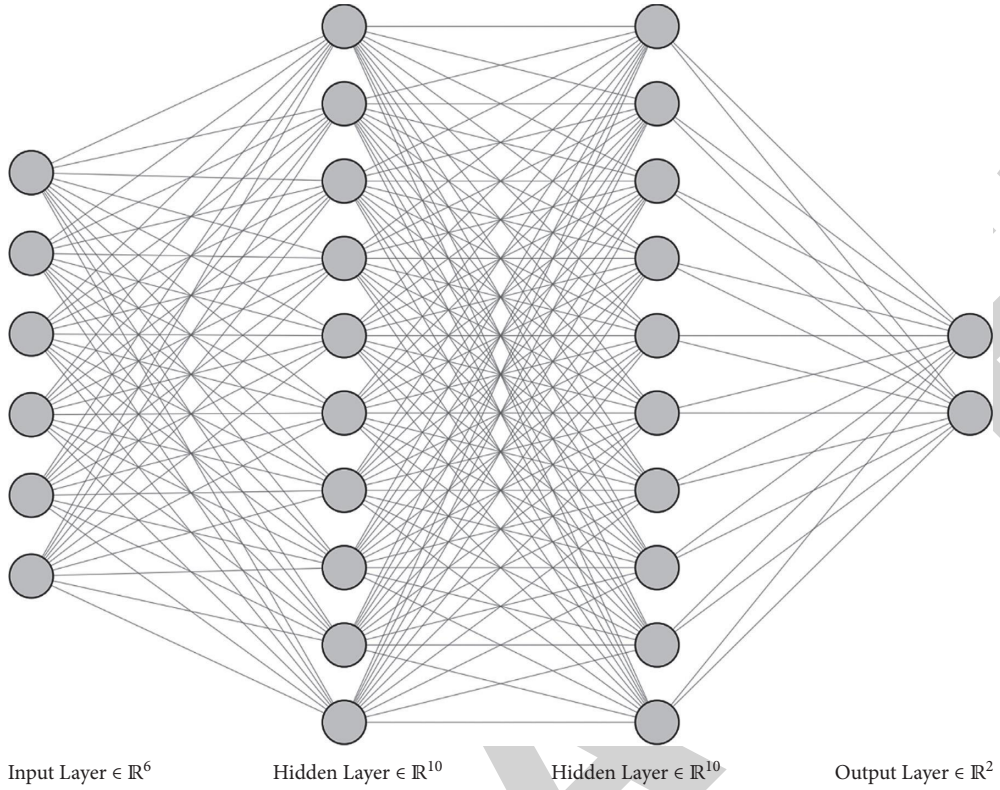

Figure 4: MLP architecture.

Global features are extracted from the lead scale. The *R-R* interval represents the heart rate variability, that is, the dynamic rhythm of the signal. We extract *R-R* intervals and their first-order differences. DWT is performed on the whole ECG lead, and sixth-order DWT coefficients are obtained as lead frequency features.

After local features and global features have been obtained, a two-stage feature fusion method is applied to form the final feature vector. First, for each lead, local and global features are combined to form the lead vector. Each lead is represented as a lead vector. Then, lead vectors are concatenated to form a record vector, *r* vector. The ECG record is represented as follows:

$$r\,\text{vector} = \left[x_i^{(1)}, x_i^{(2)}, x_i^{(3)}, \ldots, x_i^{(P)}\right] \in R^{V\times P}, \quad (1)$$

where P is the number of leads, V represents the volume of features in each lead vector, and $x_i^{(n)}$ represents the features of the n-th lead. In this work, $P = 12$.

2.4. Random Forest. Random forest is a traditional machine learning technique that shows powerful performance in many classification tasks. A random forest is constructed by building many decision trees based on bagging, and the final classification result is the average prediction or maximum vote of each decision tree. However, the random forest method does not simply combine the decision trees but randomly selects a subset of features at each split point, thereby overcoming the overfitting problem. When random selection is not used, decision trees tend to choose the most important feature set, resulting in high correlation among trees and low classification performance. One of the most important hyperparameters of the random forest method is the number of trees it builds for a given dataset. A grid search is used to determine the optimal number of trees for a record classification task. As described above, *re* vector $= \{x_i^1, x_i^2, x_i^3, \ldots, x_i^P\}$ is the input feature vector. After training, for each *r* vector, the model outputs the probabilities for each record class. The class with the highest probability is regarded as the prediction label.

2.5. Multilayer Perceptron. MLP is the predecessor of CNN and consists of neurons and weights that connect neurons in different layers. In contrast to CNN, neurons in layer L_i in the MLP connect with all neurons in layer L_{i-1}. Thus, information from the input vector can be preserved to the maximum extent in the network. For example, MLP architecture is shown in Figure 4.

Figure 4 shows a four-layer MLP. The first layer is the input layer receiving ECG feature vector $\{x_1, x_2, x_3, \ldots, x_n\}$, where n is the length of the feature vector. Except for the bias neuron, each neuron receives one feature element x_i. The last layer, which contains two neurons, is the output layer. The size of the output layer corresponds to the number of classes used for prediction. The two layers in between are hidden layers, mapping the input vector to the output classes through training and updating the weights of each perceptron. In our model, there are two hidden layers, each with 50 neurons, one input layer, and one output layer. The

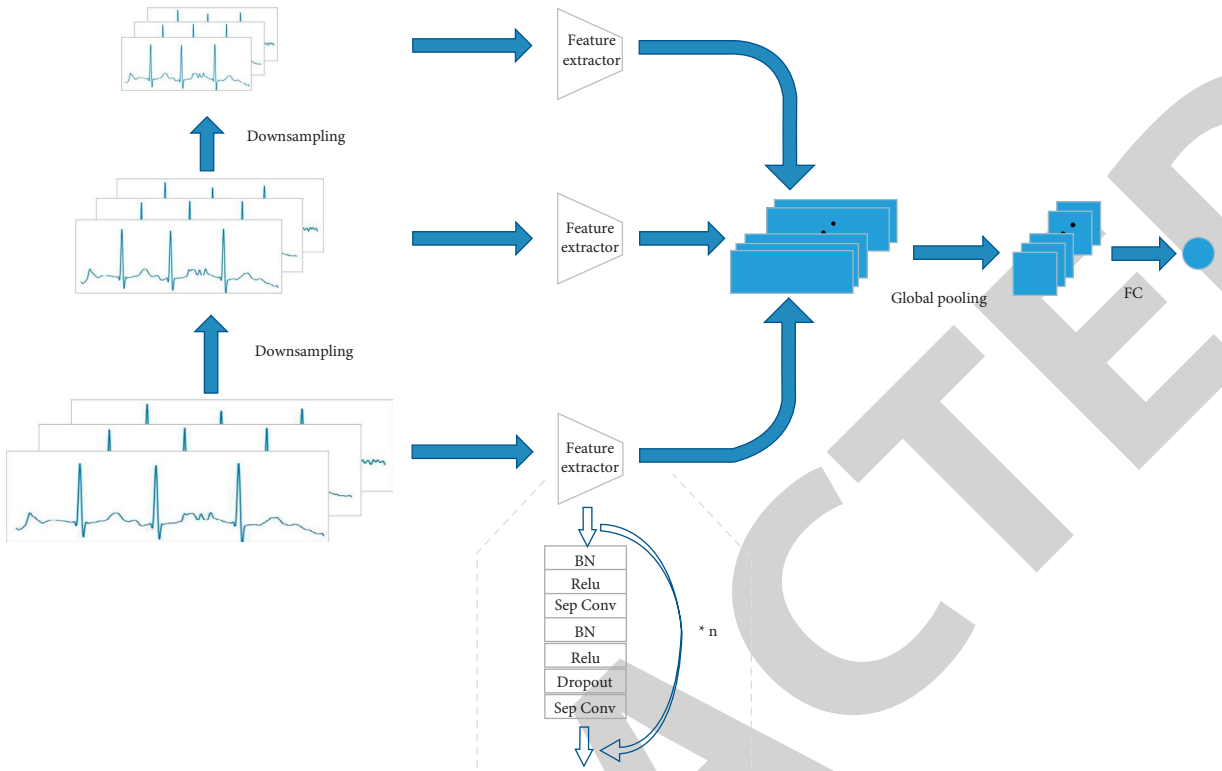

Figure 5: Modified RESNET architecture.

number of neurons in the input layer varies with the length of the feature vector extracted from the ECG record. The output layer contains two perceptrons, giving possible classes 0 and 1.

2.6. Modified RESNET. Although deep representation is vital for distinguishing different classes of objects, traditional deep neural networks suffer from difficulty in training. RESNET [33] was proposed to solve this vanishing gradient problem by using shortcut connections in the residual block. The core idea of RESNET is to enable gradients to flow to earlier layers directly through these shortcut connections. In the case of long series of ECG signals, we assume that the use of deep architecture is the most effective way to extract ECG representational features. Therefore, in this work, a novel deep CNN was designed based on residual block architecture (Figure 5).

As shown in Figure 5, for each scale, a feature extractor with 16 RESNET blocks was implemented to form the feature map, where *Sep Conv* represents separable convolution and different downsampling scales result in ECG signals at different scales. The details are given below.

Similar to images, ECG signals contain features of different levels. Inspired by ContextNet [34], we implemented a multiscale extraction module in our CNN architecture to extract multilevel ECG features. Specifically, ECG pyramids are fed into the neural network to capture ECG signal information at different scales; this information is then concatenated to form a multiscale feature vector. ECG pyramids consist of ECG signals produced by different downsampling scales, enabling the calculation of feature maps with different receptive fields. Using a multiscale extraction method, both global dynamic information and local signal rhythm can be captured in the feature vector. We defined the original ECG signal as *raw*. Different downsampling scales produce signal fragments with distinct lengths, described as *clip*. The calculation of each clip is performed using the following formula:

$$M = \frac{N}{S},$$
$$\beta_k = \frac{1}{S} \sum_{i=S*k}^{S\times(K+1)-1} \alpha_i, \tag{2}$$

where N is the length of the original signal; raw $= \{\alpha_1, \alpha_2, \alpha_3, \ldots, \alpha_n\}$, where $0 \le i \le N$; S represents the downsampling scales {1, 2, 4, 8, 16}; and M is the length of the generated ECG clip. Therefore, the generated ECG pieces are clip $= \{\beta_1, \beta_2, \beta_3, \ldots, \beta_n\}$. Specifically, when $S = 1$, clip is the same as the original signal raw. Thus, with different values of S, multiClips is obtained as the new input signal series:

$$\text{multi Clips} = \left\{\text{clip}^1, \text{clip}^2, \text{clip}^3, \ldots, \text{clip}^n\right\}, \tag{3}$$

where clip^j represents clip with a downsampling scale of j. To explore the effects of combinations of different downsampling scale clips, we performed experiments and discuss the results below.

Considering ECG leads as channels in an image, 12 leads contain information from 12 channels. In clinical scenarios, different leads reflect various details of heart activity, and all leads are vital for judging the condition of the heart. Thus, all 12 channels were fed into the neural network for feature extraction. More importantly, although different leads have the same size, they are not exactly aligned. Along the dimension of time, the same heart activity causes the 12 leads to react slightly differently. Therefore, separable convolution was used in the convolution layers for better feature extraction. The first step is depth-wise convolution. Each channel is convolved by a kernel; different channels are computed separately. Suppose the number of channels is C, that is, $C = 12$. After depth-wise convolution, C feature maps are generated. The second convolution step fuses features from different channels by convolution in the depth dimension. This point-wise convolution combines features at similar spatial points across the C channels. Another significant advantage of separable convolution is the reduction of parameters in the neural network and of the overall model size. The training time is also shortened significantly. For comparison purposes, we implemented a modified RESNET based on CNN RESNET^c from [35] to classify normal and abnormal ECG records. Our model only contains 0.74 million parameters, whereas RESNET^c has more than 16 million; that is, it has 20 times fewer parameters.

After the feature extraction module, a fully connected layer is implemented to concatenate features. The fully connected layer is followed by a softmax layer, which is used as the classifier to predict the labels of ECG records.

2.7. RF-MLP. Random forest and MLP were trained separately using the r *vector* constructed in the feature fusion step. These two models were trained via different principles. When constructing decision trees, a random subset of features is selected at each split point. In our random forest model, decision trees are trained based on information gain theory. The MLP model trains the network through updating weights of neurons. Binary cross-entropy is used to calculate the loss in each iteration; then, backpropagation is applied to transfer the loss to previous layers for updating of weights. Therefore, the random forest and MLP methods have different training and classifying criteria. Proper fusion of these two models could enable better distinguishing ability.

Random forest and MLP give probabilities for all prediction classes, where a high probability indicates a high confidence level. The class with the highest confidence level is defined as the prediction label. As mentioned above, because of the different characteristics of random forest and MLP, they may classify the same record into different classes. Thus, a probabilistic model fusion approach was implemented to make use of the advantages of both methods.

2.8. RF-RESNET. The main characteristic of our modified RESNET architecture is its ability to extract deep representations of ECG sequences. However, as it uses human-crafted features, r vector, random forest has stronger interpretability. As representatives of traditional machine learning algorithms and prevalent deep learning methods, the random forest and modified RESNET models could complement each other owing to their specific characteristics. The random forest model was trained with feature representation vector, r vector, whereas for the modified RESNET model, different ECG pyramids were used as training data. As in the case of random forest and MLP, a probabilistic model-fusion methodology was applied to make use of the advantages of the two models. During testing, the two models produced possibilities for each ECG instance, indicating the predicted class. Then, the model with the higher test accuracy was given greater weight in the final decision regarding the predicted class, and the architecture is shown in Figure 6.

3. Results and Discussion

Three independent normal/abnormal detection methods, random forest, MLP, and modified RESNET, were used as baselines. Two fusion models, RF-MLP and RF-RESNET, were evaluated with respect to their effectiveness in ECG record classification tasks. In total, five models were evaluated on the CCDD database to determine their ability to classify normal and abnormal ECG records.

The whole database was randomly partitioned into a training set, validation set, and test set using a ratio of 8 : 1 : 1. The validation set was used for early stopping and selection of hyperparameters for MLP and CNN. Then, models were evaluated on the test set to assess final performance.

For random forest evaluation, we set the parameter expressing the number of constructed trees to be 200, which has been demonstrated to be the best size for this work by a series of experiments.

The MLP used in this work consisted of four layers. Each hidden layer contained 50 neurons. *ReLU* and *sigmoid* were used as the activation functions of the hidden layer and the output layer, respectively. The MLP was trained with Adam, and β_1 and β_2 were set to 0.9 and 0.999, respectively. The input layer received record feature vectors as input data, and the output layer predicted the record classes.

Our proposed CNN contains 34 layers. Before training the network, ECG sequences were intercepted to the same lengths. Then, Z-normalization was applied to the training, validation, and testing sets, respectively. Our RESNET-based CNN was trained with a ReLU activation function and Adam optimizer. The binary cross-entropy was used as the loss function. In each residual block, the convolution layer was followed by a dropout of 0.4. The final CNN contained 33 convolution layers and a fully connected layer. A sigmoid was applied to predict the two classes. The classification results obtained with these three models are shown in Table 1.

In Table 1, specificity is defined as the proportion of correctly predicted negative samples to the total number of samples with negative labels. Negative samples are those

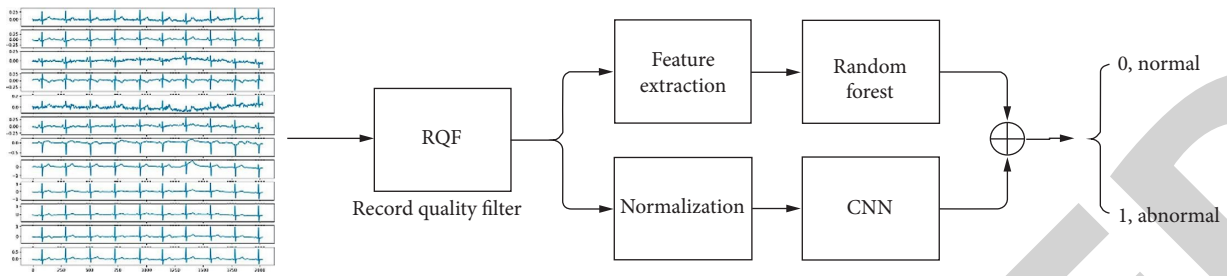

Figure 6: Model fusion architecture.

Table 1: Classification results for random forest, MLP, and modified RESNET.

Models	Precision	Recall	Specificity	F1 score	Accuracy
Random forest	0.888	0.795	0.928	0.839	0.872
MLP	0.861	0.733	0.915	0.792	0.839
Modified RESNET	0.869	0.762	0.920	0.812	0.855

ECG records with abnormal behaviors. Therefore, a high specificity value means that most of the abnormal records were detected by the model. In this work, all three baseline models yielded specificity values of over 91%, which are vital in clinical applications.

Good results were achieved for ECG classification on the CCDD database, as listed in Table 2. Our models achieved high classification accuracy, and the fusion of random forest and modified RESNET yielded the best results. Furthermore, part of the PTB diagnostic ECG database, which contains 126 records of 12-lead ECGs from 43 patients, was also used for experiments, and the classification accuracy was 0.841 for our models.

We compared the difference in performance between separable and nonseparable convolution in CNN architecture. According to our experimental results, the classification accuracy was 0.831 for nonseparable convolution but 0.842 for separable convolution. Moreover, separable convolution required 20 times fewer parameters than nonseparable convolution. Therefore, for multichannel time-series data, separable convolution had a stronger distinguishing capability.

Furthermore, we conducted experiments using different convolutional scales to determine the influence of scale on the effectiveness of multiscale convolution methods. Details of the classification results are given in Figure 7. The modified RESNET achieved the best classification accuracy when the scale was 3. This implies that using too many scales leads to information redundancy. When the downsampling rate exceeds a certain level, key information in the original signal can become indistinguishable.

To evaluate the effect of the depth of the modified RESNET, 34-layer and 50-layer modified RESNET models were implemented for comparison. The 50-layer network, which had 1.1 million parameters compared with 0.74 million in the 34-layer network, suffered from overfitting and had a training accuracy of approximately 0.9 and test accuracy less than 0.855.

Table 2: Summary of record classification performance on CCDD.

Literature	Method	Accuracy
Jin et al. [26]	LCNN	0.837
Jin et al. [27]	LCNNs and rule-based classifiers	0.862
Chen et al. [28]	MBCRNet-L	0.870
Proposed$_1$	RF-MLP	0.874
Proposed$_2$	RF-RESNET	0.880

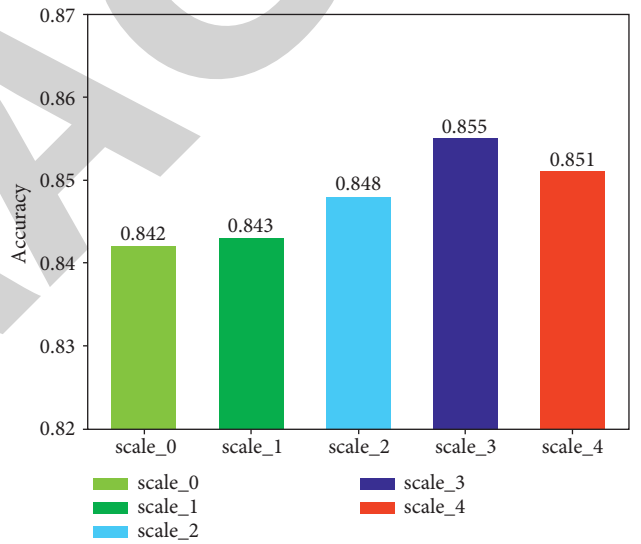

Figure 7: Classification results with different scales.

4. Conclusion

In this work, we researched methods for the detection of normal/abnormal ECG signal records, which is the essential first step in ECG diagnosis. Owing to the presence of various types of noise in the ECG data, we proposed a record filtering method to remove records seriously affected by noise. Then, we developed a feature fusion method that could extract both local and global features from different leads to construct a representation of the ECG record. Random forest, MLP, and modified RESNET were implemented to provide classification baselines. Ensemble methods were developed by fusing random forest with MLP and RESNET, respectively. Experiments were performed to further investigate the influence of multiscale convolution and separable convolution. The best results were achieved when random forest was fused with modified RESNET, with three scales and separable convolution. The classification results for our

methods were compared with those obtained with several state-of-the-art methods on the same database; our ensemble model using random forest and modified RESNET achieved the best classification results. Future work will include optimizing the algorithm and exploring the use of RNN and CNN models to enhance the accuracy of the method and its ability to extract dynamic features.

Data Availability

The data that support the findings of this study are available from the corresponding author upon reasonable request.

Conflicts of Interest

The authors declare no potential conflicts of interest with respect to the research, authorship, and/or publication of this article.

Acknowledgments

This work was partially supported by the Natural Science Foundation of Zhejiang(No. LY20F020001) and the Natural Science Foundation of Ningbo City (No. 2018A610166, 2019A610339).

References

[1] D. De Bacquer, G. De Backer, M. Kornitzer, and H. Blackburn, "Prognostic value of ECG findings for total, cardiovascular disease, and coronary heart disease death in men and women," *Heart*, vol. 80, no. 6, pp. 570–577, 1998.

[2] E. J. d. S. Luz, S. William Robson, C.-C. Guillermo, W. R. Schwartz, G. Cámara-Chávez, and D. Menotti, "ECG-based heartbeat classification for arrhythmia detection: a survey," *Computer Methods and Programs in Biomedicine*, vol. 127, pp. 144–164, 2016.

[3] G. D. Clifford, J. Behar, Q. Li, and I. Rezek, "Signal quality indices and data fusion for determining clinical acceptability of electrocardiograms," *Physiological Measurement*, vol. 33, no. 9, pp. 1419–1433, 2012.

[4] I. Silva, B. Moody George, and C. Leo, "Improving the quality of ECGs collected using mobile phones: the physionet/computing in cardiology challenge 2011," in *Proceedings of 2011 Computing in Cardiology*, pp. 273–276, IEEE, Hangzhou, China, September 2011.

[5] M. Kabir, A. Ashfanoor, and C. Shahnaz, "Denoising of ECG signals based on noise reduction algorithms in EMD and wavelet domains," *Biomedical Signal Processing and Control*, vol. 7, no. 5, pp. 481–489, 2012.

[6] C. Can Ye, B. V. K. V. Kumar, and M. T. Coimbra, "Heartbeat classification using morphological and dynamic features of ECG signals," *IEEE Transactions on Biomedical Engineering*, vol. 59, no. 10, pp. 2930–2941, 2012.

[7] S. M. Kiani and S. Asadollah, "Classification of ECG arrhythmias using discrete wavelet transform and neural networks," *International Journal of Computer Science, Engineering and Applications*, vol. 2, p. 1, 2012.

[8] S. Sani, Ö. Nalan, and K. I. Abdullahi, "Wavelet feature extraction for ECG beat classification," in *Proceedings of 2014 IEEE 6th International Conference on Adaptive Science & Technology (ICAST)*, pp. 1–6, IEEE, Ota, Nigeria, October 2014.

[9] A. S. Muhammad, M. Gul, M. Muhammad, and A. Majdi, "Arrhythmia classification of ecg signals using hybrid features," *Computational and Mathematical Methods in Medicine*, vol. 2018, Article ID 1380348, 8 pages, 2018.

[10] L. Hela and K. Raouf, *Genetic Fuzzy Logic Based System for Arrhythmia Classification in Control Theory in Biomedical Engineering*, pp. 105–127, Elsevier, Amsterdam, Netherlands, 2020.

[11] S. Sahoo, M. Mohanty, S. Behera, and S. K. Sabut, "ECG beat classification using empirical mode decomposition and mixture of features," *Journal of Medical Engineering & Technology*, vol. 41, no. 8, pp. 652–661, 2017.

[12] S. Kiranyaz, T. Ince, and M. Gabbouj, "Real-time patient-specific ECG classification by 1-D convolutional neural networks," *IEEE Transactions on Biomedical Engineering*, vol. 63, no. 3, pp. 664–675, 2016.

[13] K. Mohammad, F. Shayan, and S. Majid, "ECG heartbeat classification: a deep transferable representation," in *Proceedings of 2018 IEEE International Conference on Healthcare Informatics (ICHI)*, pp. 443-444, IEEE, New York, NY, USA, June 2018.

[14] J. AlAref Subhi, A. Khalil, G. Singh et al., "Clinical applications of machine learning in cardiovascular disease and its relevance to cardiac imaging," *European Heart Journal*, vol. 40, pp. 1975–1986, 2019.

[15] Ü. E. Derya, "ECG beats classification using multiclass support vector machines with error correcting output codes," *Digital Signal Processing*, vol. 17, pp. 675–684, 2007.

[16] M. Majid and K. Hamid, "A qualitative comparison of artificial neural networks and support vector machines in ECG arrhythmias classification," *Expert Systems with Applications*, vol. 37, pp. 3088–3093, 2010.

[17] T. Li and M. Zhou, "ECG classification using wavelet packet entropy and random forests," *Entropy*, vol. 18, no. 8, p. 285, 2016.

[18] E. Nahit, "ECG beat classification by using discrete wavelet transform and Random Forest algorithm," in *Proceedings of 2009 5th International Conference on Soft Computing, Computing with Words and Perceptions in System Analysis, Decision and Control*, pp. 1–4, IEEE, Famagusta, North Cyprus, 2009.

[19] Z. Morteza, R. Ali Bahrami, K. Katsaggelos Aggelos, K. Serkan, N. Susanna, and G. Moncef, "Detection of atrial fibrillation in ecg hand-held devices using a random forest classifier," in *Proceedings of 2017 Computing in Cardiology (CinC)*, pp. 1–4, IEEE, Rennes, France, September 2017.

[20] D. Clifford Gari, C. Liu, M. Benjamin et al., "AF classification from a short single lead ECG recording: the physionet/computing in cardiology challenge 2017," in *Proceedings of 2017 Computing in Cardiology (CinC)*, pp. 1–4, IEEE, Rennes, France, September 2017.

[21] T. Tomás, A. Garc'ıa Constantino, C. Daniel, and F. Paulo, "Arrhythmia classification from the abductive interpretation of short single-lead ECG records," in *Proceedings of 2017 Computing in Cardiology (CinC)*, pp. 1–4, IEEE, Rennes, France, September 2017.

[22] S. Hong, M. Wu, Y. Zhou et al., "ENCASE: an ensemble classifier for ECG classification using expert features and deep neural networks," in *Proceedings of 2017 Computing in Cardiology (CinC)*, pp. 1–4, IEEE, Rennes, France, September 2017.

[23] S. Datta, P. Chetanya, A. Mukherjee et al., "Identifying normal, AF and other abnormal ECG rhythms using a cascaded binary classifier," in *Proceedings of 2017 Computing in*